THE SOLAR REFLECTANCE AND/OR HEMISPHERICAL EMITTANCE OF SELECTED SPACE SUIT MATERIALS

Contract No. NAS 9-3684
NASA Manned Spacecraft Center
Control No. PR4-19-8009

5324-6001-SU000

15 July 1965

Signed: Jerry T. Bevans
Head, Thermophysics Laboratory

Approved: for Robert P. Lipkis
Manager, Spacecraft Heat Transfer Dept.

TRW INC.
TRW SYSTEM GROUP
One Space Park . Redondo Beach, California

TABLE OF CONTENTS

LIST OF TABLES

LIST OF FIGURES

LIST OF FIGURES (CONT.)

Page

LIST OF FIGURES (CONT.)

Page

LIST OF FIGURES (CONT.)

Page

SUMMARY

The solar reflectance and/or hemispherical emittance of a number of selected space suit materials are reported. This work was performed for the NASA Manned Spacecraft Center under Contract No. NAS 9-3684, Control No. PR No. 4-19-8009.

1. INTRODUCTION

The thermal design of a space suit is strongly dependent upon the thermal radiation properties of the materials used in its construction. The particular thermal radiation properties of primary concern are the solar reflectance as a function of the angle of incidence ($\rho(\theta)$) and the total hemispherical emittance (ε_H). The following is a report of the results of a program to measure these properties for a number of probable space suit materials. This accumulation of information should be valuable in the evaluation and selection of candidate materials for future space suit designs.

MATERIALS TESTED

The materials tested in the program were supplied by the NASA Manned Spacecraft Center. Tables 1 and 2 summarize the descriptions of these materials as provided by the Manned Spacecraft Center.

2. MEASUREMENT PROCEDURES

2.1 SOLAR REFLECTANCE MEASUREMENTS

The directional spectral reflectance was measured in an integrating sphere reflectometer similar to that described by Edwards (1). The measurements were performed with the reflectometer operated in the "abolute mode" as described by Edwards, i.e., the measurements were not relative. The polar angles of incidence (measured from the surface normal) were 10, 22, 33, 44, 55, 66, and 80 degrees; azimuthal angles, as measured from a reference point marked on the sample, were 0, 45, 60, and 90 degrees.

The value of solar reflectance for each angular setting was calculated using the solar energy spectrum described by Johnson (2). The hemispherical solar reflectance was computed by numerically integrating the expression:

$$\rho_H = \frac{1}{\pi} \int_0^{2\pi} \int_0^{\pi/2} \rho(\theta,\varphi) \sin\theta \cos\theta \, d\theta \, d\varphi$$

where

θ = polar angle of incidence

φ = azimuthal angle of incidence

As will be shown in the results, the azimuthal variations were negligible for all test surfaces and the above expression reduced to

$$\rho_H = \int_0^{\pi/2} \rho(\theta) \, d\,(\sin^2\theta)$$

2.2 TOTAL HEMISPHERICAL EMITTANCE MEASUREMENTS

The total hemispherical emittance was determined by cementing the test samples to the large sides of a heater assembly. This heater assembly consisted of a constantan wire resistor sandwiched between two pieces of Mylar (0.001 inches thick). This resistance was again sandwiched between two face sheets of 1100 Alloy aluminum and the whole unit bonded together with epoxy cement. When completed, the heater assembly was approximately 4 inches square (10 cm.) and 0.063 inches (0.16 cm.) thick. Measurement of cloth surface temperature is a difficult experimental problem and probably will never be solved satisfactorily. For these tests, thermocouples were placed on the aluminum heater surfaces prior to the cementing of the samples to the heater.

The sample-heater unit was suspended by the heater and thermocouple wires within a liquid nitrogen cooled enclosure and housed in a vacuum bell jar. This bell jar was evacuated to a pressure of 10^{-6} torr or less. Sample temperatures of approximately - 150, 0, 100, and 250°F were set by adjusting the heat supplied to the samples. Equilibrium was established by monitoring the temperatures indicated by the thermocouples and data was not recorded until the readings were constant over a 20-40 minute time period.

The technique described above is essentially that given by Nelson and Bevans (3) and is based upon minimizing the errors described in that reference. Precautions were taken to minimize the edge effects by covering the edges of the sample-heater assembly with aluminum tape. The power was monitored by the usual four terminal resistor technique.

3. TEST RESULTS

3.1 SOLAR REFLECTANCE RESULTS

The directional solar reflectance measurements for the samples listed in Table 1 are summarized in Tables 3 through 13. The calculated hemispherical solar reflectances are given in Table 14. Note that no azimuthal variations in this hemispherical property are given since for the samples tested no azimuthal variation was found within the accuracy of the measurements. The spectral directional reflectances for these samples are given in Figures 14 through 57.

The effect of the degradation of ultraviolet and vacuum exposure is quite evident upon comparison of Samples 5B and 12B and Sample 16 and 17.

3.2 TOTAL HEMISPHERICAL EMITTANCE MEASUREMENTS

The total hemispherical emittance of the samples listed in Table 2 are given as a function of temperature in Figure 1 through 13. Two samples, No.'s 6.1 and 13.1, gave some difficulty in the measurement process. Both samples were a polypropylene laminated to an aluminum foil. Separation of the aluminum from the polypropylene occurred on the first sample tested, i.e., sample degradation. There was also some difficulty in securing a satisfactory bond between the sample and the aluminum heater surface. This latter problem was solved in succeeding samples by applying a primer to the aluminum heater surface, but the measurement at 250°F may have been affected by some material degradation.

The ultraviolet and vacuum degradation effects varied markedly between the different samples. Samples 4.1 and 11.1 indicate a small increase in emittance after exposure and a change in the temperature dependency. The same exposure apparently cleaned the aluminum surface of Samples 5.1A and 12.1A with consequent decrease in emissivity. For the Mylar side of these samples (5.1B and 12.1B), no significant change was indicated. Samples 6.1 and 13.1 were the two that were difficult to test but below 200°F, the effects of degradation were slight. A comparison of the results for Samples 16.1 and 17.1 show the degradation effects to have been very slight.

4. CONCLUSIONS

The study reported herein was essentially a testing program and, as such, the test results offer no conclusions. One point should be made, however. The spectral reflectance measurements indicated little azimuthal variation for the materials tested. This should not be considered to be a general conclusion for all space suit materials. Degradation by exposure to ultraviolet and vacuum conditions had an effect which depended upon the sample material. Each material must be tested for this condition and no generalization should be made.

5. ACKNOWLEDGEMENTS

Mr. G. Poradek of NASA Manned Spacecraft Center greatly assisted in the conduct of this program. Mr. G. Brown and F. Turnbow of TRW Systems directed and assisted in the performance of the measurements.

REFERENCES

1. Edward, D. K., et al., J. of the Optical Soc. Am., 51:1279-88 (1961).

2. Johnson, F. S., J. of Meteorology, 11:431-439 (1954).

3. Nelson, K. E., and Bevans, J. T., "Errors of the Calorimetric Method of Total Emittance Measurement," Measurement of Thermal Radiation Properties of Solids NASA SP-31, 1963.

Sample No.*	Description	Side Measured
4	Two 1/8 inch layers of open celled polyurethane foam sandwiched between a layer of rayon dipped in teflon containing a pigmentation of magnesium oxide (Side A), and a layer of nylon treco (Side B).	A
5	Seven layers of 1/4 mil Mylar uncoated on one side (Side B) and coated on the other side with monomolecular aluminum (Side A), separated with six layers of unwoven dacron spacers.	A, B
9	Fine weave DuPont HT-1 nylon (nomex) fabric with 3M aluminized coating in one side (Side A). This sample has been exposed for 12 hours to a high vacuum (10^{-7} torr) and the aluminized side (A) was exposed to a UV rich solar simulation source.	A
11	This sample is the same as Sample 4 except that the sample has been exposed for 12 hours to a high vacuum (10^{-7} torr) and the rayon dipped in teflon side was subjected to UV rich solar simulation for 12 hours.	A
12	This sample is the same as Sample 5 except that the sample was exposed to vacuum and the Mylar side subjected to 12 hours of UV rich solar simulation.	A, B
15	This sample is a medium weave DuPont HT-1 nylon (nomex) fabric with one side coated with 3M aluminum (Side A).	A, B
16	This is an uncoated DuPont HT-1 nylon (nomex) fabric (Side A) backed by 7 layers of NRC-2 aluminized Mylar separated by 7 layers of unwoven dacron spacers.	A
17	This sample is the same as Sample No. 16 except the sample has been exposed to vacuum (10^{-7}) and the nylon has been subjected to a UV rich solar source for 12 hours.	A

Table 1: Description of Sample Materials Measured for Solar Reflectance

*NASA Manned Spacecraft Center designation and description.

Sample No.*	Description	Side Measured
4.1	This is rayon fabric dipped in teflon containing a pigmentation of magnesium oxide.	A
5.1	This is a sheet of 1/4 mil Mylar with one side covered with a monomolecular layer of aluminum (Side A).	A, B
6.1	This is a 0.45 mil polypropylene layer (Side B) laminated to a 0.18 mil layer of aluminum foil (Side A).	B
8.1	This is a sheet of 1/4 mil Mylar with one side covered with a monomolecular layer of gold (Side A).	A
9	Fine weave DuPont HT-1 nylon (nomex) fabric with 3M aluminized coating in one side (Side A). This sample has been exposed for 12 hours to a high vacuum (10^{-7} torr) and the aluminized side (A) was exposed to a UV rich solar simulation source.	A
11.1	This is the same as Sample No. 4.1 except that the sample was exposed to high vacuum (10^{-7} torr) and (Side A) subjected to UV rich solar simulation for 12 hours.	A
12.1	This is the same as Sample No. 5.1 except that the sample was exposed to high vacuum (10^{-7} torr) and the Mylar side subjected to UV rich solar simulation for 12 hours.	A, B
13.1	This is the same as Sample No. 6.1 except that the sample was exposed to high vacuum (10^{-7} torr) for 12 hours.	B
15	This sample is a medium weave DuPont HT-1 nylon (nomex) fabric with one side coated with 3M aluminum (Side A).	B
16.1	This is uncoated HT-1 nylon fabric.	A
17.1	This is the same as Sample No. 16.1 except the sample has been exposed to high vacuum (10^{-7} torr) and UV rich solar simulation for 12 hours.	A

*NASA Manned Spacecraft designation and description.

Table 2: Description of Sample Materials Measured for Total Hemispherical Emittance

Azimuthal Angle* of Energy Incidence φ	Polar Angle of** Energy Incidence θ	Directional Solar Reflectance $\bar{\rho}_s$
0°	10	0.76
	22	0.76
	33	0.77
	44	0.77
	55	0.78
	66	0.79
	80	0.82
45°	10	0.76
	22	0.77
	33	0.77
	44	0.78
	55	0.78
	66	0.79
	80	0.82
60°	10	0.76
	22	0.77
	33	0.78
	44	0.78
	55	0.78
	66	0.79
	80	0.81
90°	10	0.76
	22	0.76
	33	0.76
	44	0.76
	55	0.79
	66	0.80
	80	0.81

Table 3: Values of Directional Solar Reflectance, $\bar{\rho}_s$, of Sample No. 4, Polyurethane Foam Sandwiched between a Rayon Dipped in Teflon Pigmented with MgO (Side Measured) and Nylon Treco

*The angle swept when a line in the plane of the sample is rotated counter-clockwise about the sample normal. The zero reference angle was arbitrarily chosen as the direction of the warp.

**The angle between the surface normal and the incident energy beam.

Azimuthal Angle* of Energy Incidence φ	Polar Angle of** Energy Incidence θ	Directional Solar Reflectance $\bar{\rho}_s$
0°	10°	.91
	22°	.91
	33°	.91
	44°	.91
	55°	.90
	66°	.90
	80°	.88
45°	10°	.91
	22°	.91
	33°	.91
	44°	.90
	55°	.90
	66°	.89
	80°	.88
60°	10°	.91
	22°	.91
	33°	.91
	44°	.90
	55°	.89
	66°	.89
	80°	.88
90°	10°	.91
	22°	.91
	33°	.90
	44°	.90
	55°	.90
	66°	.89
	80°	.88

Table 4: Values of Directional Solar Reflectance, $\bar{\rho}_s$, of MSC Sample No. 5A, 1/4 mil Aluminized Mylar (Aluminum Side)

* The angle sept when a line the plane of the sample is rotated counterclockwise about the sample normal. The zero reference angle was arbitrarily chosen.

** The angle between the surface normal and the incident energy beam.

Azimuthal Angle* of Energy Incidence φ	Polar Angle of** Energy Incidence θ	Directional Solar Reflectance $\bar{\rho}_s$
0°	10°	.86
	22	.86
	33	.85
	44	.85
	55	.84
	66	.82
	80	.80
45°	10°	.86
	22	.86
	33	.85
	44	.85
	55	.84
	66	.83
	80	.79
60°	10°	.86
	22	.86
	33	.86
	44	.85
	55	.85
	66	.83
	80	.78
90°	10°	.86
	22	.86
	33	.85
	44	.84
	55	.84
	66	.83
	80	.78

Table 5: Values of Directional Solar Reflectance, $\bar{\rho}_s$, of MSC Sample No. 5B, 1/4 mil Aluminized Mylar (Mylar Side)

* The angle swept when a line in the plane of the sample is rotated counter-clockwise about the sample normal. The zero reference angle was arbitrarily chosen.

** The angle between the surface normal and the incident energy beam.

Azimuthal Angle* of Energy Incidence φ	Polar Angle of** Energy Incidence θ	Directional Solar Reflectance $\bar{\rho}_s$
0°	10	.90
	22	.91
	33	.91
	44	.90
	55	.88
	66	.87
	80	.84
45°	10	.91
	22	.92
	33	.91
	44	.90
	55	.89
	66	.88
	80	.84
60°	10	.88
	22	.91
	33	.90
	44	.89
	55	.88
	66	.88
	80	.84
90°	10	.88
	22	.91
	33	.90
	44	.89
	55	.89
	66	.87
	80	.84

Table 6: Values of Directional Solar Reflectance, $\bar{\rho}_s$, of Sample No. 9, Aluminized DuPont HT-1 Nylon Fabric Exposed to Ultraviolet and Vacuum

*The angle swept when a line in the plane of the sample is rotated counter-clockwise about the sample normal. The zero reference angle was arbitrarily chosen as the direction of the woof for Sample 9 and the warp for Sample 4.

**The angle between the surface normal and the incident energy beam.

Azimuthal Angle* of Energy Incidence φ	Polar Angle** of Energy Incidence θ	Directional Solar Reflectance $\bar{\rho}_s$
0°	10	0.71
	22	0.71
	33	0.73
	44	0.73
	55	0.74
	66	0.75
	80	0.77
45°	10	0.72
	22	0.72
	33	0.73
	44	0.72
	55	0.73
	66	0.76
	80	0.77
60°	10	0.71
	22	0.71
	33	0.72
	44	0.72
	55	0.73
	66	0.74
	80	0.77
90°	10	0.71
	22	0.71
	33	0.71
	44	0.72
	55	0.74
	66	0.74
	80	0.77

Table 7: Values of Directional Solar Reflectance, $\bar{\rho}_s$, of Sample No. 11

*The angle swept when a line in the plane of the sample is rotated counter-clockwise about the sample normal. The zero reference angle was arbitrarily chosen as the direction of the warp.

**The angle between the surface normal and the incident energy beam.

Azimuthal Angle* of Energy Incidence φ	Polar Angle of** Energy Incidence θ	Directional Solar Reflectance $\bar{\rho}_s$
0°	10°	.88
	22°	.88
	33°	.88
	44°	.88
	55°	.87
	66°	.86
	80°	.82
45°	10°	.89
	22°	.89
	33°	.88
	44°	.87
	55°	.87
	66°	.86
	80°	.83
60°	10°	.89
	22°	.88
	33°	.88
	44°	.88
	55°	.86
	66°	.86
	80°	.83
90°	10°	.88
	22°	.88
	33°	.88
	44°	.87
	55°	.86
	66°	.86
	80°	.83

Table 8: Tabulated Values of Directional Solar Reflectance, $\bar{\rho}_s$, for Sample 12A, 1/4 mil Aluminized Mylar (Aluminized Side)

* The angle swept when a line in the plane of the sample is rotated counter-clockwise about the sample normal. The zero reference angle was arbitarily chosen.

** The angle between the surface normal and the incident energy beam.

Azimuthal Angle* of Energy Incidence φ	Polar Angle of** Energy Incidence θ	Directional Solar Reflectance $\bar{\rho}_s$
0°	10°	.79
	22°	.79
	33°	.78
	44°	.77
	55°	.77
	66°	.76
	80°	.74
45°	10°	.79
	22°	.79
	33°	.78
	44°	.79
	55°	.77
	66°	.77
	80°	.75
60°	10°	.79
	22°	.79
	33°	.79
	44°	.78
	55°	.77
	66°	.76
	80°	.74
90°	10°	.79
	22°	.79
	33°	.78
	44°	.78
	55°	.77
	66°	.76
	80°	.73

Table 9: Tabulated Values of Directional Solar Reflectance, $\bar{\rho}_s$, for Sample 12B, 1/4 mil Aluminized Mylar (Mylar Side)

* The angle swept when a line in the plane of the sample is rotated counter-clockwise about the sample normal. The zero reference angle was arbitrarily chosen.

** The angle between the surface normal and the incident energy beam.

Azimuthal Angle* of Energy Incidence φ	Polar Angle of** Energy Incidence θ	Directional Solar Reflectance $\bar{\rho}_s$
0°	10°	.87
	22	.88
	33	.88
	44	.86
	55	.86
	66	.84
	80	.79
45°	10°	.87
	22	.88
	33	.88
	44	.86
	55	.85
	66	.83
	80	.79
60°	10°	.86
	22	.88
	33	.87
	44	.86
	55	.86
	66	.83
	80	.79
90°	10°	.86
	22	.88
	33	.87
	44	.86
	55	.86
	66	.84
	80	.79

Table 10: Values of Directional Solar Reflectance, $\bar{\rho}_s$, of MSC Sample No. 15A Medium Weave DuPont HT-1 Nylon (Nomex) Fabric with One Side Coated with 3M Aluminum (Aluminum Side), Aluminum Side Measured

* The angle swept when a line in the plane of the sample is rotated counter-clockwise about the sample normal. The zero reference angle was chosen as the direction of the warp.

** The angle between the surface normal and the incident energy beam.

Azimuthal Angle* of Energy Incidence φ	Polar Angle of** Energy Incidence θ	Directional Solar Reflectance $\bar{\rho}_s$
0°	10°	.62
	22	.62
	33	.62
	44	.62
	55	.64
	66	.66
	80	.71
45°	10°	.61
	22	.61
	33	.62
	44	.63
	55	.65
	66	.67
	80	.72
60°	10°	.62
	22	.62
	33	.62
	44	.64
	55	.65
	66	.67
	80	.71
80°	10°	.61
	22	.62
	33	.62
	44	.64
	55	.65
	66	.67
	80	.71

Table 11: Values of Directional Solar Reflectance, $\bar{\rho}_s$, of MSC Sample No. 15B, Medium Weave DuPont HT-1 Nylon (Nomex) Fabric with One Side Coated with 3M Aluminum (Nylon Side), Nylon Side Measured

* The angle swept when a line in the plane of the sample is rotated counter-clockwise about the sample normal. The zero reference angle was chosen as the direction of the warp.

** The angle between the surface normal and the incident energy beam.

Azimuthal Angle* of Energy Incidence φ	Polar Angle of** Energy Incidence θ	Directional Solar Reflectance $\bar{\rho}_s$
0°	10	.70
	22	.71
	33	.71
	44	.72
	55	.73
	66	.73
	80	.77
45°	10	.71
	22	.71
	33	.71
	44	.72
	55	.73
	66	.74
	80	.78
60°	10	.71
	22	.71
	33	.71
	44	.72
	55	.73
	66	.74
	80	.77
90°	10	.71
	22	.71
	33	.71
	44	.72
	55	.72
	66	.74
	80	.77

Table 12: Values of Directional Solar Reflectance, $\bar{\rho}_s$ of Sample No. 16, Uncoated DuPont HT-1 Nylon Fabric

*The angle swept when a line in the plane of the sample is rotated counter-clockwise about the sample normal. The zero reference angle was arbitrarily chosen as the direction of the warp.

**The angle between the surface normal and the incident energy beam.

Azimuthal Angle* of Energy Incidence φ	Polar Angle of** Energy Incidence θ	Directional Solar Reflectance $\bar{\rho}_s$
0°	10	.67
	22	.67
	33	.68
	44	.68
	55	.71
	66	.72
	80	.71
45°	10	.68
	22	.68
	33	.68
	44	.69
	55	.70
	66	.71
	80	.72
60°	10	.67
	22	.68
	33	.68
	44	.68
	55	.70
	66	.71
	80	.72
90°	10	.67
	22	.68
	33	.68
	44	.68
	55	.67
	66	.72
	80	.70

Table 13: Values of Directional Solar Reflectance, $\bar{\rho}_s$, of Sample No. 17, Uncoated DuPont Nylon Fabric Exposed to an Ultraviolet Source in a Vacuum

*The angle swept when a line in the plane of the sample is rotated counter-clockwise about the sample normal. The zero reference angle was arbitrarily chosen as the direction of the warp.

**The angle between the surface normal and the incident energy beam.

SAMPLE NO. (See Table 1 for description.)	HEMISPHERICAL SOLAR REFLECTANCE ρ_H
4	.78
5A	.90
5B	.84
9	.89
11	.74
12A	.87
12B	.77
15A	.86
15B	.64
16	.72
17	.69

Table 14: Tabulated Values of Hemispherical Reflectance for Solar Radiation

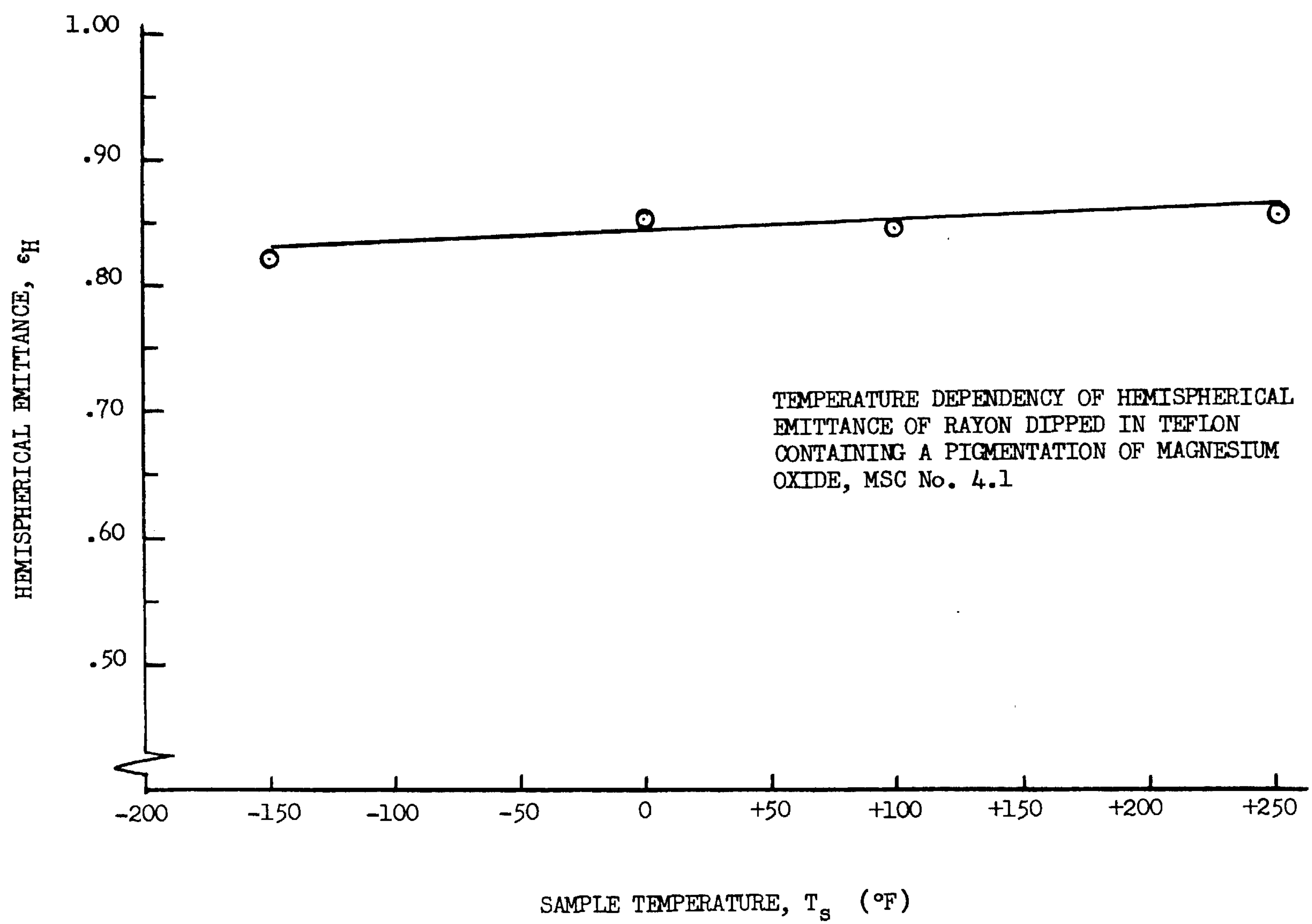
TEMPERATURE DEPENDENCY OF HEMISPHERICAL EMITTANCE OF RAYON DIPPED IN TEFLON CONTAINING A PIGMENTATION OF MAGNESIUM OXIDE, MSC No. 4.1
HEMISPHERICAL EMITTANCE, ϵ_H
1.00
.90
.80
.70
.60
.50
-200
-150
-100
-50
0
+50
+100
+150
+200
+250
SAMPLE TEMPERATURE, T_s (°F)

FIGURE 1

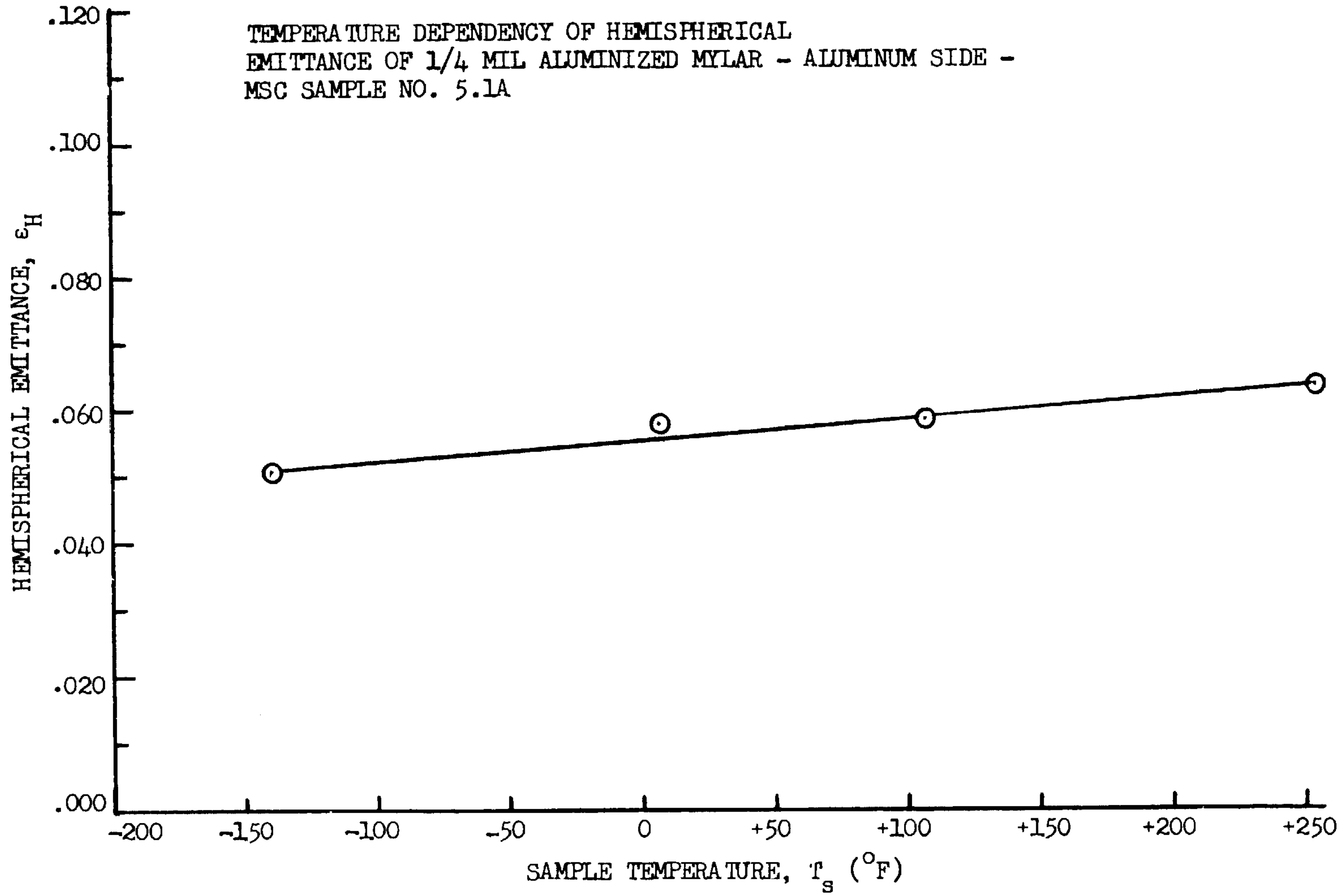

TEMPERATURE DEPENDENCY OF HEMISPHERICAL
EMITTANCE OF 1/4 MIL ALUMINIZED MYLAR - ALUMINUM SIDE -
MSC SAMPLE NO. 5.1A
.120
.100
.080
.060
.040
.020
.000
HEMISPHERICAL EMITTANCE, εH
-200
-150
-100
-50
0
+50
+100
+150
+200
+250
SAMPLE TEMPERATURE, Ts (°F)

FIGURE 2

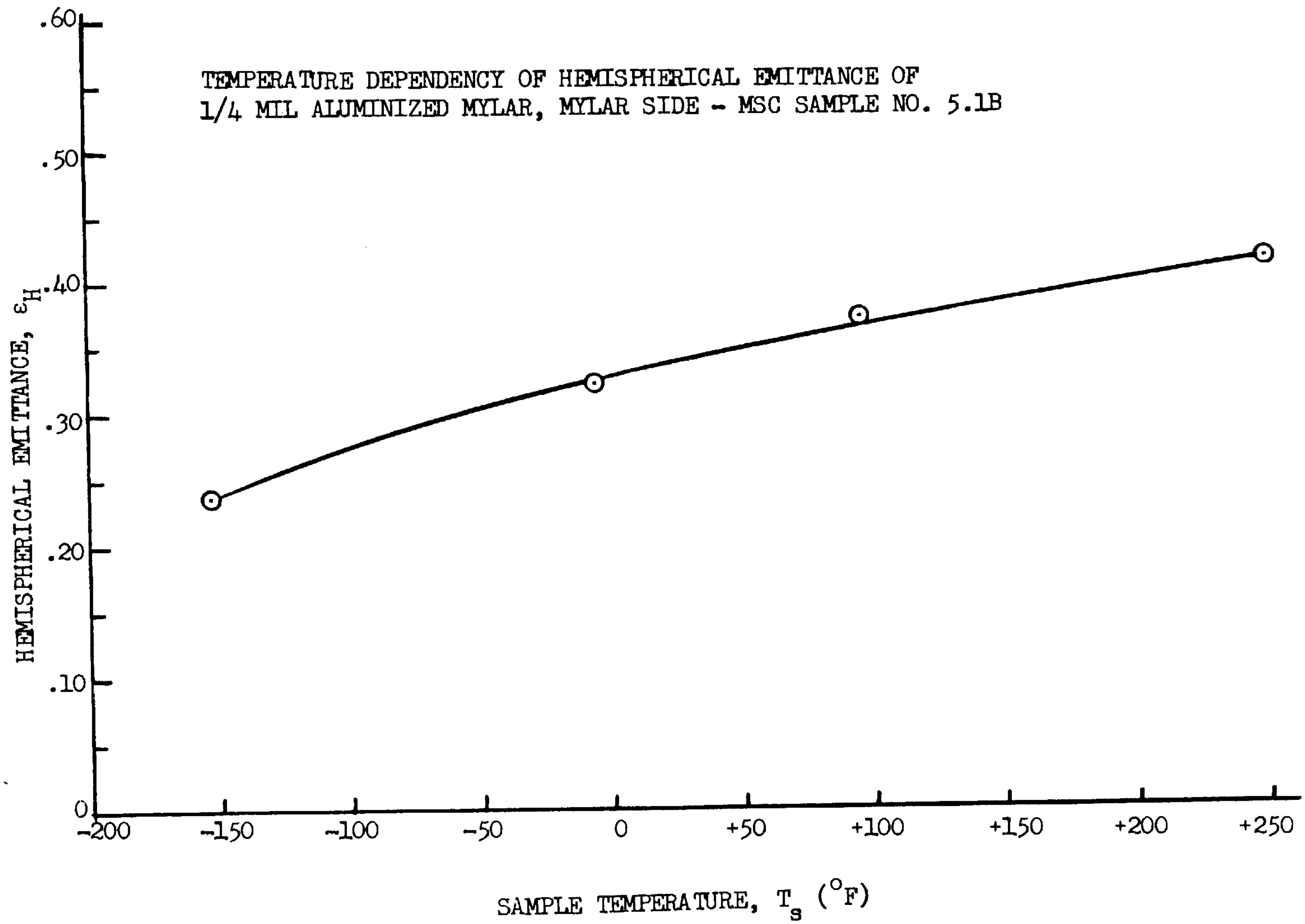
TEMPERATURE DEPENDENCY OF HEMISPHERICAL EMITTANCE OF
1/4 MIL ALUMINIZED MYLAR, MYLAR SIDE - MSC SAMPLE NO. 5.1B
.60
.50
.40
.30
.20
.10
0
HEMISPHERICAL EMITTANCE, ε_H
-200
-150
-100
-50
0
+50
+100
+150
+200
+250
SAMPLE TEMPERATURE, T_s (^oF)

FIGURE 3

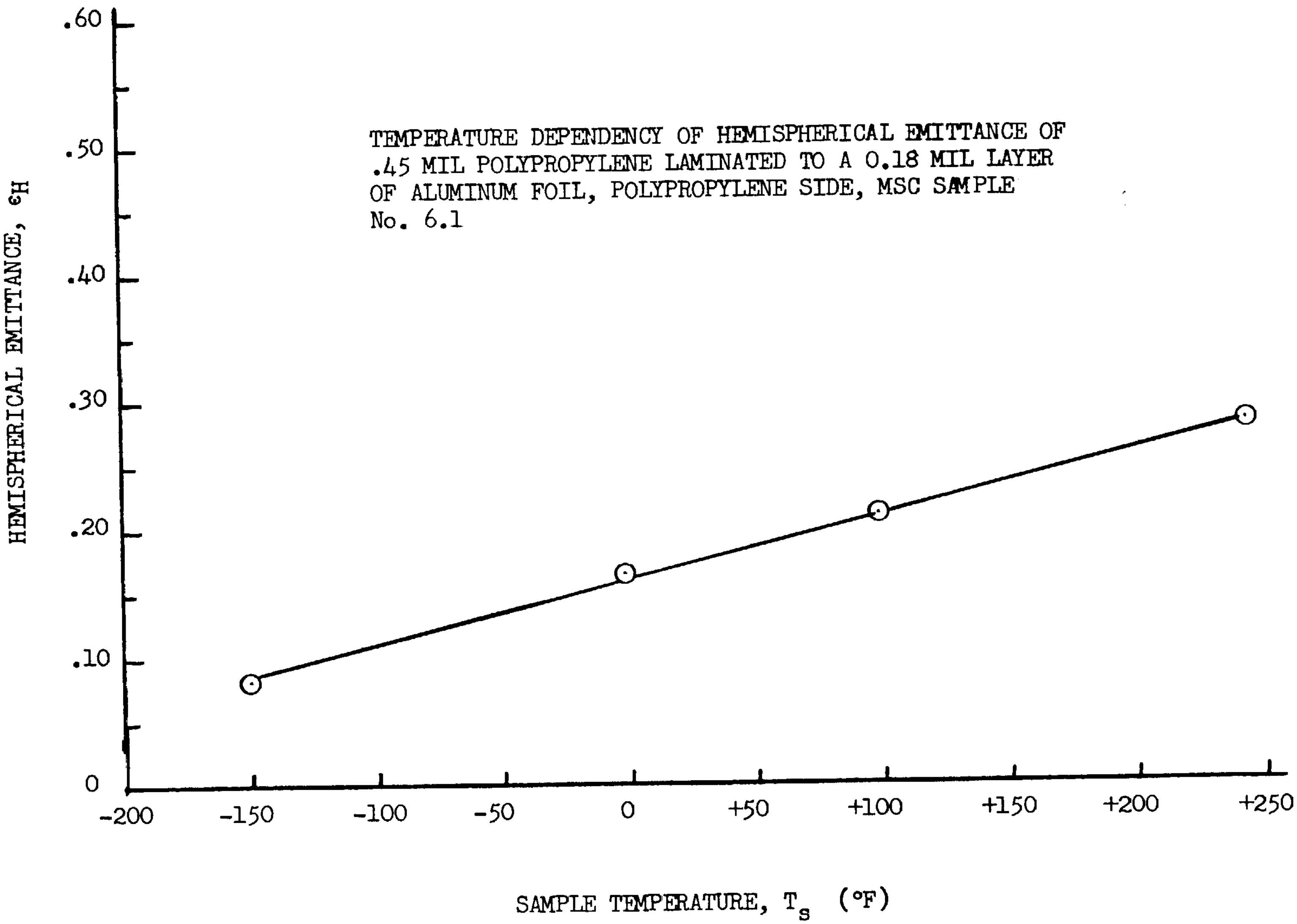
TEMPERATURE DEPENDENCY OF HEMISPHERICAL EMITTANCE OF .45 MIL POLYPROPYLENE LAMINATED TO A 0.18 MIL LAYER OF ALUMINUM FOIL, POLYPROPYLENE SIDE, MSC SAMPLE No. 6.1
HEMISPHERICAL EMITTANCE, ϵ_H
.60
.50
.40
.30
.20
.10
0
-200
-150
-100
-50
0
+50
+100
+150
+200
+250
SAMPLE TEMPERATURE, T_s (°F)

FIGURE 4

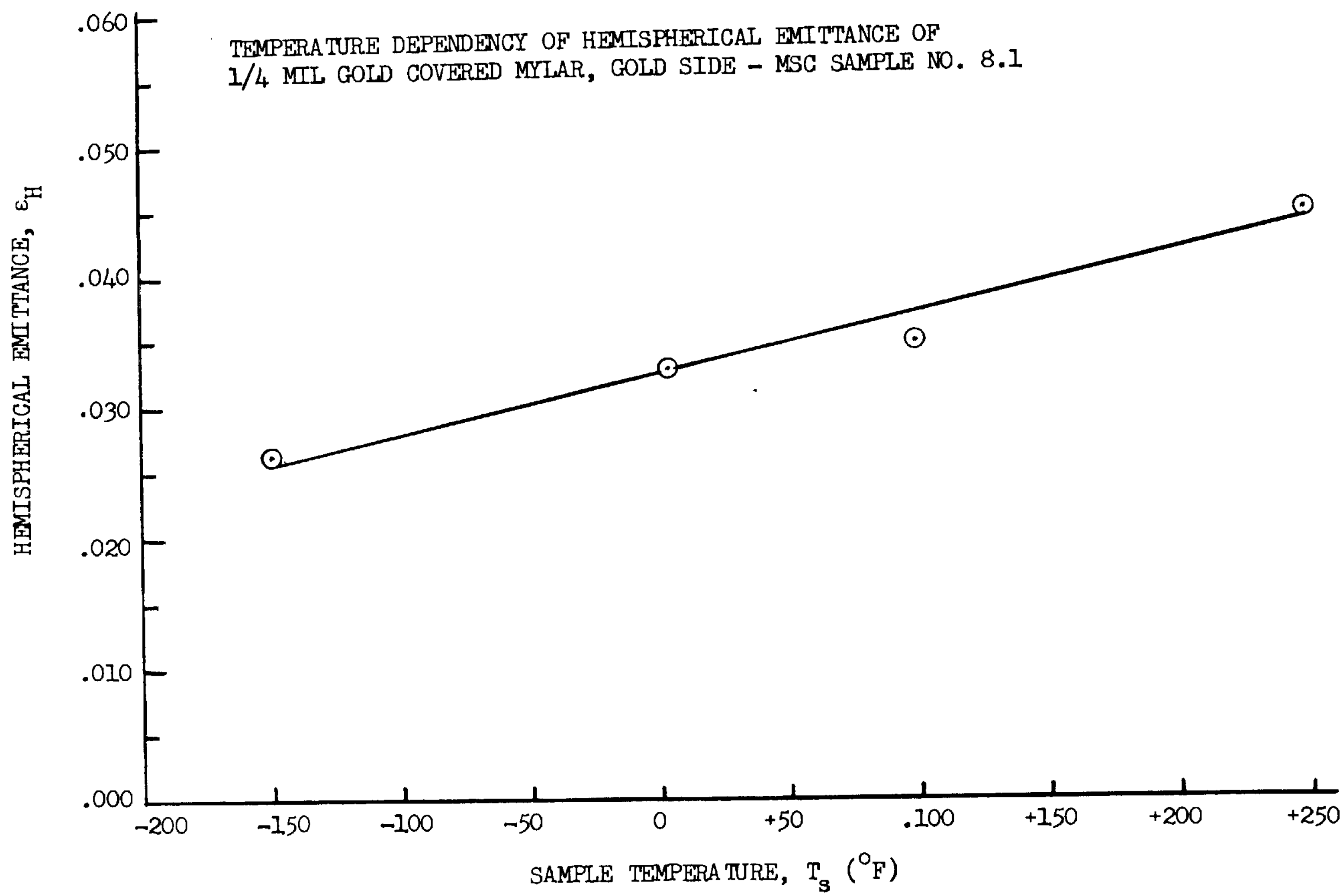
TEMPERATURE DEPENDENCY OF HEMISPHERICAL EMITTANCE OF
1/4 MIL GOLD COVERED MYLAR, GOLD SIDE - MSC SAMPLE NO. 8.1
HEMISPHERICAL EMITTANCE, εH
.060
.050
.040
.030
.020
.010
.000
-200
-150
-100
-50
0
+50
.100
+150
+200
+250
SAMPLE TEMPERATURE, Ts (°F)

FIGURE 5

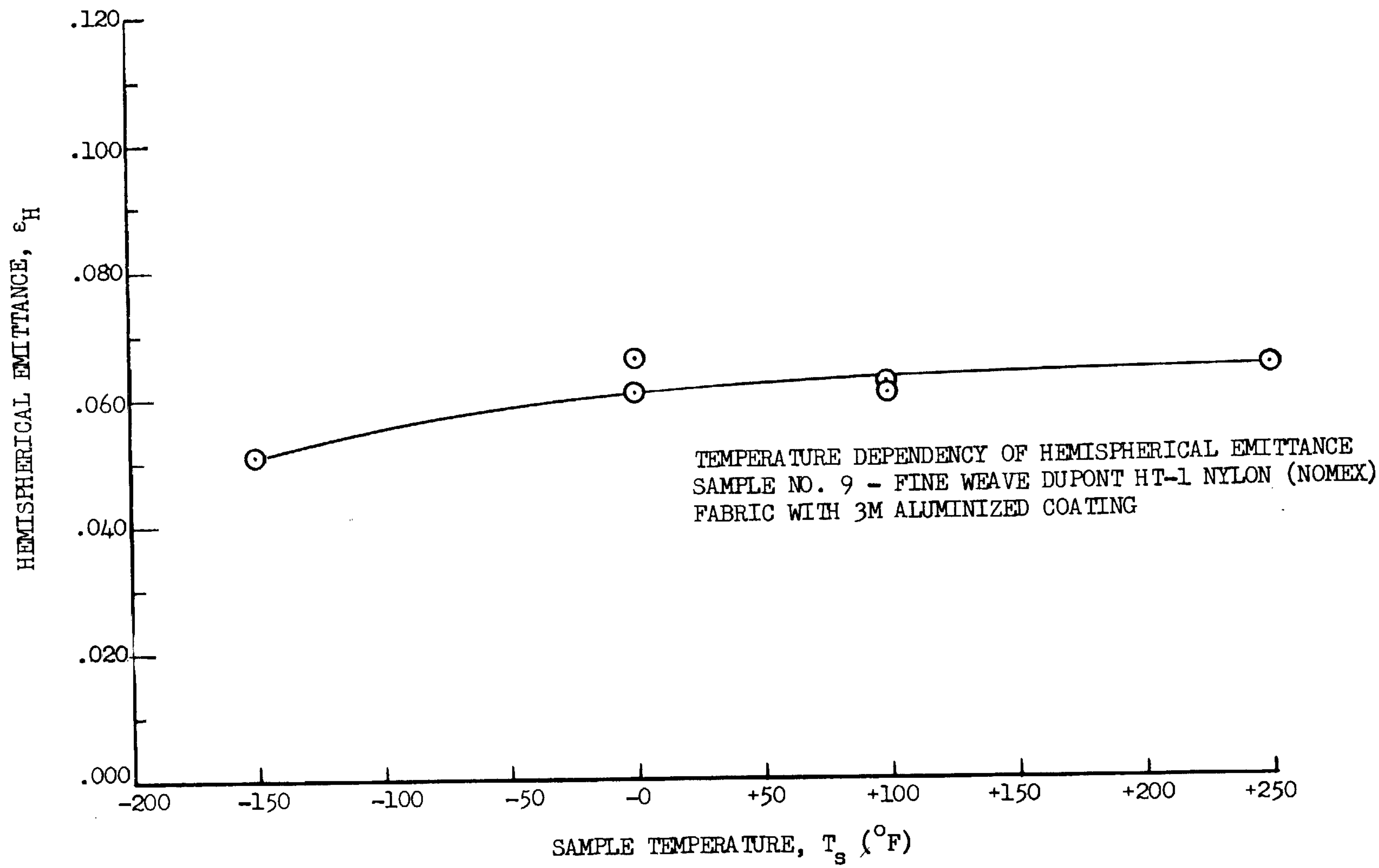
TEMPERATURE DEPENDENCY OF HEMISPHERICAL EMITTANCE
SAMPLE NO. 9 - FINE WEAVE DUPONT HT-1 NYLON (NOMEX)
FABRIC WITH 3M ALUMINIZED COATING
HEMISPHERICAL EMITTANCE, ε_H
.120
.100
.080
.060
.040
.020
.000
-200
-150
-100
-50
-0
+50
+100
+150
+200
+250
SAMPLE TEMPERATURE, T_s (°F)

FIGURE 6

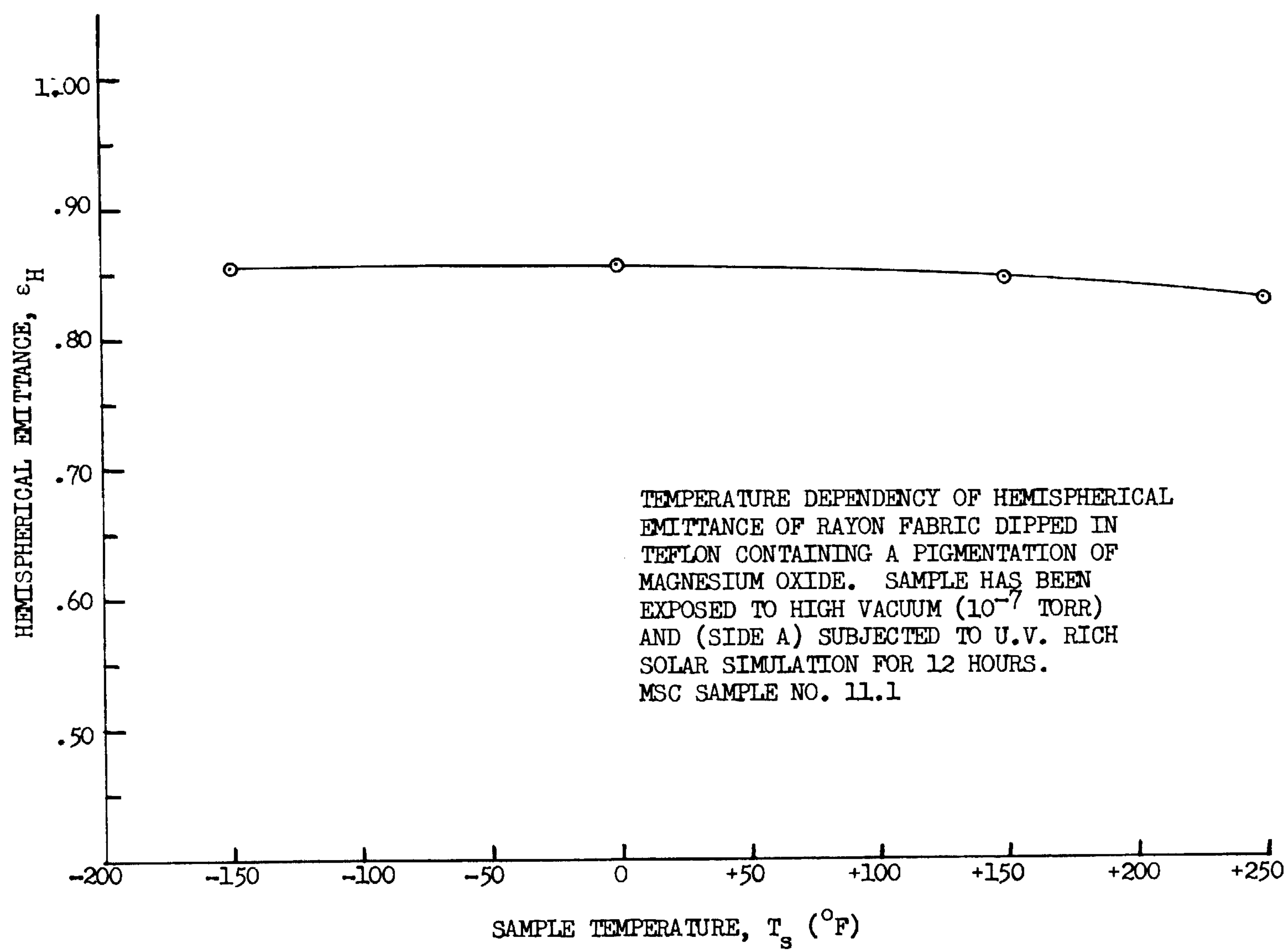
1.00
.90
.80
.70
.60
.50
HEMISPHERICAL EMITTANCE, ε_H
-200
-150
-100
-50
0
+50
+100
+150
+200
+250
SAMPLE TEMPERATURE, T_s (°F)
TEMPERATURE DEPENDENCY OF HEMISPHERICAL
EMITTANCE OF RAYON FABRIC DIPPED IN
TEFLON CONTAINING A PIGMENTATION OF
MAGNESIUM OXIDE. SAMPLE HAS BEEN
EXPOSED TO HIGH VACUUM (10^{-7} TORR)
AND (SIDE A) SUBJECTED TO U.V. RICH
SOLAR SIMULATION FOR 12 HOURS.
MSC SAMPLE NO. 11.1

FIGURE 7

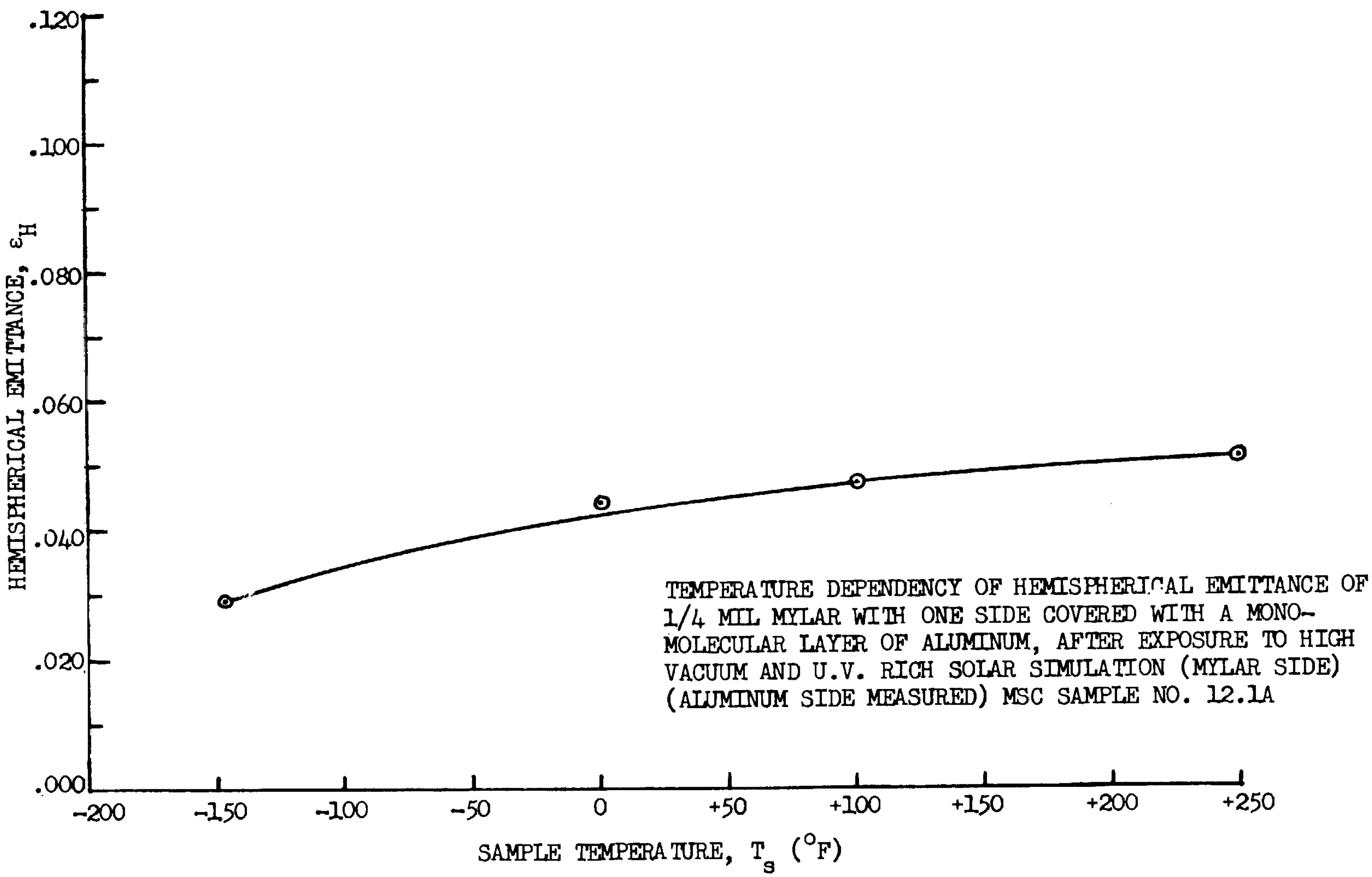
.120
.100
.080
.060
.040
.020
.000
HEMISPHERICAL EMITTANCE, ε_H
-200
-150
-100
-50
0
+50
+100
+150
+200
+250
SAMPLE TEMPERATURE, T_s (°F)
TEMPERATURE DEPENDENCY OF HEMISPHERICAL EMITTANCE OF 1/4 MIL MYLAR WITH ONE SIDE COVERED WITH A MONO-MOLECULAR LAYER OF ALUMINUM, AFTER EXPOSURE TO HIGH VACUUM AND U.V. RICH SOLAR SIMULATION (MYLAR SIDE) (ALUMINUM SIDE MEASURED) MSC SAMPLE NO. 12.1A

FIGURE 8

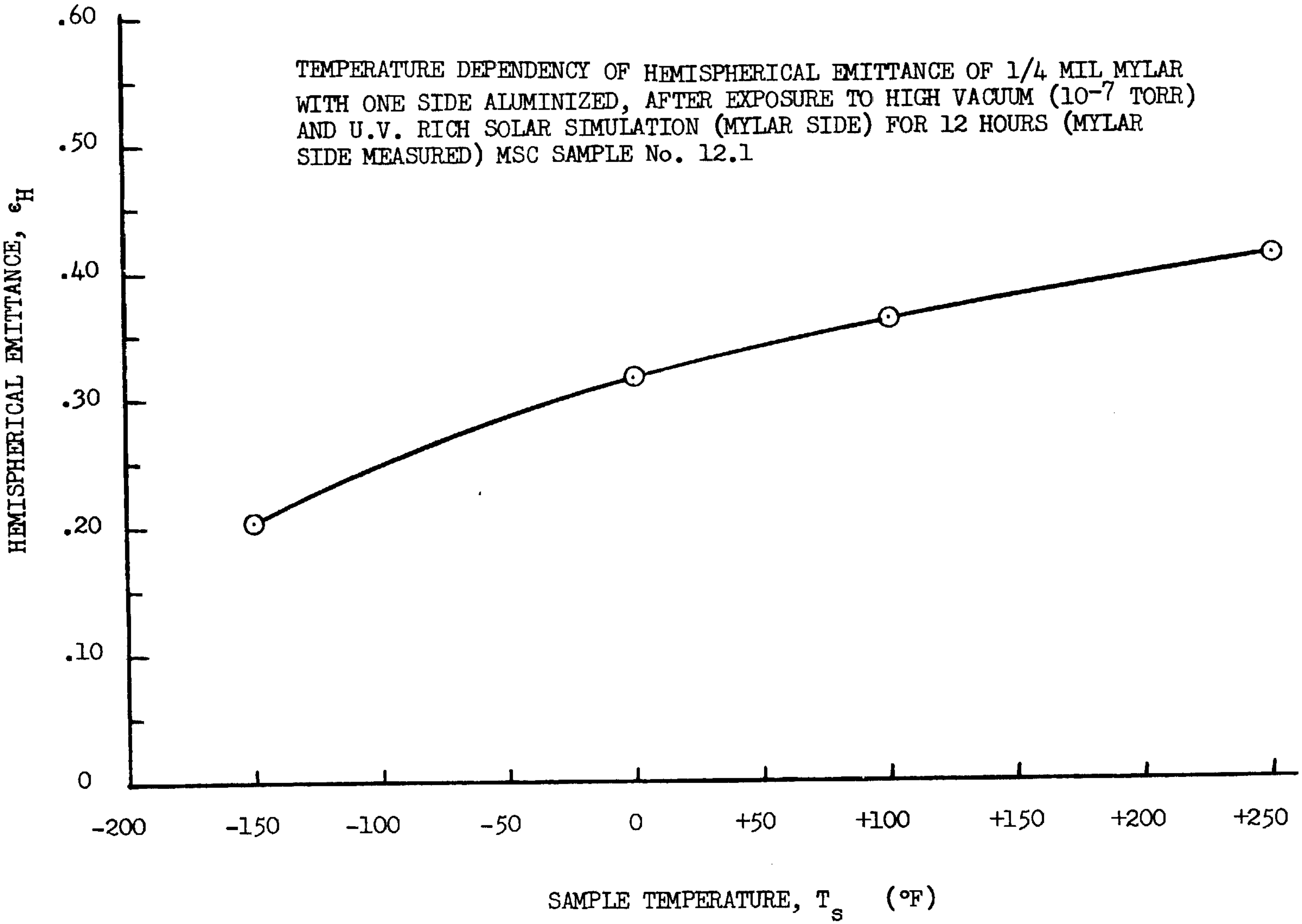
TEMPERATURE DEPENDENCY OF HEMISPHERICAL EMITTANCE OF 1/4 MIL MYLAR WITH ONE SIDE ALUMINIZED, AFTER EXPOSURE TO HIGH VACUUM (10-7 TORR) AND U.V. RICH SOLAR SIMULATION (MYLAR SIDE) FOR 12 HOURS (MYLAR SIDE MEASURED) MSC SAMPLE No. 12.1
HEMISPHERICAL EMITTANCE, εH
.60
.50
.40
.30
.20
.10
0
-200
-150
-100
-50
0
+50
+100
+150
+200
+250
SAMPLE TEMPERATURE, Ts (°F)

FIGURE 9

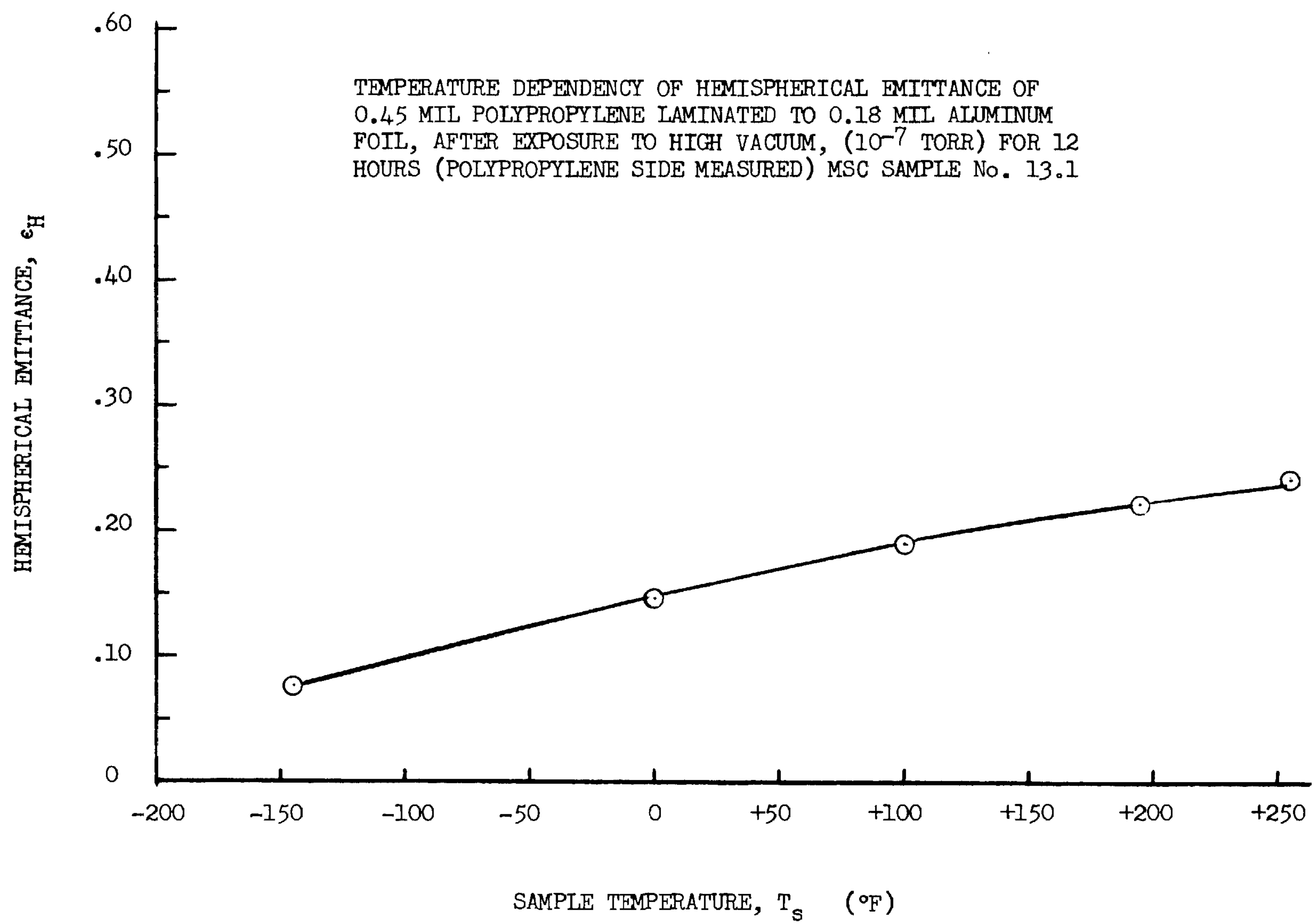
TEMPERATURE DEPENDENCY OF HEMISPHERICAL EMITTANCE OF
0.45 MIL POLYPROPYLENE LAMINATED TO 0.18 MIL ALUMINUM
FOIL, AFTER EXPOSURE TO HIGH VACUUM, (10^{-7} TORR) FOR 12
HOURS (POLYPROPYLENE SIDE MEASURED) MSC SAMPLE No. 13.1
HEMISPHERICAL EMITTANCE, ϵ_H
.60
.50
.40
.30
.20
.10
0
-200
-150
-100
-50
0
+50
+100
+150
+200
+250
SAMPLE TEMPERATURE, T_s (°F)

FIGURE 10

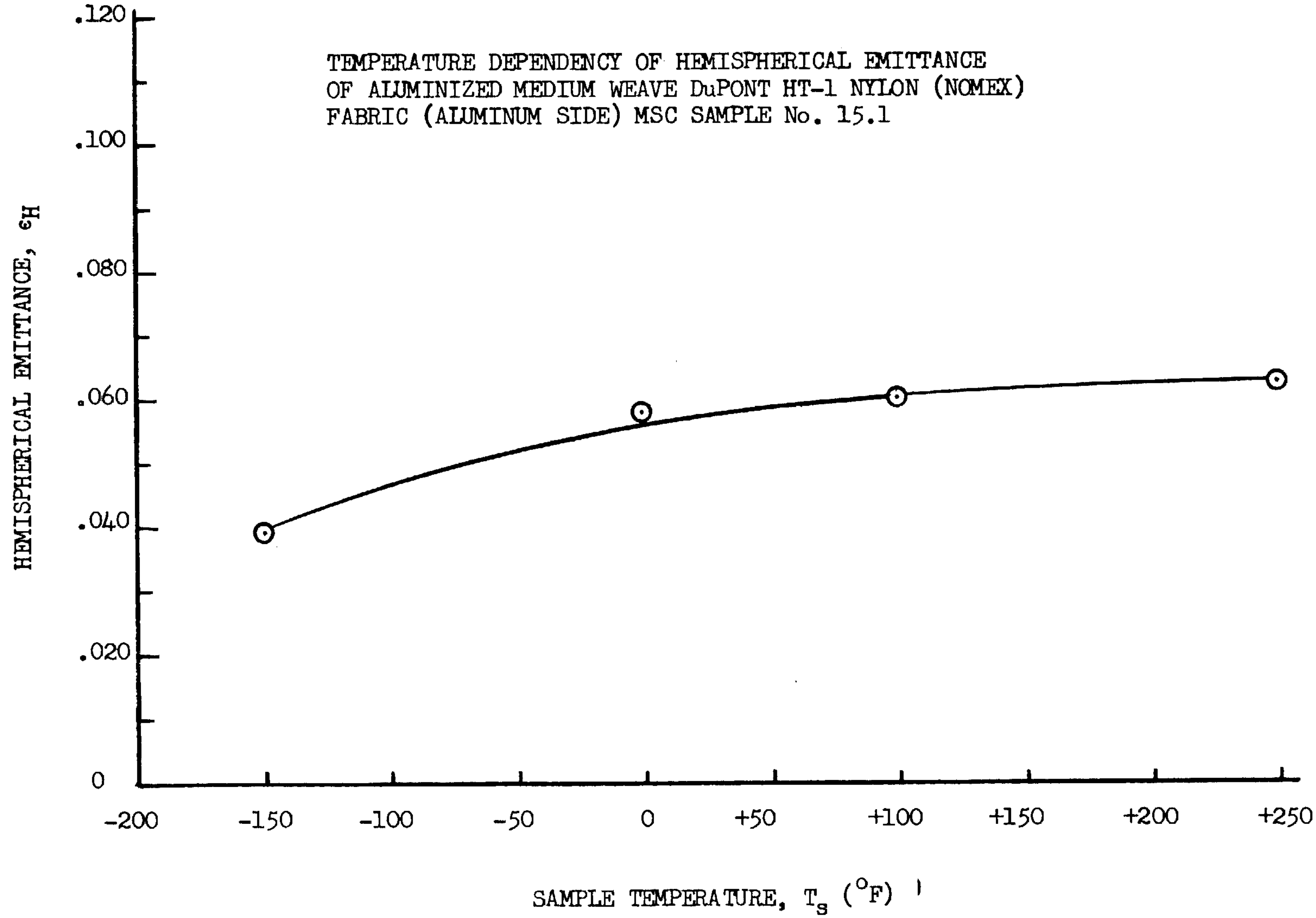
TEMPERATURE DEPENDENCY OF HEMISPHERICAL EMITTANCE
OF ALUMINIZED MEDIUM WEAVE DuPONT HT-1 NYLON (NOMEX)
FABRIC (ALUMINUM SIDE) MSC SAMPLE No. 15.1
HEMISPHERICAL EMITTANCE, ϵ_H
.120
.100
.080
.060
.040
.020
0
-200
-150
-100
-50
0
+50
+100
+150
+200
+250
SAMPLE TEMPERATURE, T_s (^oF)

FIGURE 11

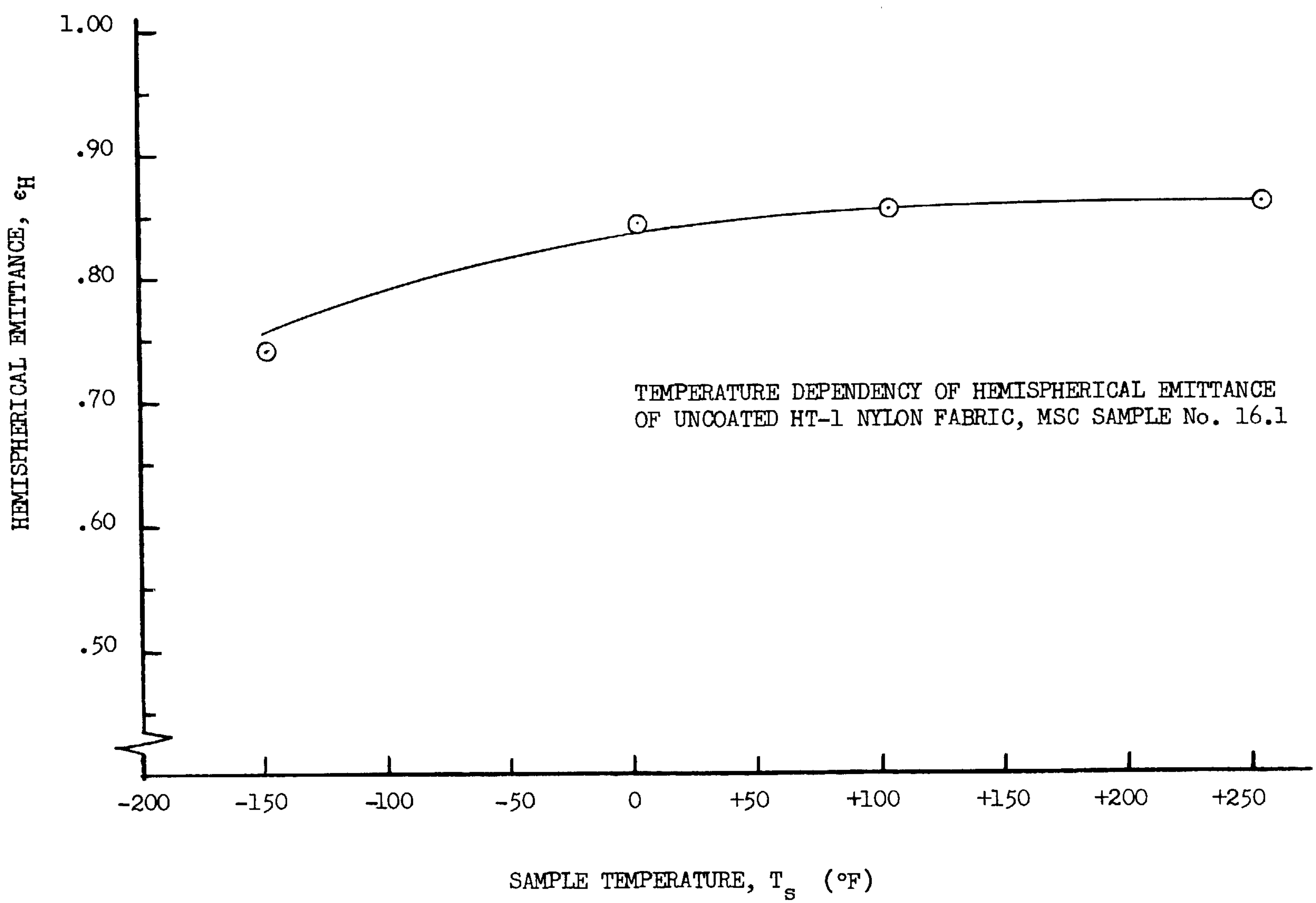
TEMPERATURE DEPENDENCY OF HEMISPHERICAL EMITTANCE
OF UNCOATED HT-1 NYLON FABRIC, MSC SAMPLE No. 16.1
HEMISPHERICAL EMITTANCE, ϵ_H
1.00
.90
.80
.70
.60
.50
-200
-150
-100
-50
0
+50
+100
+150
+200
+250
SAMPLE TEMPERATURE, T_s (°F)

FIGURE 12

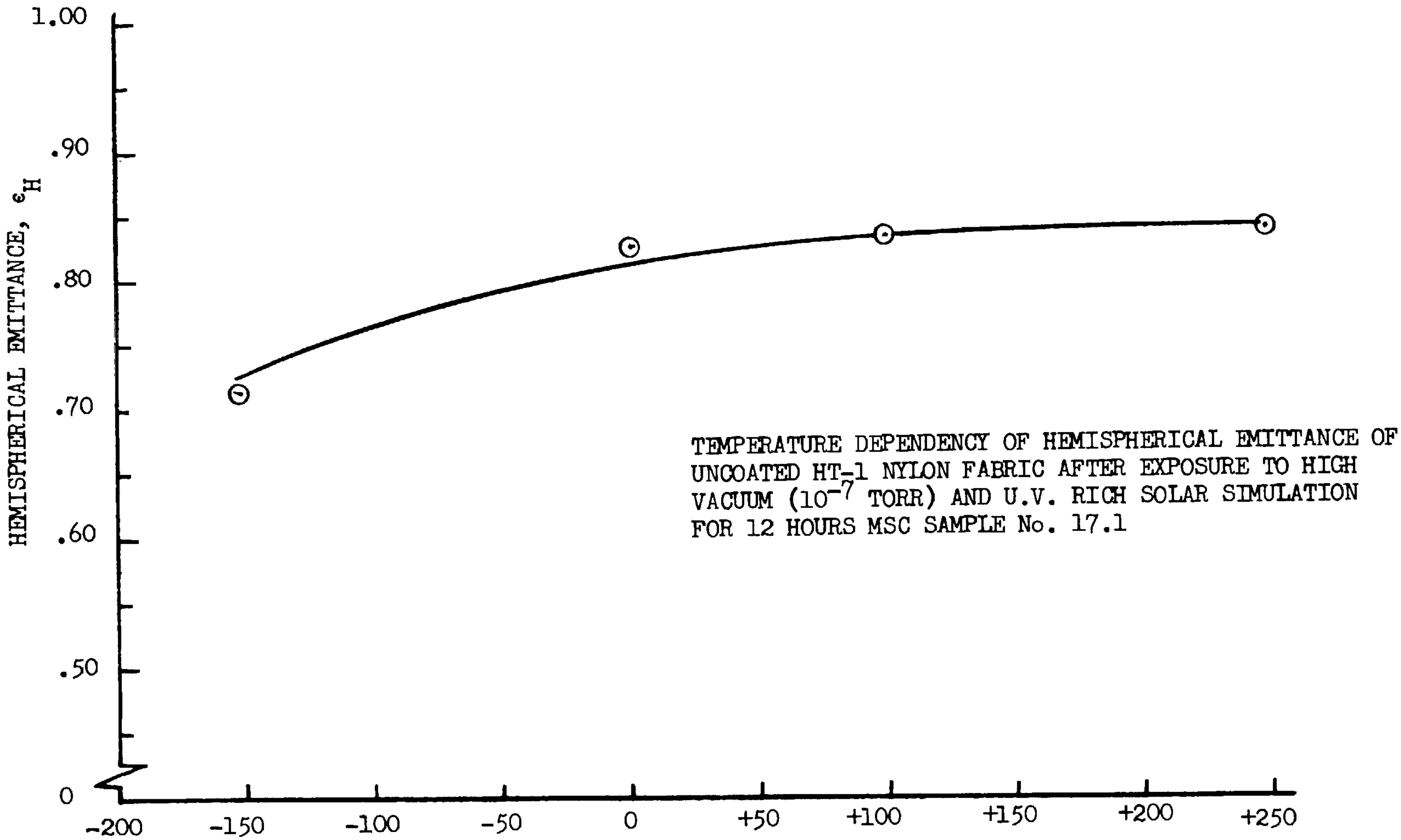

SAMPLE TEMPERATURE, T_s (°F)

FIGURE 13

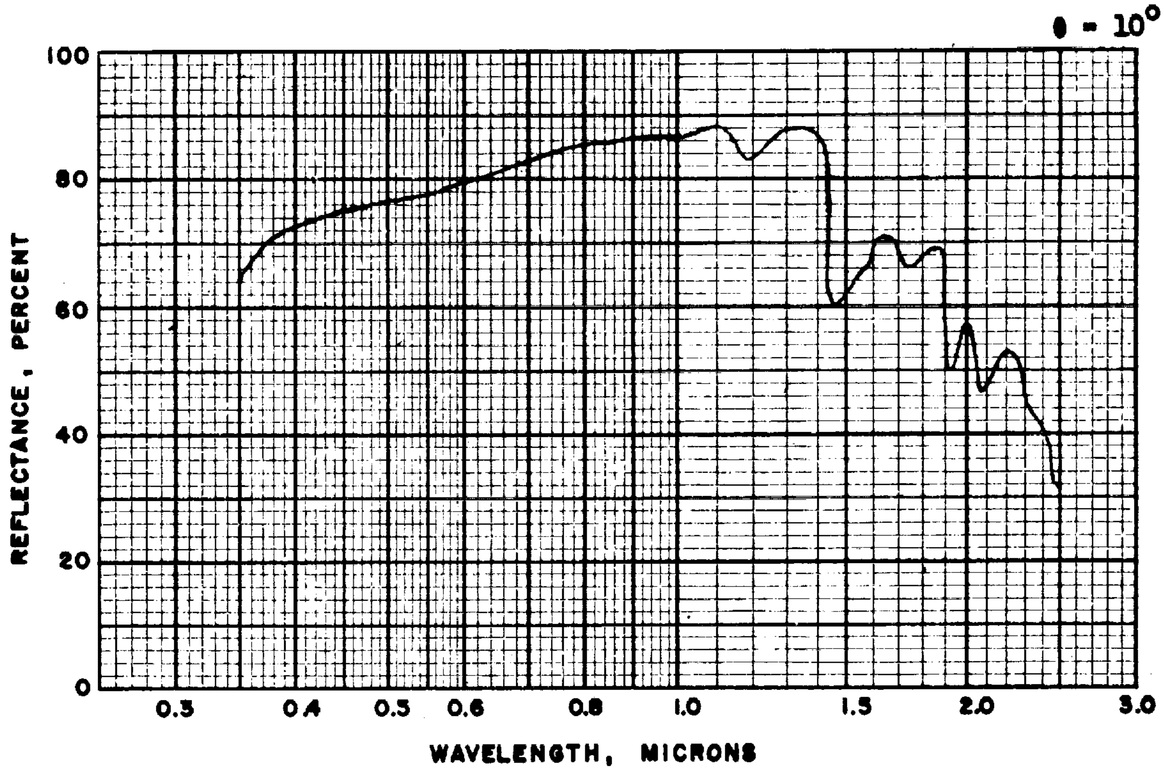

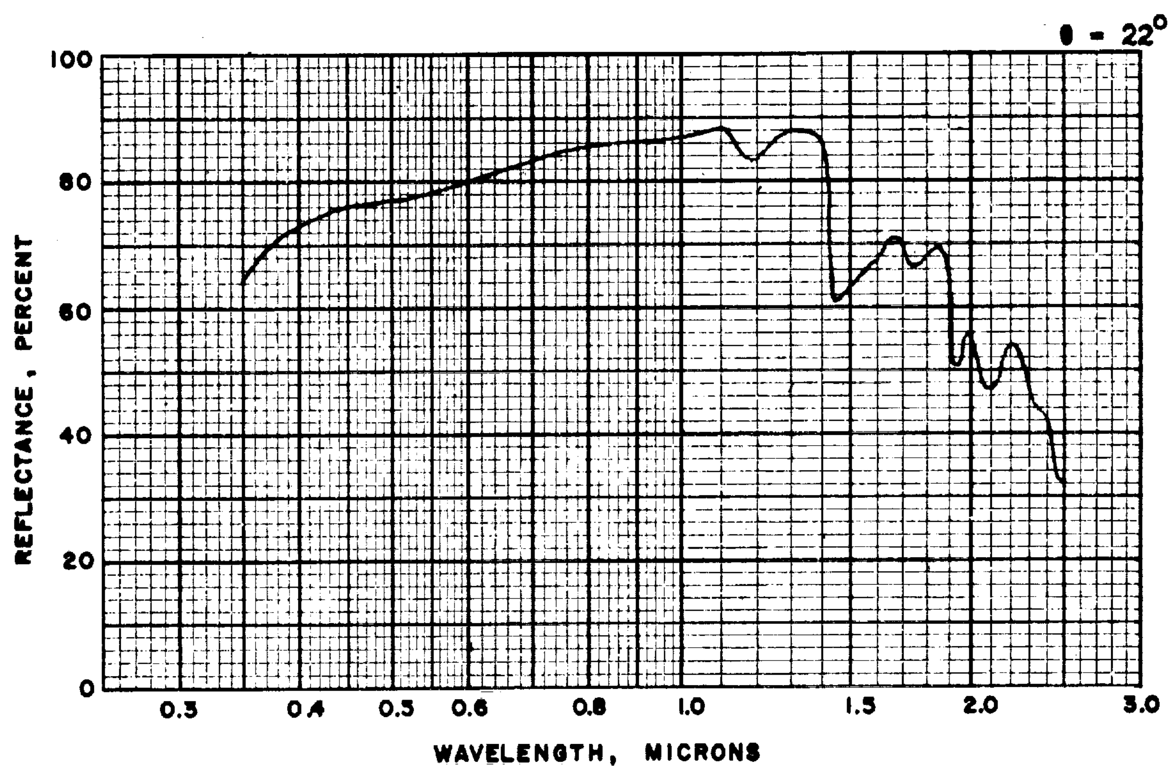

Figure 14: Sample 4, Azimuthal Angle 0°, Angles of Incidence 10° and 22°

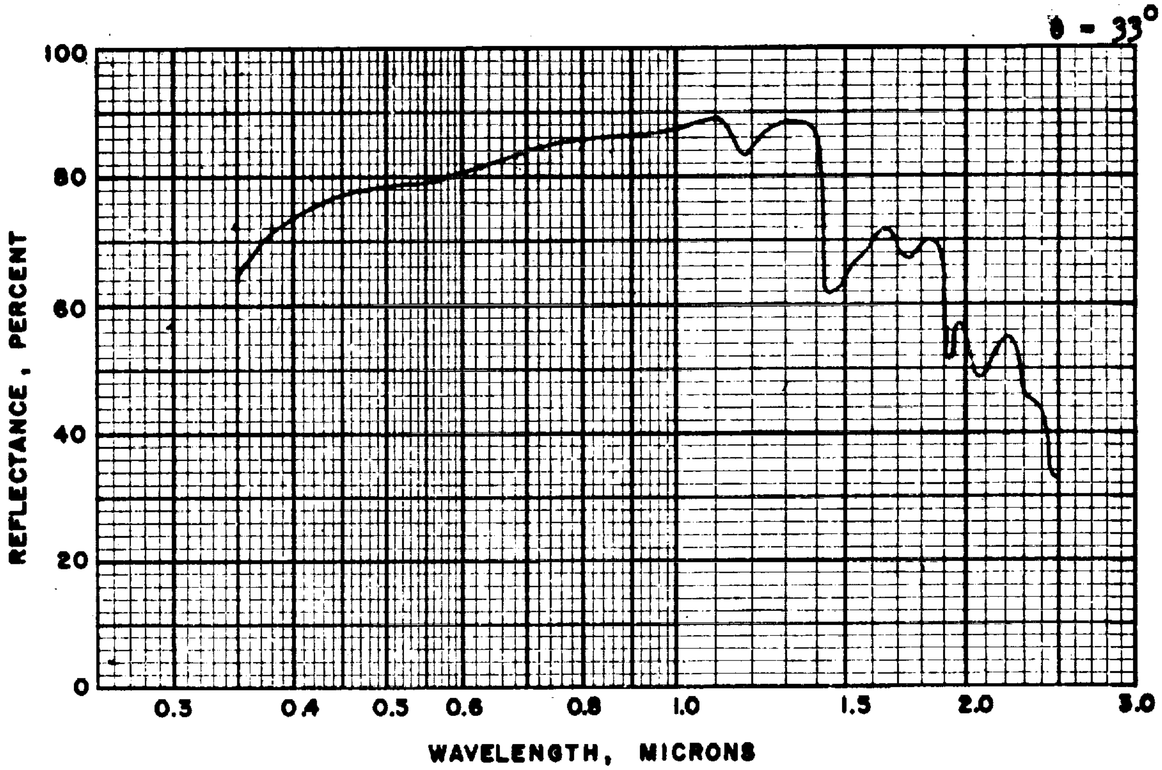

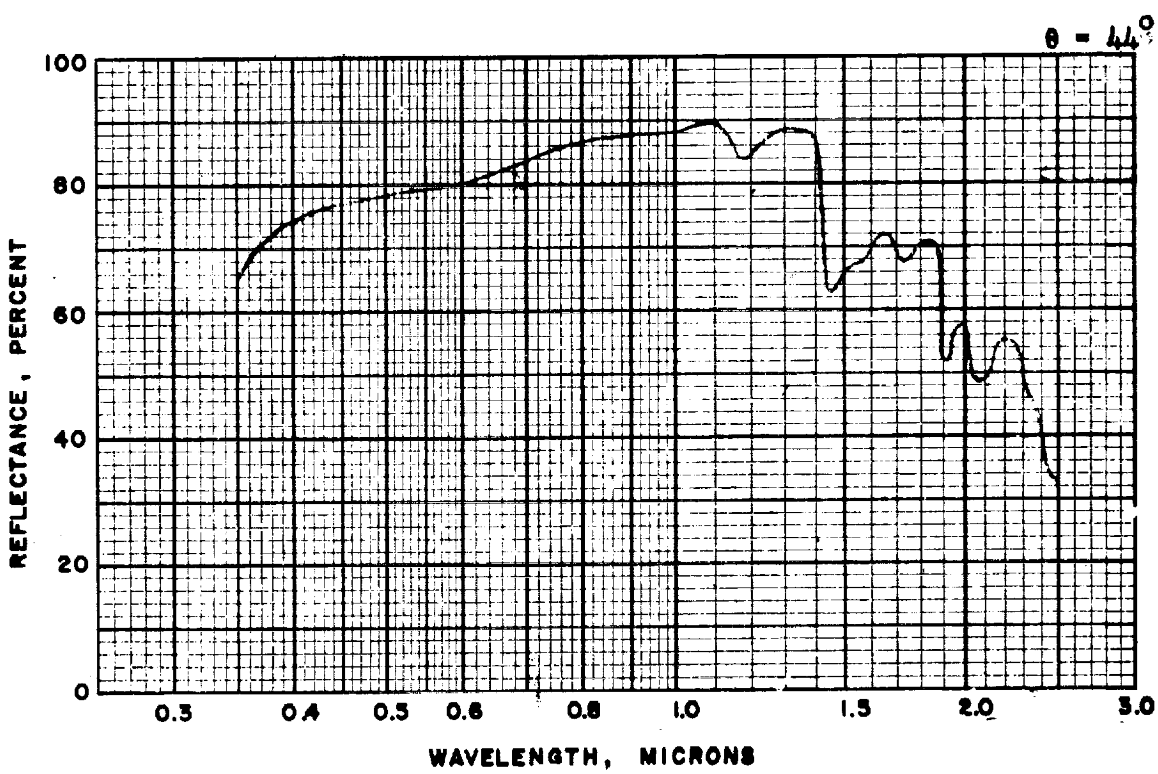

Figure 14 (Cont.): Sample 4, Azimuthal Angle 0°, Angles of Incidence 33° and 44°

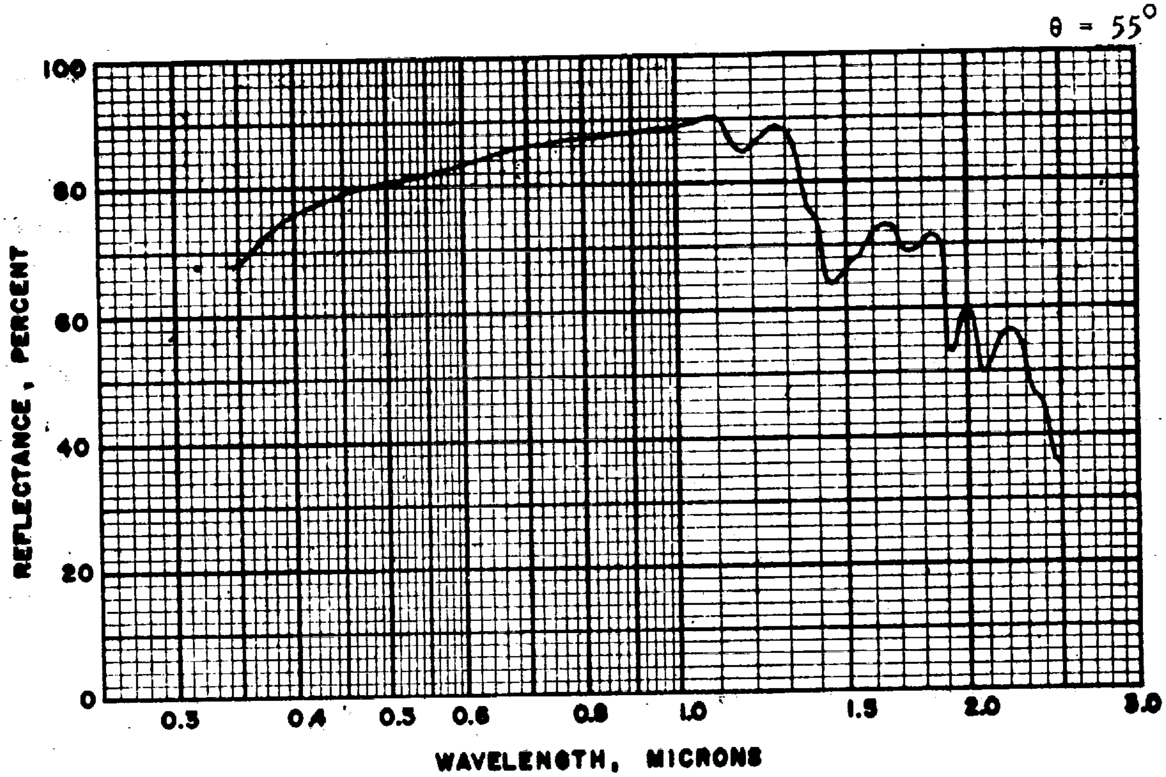

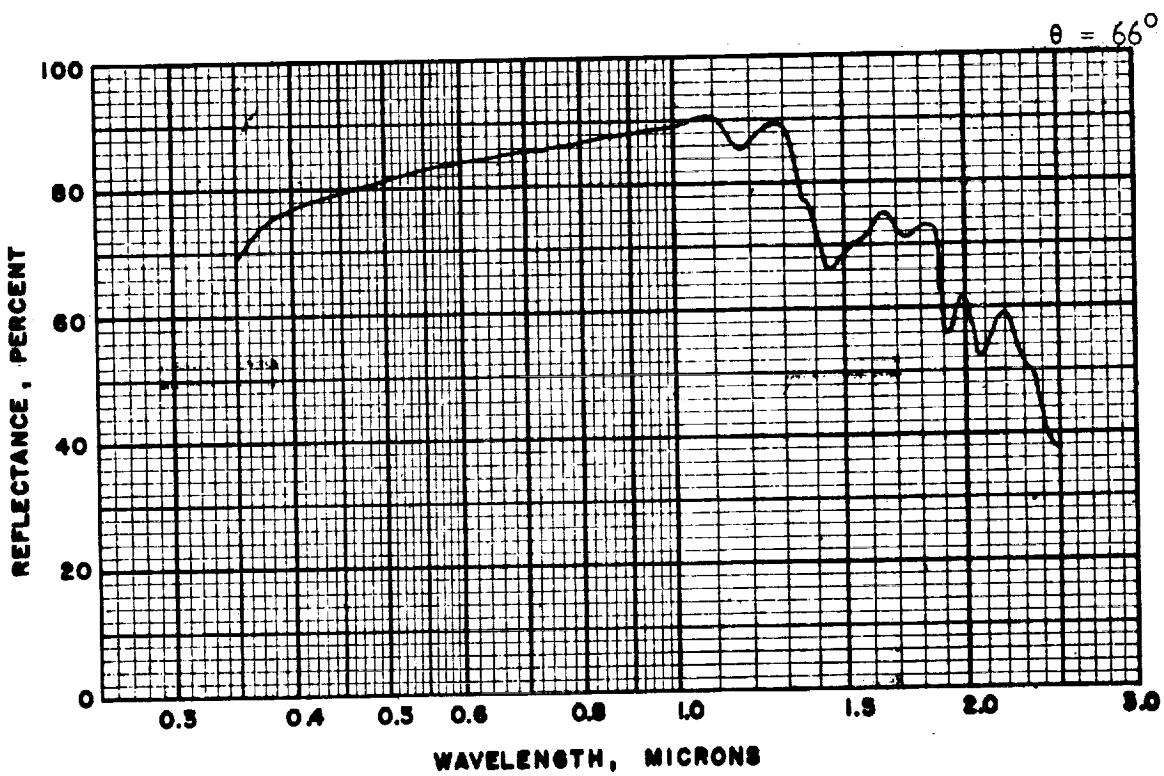

Figure 14 (Cont.): Sample 4, Azimuthal Angle 0°, Angles of Incidence 55° and 66°

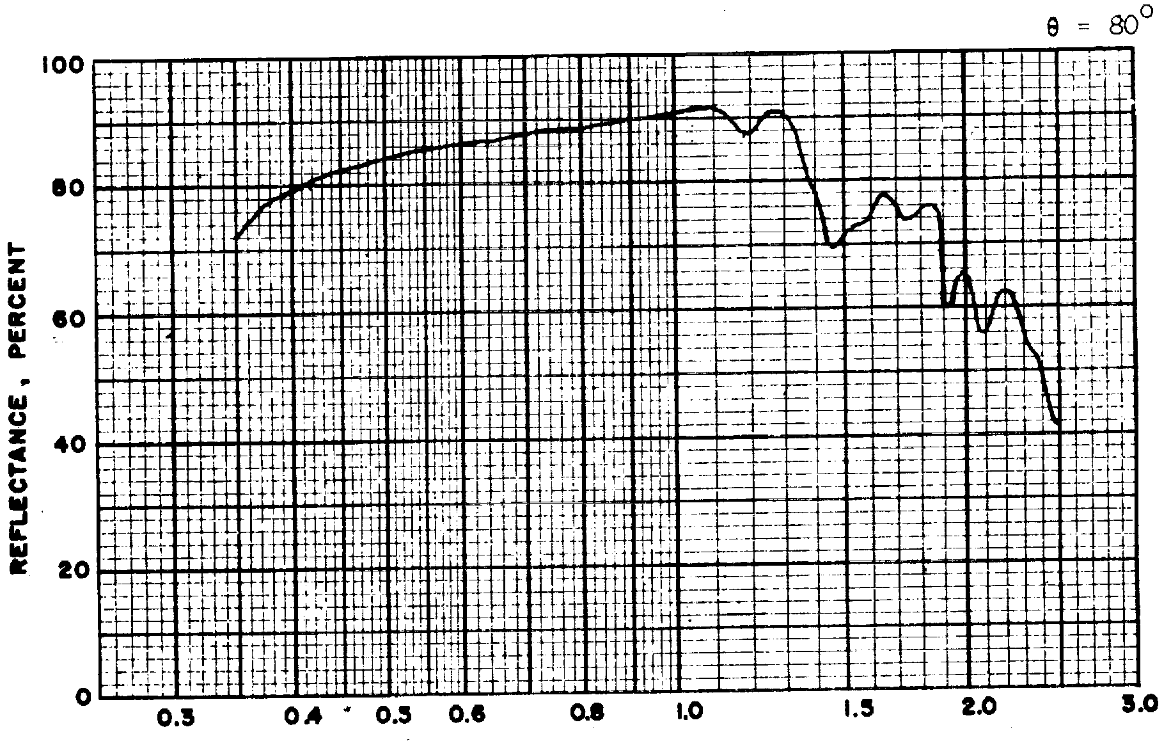

Figure 14 (Cont.): Sample 4, Azimuthal Angle 0°
Angle of Incidence 80°

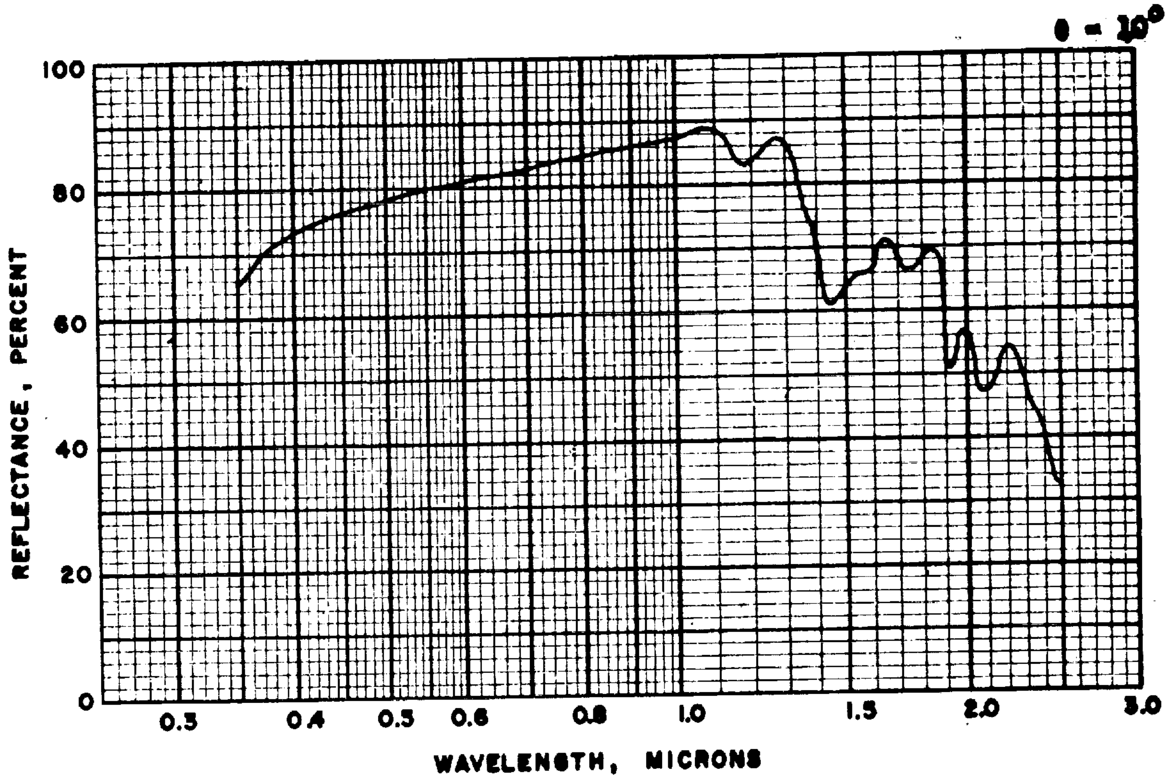

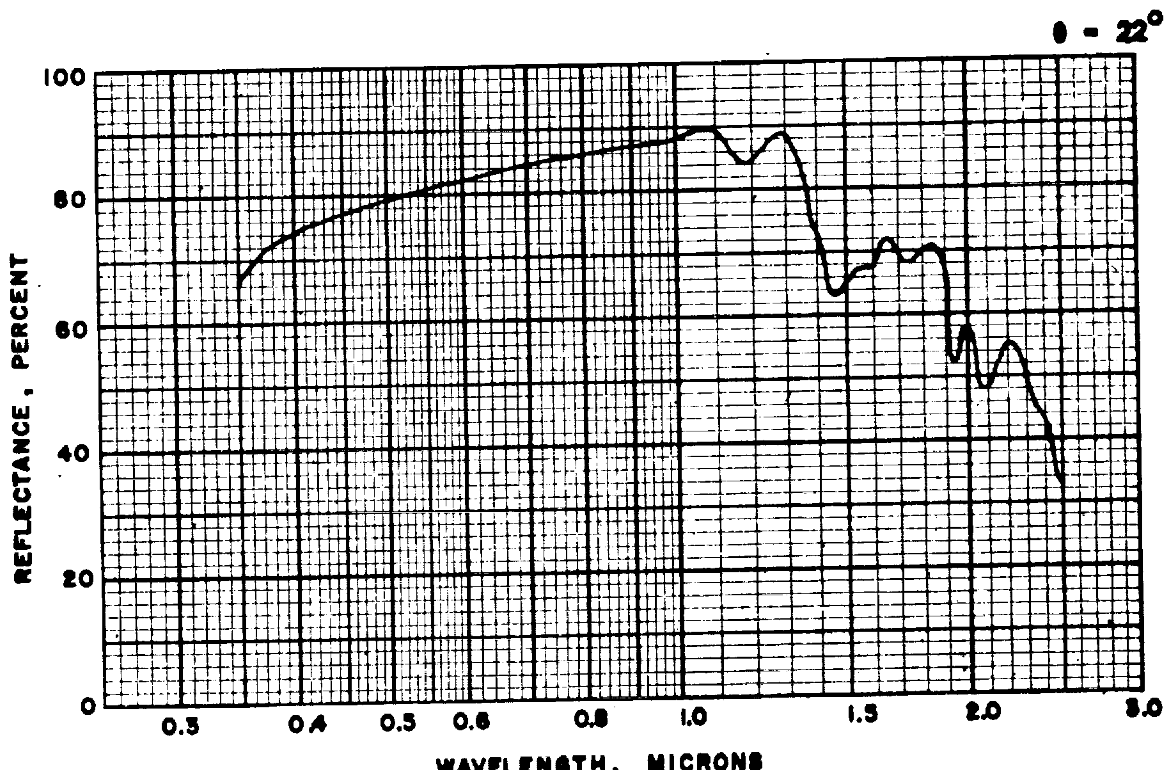

Figure 15: Sample 4, Azimuthal Angle 45°, Angles of Incidence 10° and 22°

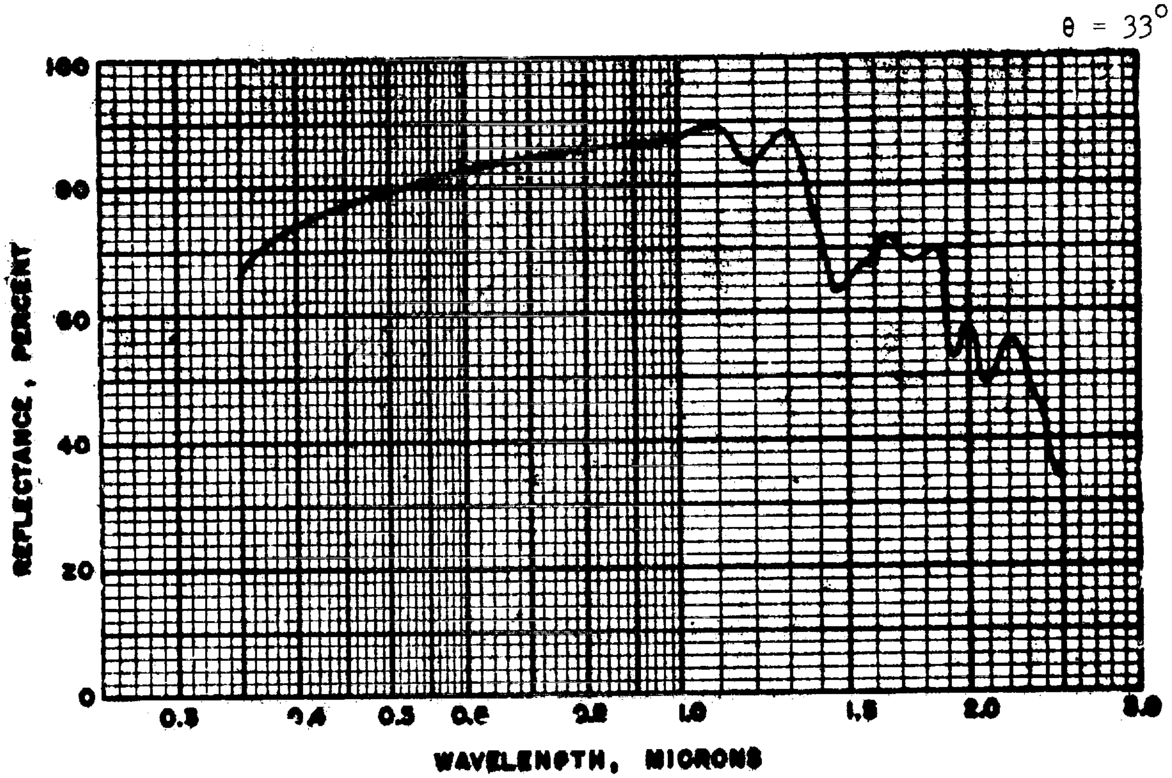

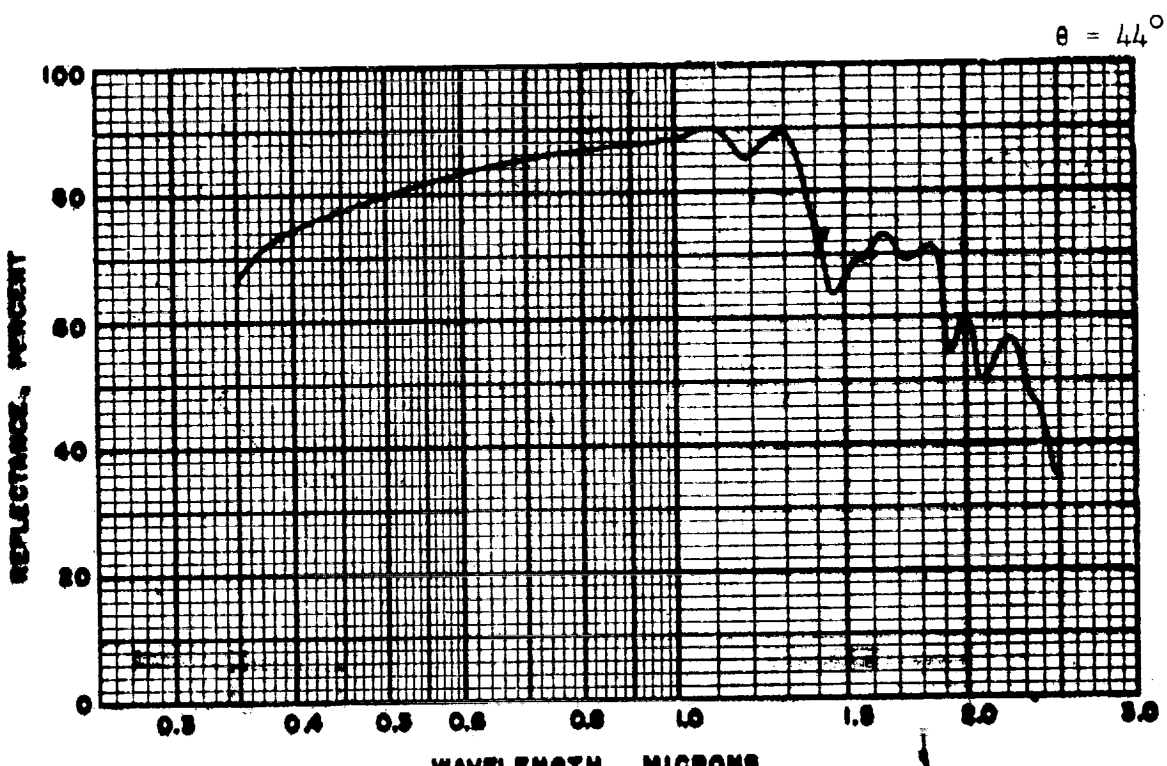

Figure 15 (Cont.): Sample 4, Azimuthal Angle 45°, Angles of Incidence 33° and 44°

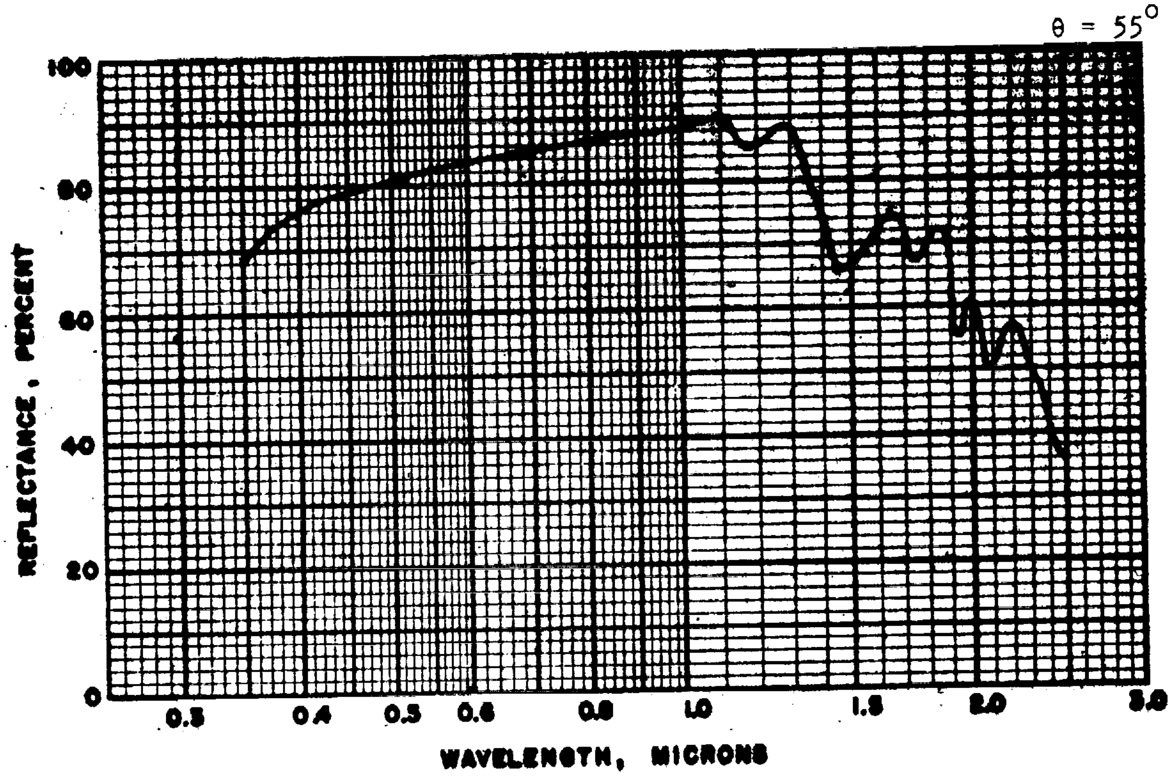

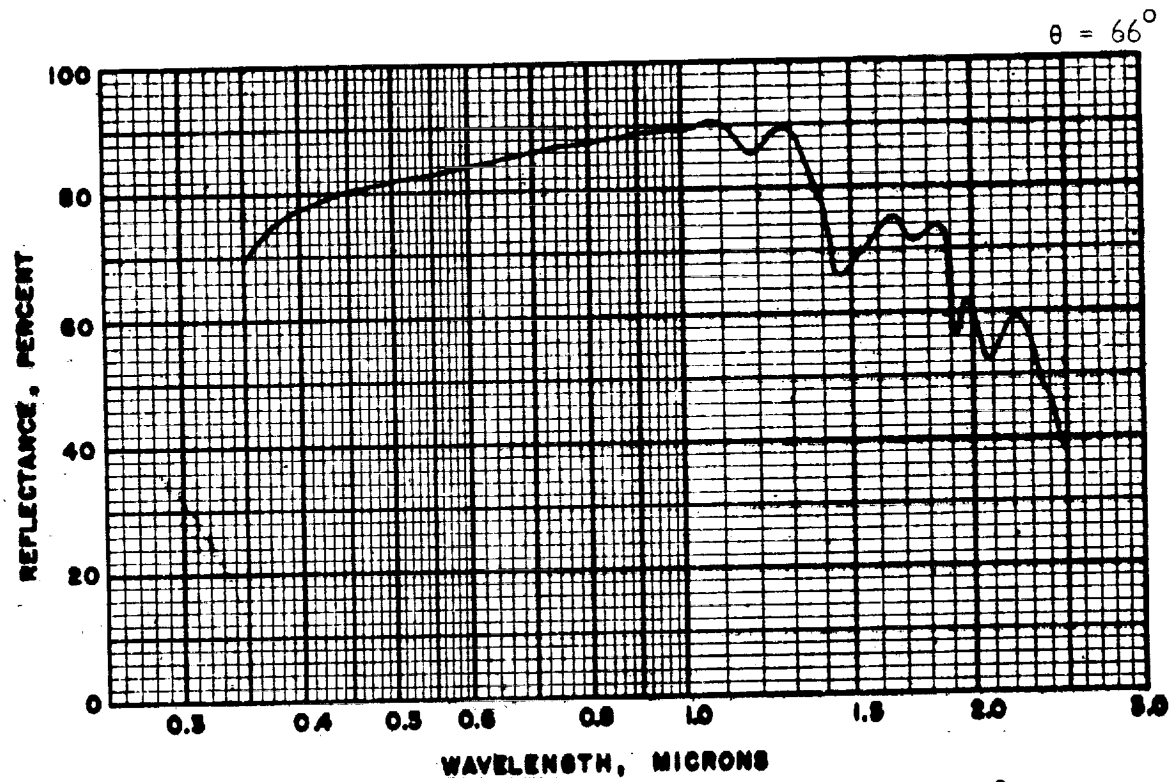

Figure 15 (Cont.): Sample 4, Azimuthal Angle 45°, Angles of Incidence 55° and 66°

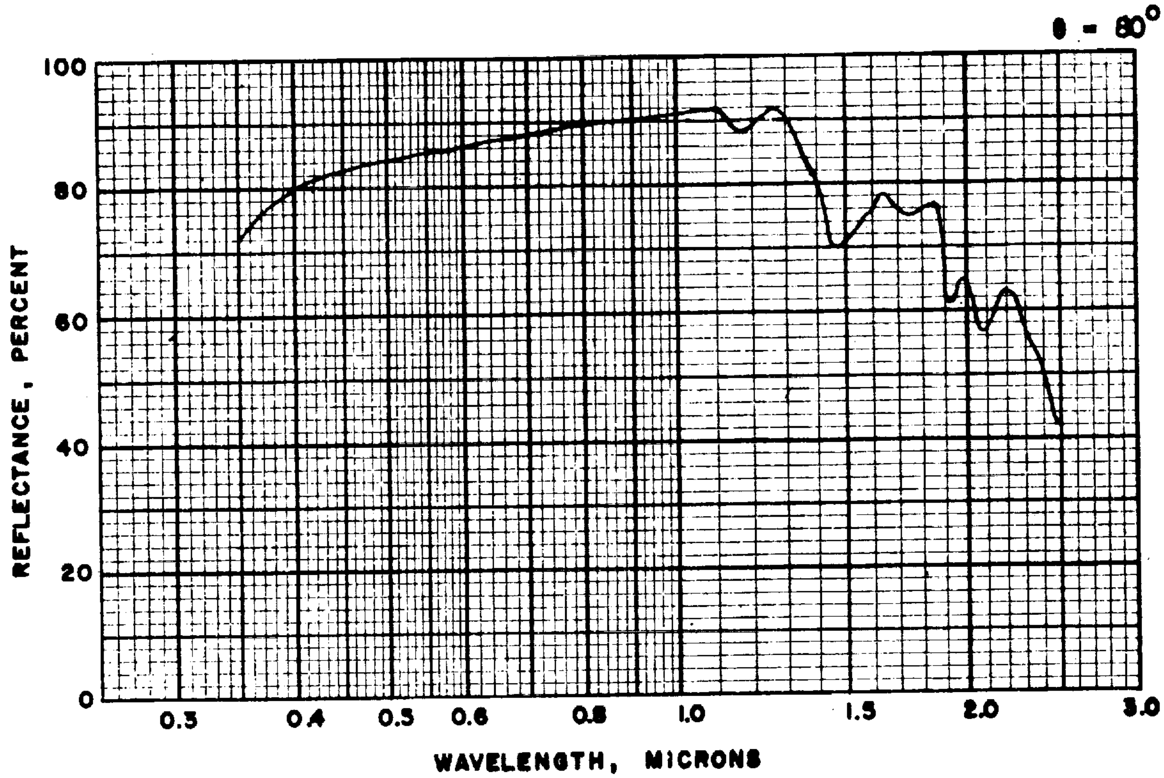

Figure 15 (Cont.): Sample 4, Azimuthal Angle 45°
Angle of Incidence 80°

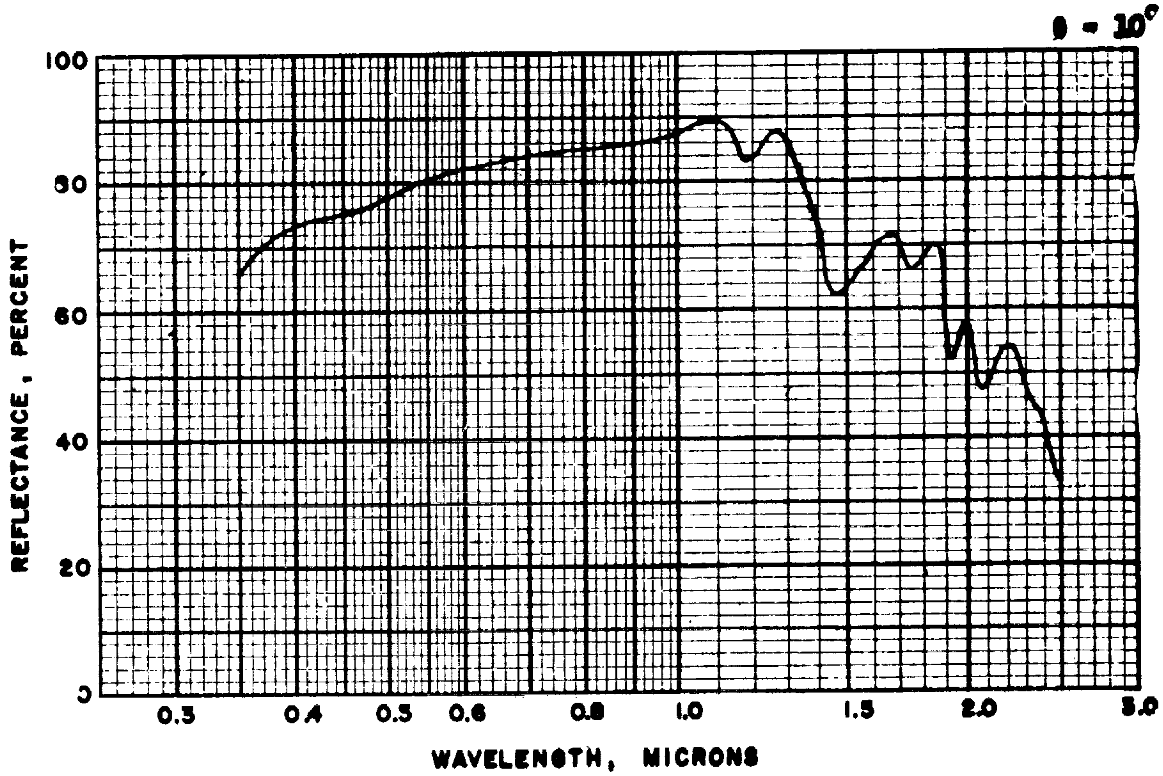

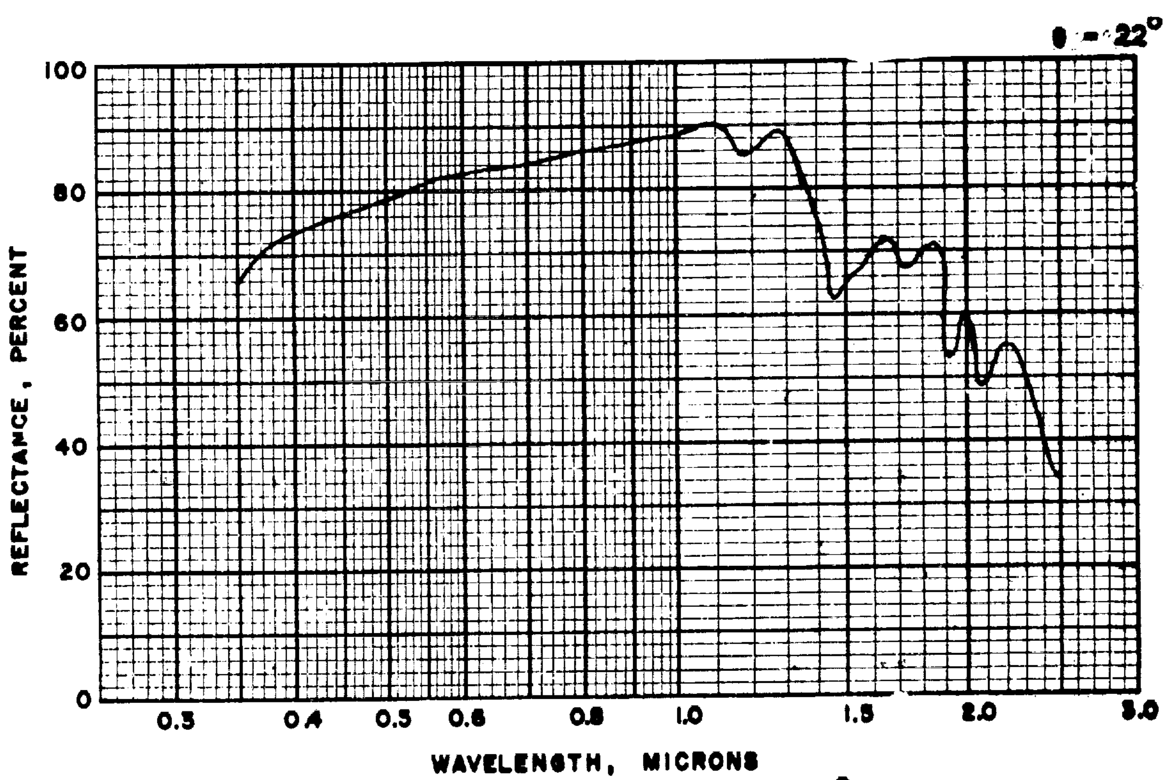

Figure 16: Sample 4, Azimuthal Angle 60°, Angles of Incidence 10° and 22°

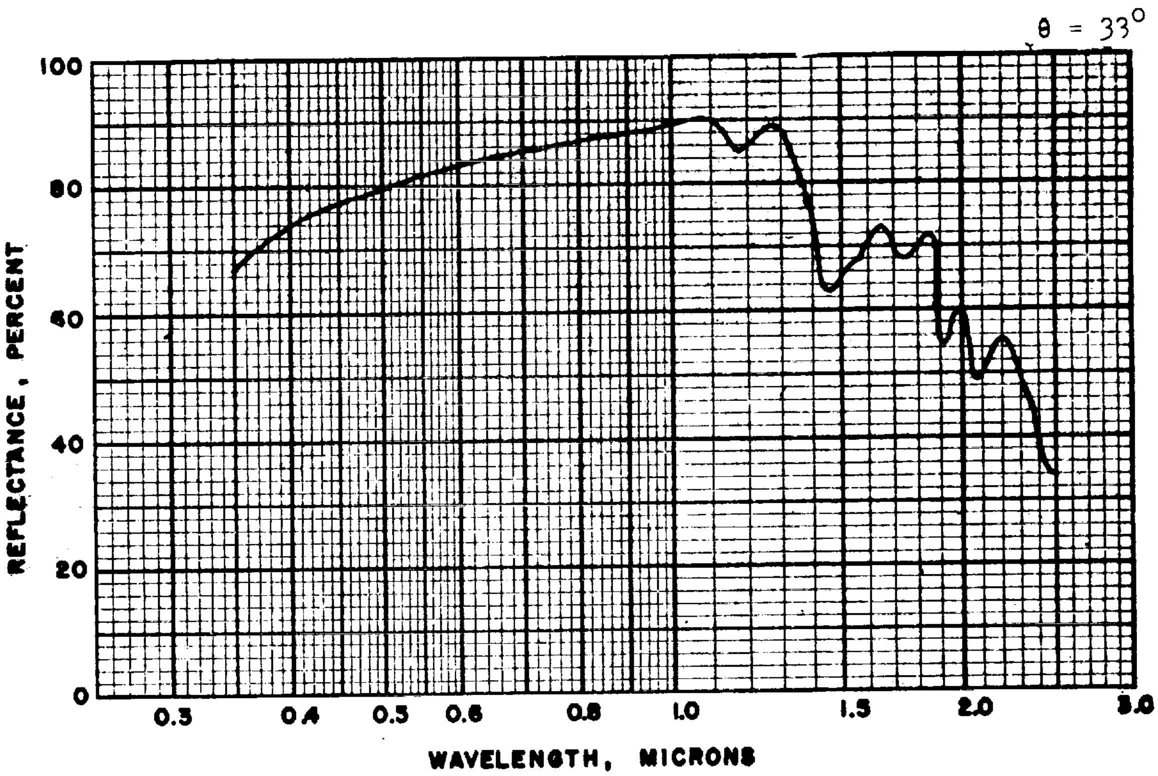

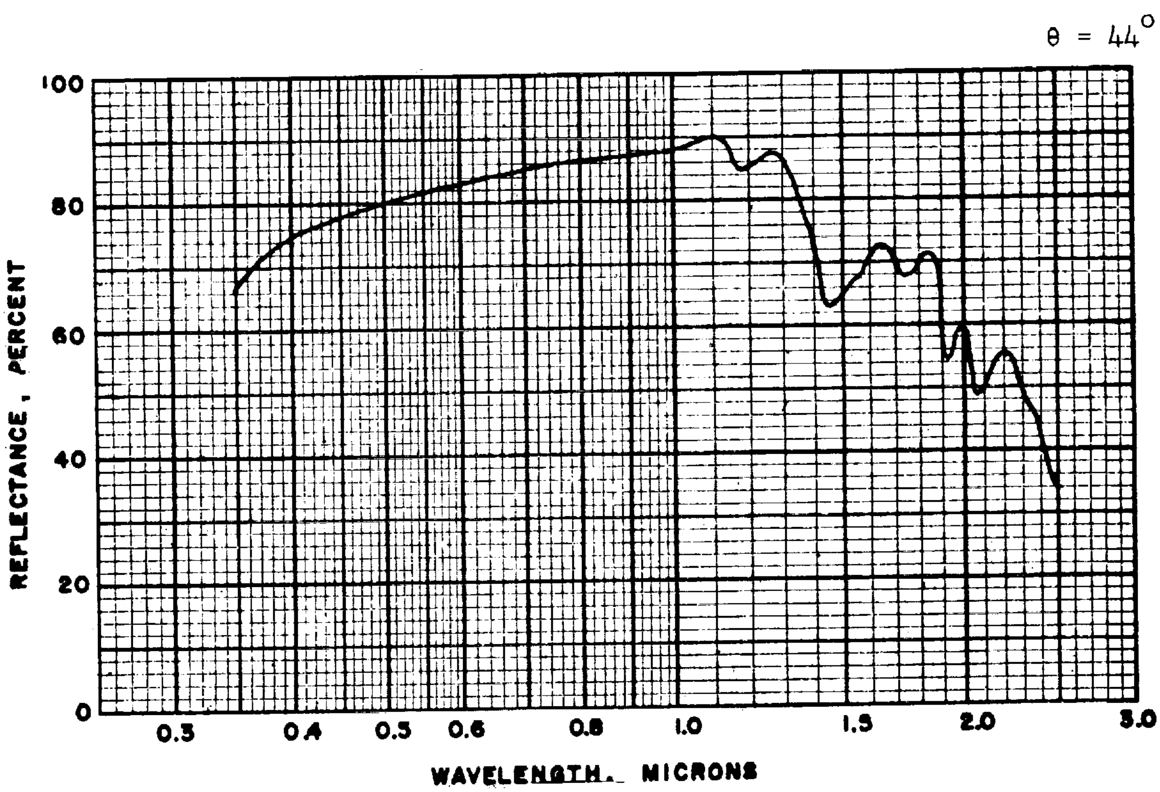

Figure 16 (Cont.): Sample 4, Azimuthal Angle 60°, Angles of Incidence 33° and 44°

θ = 55°

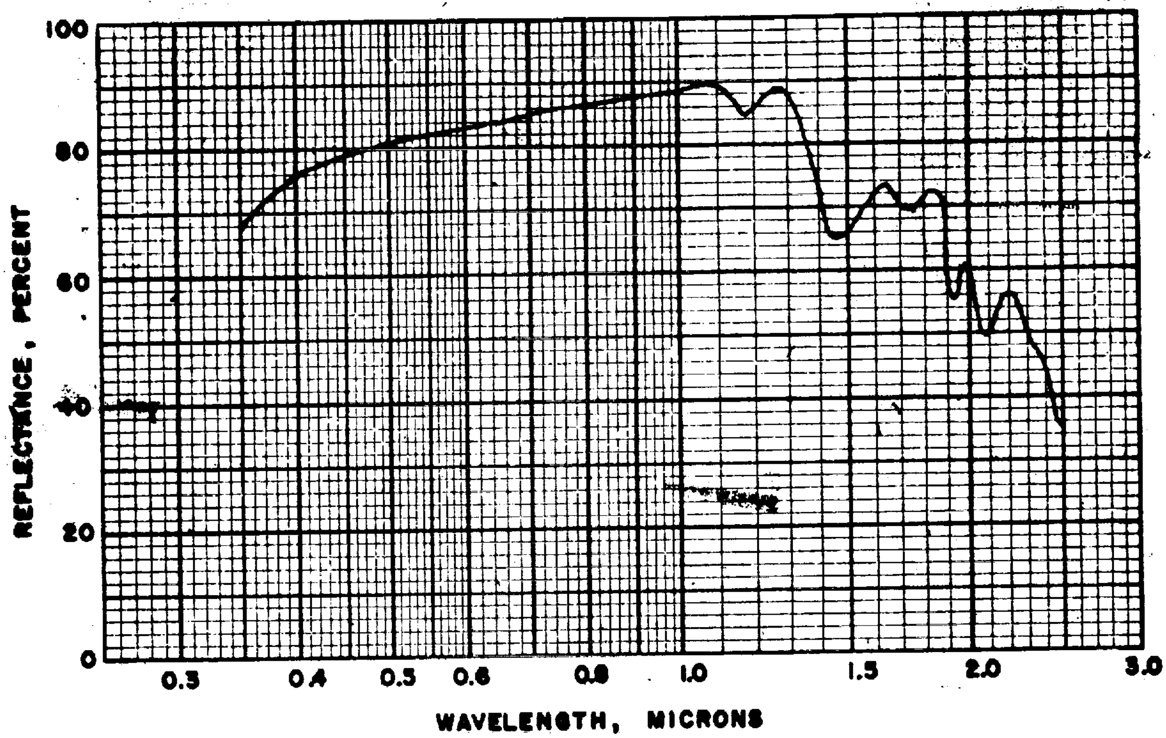

θ = 66°

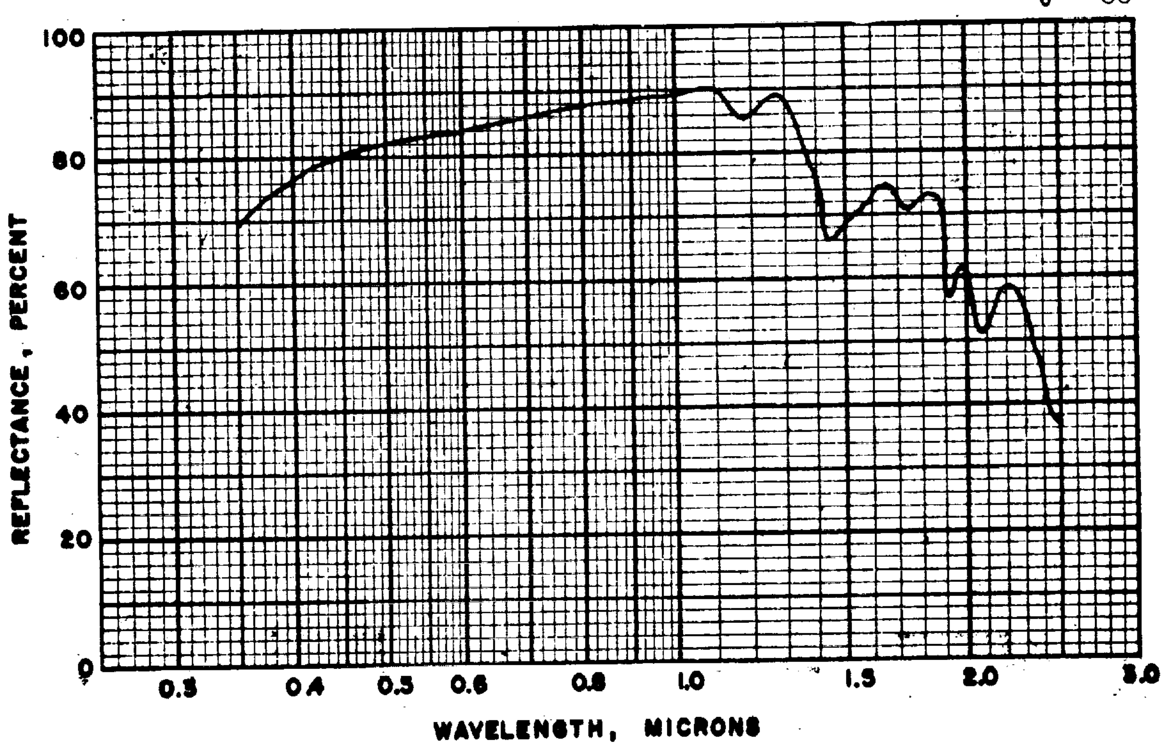

Figure 16 (Cont.): Sample 4, Azimuthal Angle 60°, Angles of Incidence 55° and 66°

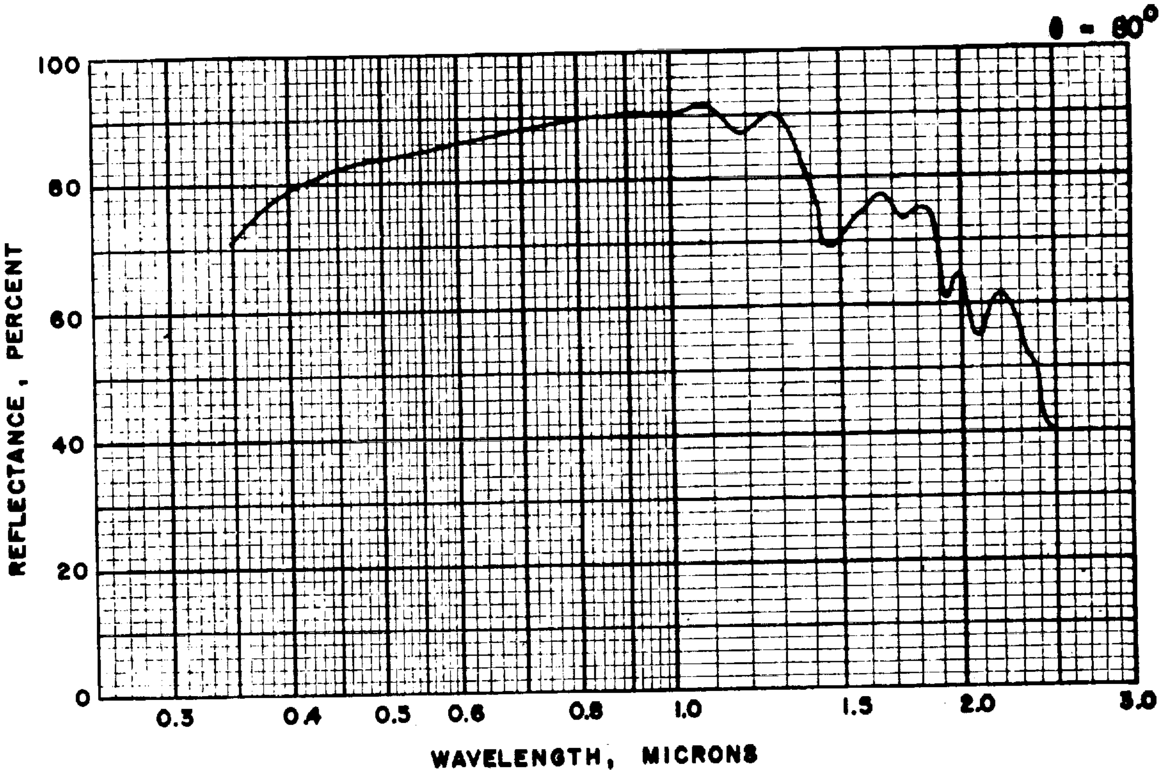

Figure 16 (Cont.): Sample 4, Azimuthal Angle 60°, Angle of Incidence 80°

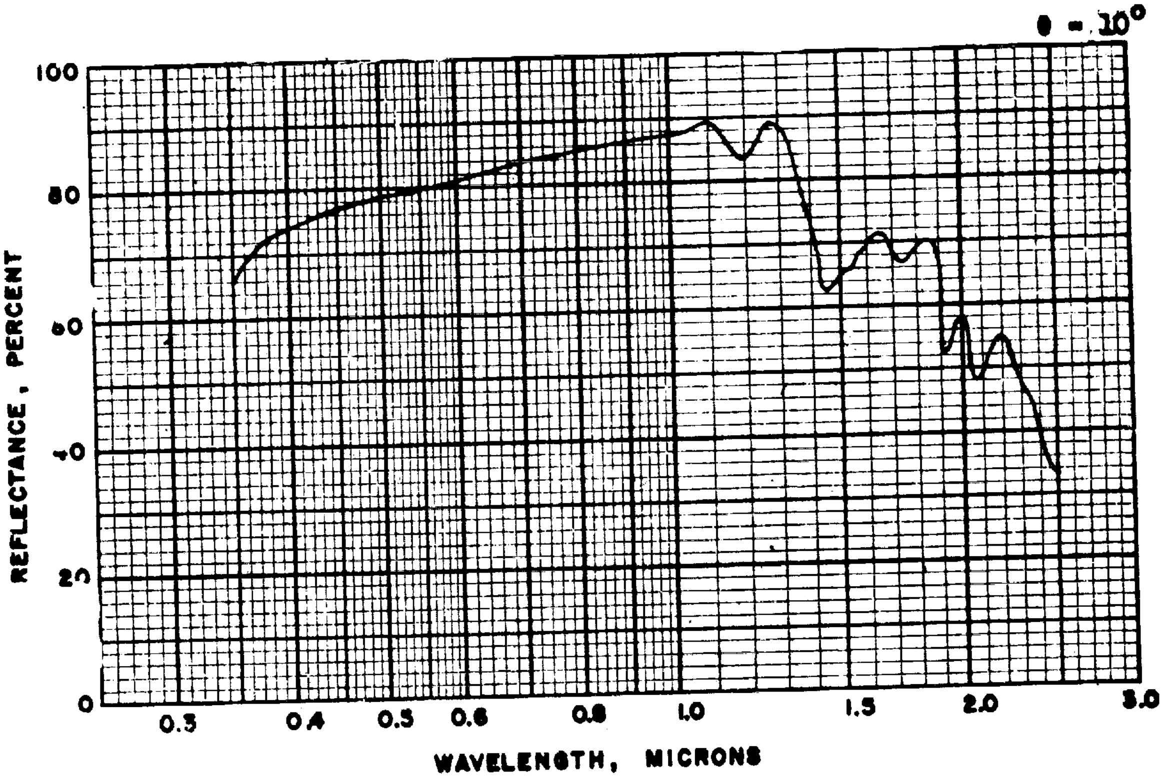

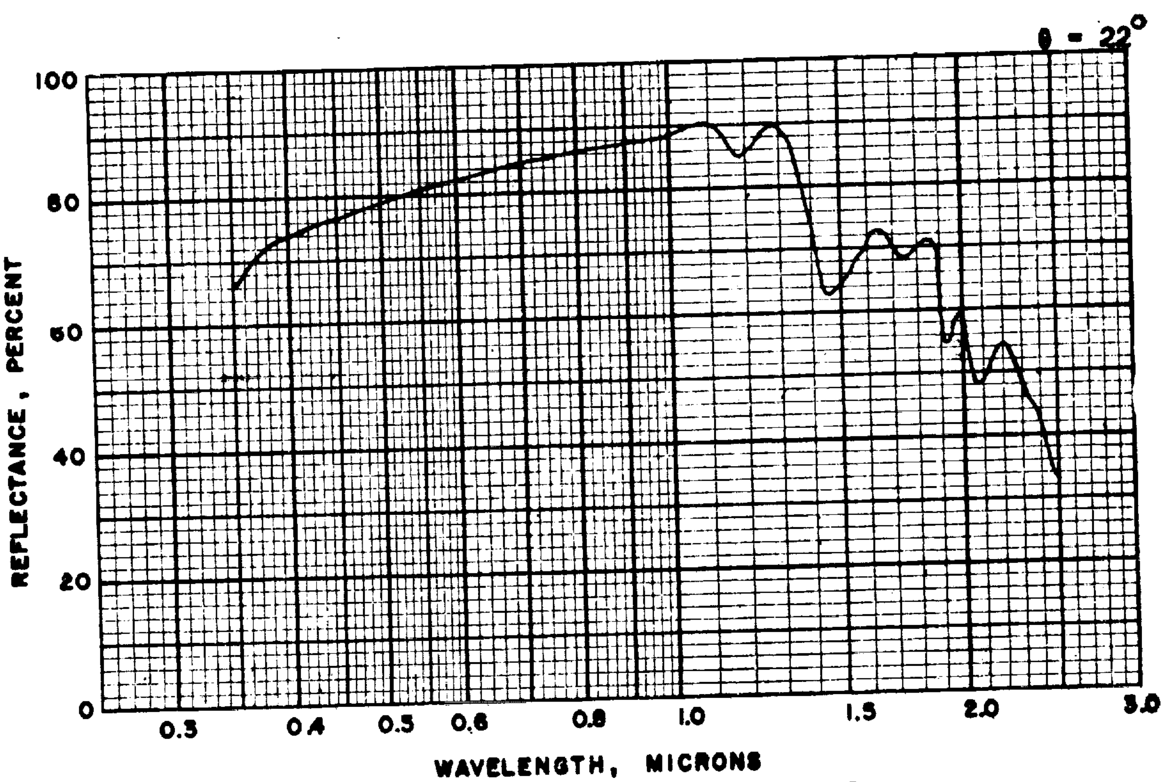

Figure 17: Sample 4, Azimuthal Angle 90°, Angles of Incidence 10° and 22°

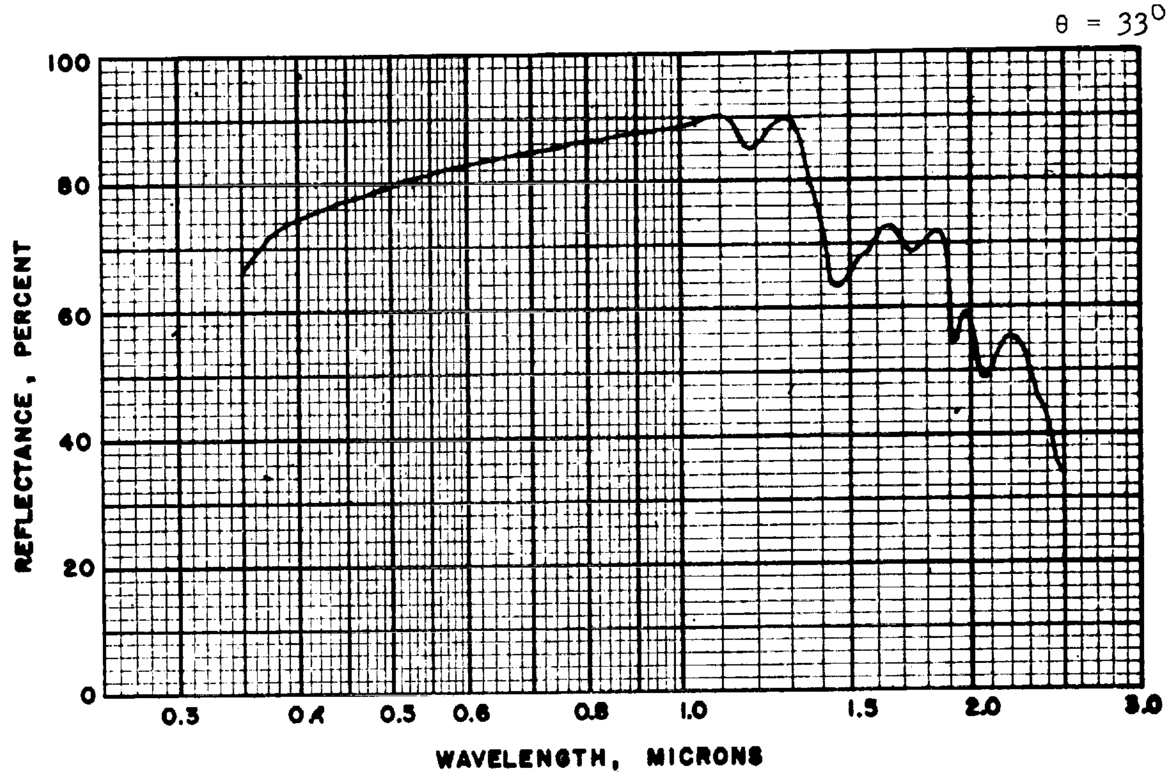

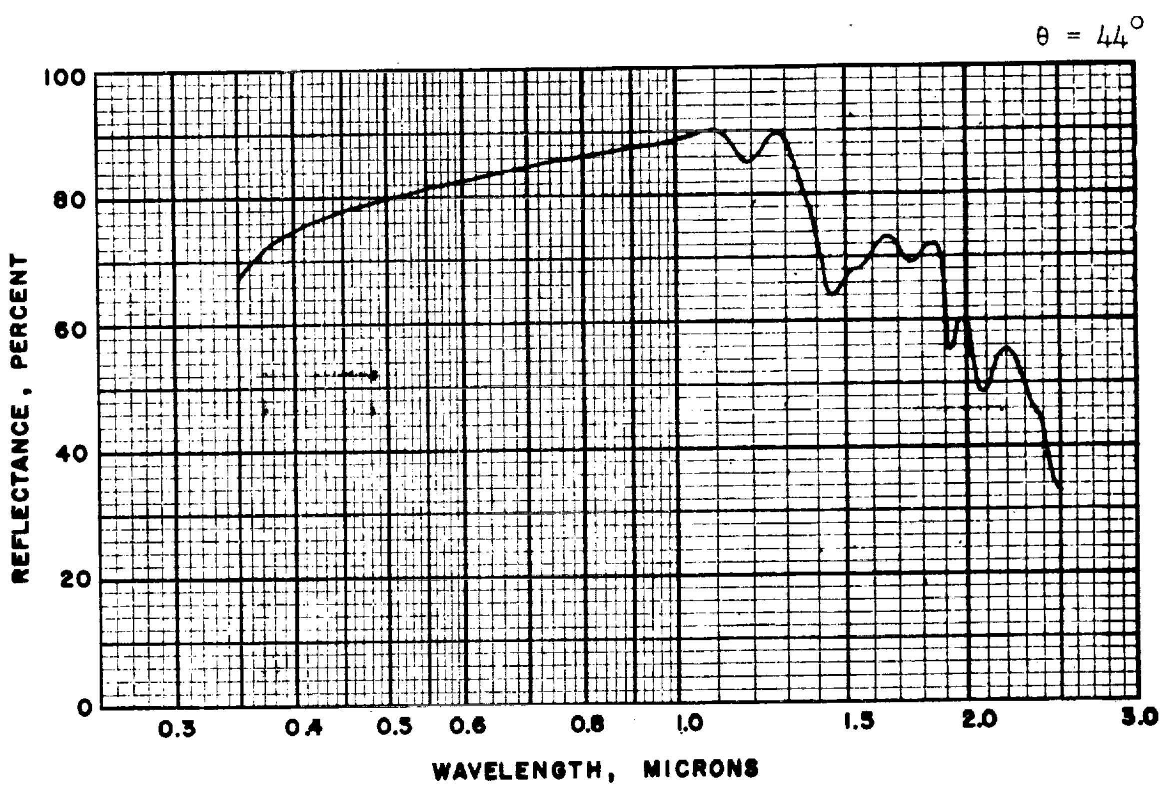

Figure 17 (Cont.): Sample 4, Azimuthal Angle 90°, Angles of Incidence 33° and 44°

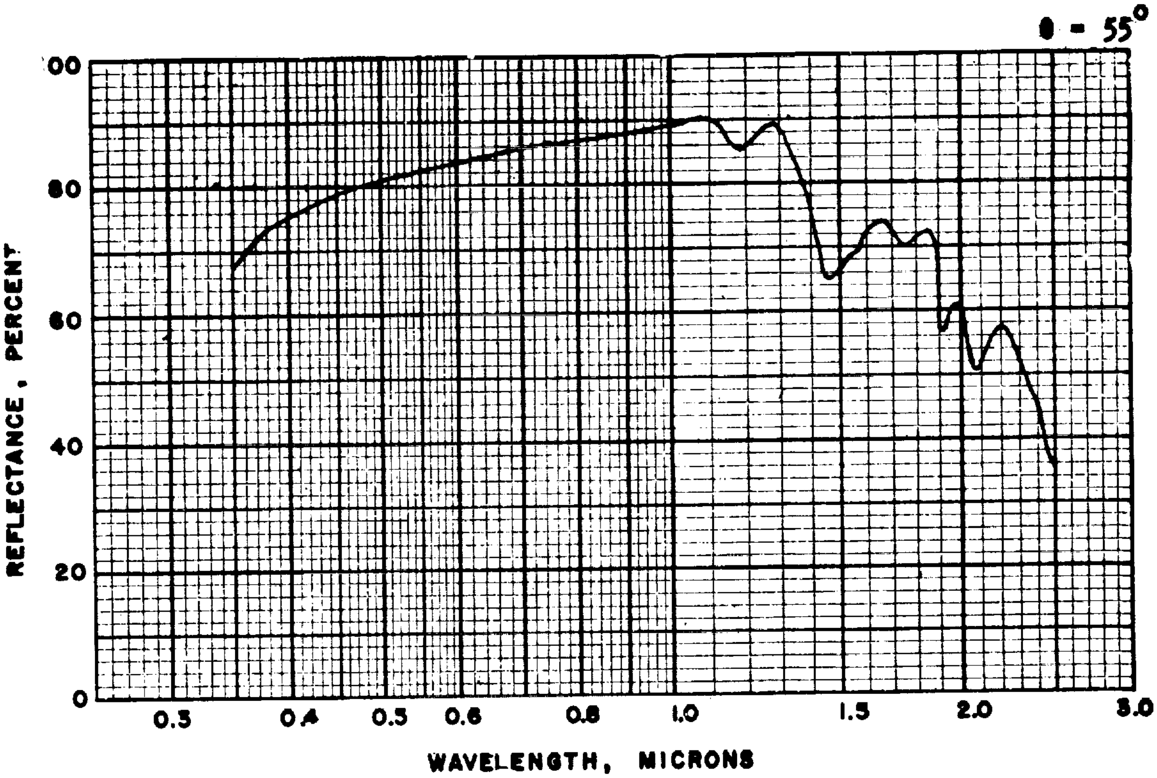

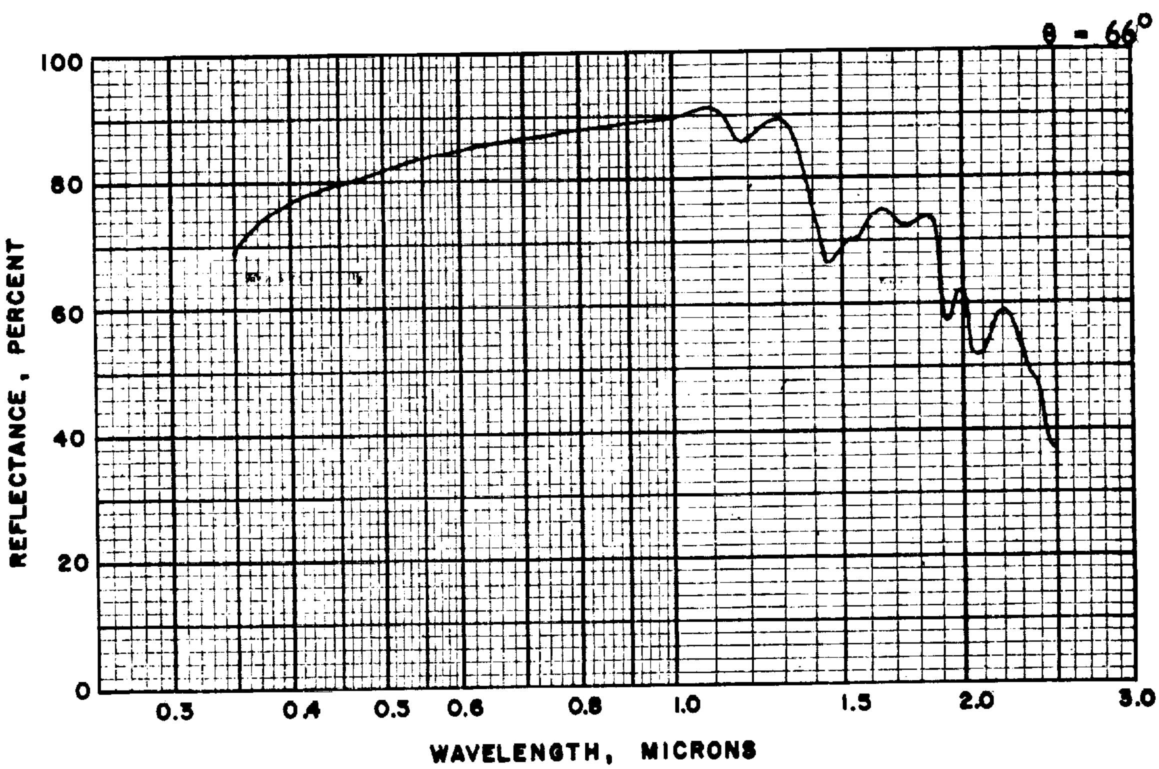

Figure 17 (Cont.): Sample 4, Azimuthal Angle 90°,
Angles of Incidence 55° and 66°

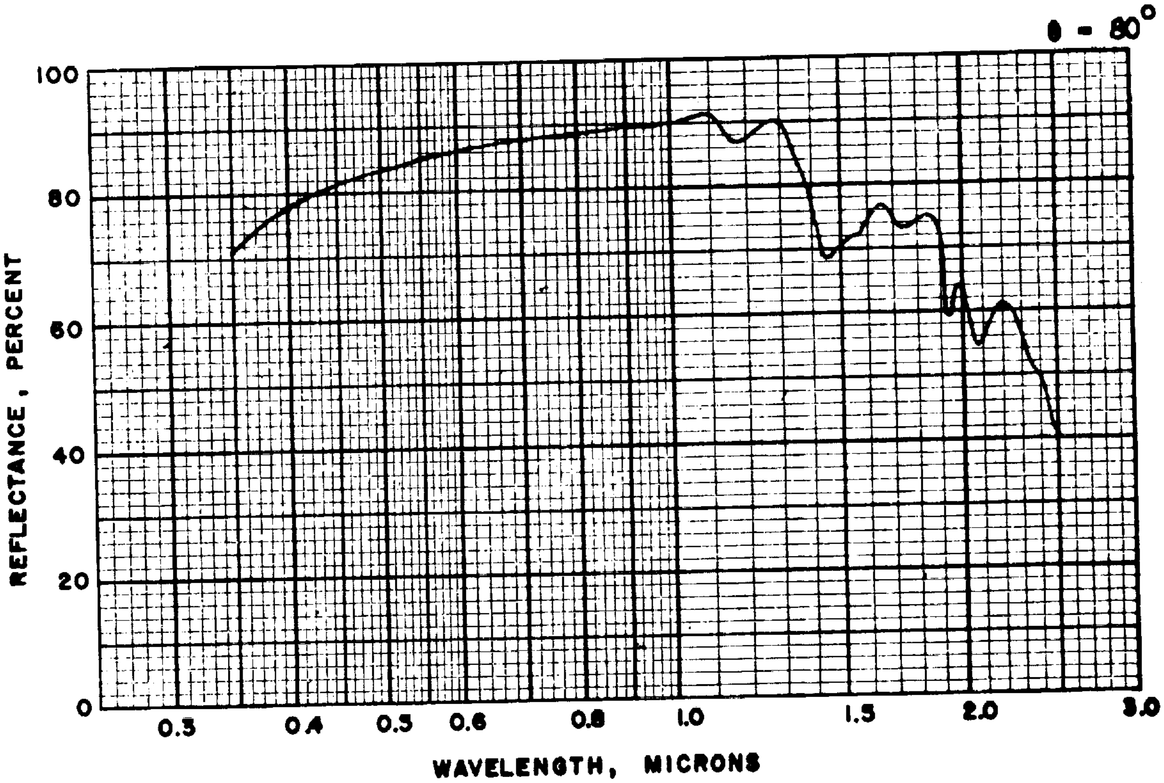

Figure 17 (Cont.): Sample 4, Asimuthal Angle 90°
Angle of Incidence 80°

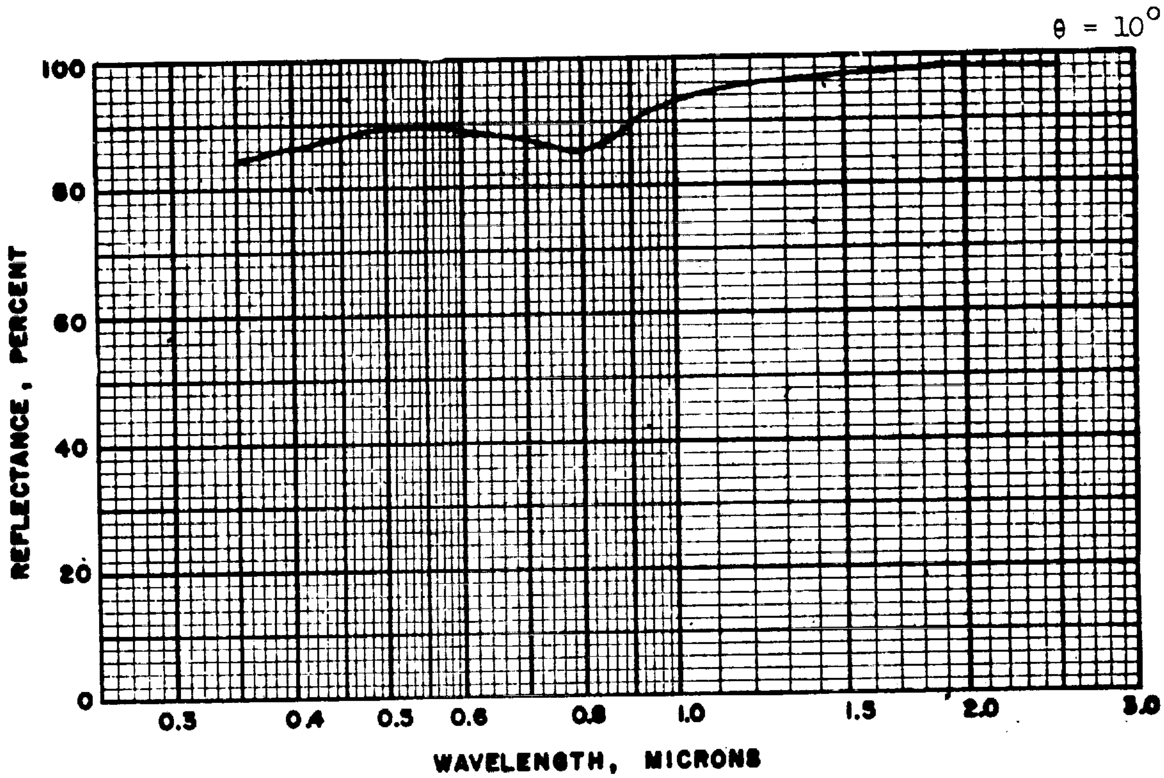

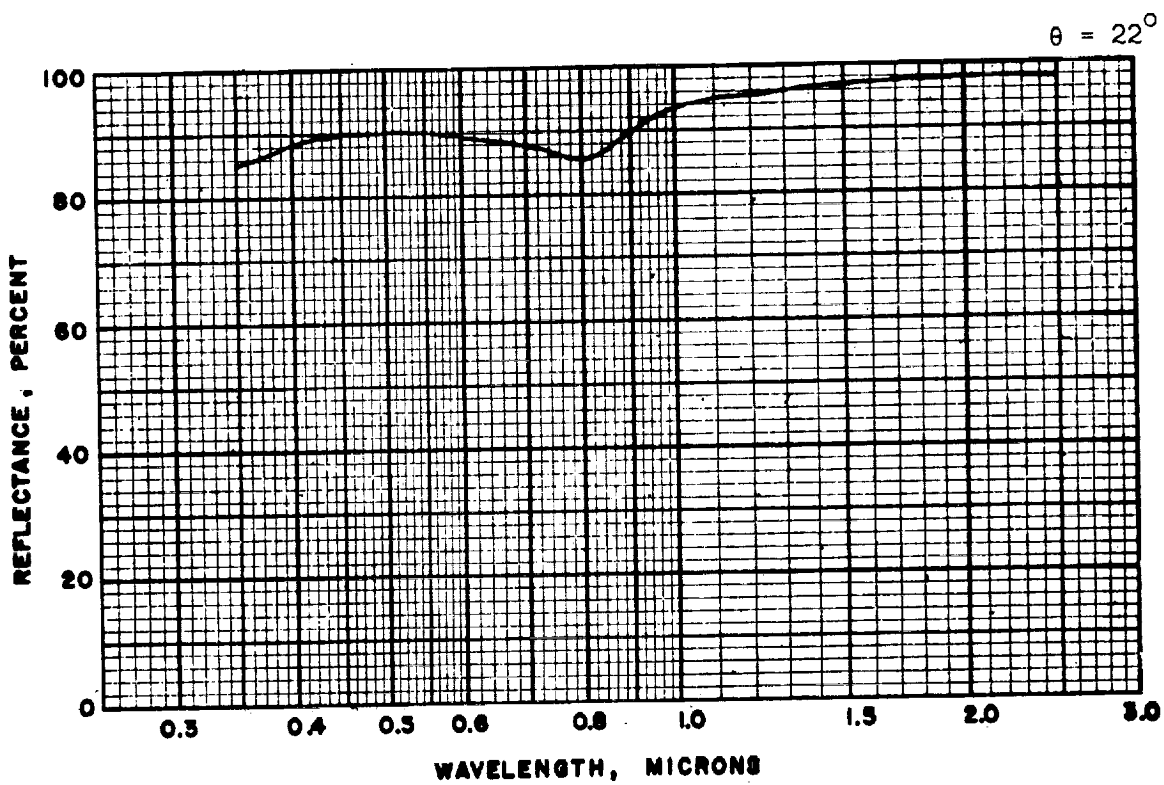

Figure 18: Sample 5A, Azimuthal Angle 0°,
Angles of Incidence 10° and 22°

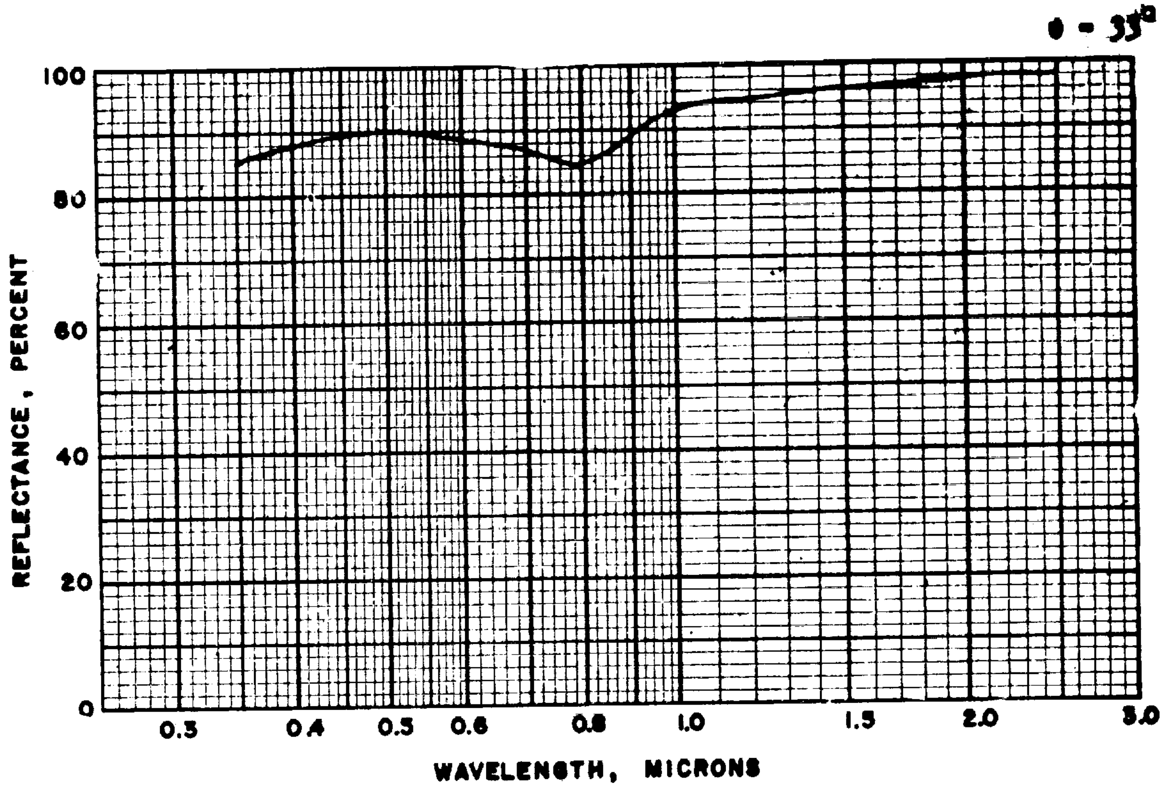

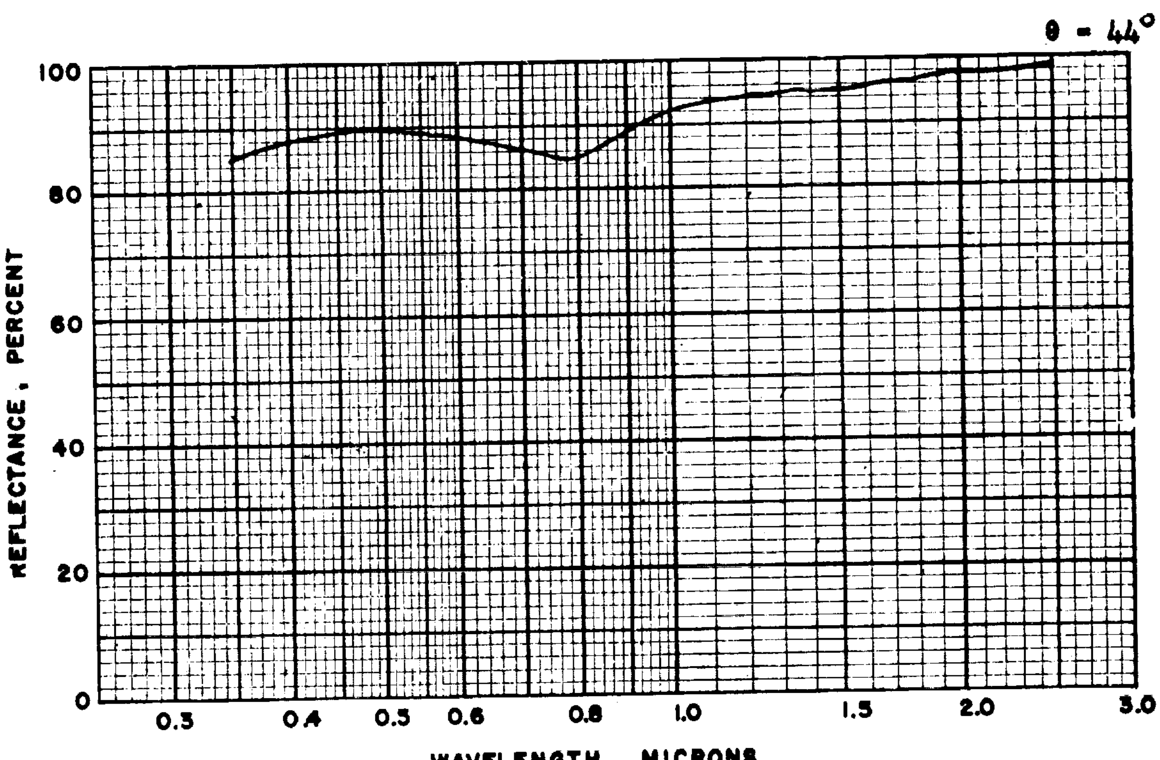

Figure 18 (Cont.): Sample 5A, Azimuthal Angle 0°, Angles of Incidence 33° and 44°

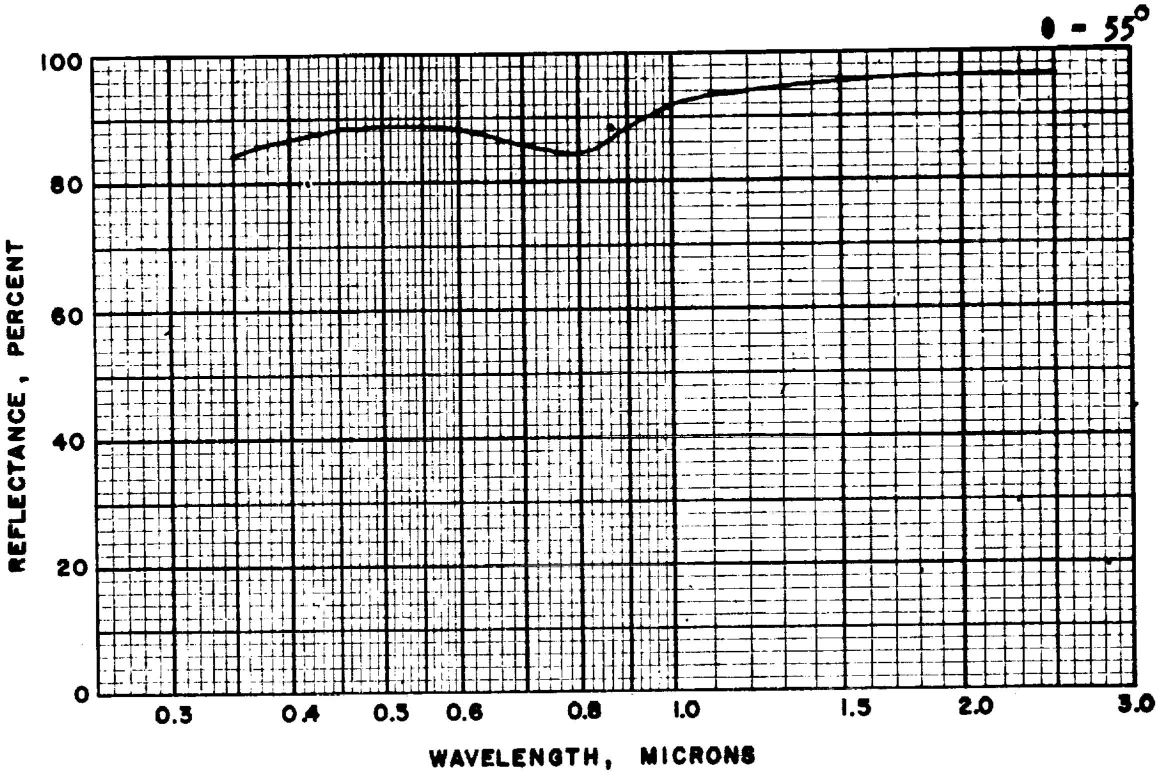

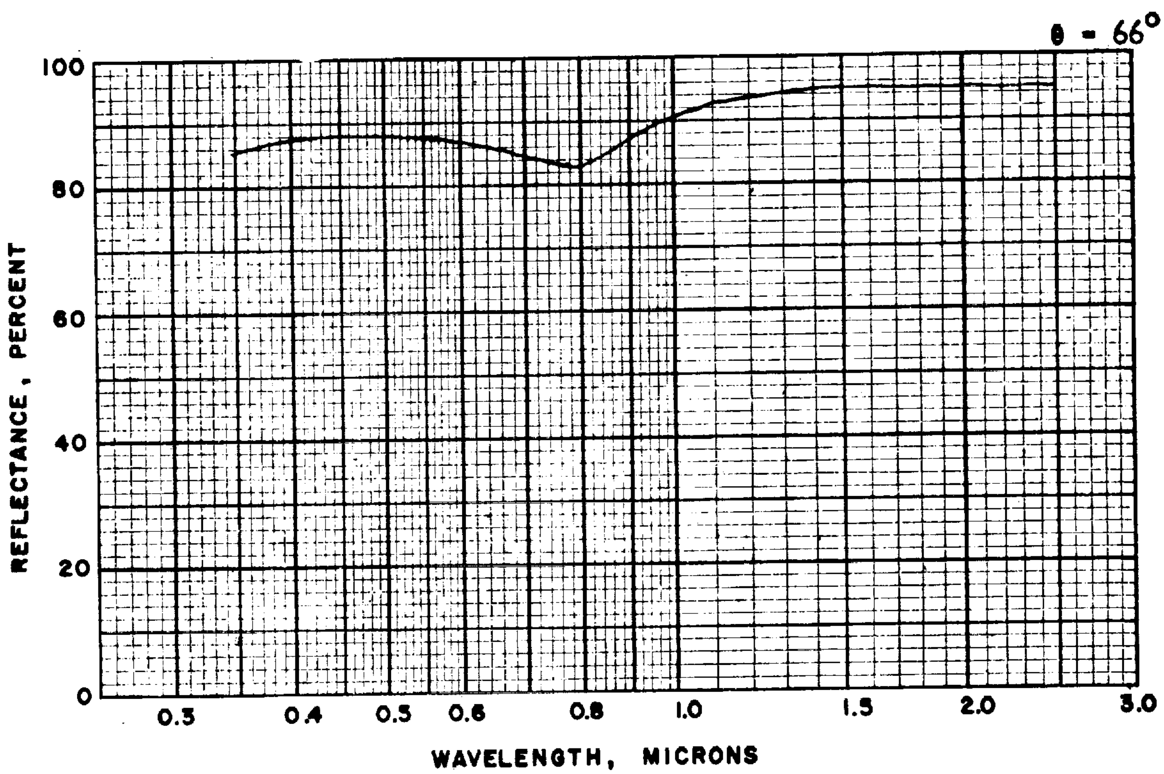

Figure 18 (Cont.): Sample 5A, Azimuthal Angle 0°,
Angles of Incidence 55° and 66°

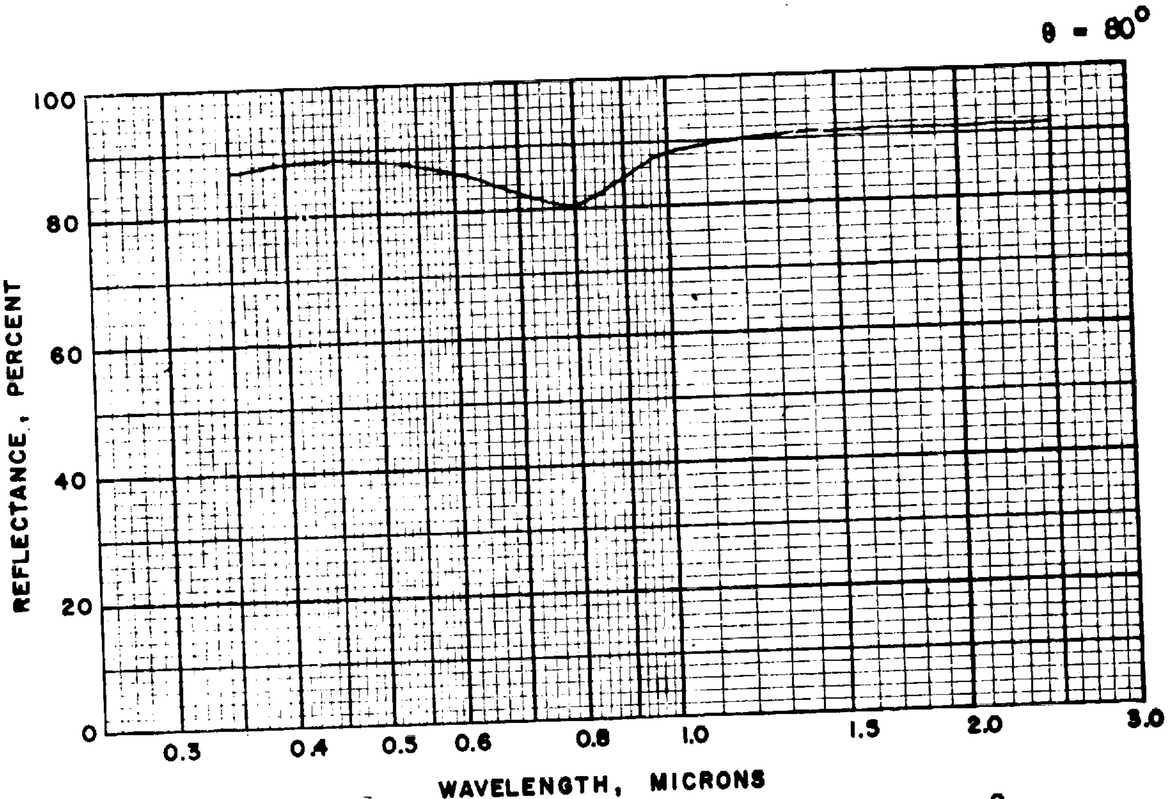

Figure 18 (Cont.): Sample 5A, Azimuthal Angle 0°, Angle of Incidence 80°

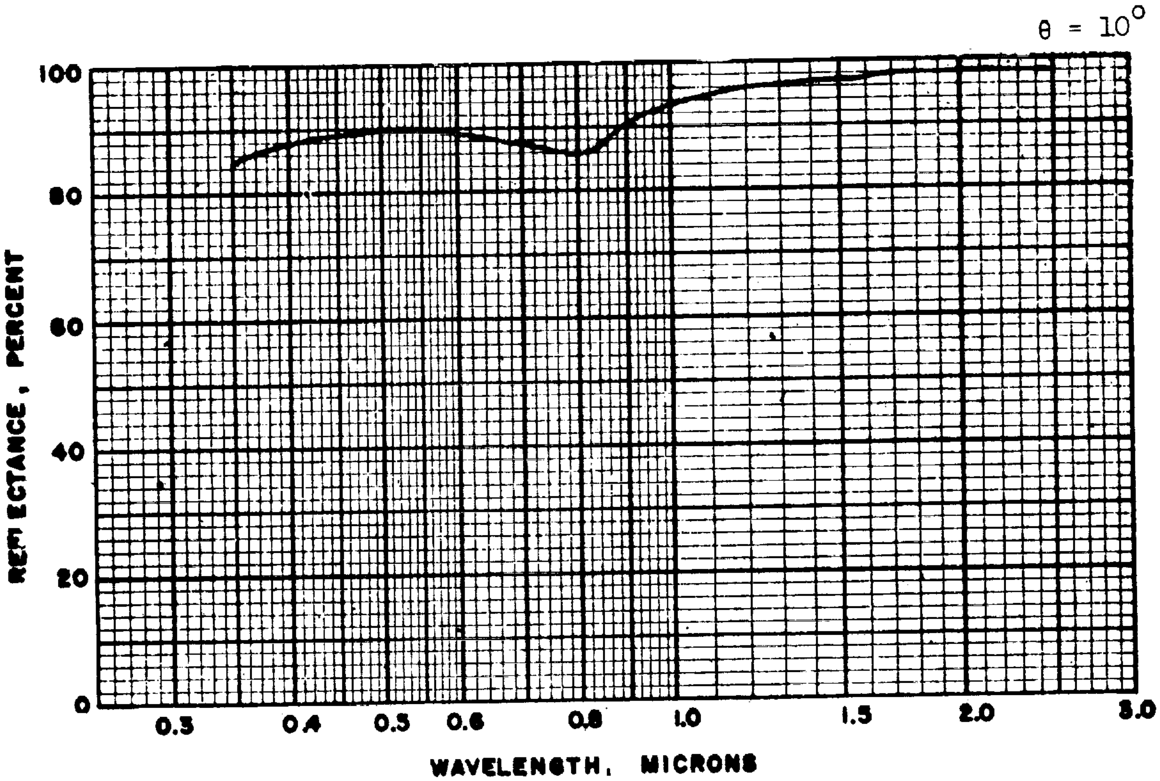

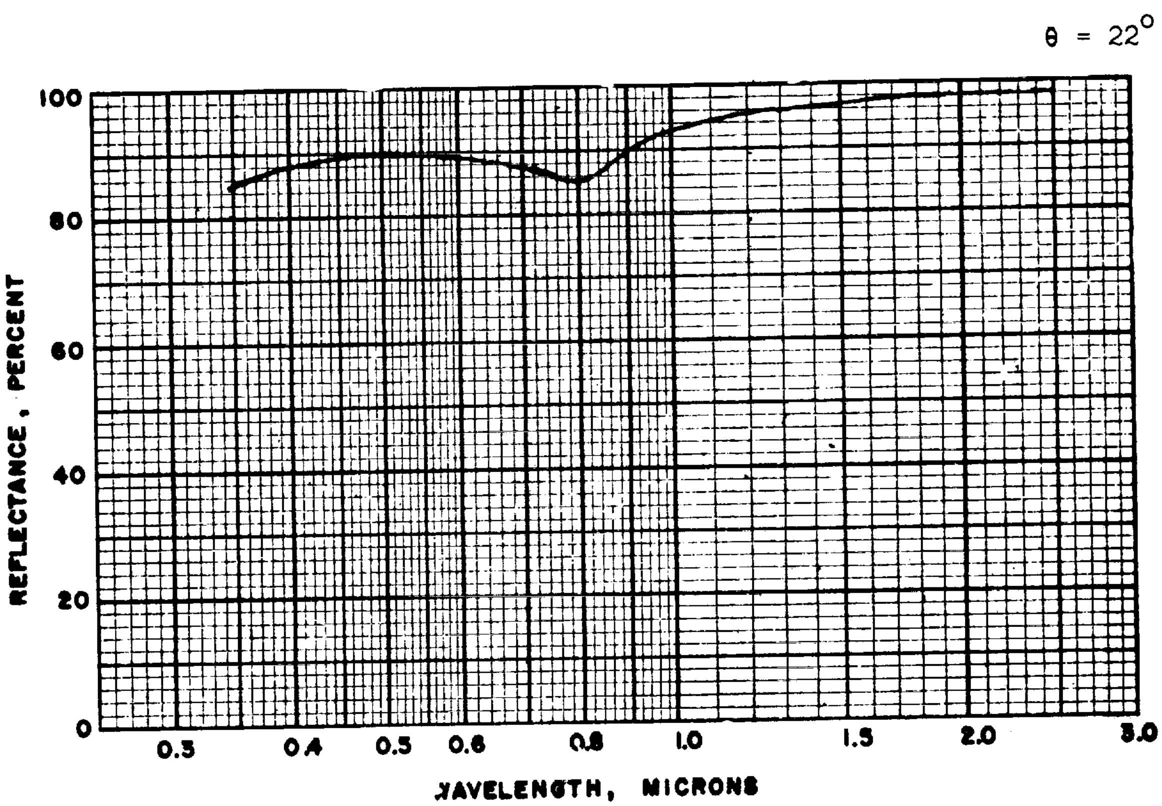

Figure 19: Sample 5A, Azimuthal Angle 45°
Angles of Incidence 10° and 22°

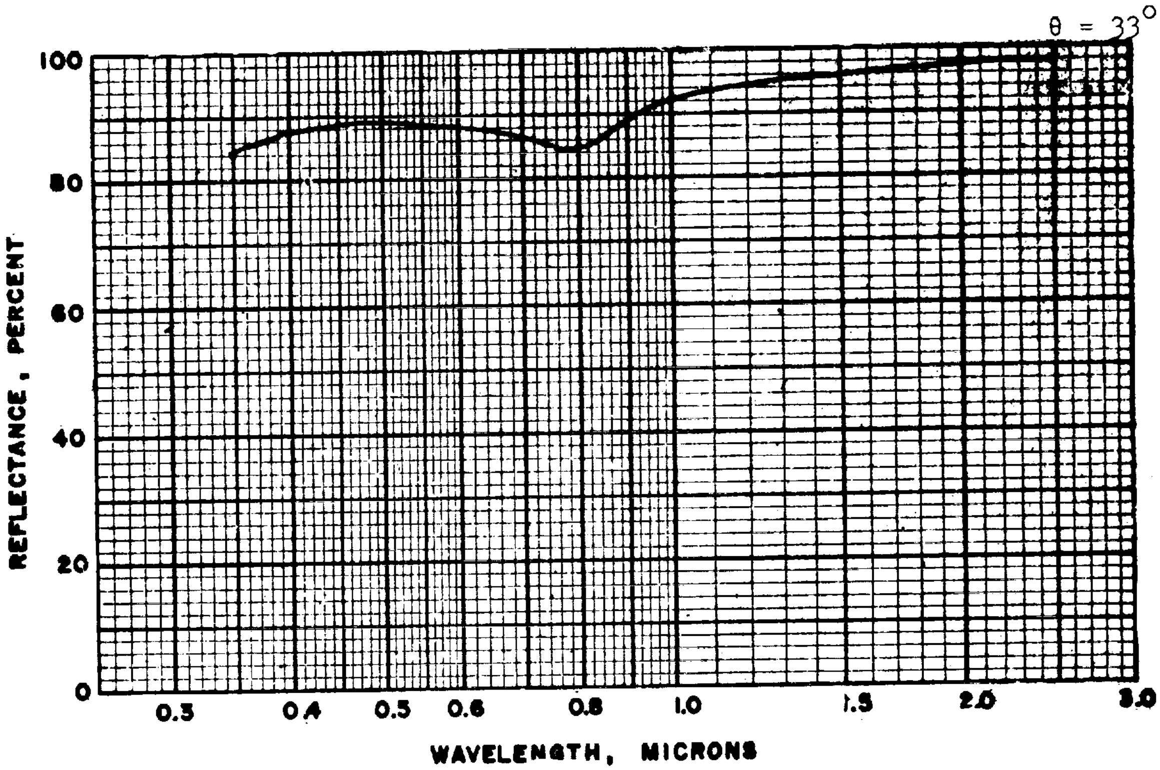

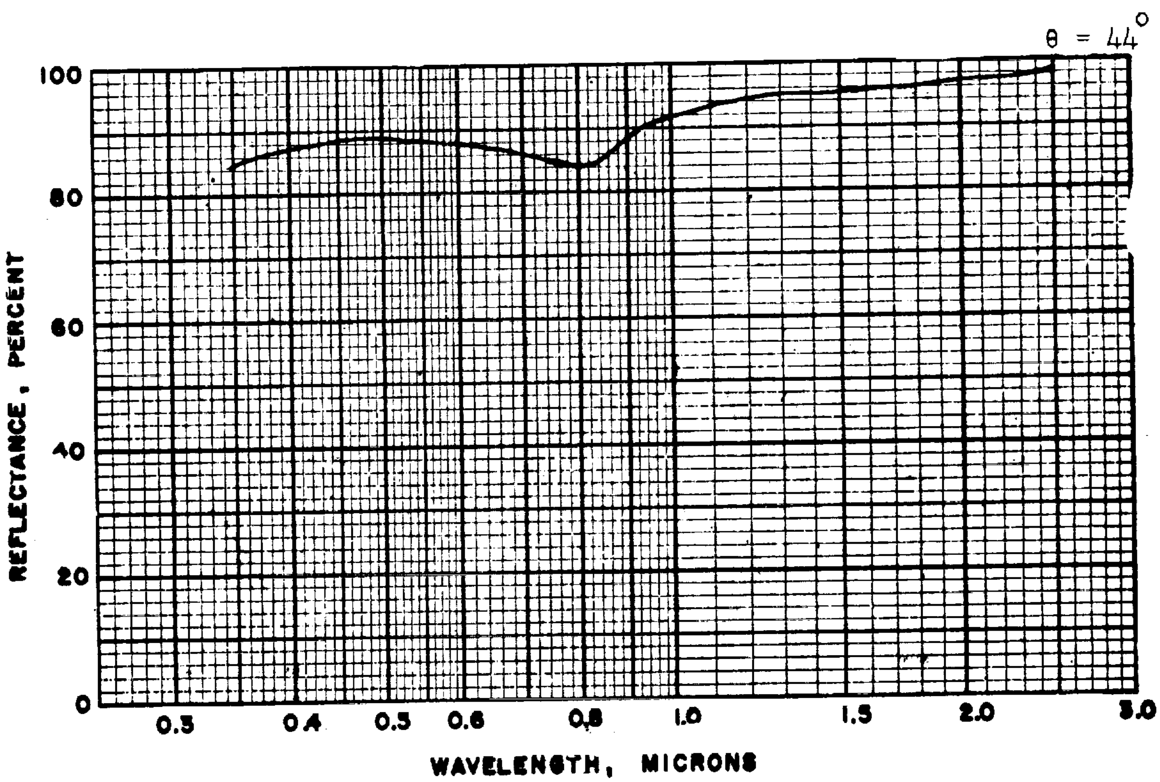

Figure 19 (Cont.): Sample 5A, Azimuthal Angle 45°, Angles of Incidence 33° and 44°

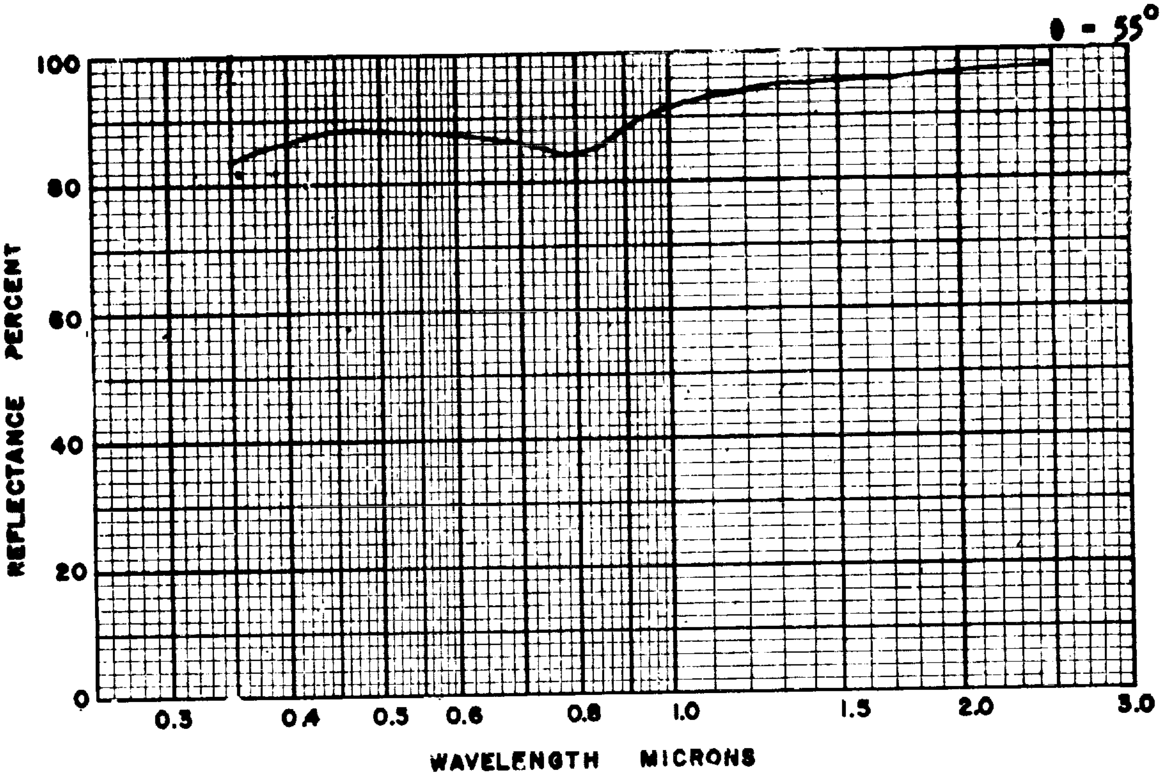

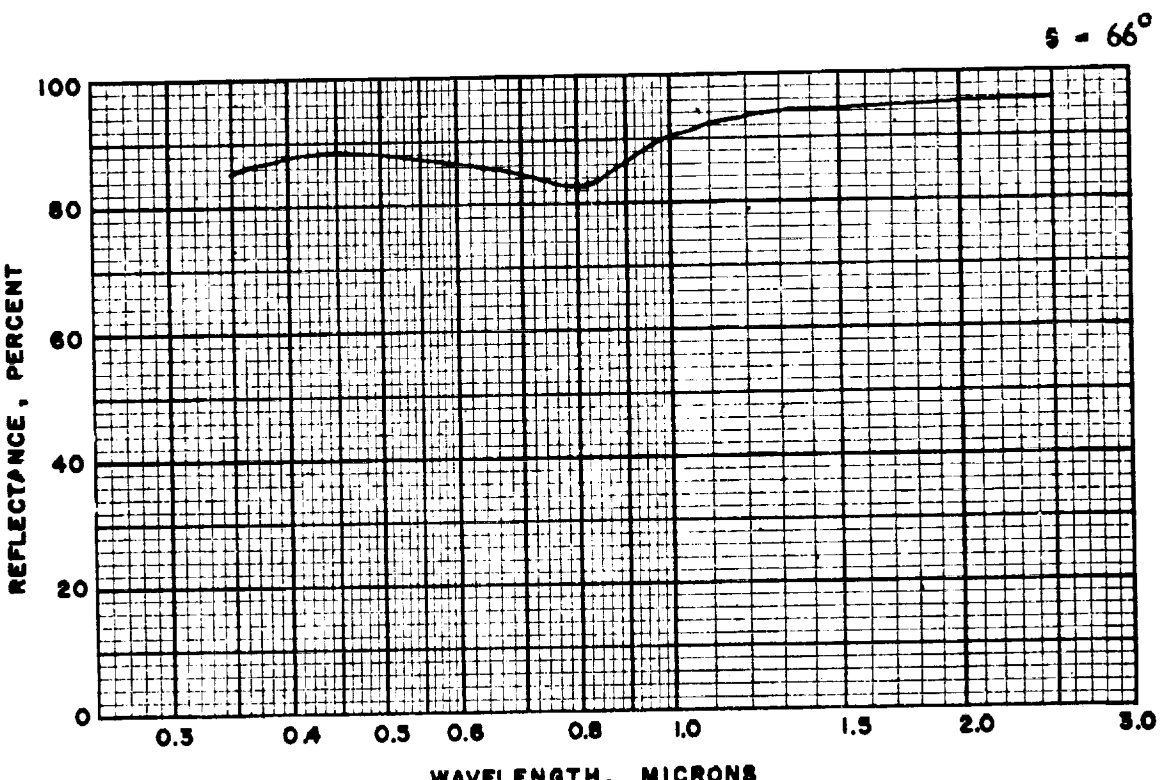

Figure 19 (Cont.): Sample 5A, Azimuthal Angle 45°, Angles of Incidence 55° and 66°

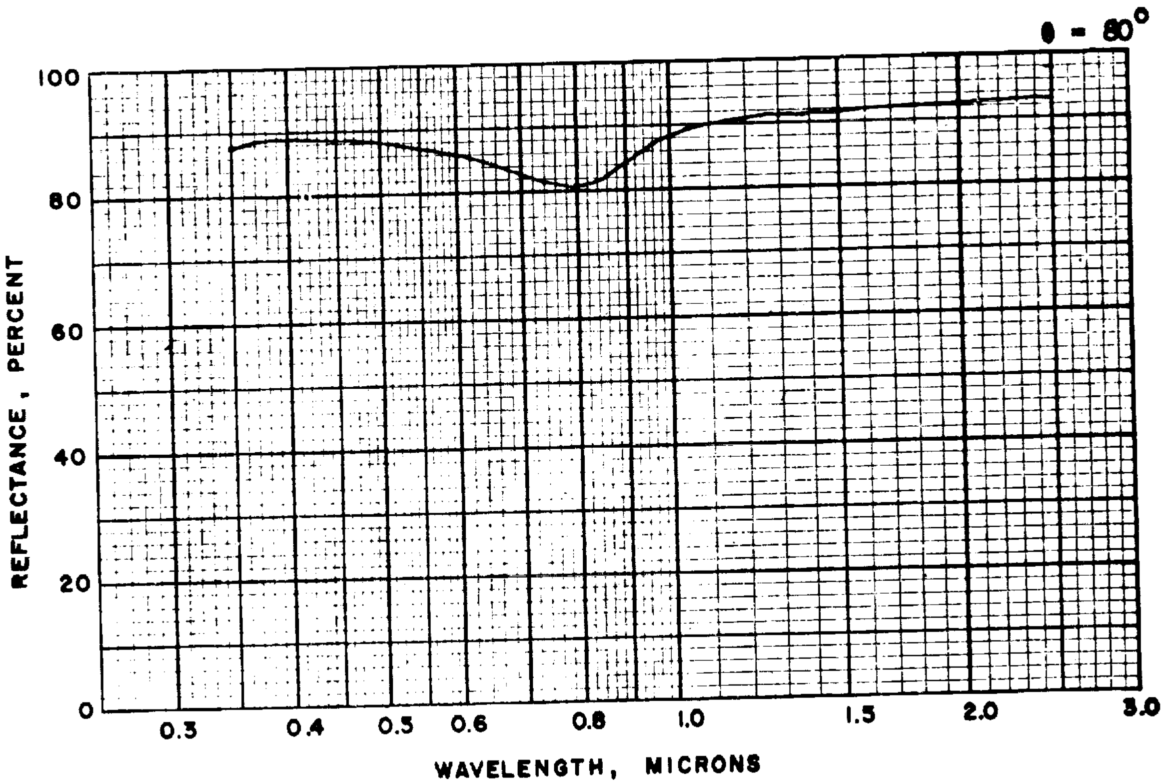

Figure 19 (Cont.): Sample 5A, Azimuthal Angle 45°, Angle of Incidence 80°

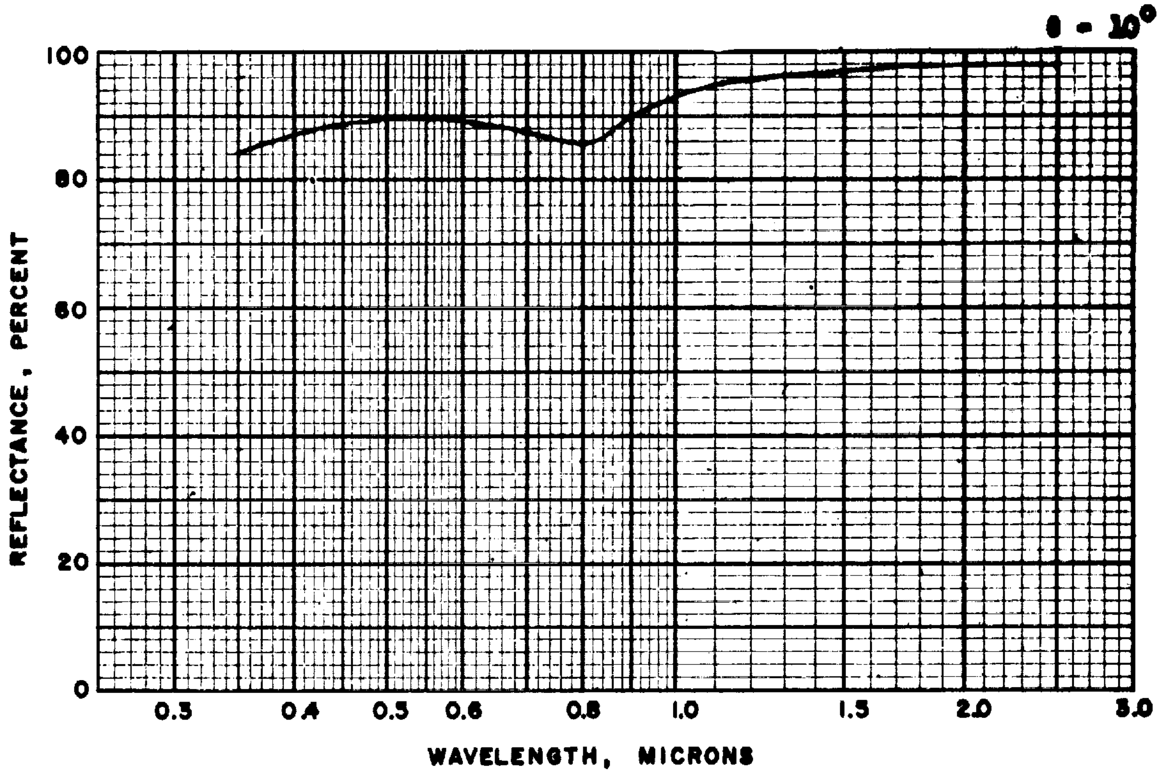

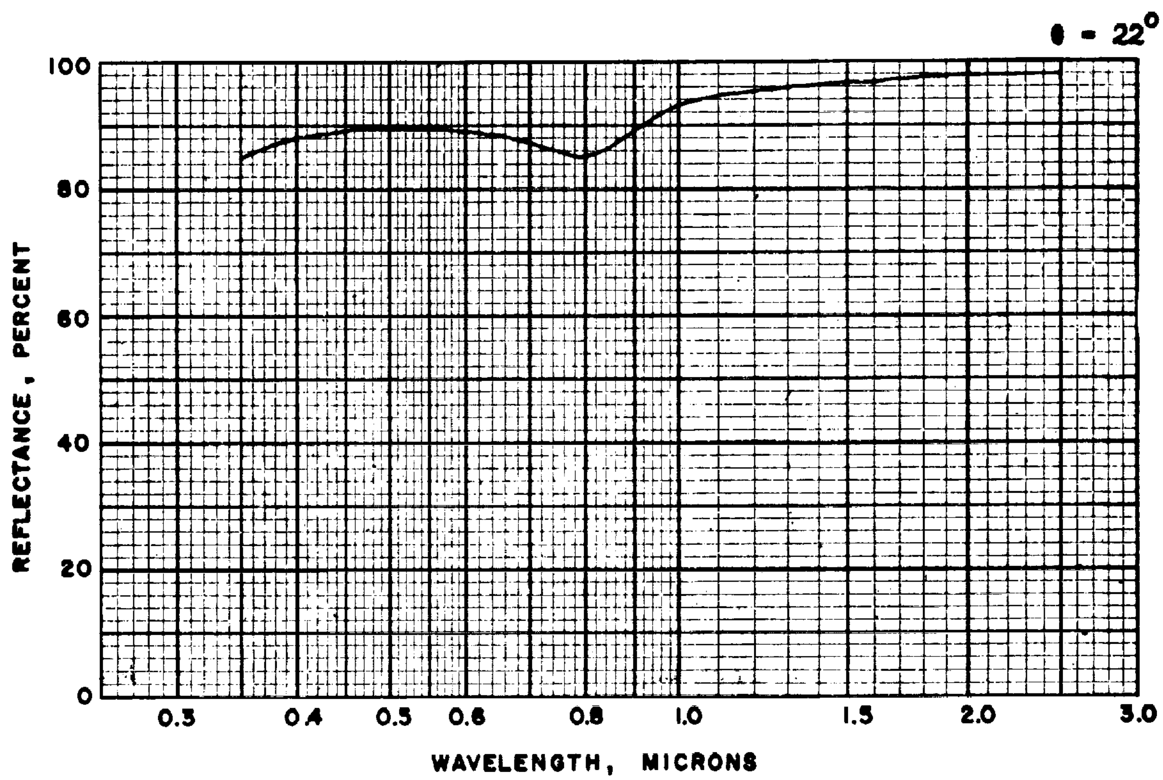

Figure 20: Sample 5A, Azimuthal Angle 60°, Angles of Incidence 10° and 22°

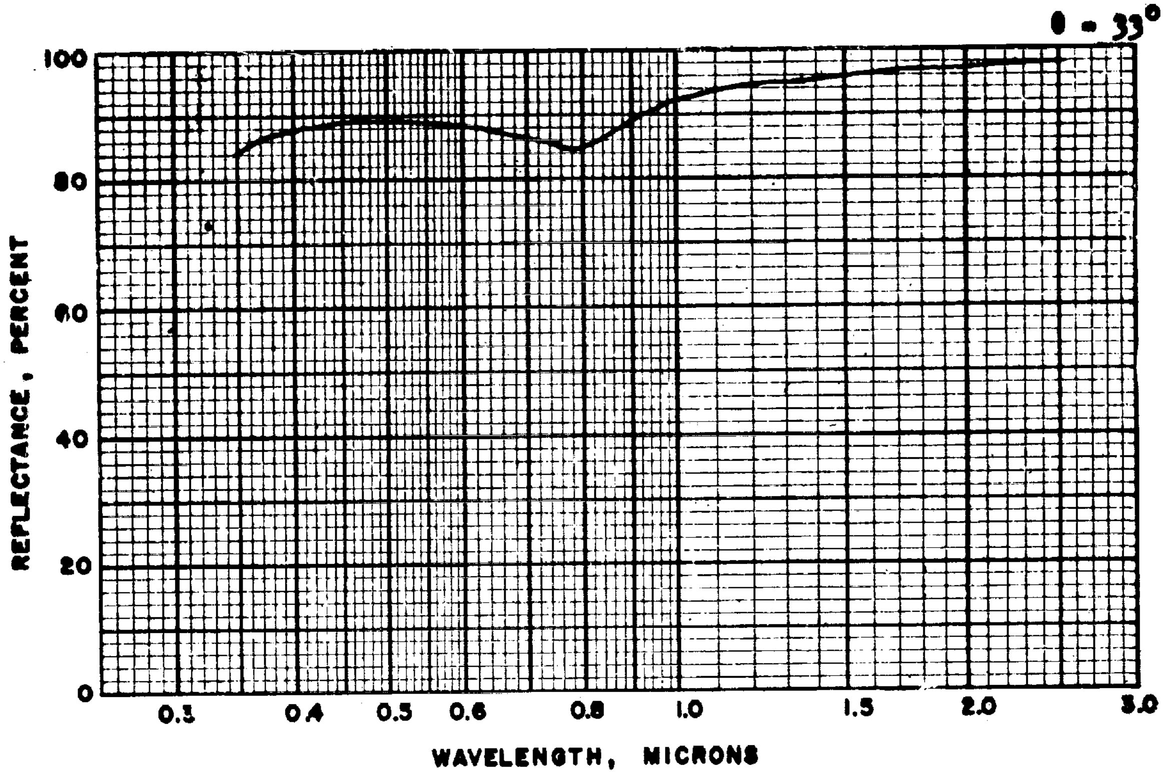

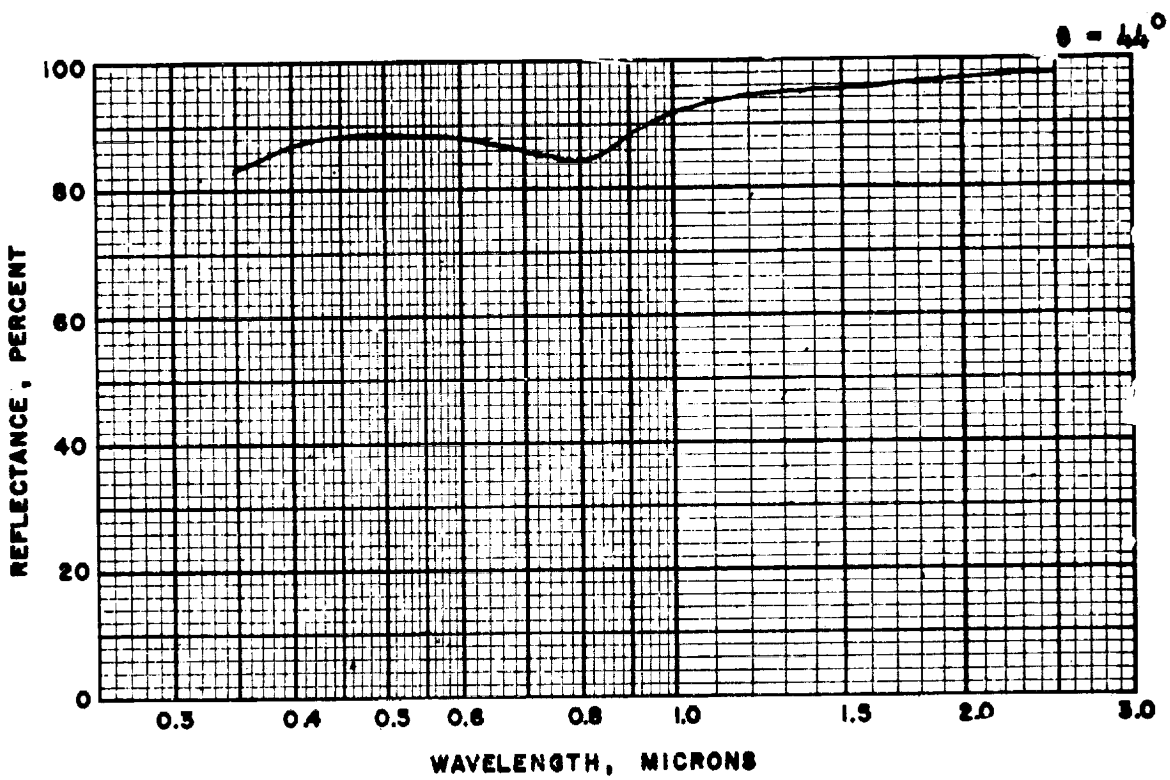

Figure 20 (Cont.): Sample 5A, Azimuthal Angle 60°, Angles of Incidence 33° and 44°

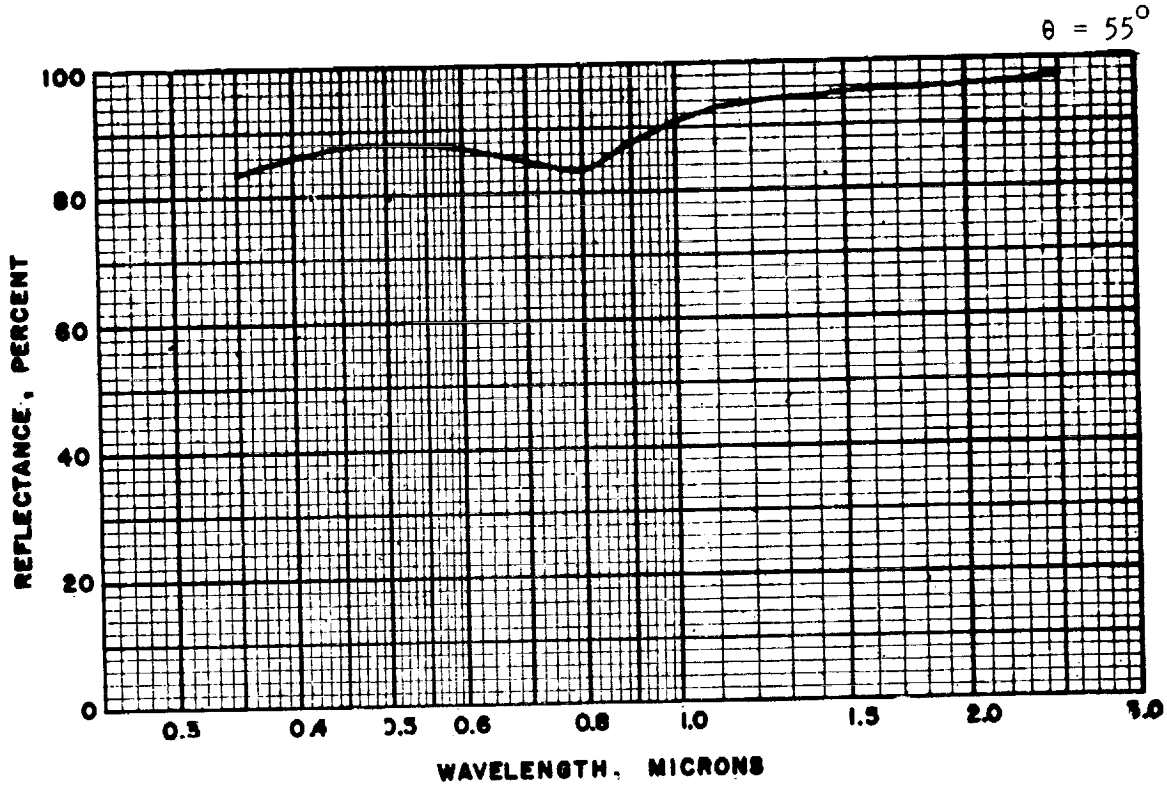

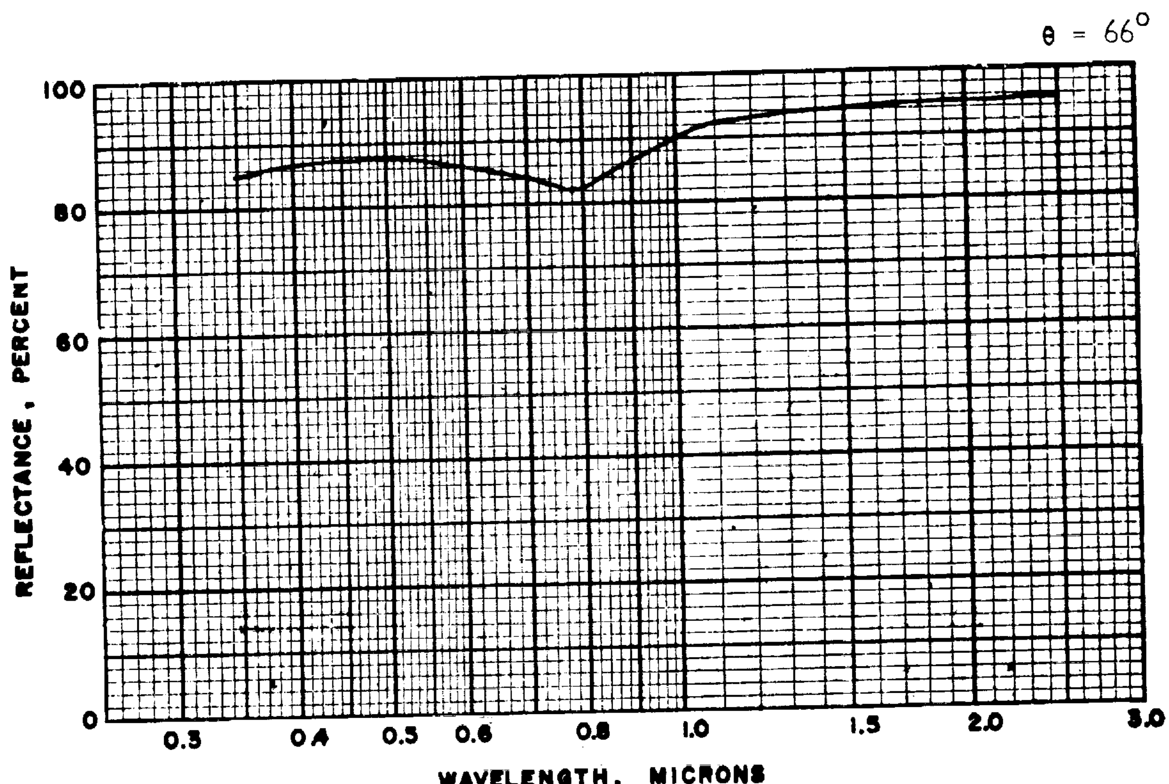

Figure 20 (Cont.): Sample 5A, Azimuthal Angle 60°, Angles of Incidence 55° and 66°

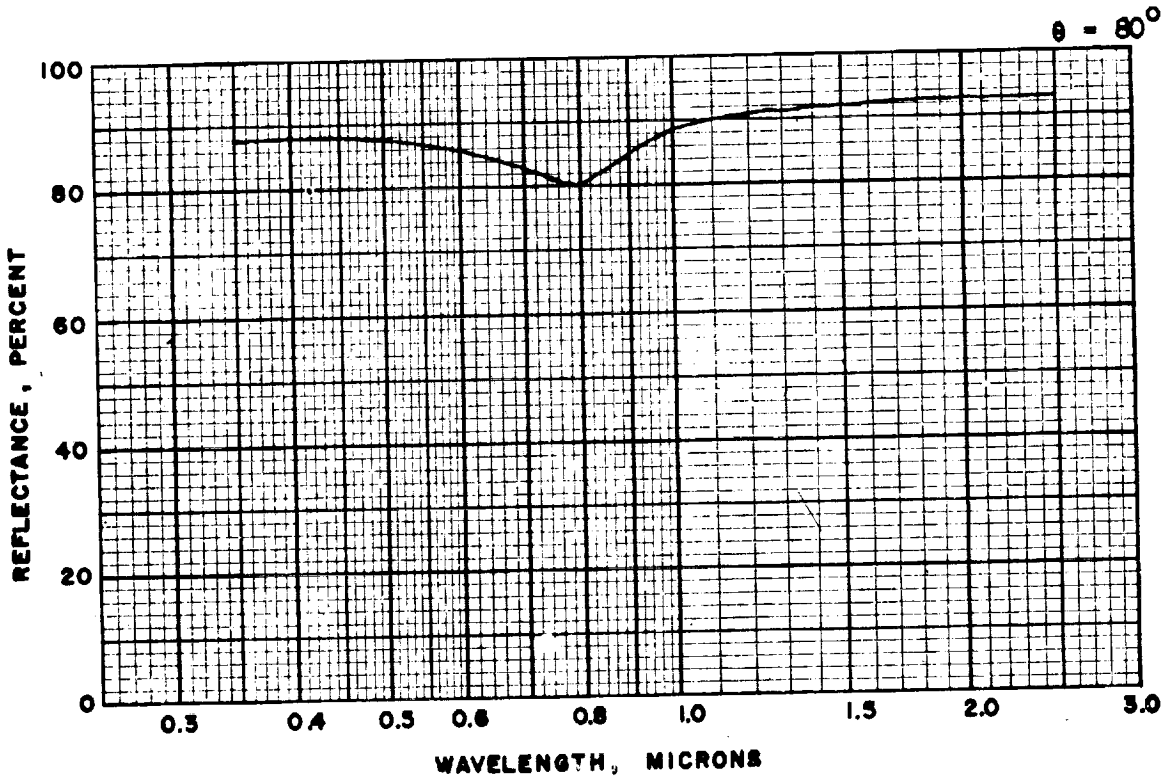

Figure 20 (Cont.): Sample 5A, Azimuthal Angle 60°, Angle of Incidence 80°

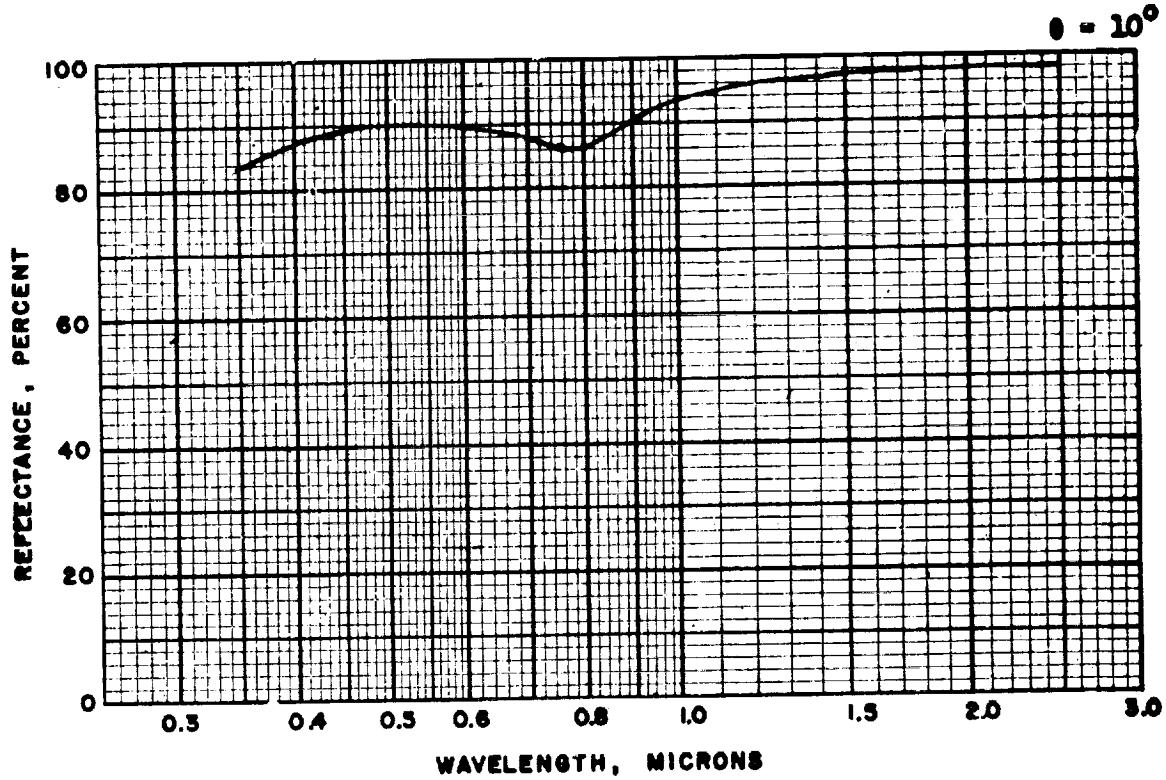

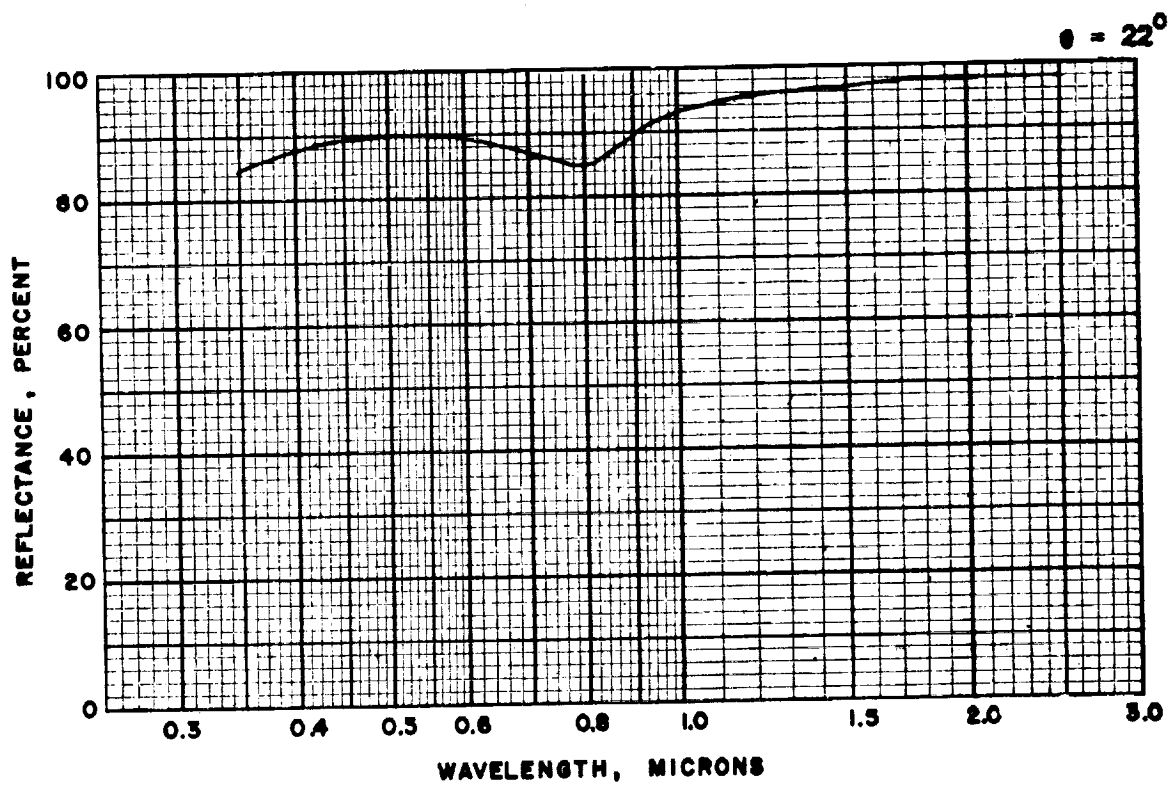

Figure 21: Sample 5A, Azimuthal Angle 90°, Angles of Incidence 10° and 22°

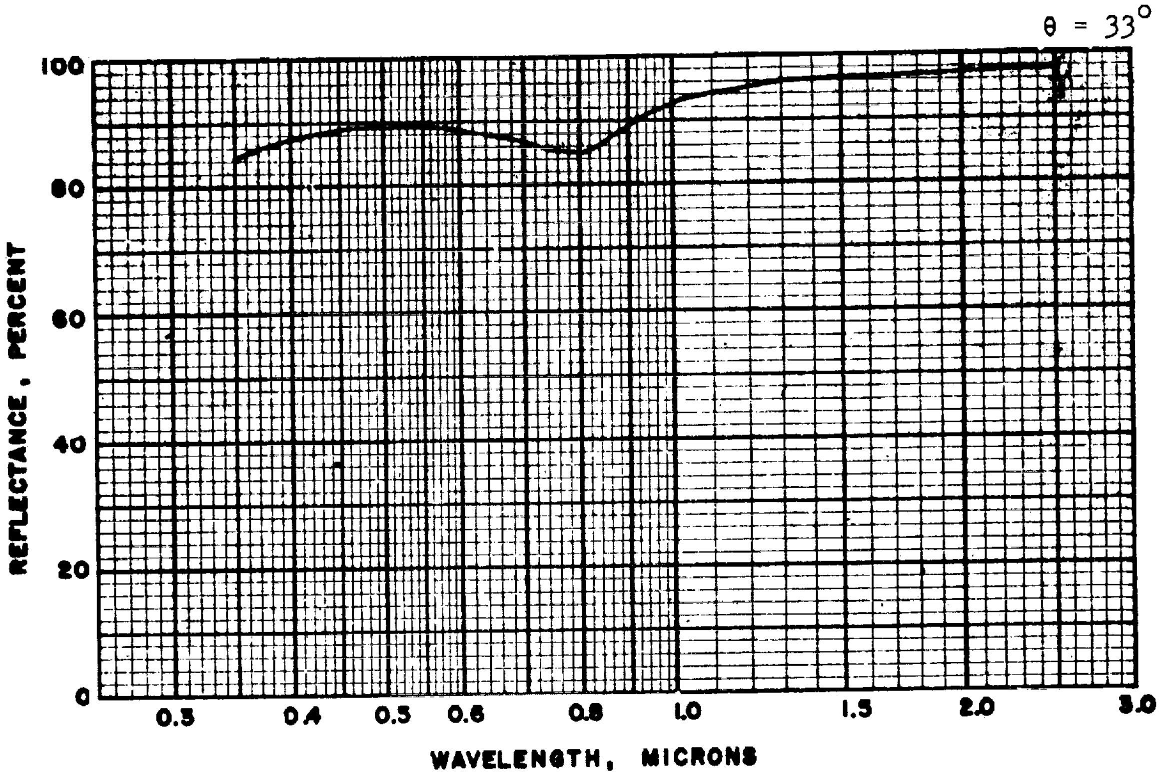

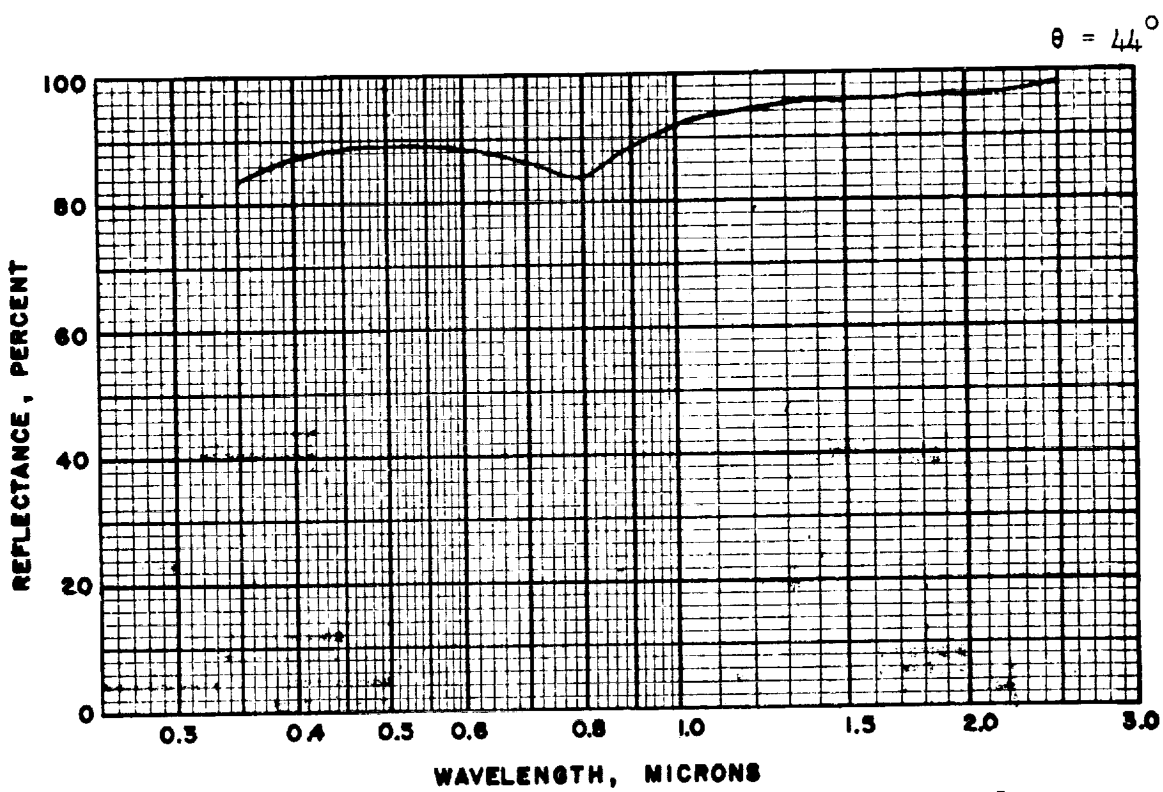

Figure 21 (Cont.): Sample 5A, Azimuthal Angle 90°, Angles of Incidence 33° and 44°

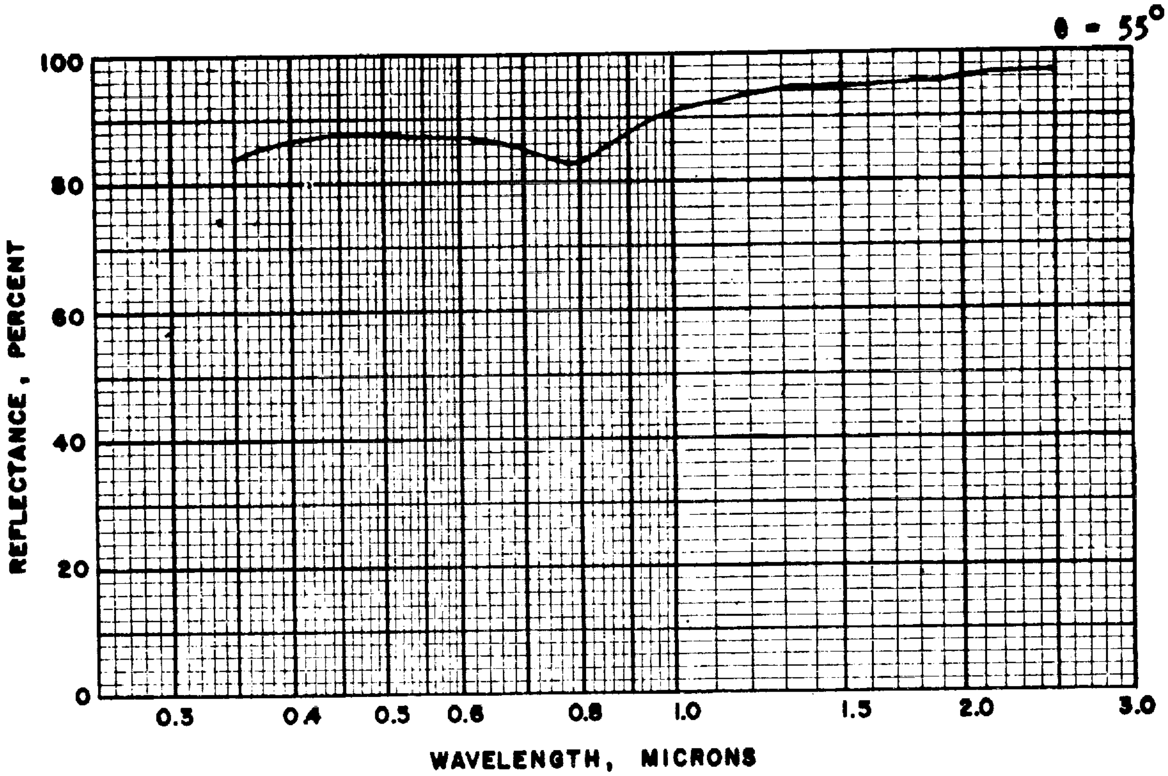

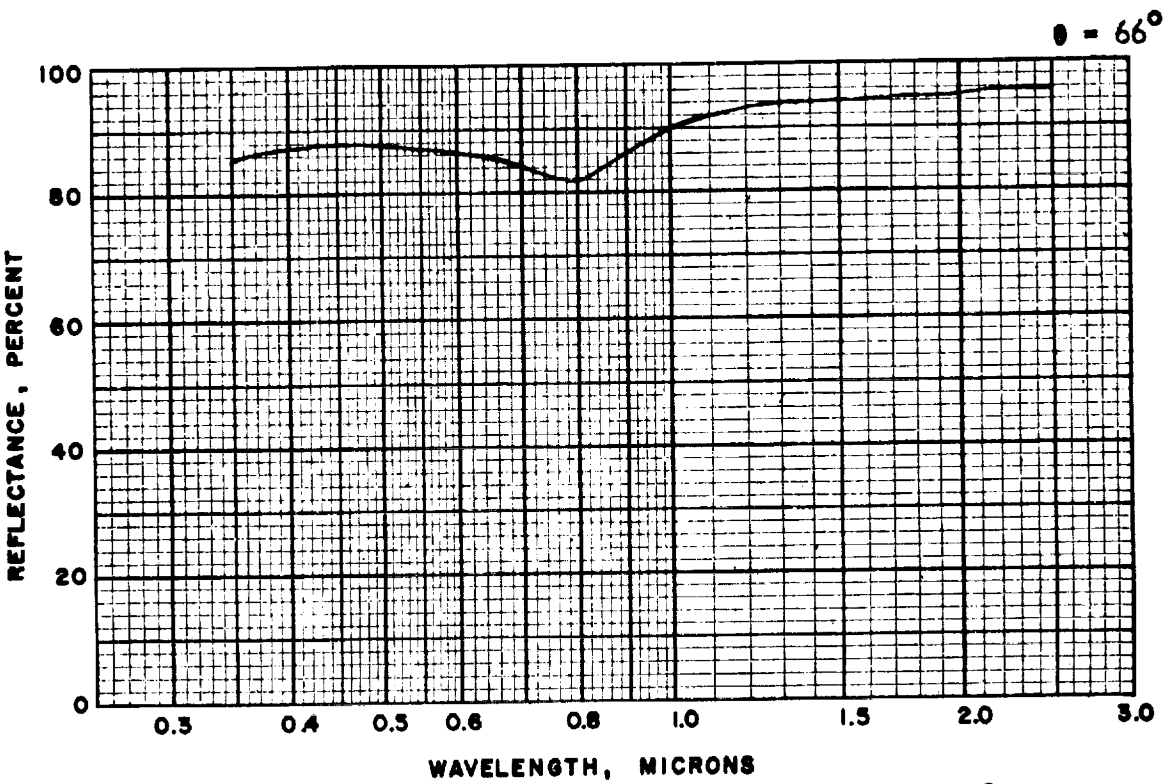

Figure 21 (Cont.): Sample 5A, Azimuthal Angle 90°, Angles of Incidence 55° and 66°

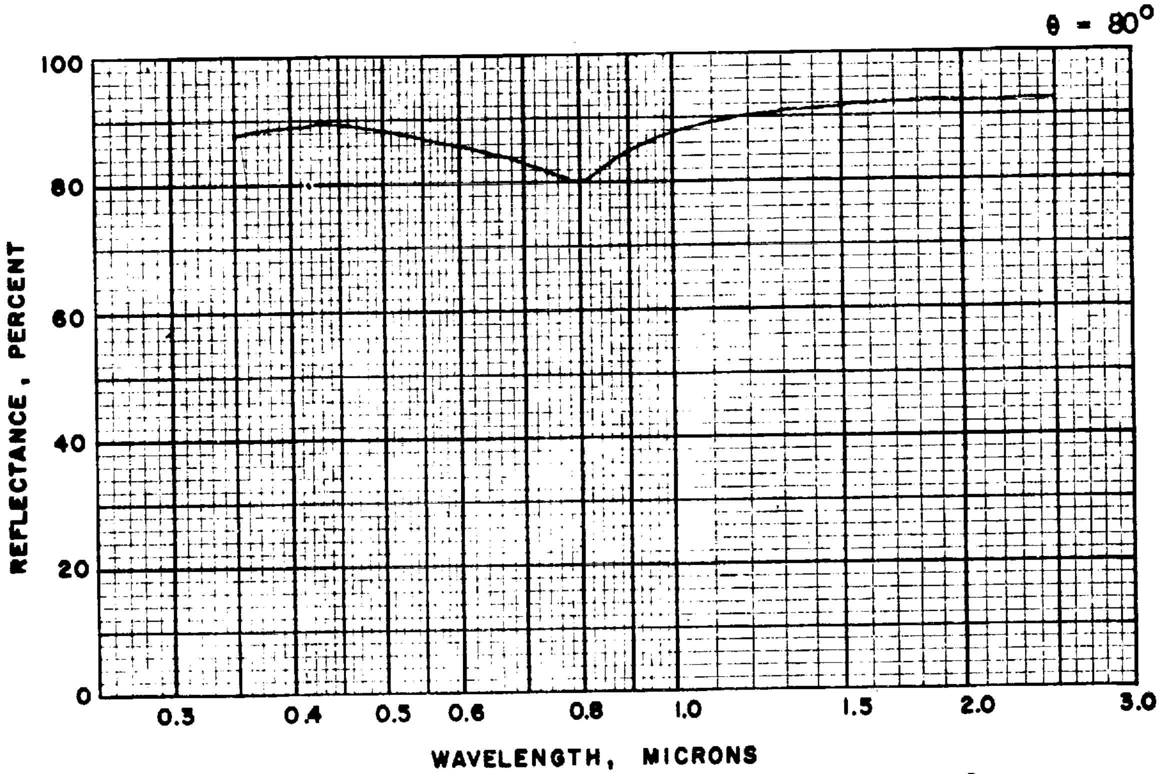

Figure 21 (Cont.): Sample 5A Azimuthal Angle 90°, Angle of Incidence 80°

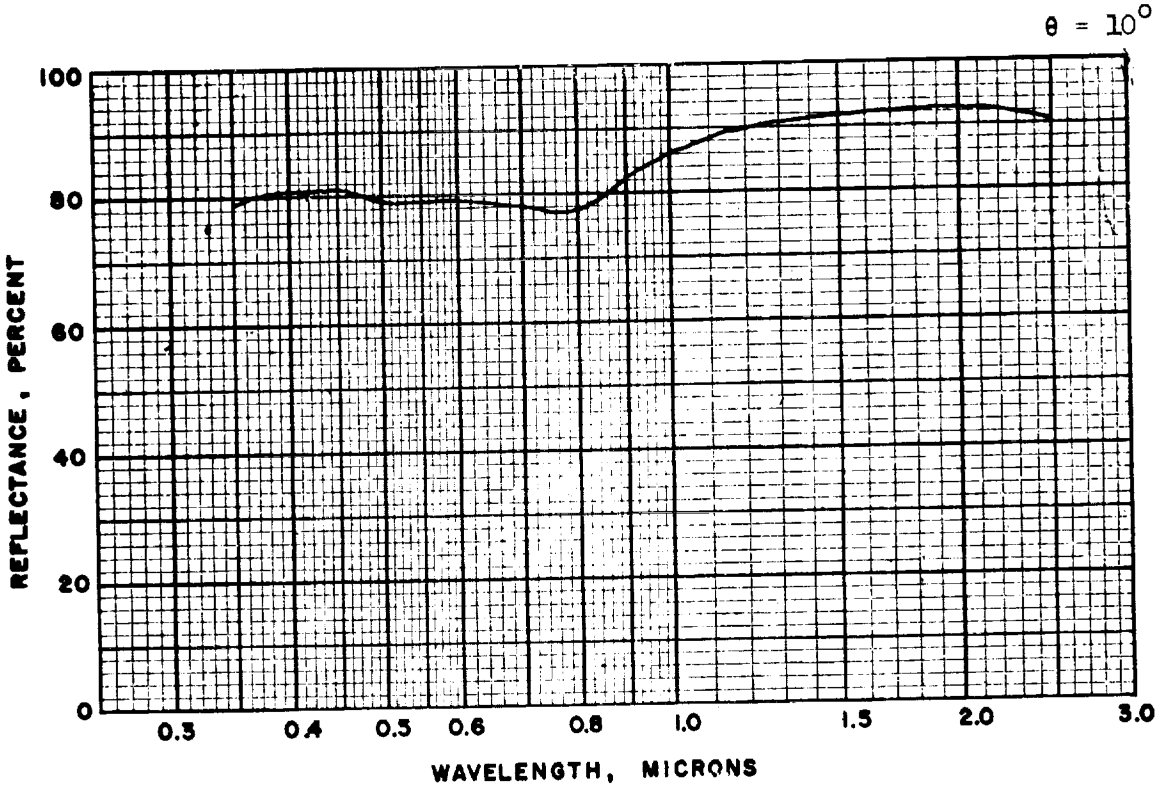

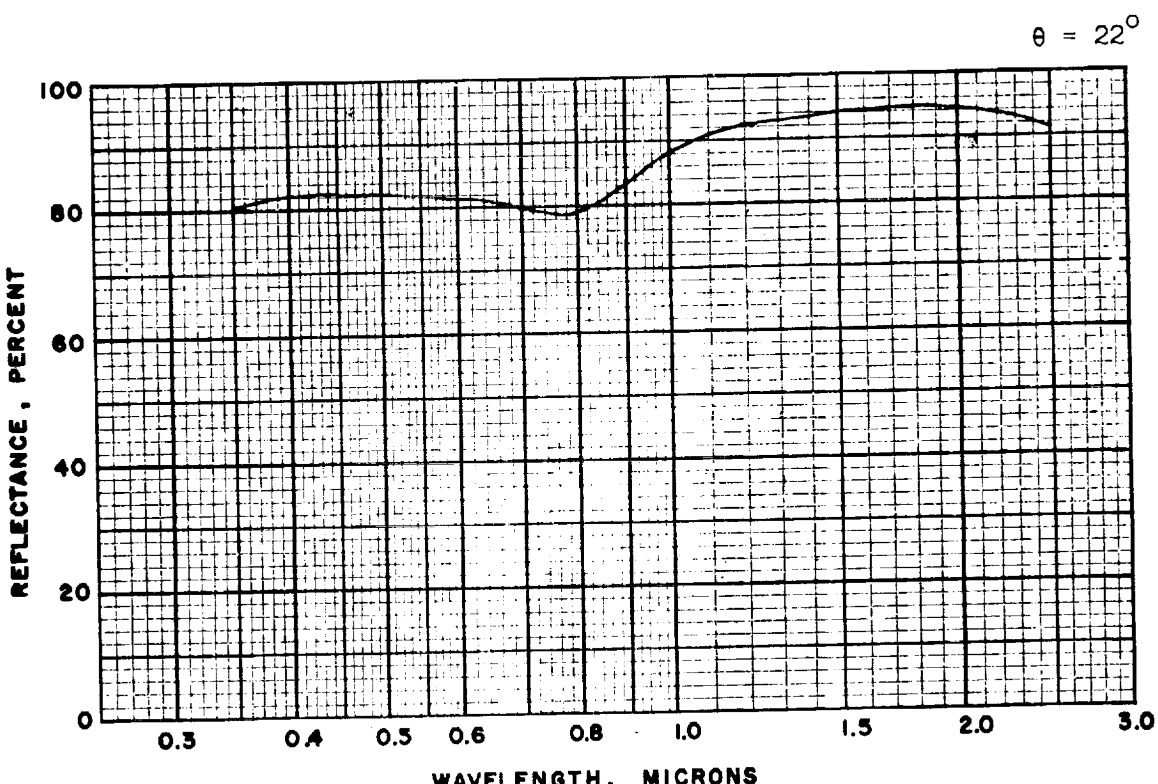

Figure 22: Sample 5B, Azimuthal Angle 0°, Angles of Incidence 10° and 22°

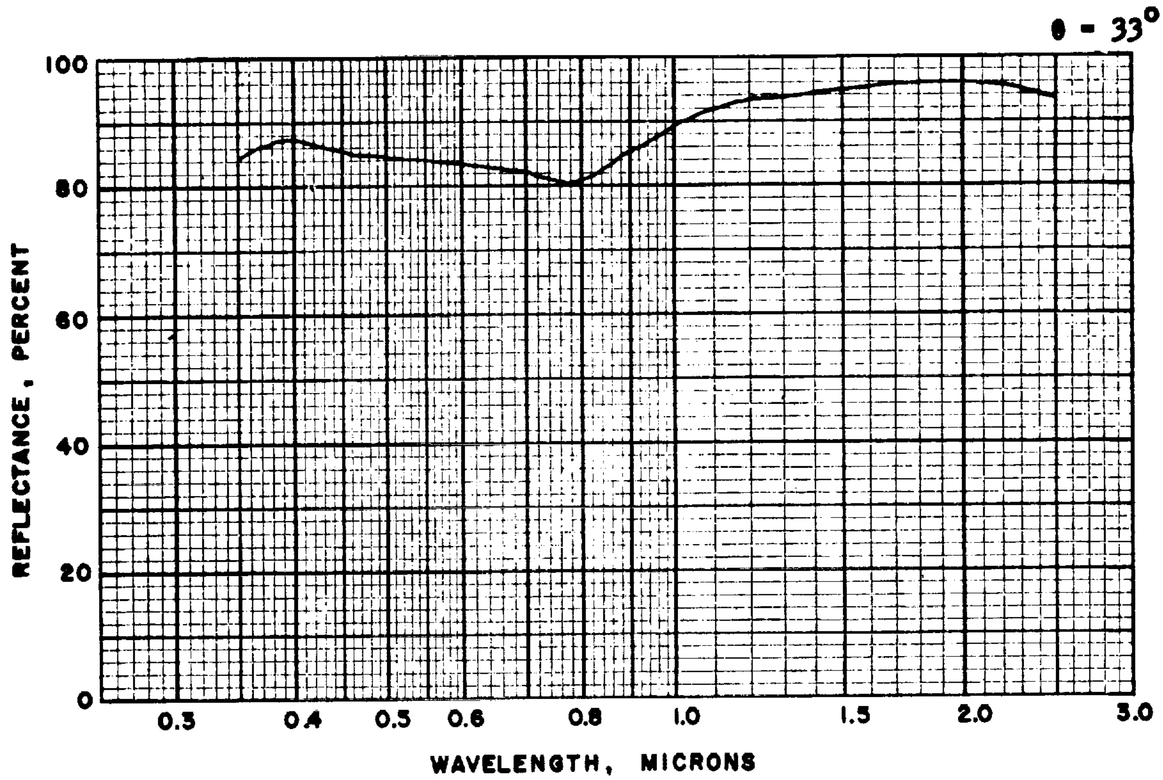

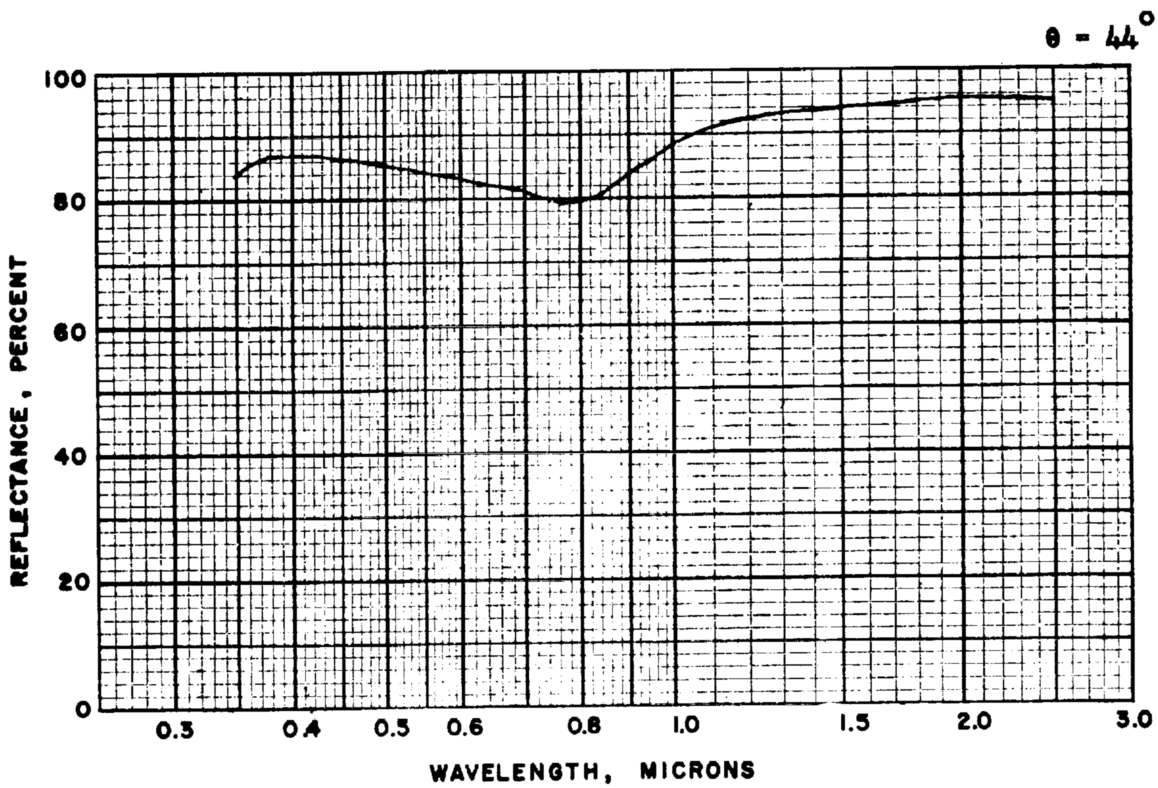

Figure 22 (Cont.): Sample 5B, Azimuthal Angle 0°, Angles of Incidence 33° and 44°

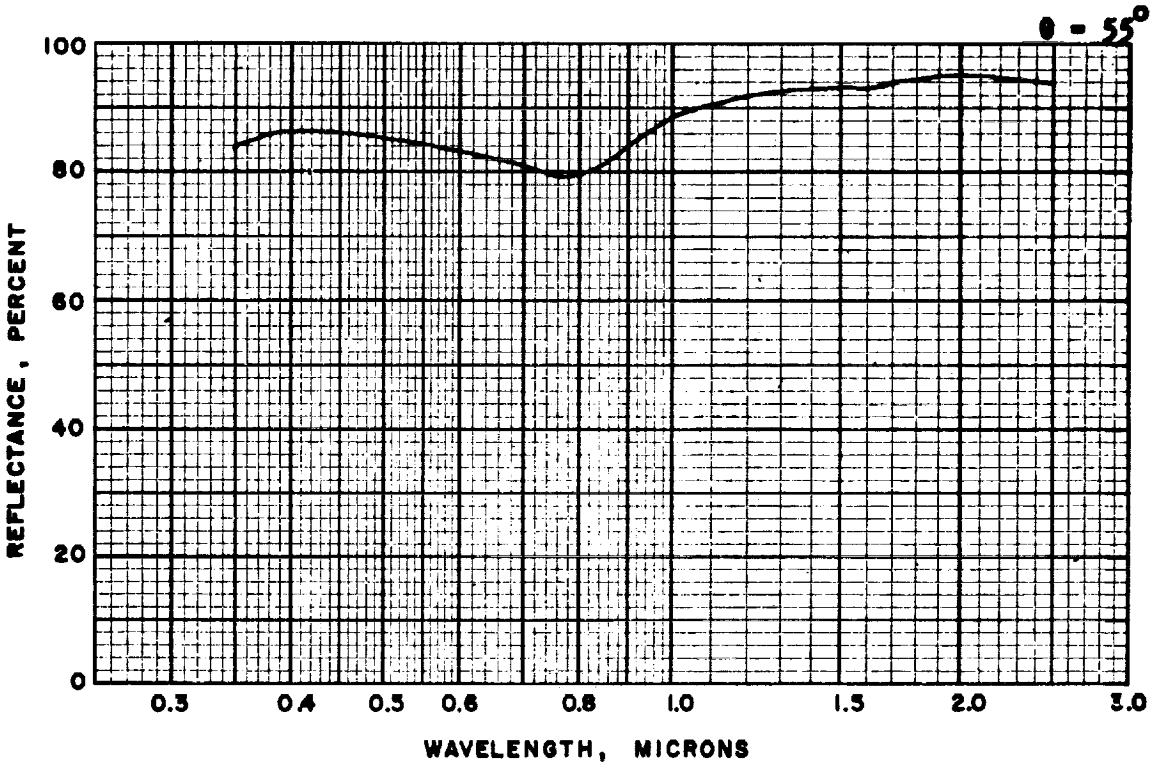

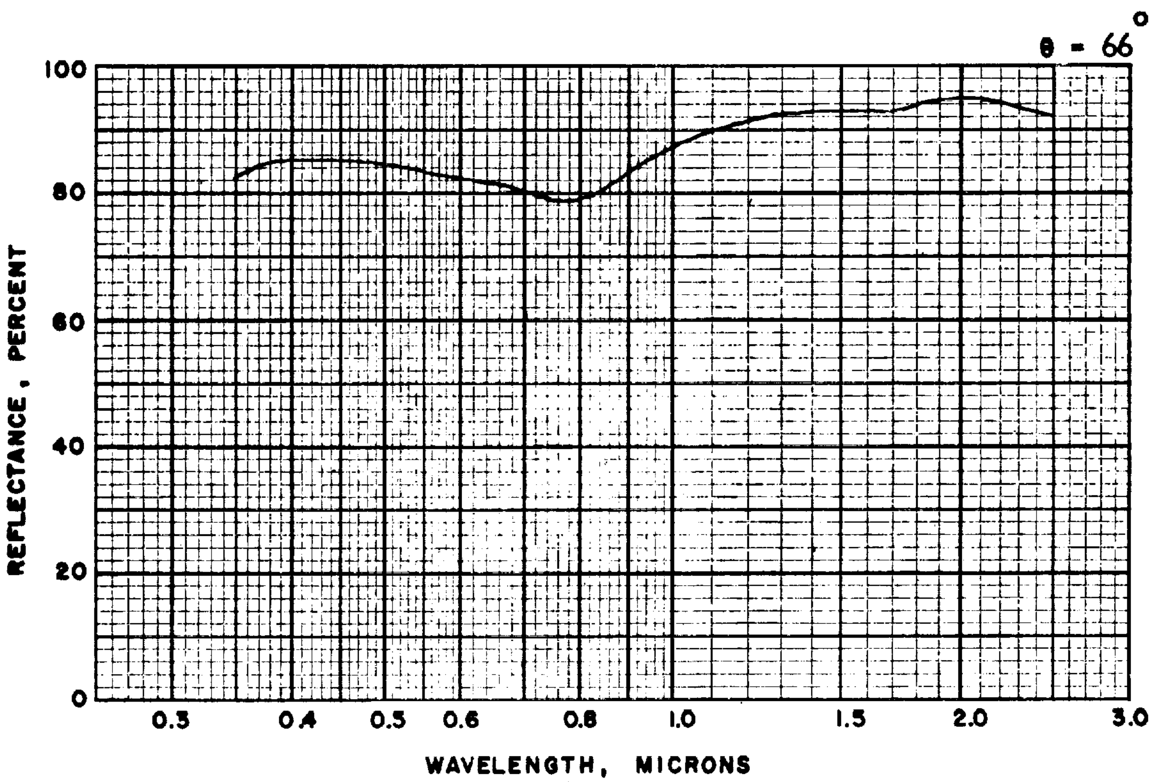

Figure 22 (Cont.): Sample 5B, Azimuthal Angle 0°, Angles of Incidence 55° and 66°

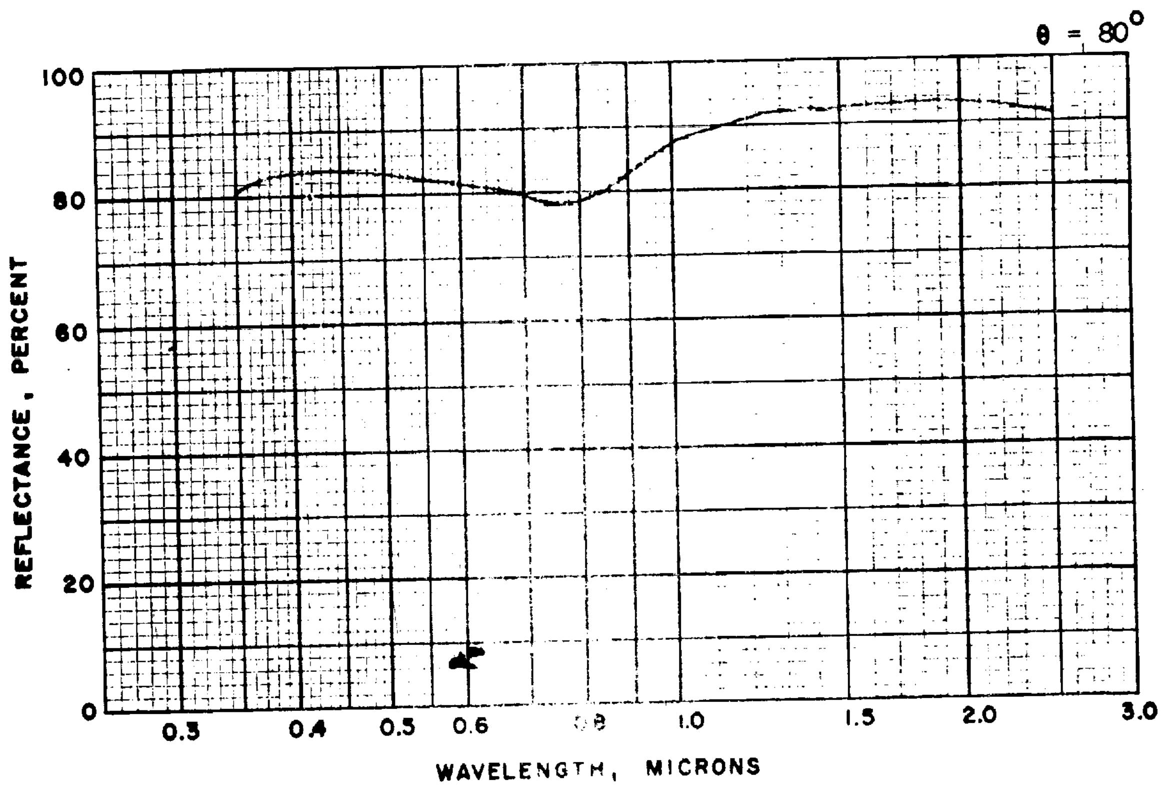

Figure 22 (Cont.): Sample 5B, Azimuthal Angle 0°, Angle of Incidence 80°

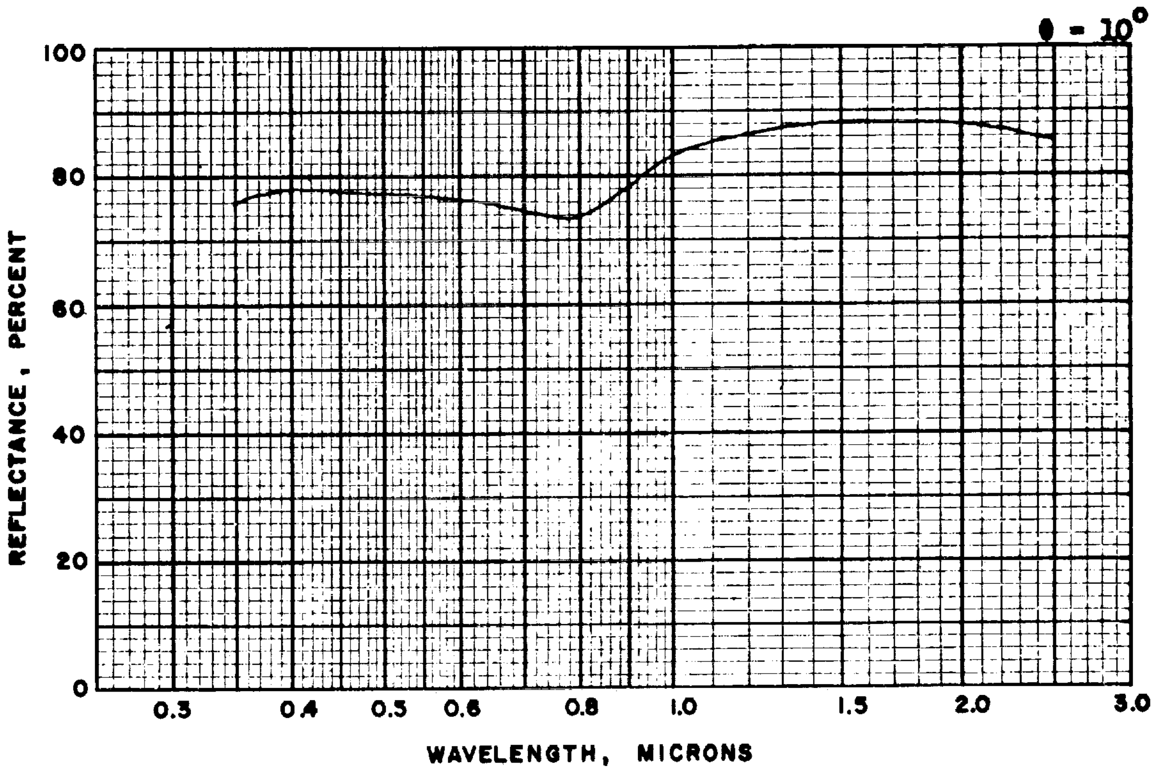

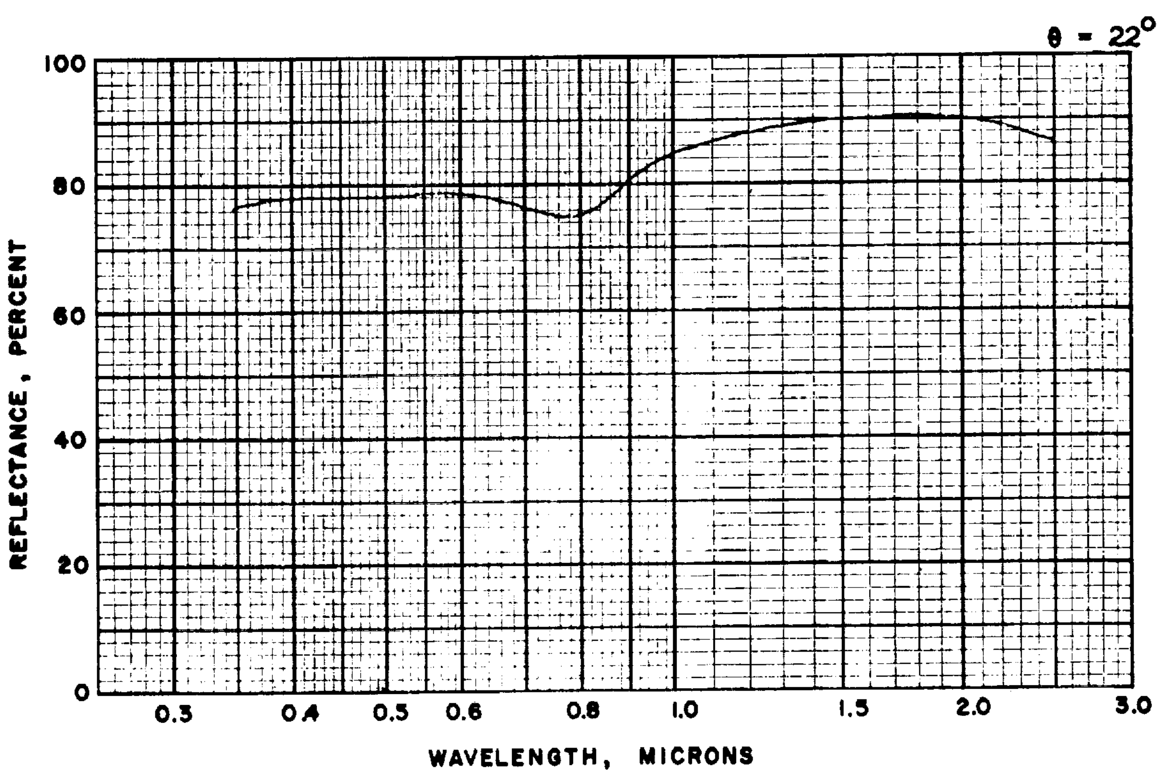

Figure 23: Sample 5B, Azimuthal Angle 45°, Angles of Incidence 10° and 22°

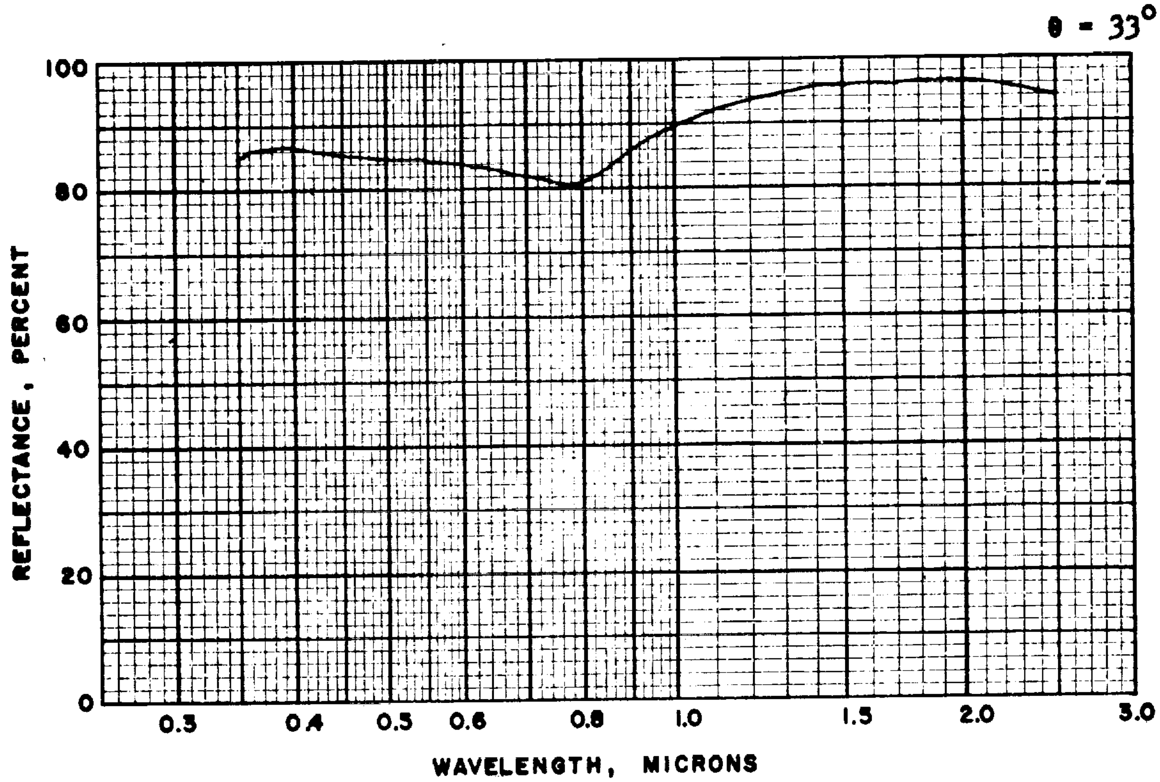

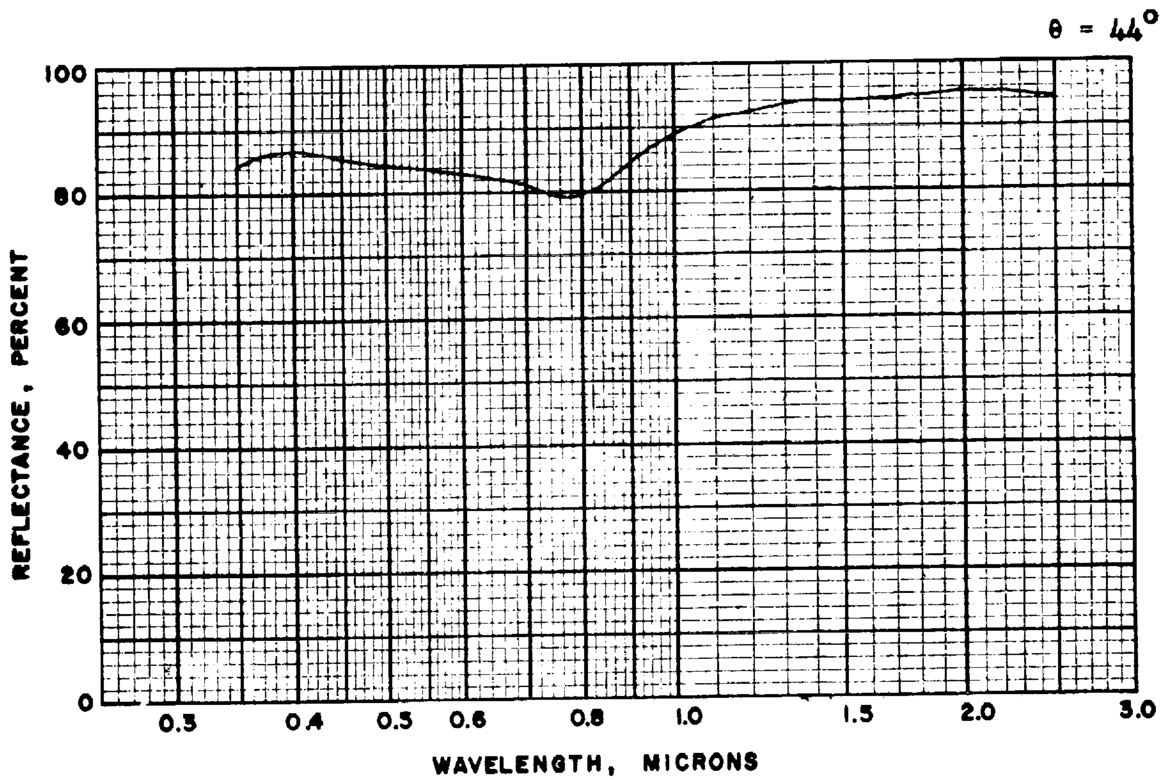

Figure 23 (Cont.): Sample 5B, Azimuthal Angle 45°, Angles of Incidence 33° and 44°

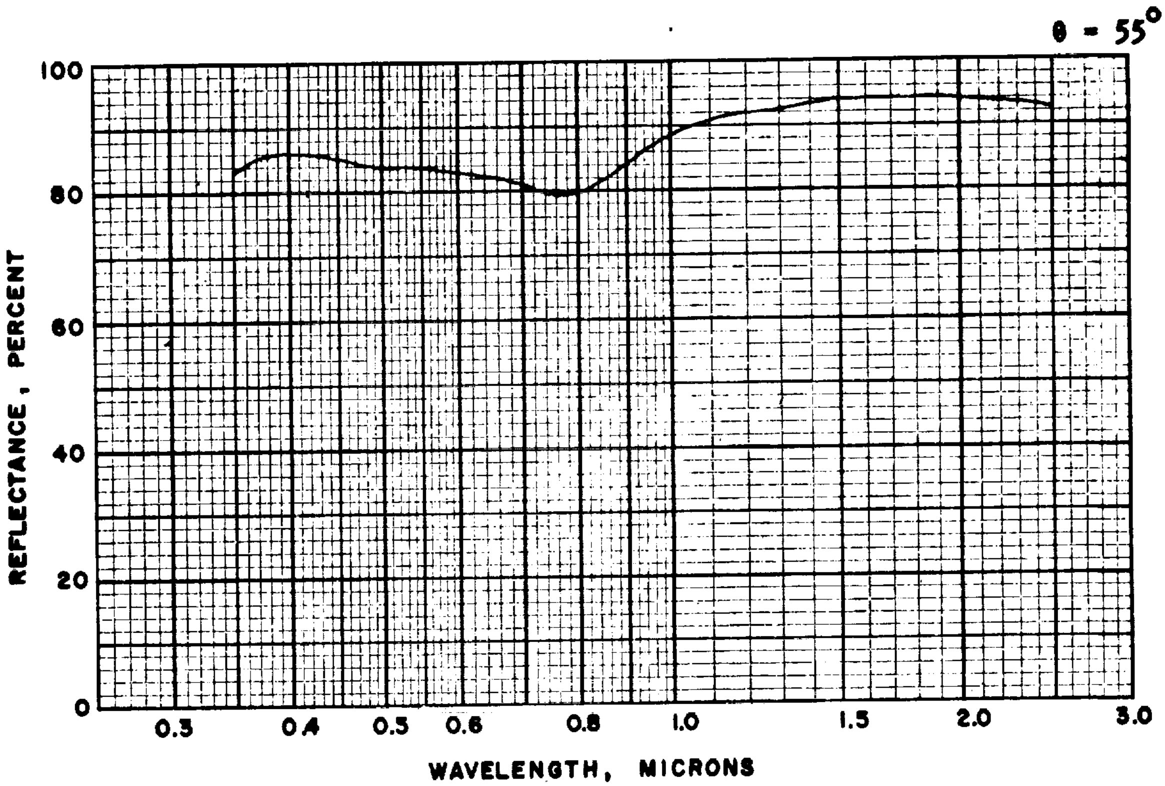

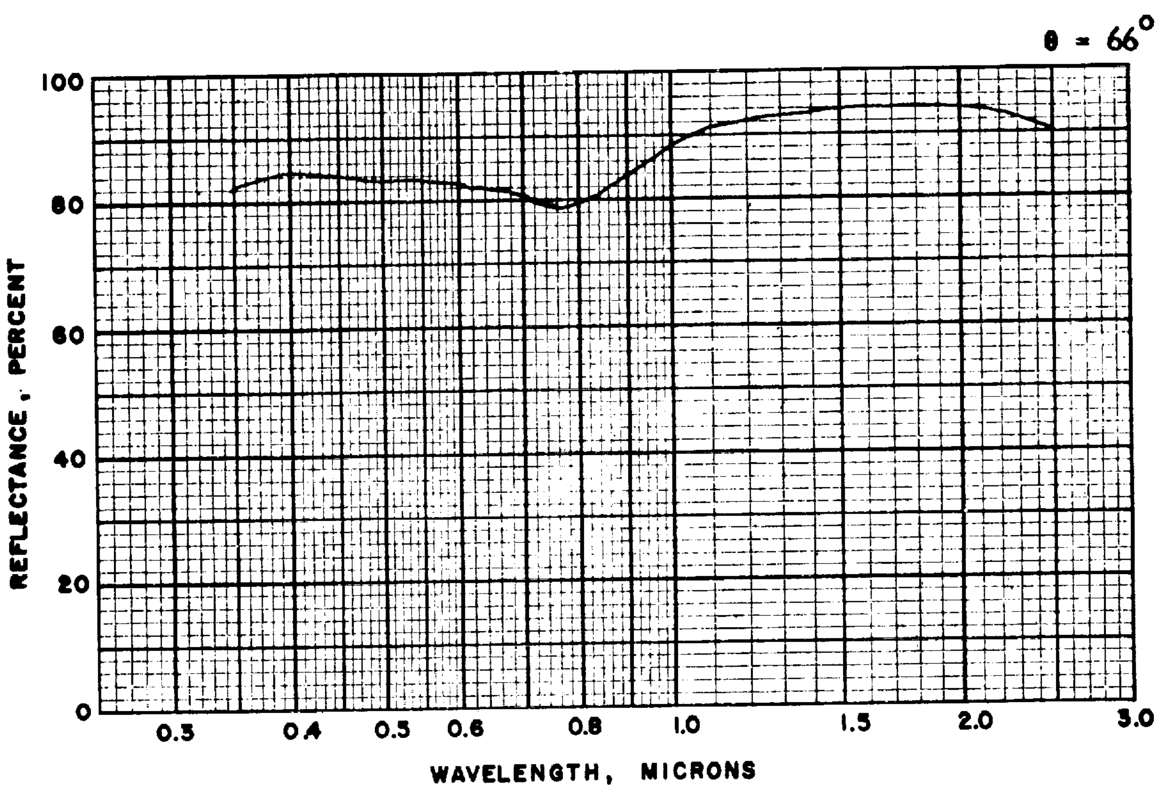

Figure 23 (Cont.): Sample 5B, Azimuthal Angle 45°
Angles of Incidence 55° and 66°

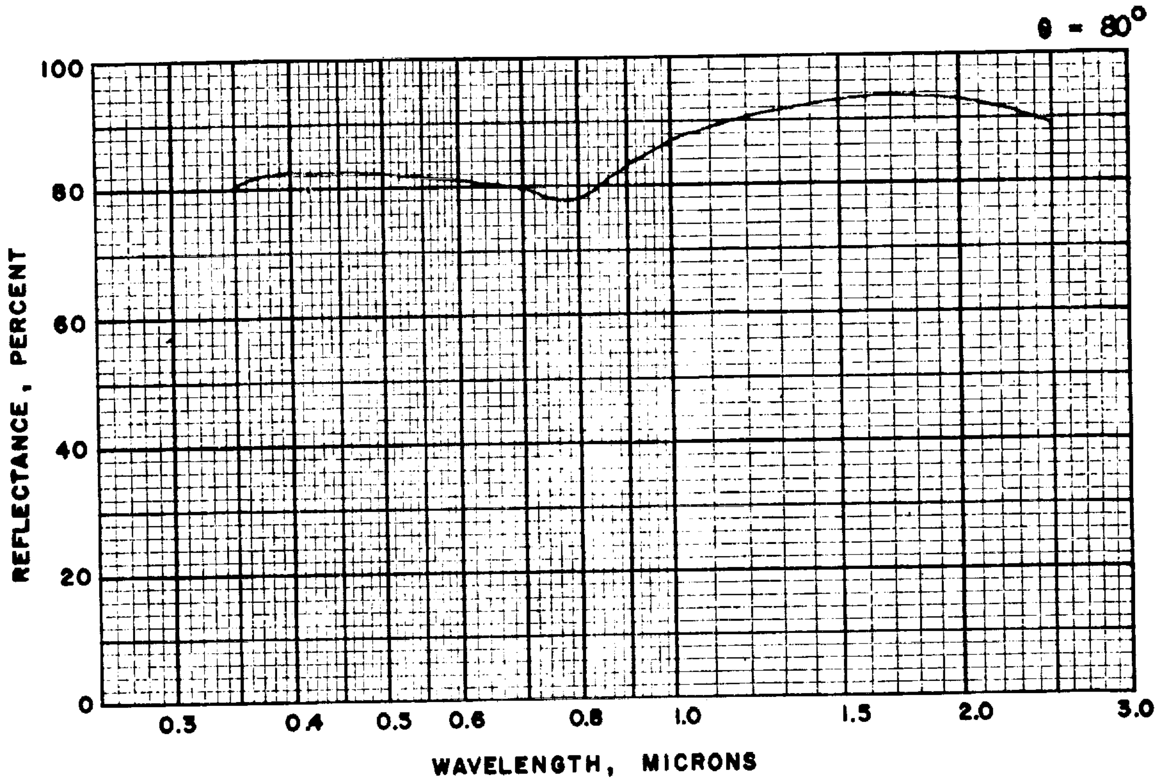

Figure 23 (Cont.): Sample 5B, Azimuthal Angle 45°, Angle of Incidence 80°

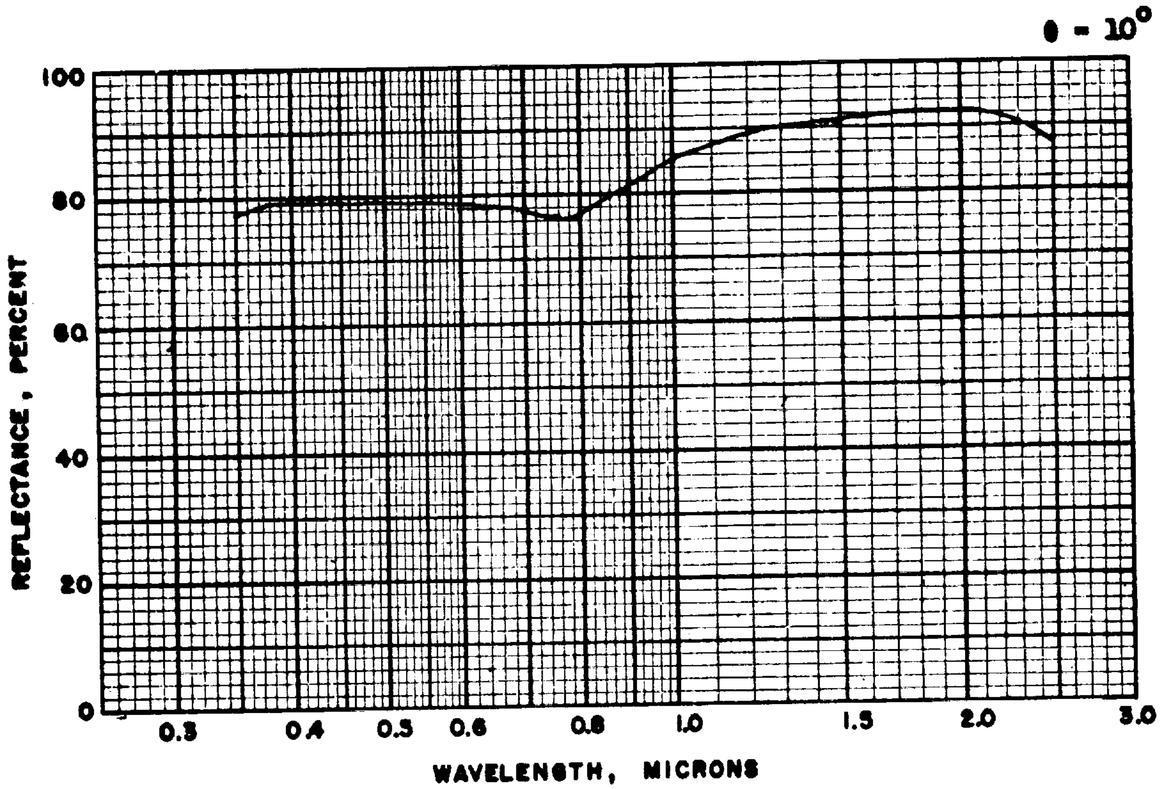

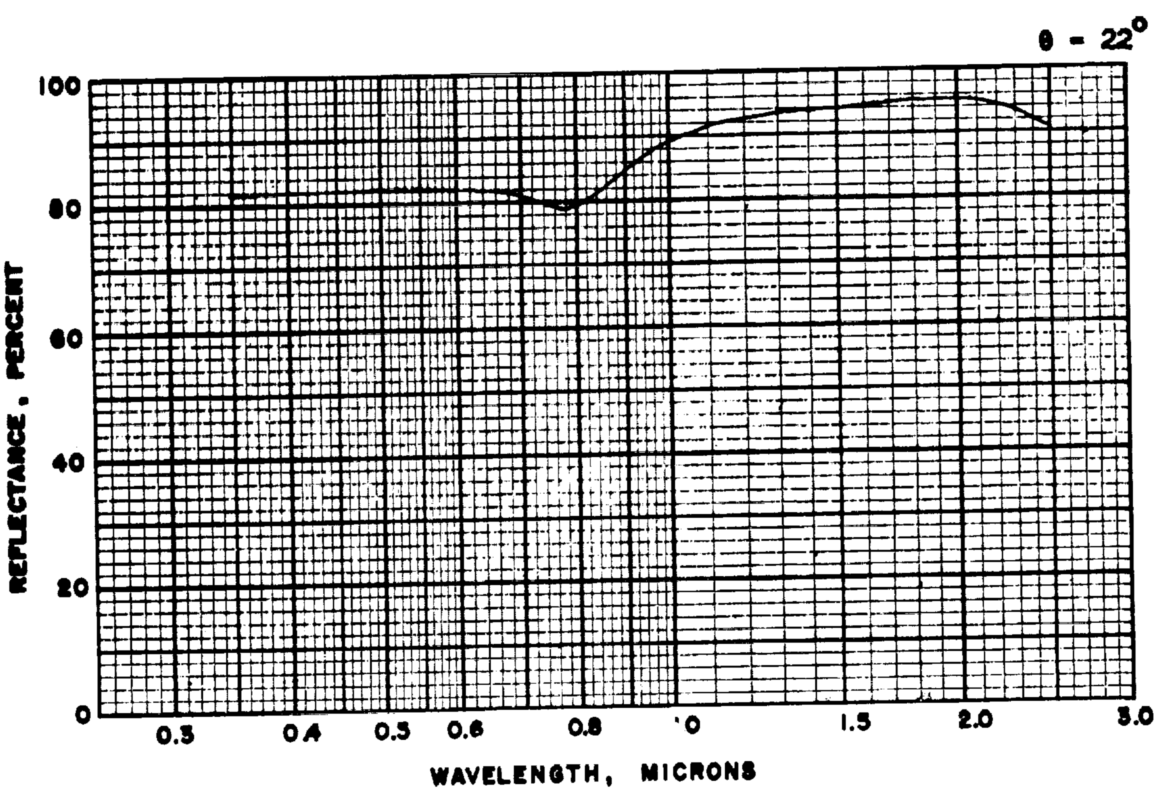

Figure 24: Sample 5B, Azimuthal Angle 60°, Angles of Incidence 10° and 22°

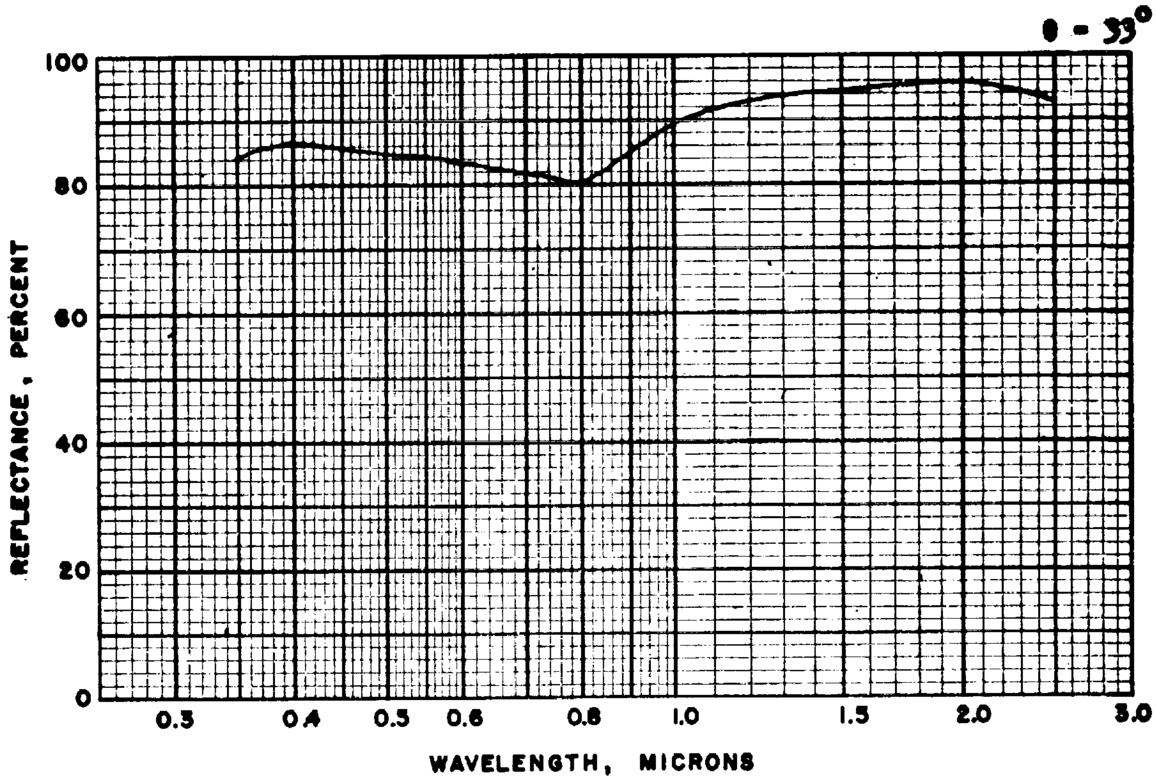

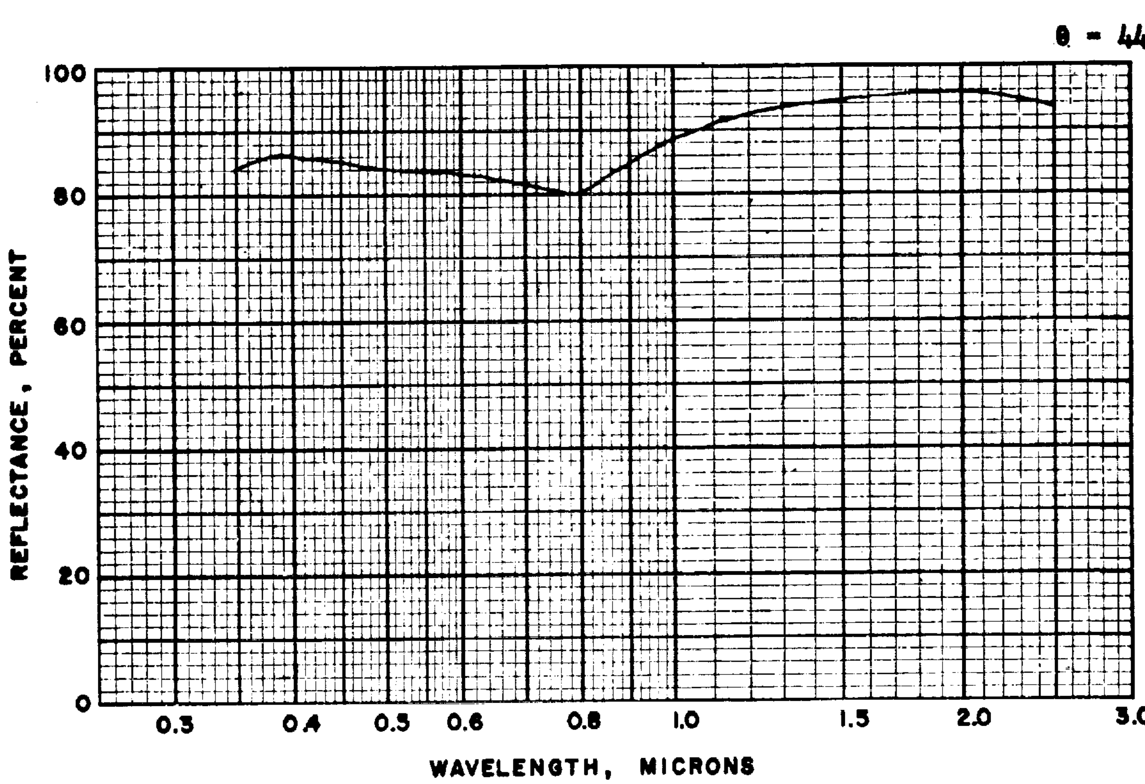

Figure 24 (Cont.): Sample 5B, Asimuthal Angle 60°, Angles of Incidence 33° and 44°

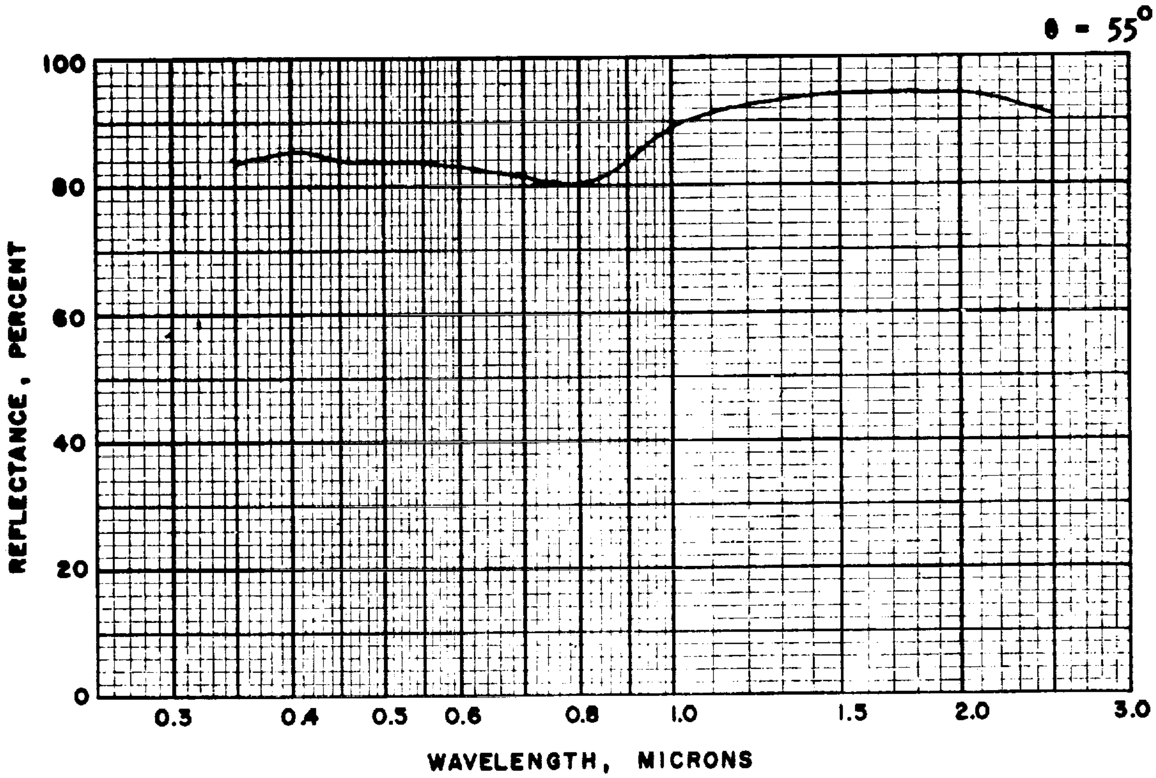

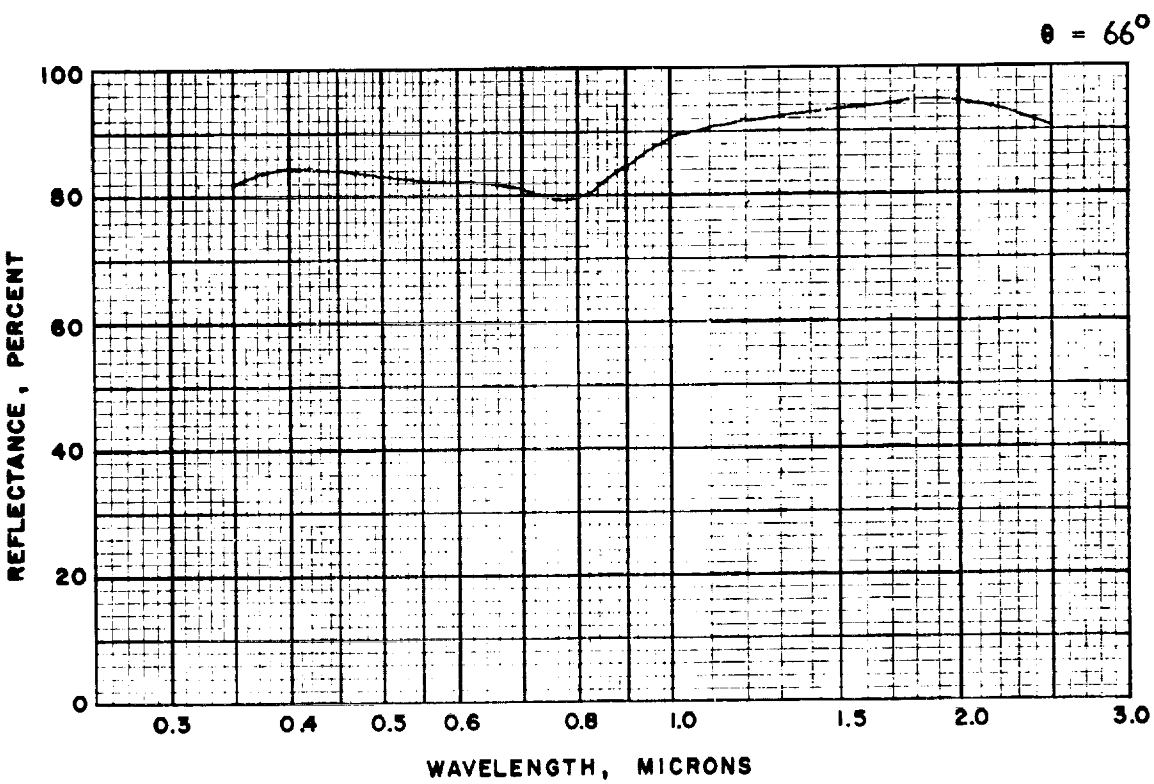

Figure 24 (Cont.): Sample 5B, Azimuthal Angle 60°, Angles of Incidence 55° and 66°

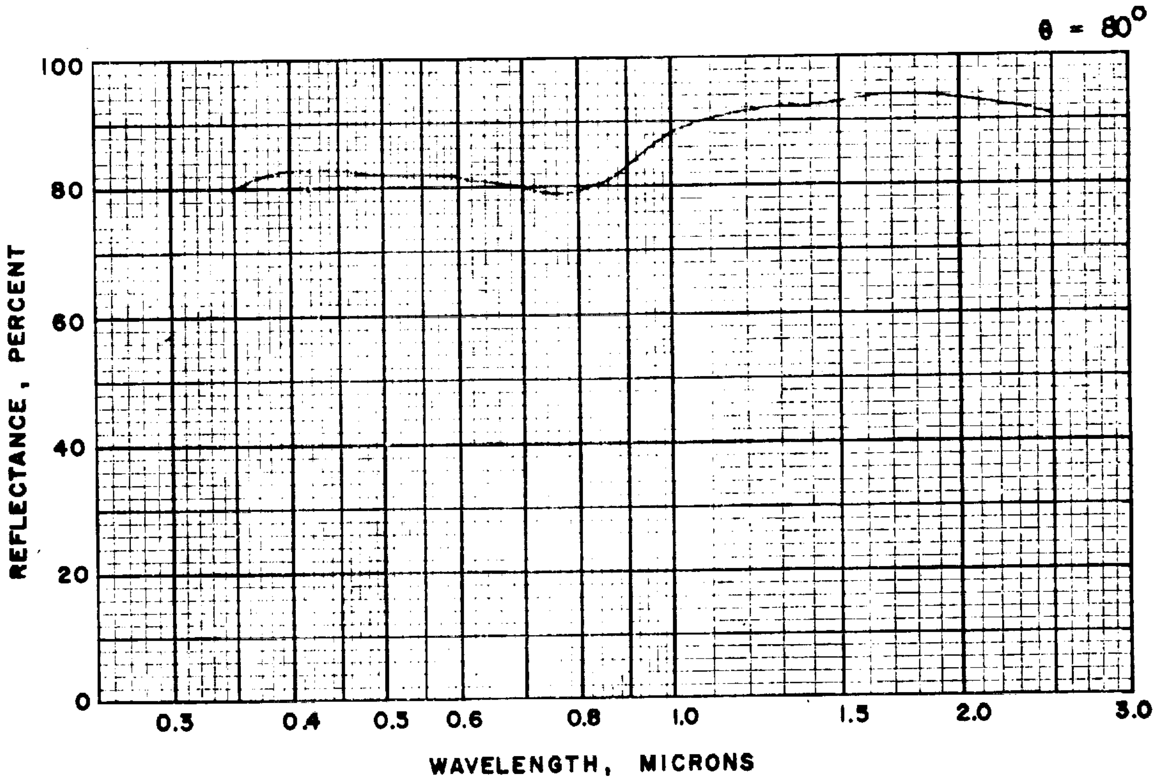

Figure 24 (Cont.): Sample 5B, Azimuthal Angle 60°, Angle of Incidence 80°

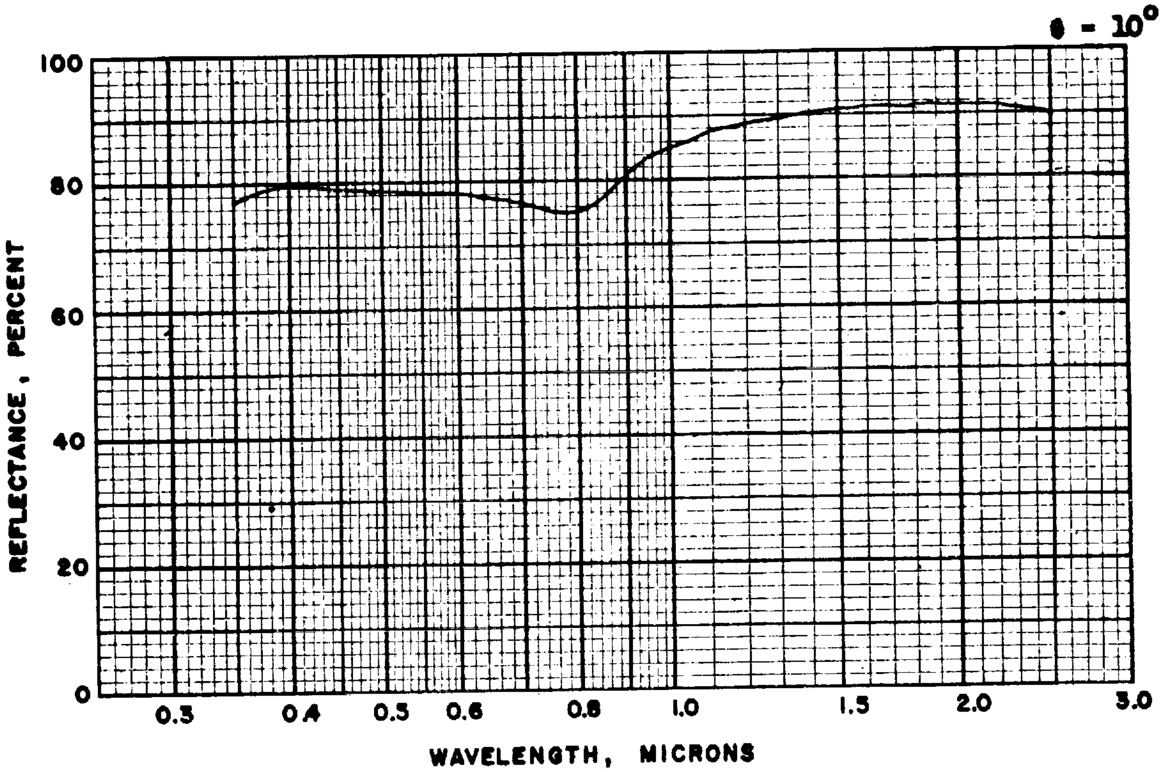

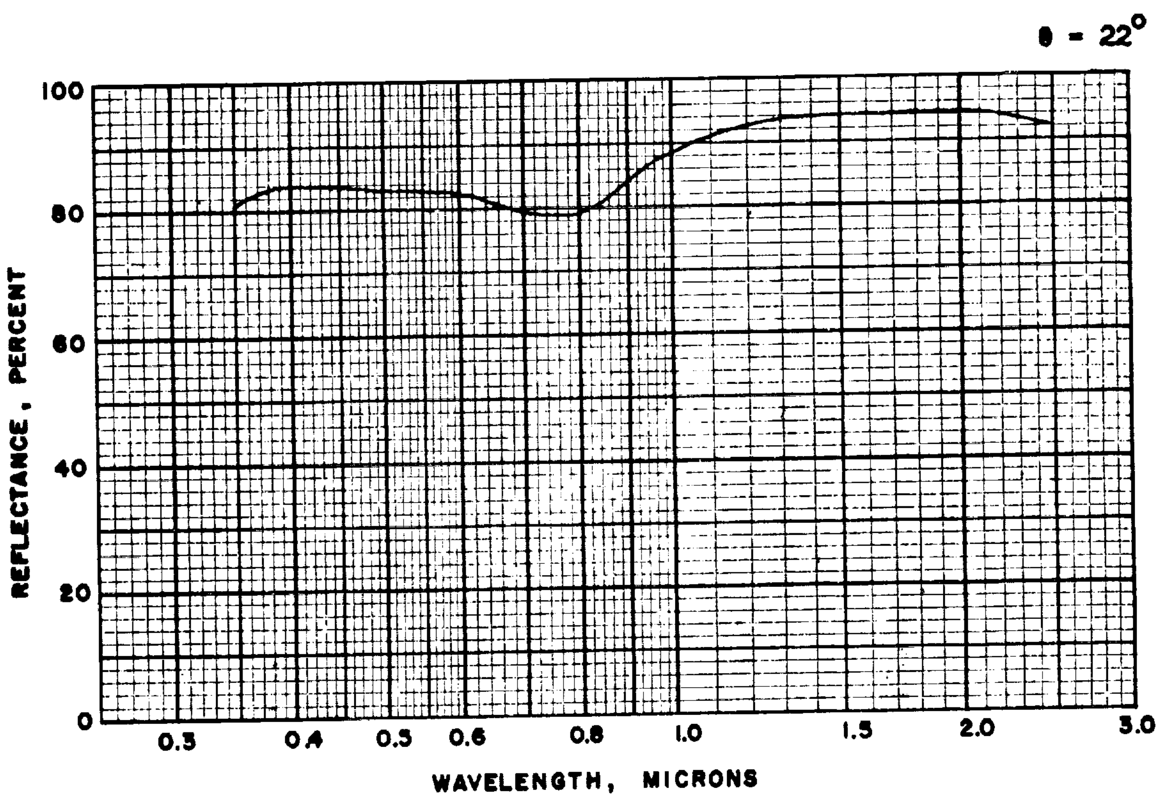

Figure 25: Sample 5B, Azimuthal Angle 90°, Angles of Incidence 10° and 22°

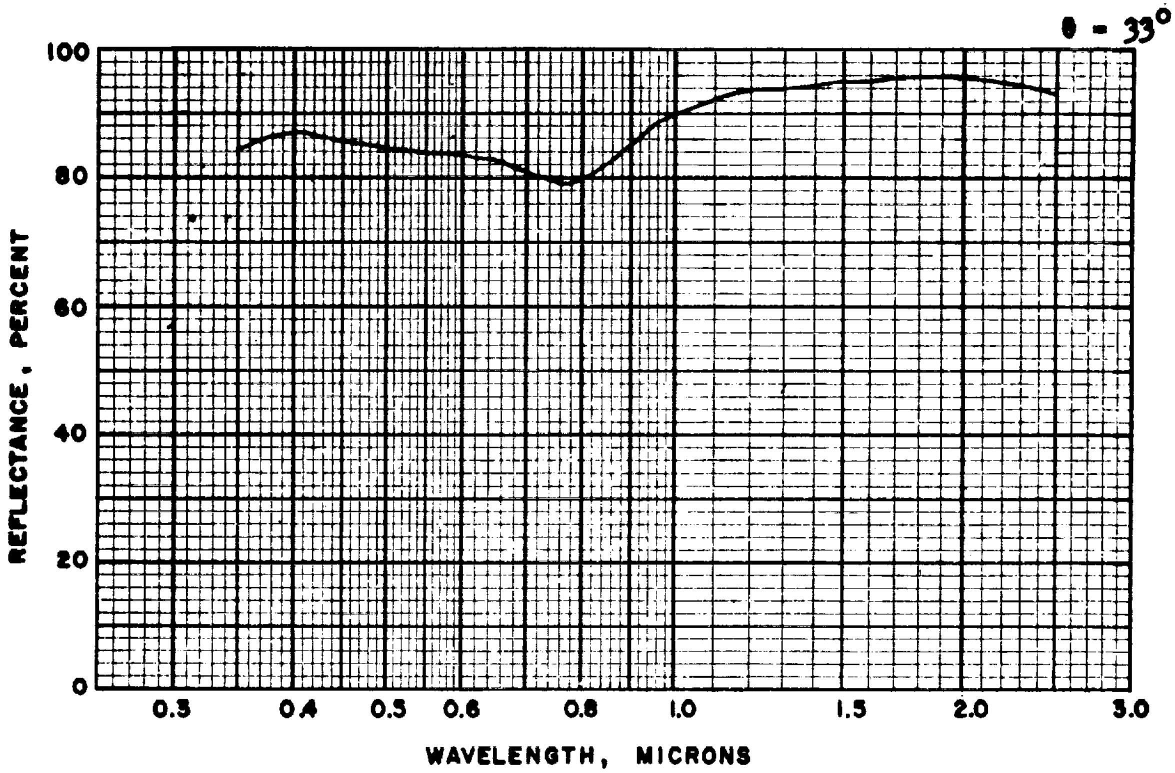

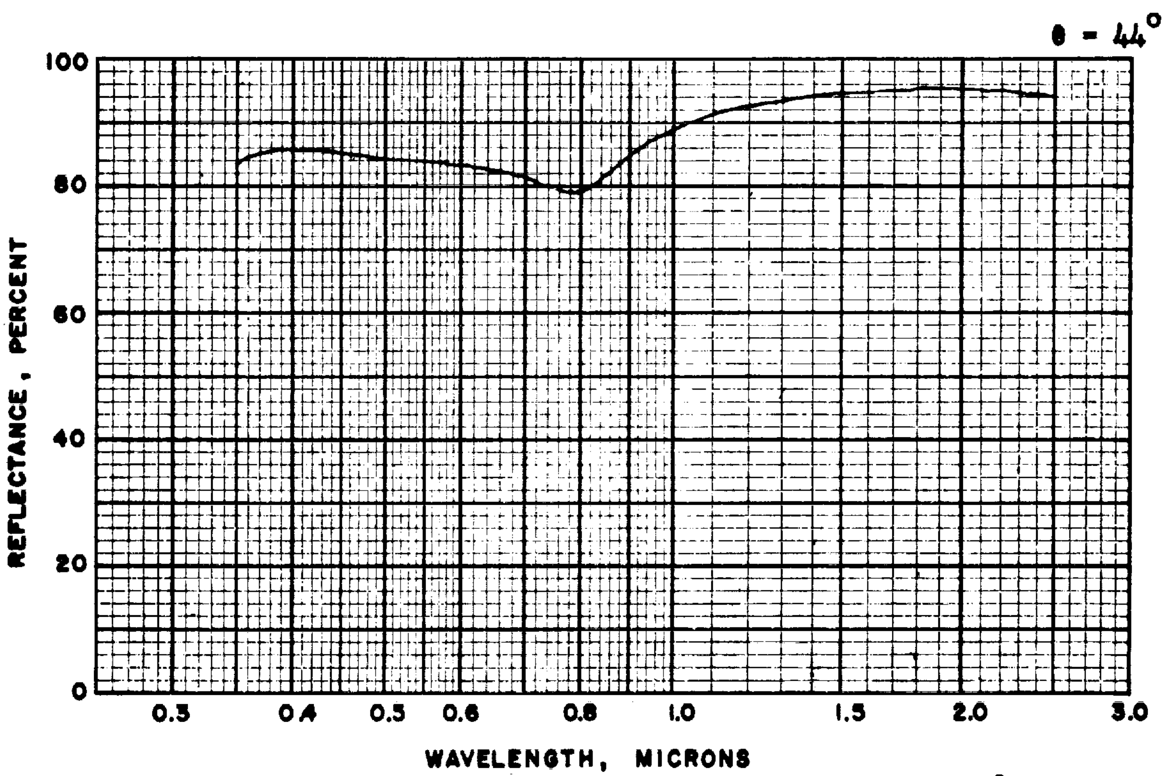

Figure 25 (Cont.): Sample 5B, Azimuthal Angle 90°, Angles of Incidence 33° and 44°

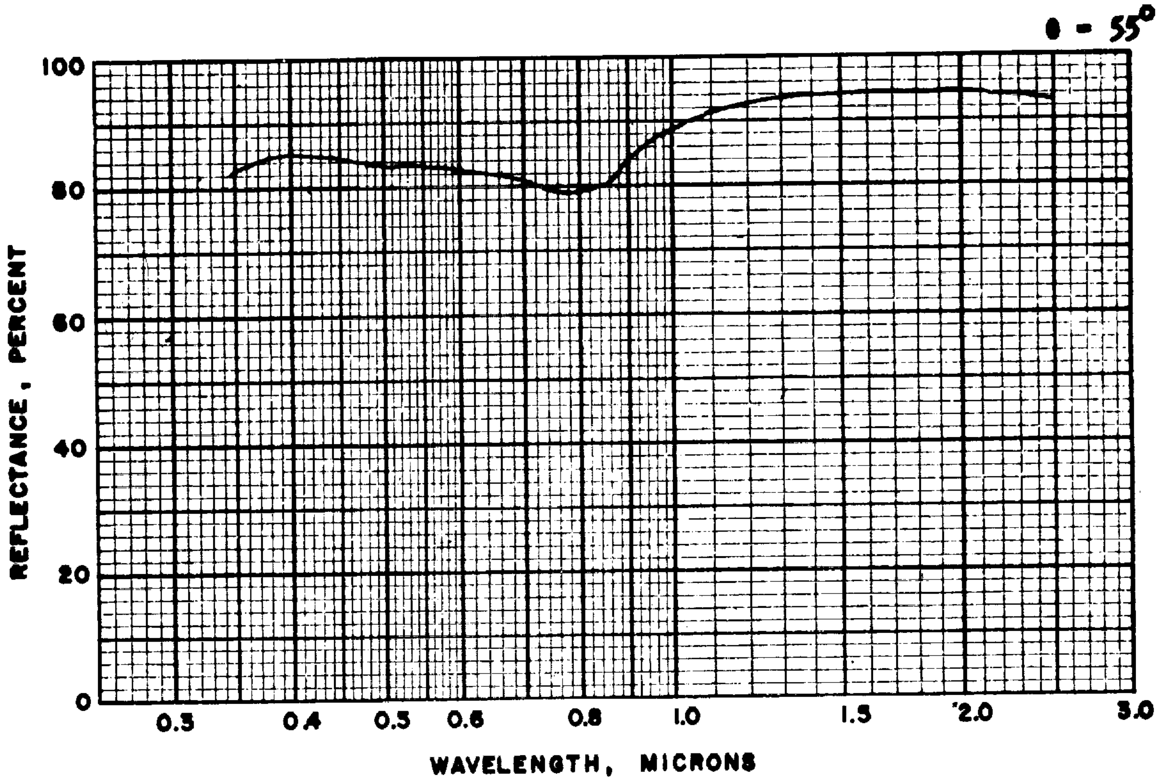

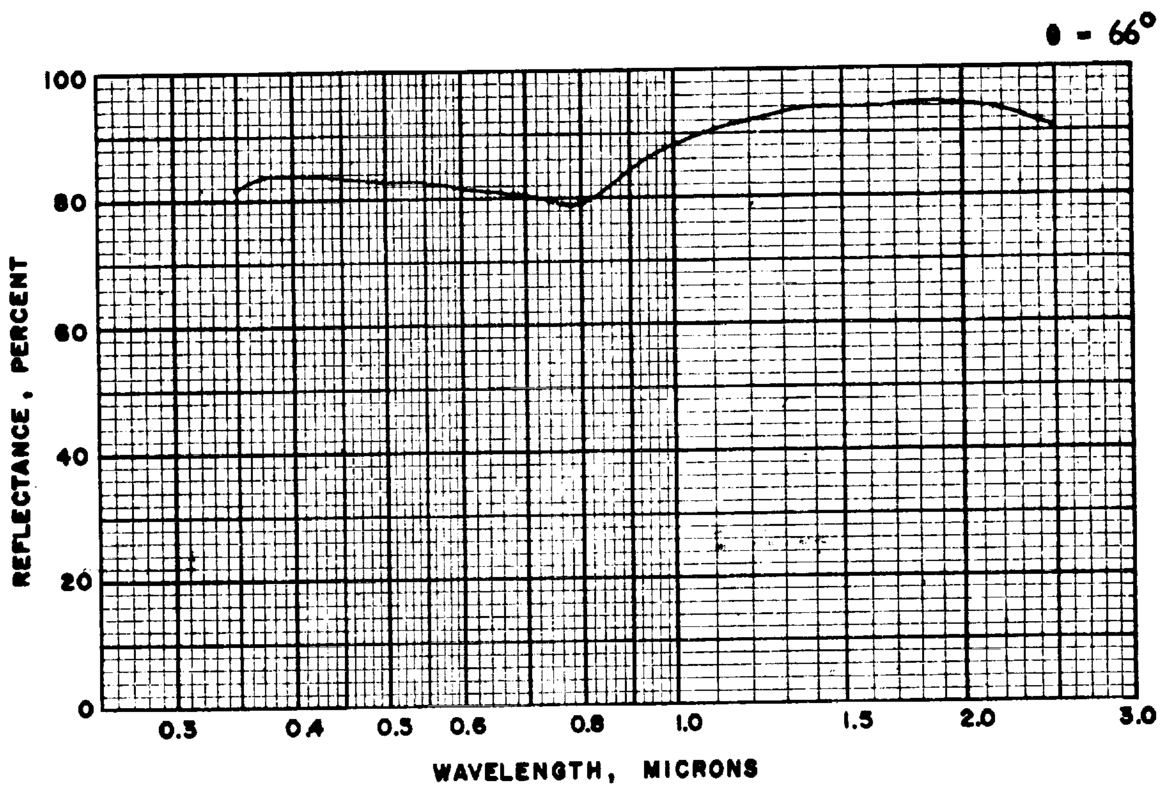

Figure 25 (Cont.): Sample 5B, Azimuthal Angle 90°, Angles of Incidence 55° and 66°

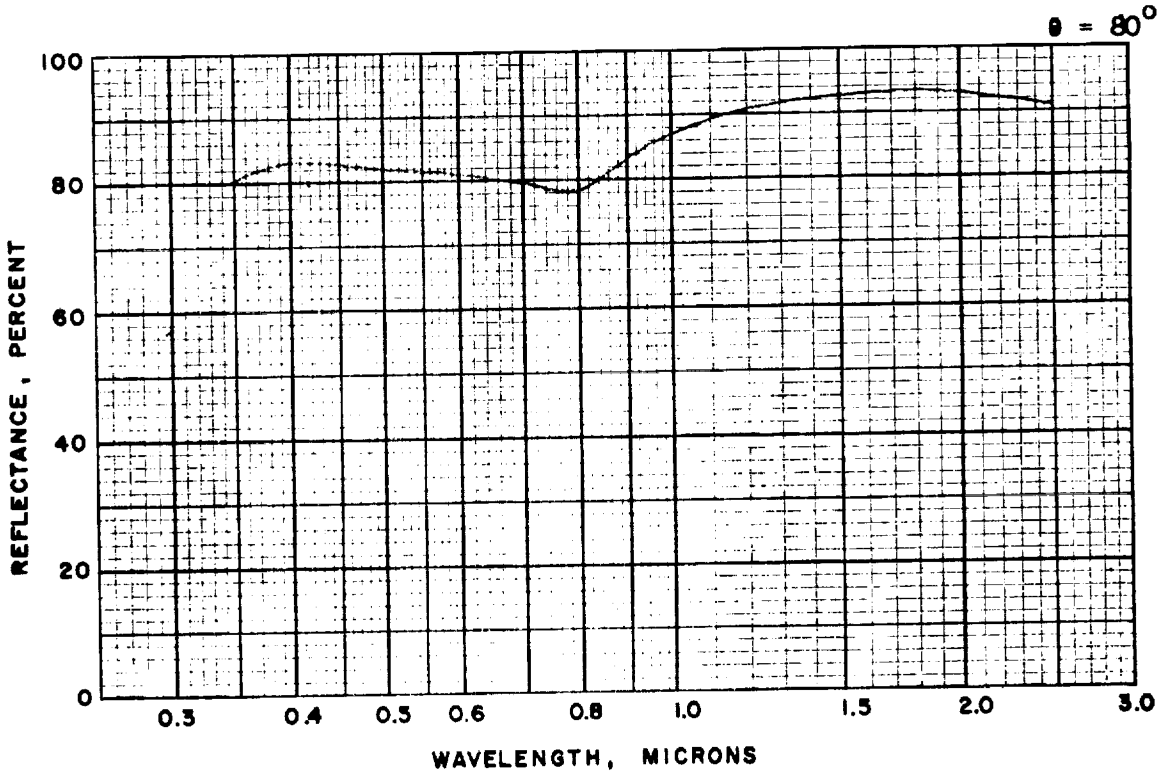

Figure 25 (Cont.): Sample 5B, Azimuthal Angle 90°, Angle of Incidence 80°

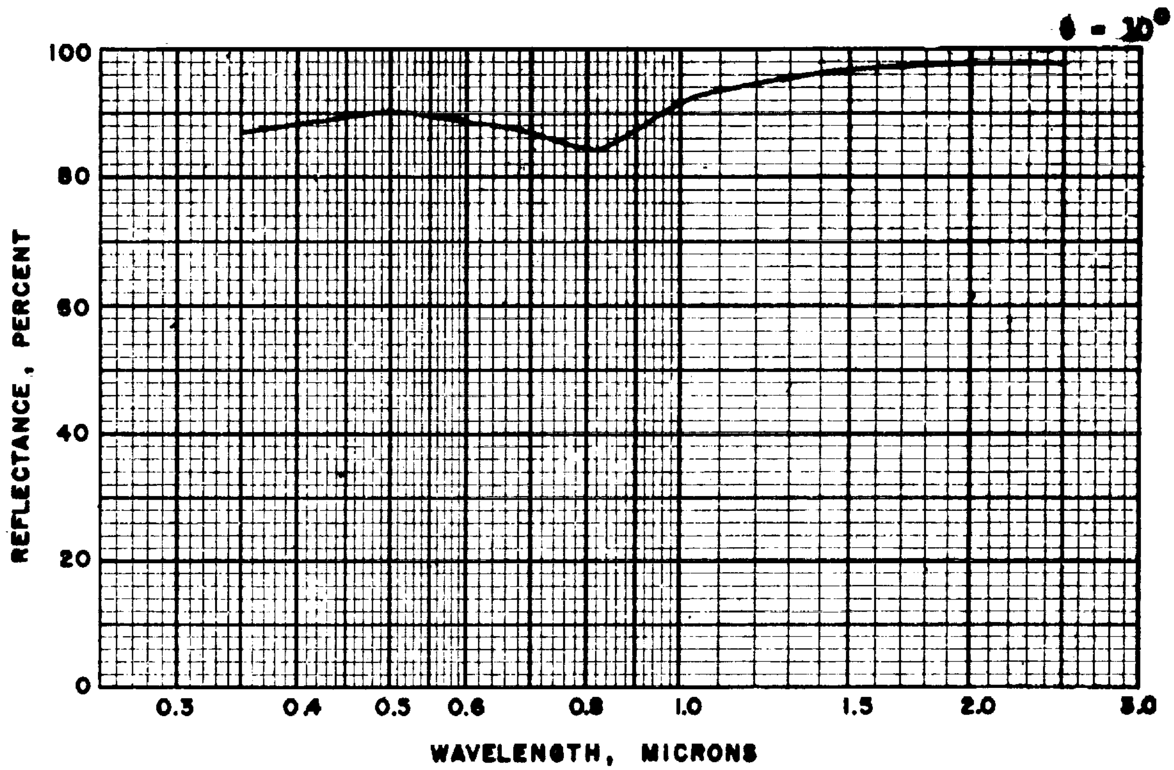

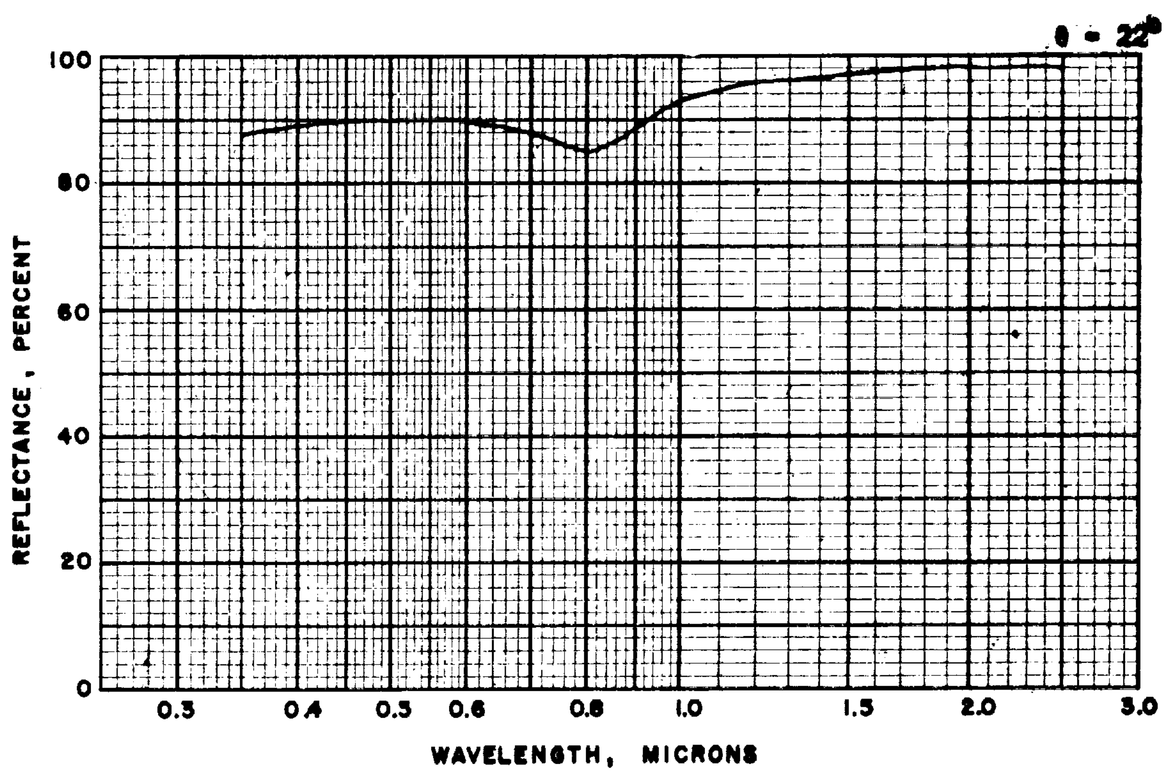

Figure 26: Sample 9, Azimuthal Angle 0°, Angles of Incidence 10° and 22°

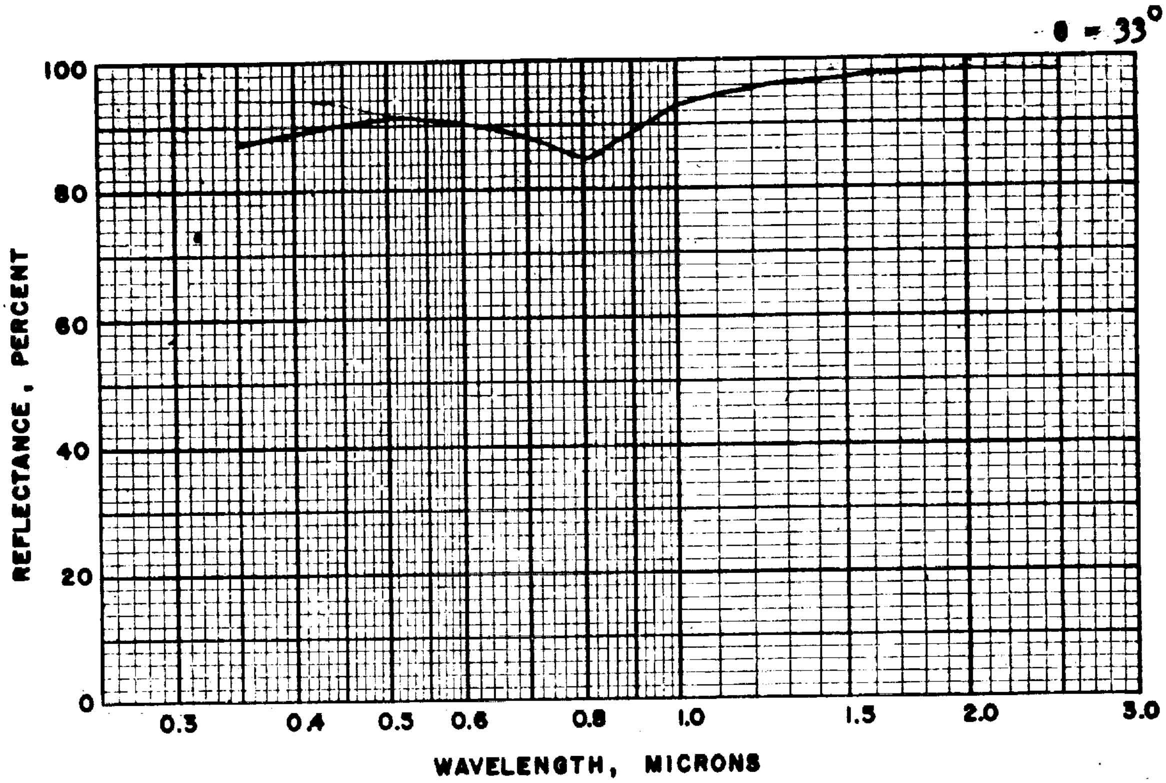

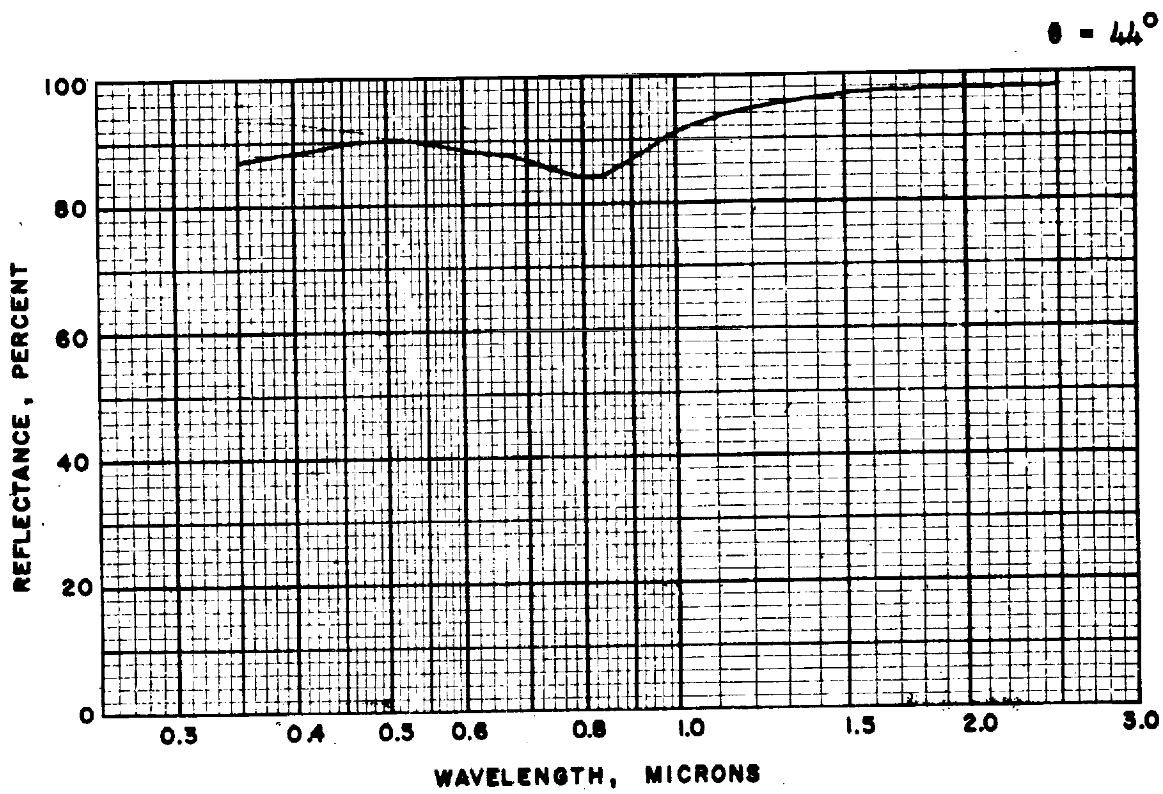

Figure 26 (Cont.): Sample 9, Azimuthal Angle 0°, Angles of Incidence 33° and 44°

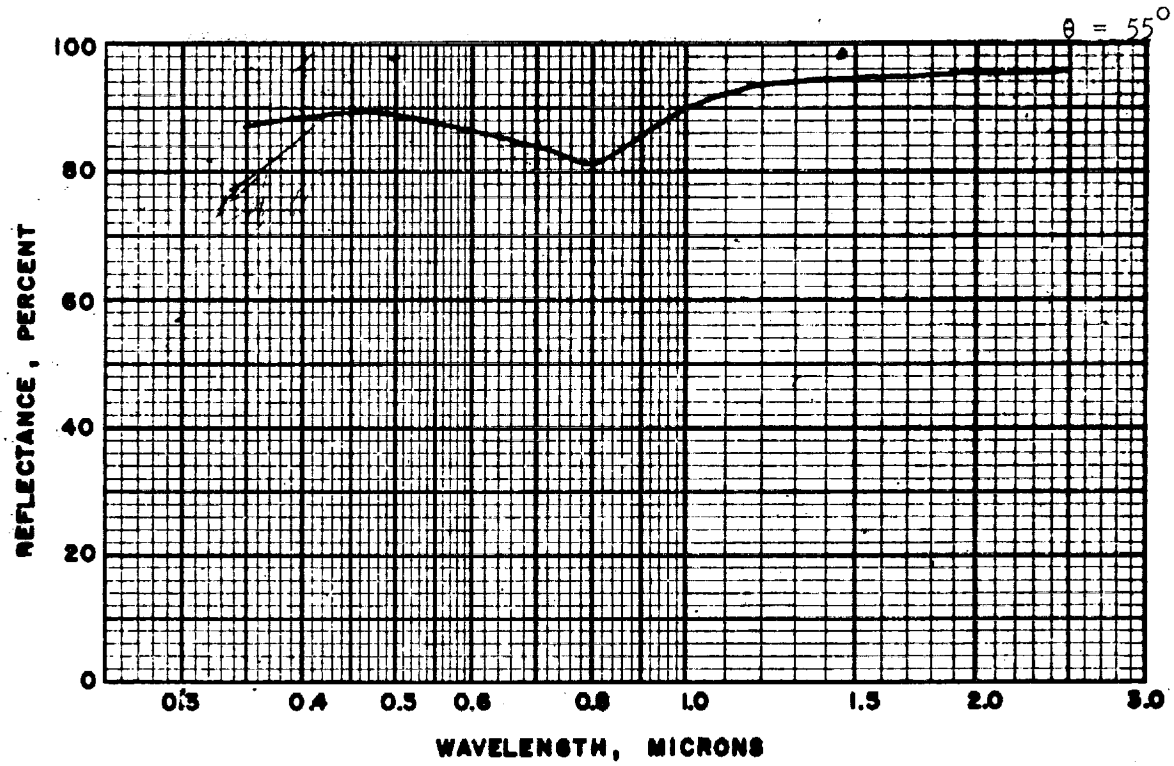

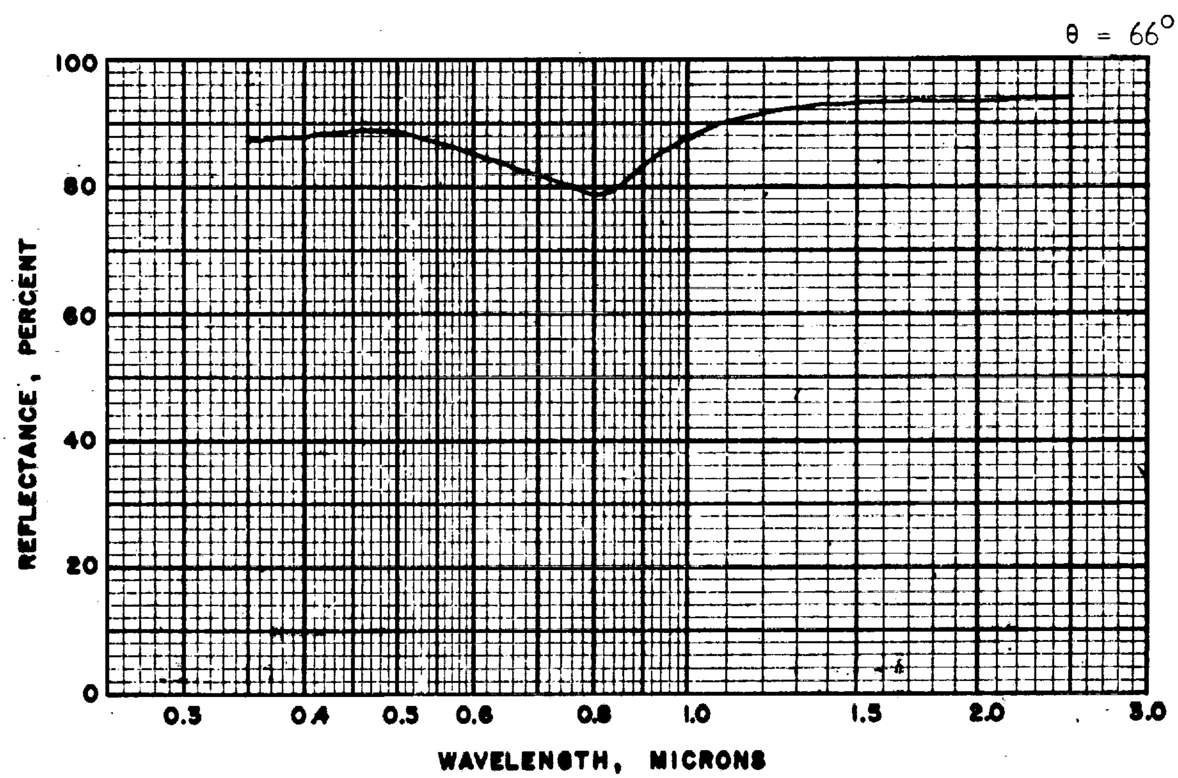

Figure 26 (Cont.): Sample 9, Azimuthal Angle 0°, Angles of Incidence 55° and 66°

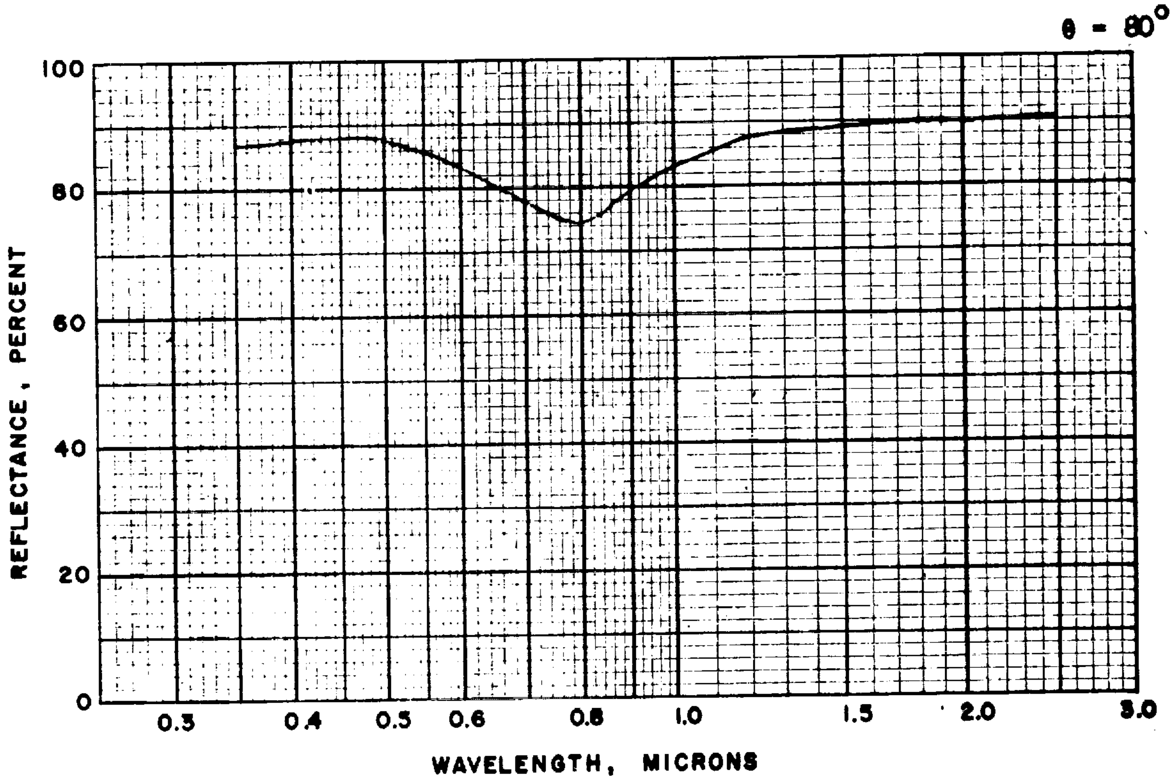

Figure 26 (Cont.): Sample 9, Azimuthal Angle 0°, Angle of Incidence 80°

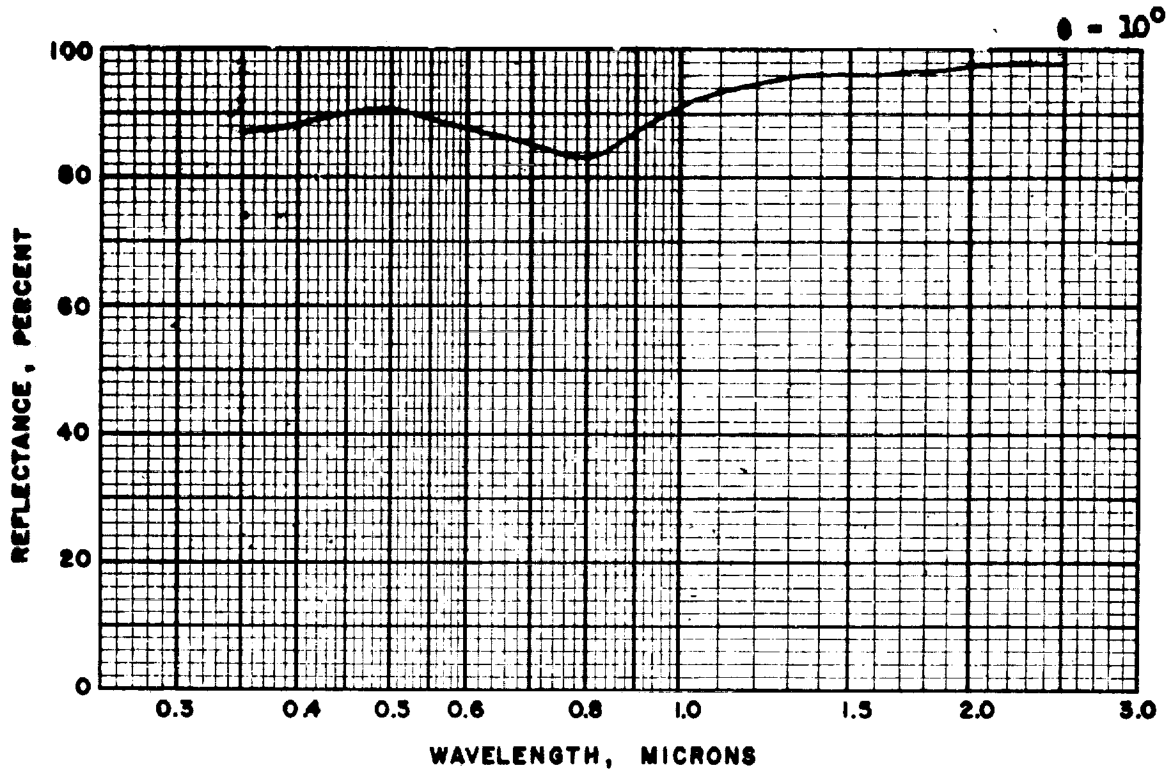

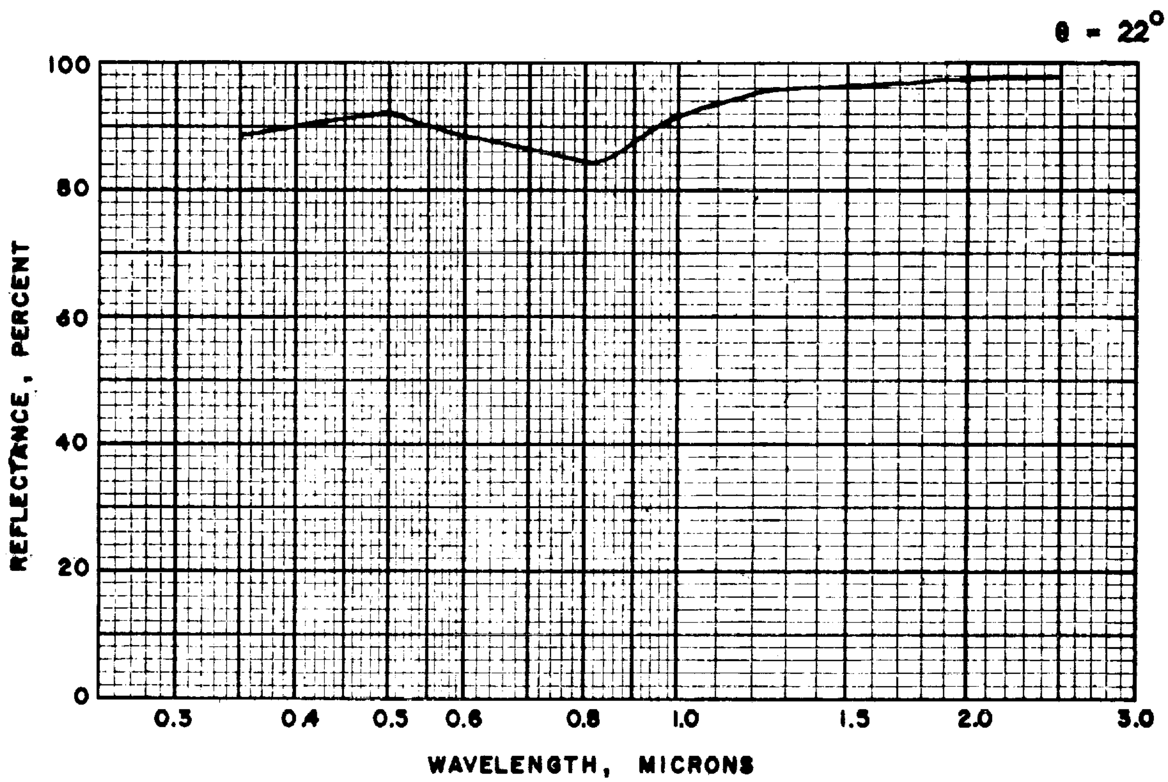

Figure 27: Sample 9, Azimuthal Angle 45°, Angles of Incidence 10° and 22°

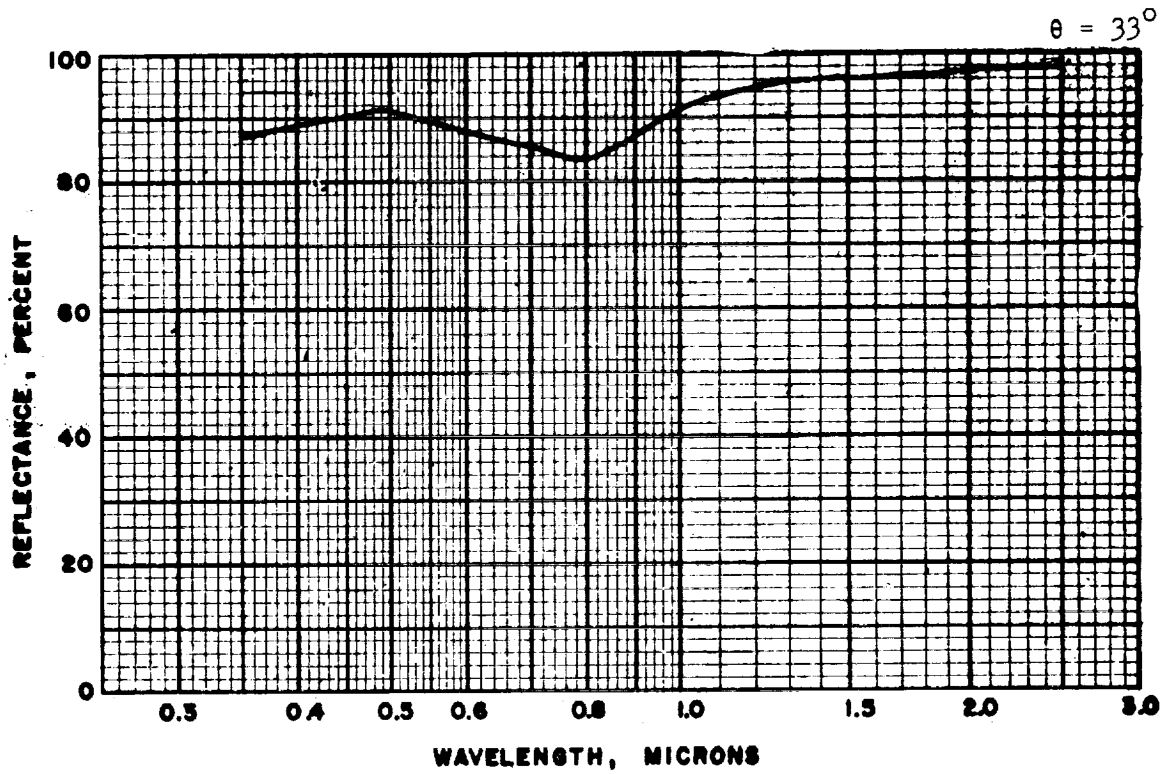

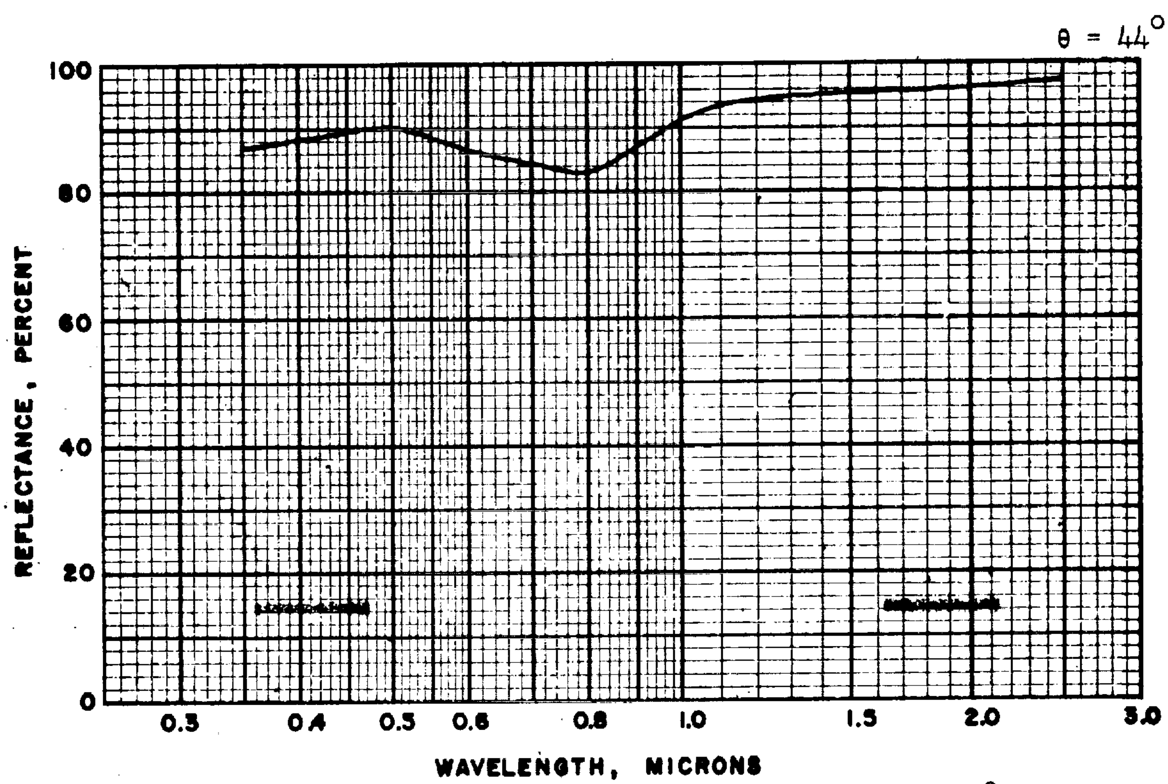

Figure 27 (Cont.): Sample 9, Azimuthal Angle 45°, Angles of Incidence 33° and 44°

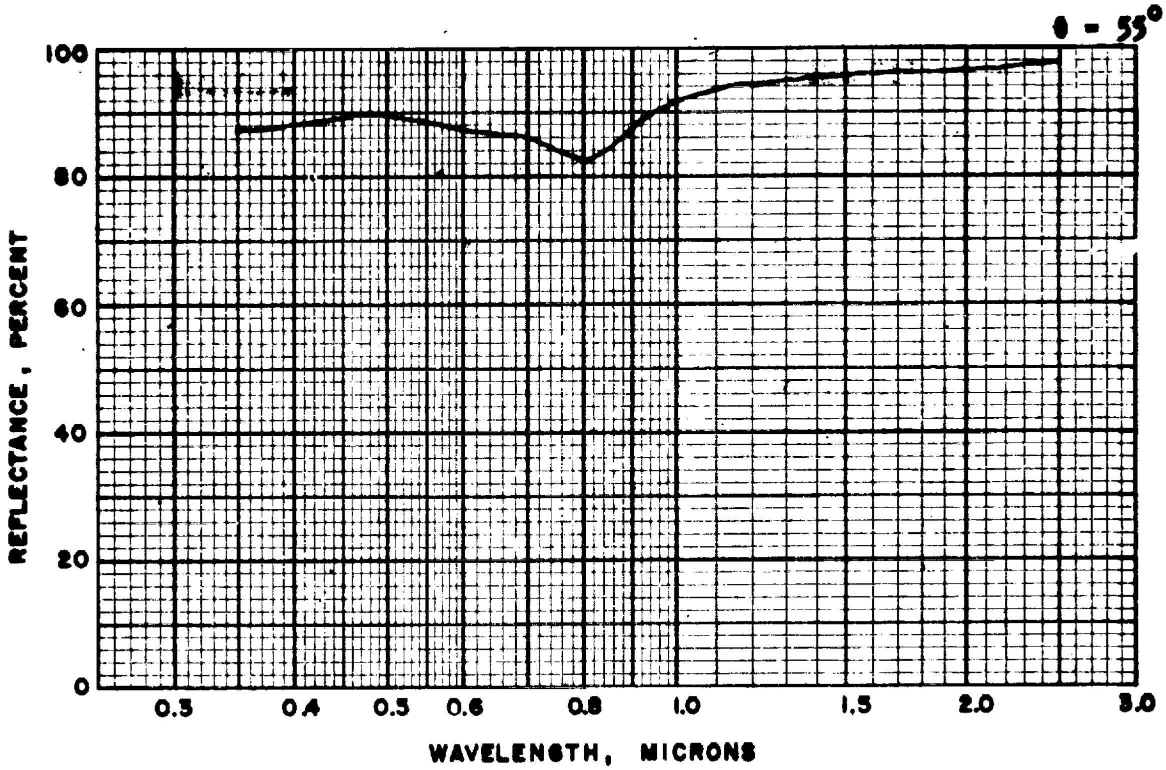

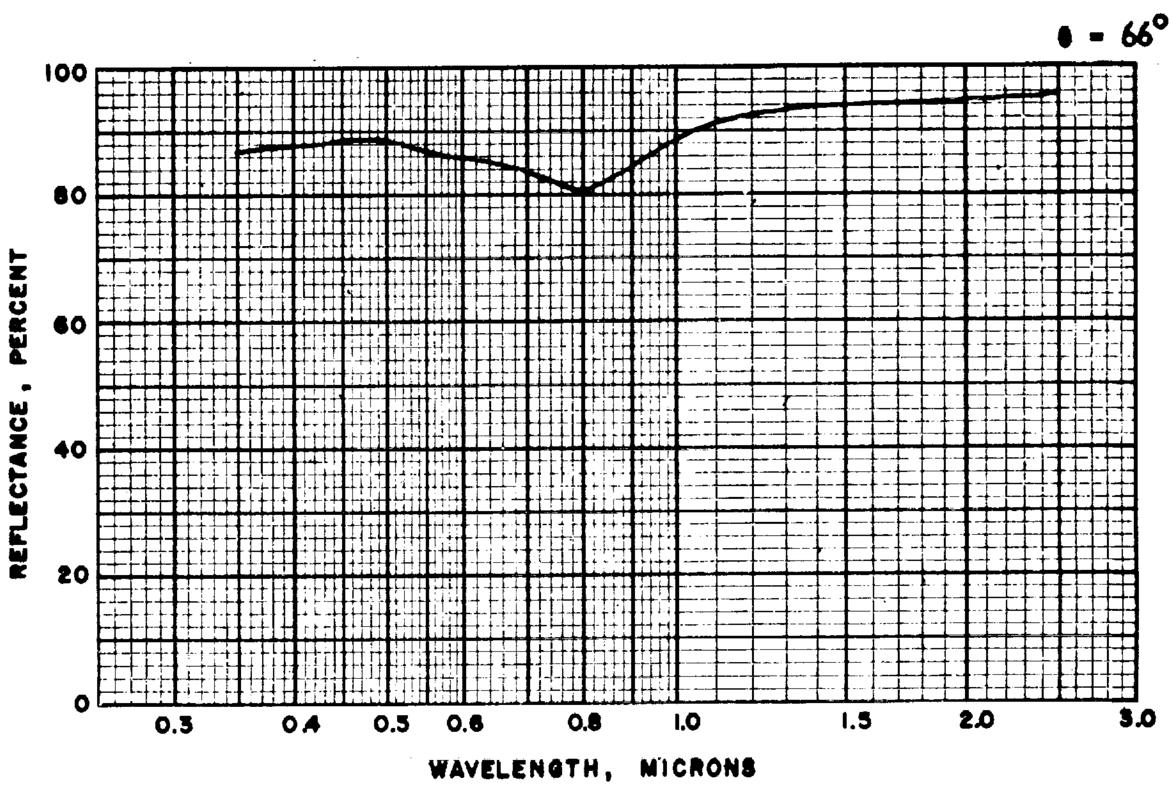

Figure 27 (Cont.): Sample 9, Azimuthal Angle 45°, Angles of Incidence 55° and 66°

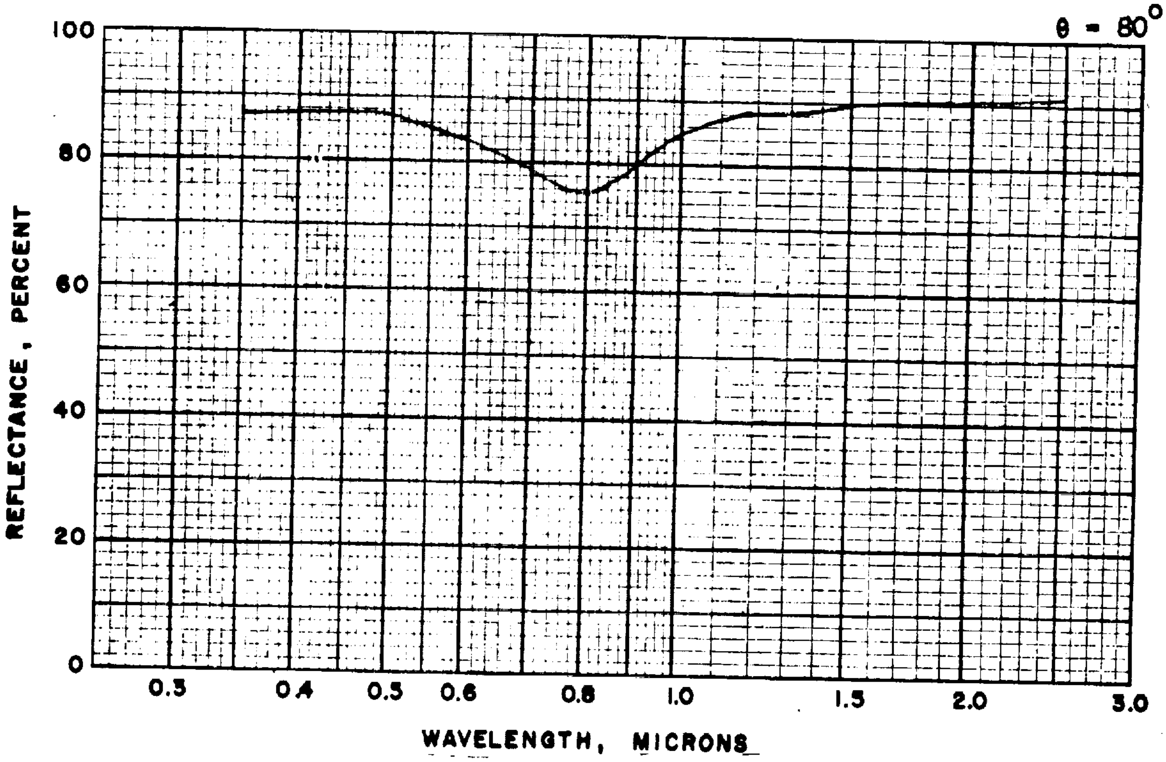

Figure 27 (Cont.): Sample 9, Azimuthal Angle 45°, Angle of Incidence 80°

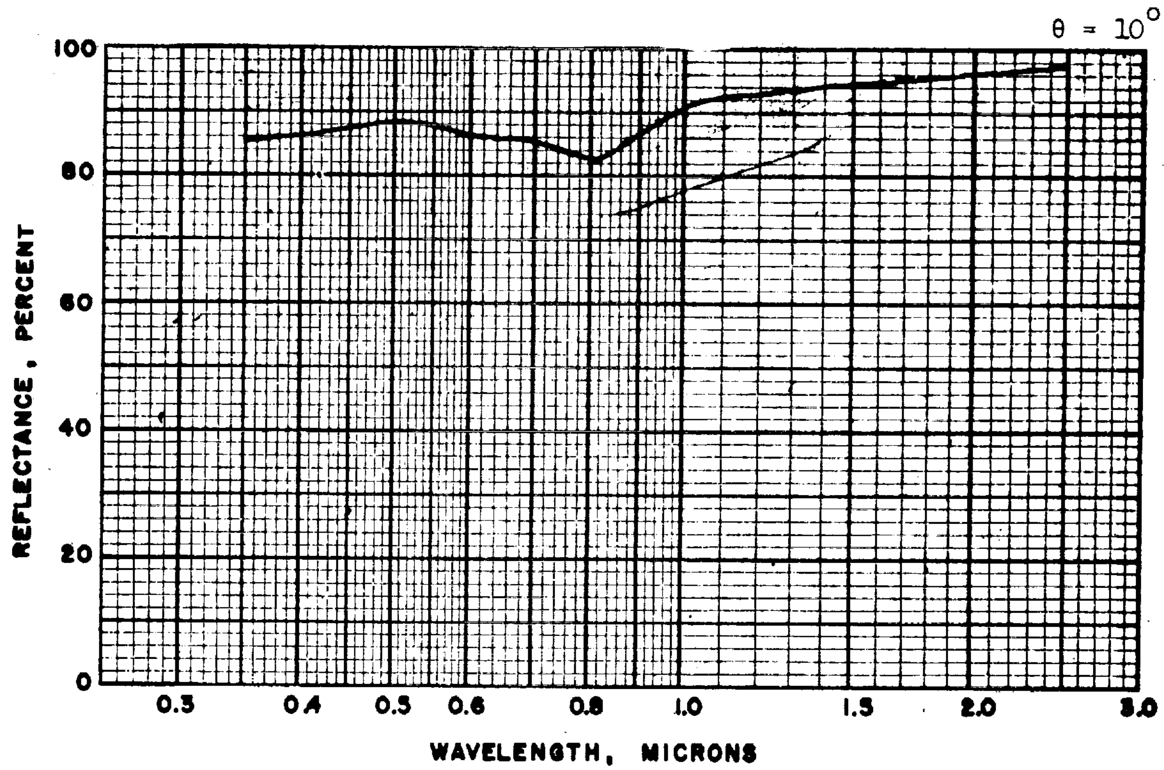

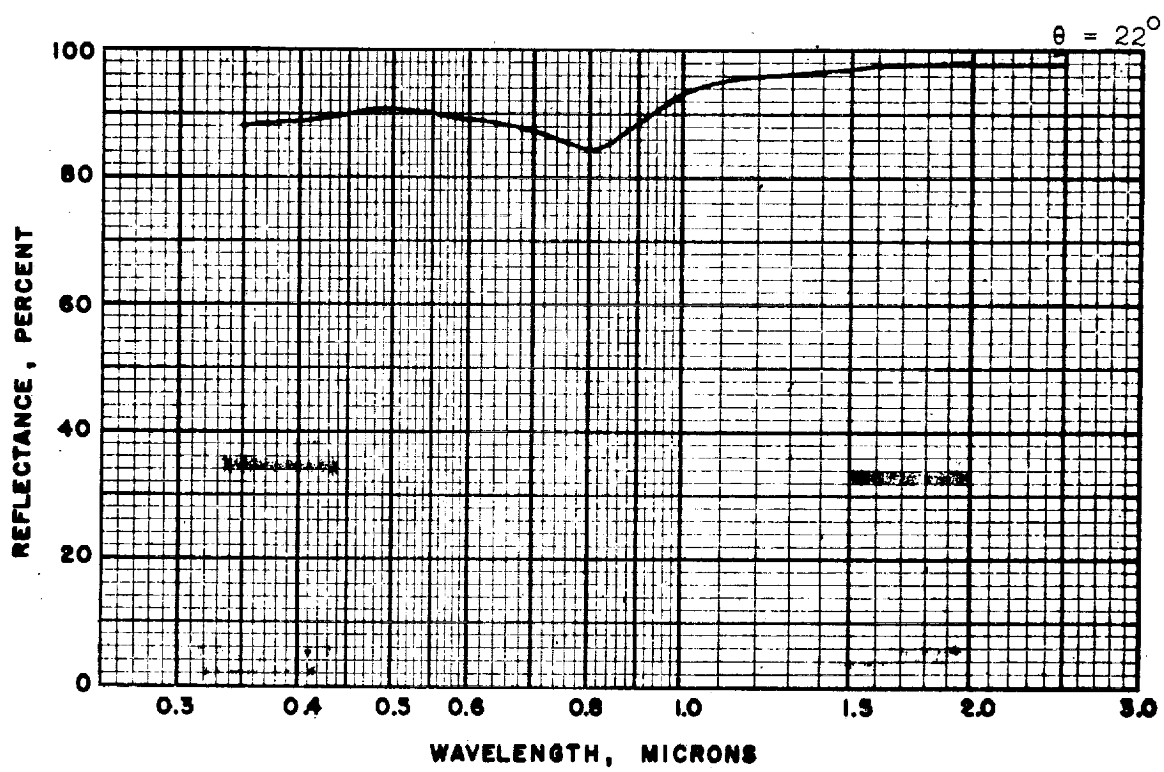

Figure 28: Sample 9, Azimuthal Angle 60°, Angles of Incidence 10° and 22°

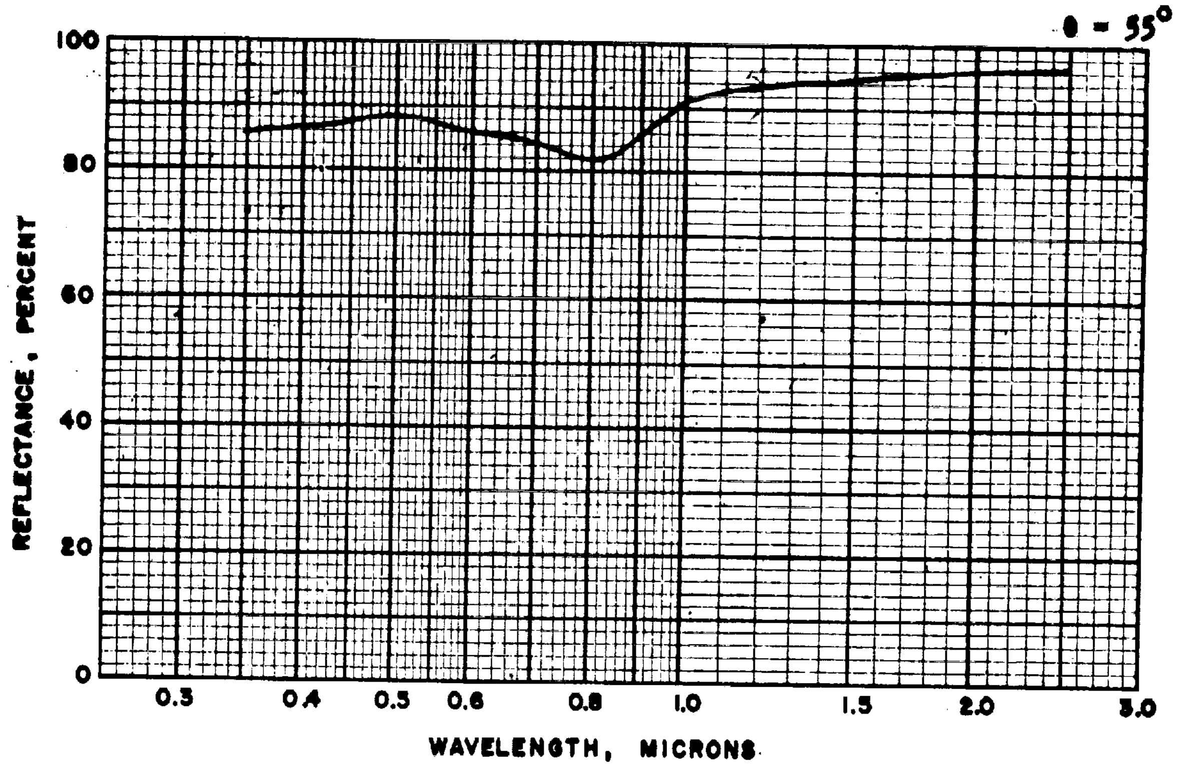

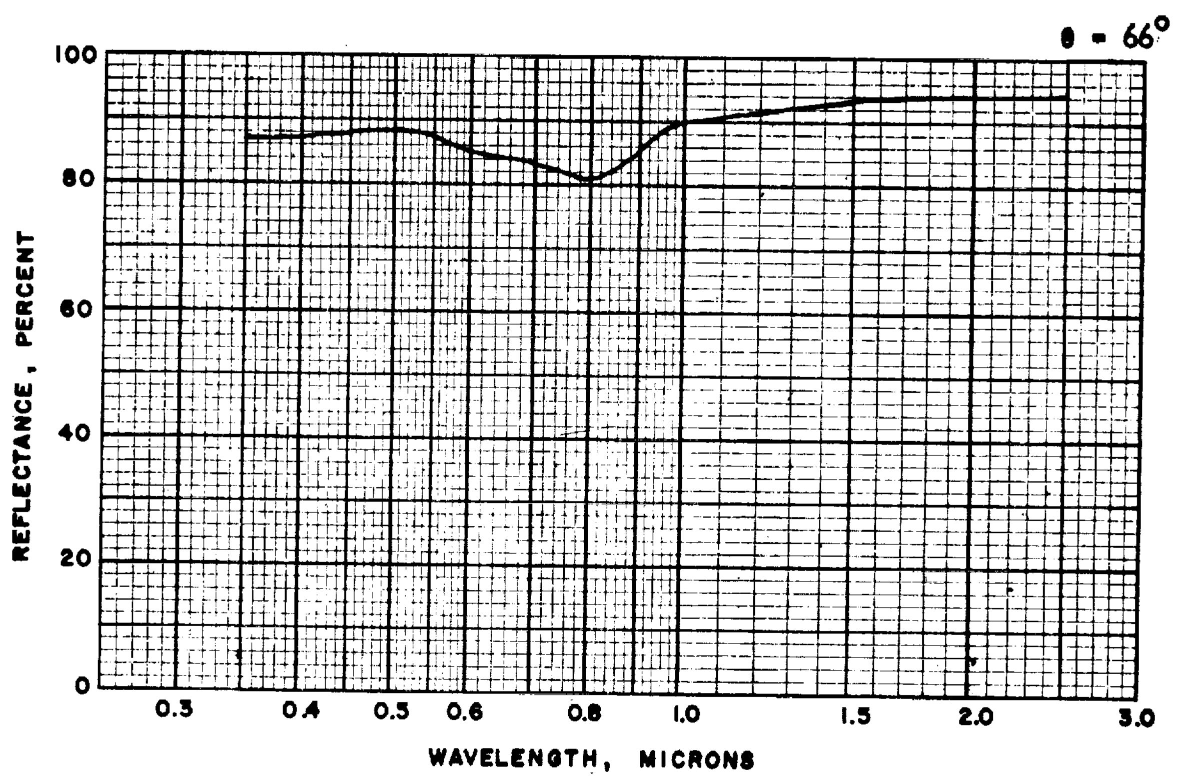

Figure 28 (Cont.): Sample 9, Azimuthal Angle 60°, Angles of Incidence 55° and 66°

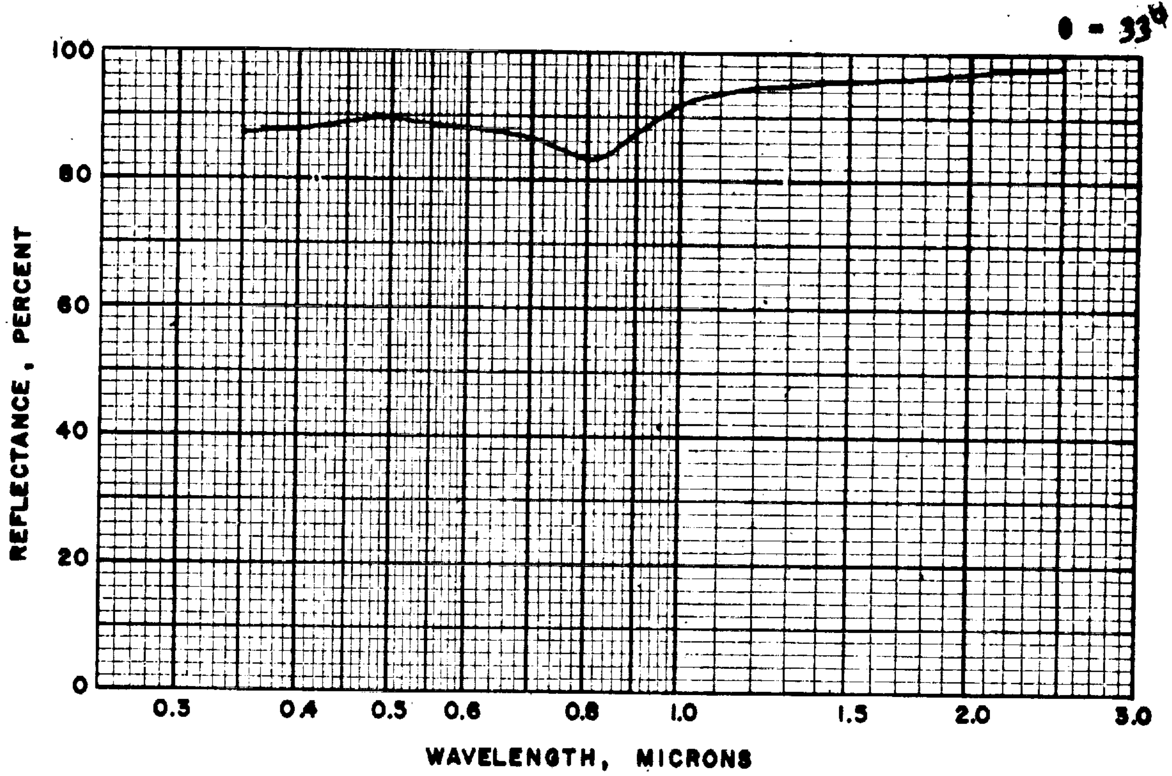

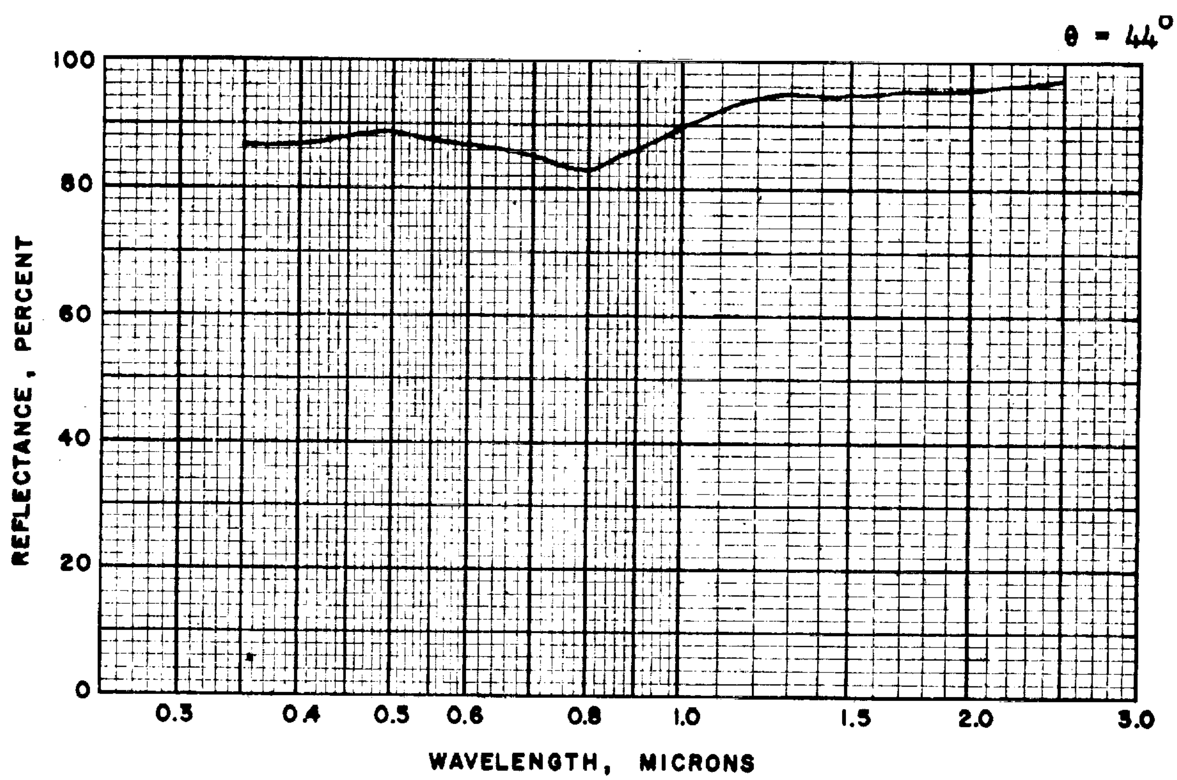

Figure 28 (Cont.): Sample 9, Azimuthal Angle 60°, Angles of Incidence 33° and 44°

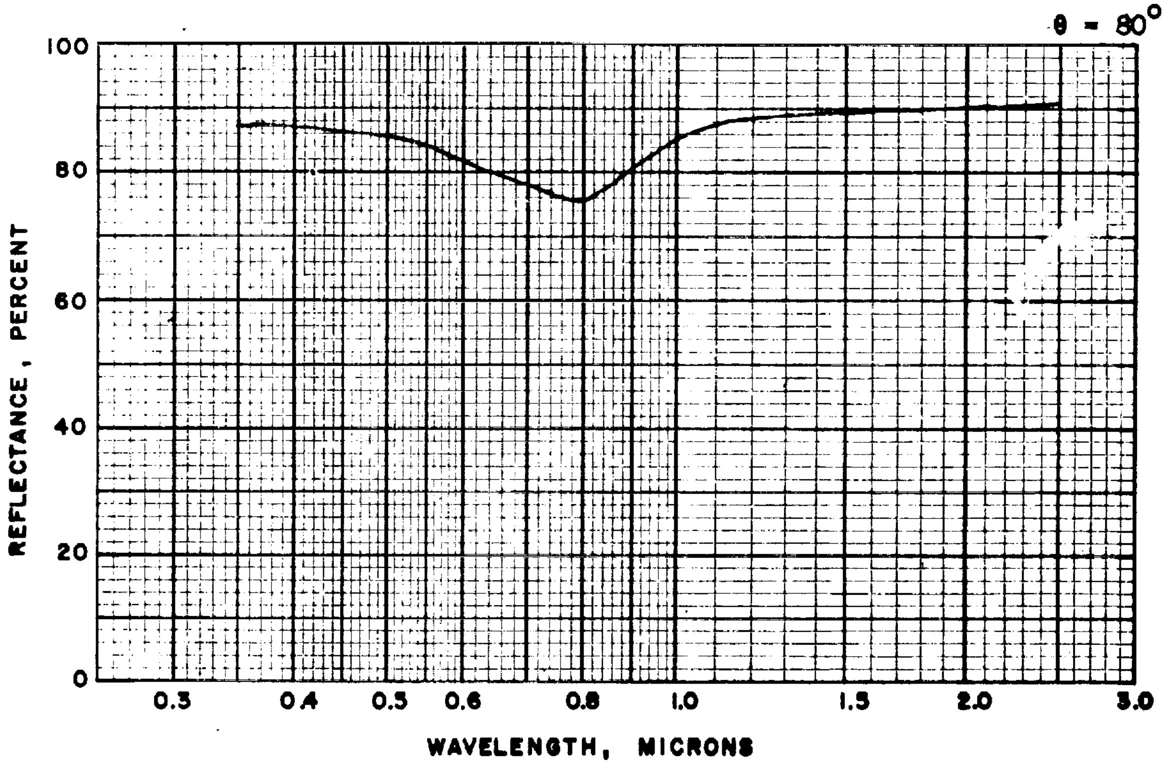

Figure 28 (Cont.): Sample 9, Azimuthal Angle 60°,
Angle of Incidence 80°

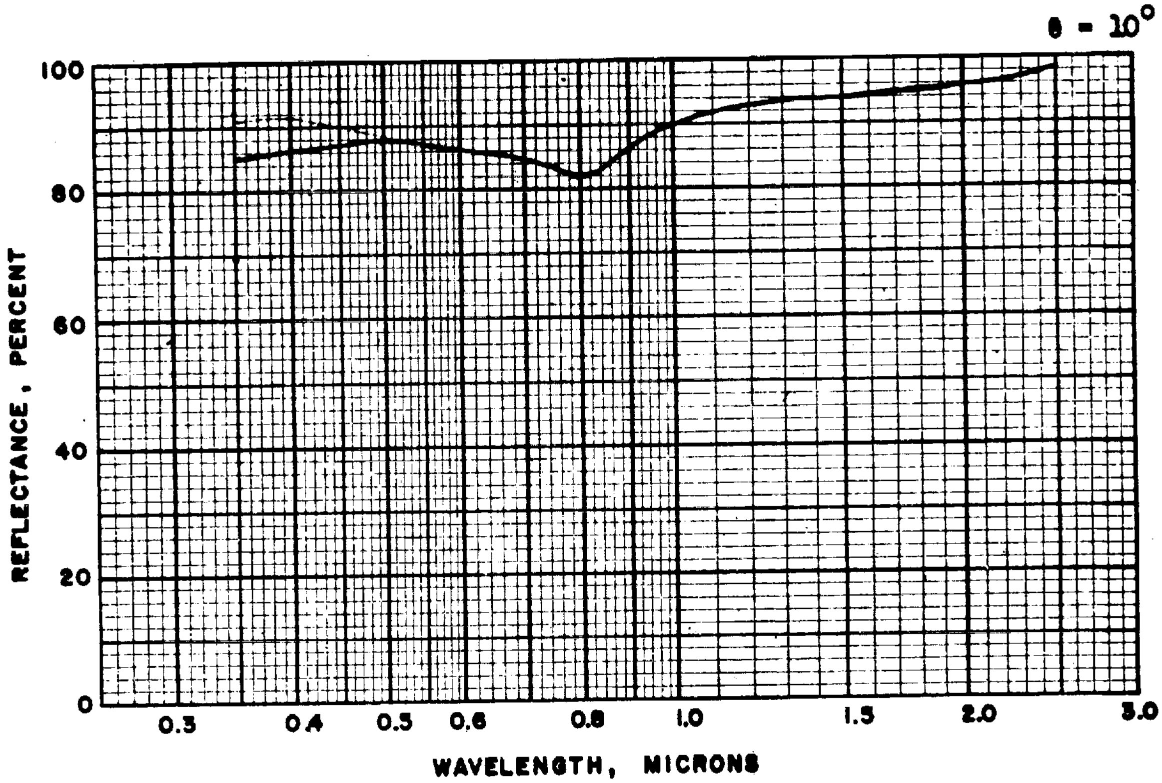

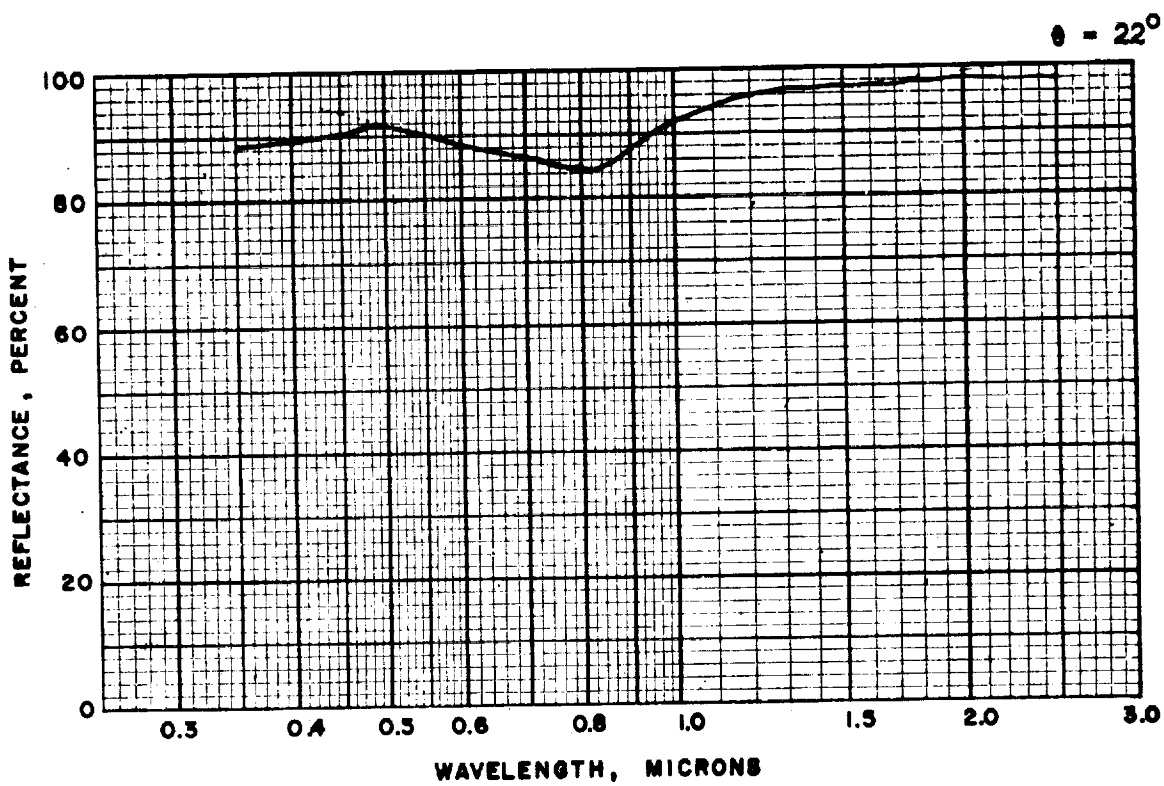

Figure 29: Sample 9, Azimuthal Angle 90°, Angles of Incidence 10° and 22°

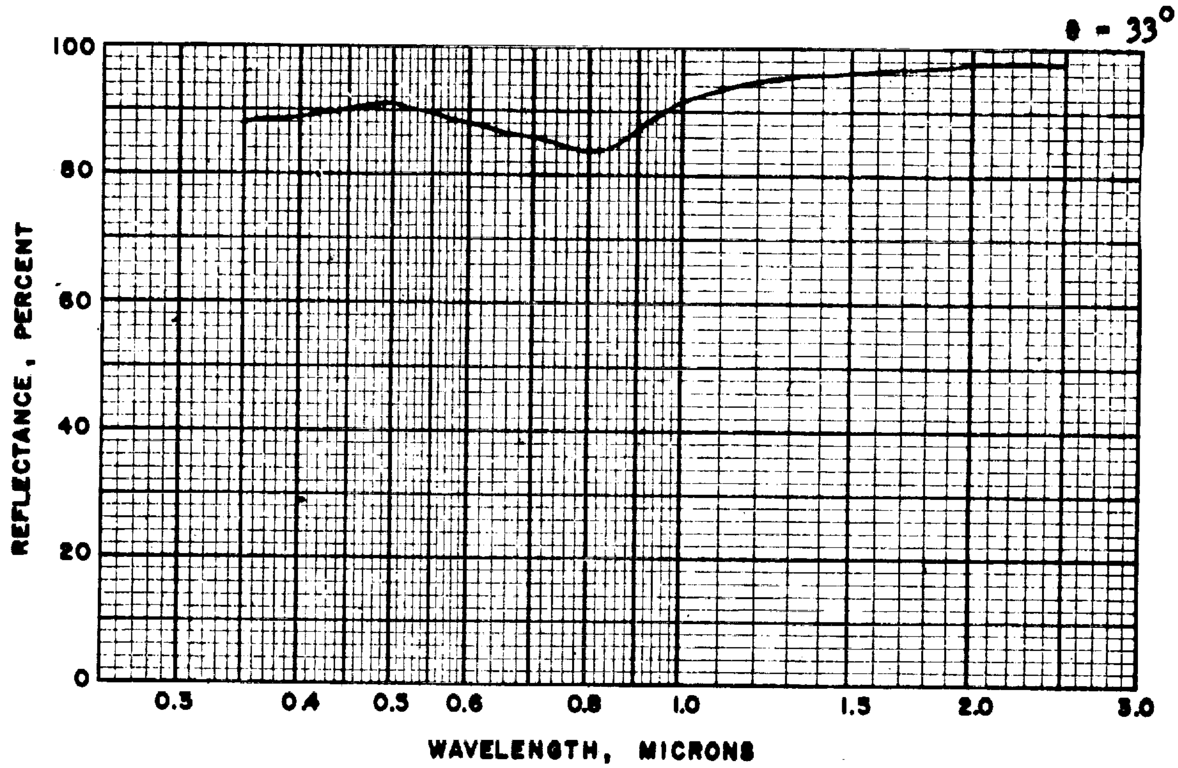

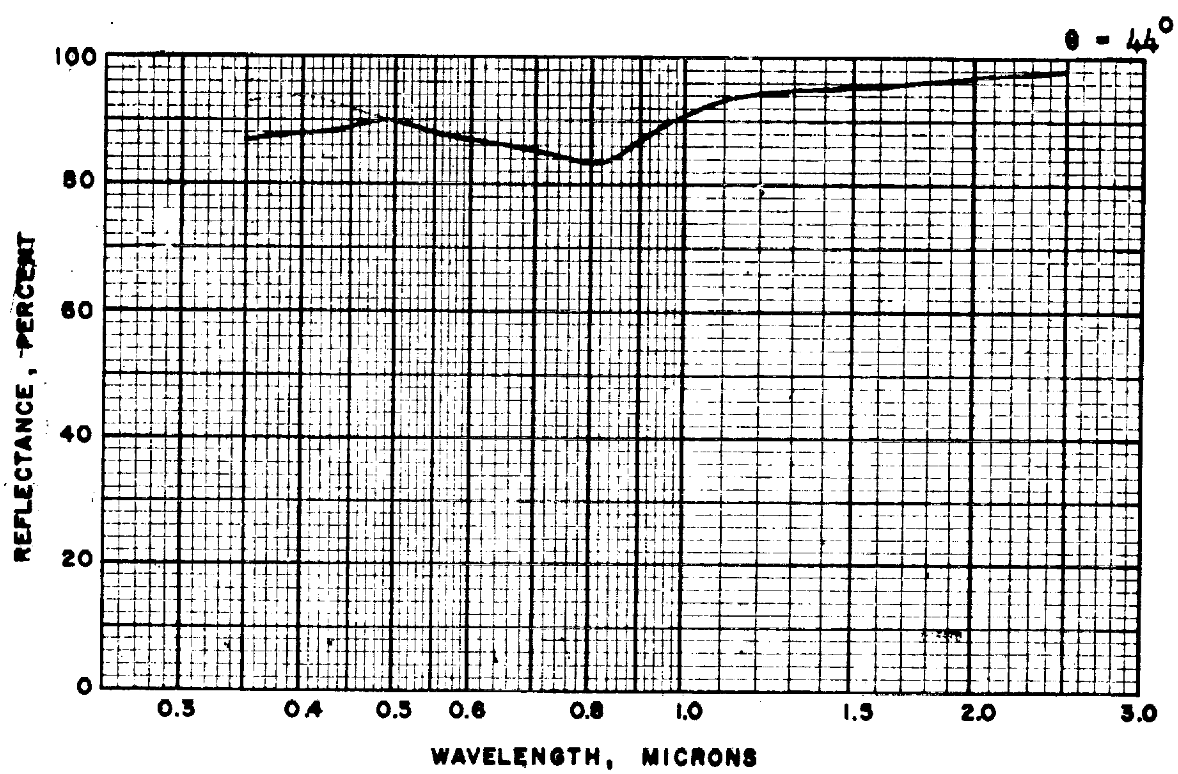

Figure 29 (Cont.): Sample 9, Azimuthal Angle 90°, Angles of Incidence 33° and 44°

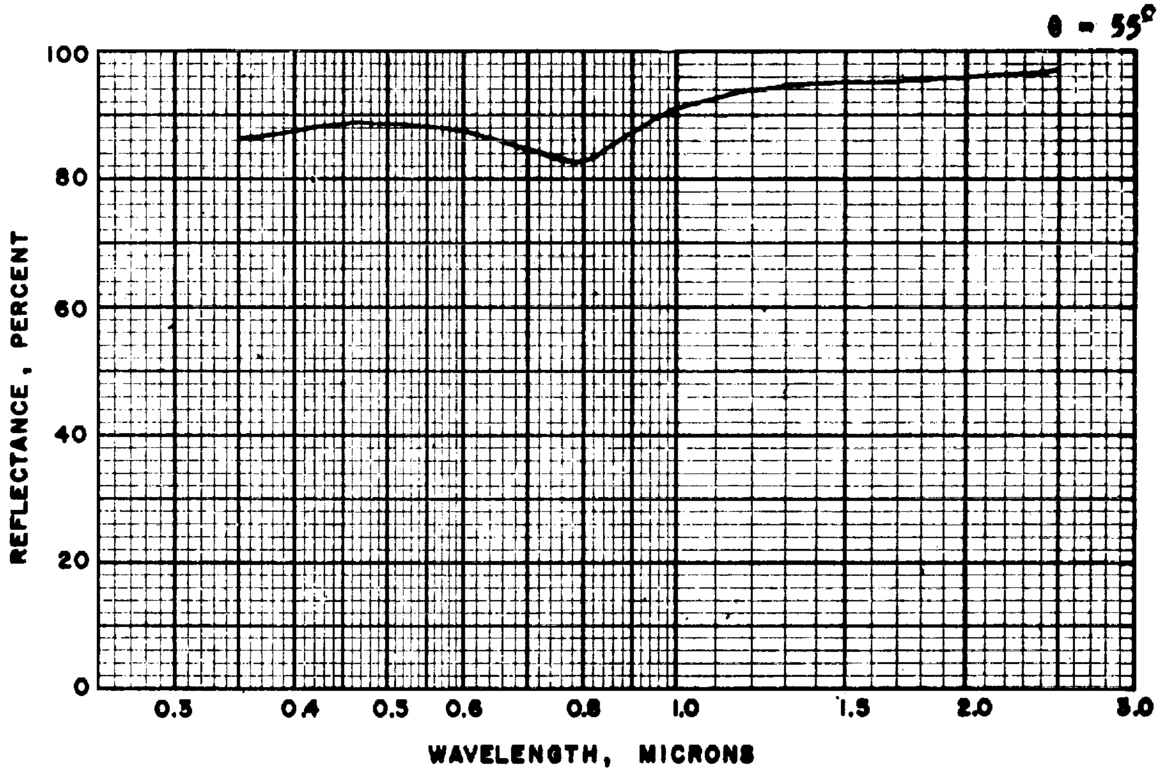

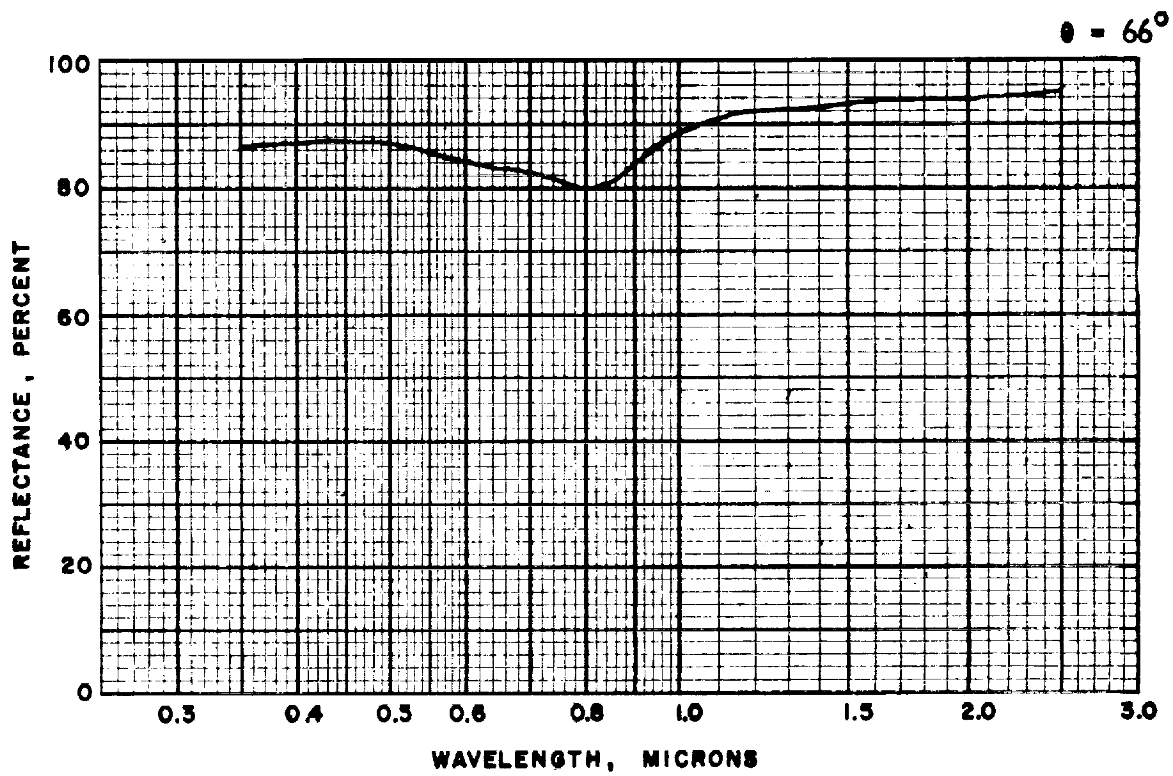

Figure 29 (Cont.): Sample 9, Azimuthal Angle 90°, Angles of Incidence 55° and 66°

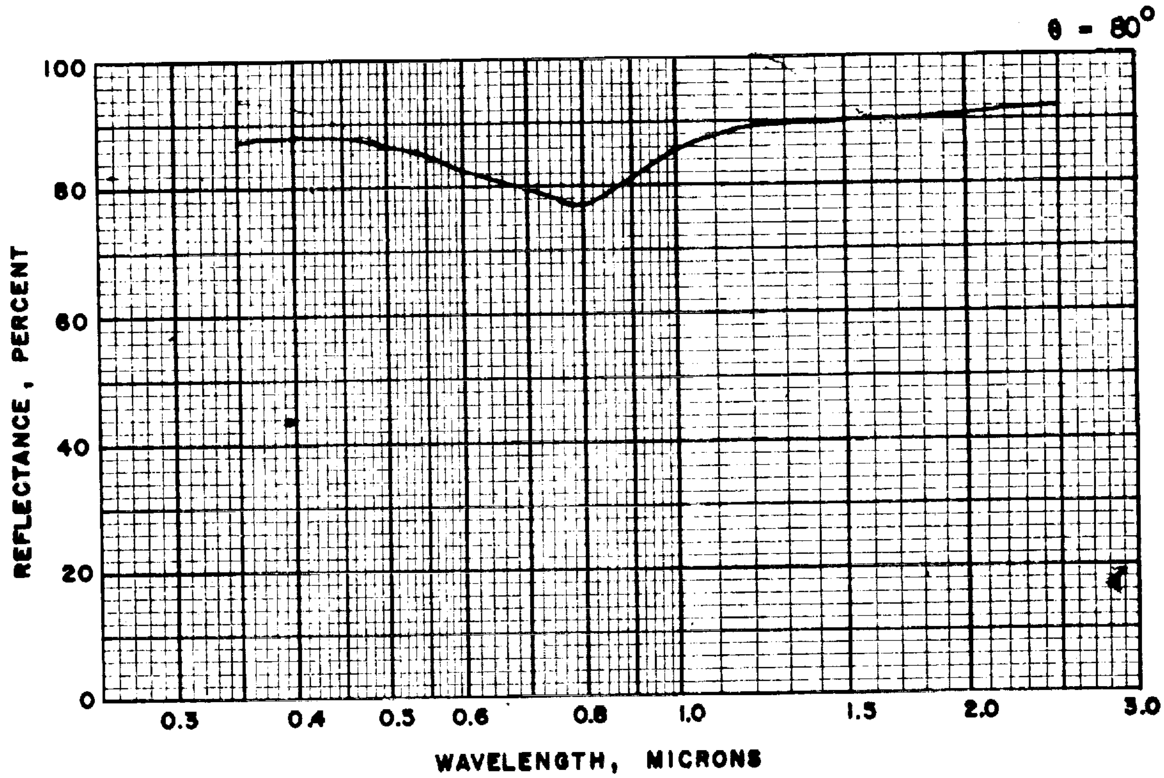

Figure 29 (Cont.): Sample 9, Azimuthal Angle 90°, Angle of Incidence 80°

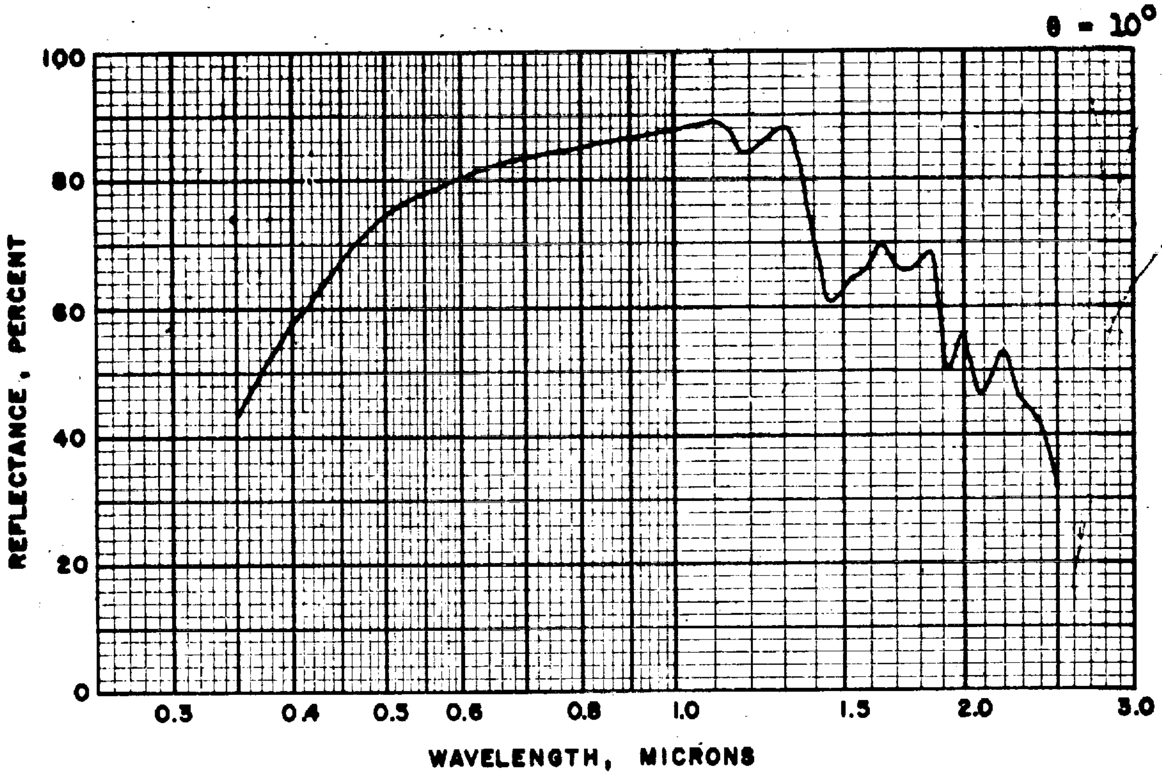

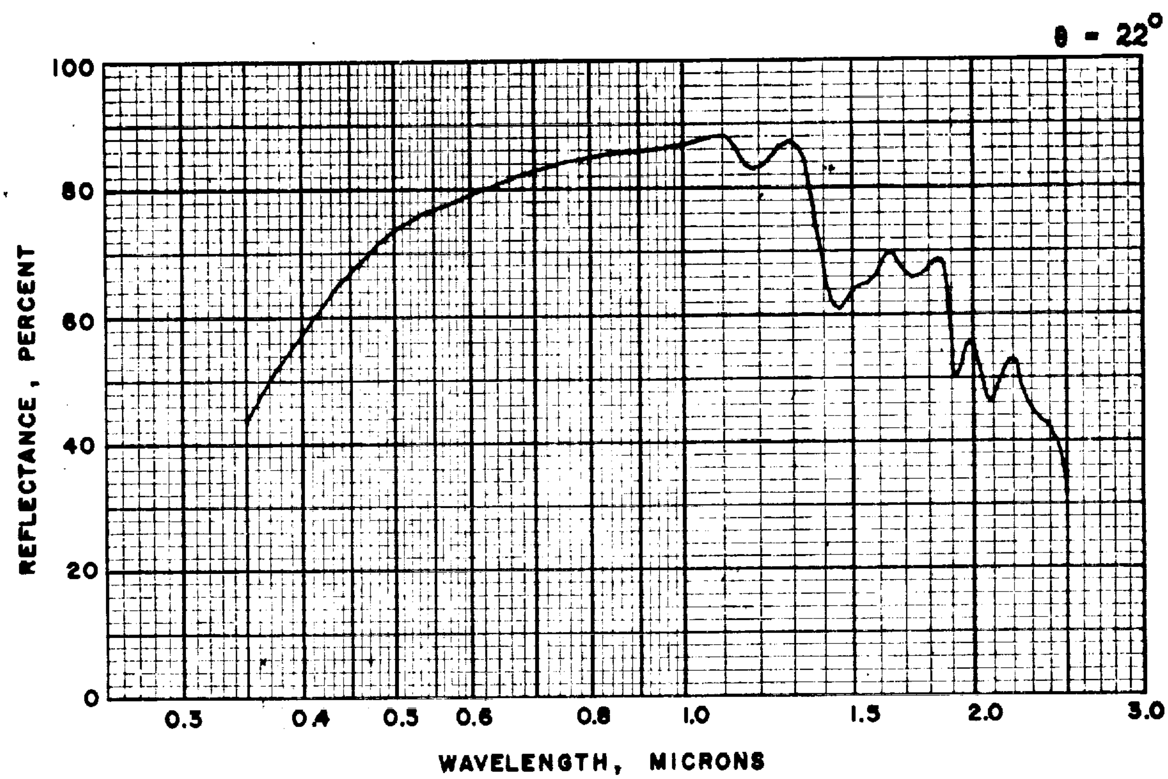

Figure 30: Sample 11, Azimuthal Angle 0°, Angles of Incidence 10° and 22°

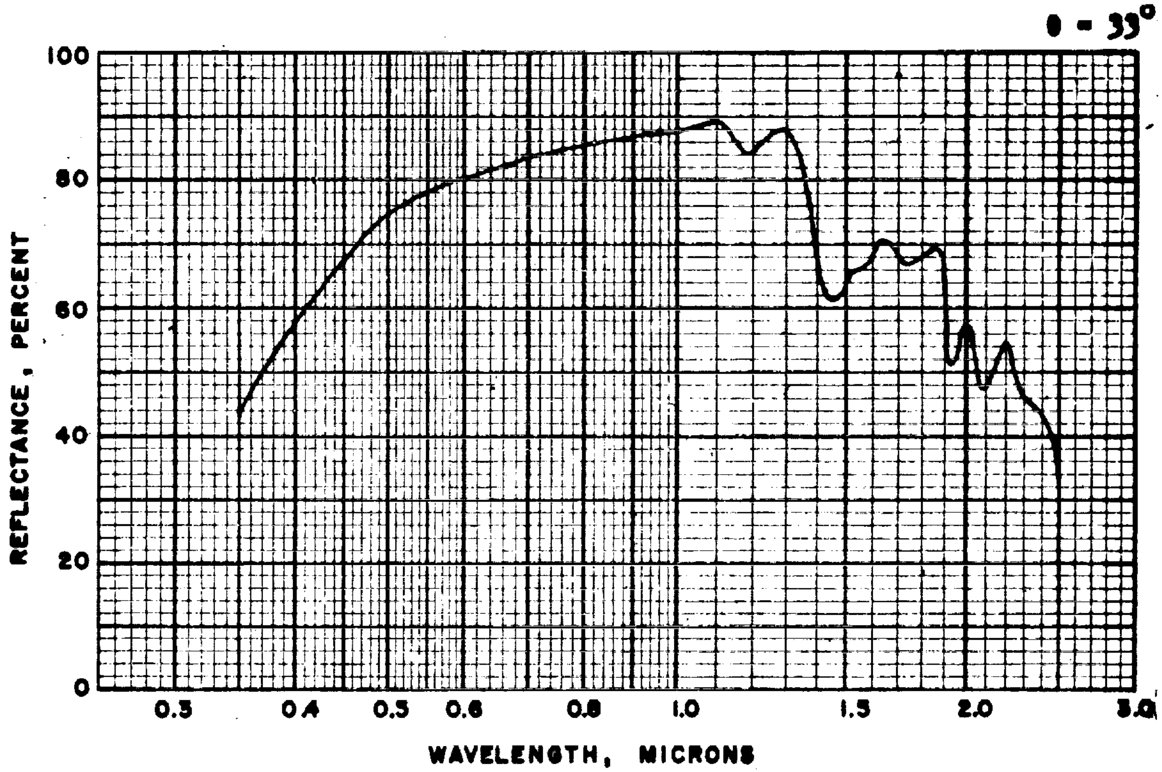

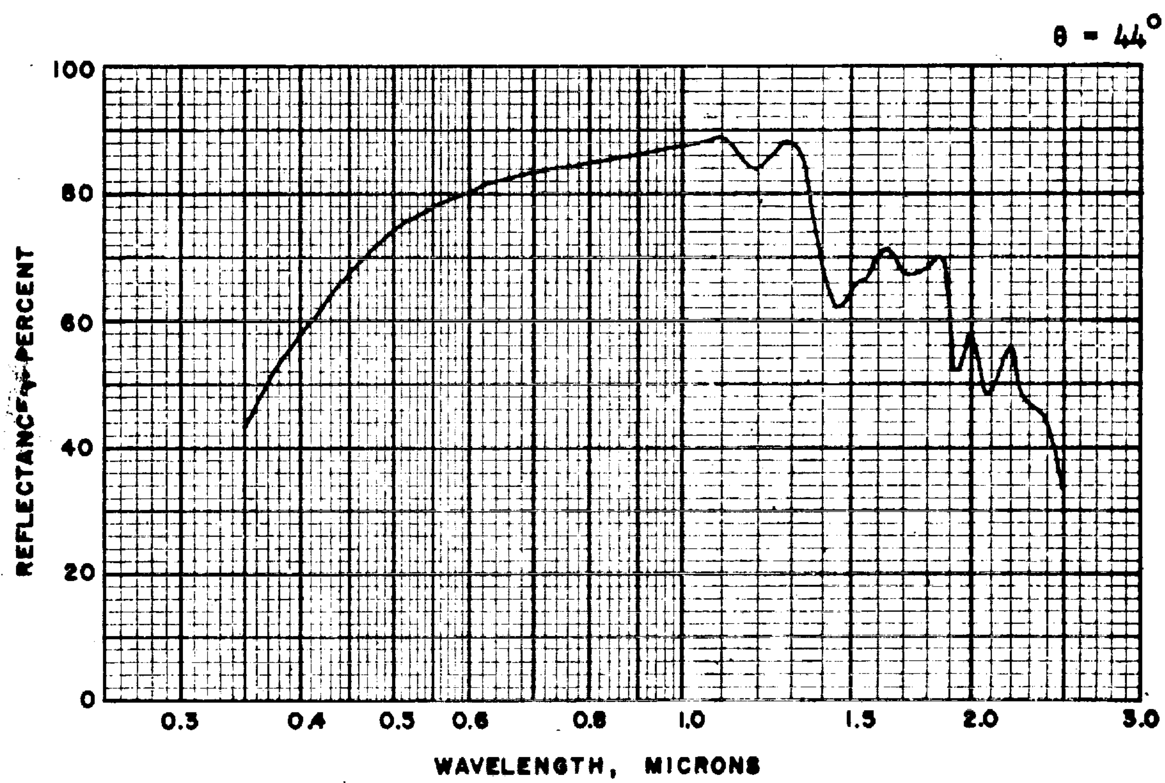

Figure 30 (Cont.): Sample 11, Azimuthal Angle 0°, Angles of Incidence 33° and 44°

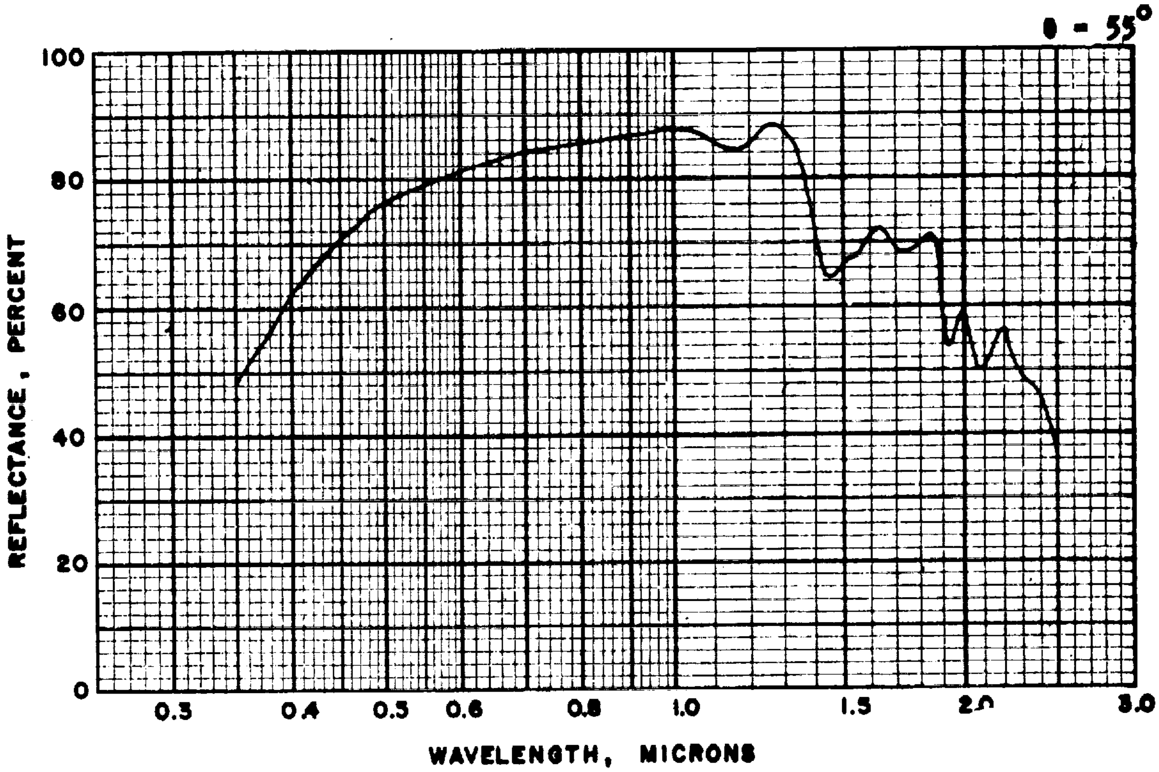

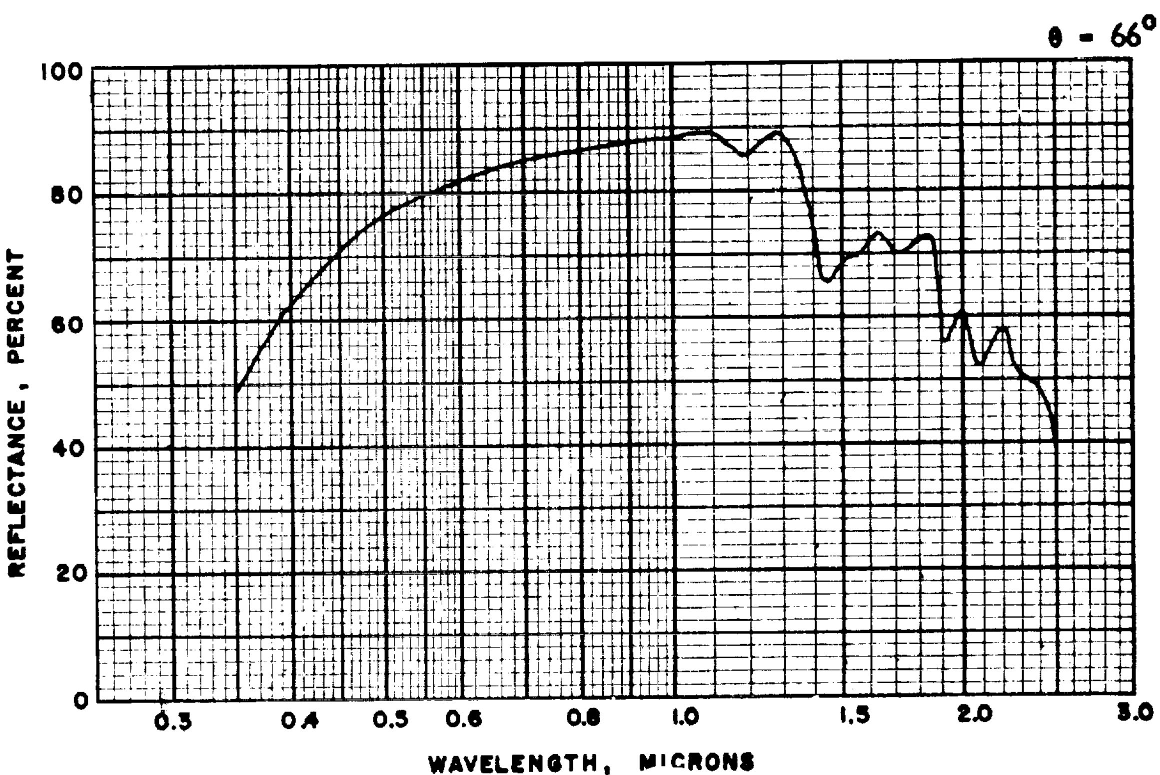

Figure 30 (Cont.): Sample 11, Azimuthal Angle 0°, Angles of Incidence 55° and 66°

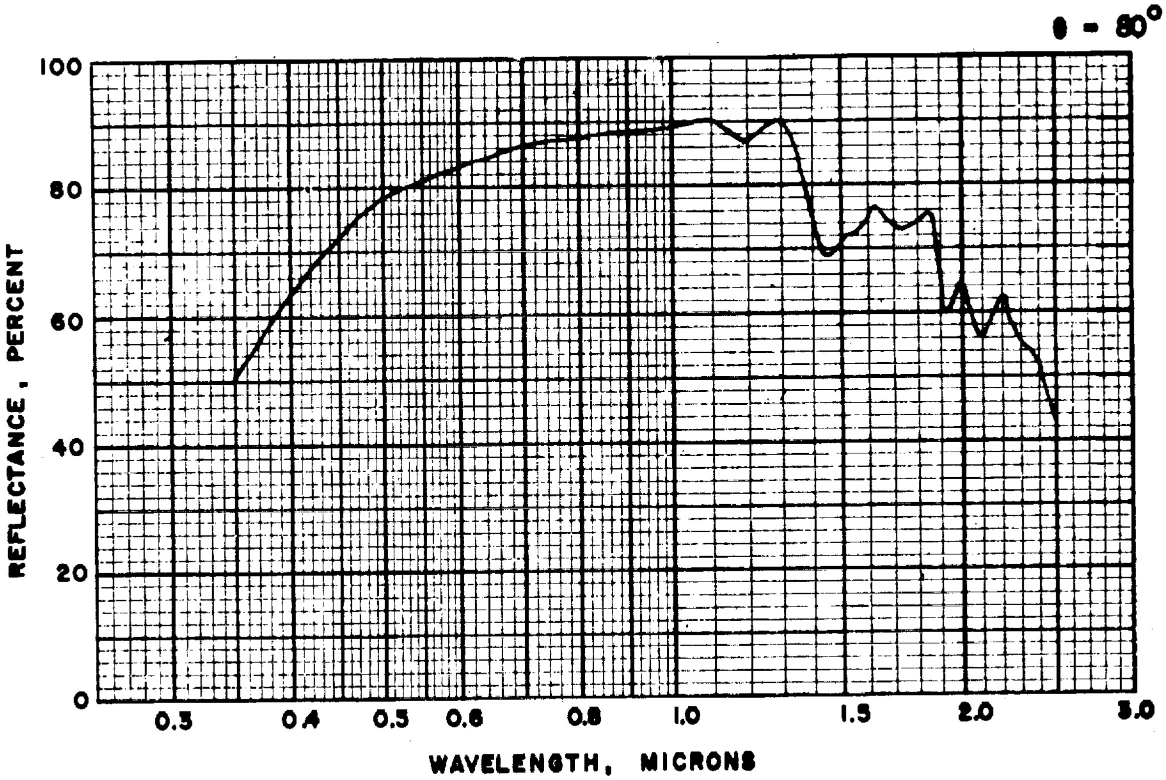

Figure 30 (Cont.) Sample 11, Azimuthal Angle 0°
Angle of Incidence 80°

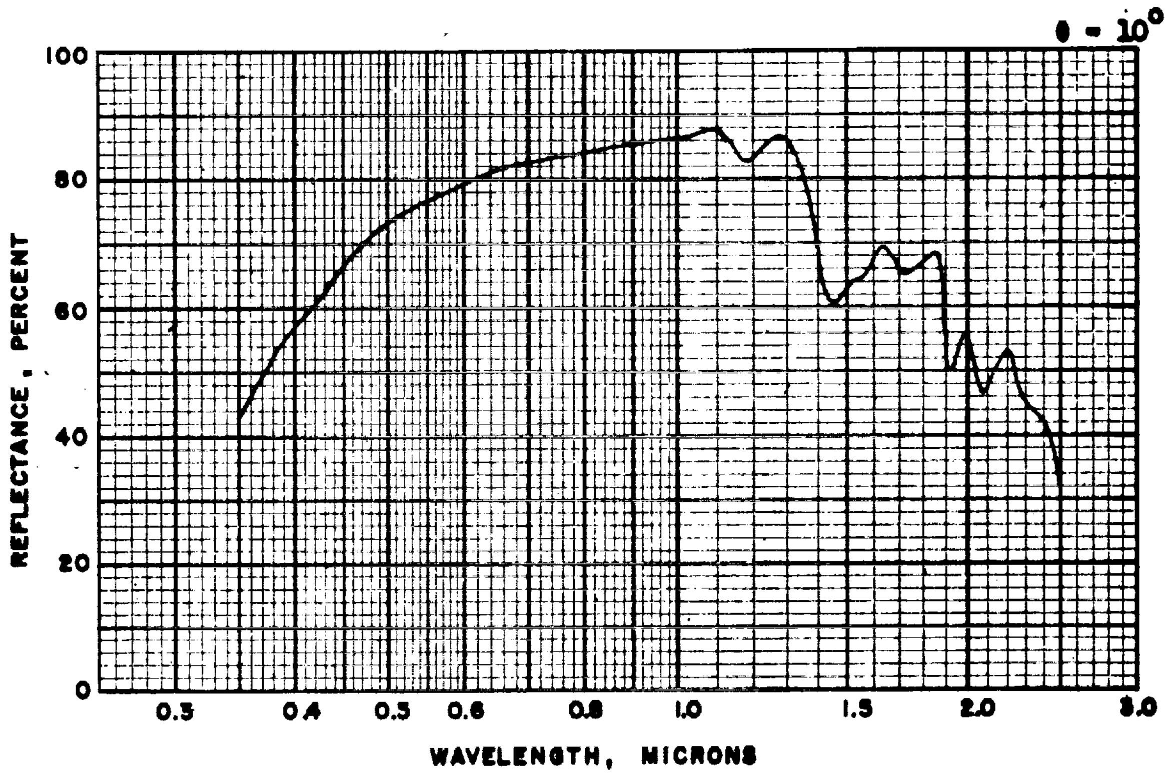

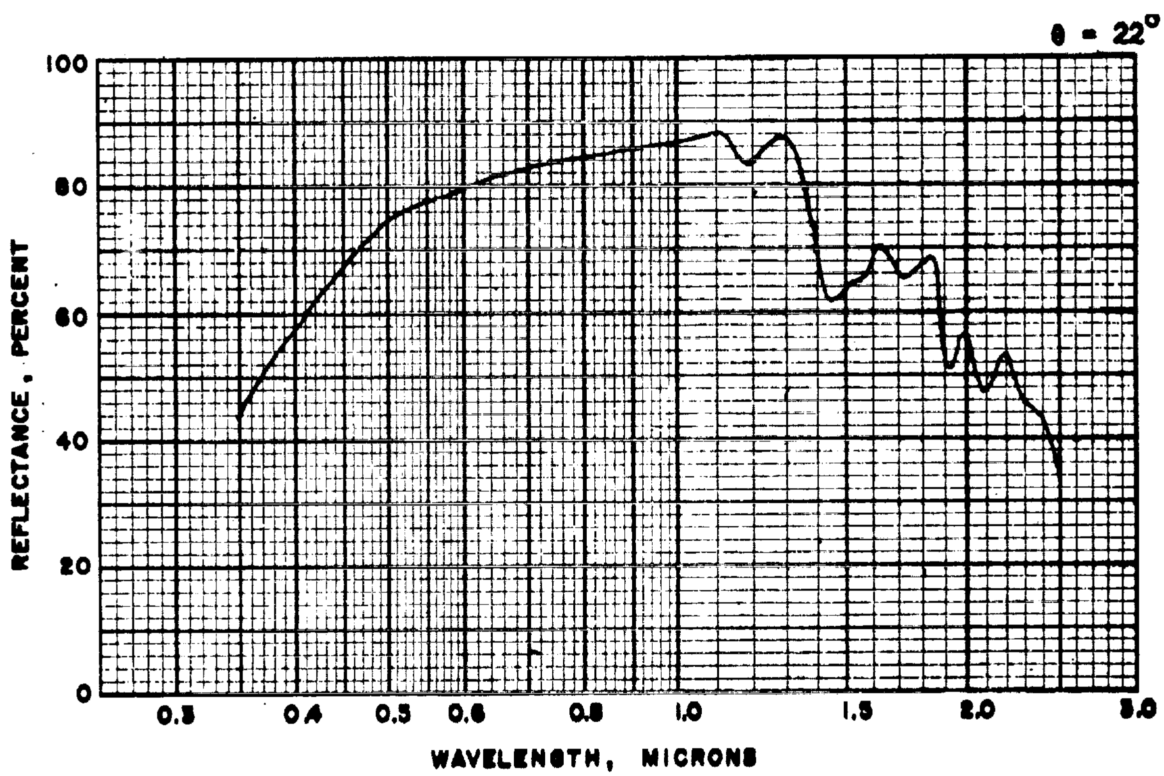

Figure 31: Sample 11, Azimuthal Angle 45°, Angles of Incidence 10° and 22°

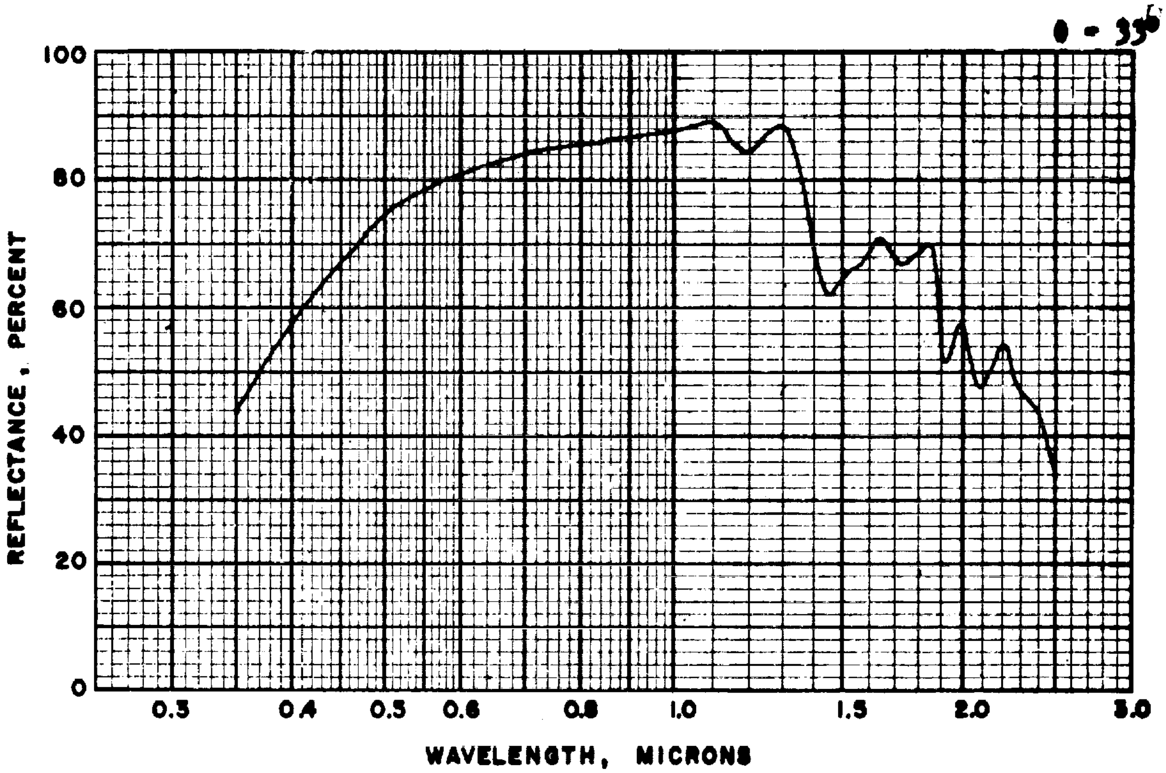

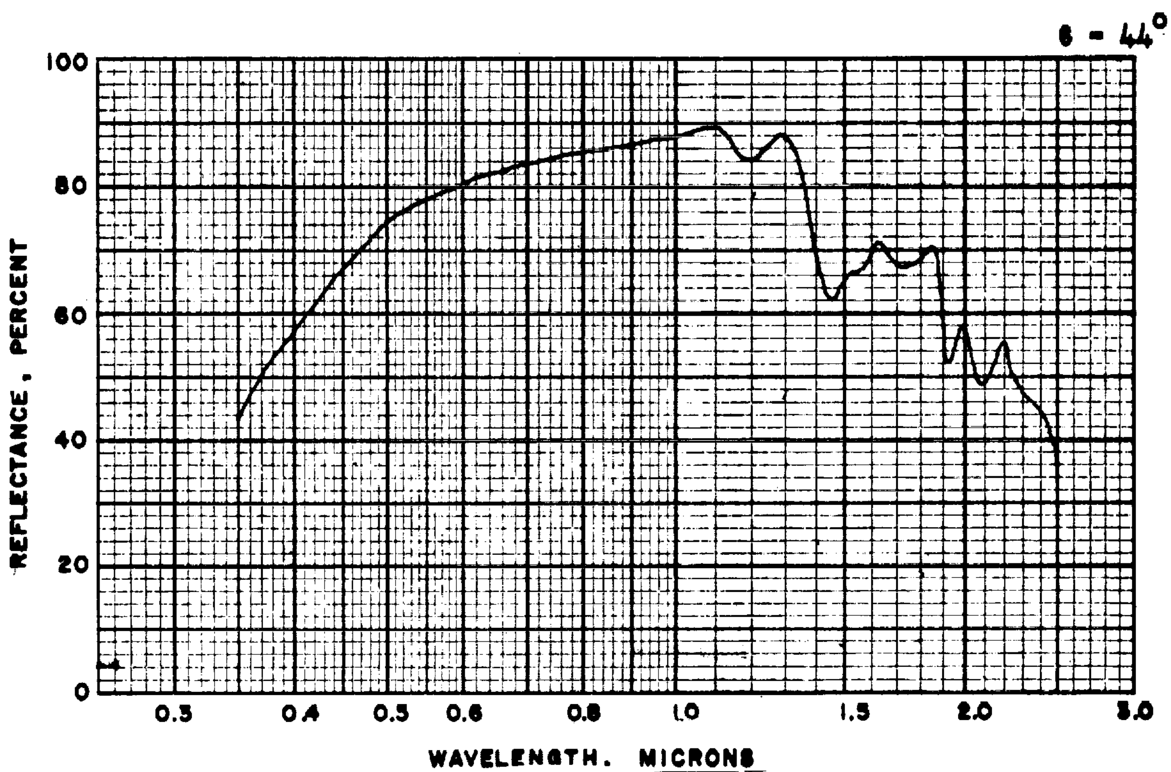

Figure 31 (Cont.): Sample 11, Azimuthal Angle 45°, Angles of Incidence 33° and 44°

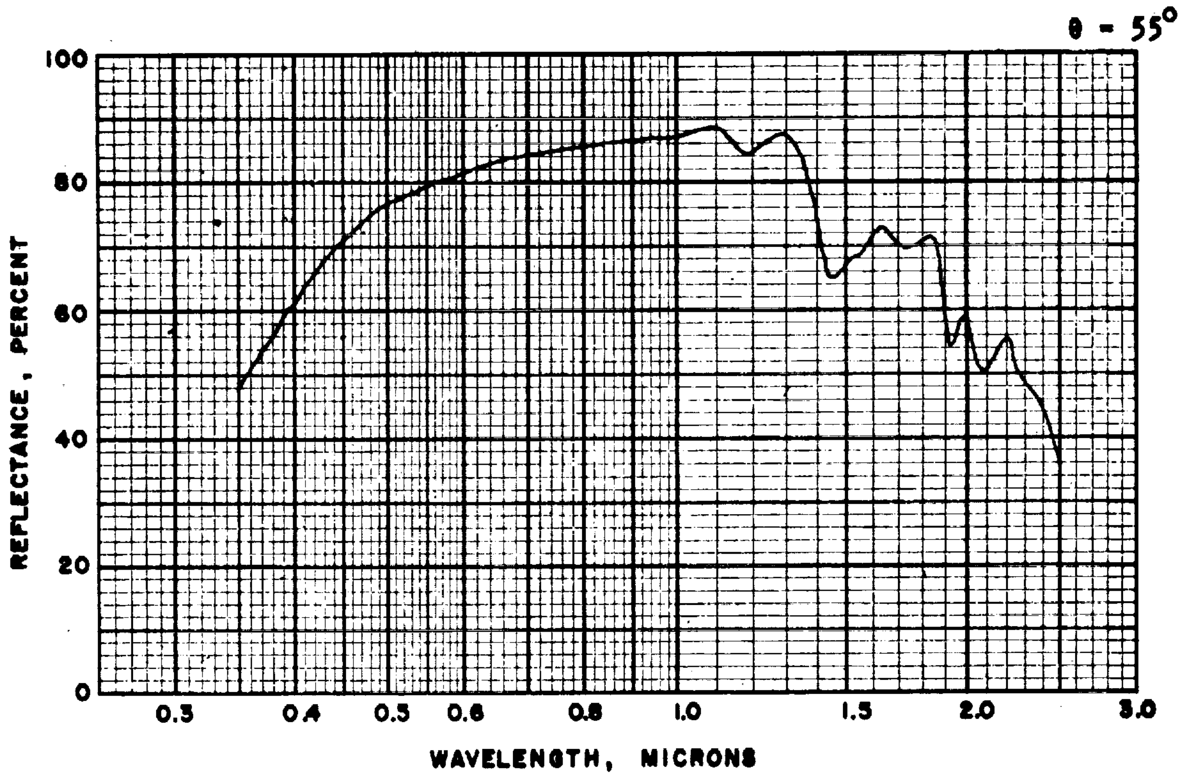

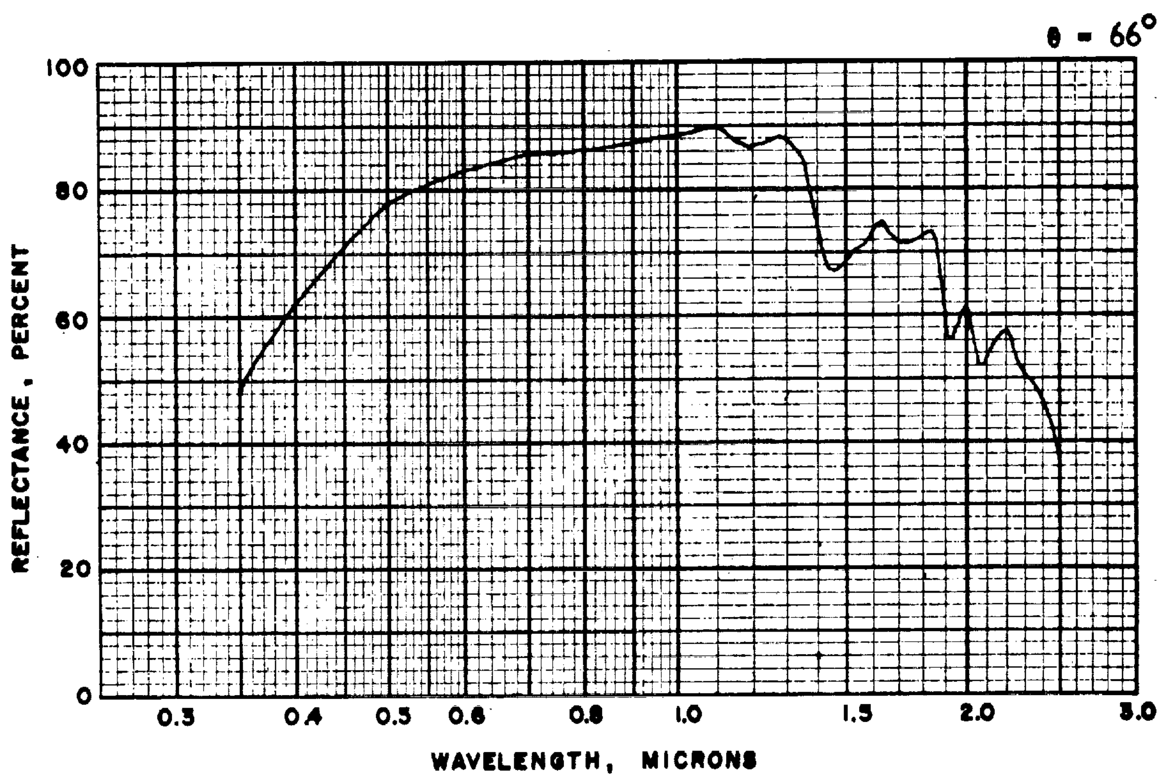

Figure 31 (Cont.): Sample 11, Azimuthal Angle 45°, Angles of Incidence 55° and 66°

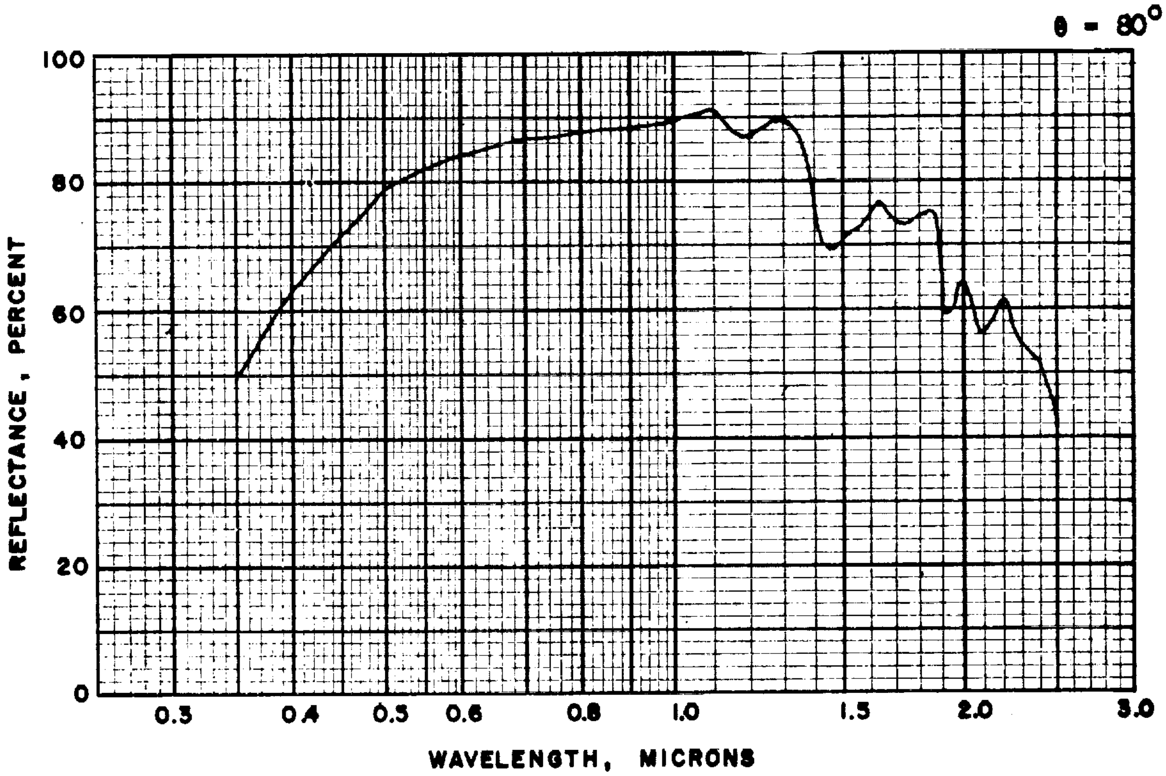

Figure 31 (Cont.): Sample 11, Azimuthal Angle 45°,
Angle of Incidence 80°

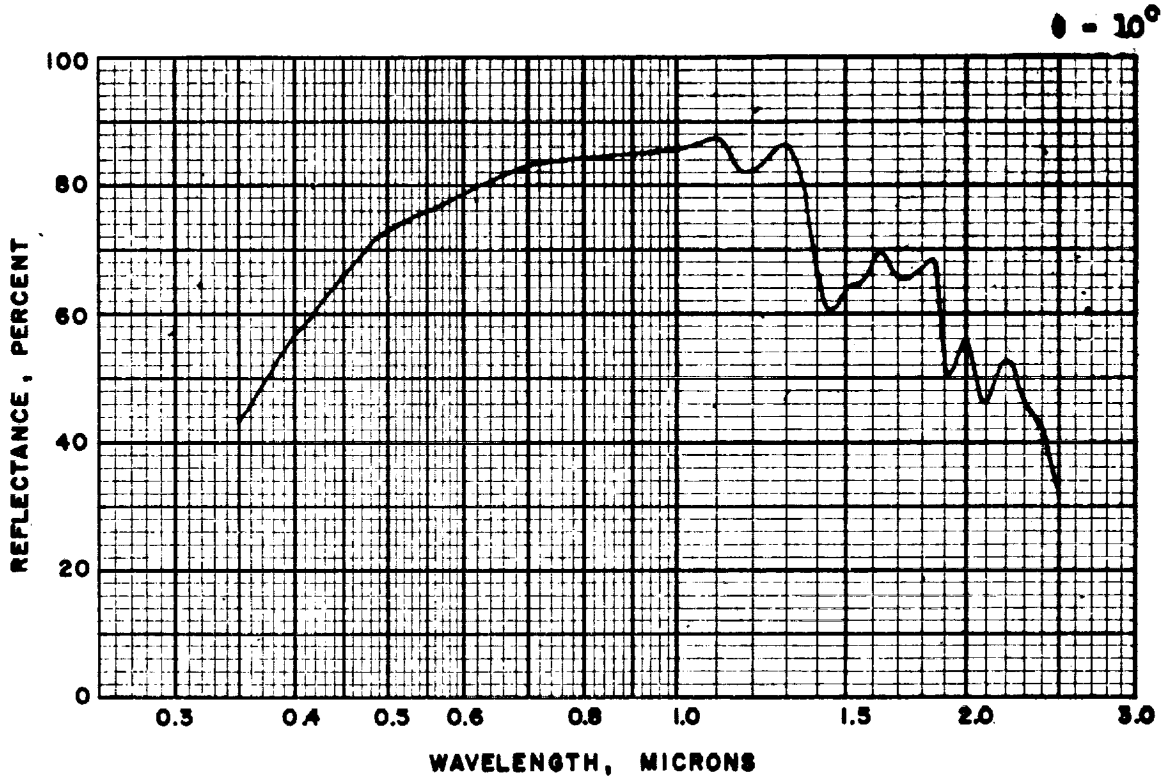

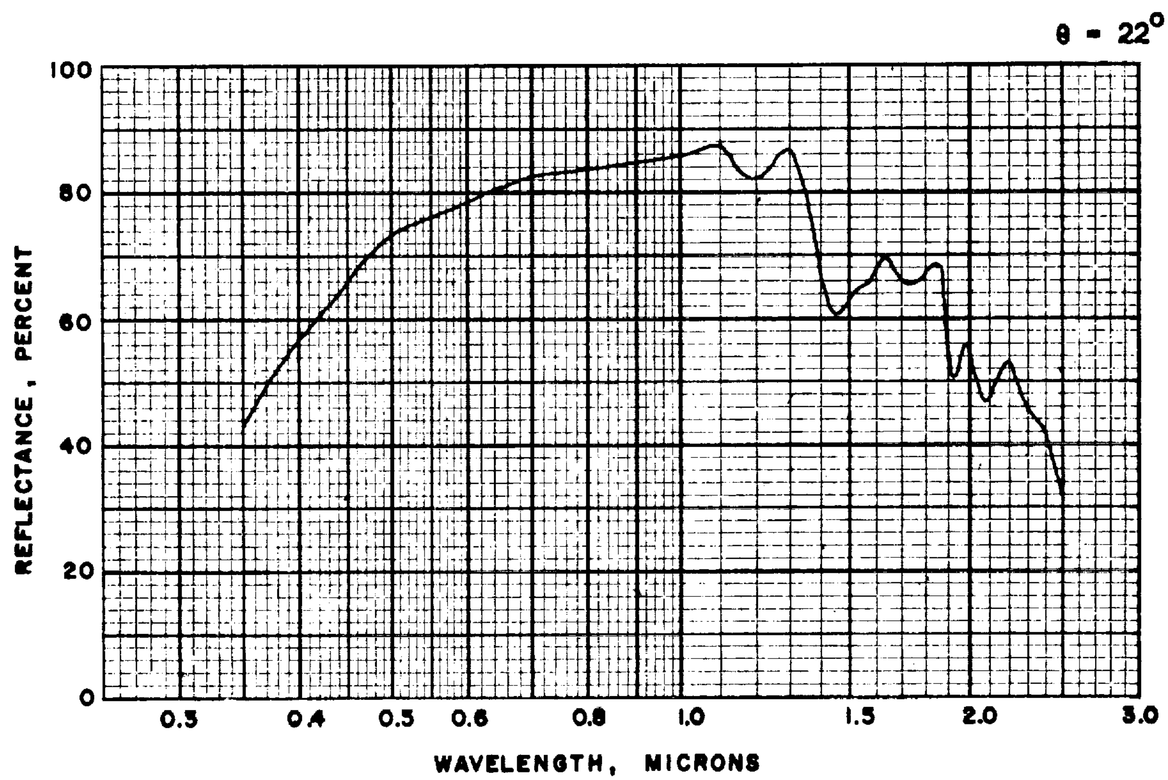

Figure 32: Sample 11, Azimuthal Angle 60°, Angles of Incidence 10° and 22°

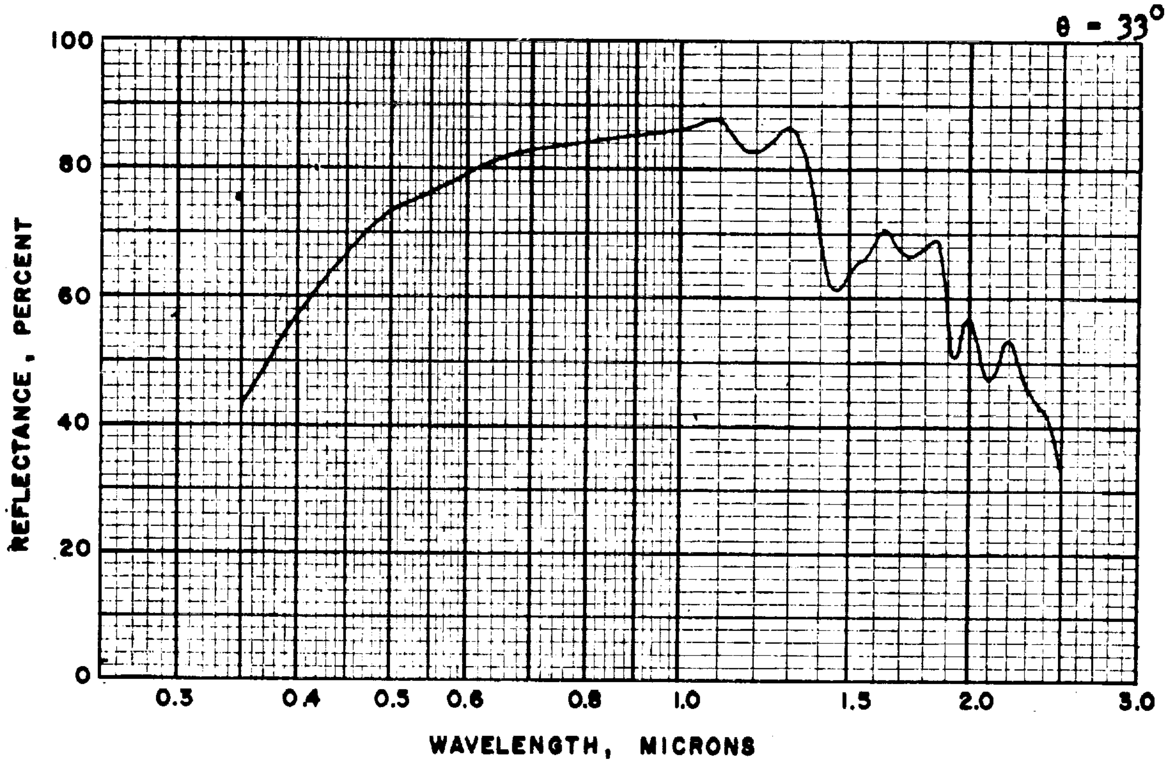

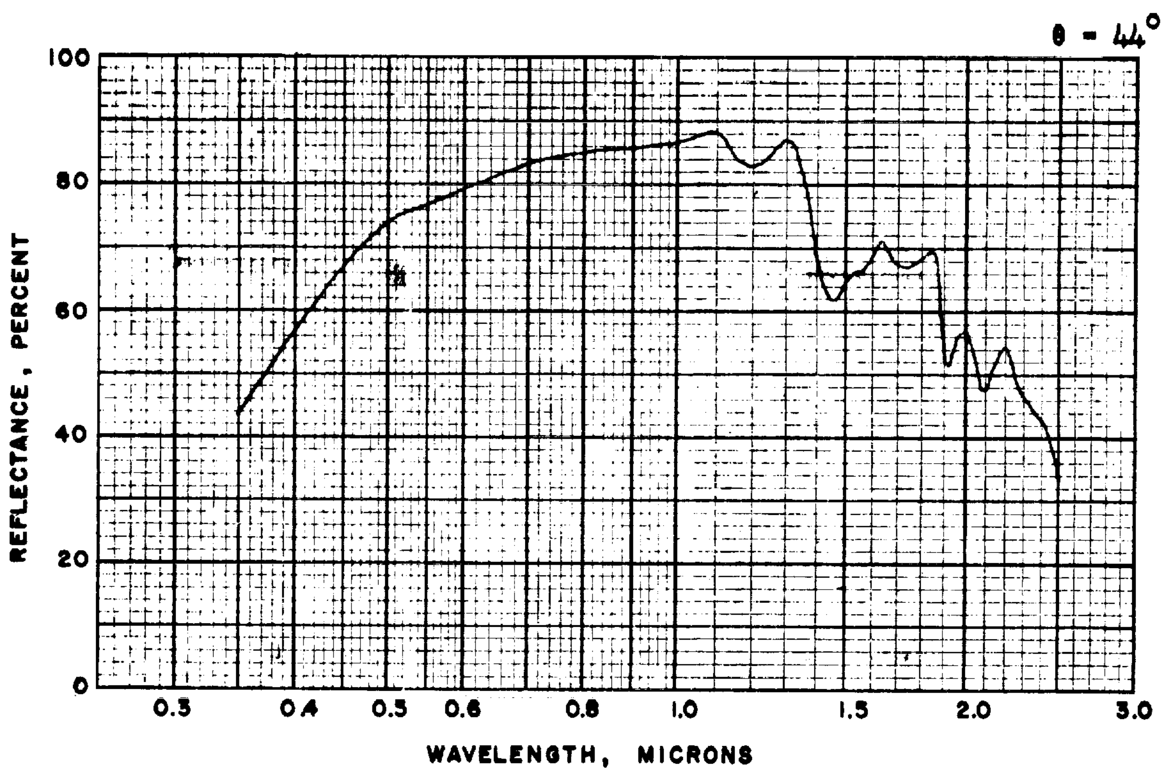

Figure 32 (Cont.): Sample 11, Azimuthal Angle 60°, Angles of Incidence 33° and 44°

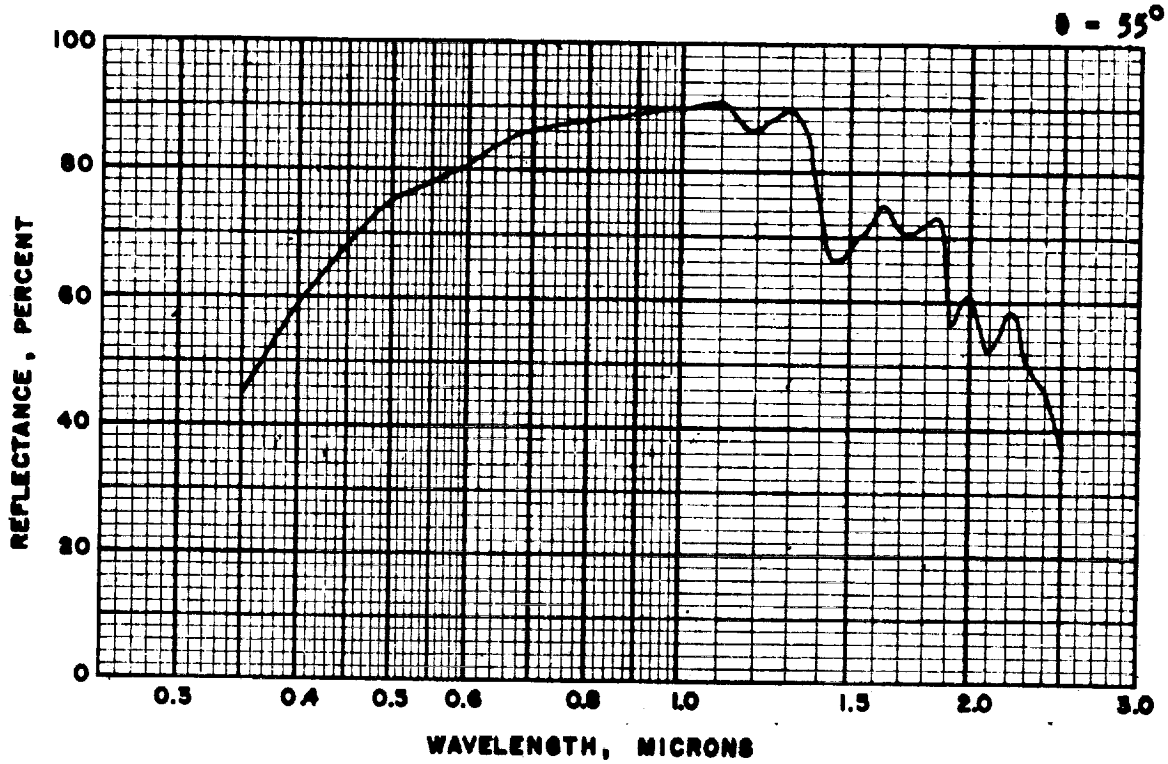

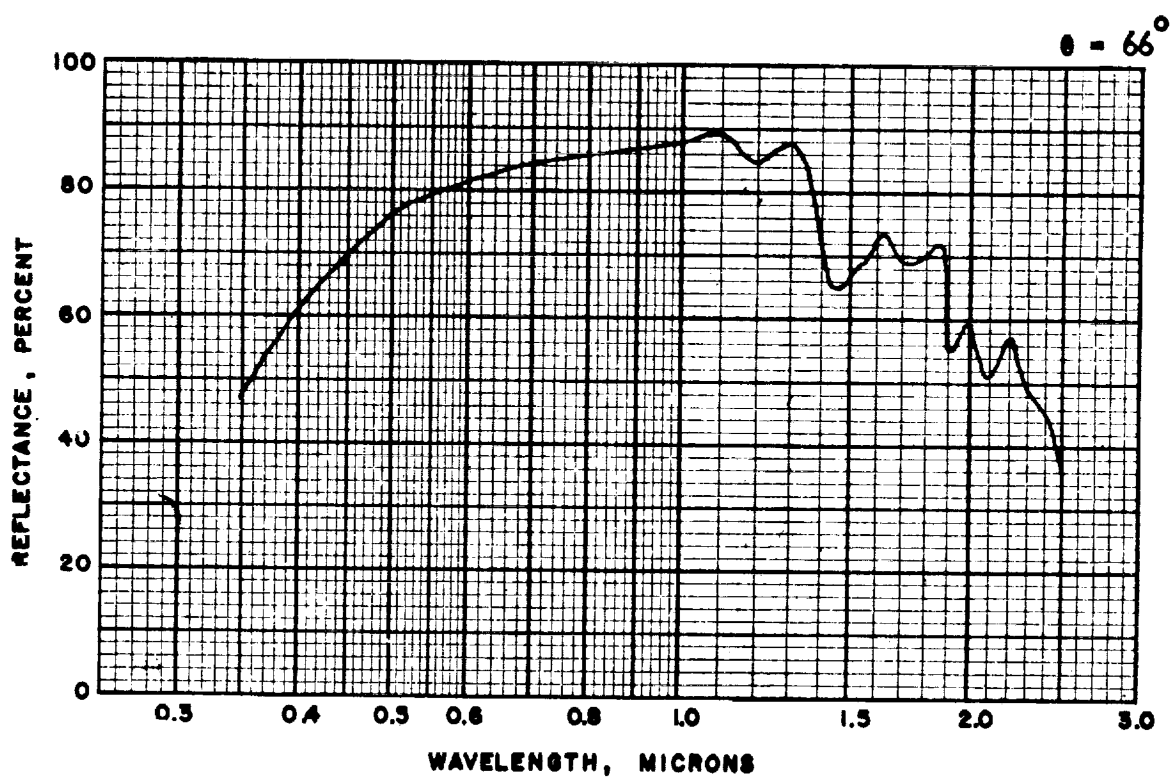

Figure 32 (Cont.): Sample 11, Azimuthal Angle 60°
Angles of Incidence 55° and 66°

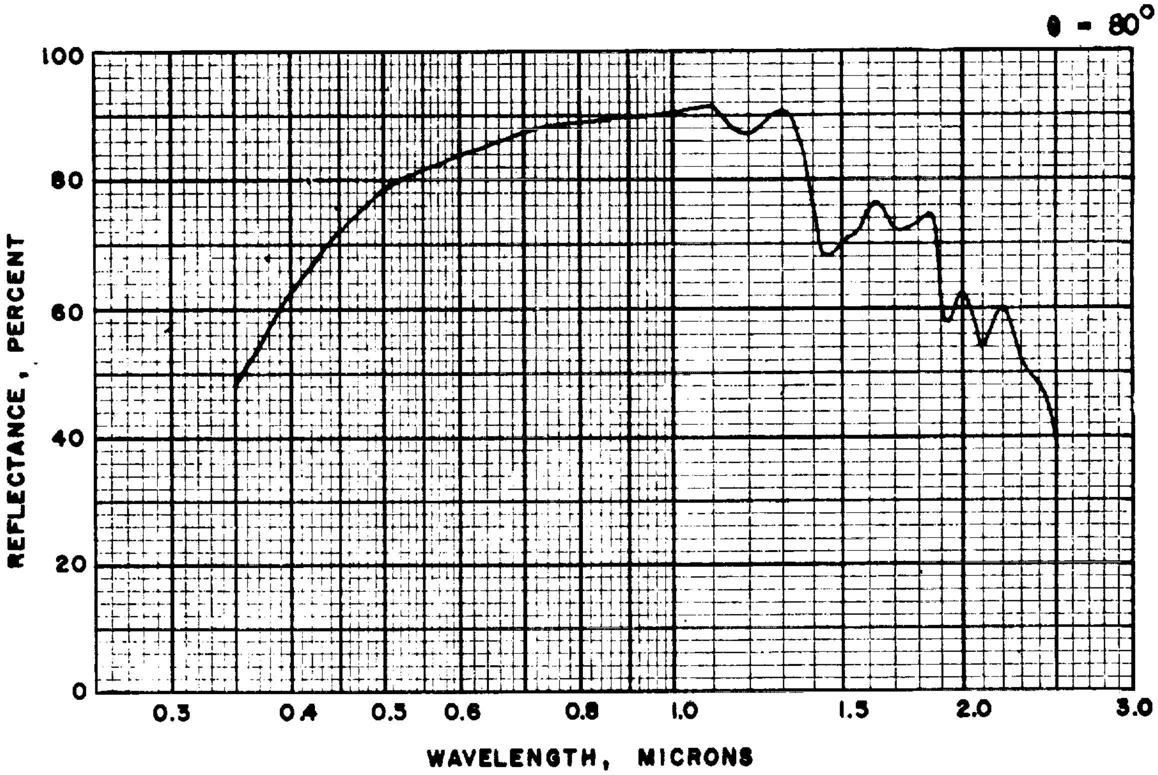

Figure 32 (Cont.): Sample 11, Azimuthal Angle 60°, Angle of Incidence 80°

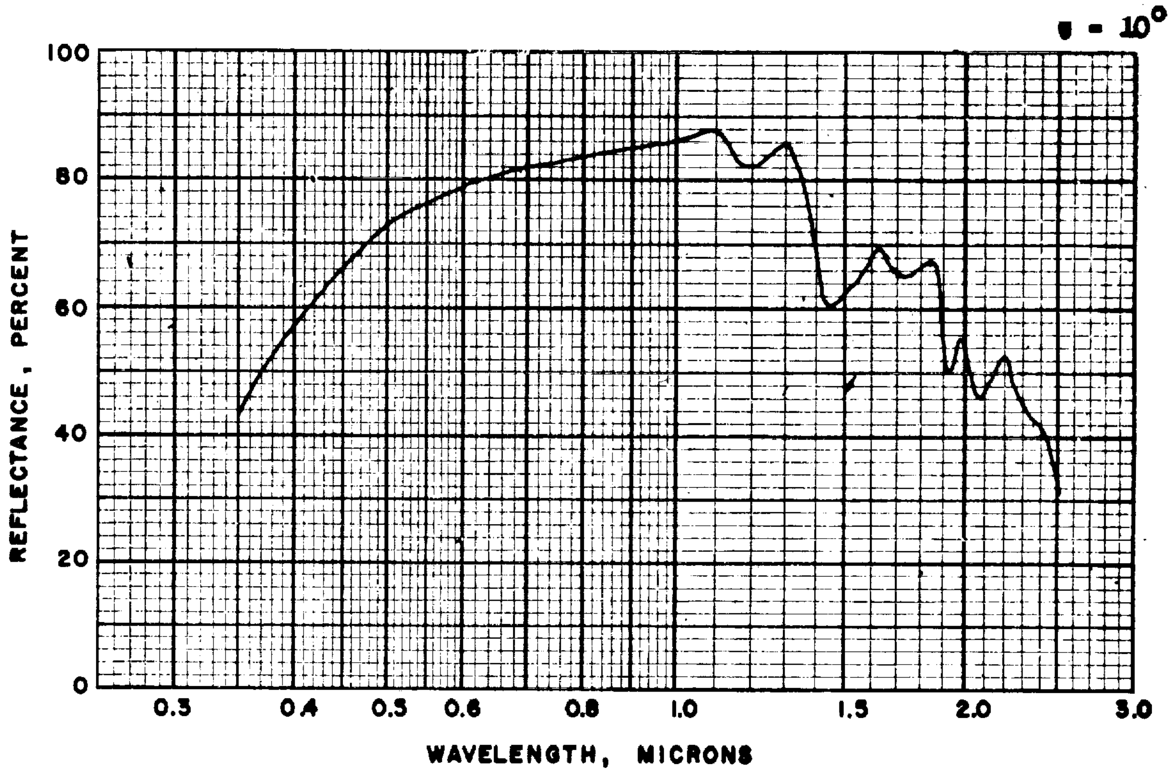

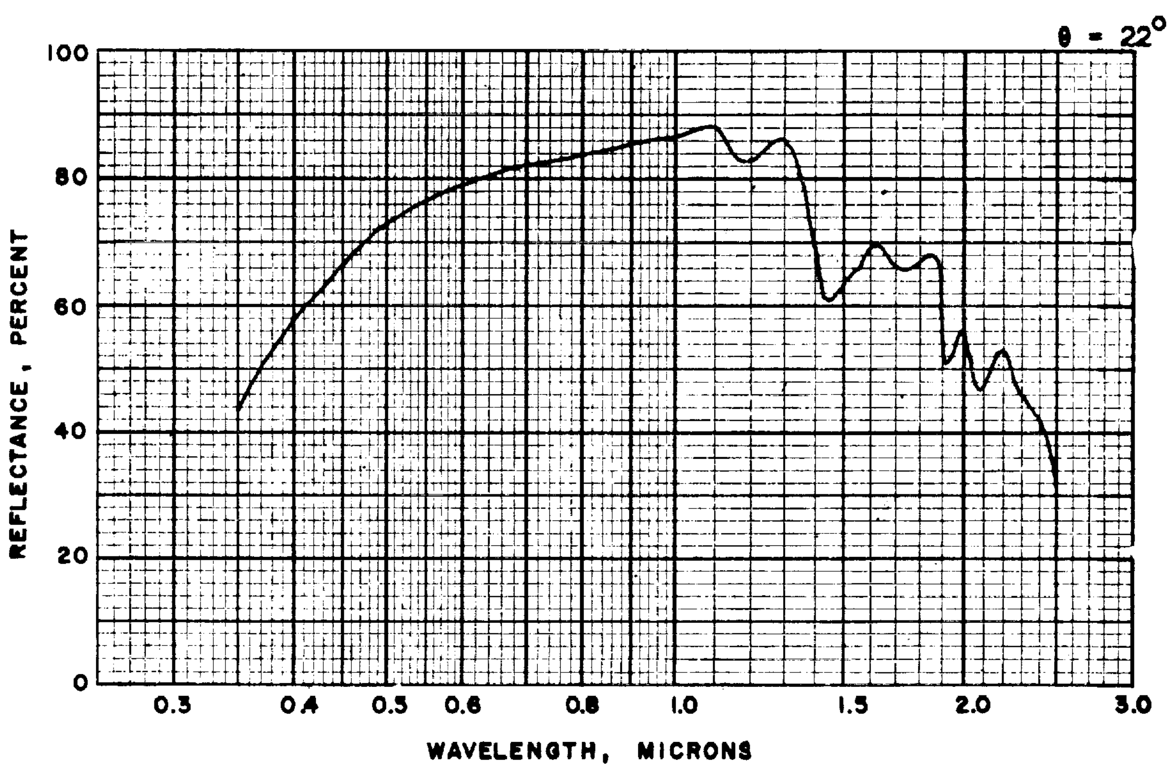

Figure 33: Sample 11, Azimuthal Angle 90°, Angles of Incidence 10° and 22°

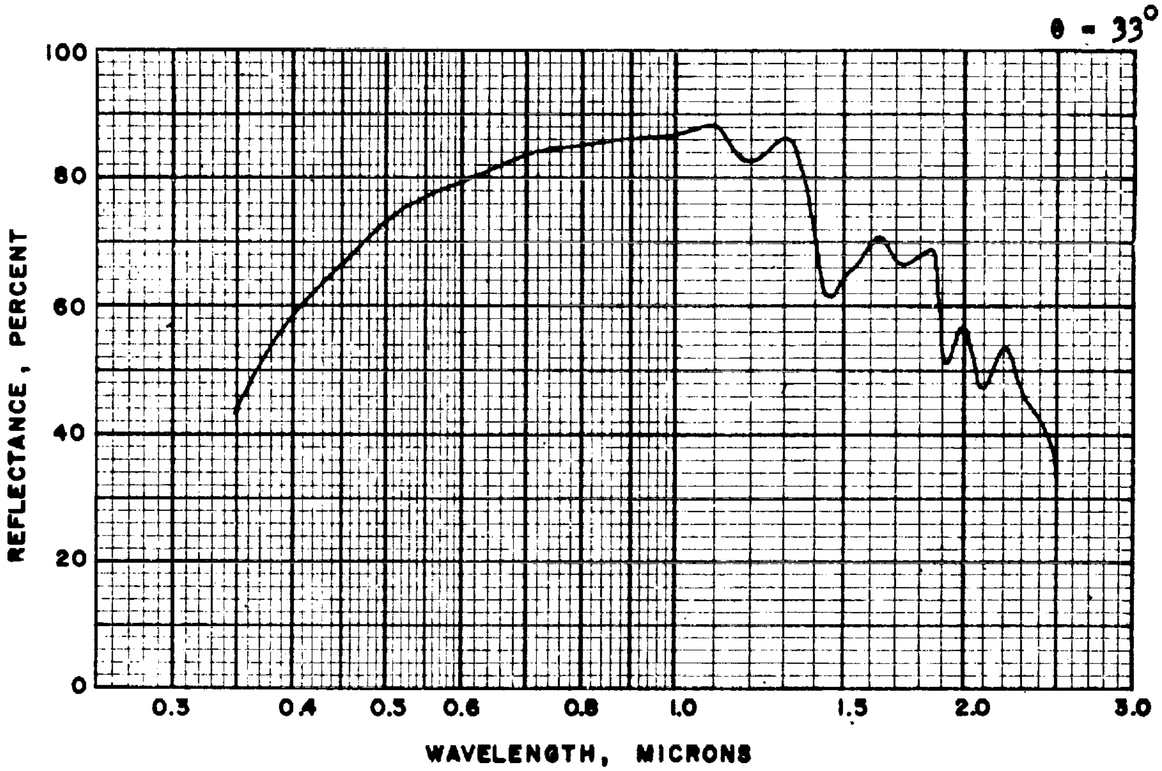

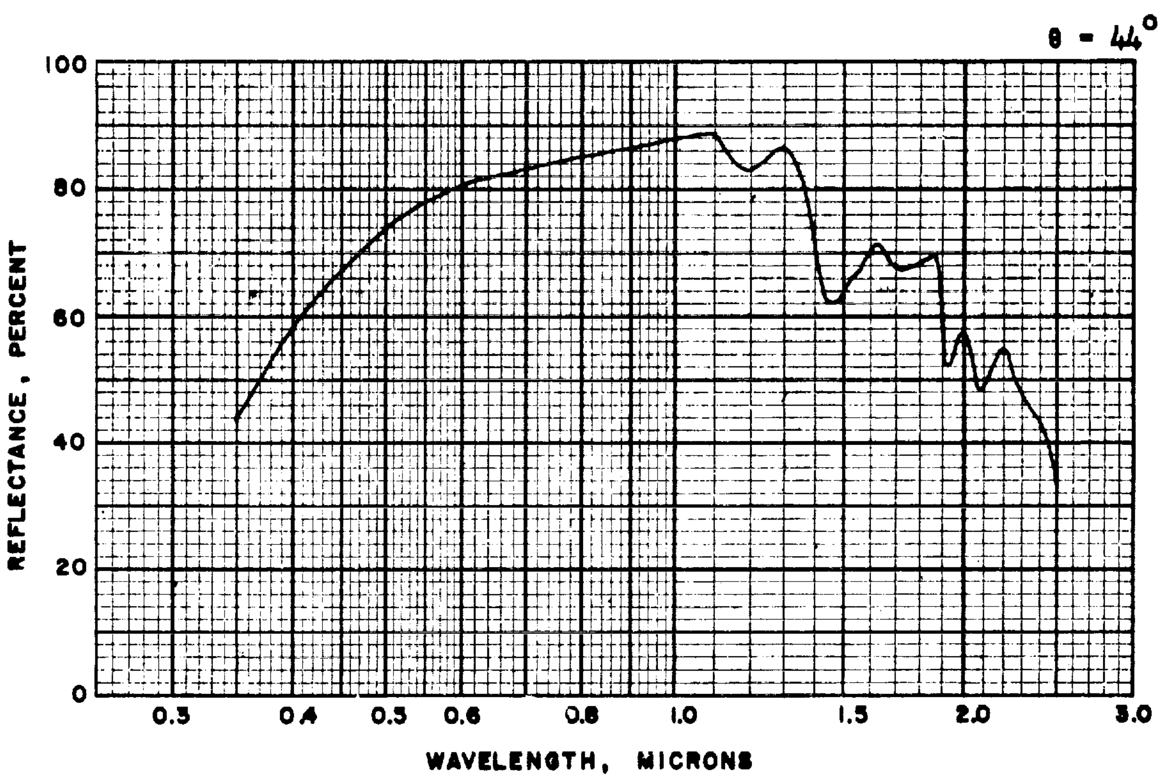

Figure 33 (Cont.): Sample 11, Azimuthal Angle 90°, Angles of Incidence 33° and 44°

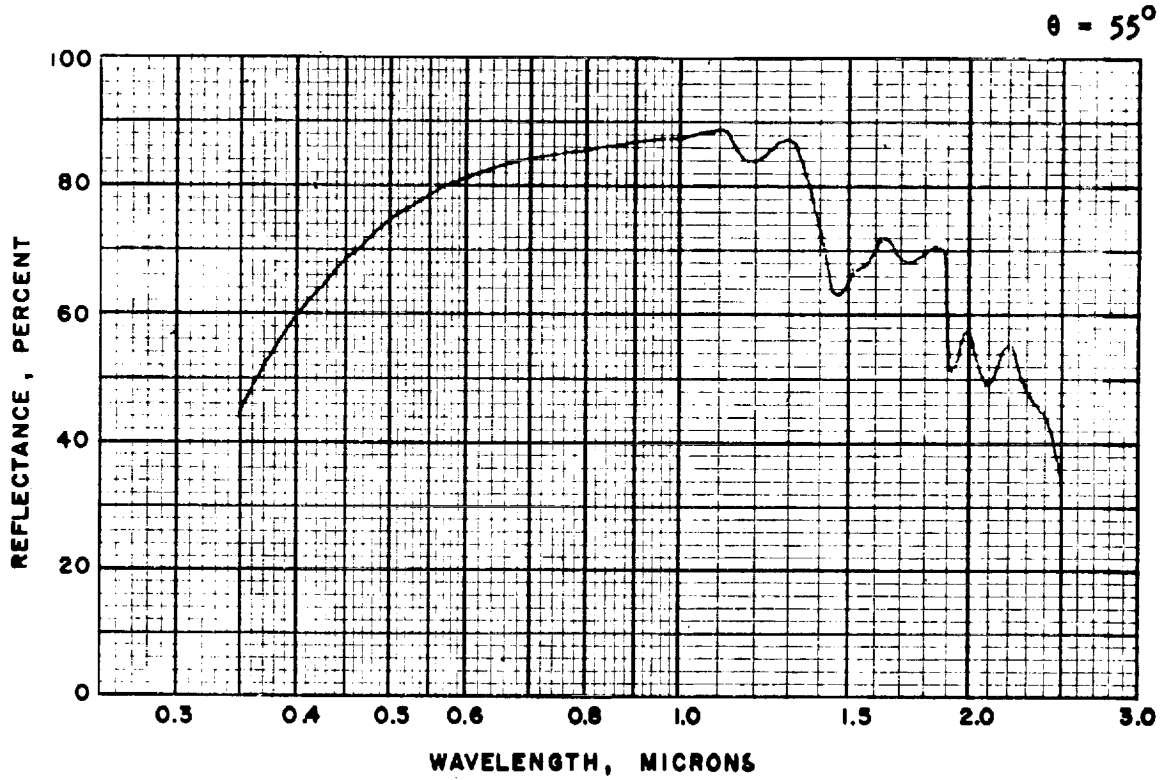

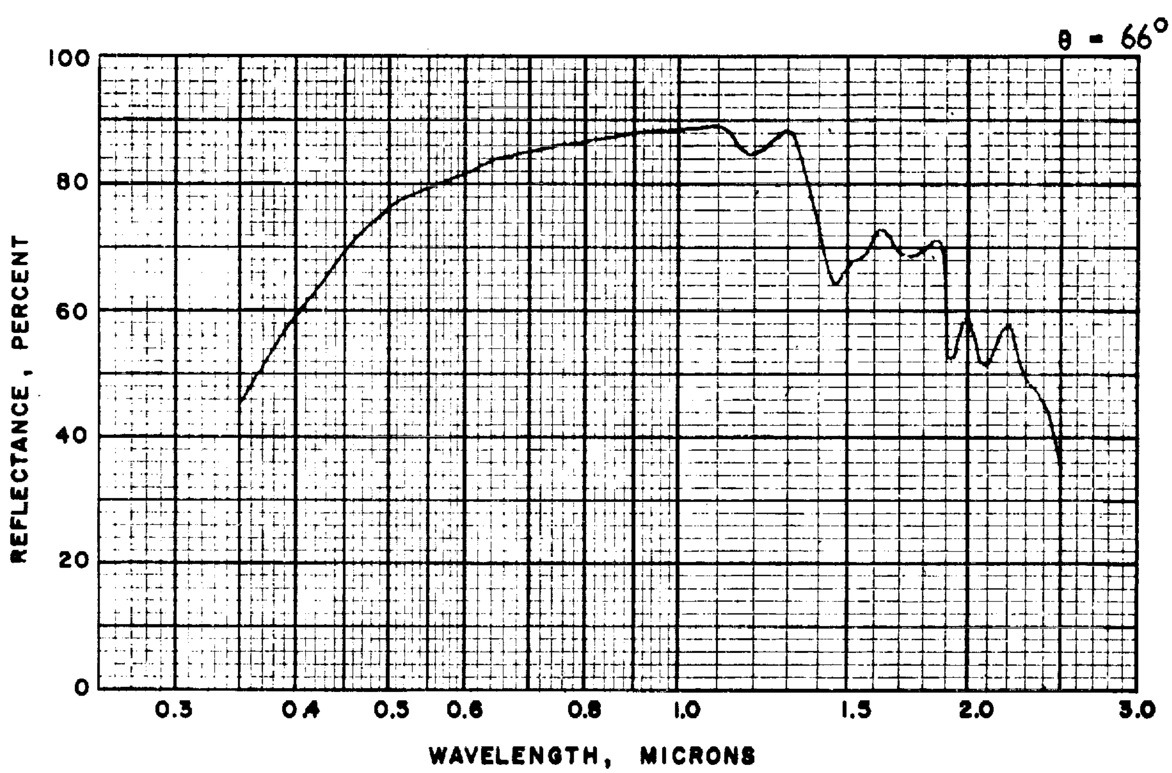

Figure 33 (Cont.): Sample 11, Azimuthal Angle 90°, Angles of Incidence 55° and 66°

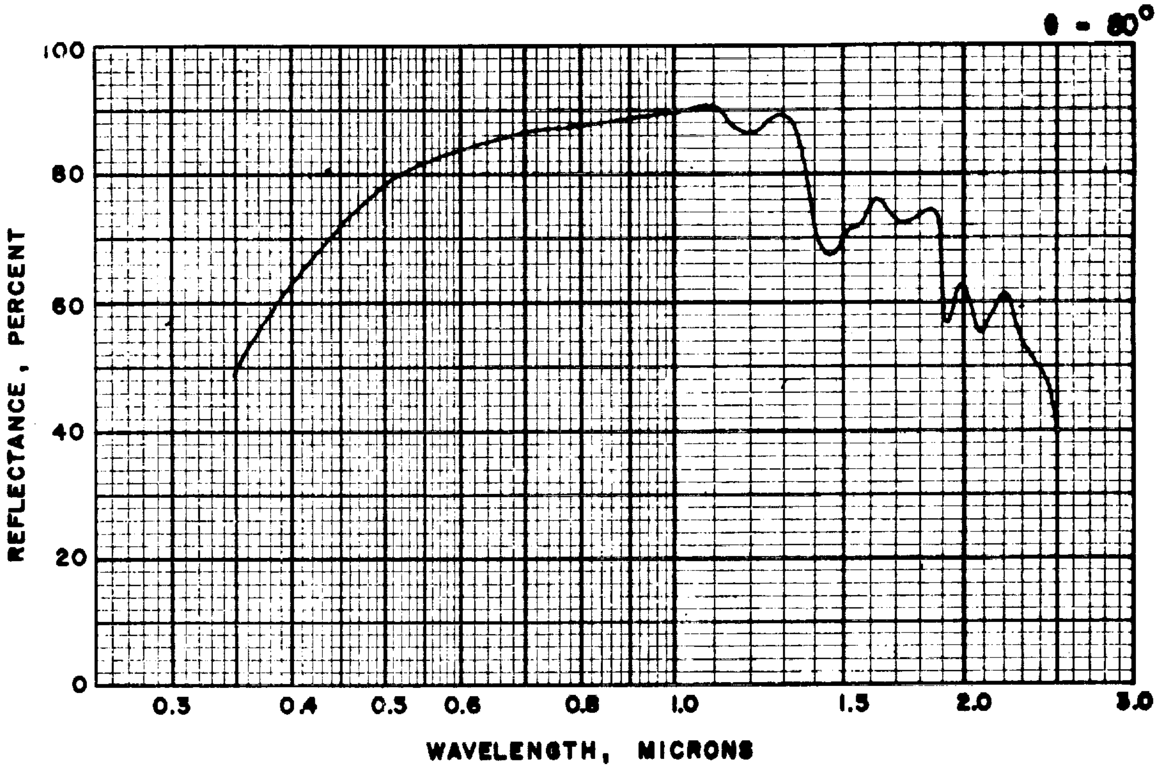

Figure 33 (Cont.): Sample 11, Azimuthal Angle 90°
Angle of Incidence 80°

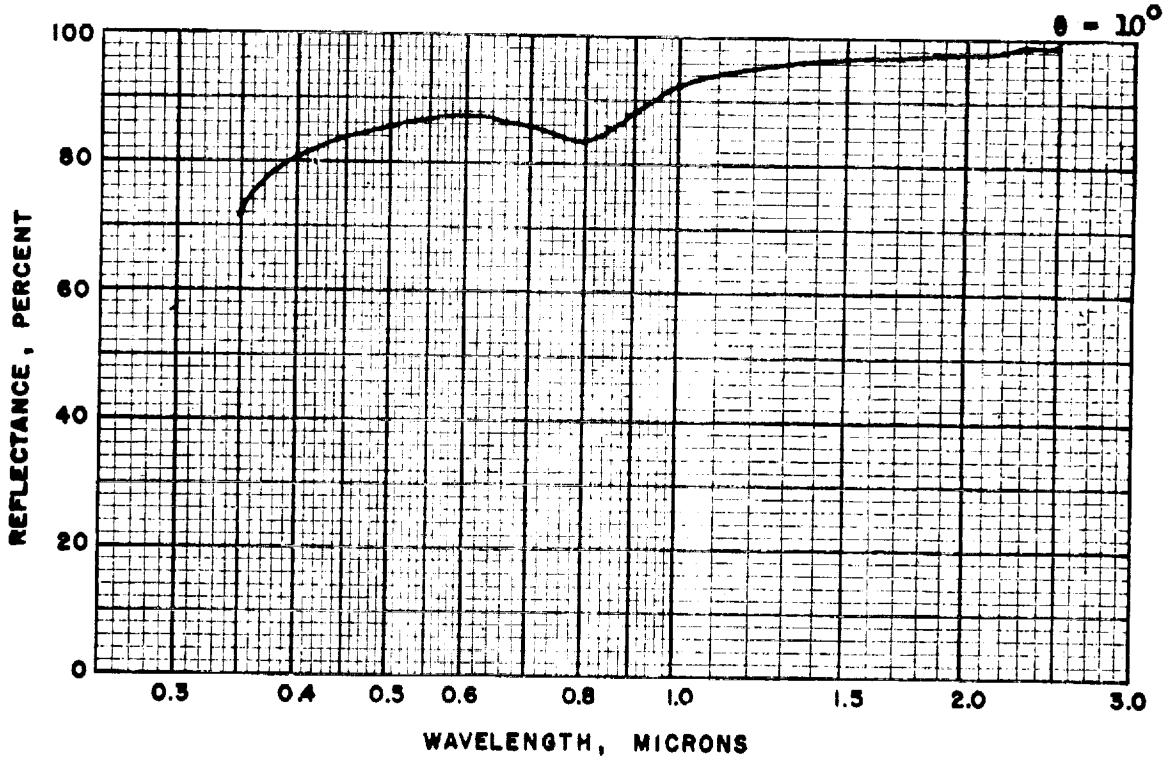

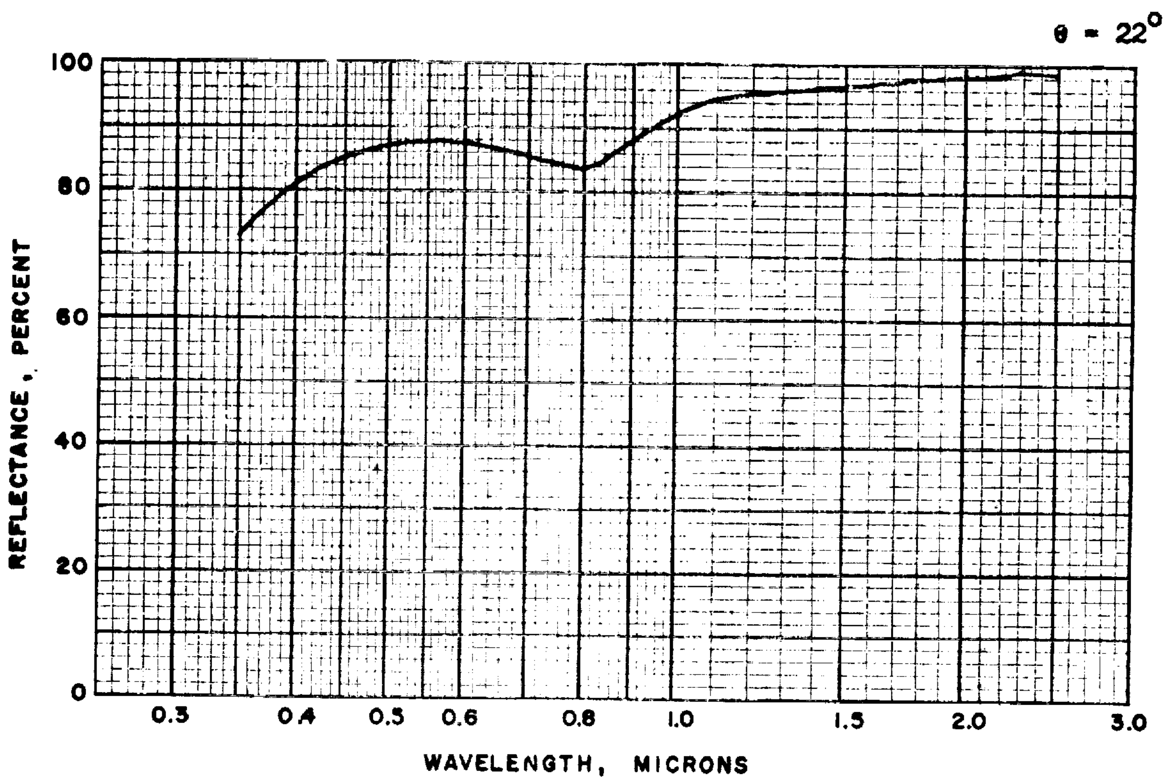

Figure 94: Sample 12A, Azimuthal Angle 0°, Angles of Incidence 10° and 22°

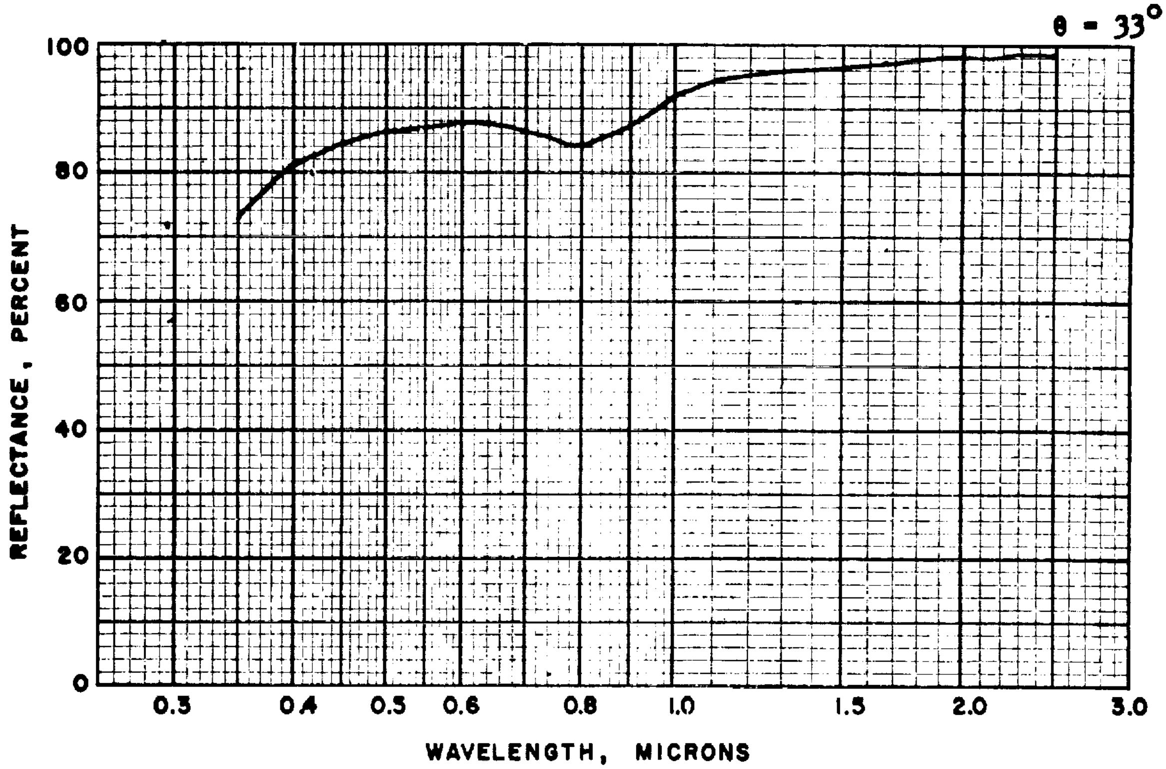

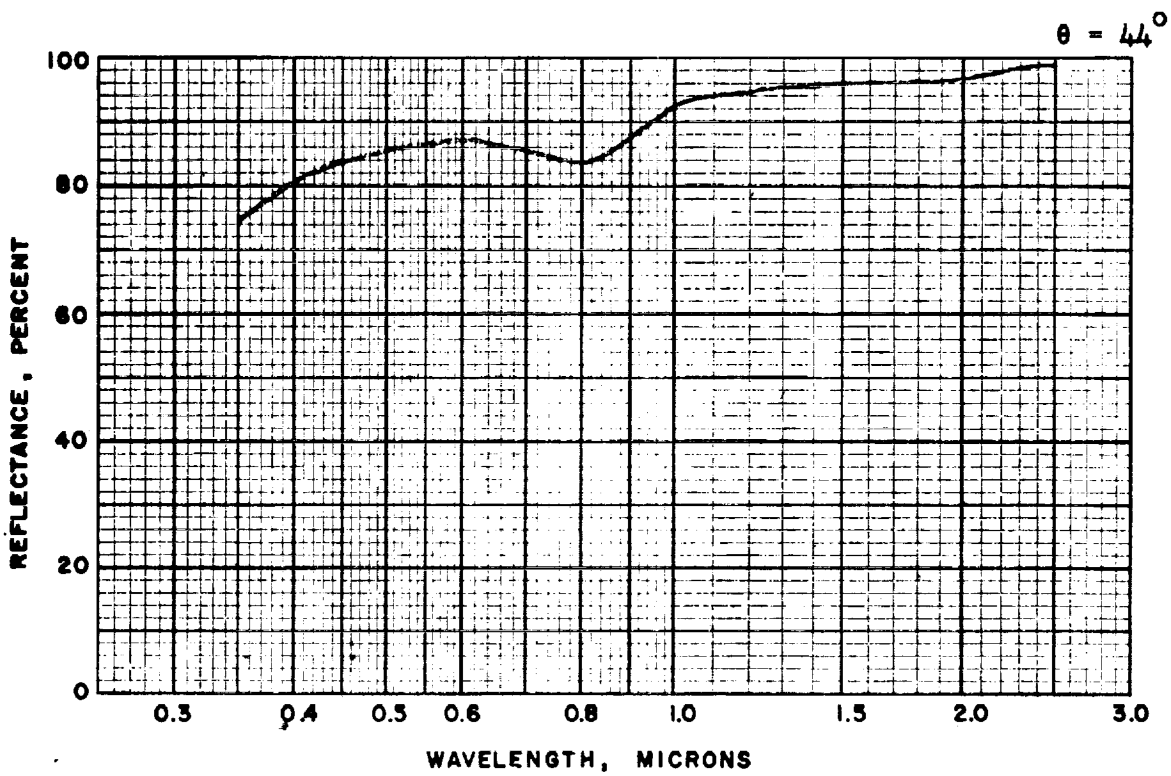

Figure 34 (Cont.): Sample 12A, Azimuthal Angle 0°, Angles of Incidence 33° and 44°

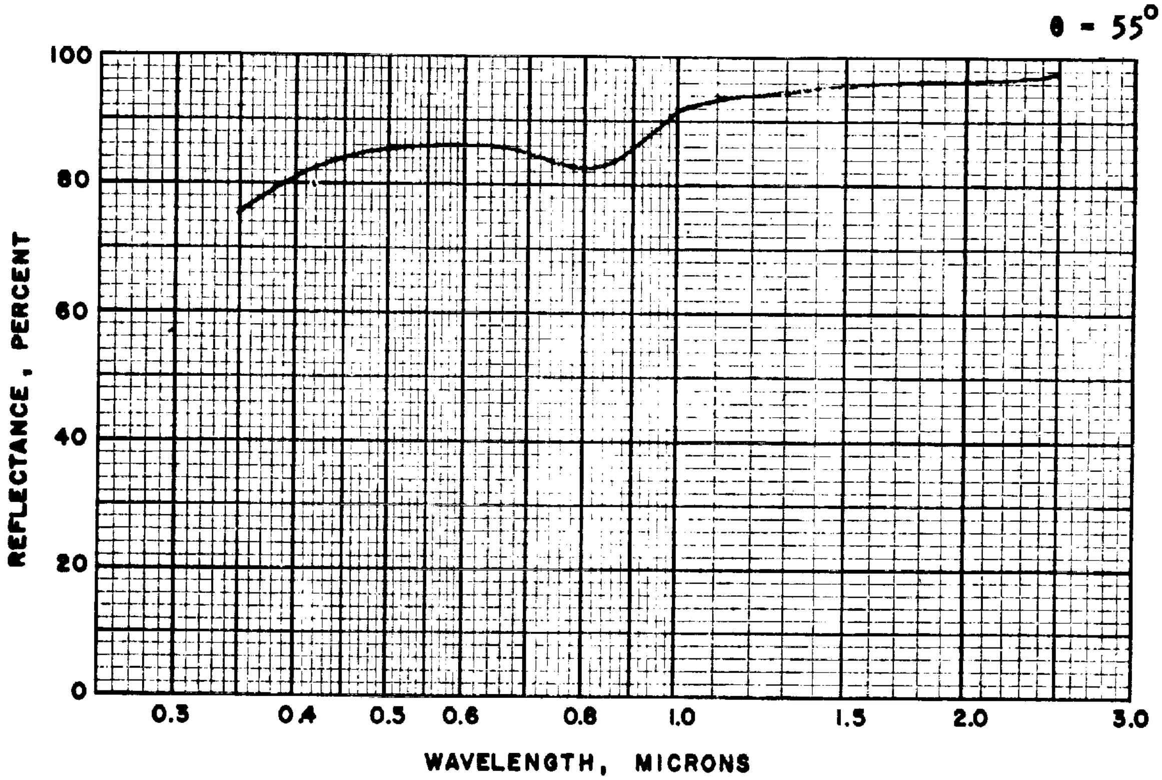

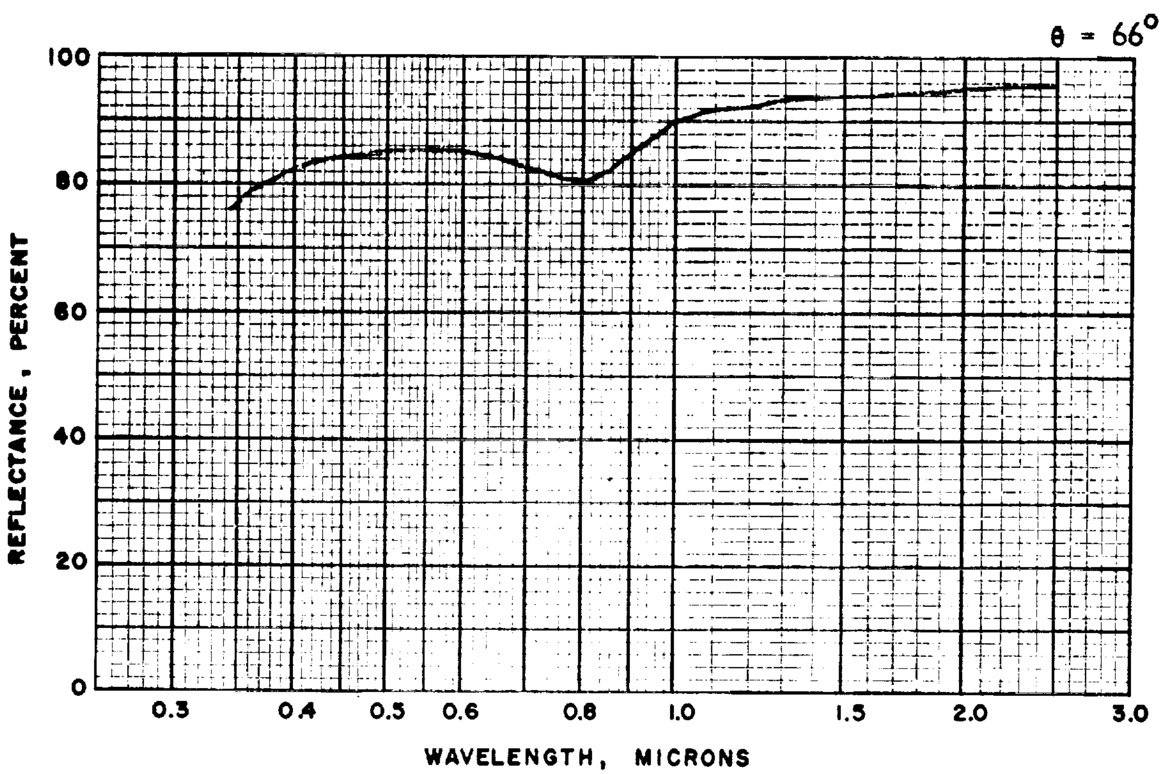

Figure 34 (Cont.): Sample 12A, Azimuthal Angle 0°
Angles of Incidence 55° and 66°

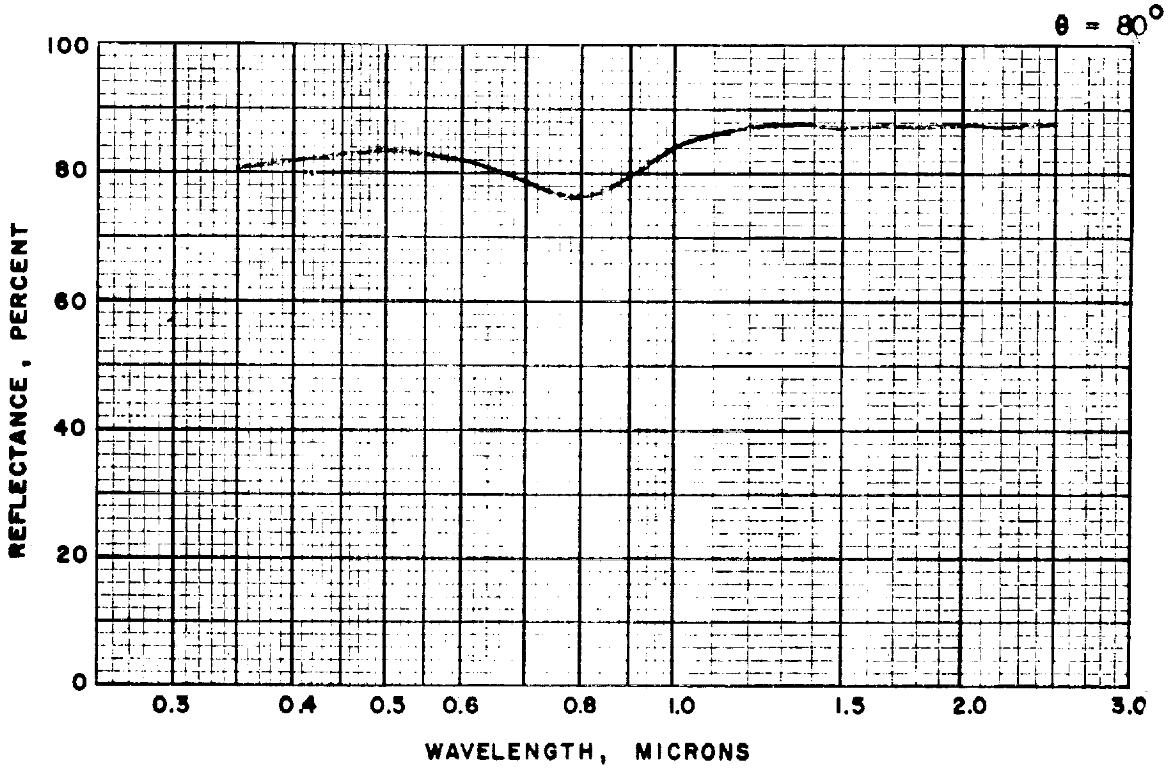

Figure 34 (Cont.): Sample 12A, Azimuthal Angle 0°
Angle of Incidence 80°

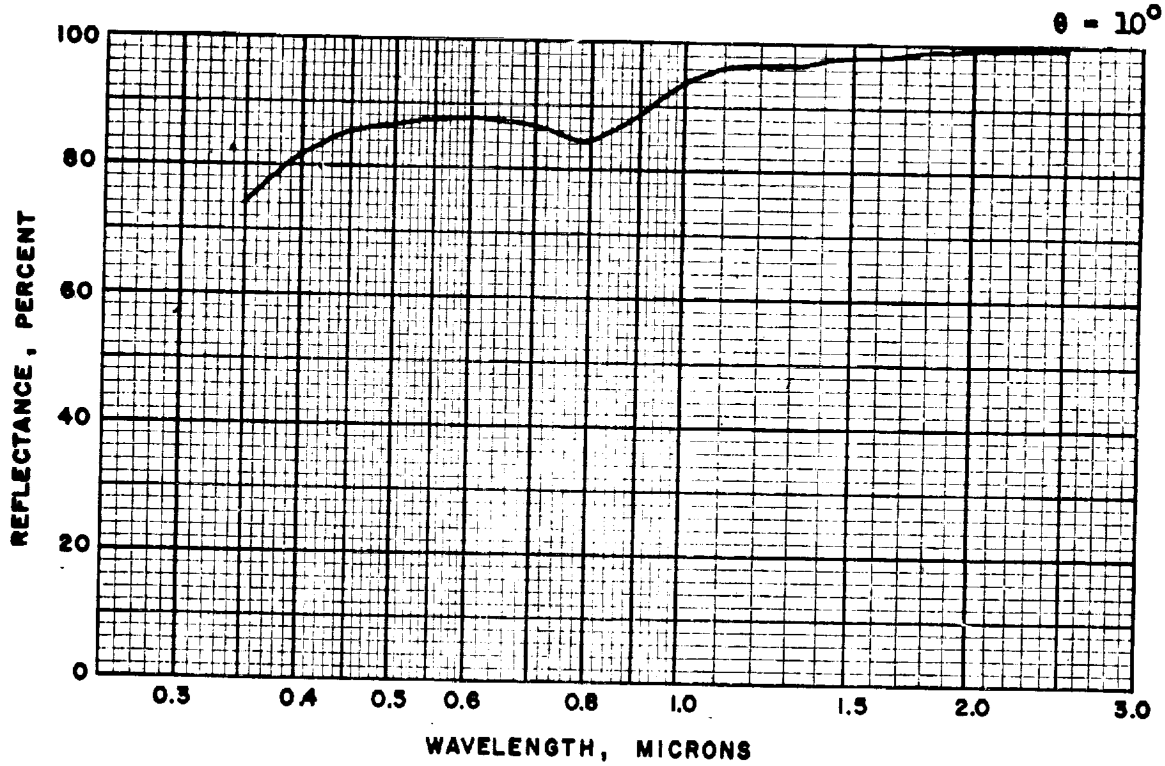

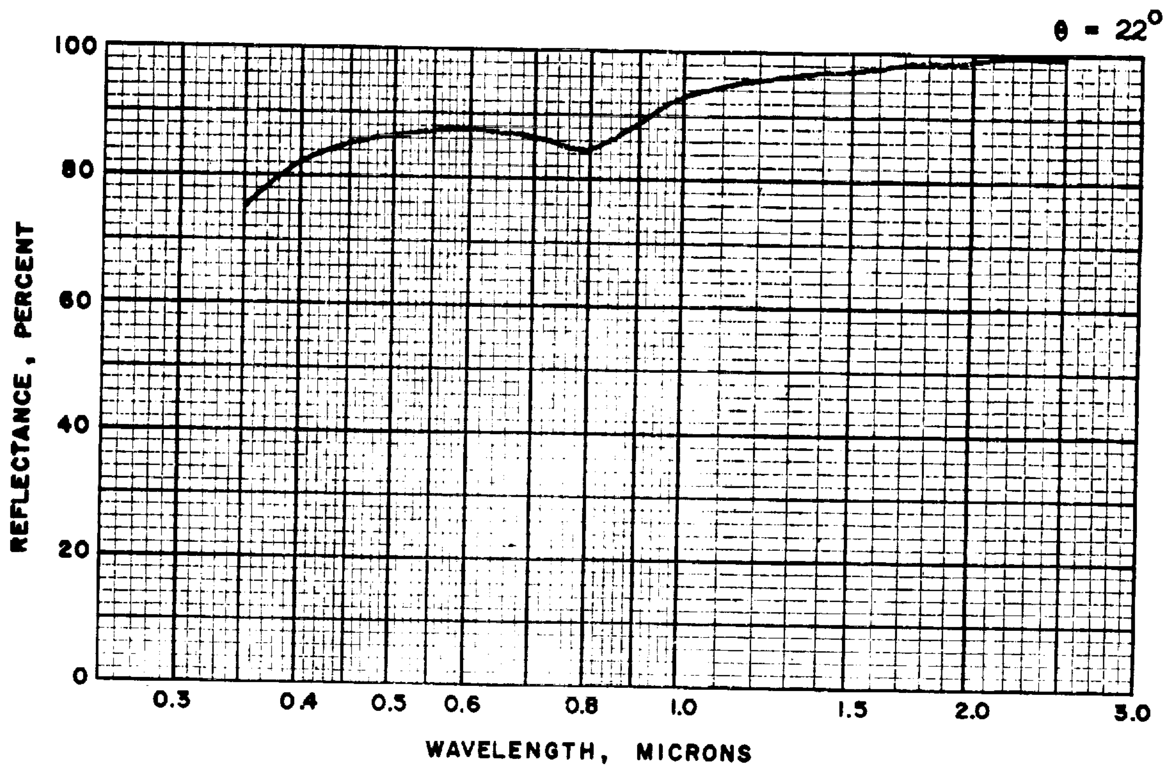

Figure 35: Sample 12A, Azimuthal Angle 45°, Angles of Incidence 10° and 22°

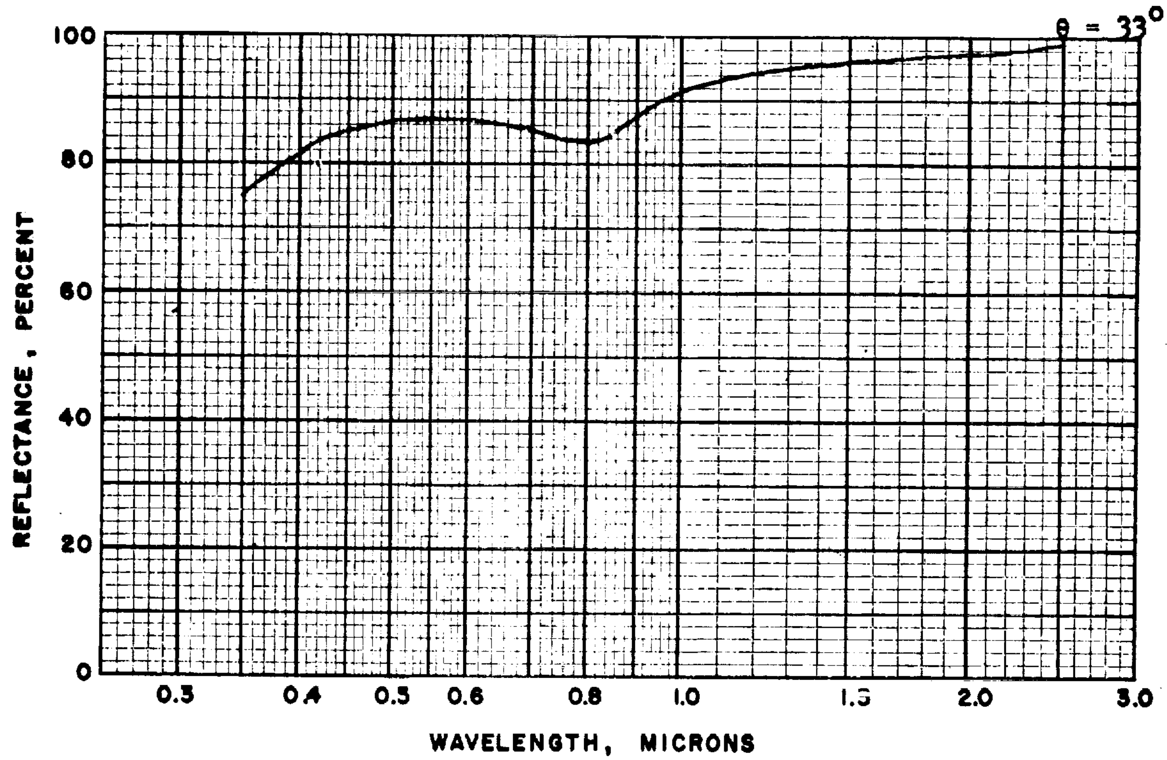

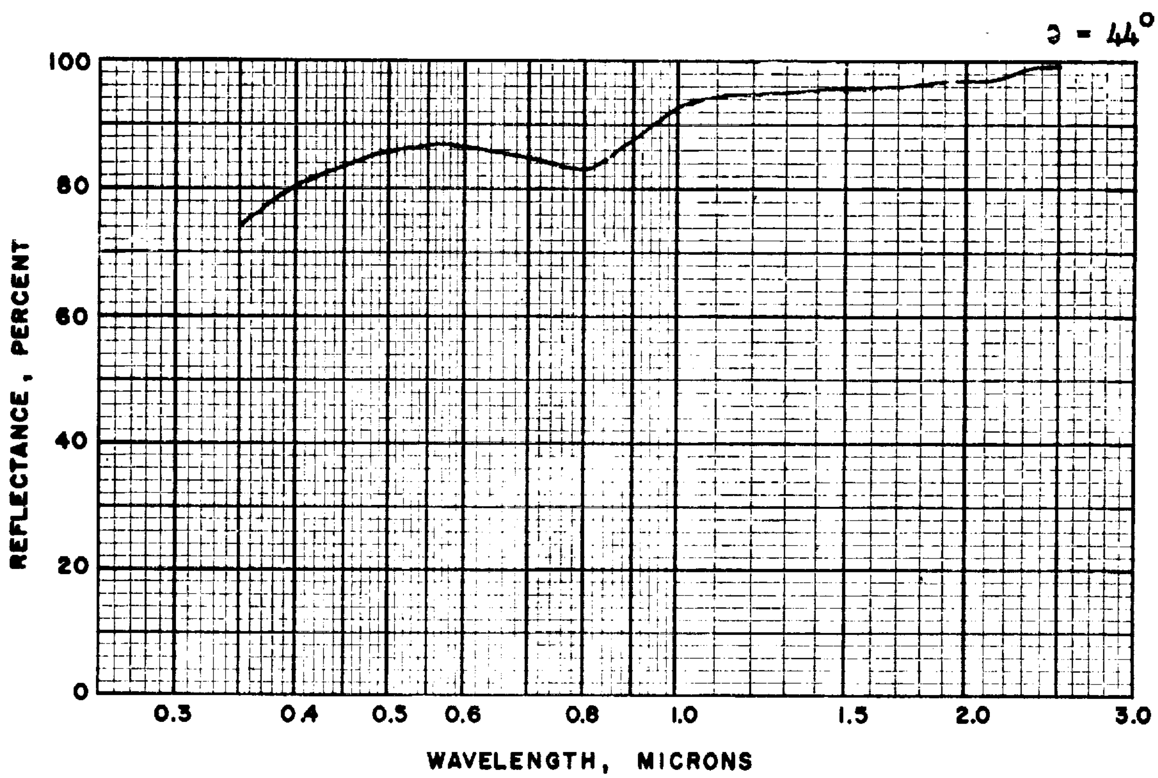

Figure 35 (Cont.): Sample 12A, Azimuthal Angle 45°, Angles of Incidence 33° and 44°

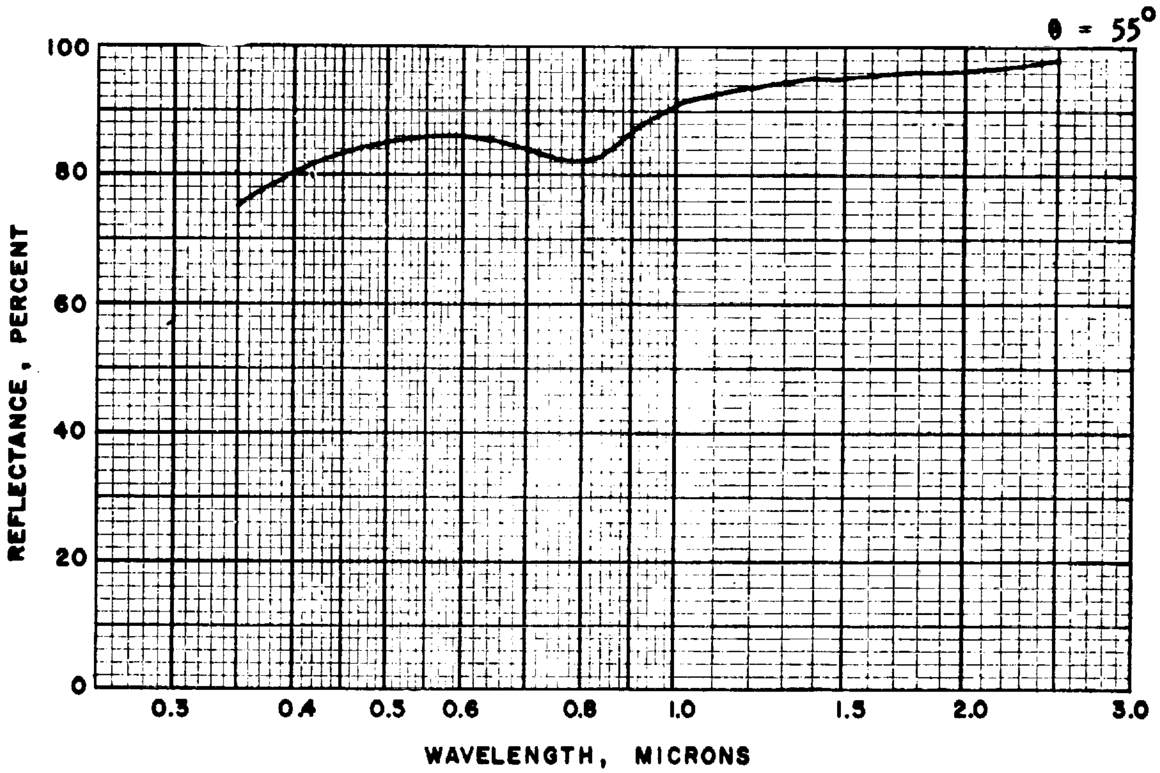

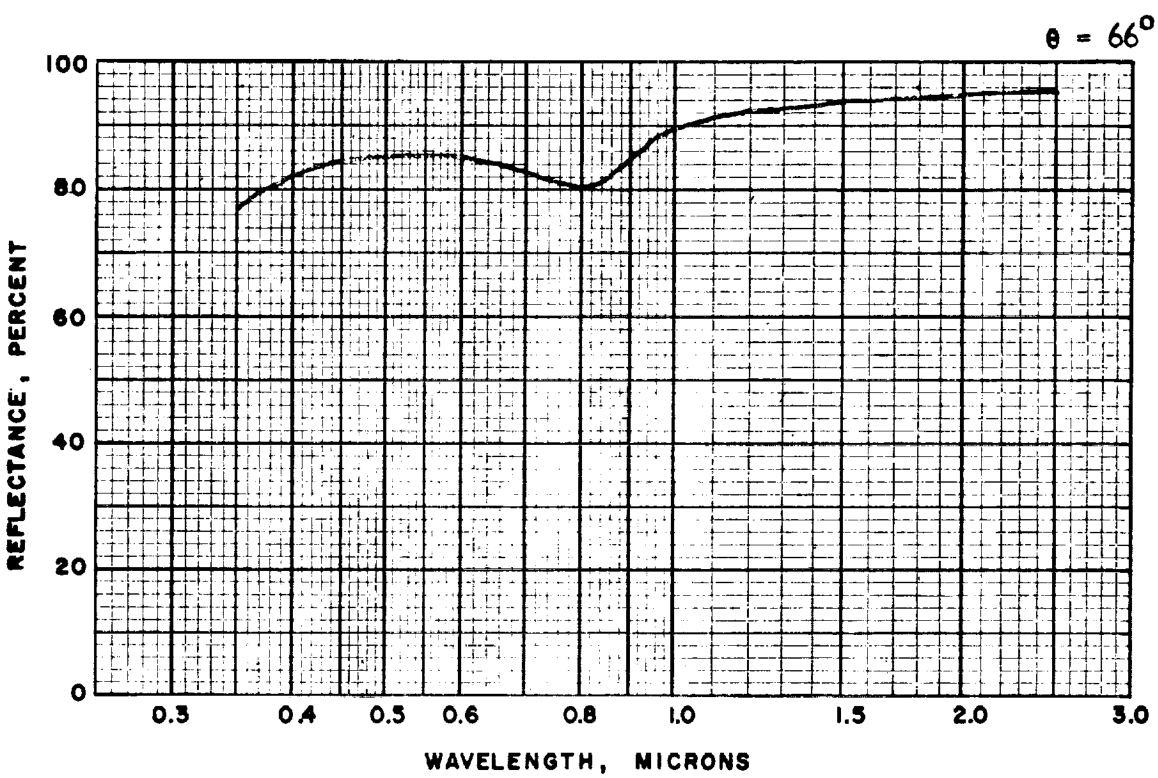

Figure 35 (Cont.): Sample 12A, Azimuthal Angle 45°, Angles of Incidence 55° and 66°

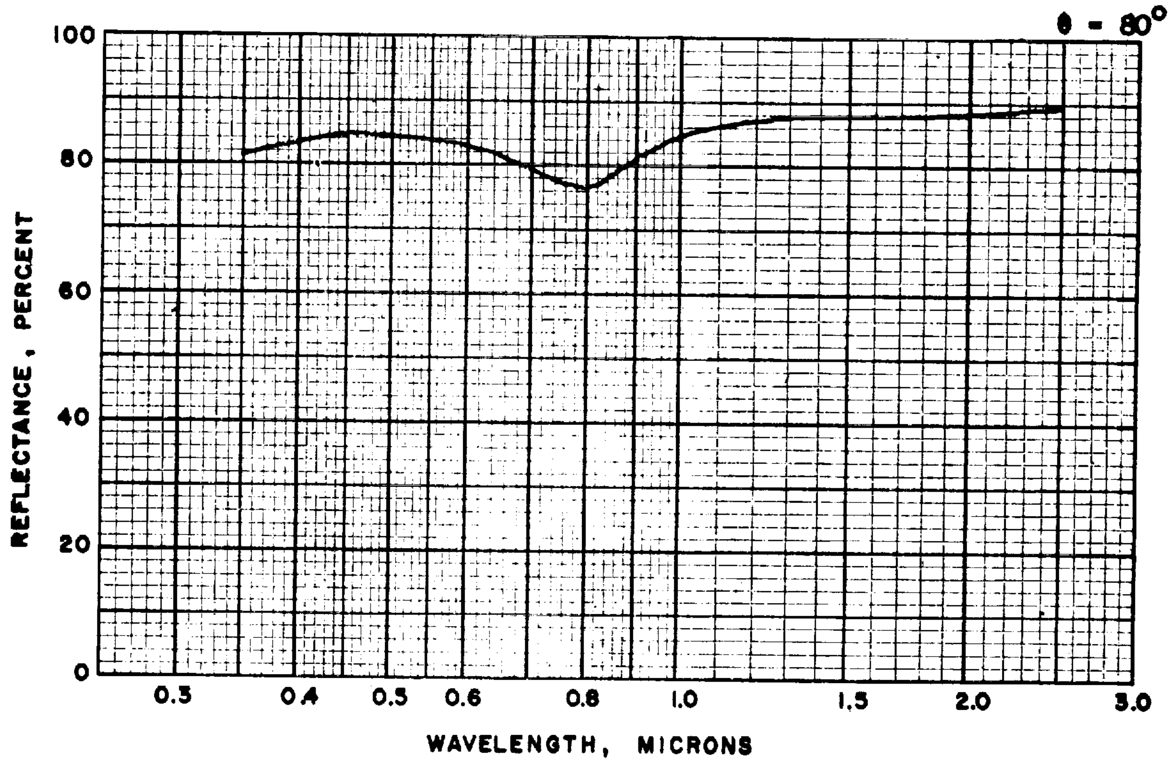

Figure 35 (Cont.): Sample 12A, Azimuthal Angle 45°, Angle of Incidence 80°

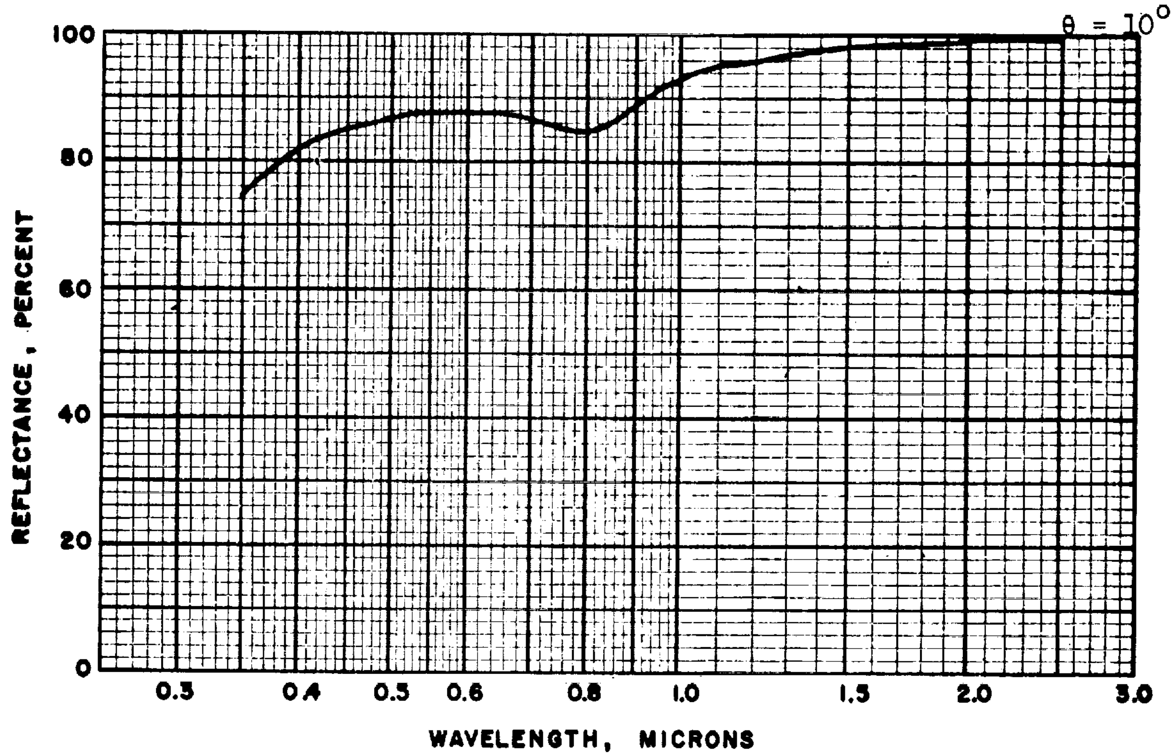

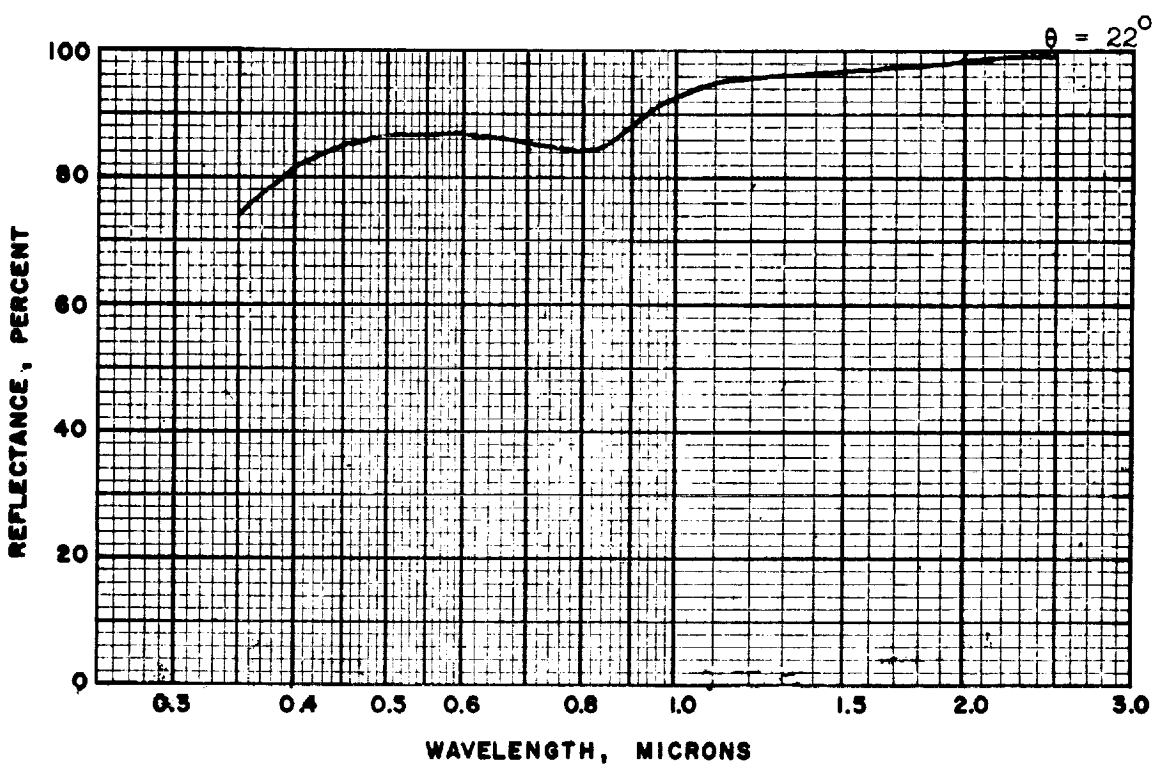

Figure 36: Sample 12A, Azimuthal Angle 60°, Angles of Incidence 10° and 22°

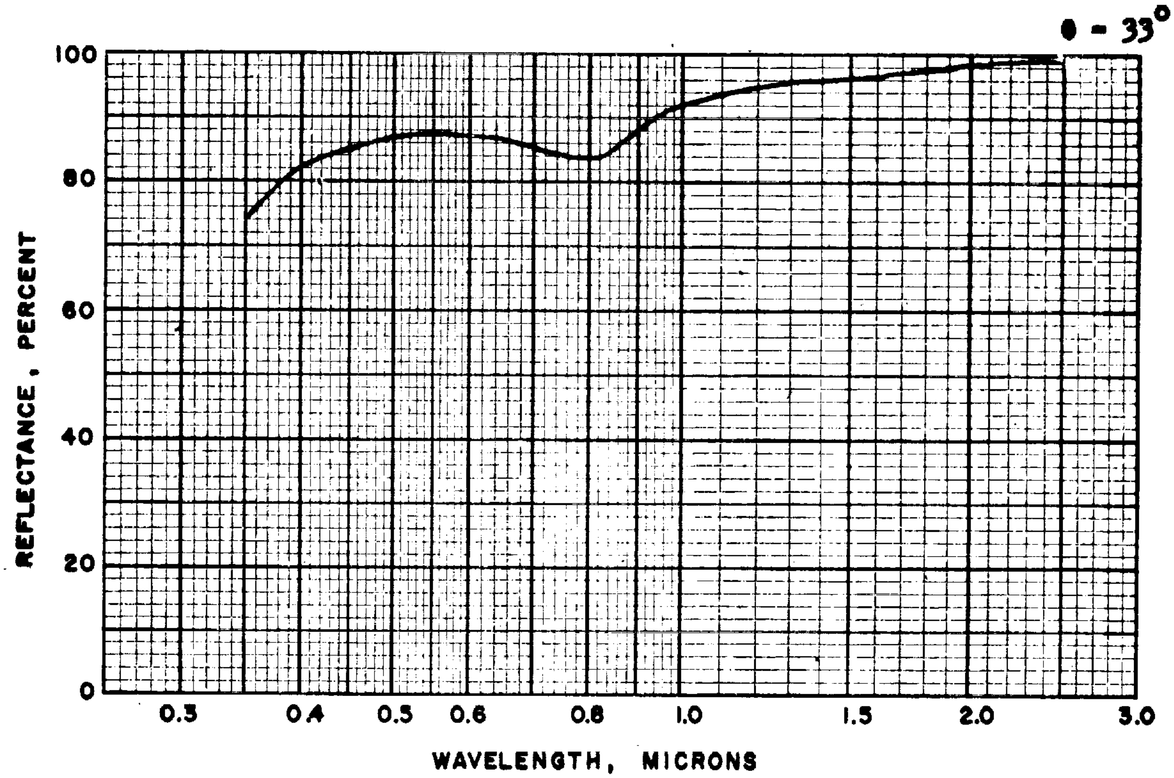

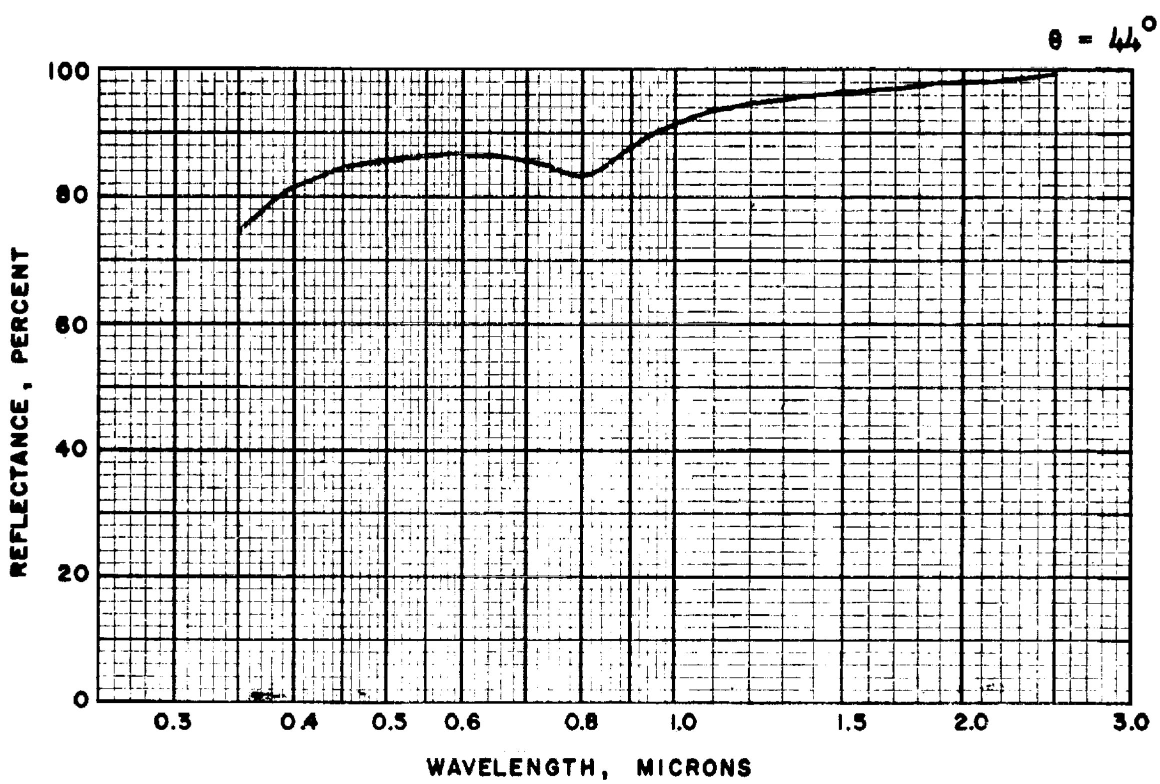

Figure 36 (Cont.): Sample 12A, Azimuthal Angle 60°, Angles of Incidence 33° and 44°

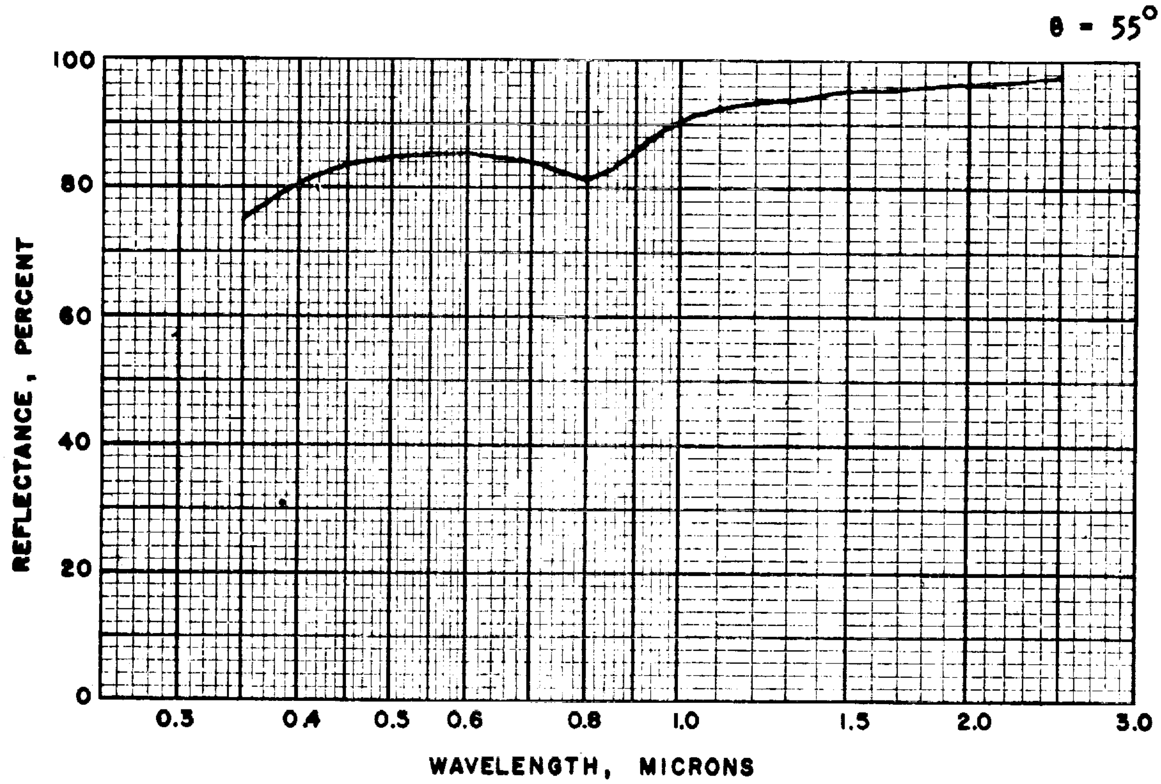

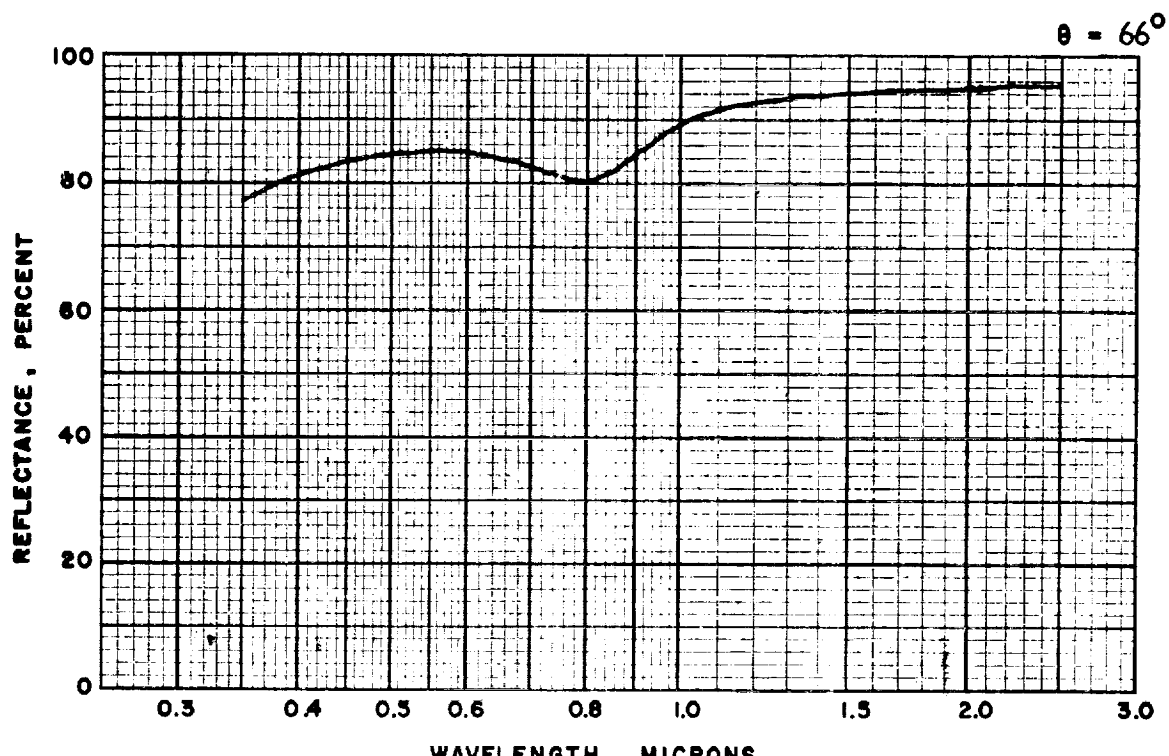

Figure 36 (Cont.): Sample 12A, Azimuthal Angle 60°, Angles of Incidence 55° and 66°

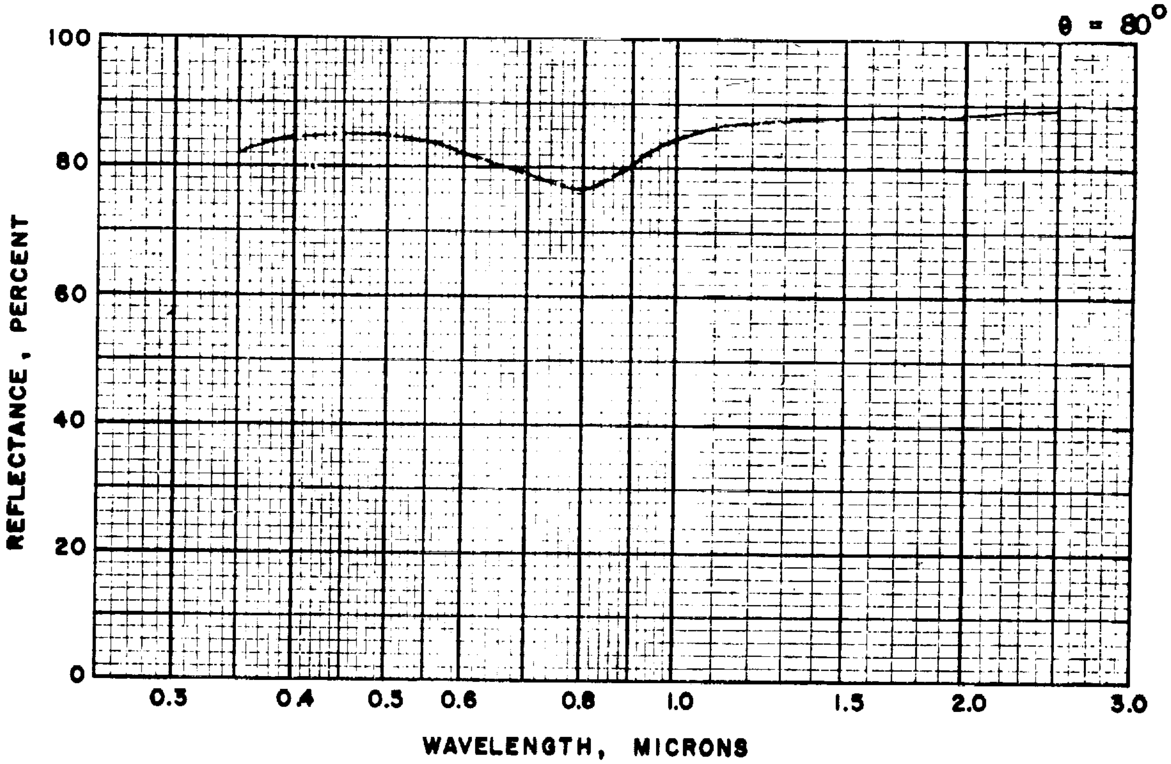

Figure 36 (Cont.): Sample 12A, Azimuthal Angle 60°, Angle of Incidence 80°

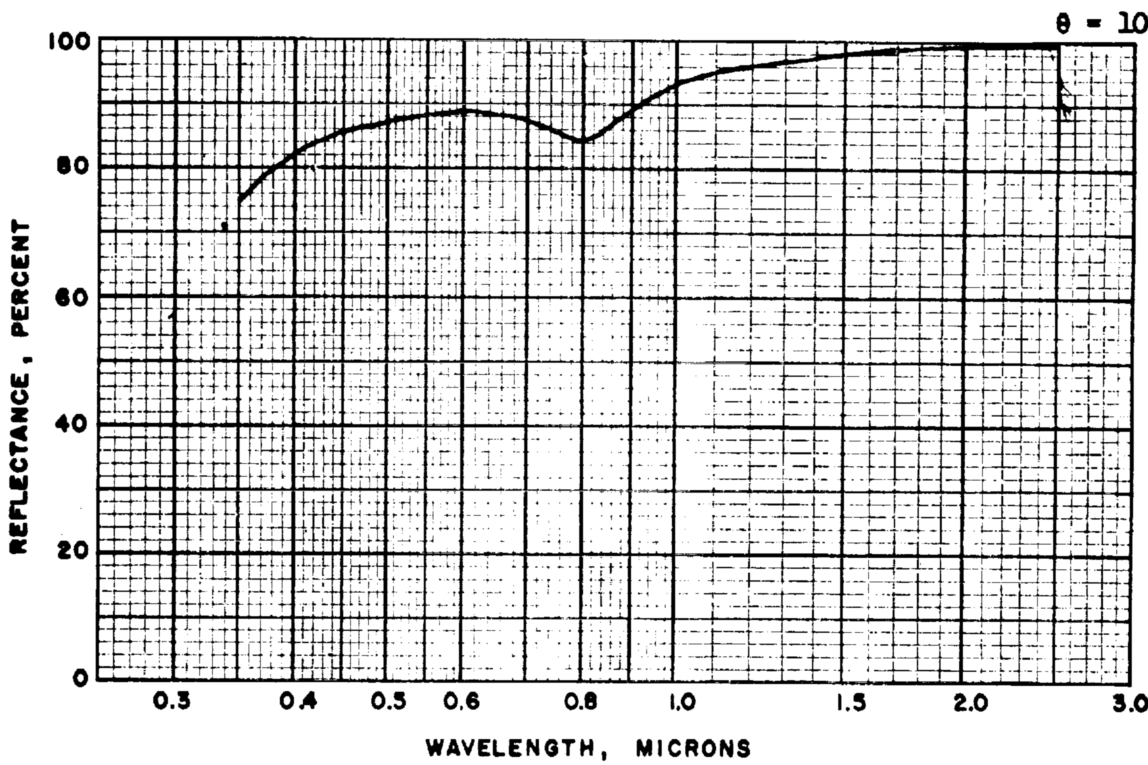

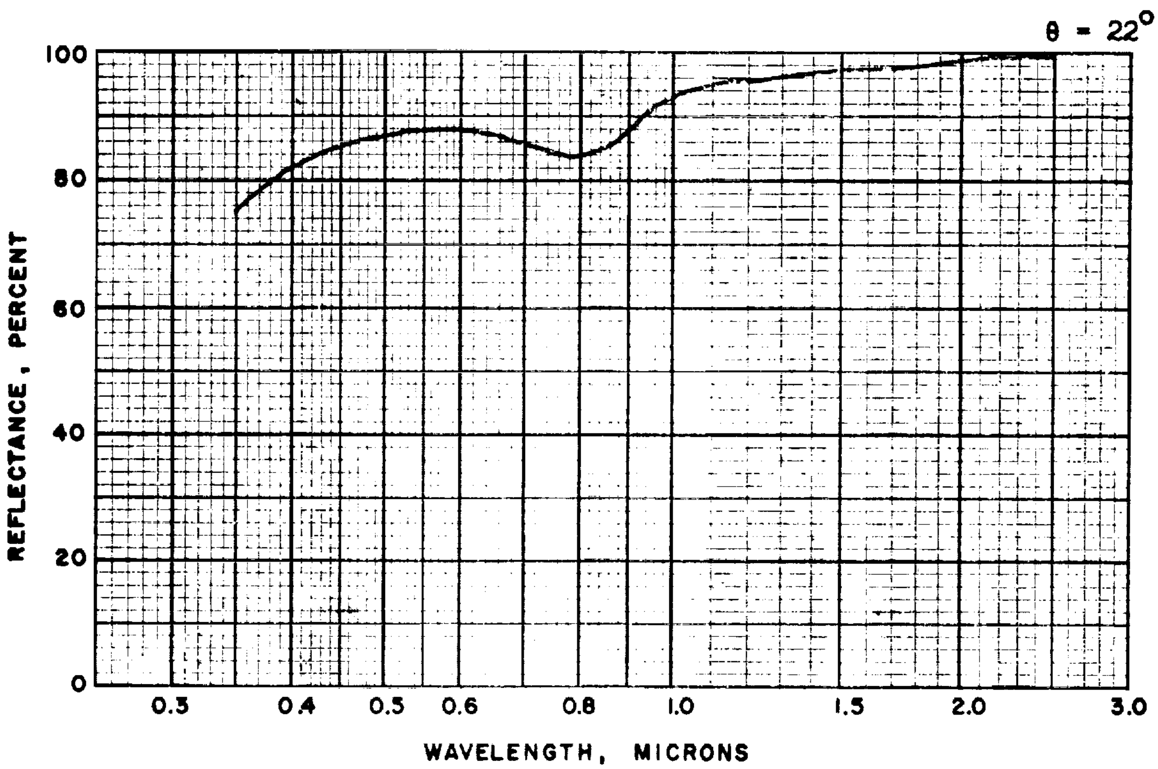

Figure 37: Sample 12A, Azimuthal Angle 90°,
Angles of Incidence 10° and 22°

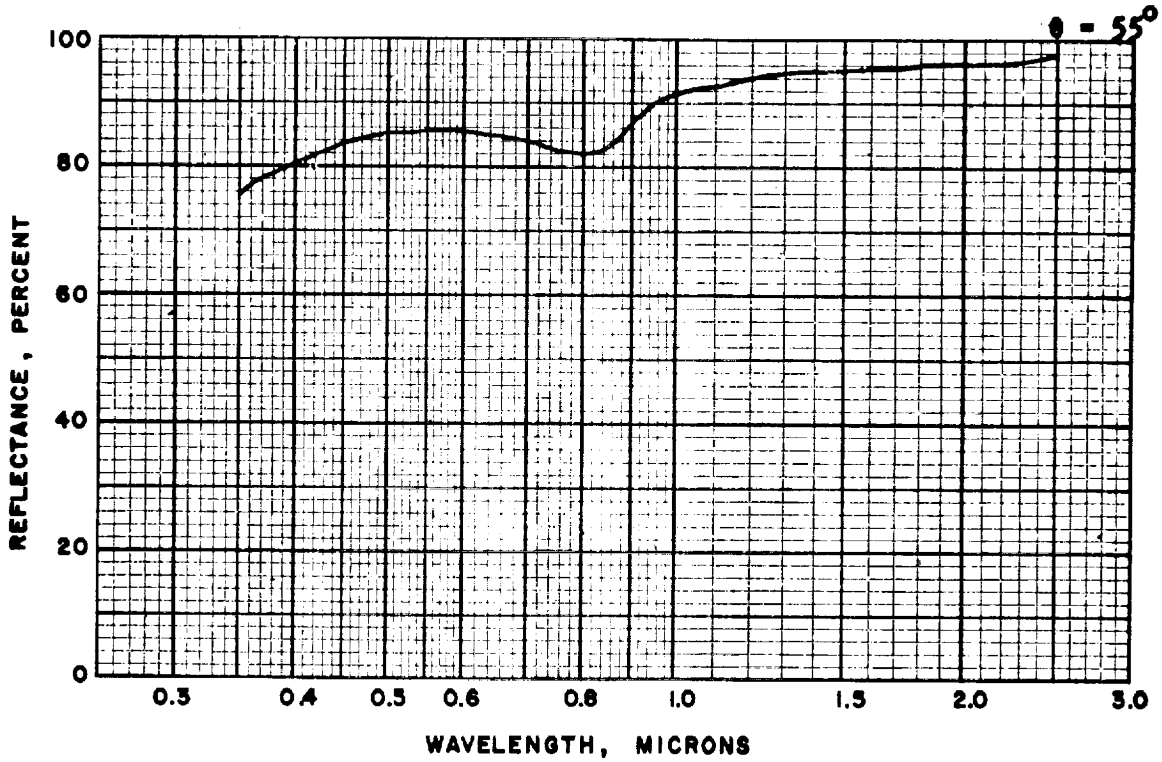

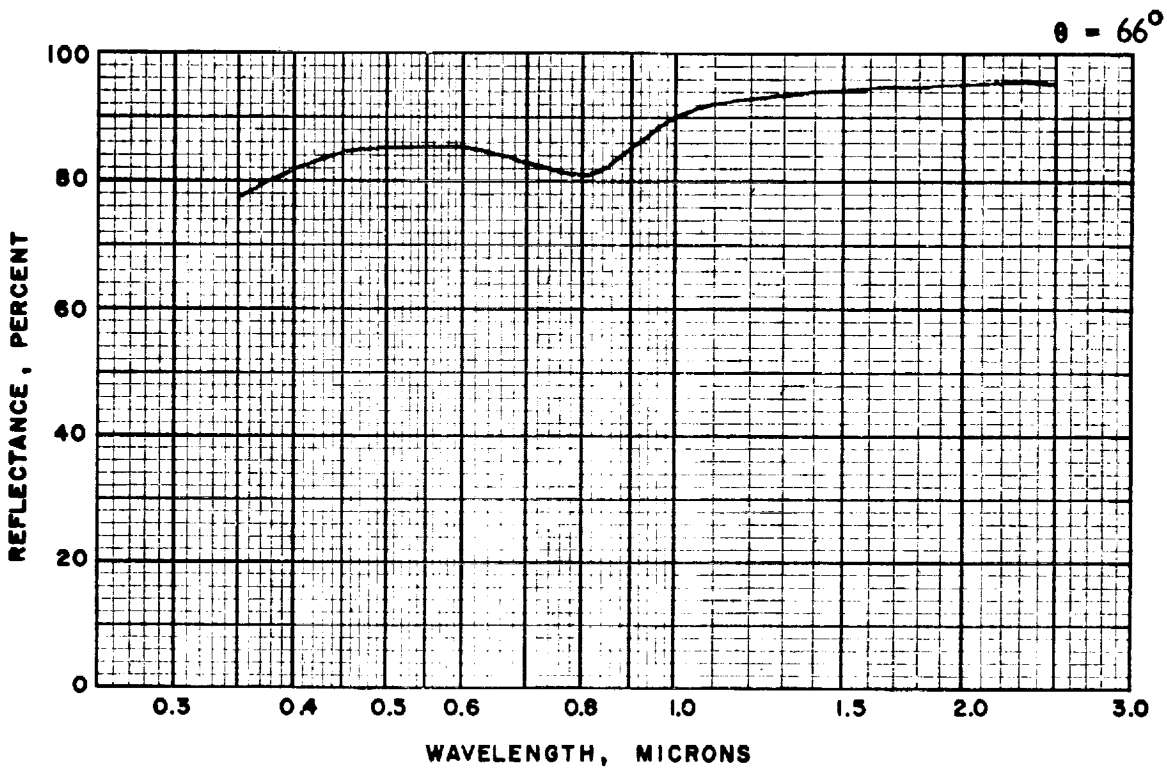

Figure 37 (Cont.): Sample 12A, Azimuthal Angle 90°, Angles of Incidence 55° and 66°

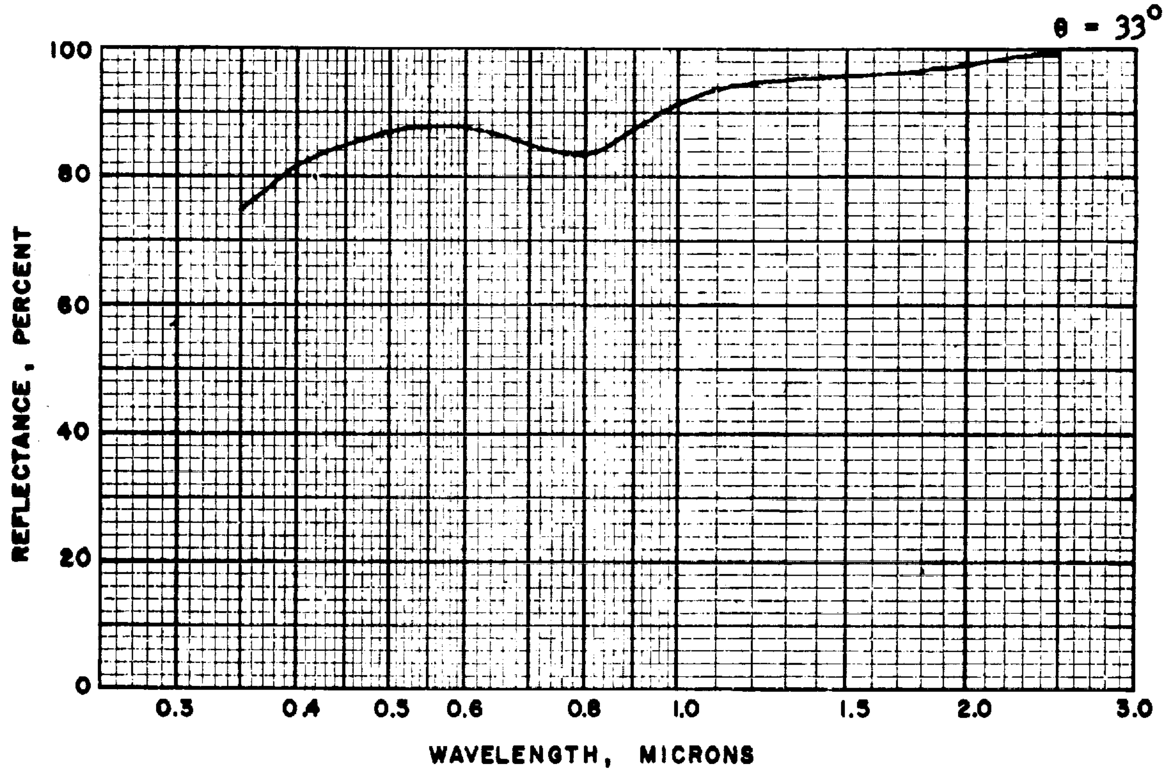

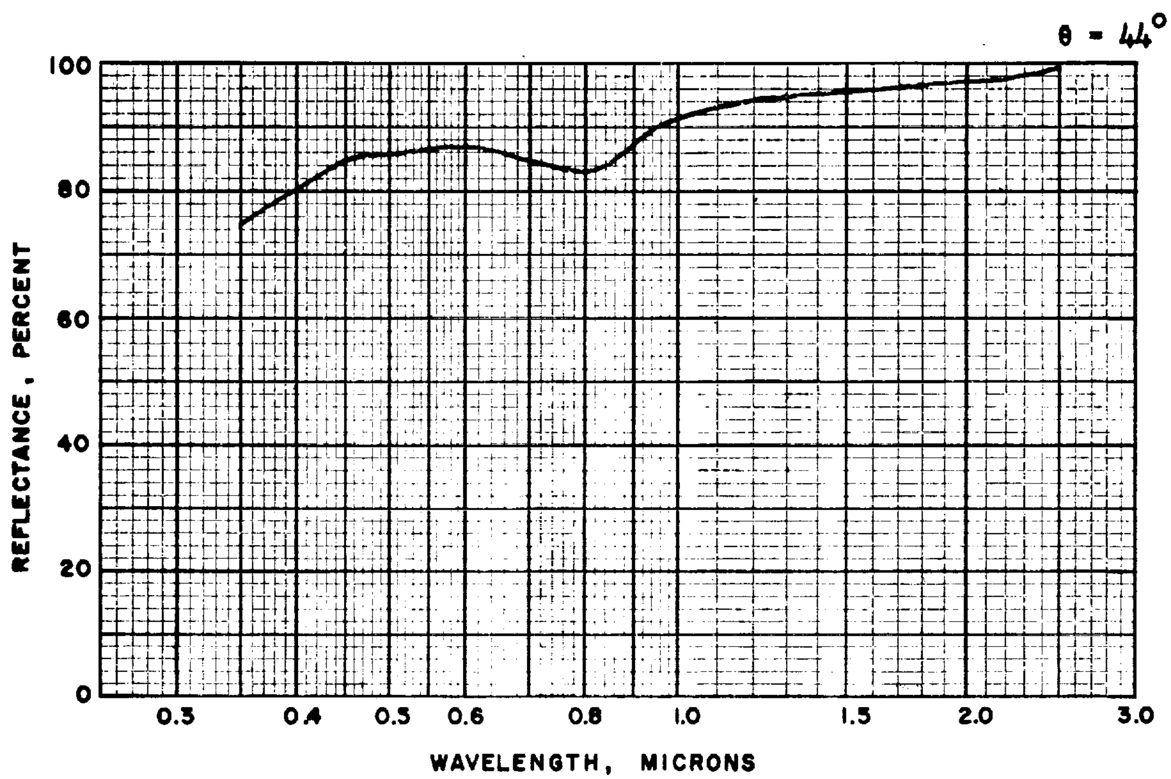

Figure 37 (Cont.): Sample 12A, Azimuthal Angle 90°, Angles of Incidence 33° and 44°

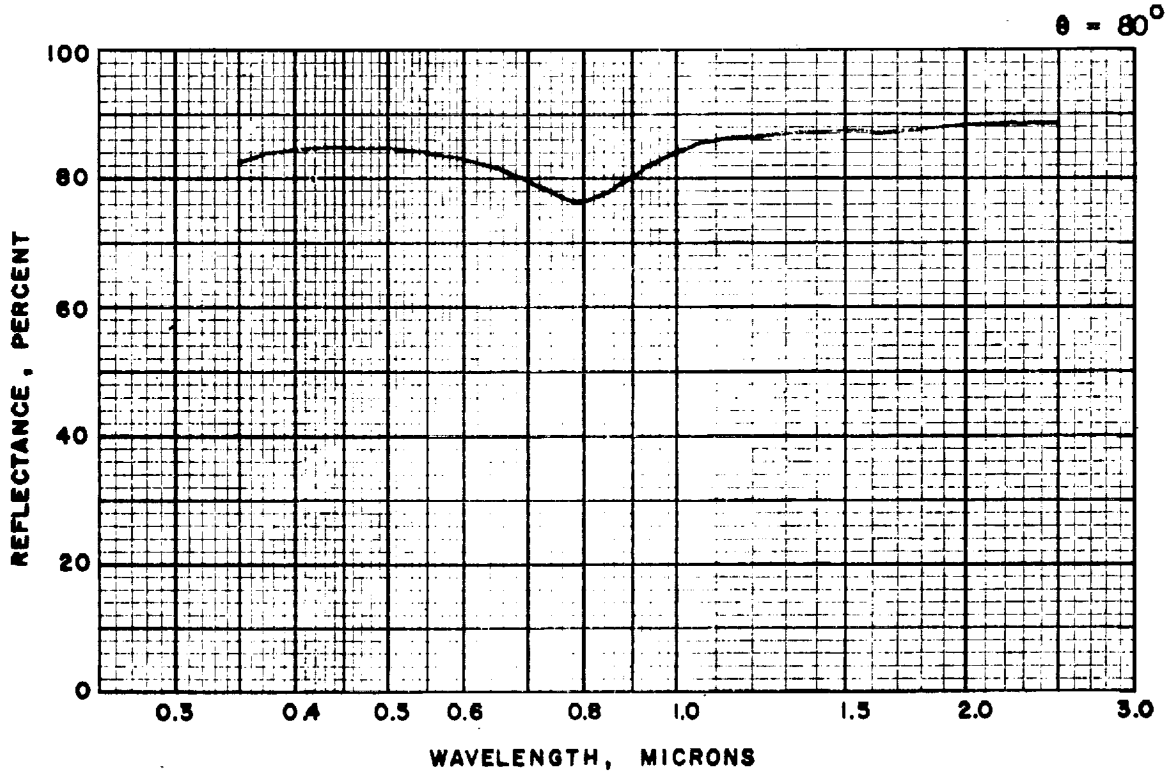

Figure 37 (Cont.): Sample 12A, Azimuthal Angle 90°, Angle of Incidence 80°

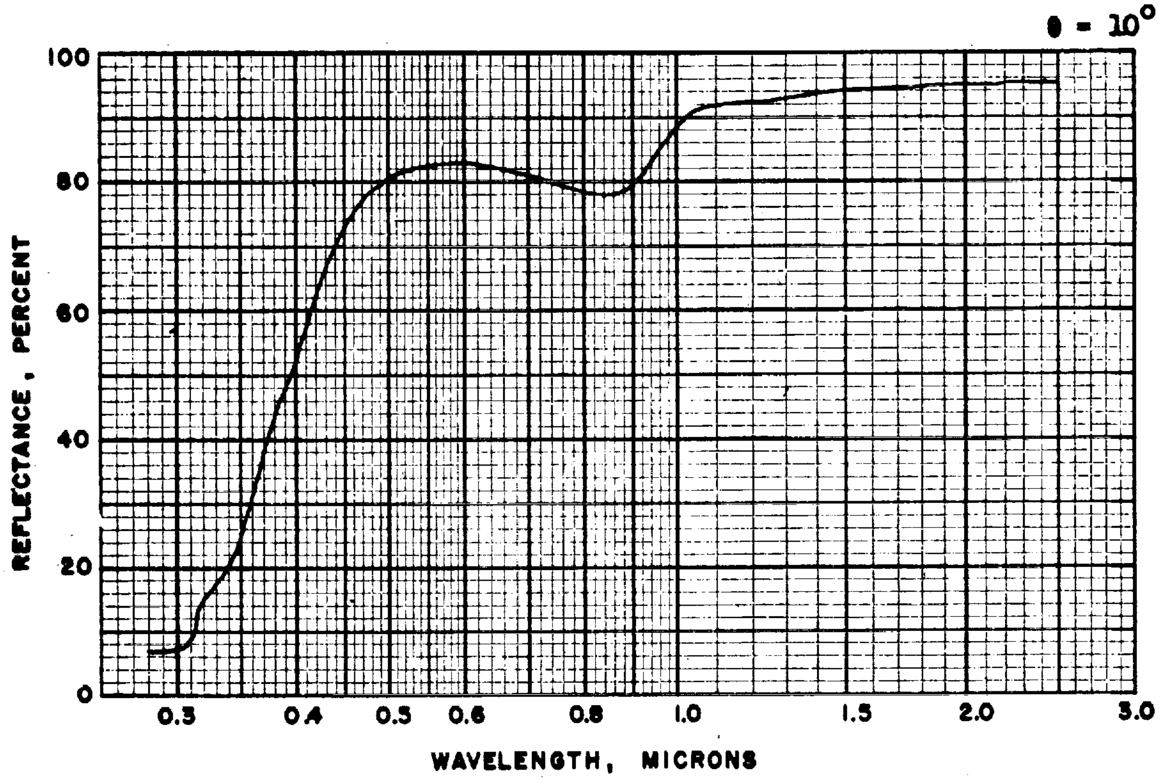

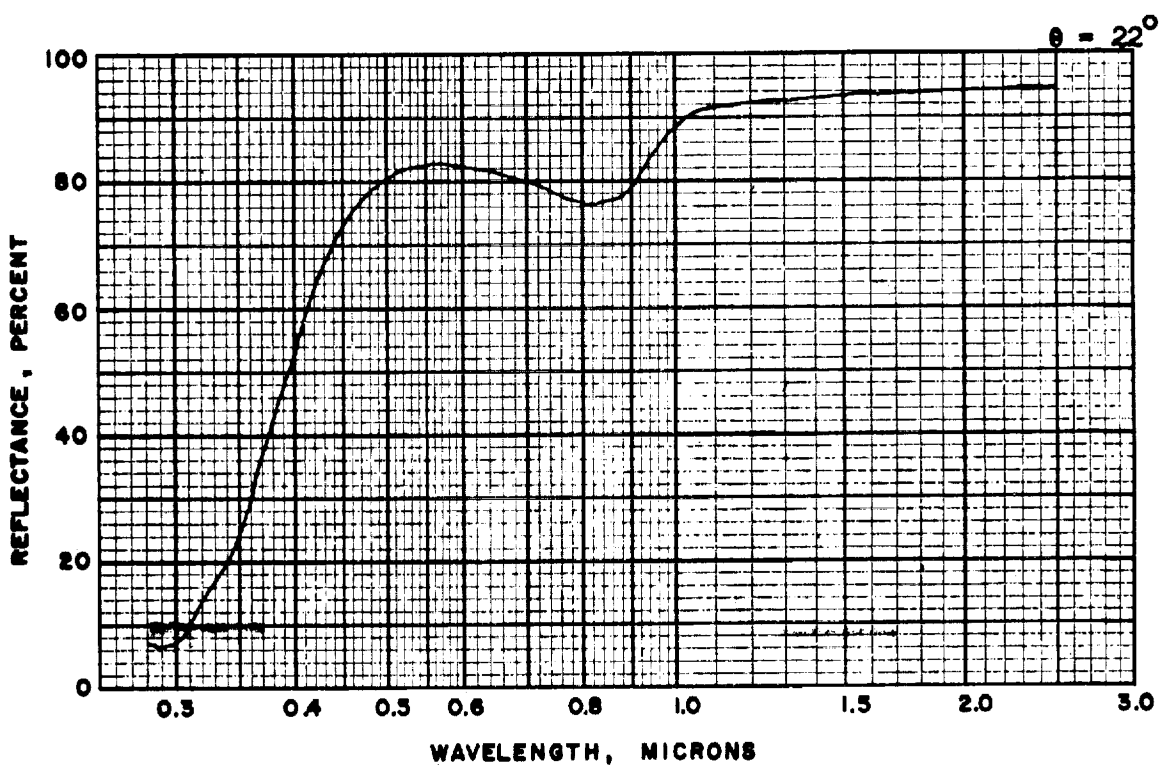

Figure 38: Sample 12B, Azimuthal Angle 0°, Angles of Incidence 10° and 22°

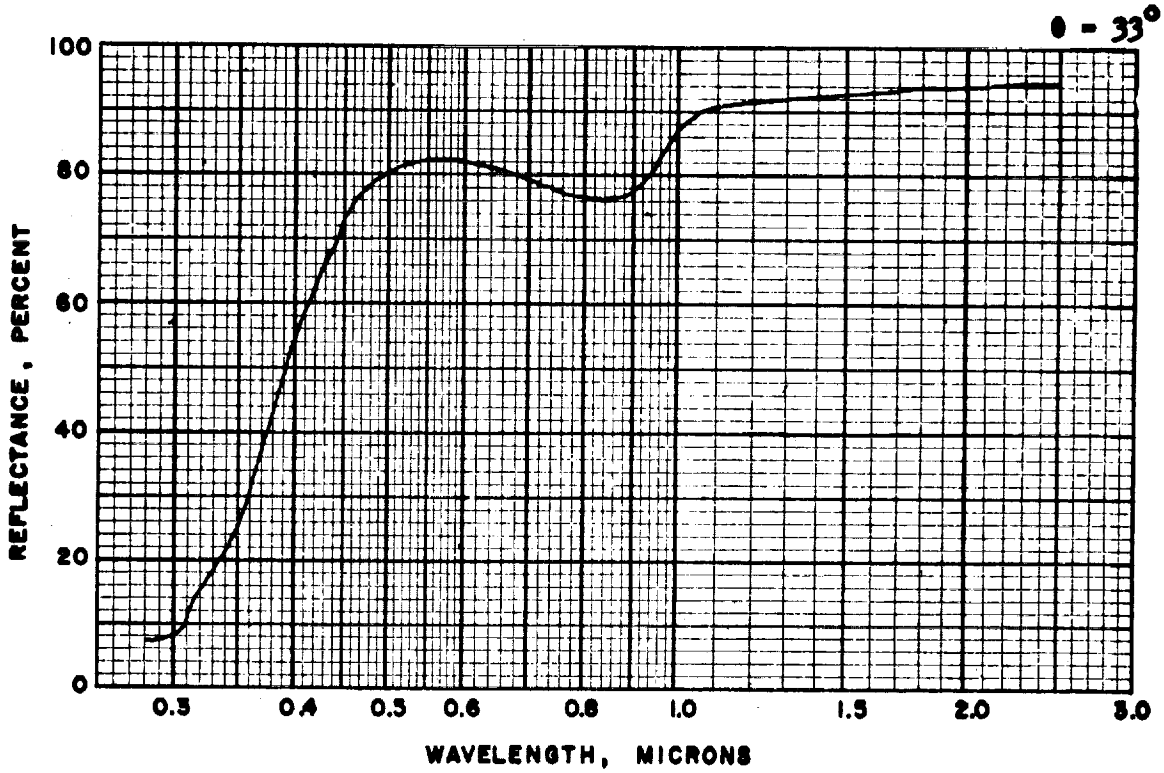

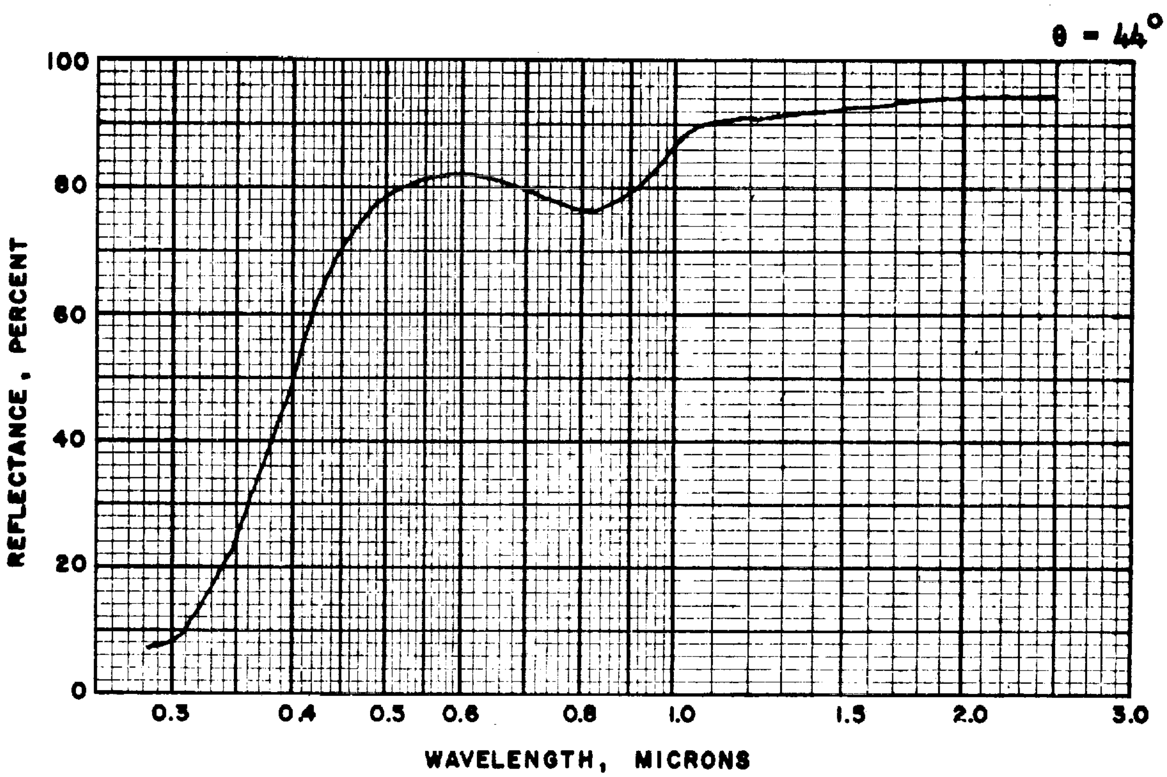

Figure 38: Sample 12B, Azimuthal Angle 0°,
(Cont.) Angles of Incidence 33° and 44°

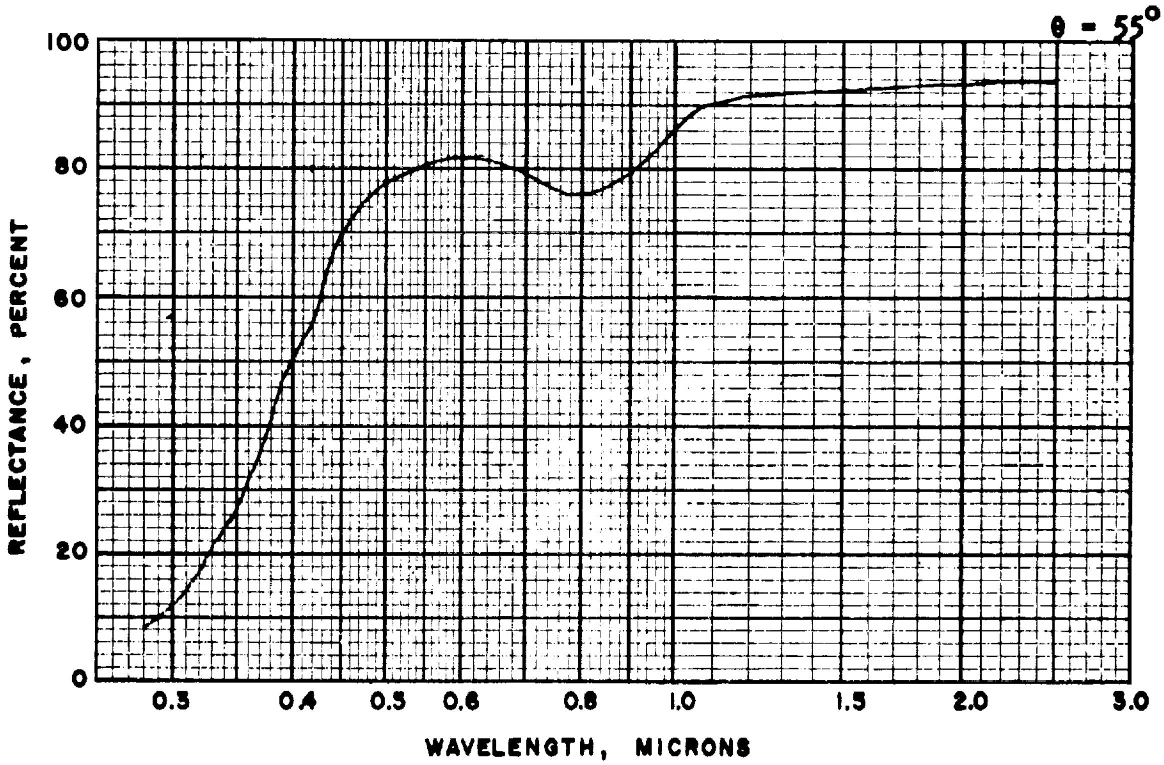

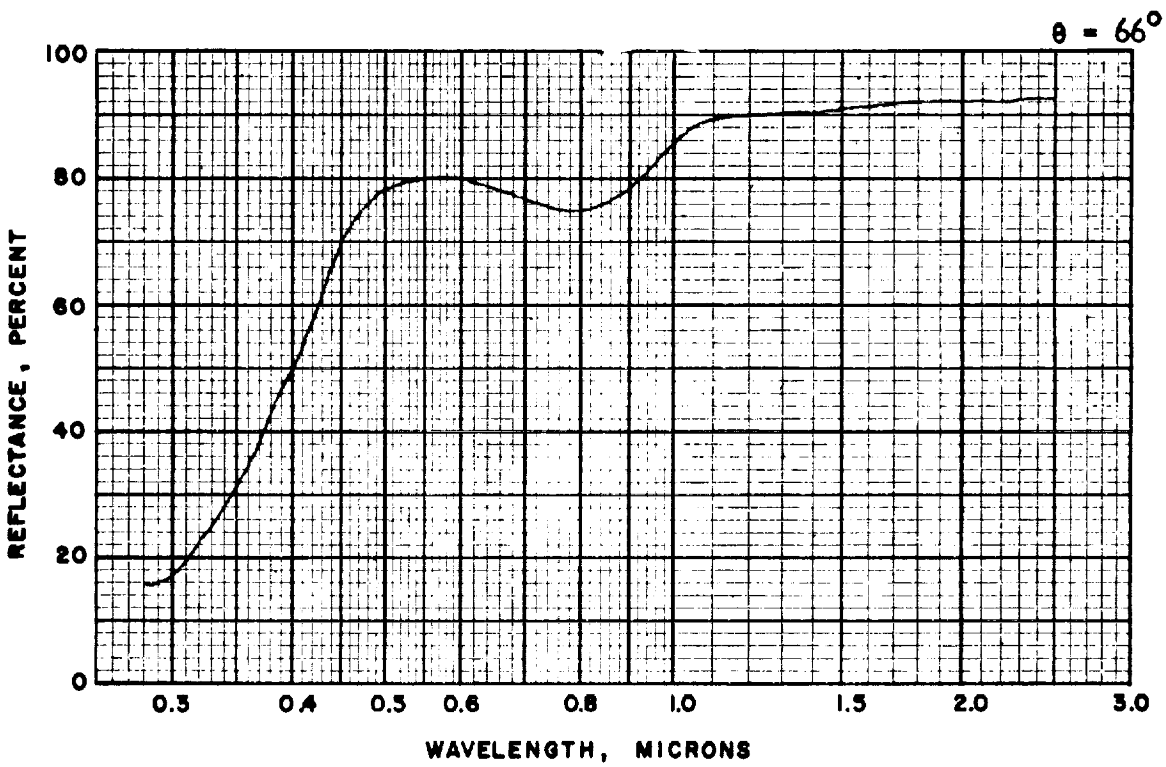

Figure 38 (Cont.): Sample 12B, Azimuthal Angle 0°, Angles of Incidence 55° and 66°

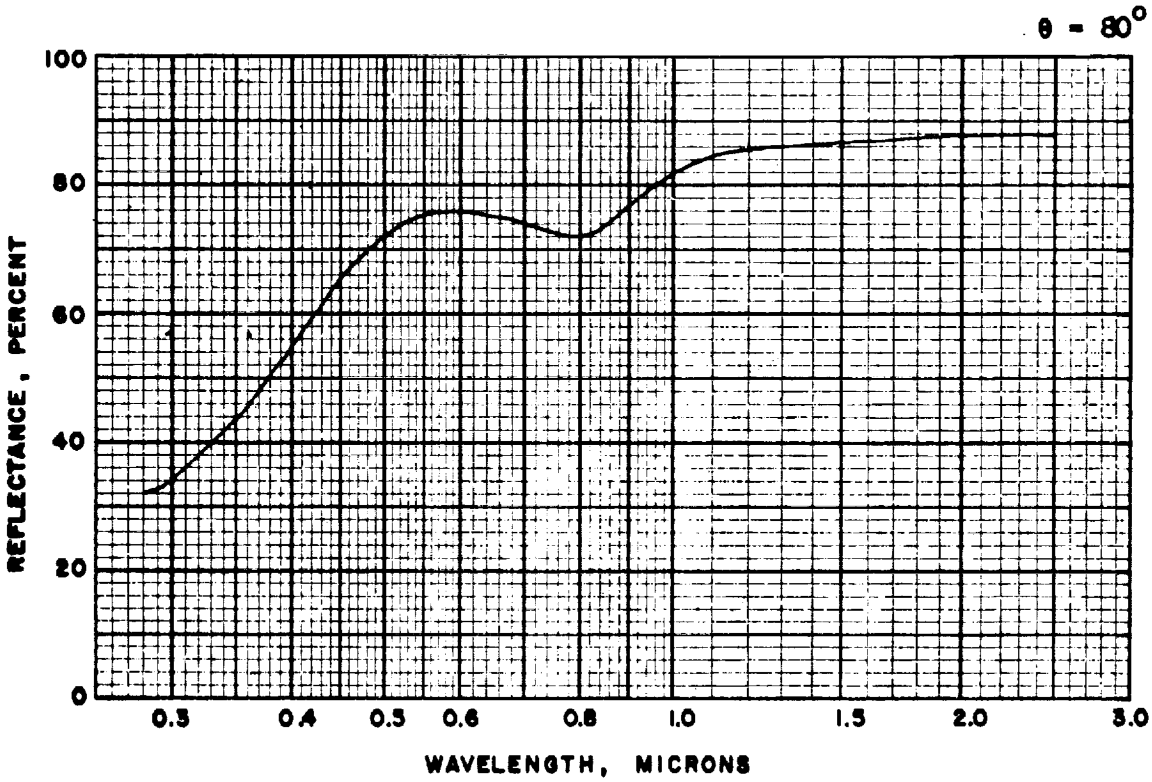

Figure 38 (Cont.): Sample 12B, Azimuthal Angle 0°, Angle of Incidence 80°

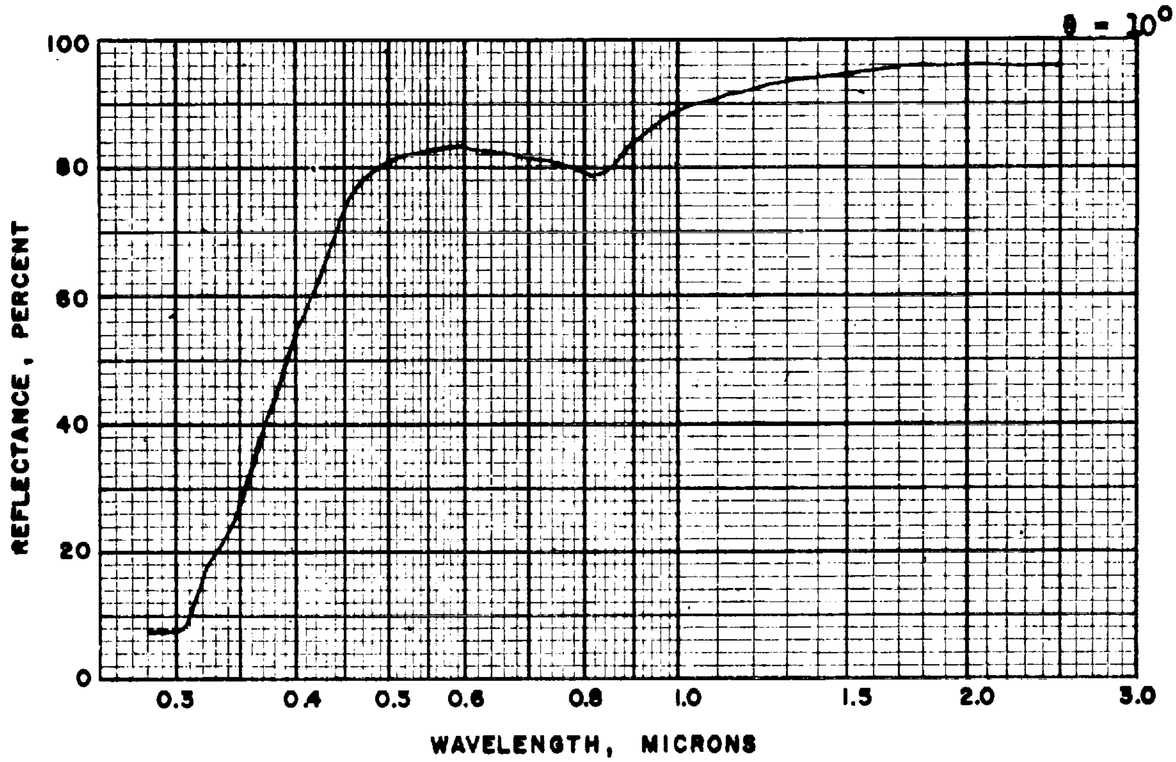

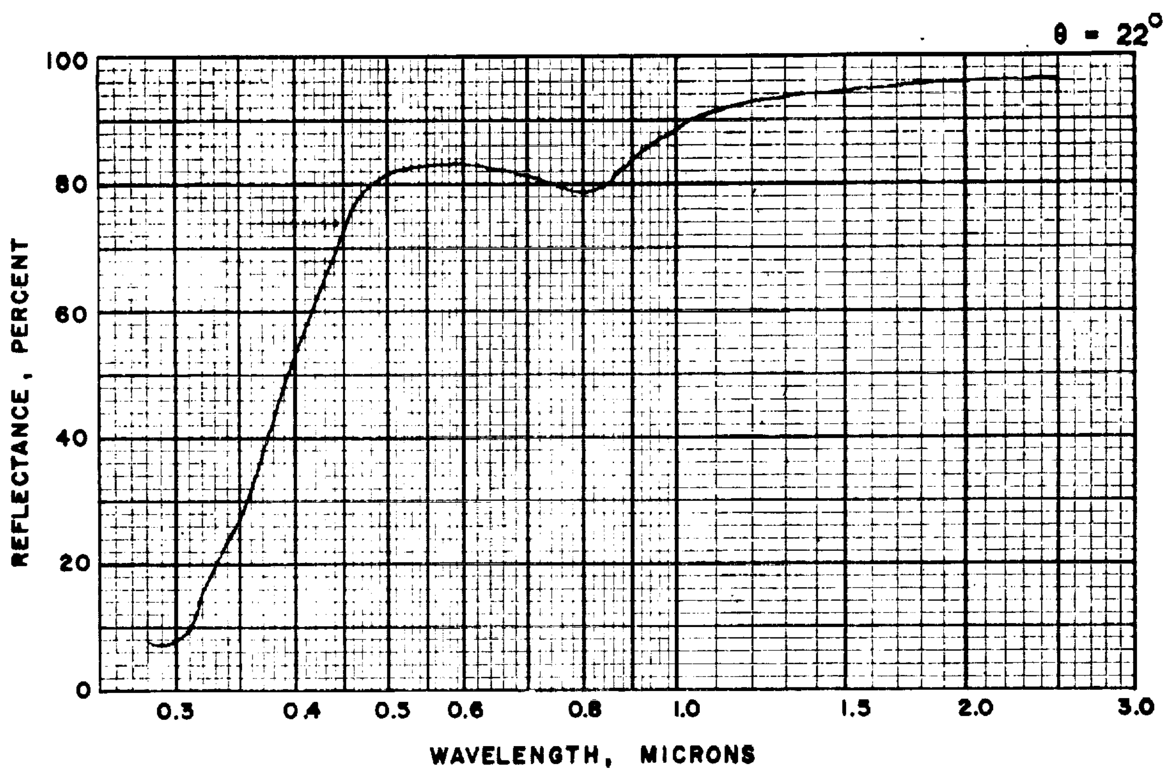

Figure 39: Sample 12B, Azimuthal Angle 45°, Angles of Incidence 10° and 22°

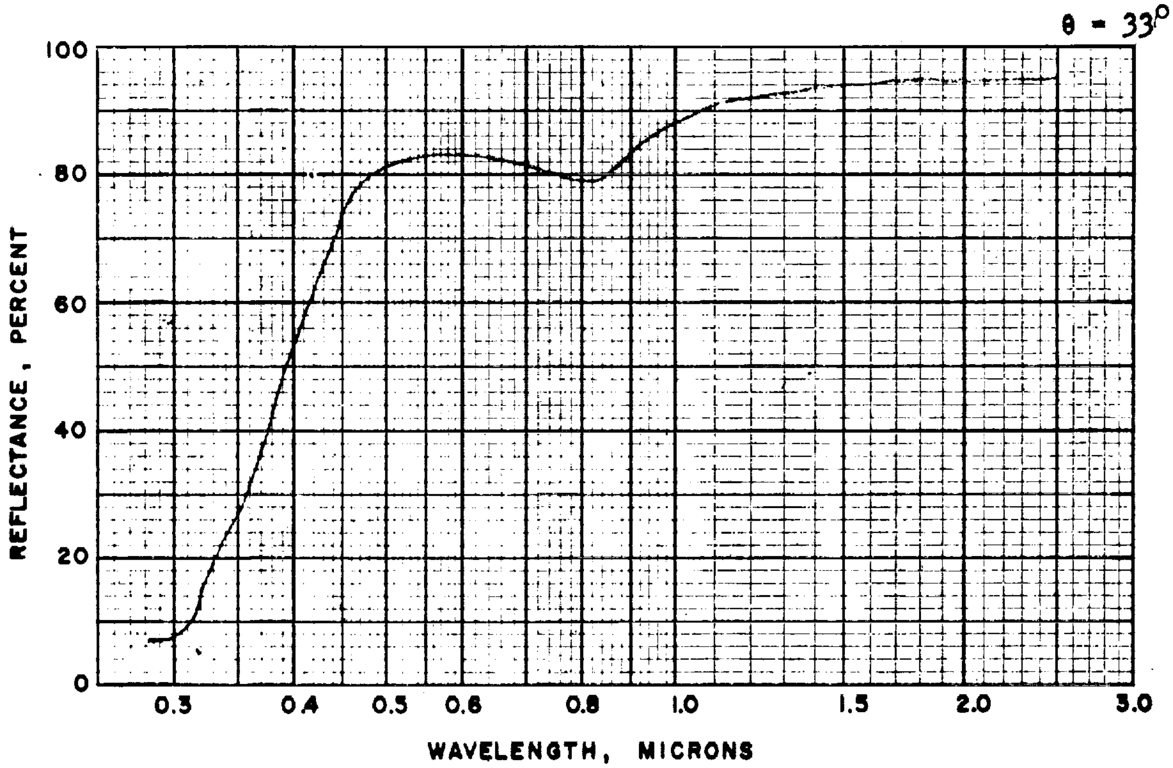

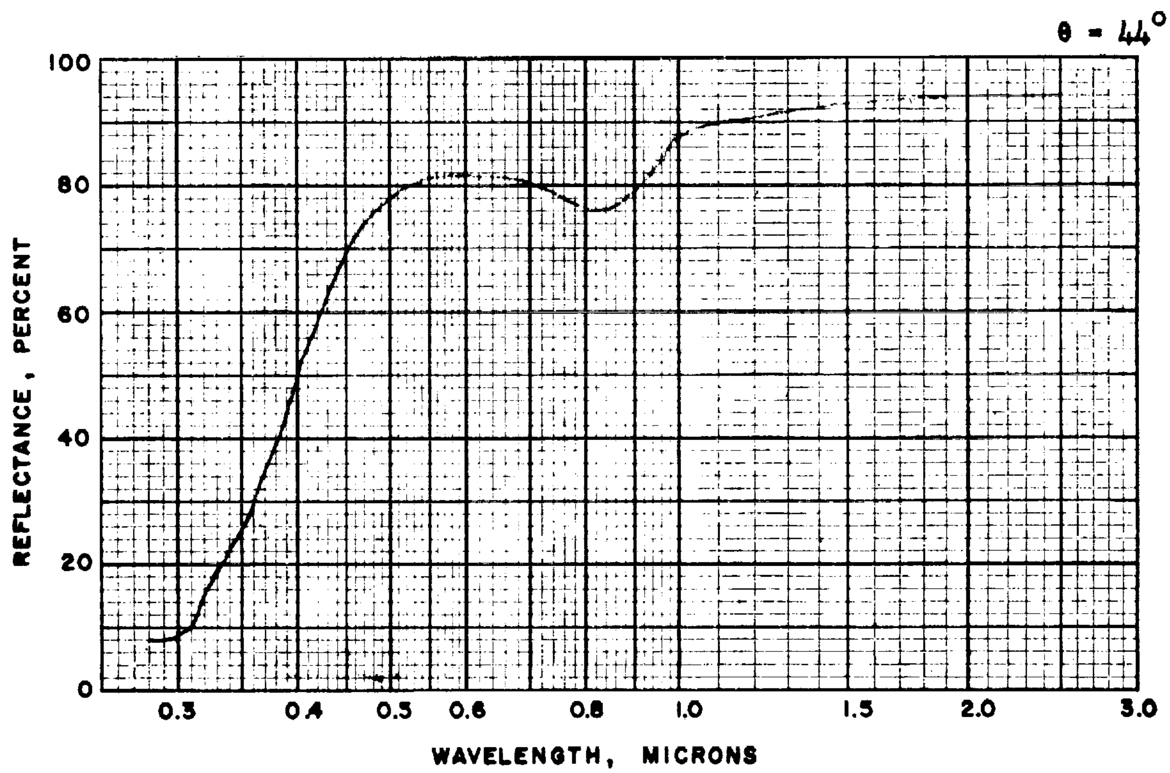

Figure 39 (Cont.): Sample 12B, Azimuthal Angle 45°, Angles of Incidence 33° and 44°

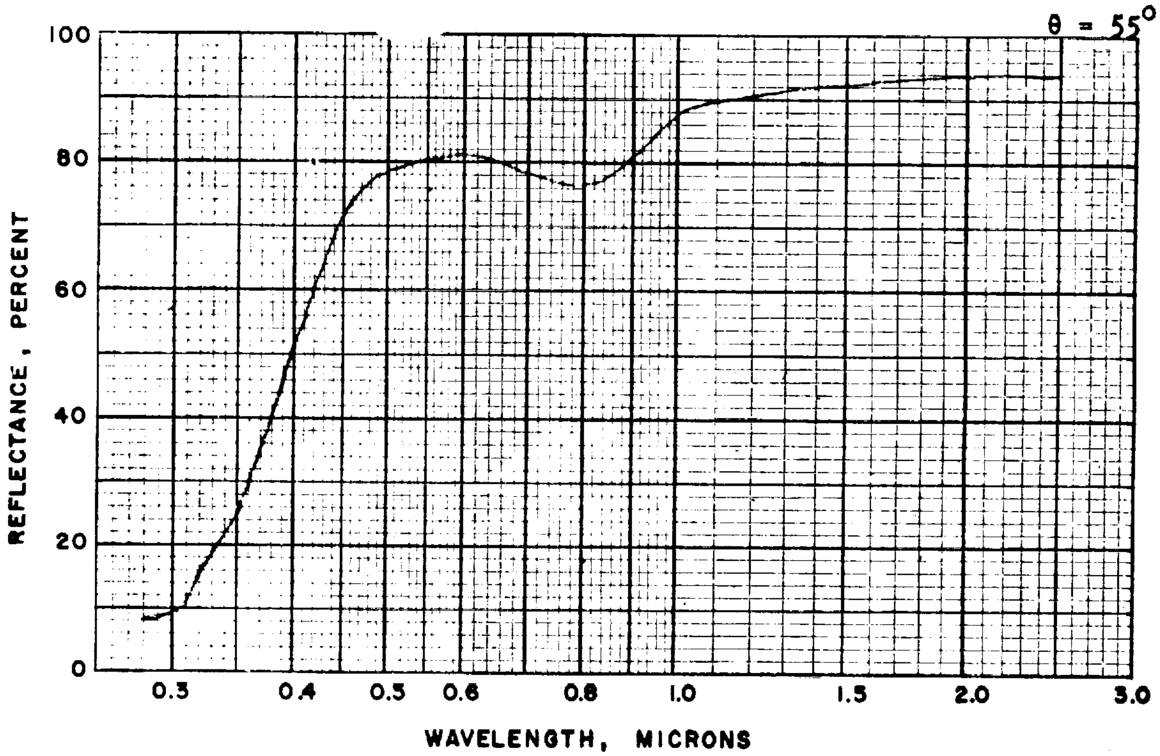

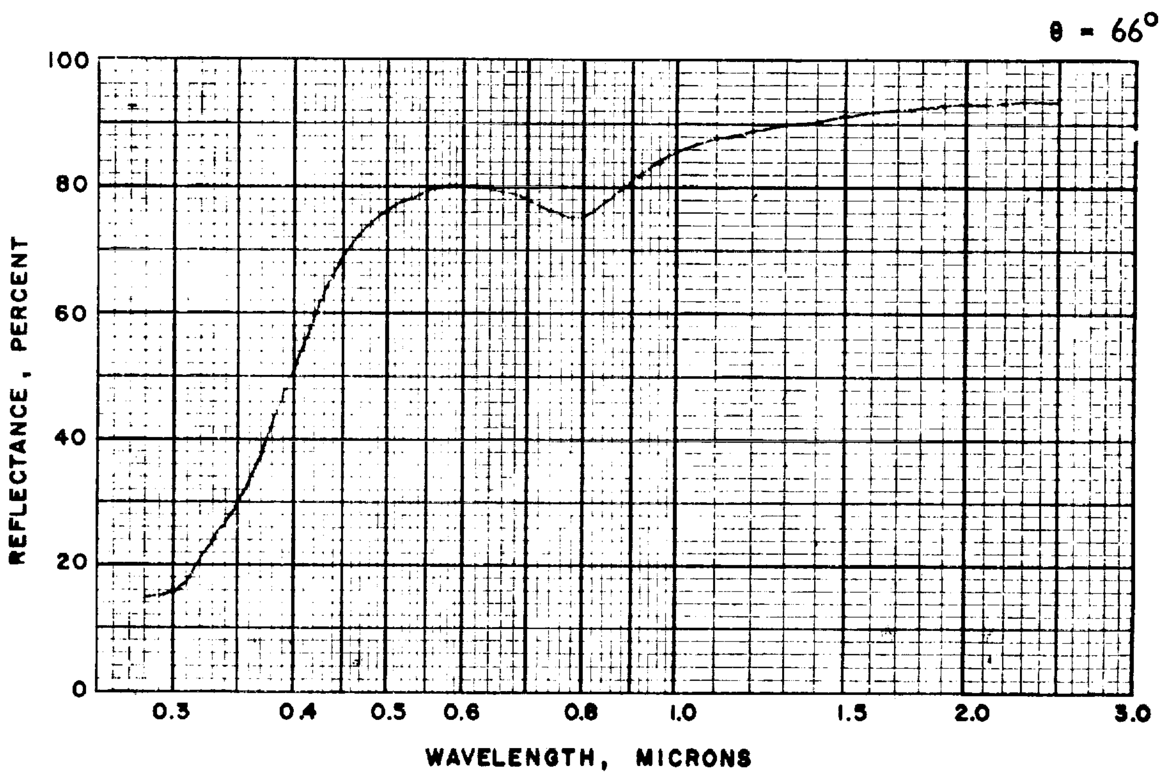

Figure 39 (Cont.): Sample 12B, Azimuthal Angle 45°, Angles of Incidence 55° and 66°

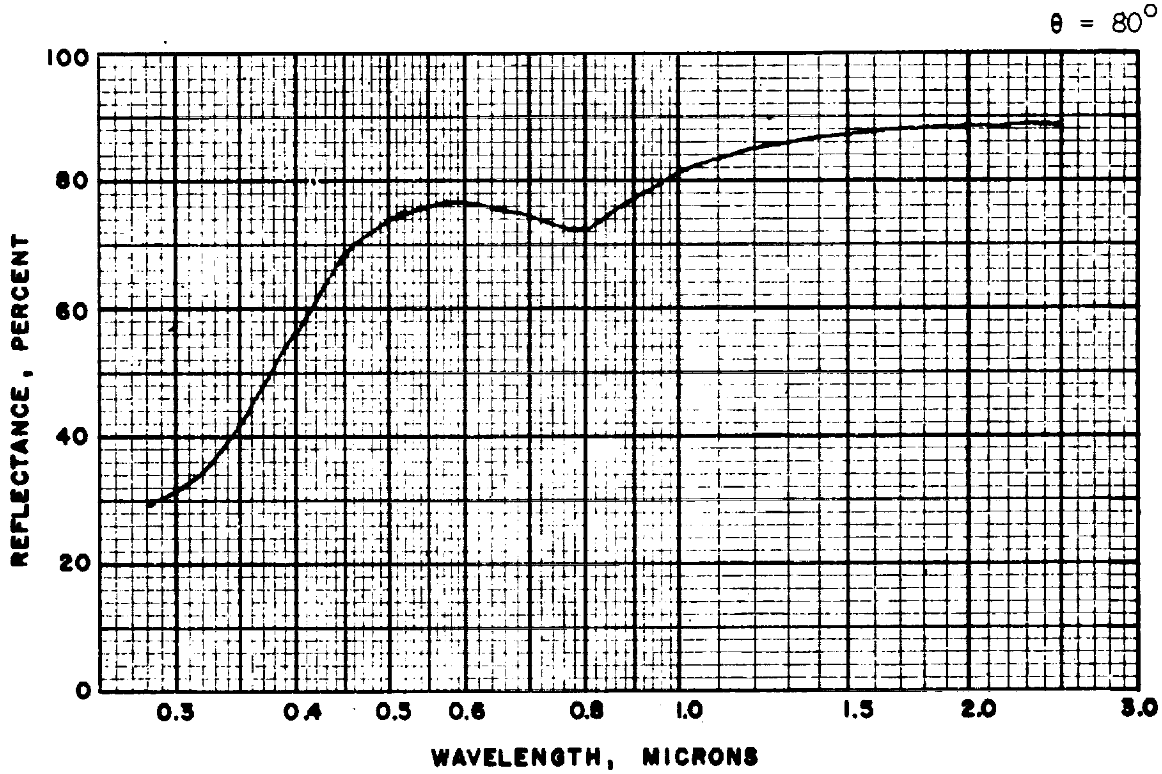

Figure 39 (Cont.): Sample 12B, Azimuthal Angle 45°
Angle of Incidence 80°

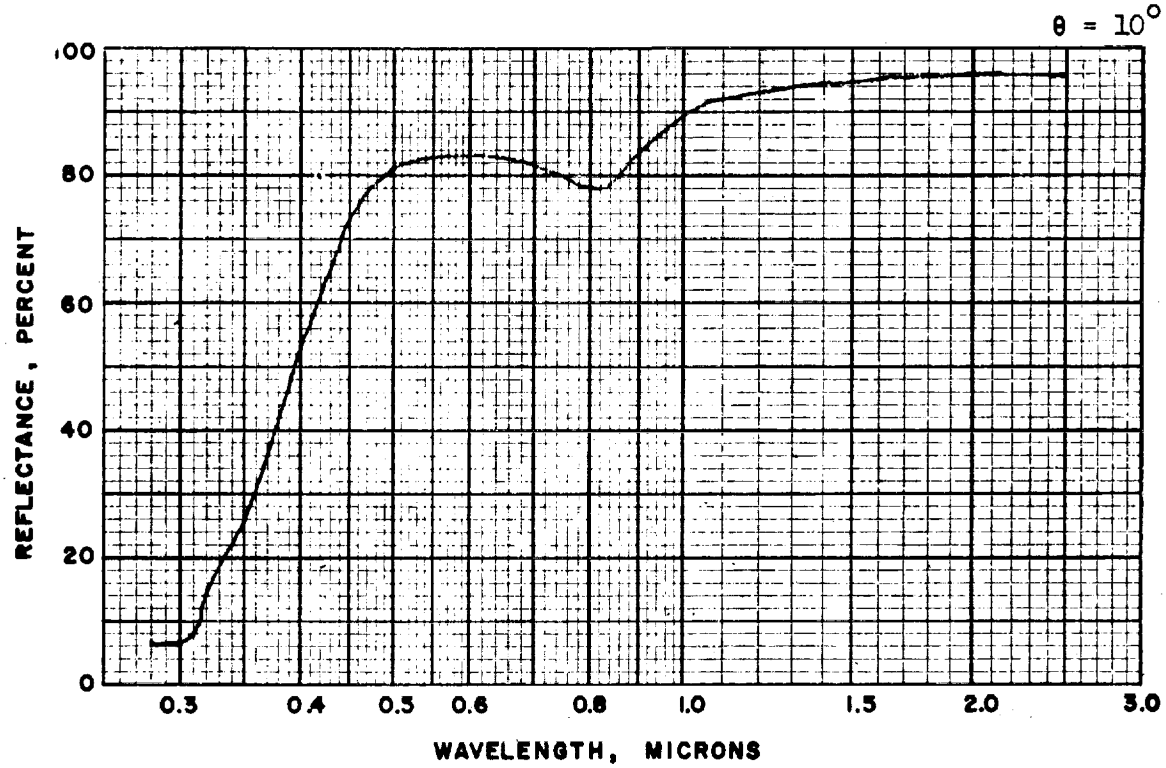

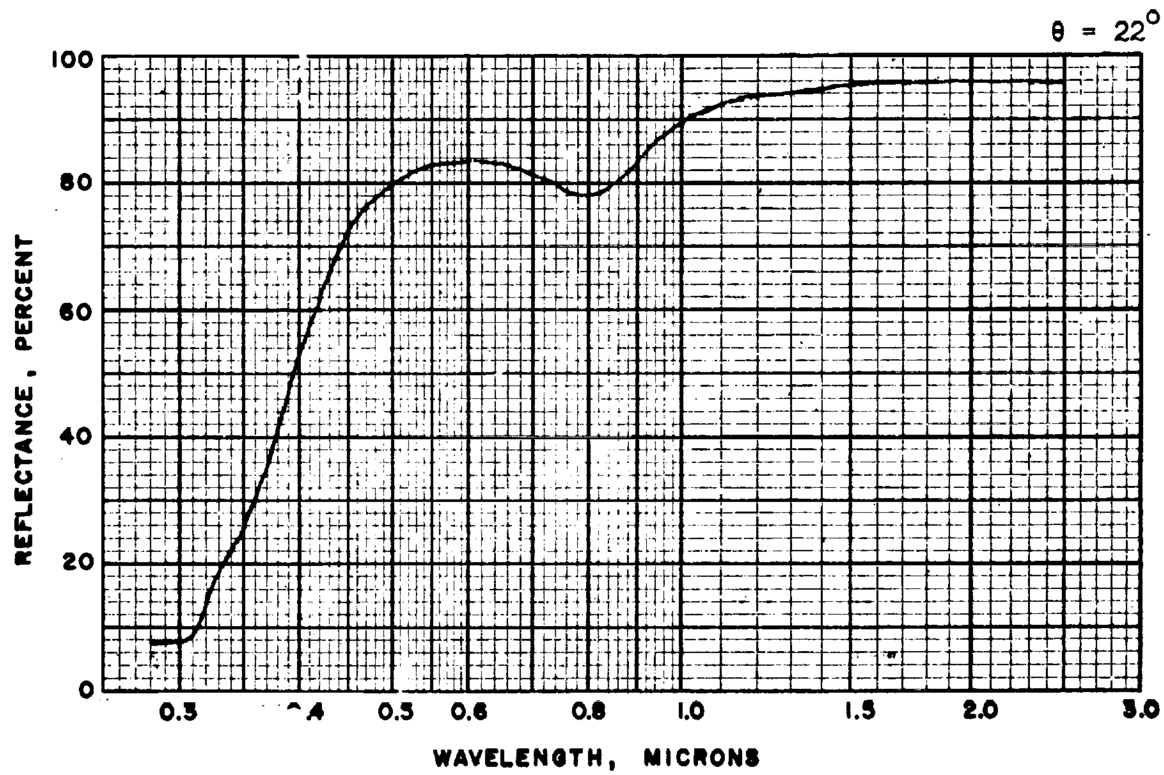

Figure 40: Sample 12B, Azimuthal Angle 60°,
Angles of Incidence 10° and 22°

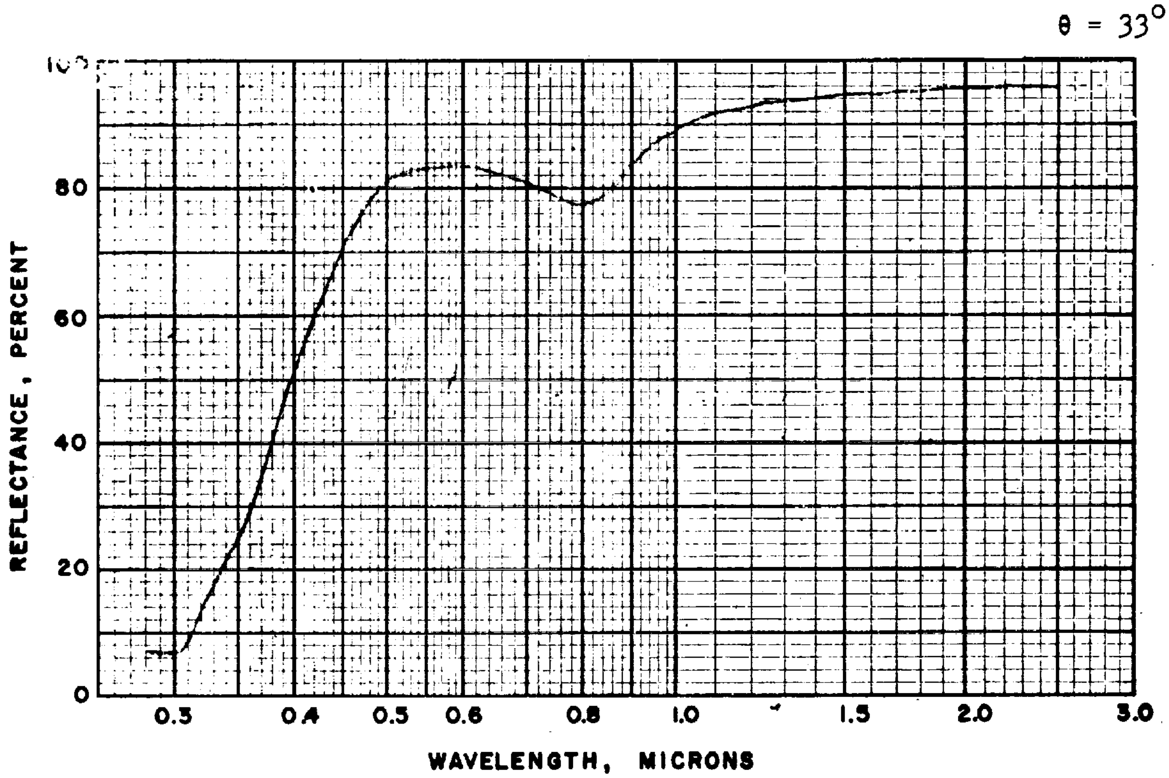

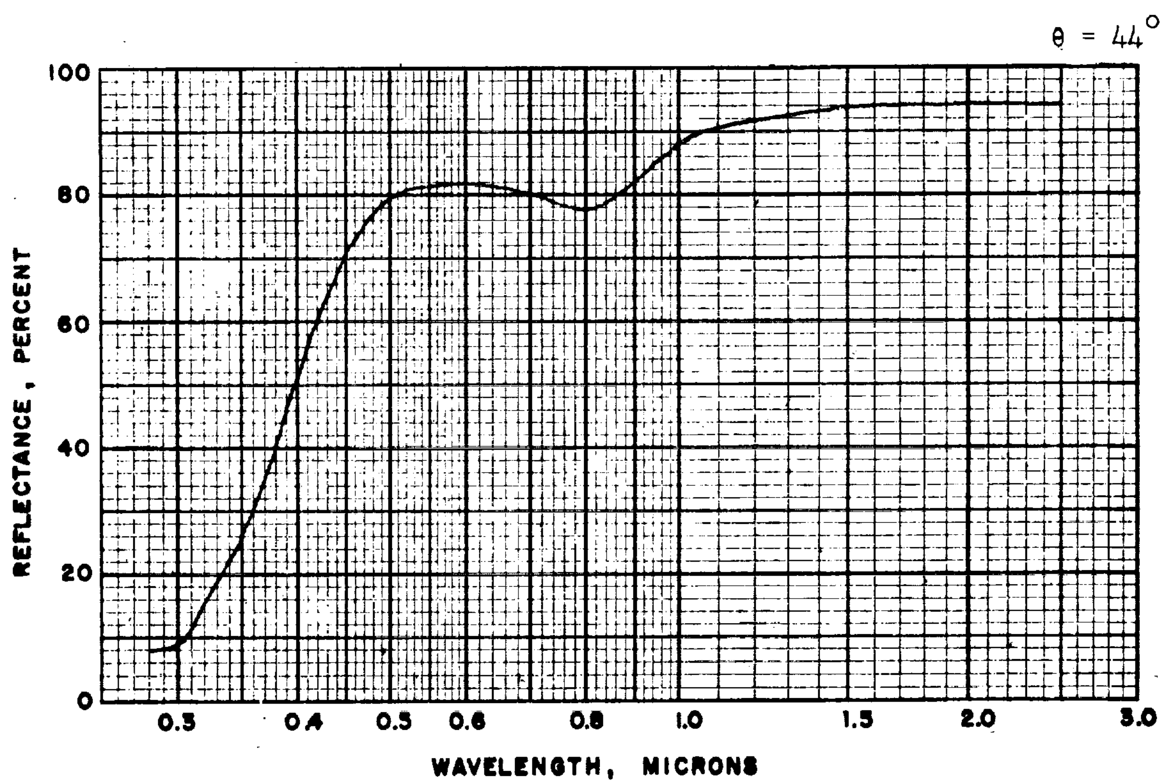

Figure 40 (Cont.): Sample 12B, Azimuthal Angle 60°, Angles of Incidence 33° and 44°

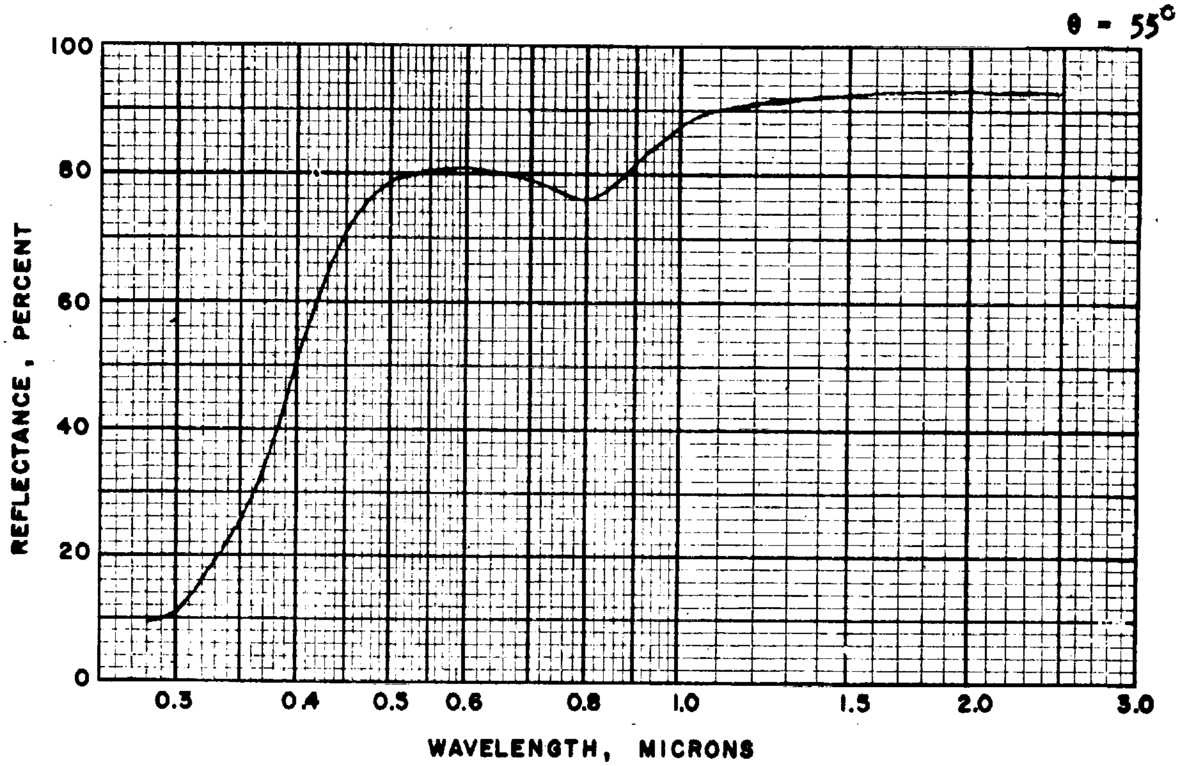

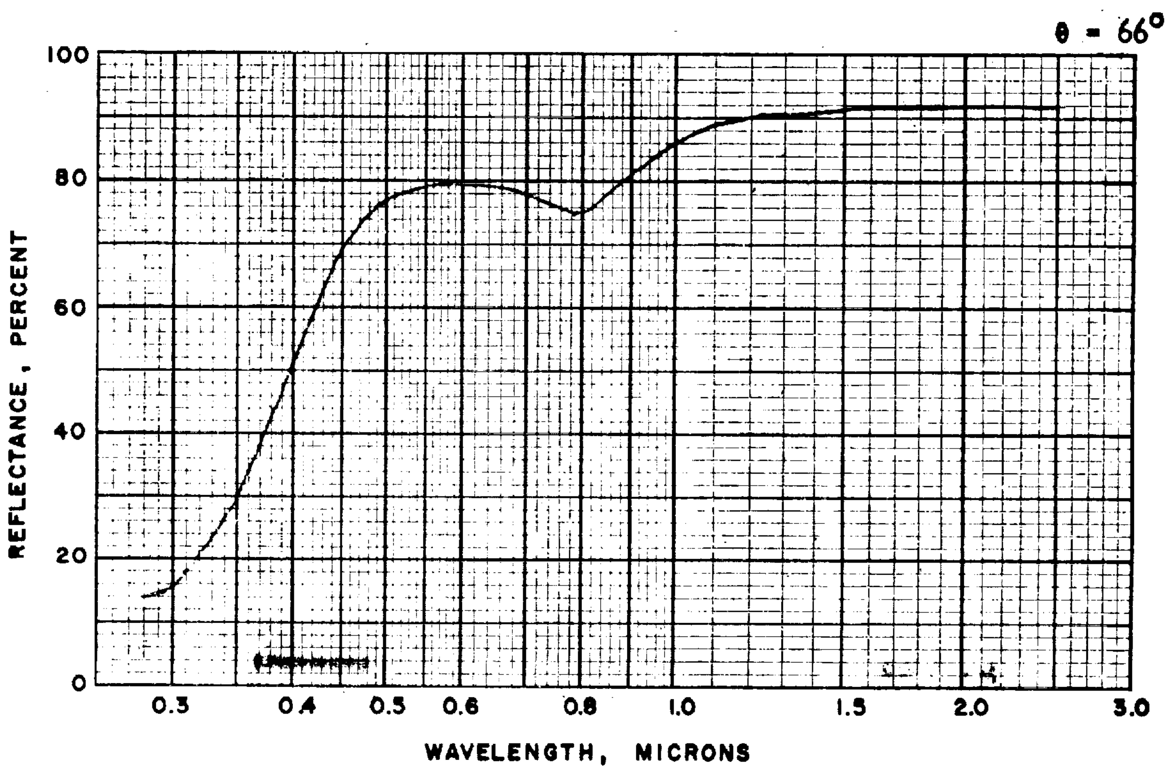

Figure 40 (Cont.): Sample 12B, Azimuthal Angle 60°, Angles of Incidence 55° and 66°

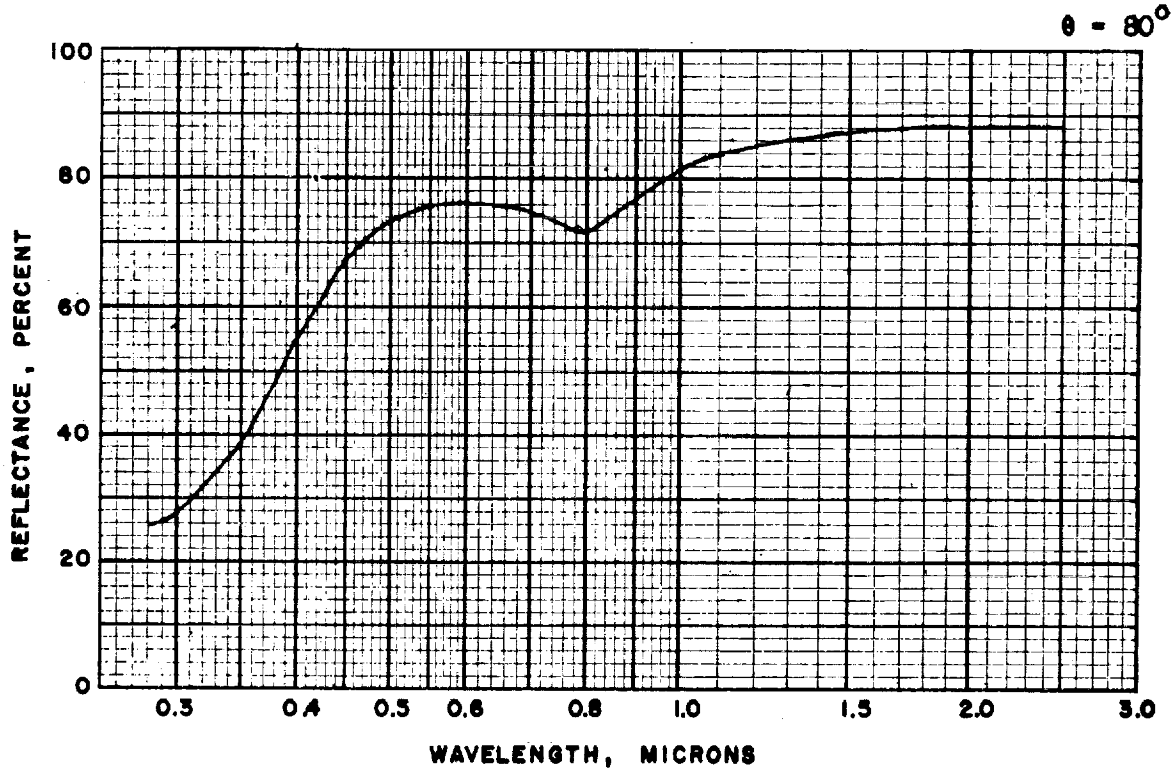

Figure 40 (Cont.): Sample 12B, Azimuthal Angle 60°
Angle of Incidence 80°

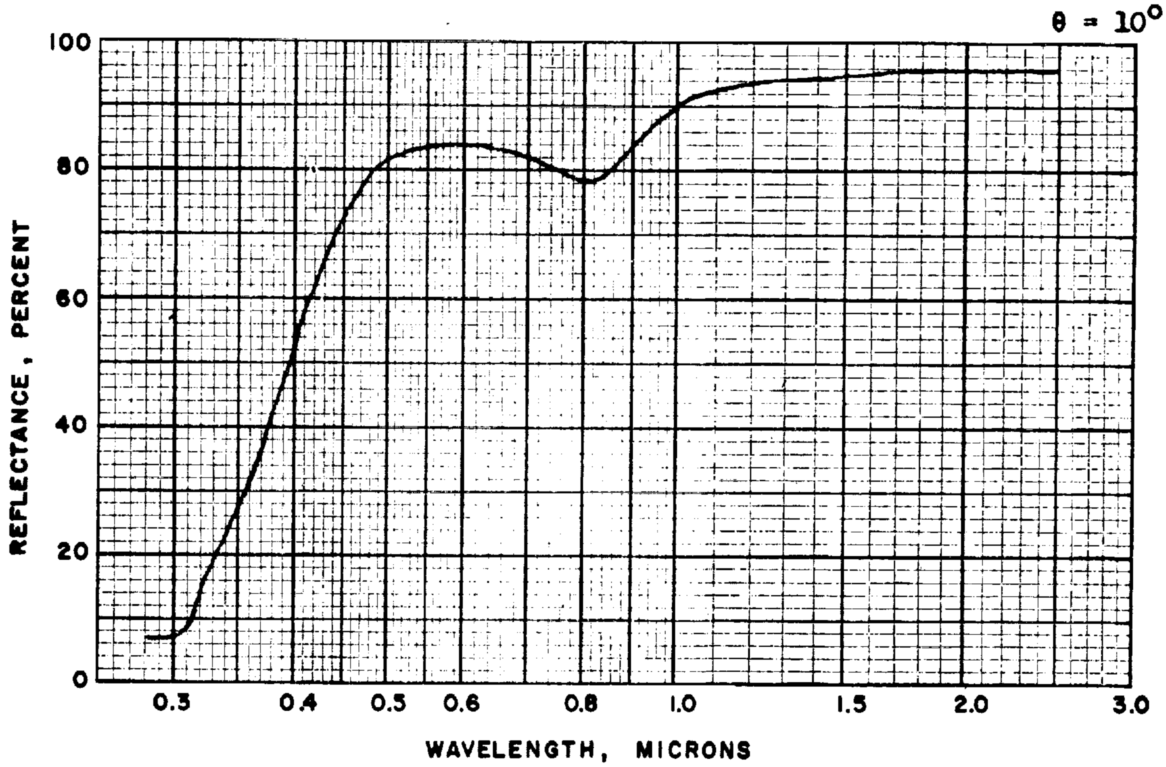

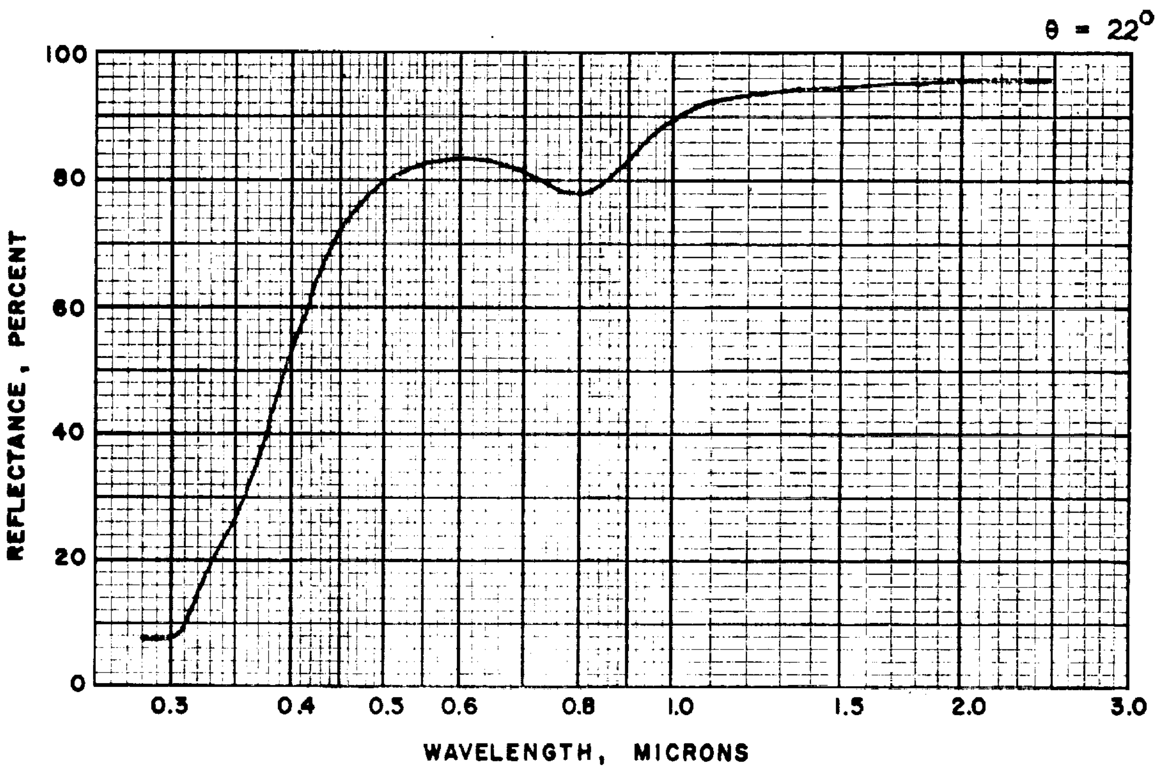

Figure 41: Sample 12B, Azimuthal Angle 90°, Angles of Incidence 10° and 22°

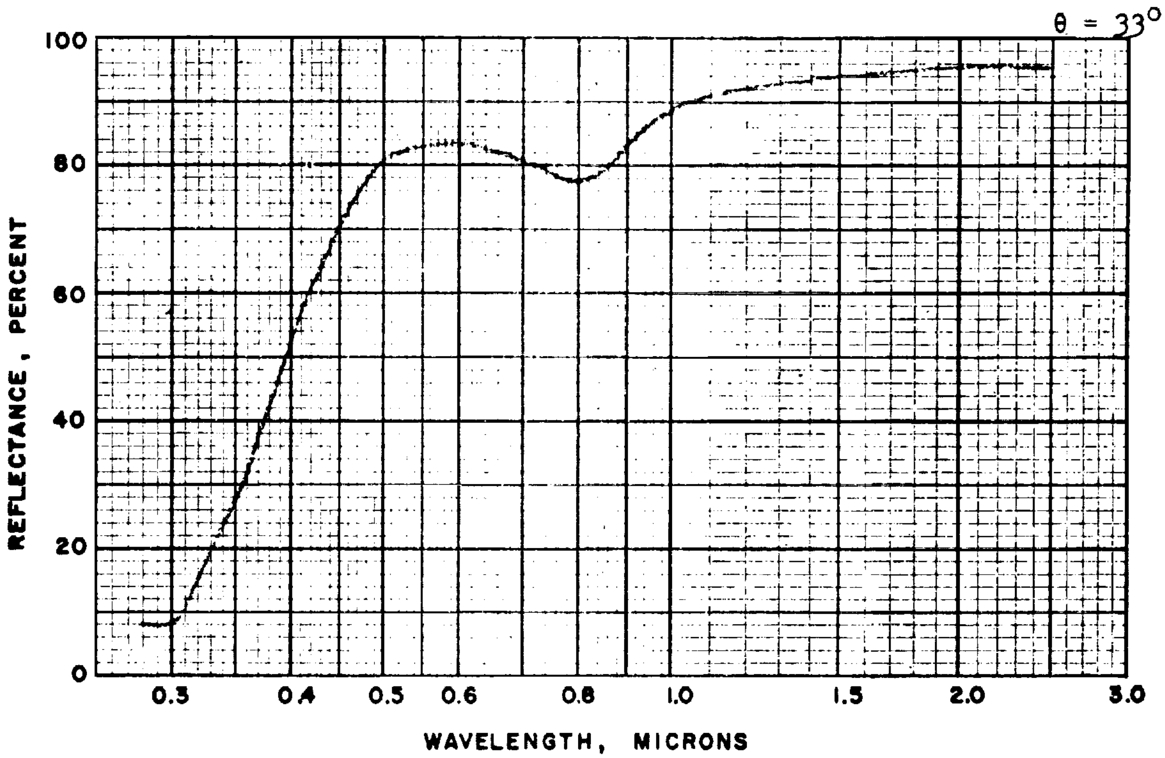

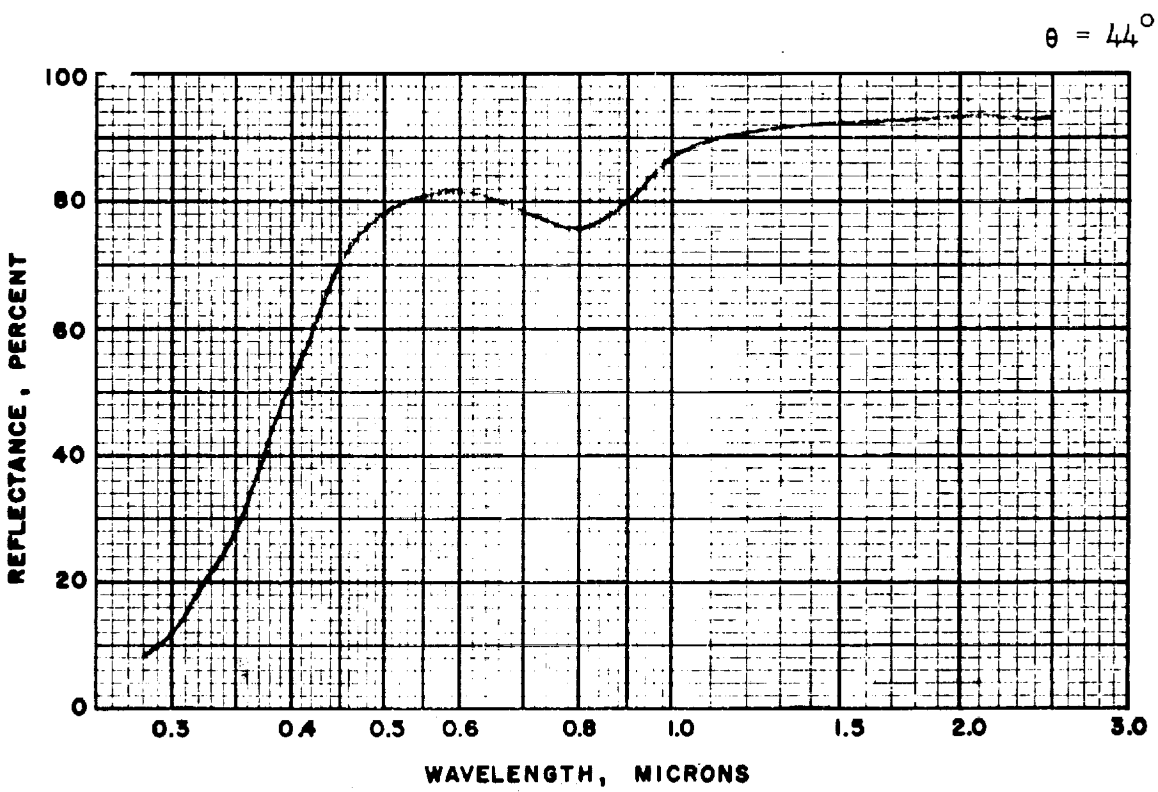

Figure 41 (Cont.): Sample 12B, Azimuthal Angle 90°
Angles of Incidence 33° and 44°

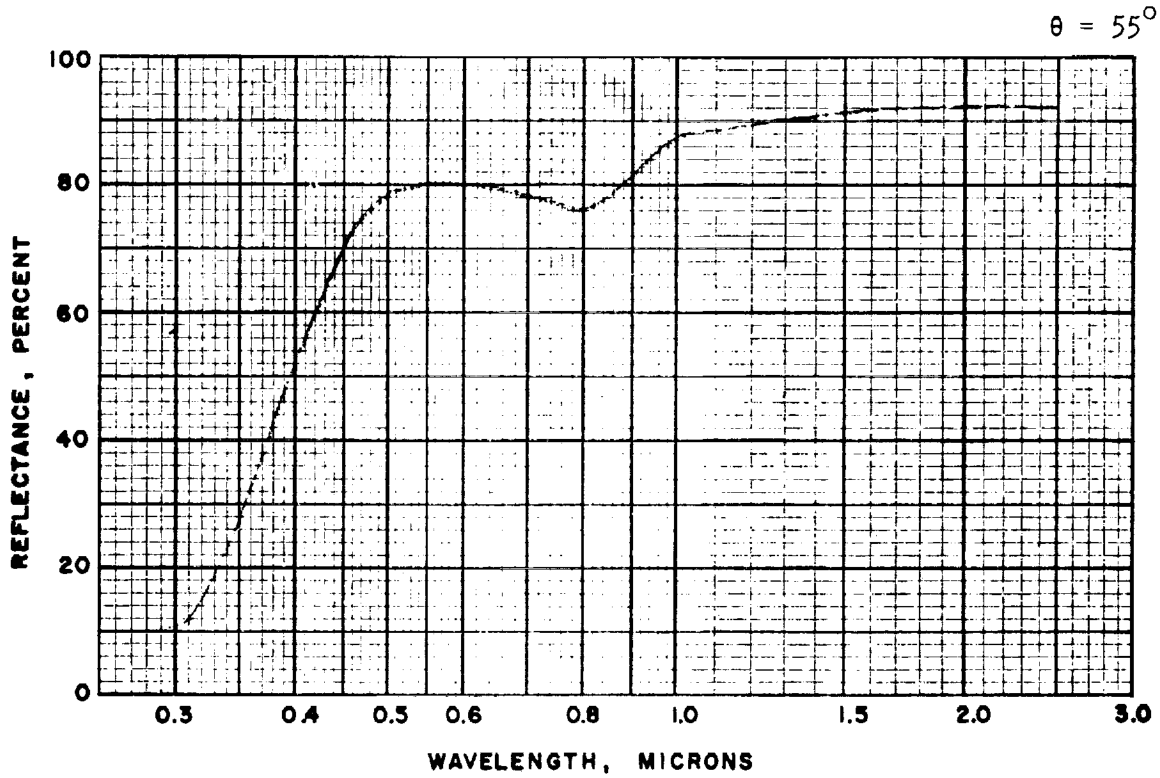

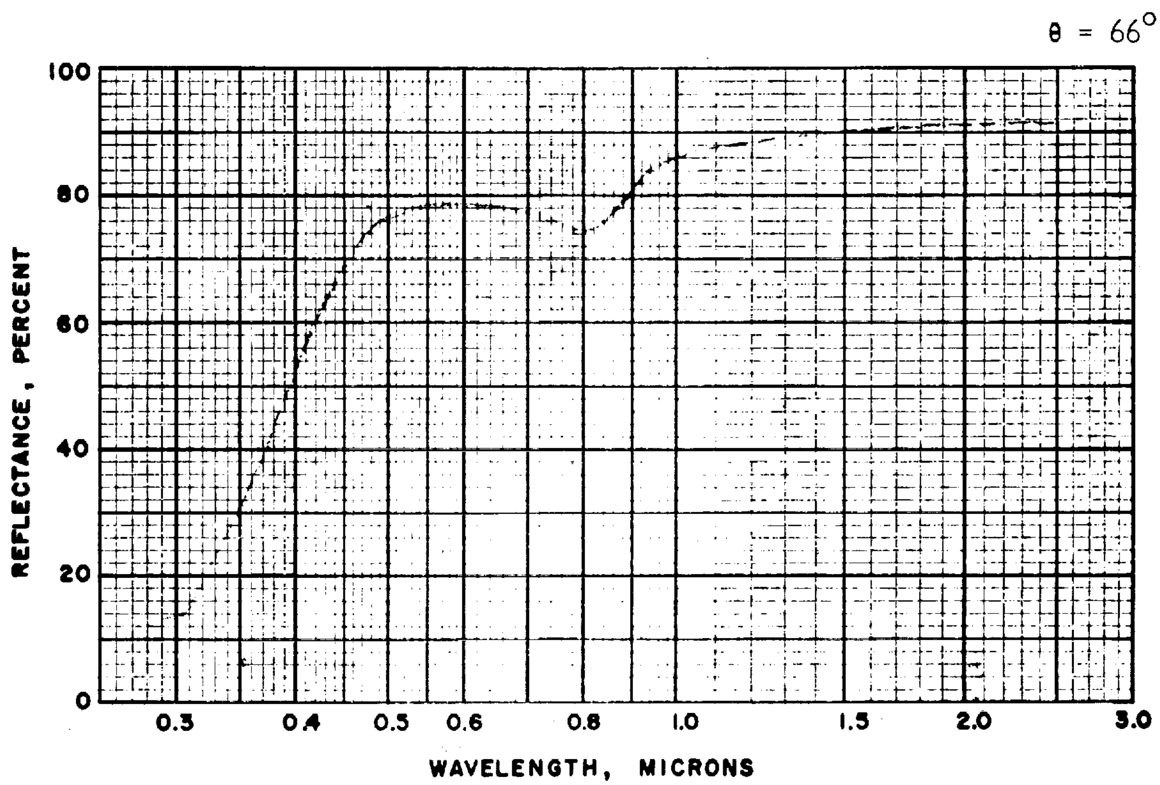

Figure 41 (Cont.): Sample 12B, Azimuthal Angle 90°, Angles of Incidence 55° and 66°

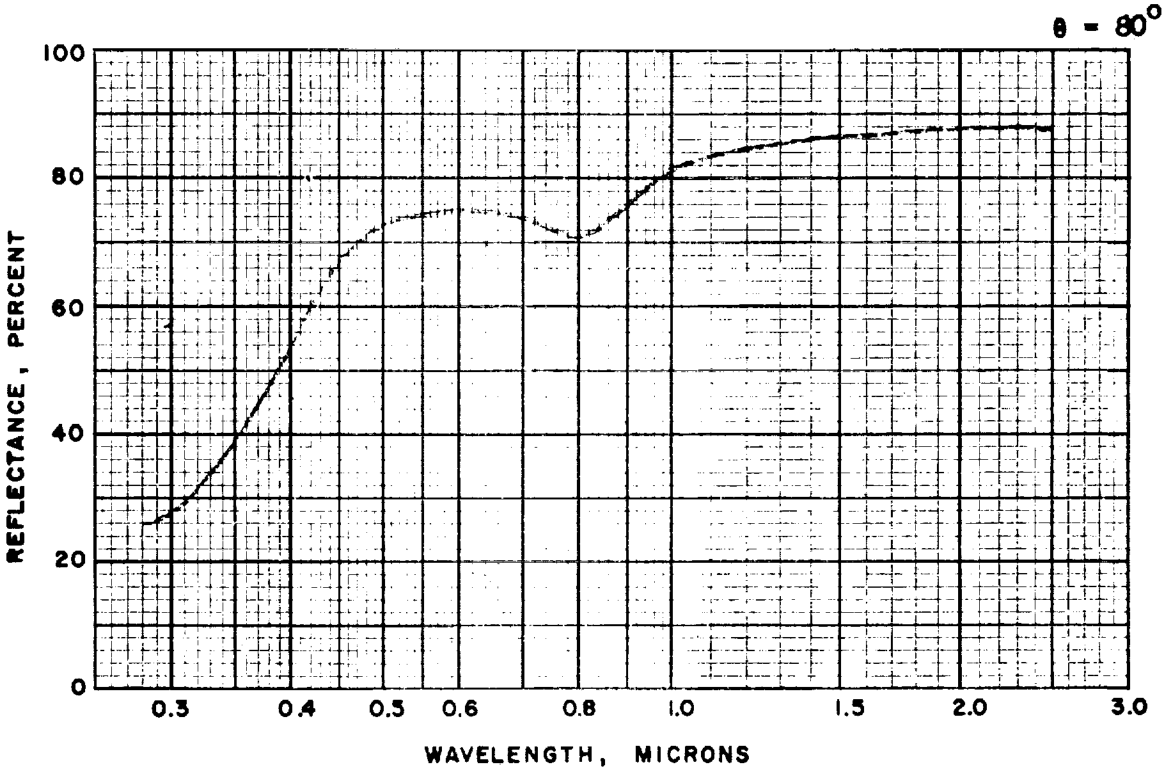

Figure 41 (Cont.): Sample 12B, Azimuthal Angle 90°, Angle of Incidence 80°

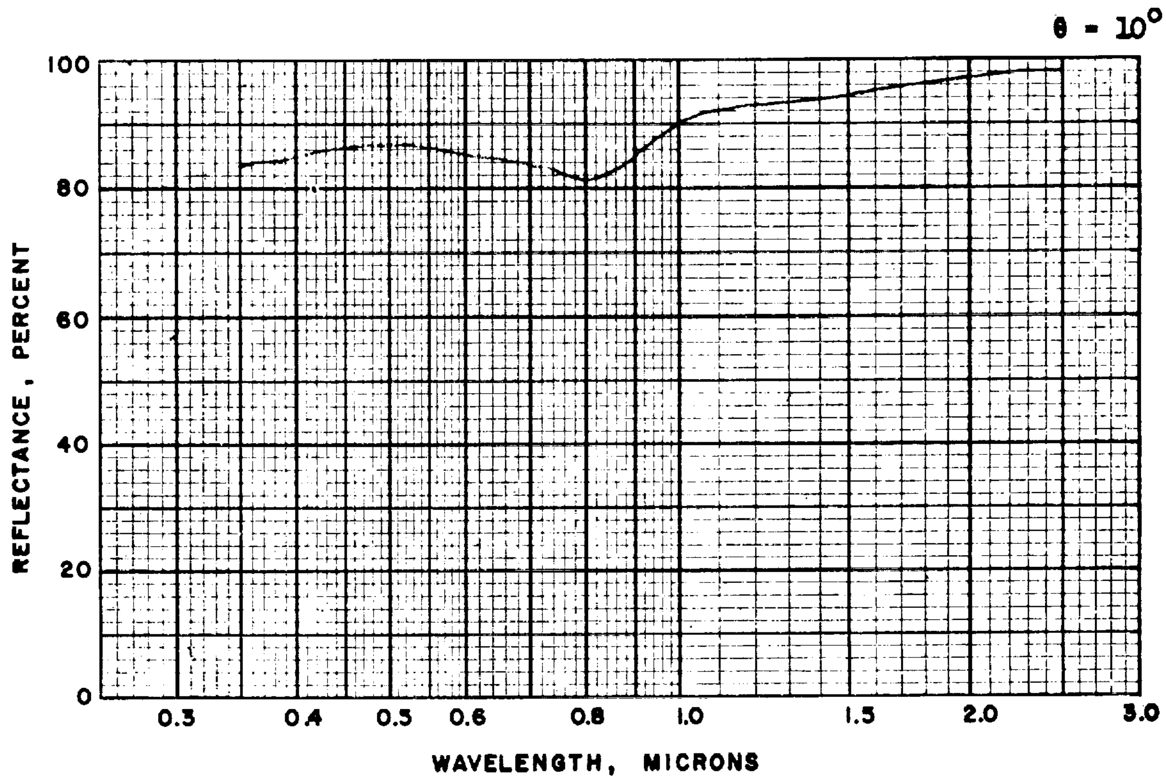

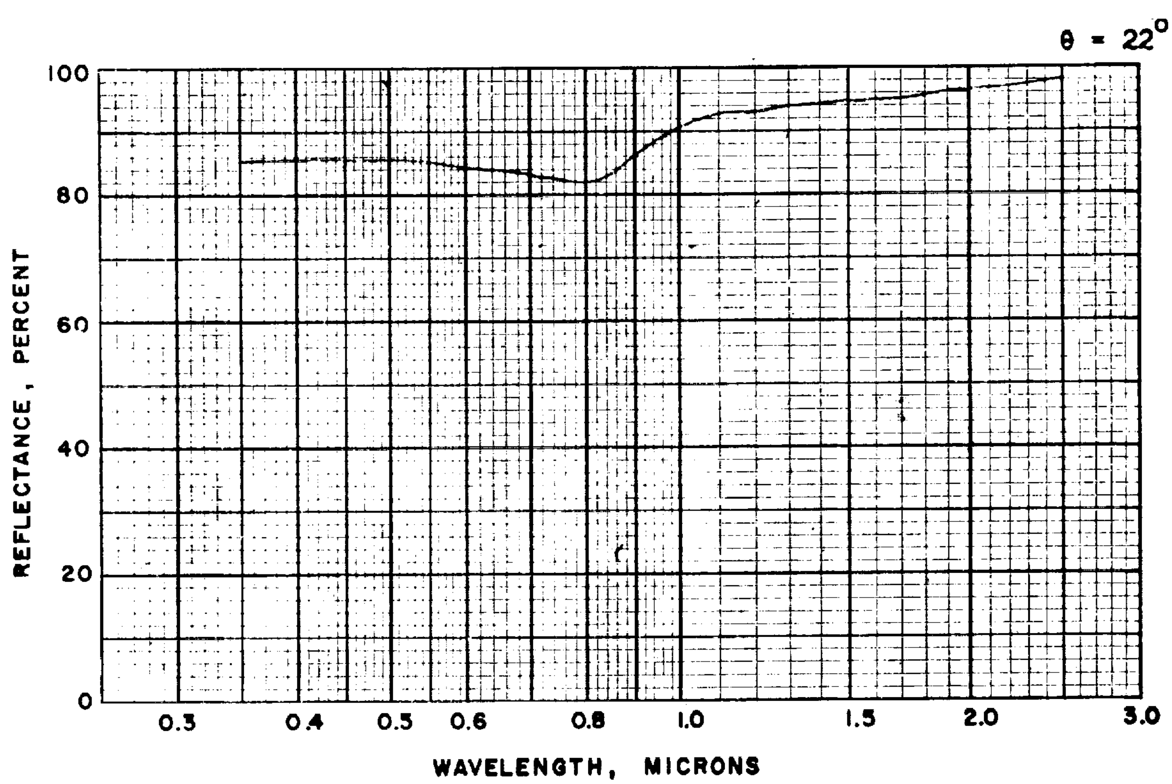

Figure 42: Sample 15A, Azimuthal Angle 0°, Angles of Incidence 10° and 22°

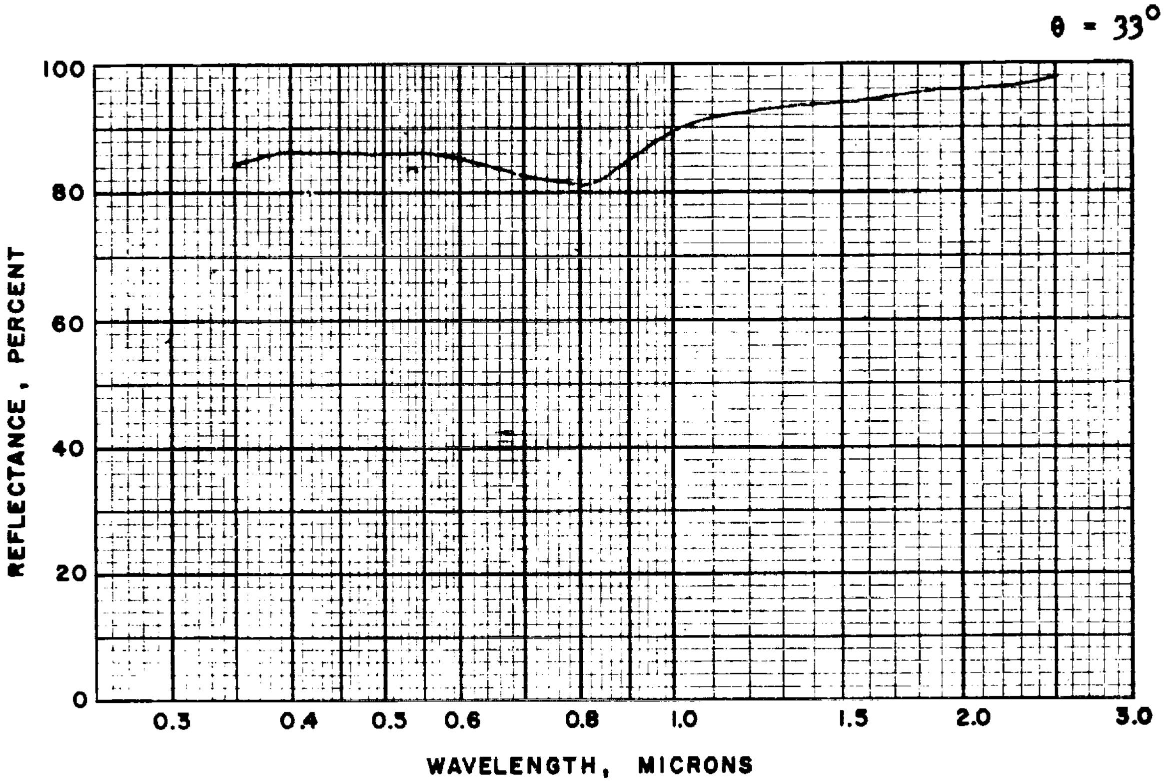

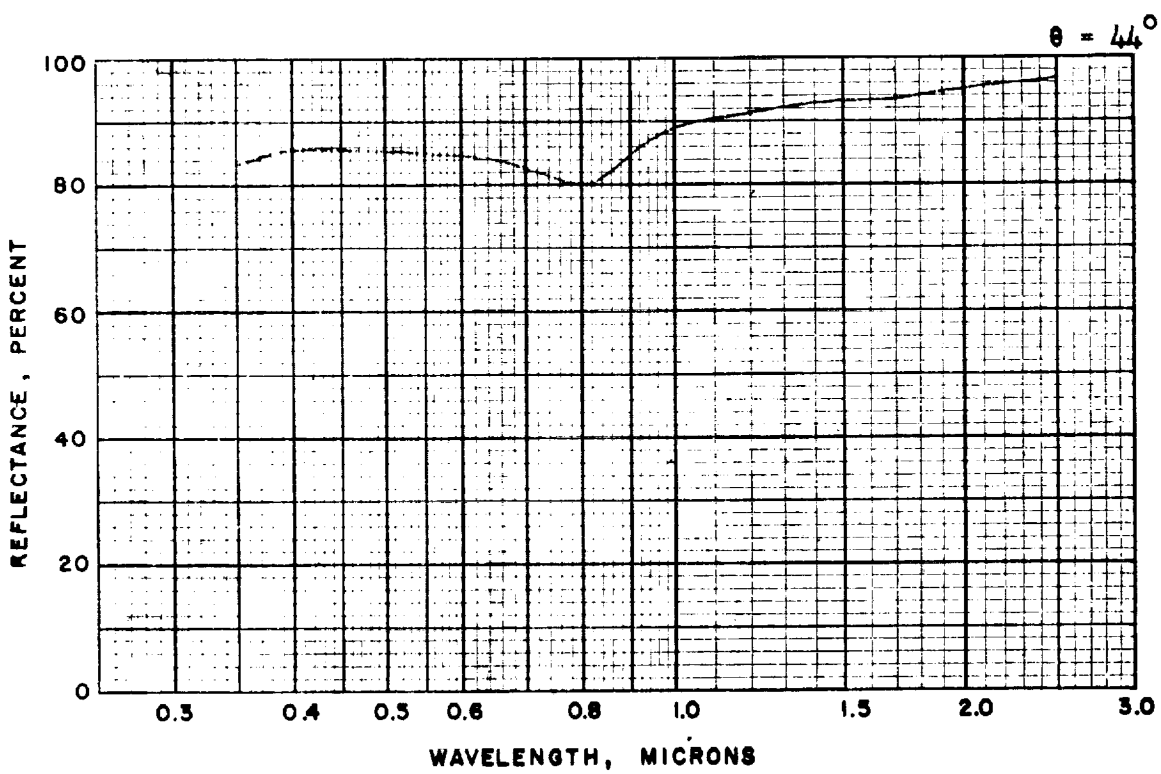

Figure 42 (Cont.): Sample 15A, Azimuthal Angle 0°, Angles of Incidence 33° and 44°

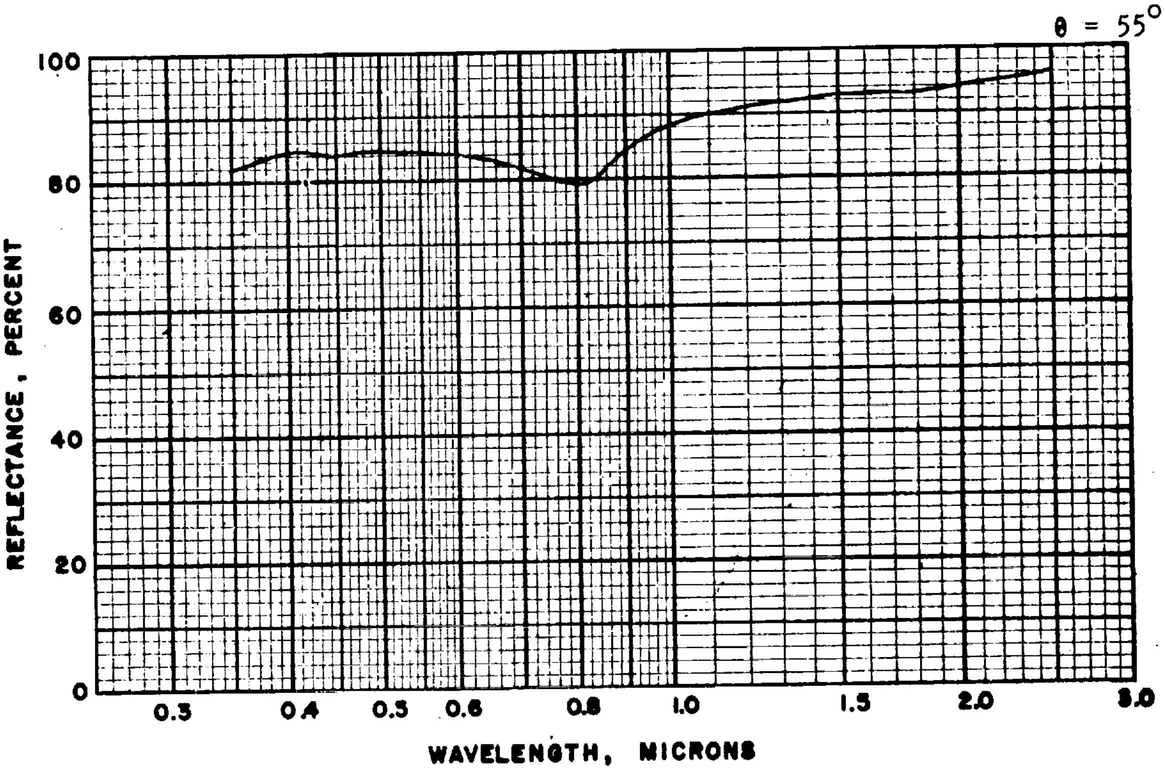

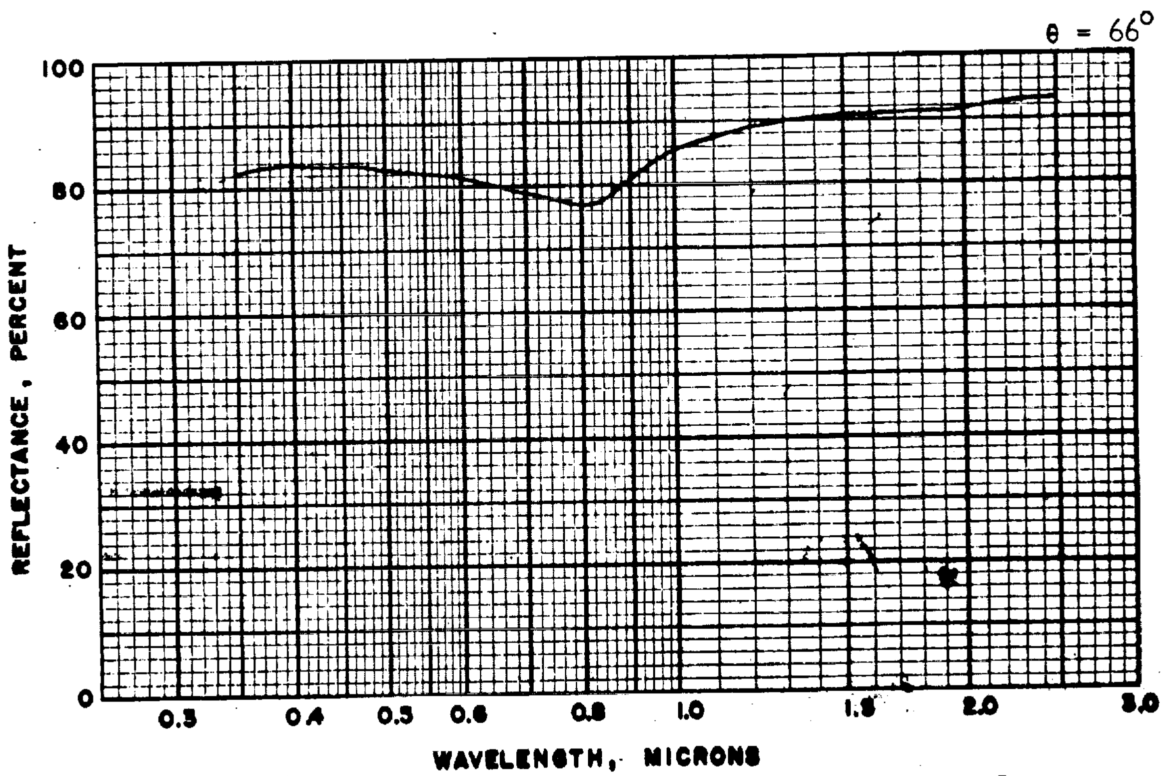

Figure 42 (Cont.): Sample 15A, Azimuthal Angle 0°, Angles of Incidence 55° and 66°

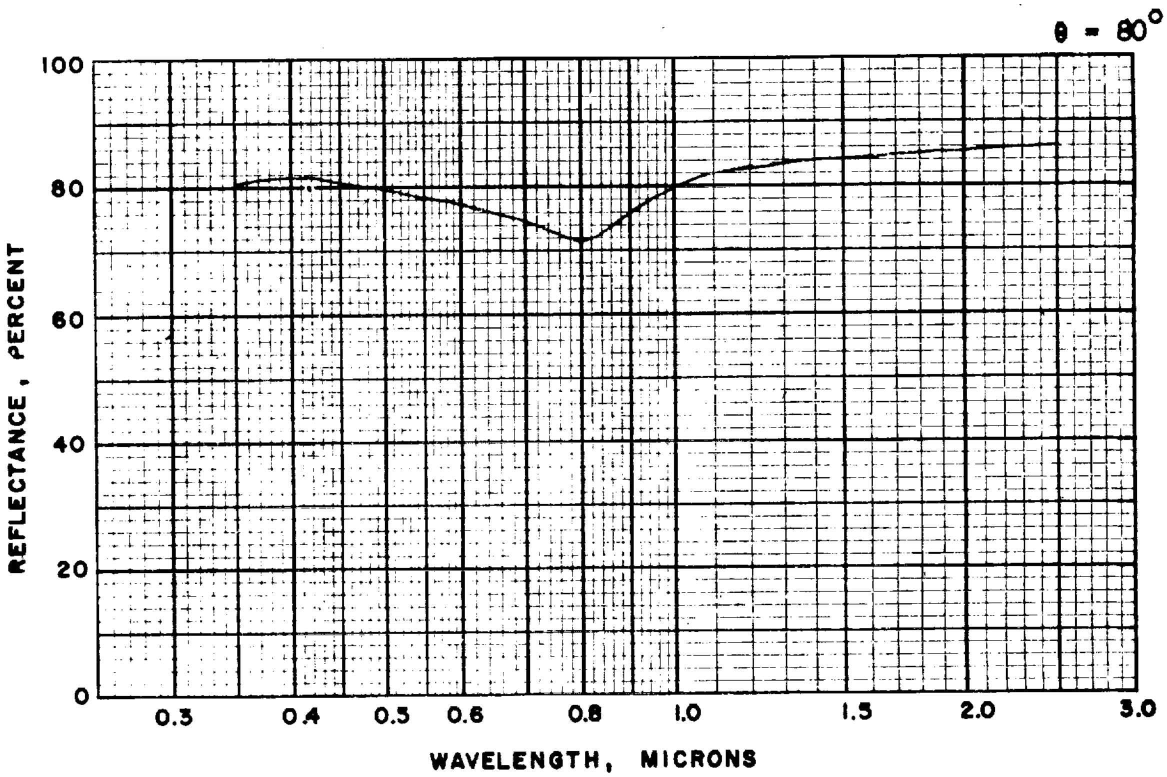

Figure 42 (Cont.): Sample 15A, Azimuthal Angle 0°, Angle of Incidence 80°

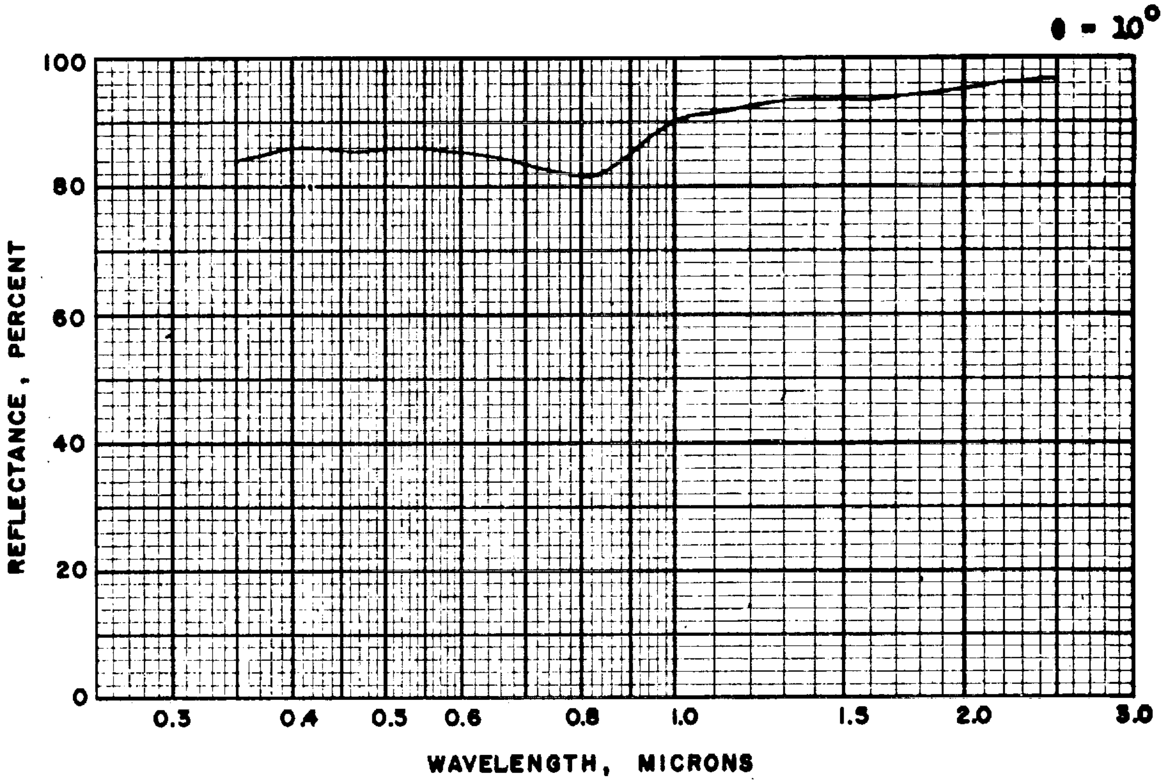

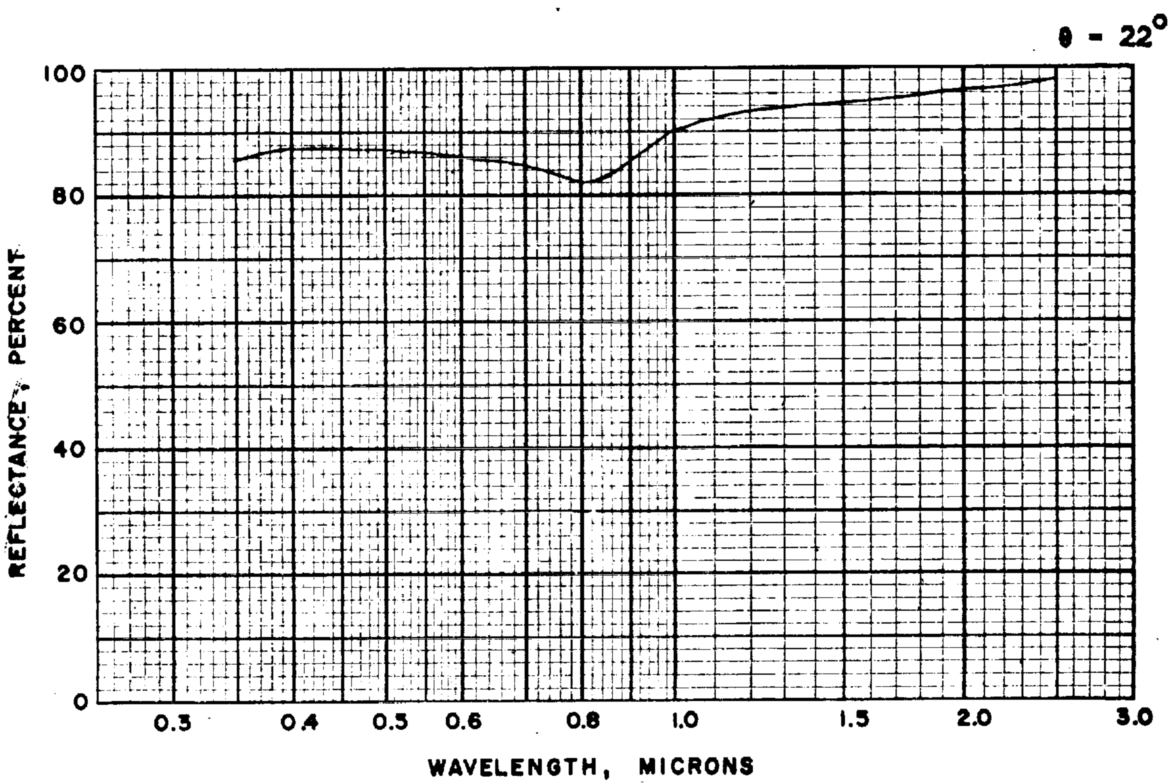

Figure 43: Sample 15A, Azimuthal Angle 45°,
Angles of Incidence 10° and 22°

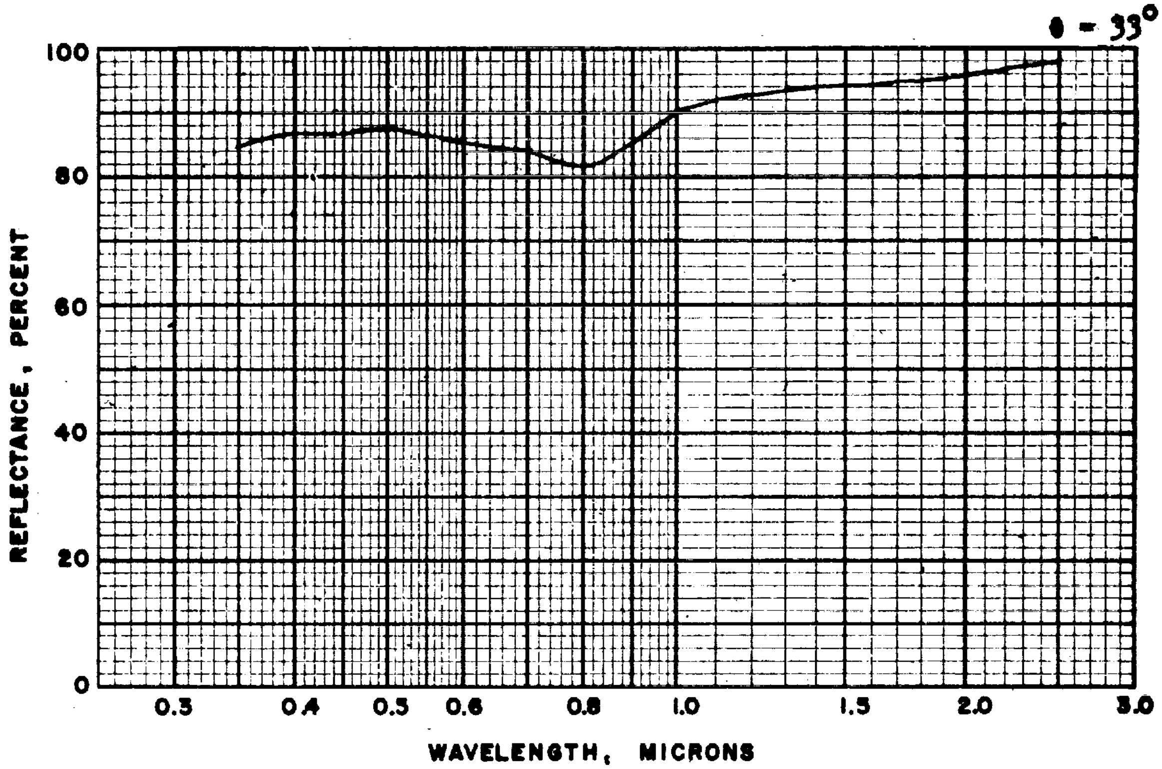

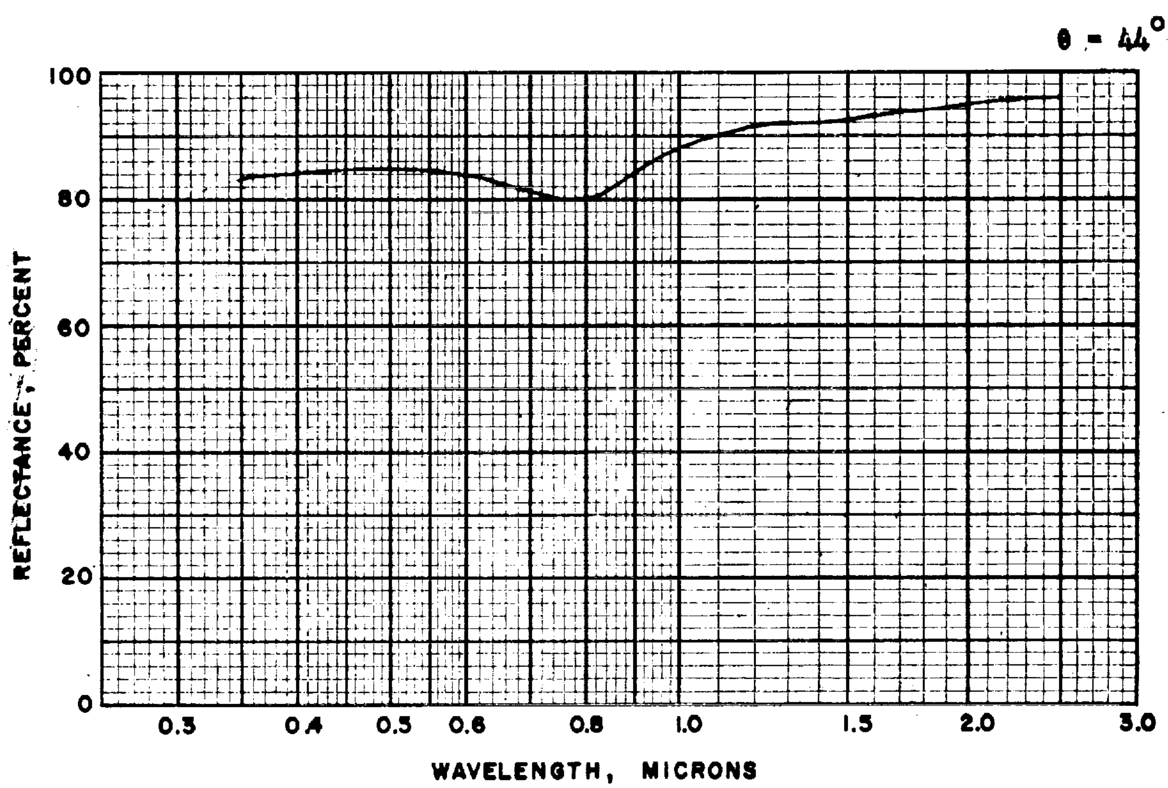

Figure 43 (Cont.): Sample 15A, Azimuthal Angle 45°, Angles of Incidence 33° and 44°

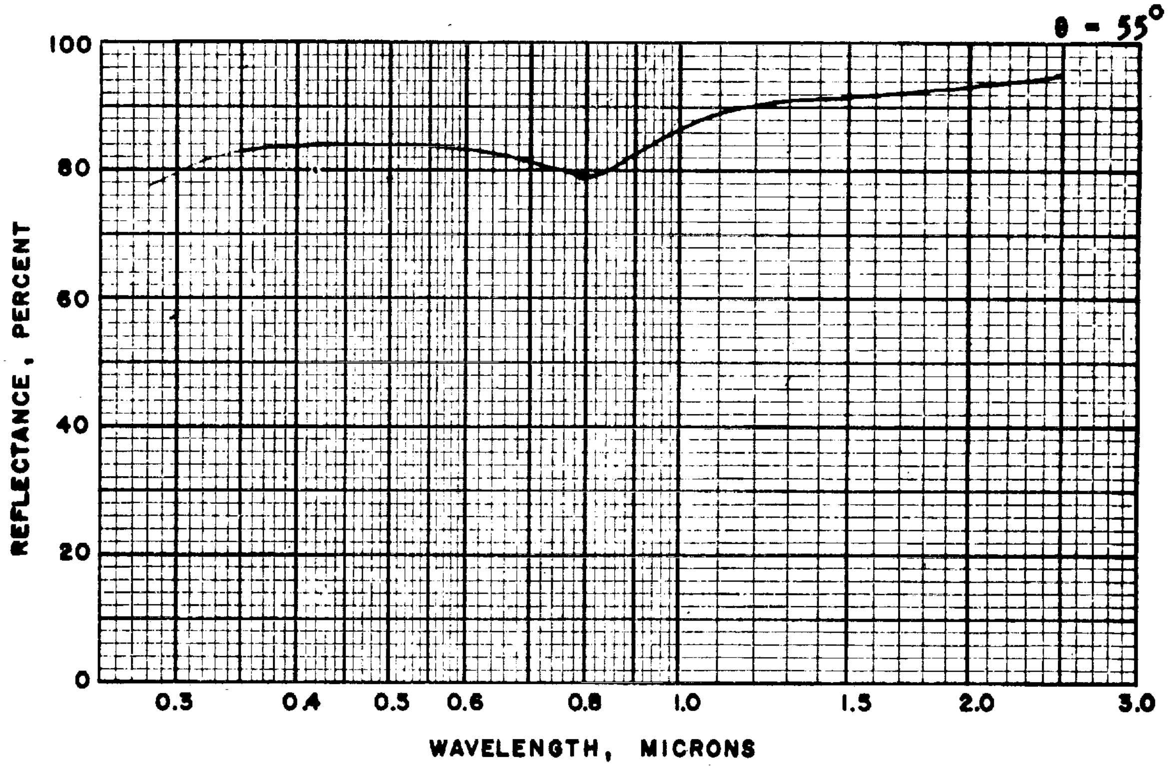

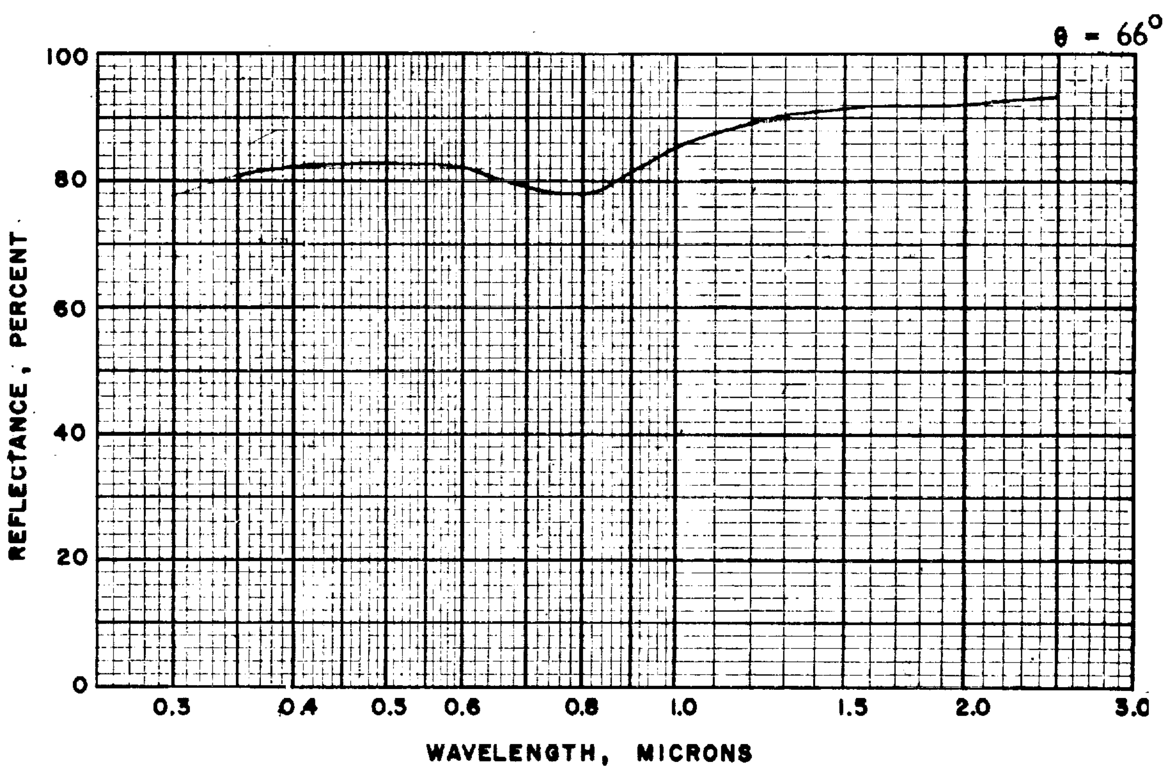

Figure 43 (Cont.): Sample 15A, Azimuthal Angle 45°, Angles of Incidence 55° and 66°

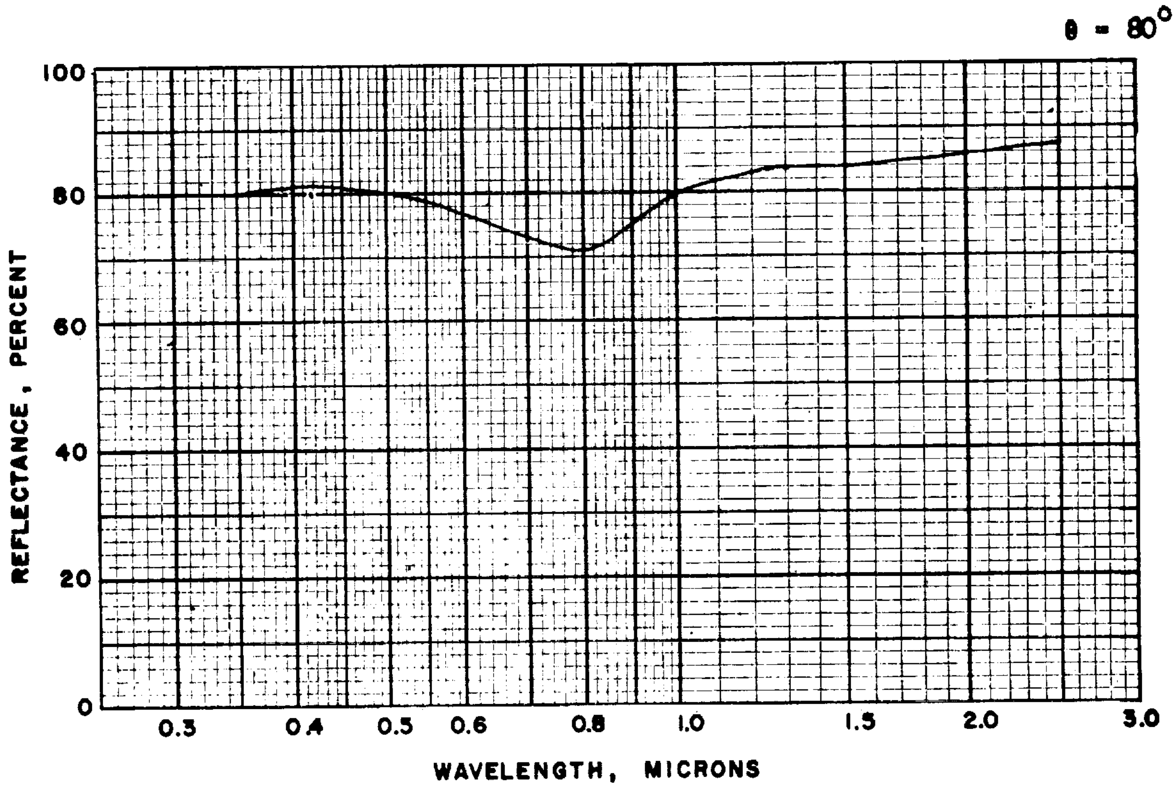

Figure 43 (Cont.): Sample 15A, Azimuthal Angle 45°, Angle of Incidence 80°

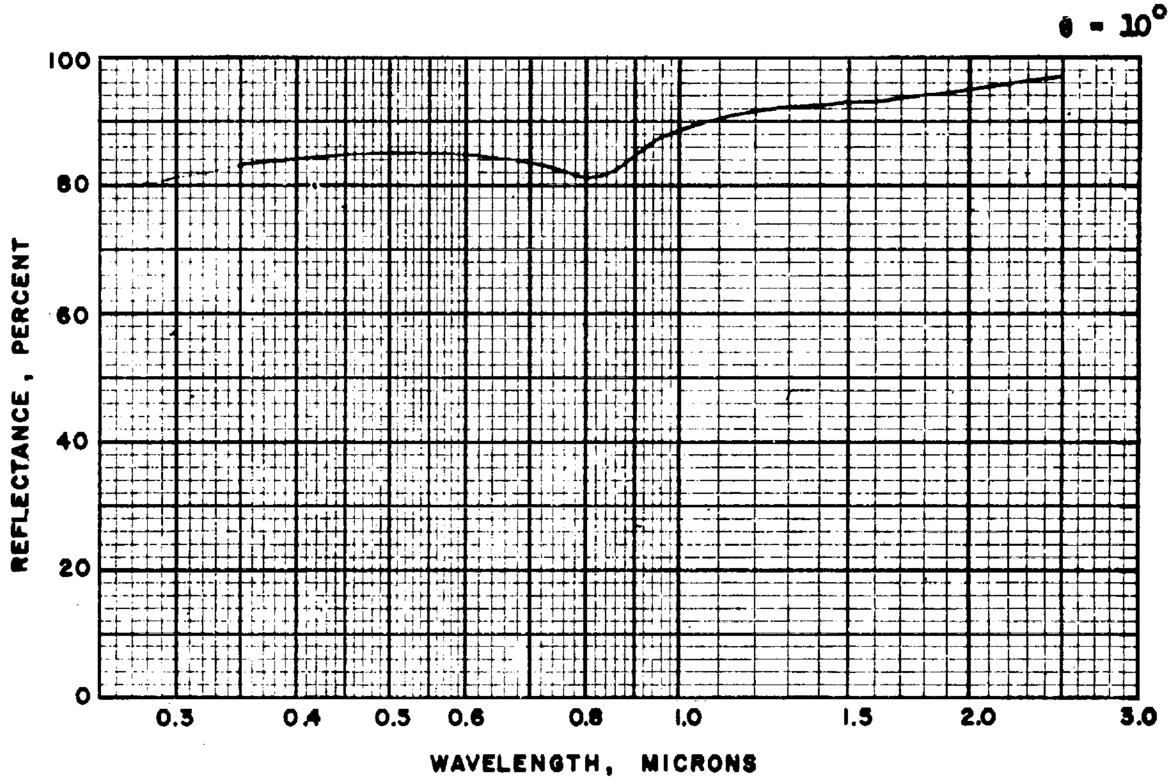

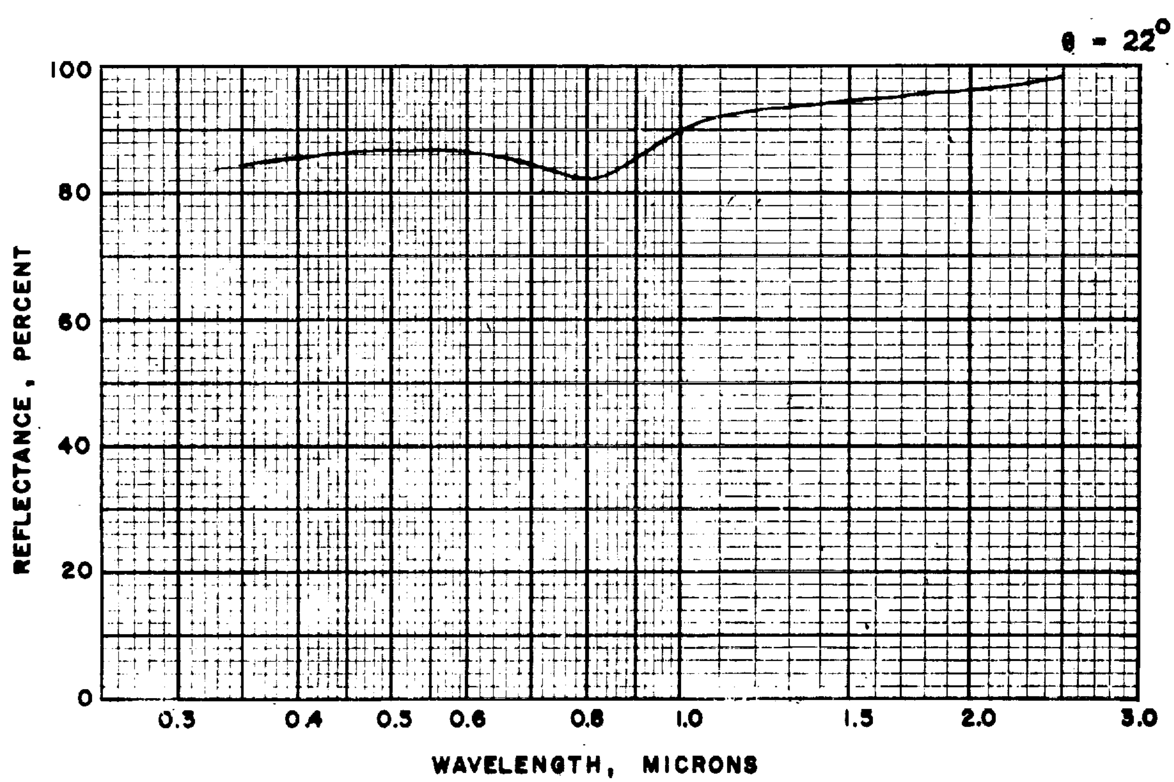

Figure 44: Sample 15A, Azimuthal Angle 60°, Angles of Incidence 10° and 22°

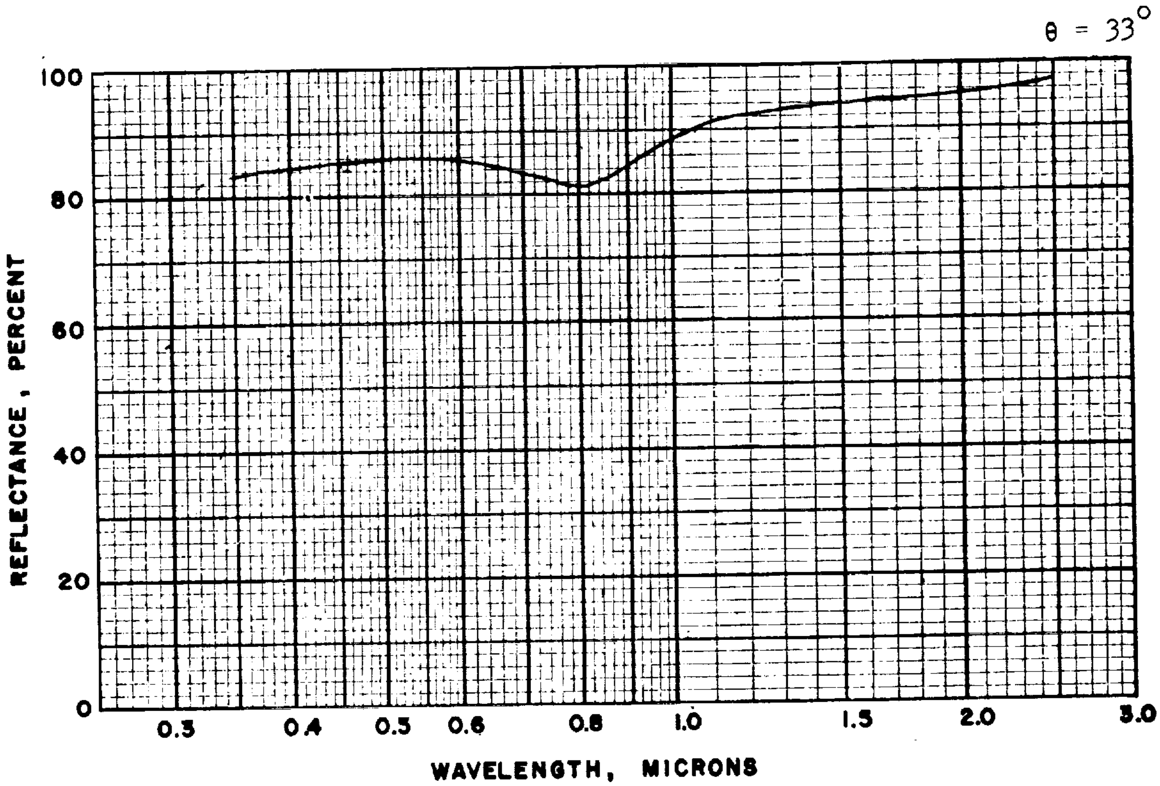

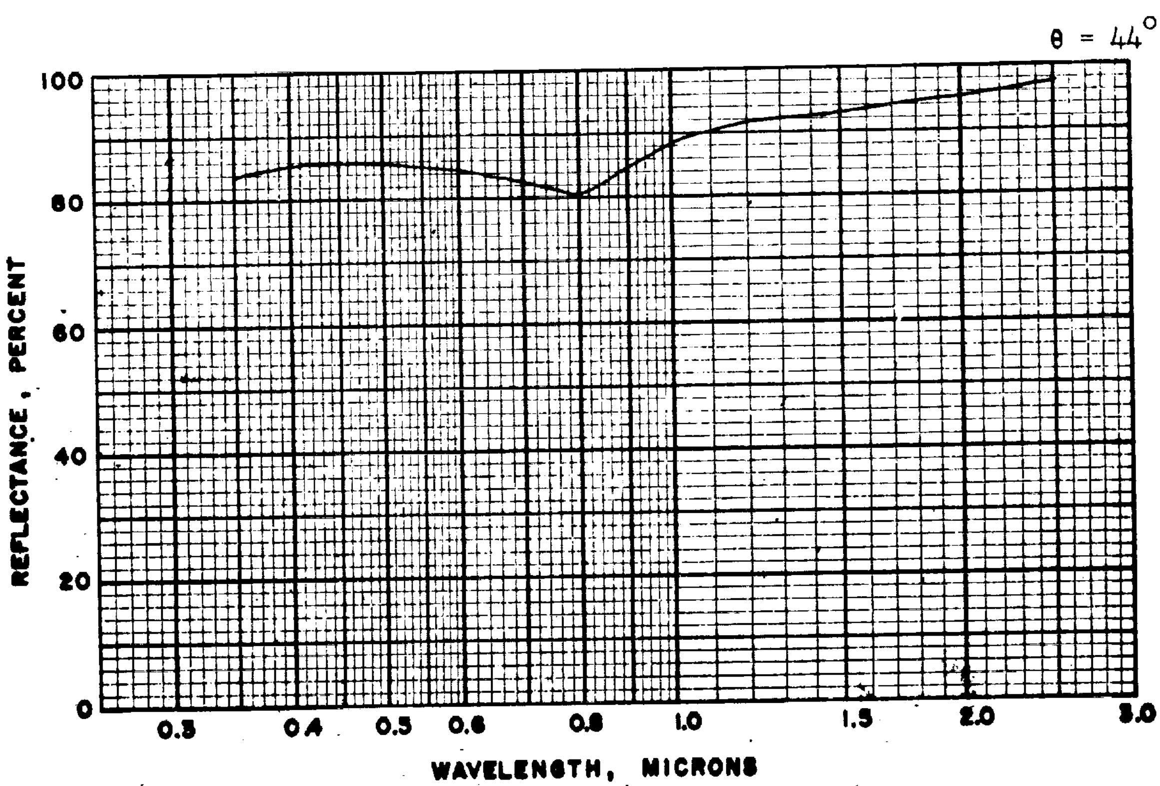

Figure 44 (Cont.): Sample 15A, Azimuthal Angle 60°, Angles of Incidence 33° and 44°

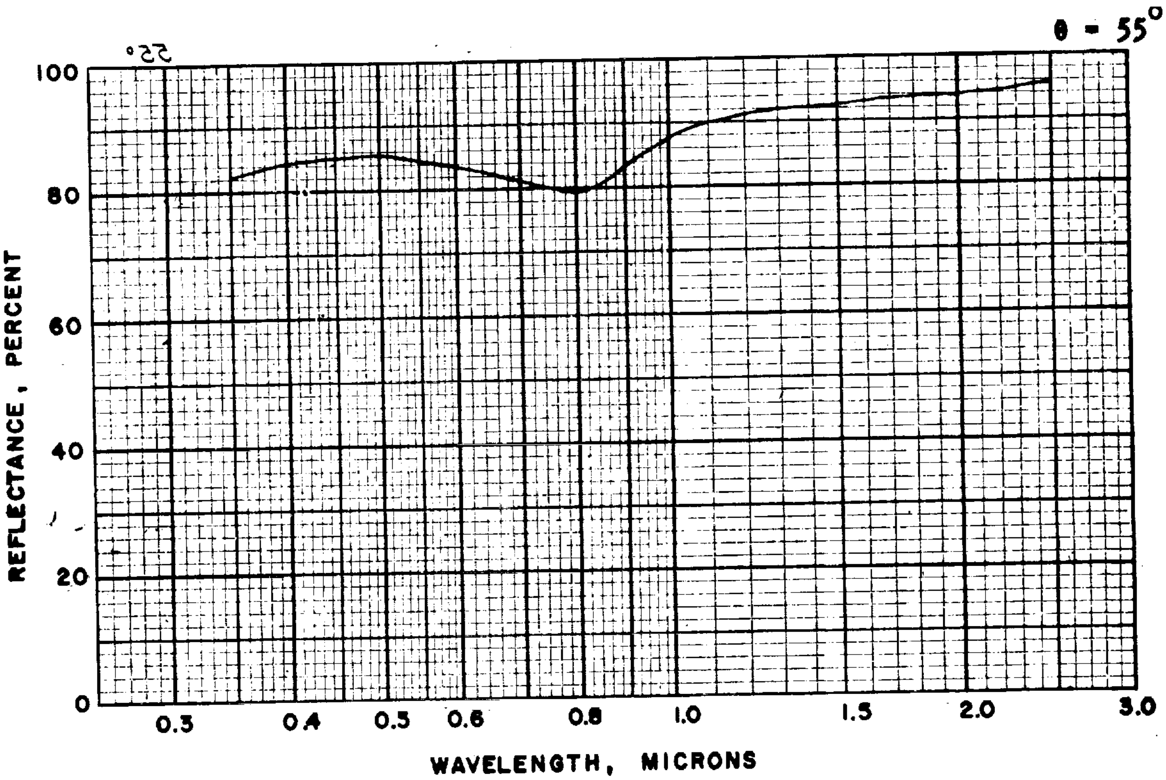

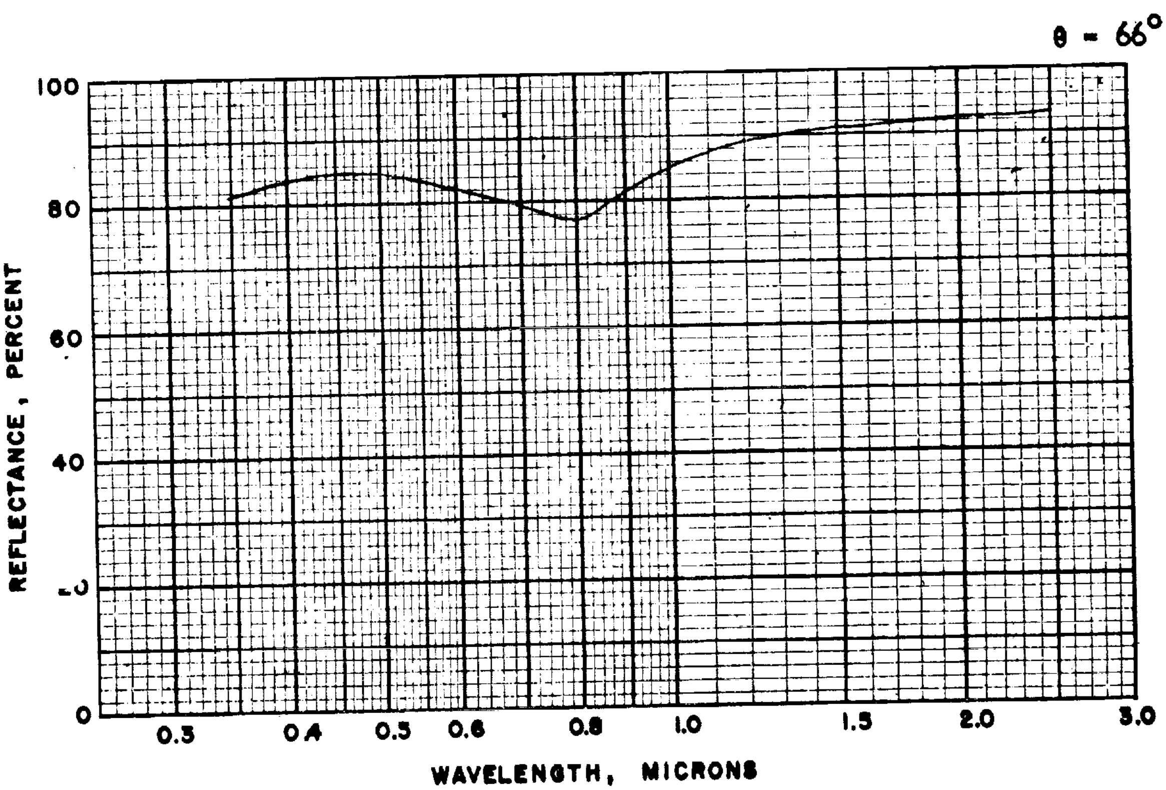

Figure 44 (Cont.): Sample 15A, Azimuthal Angle 60°, Angles of Incidence 55° and 66°

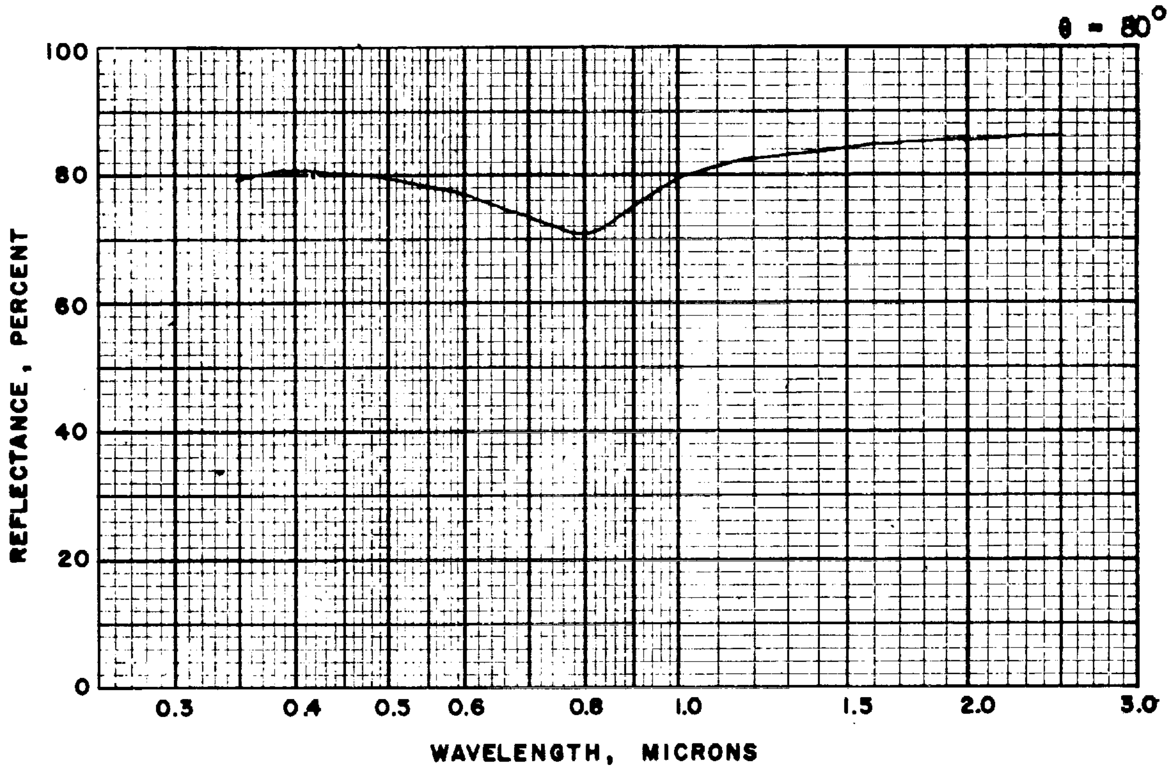

Figure 44 (Cont.): Sample 15A, Azimuthal Angle 60°
Angle of Incidence 80°

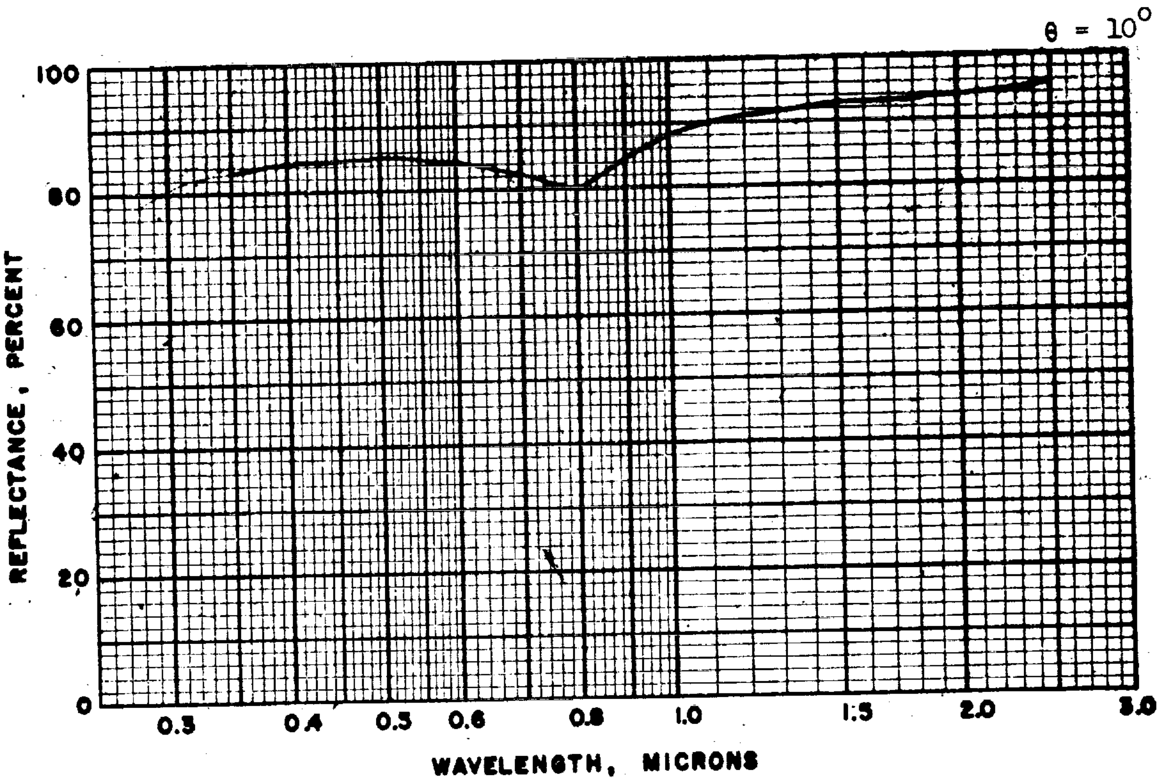

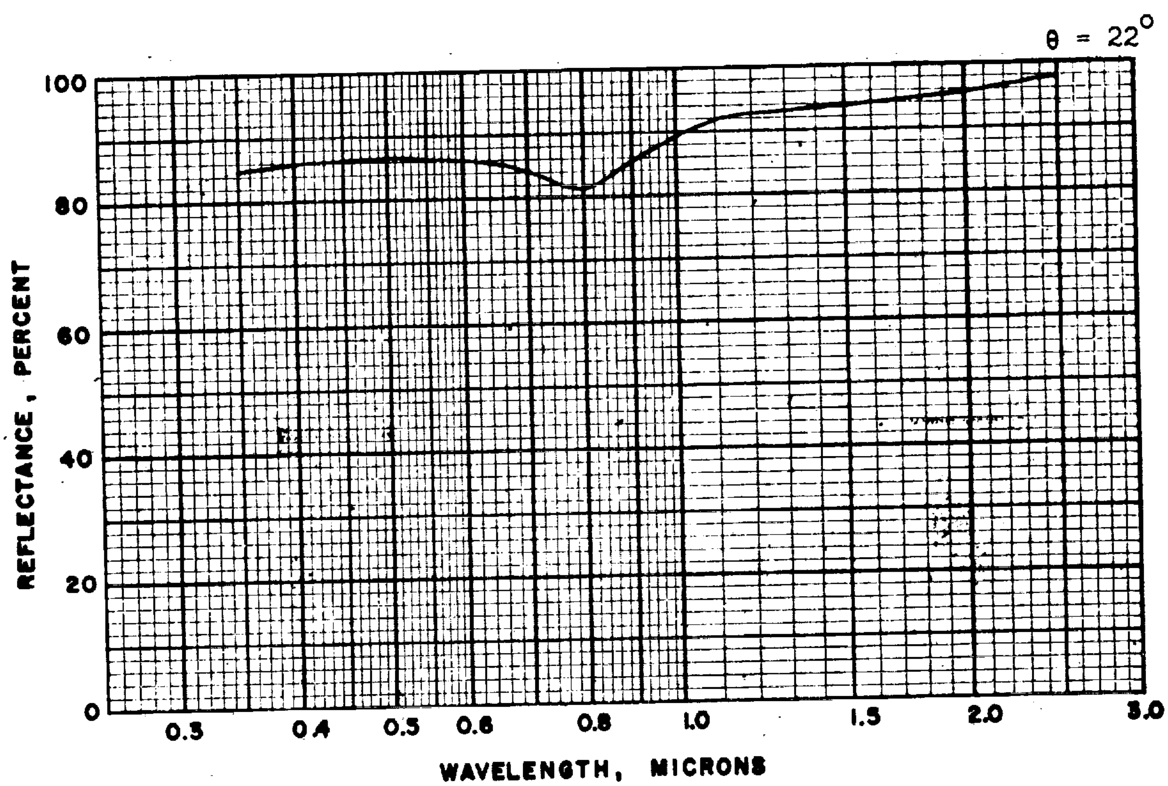

Figure 45: Sample 15A, Azimuthal Angle 90°, Angles of Incidence 10° and 22°

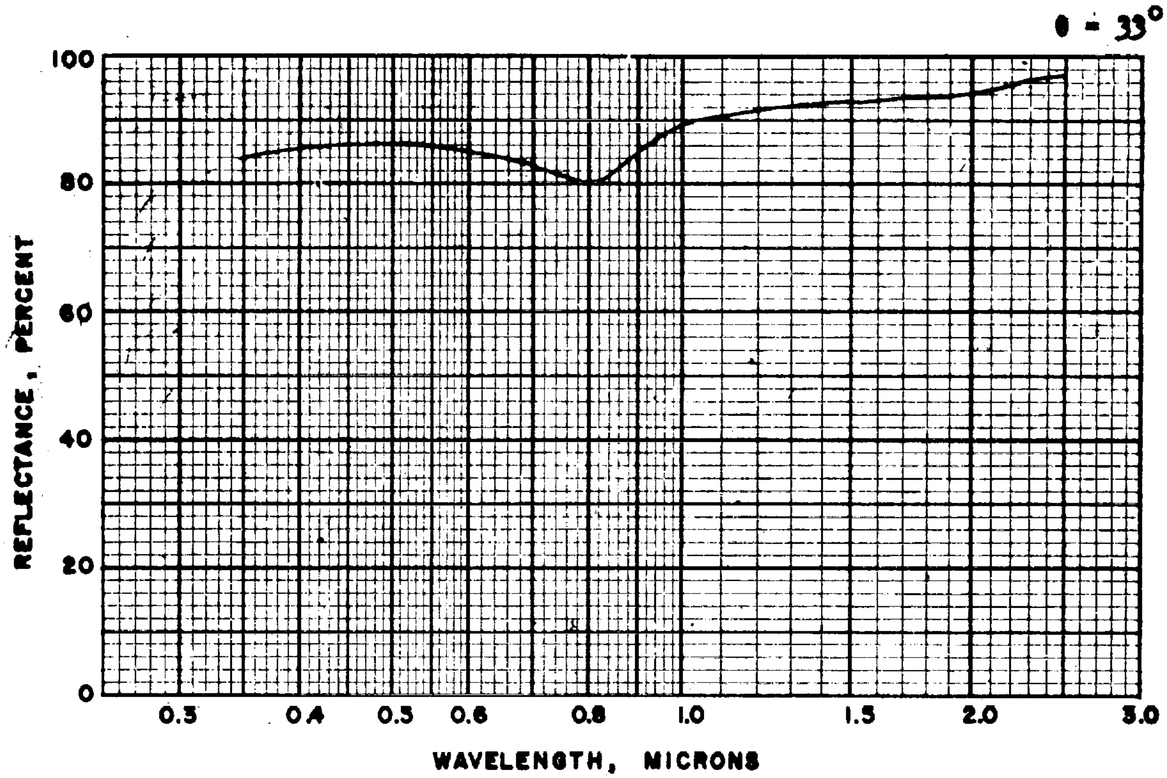

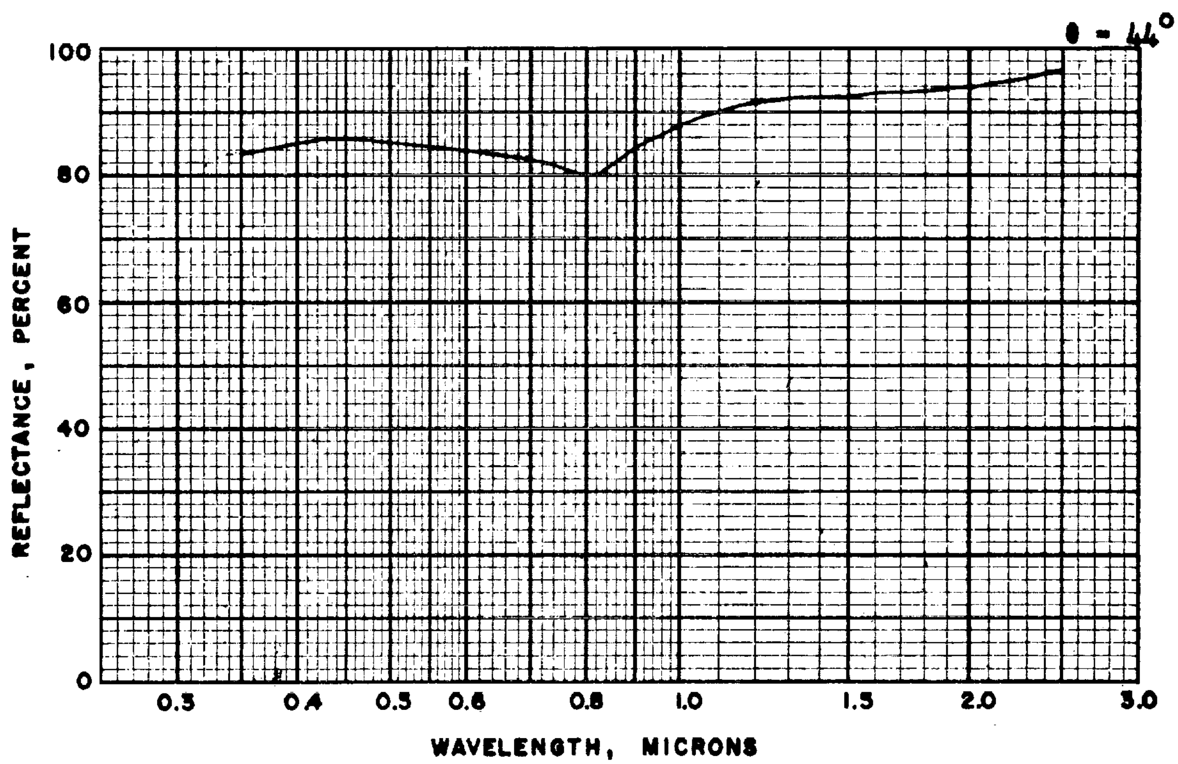

Figure 45 (Cont.): Sample 15A, Azimuthal Angle 90°, Angles of Incidence 33° and 44°

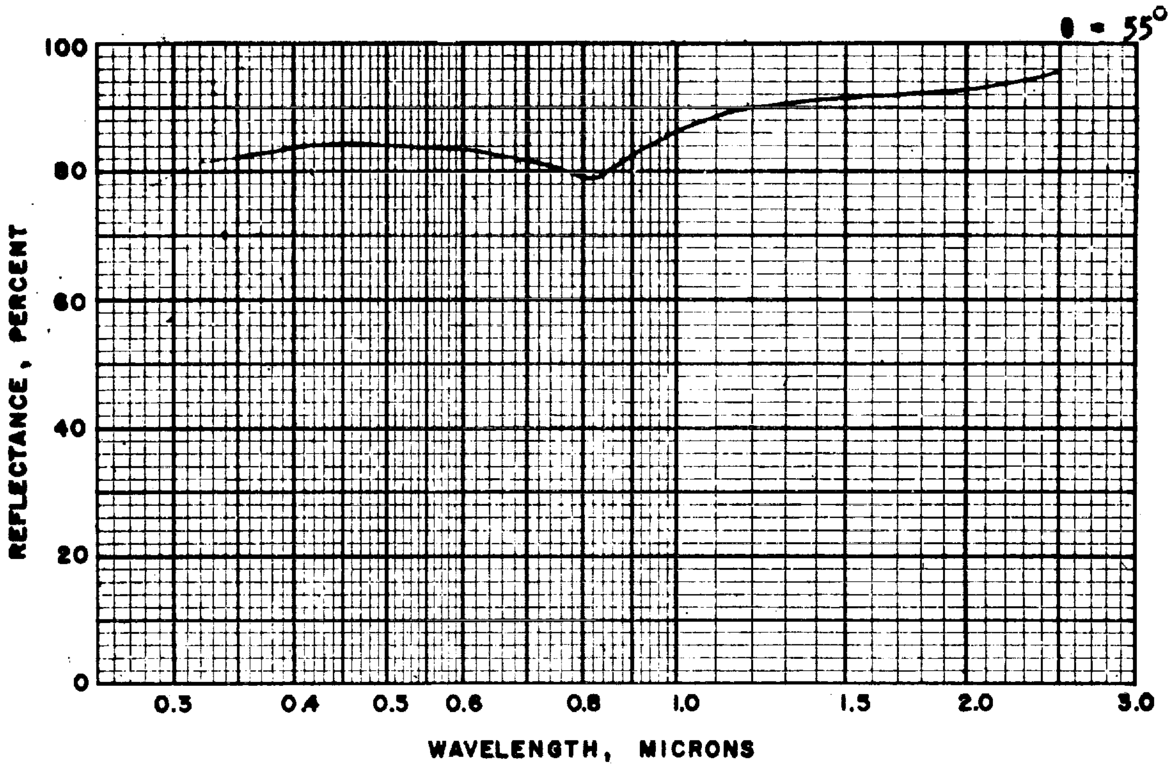

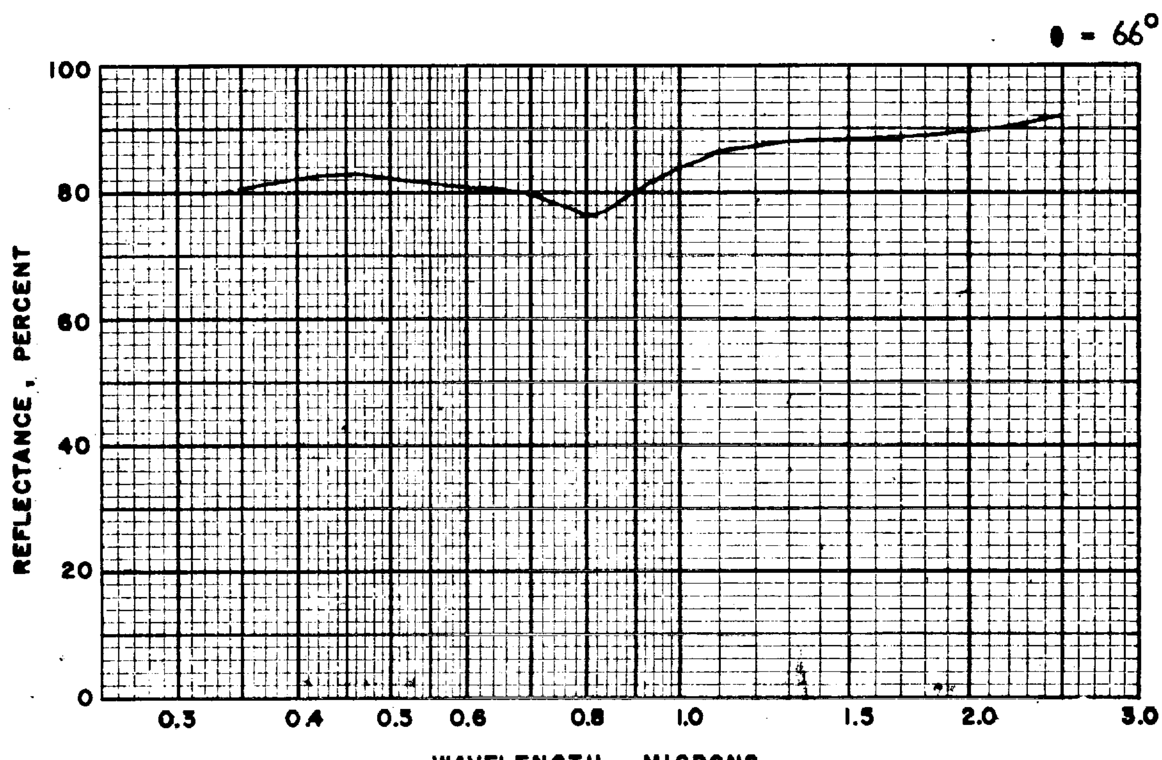

Figure 45 (Cont.): Sample 15A, Azimuthal Angle 90°, Angles of Incidence 55° and 66°

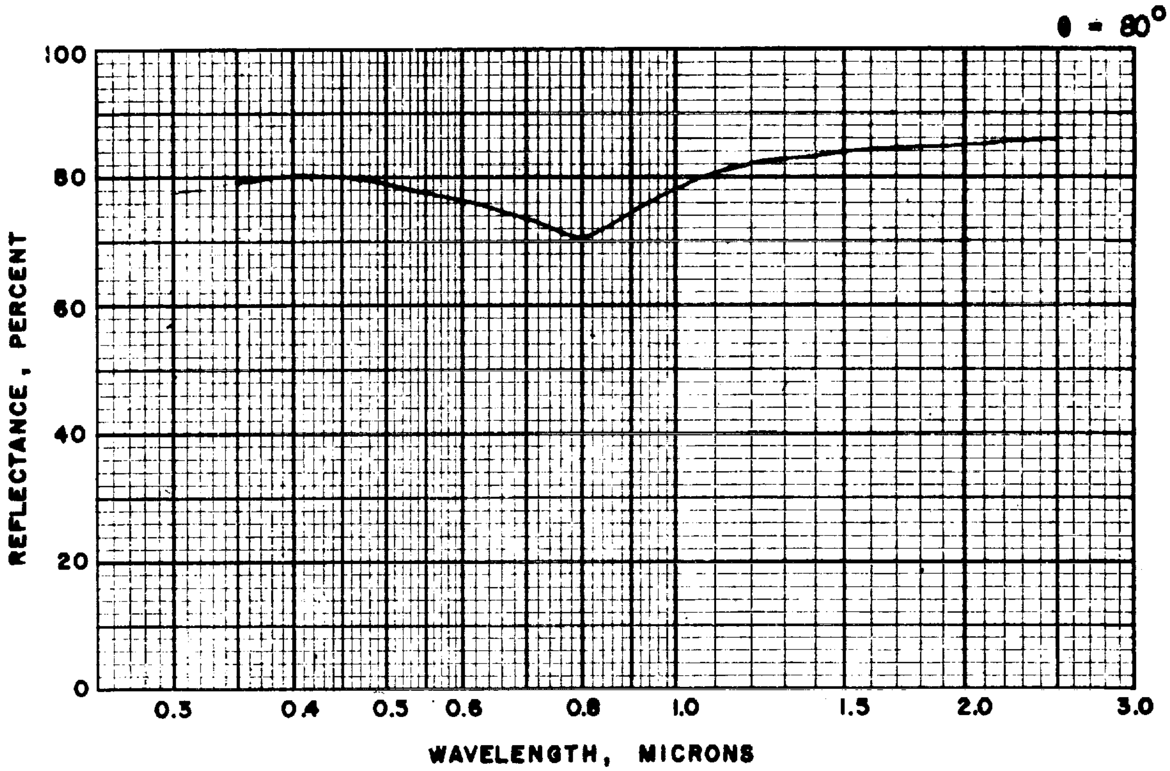

Figure 45 (Cont.): Sample 15A, Azimuthal Angle 90°
Angle of Incidence 80°

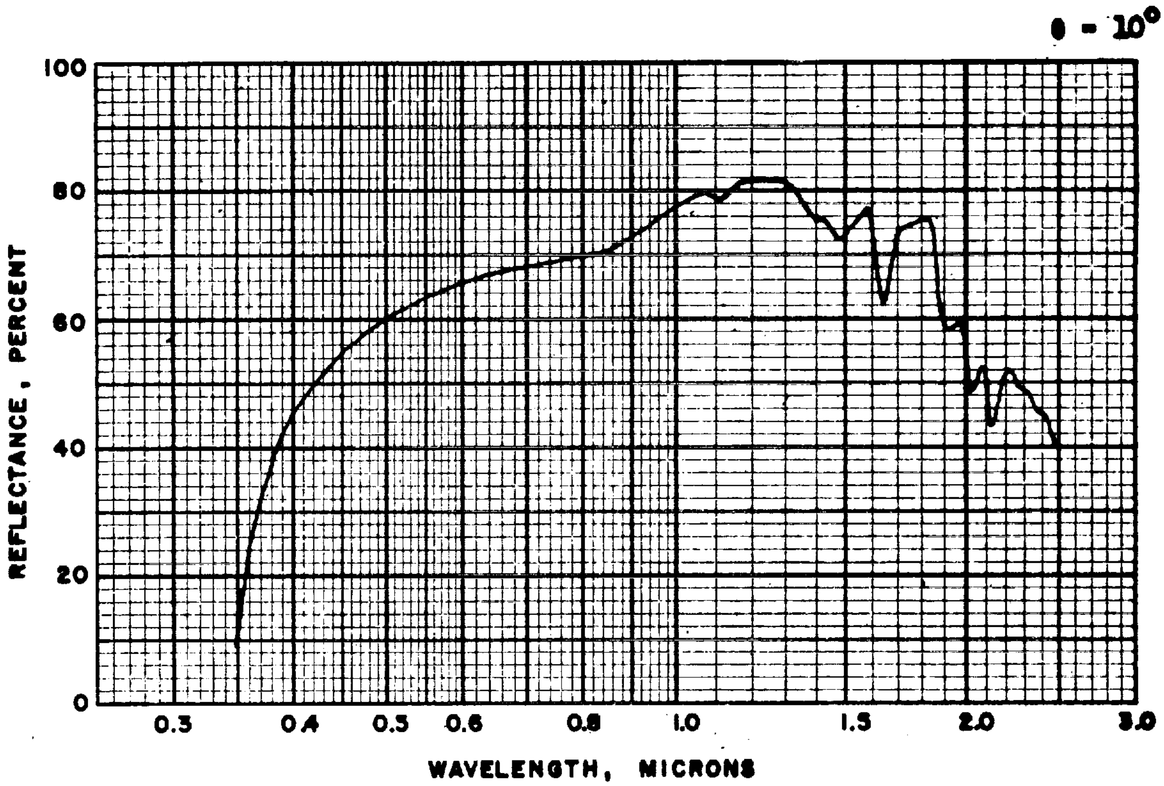

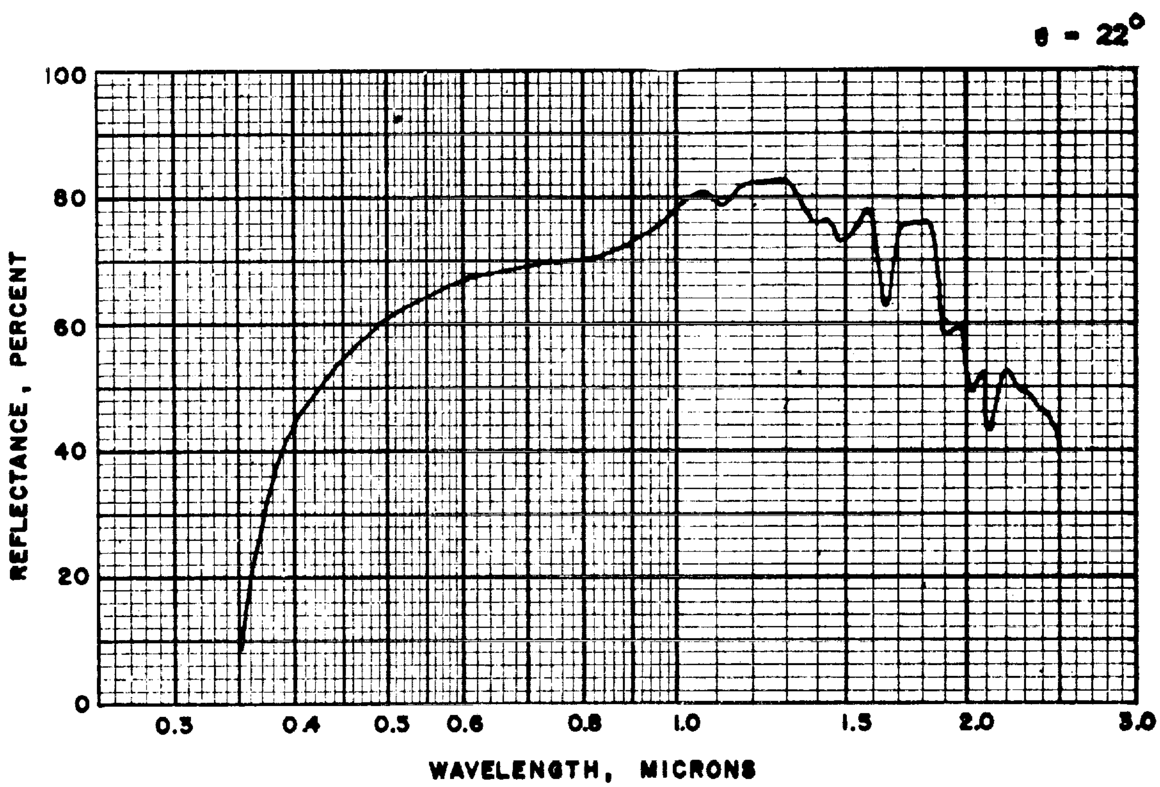

Figure 46: Sample 15B, Azimuthal Angle 0°,
Angles of Incidence 10° and 22°

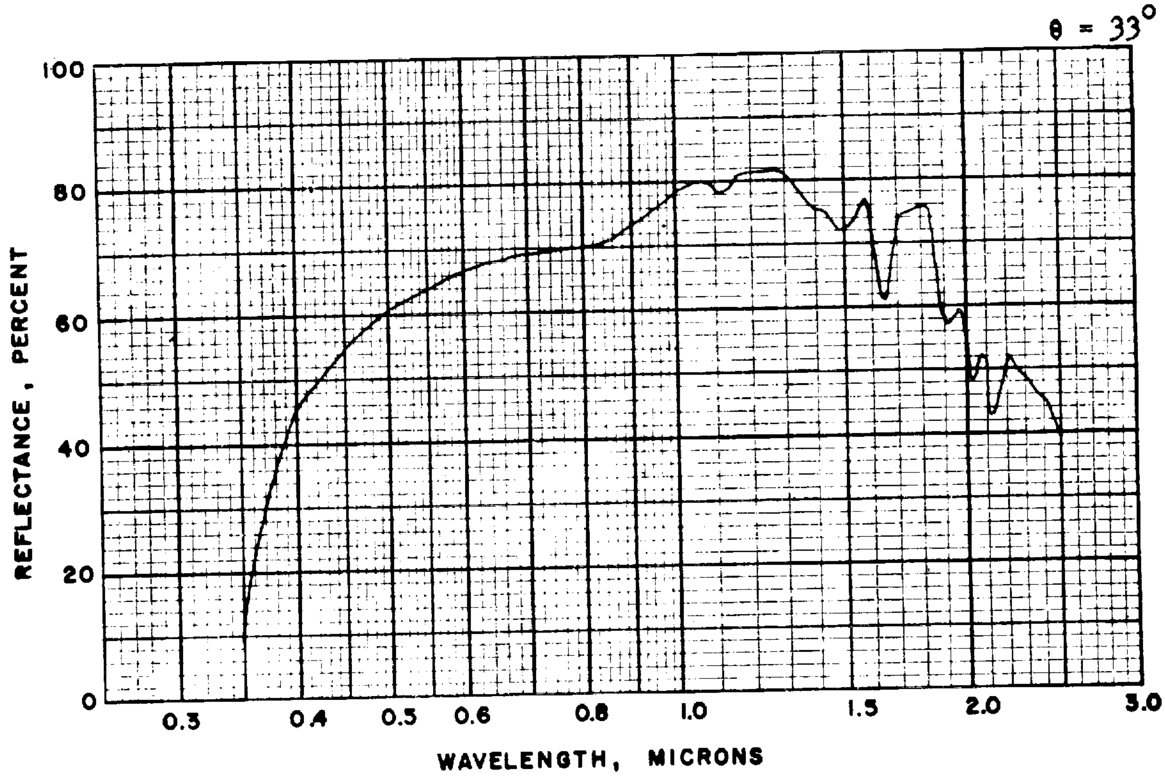

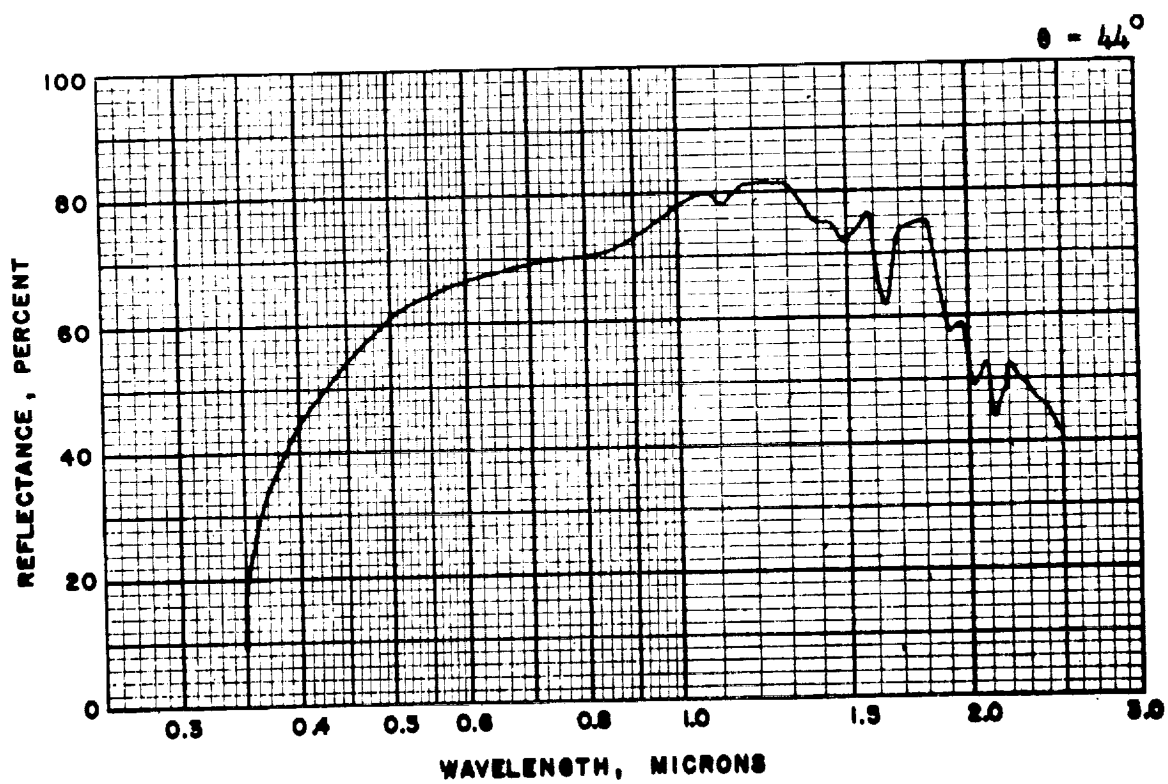

Figure 46 (Cont.): Sample 15B, Azimuthal Angle 0°, Angles of Incidence 33° and 44°

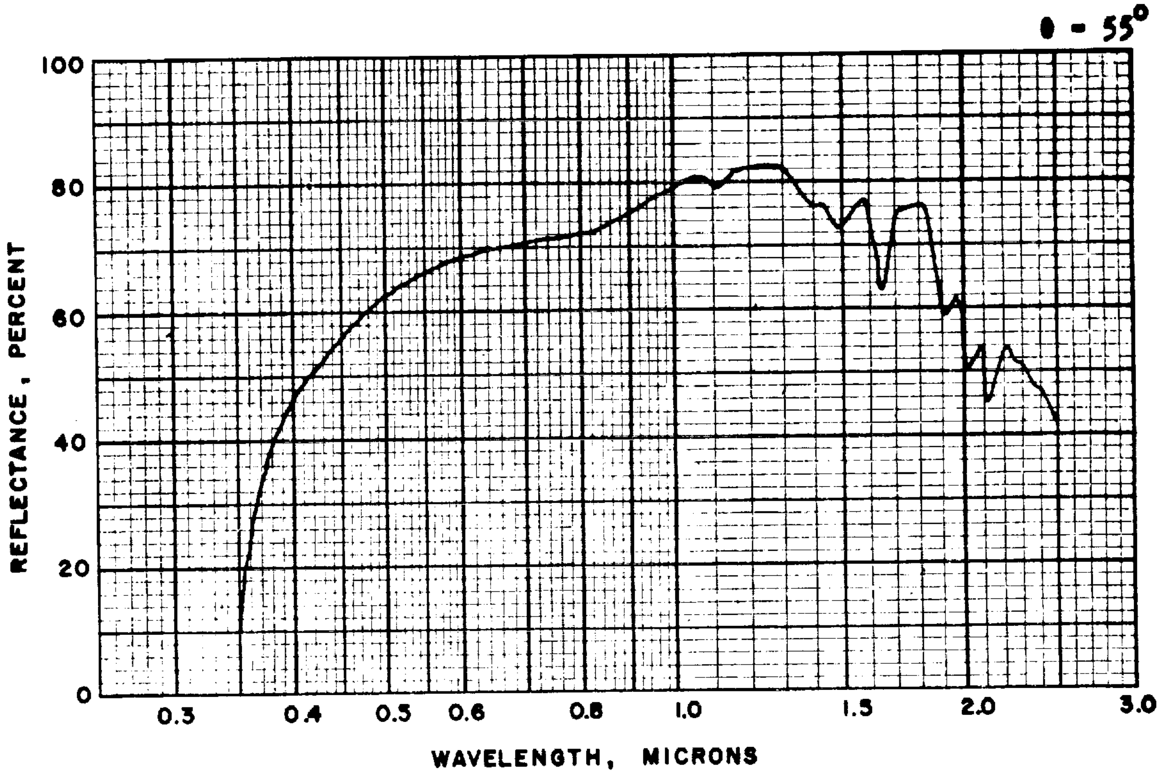

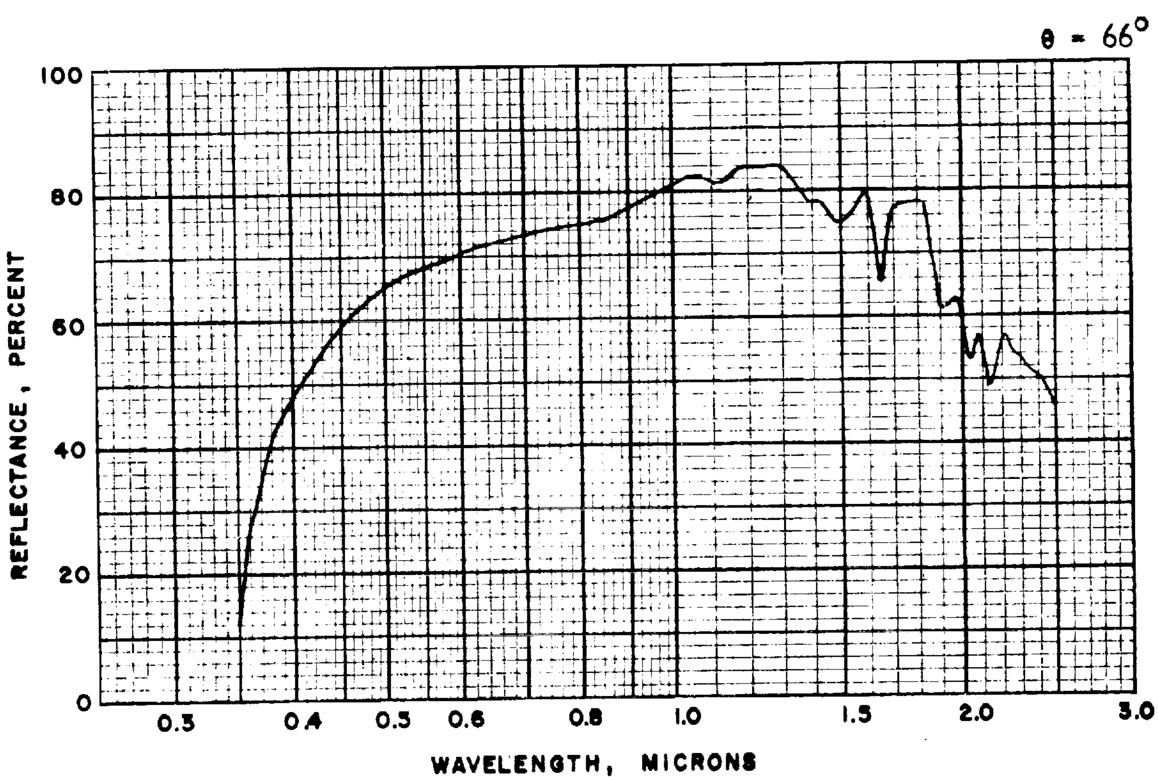

Figure 46 (Cont.): Sample 15B, Azimuthal Angle 0°
Angles of Incidence 55° and 66°

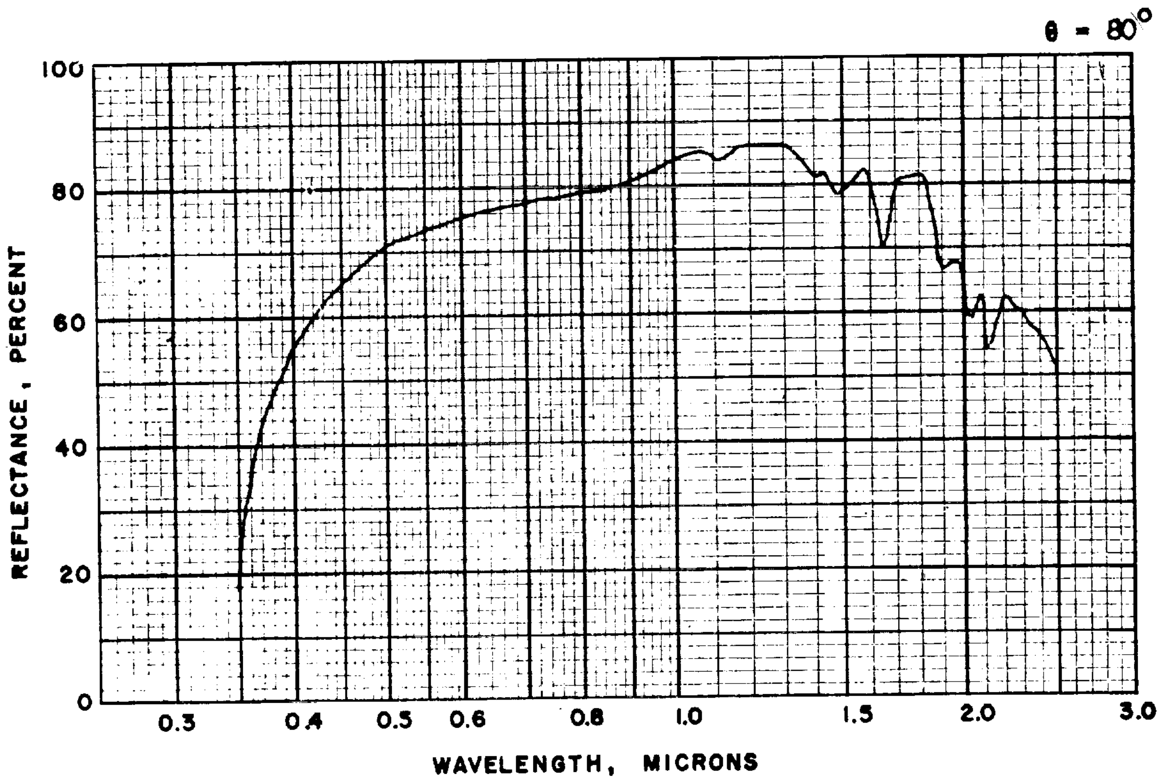

Figure 46 (Cont.): Sample 15B, Azimuthal Angle 0°
Angle of Incidence 80°

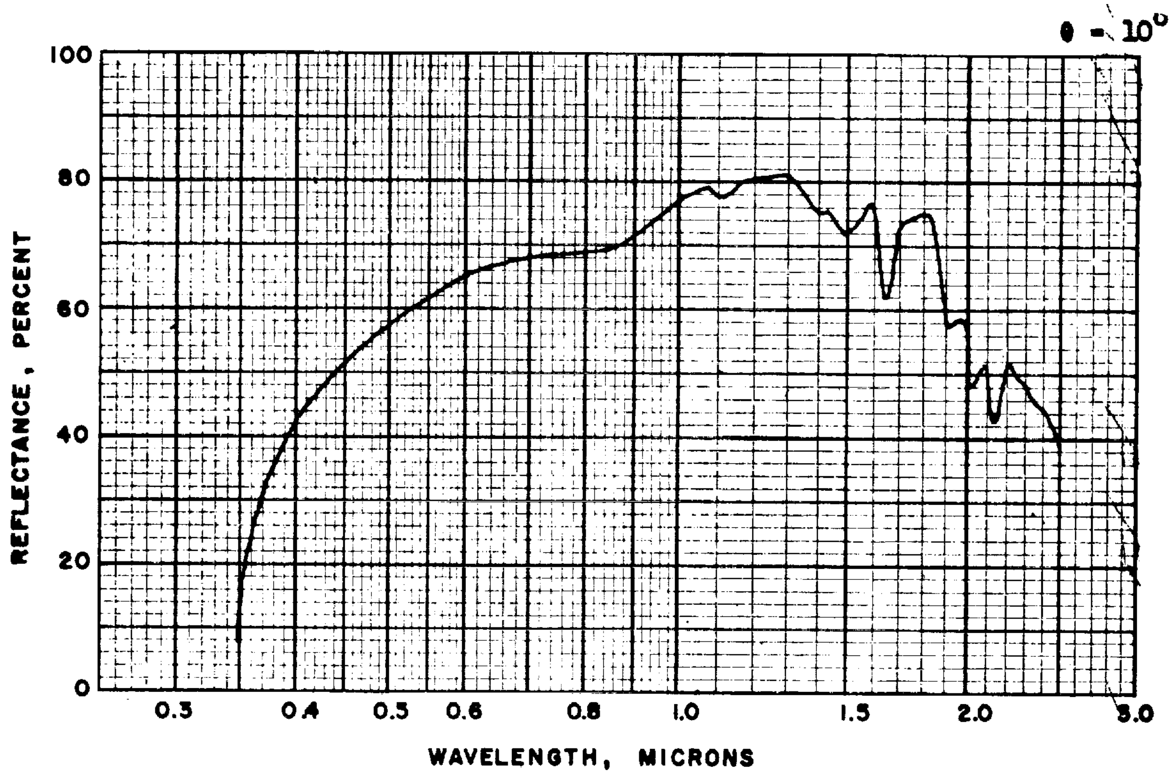

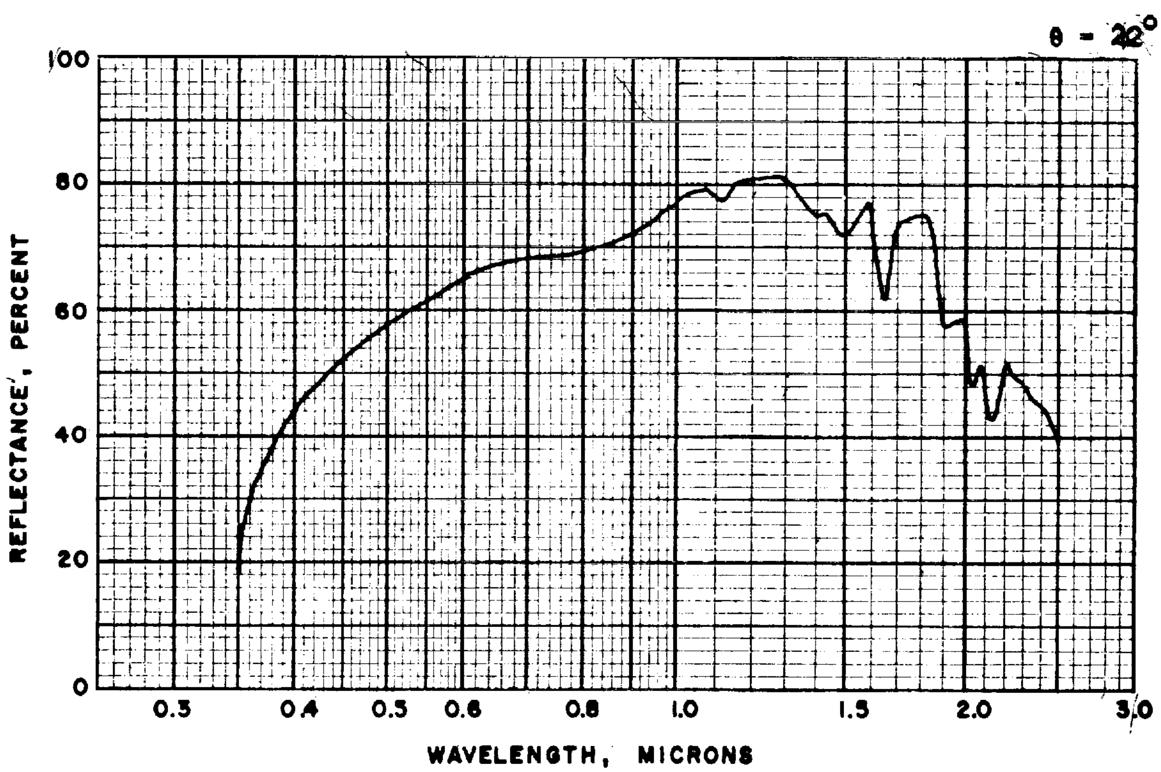

Figure 47: Sample 15B, Azimuthal Angle 45°, Angles of Incidence 10° and 22°

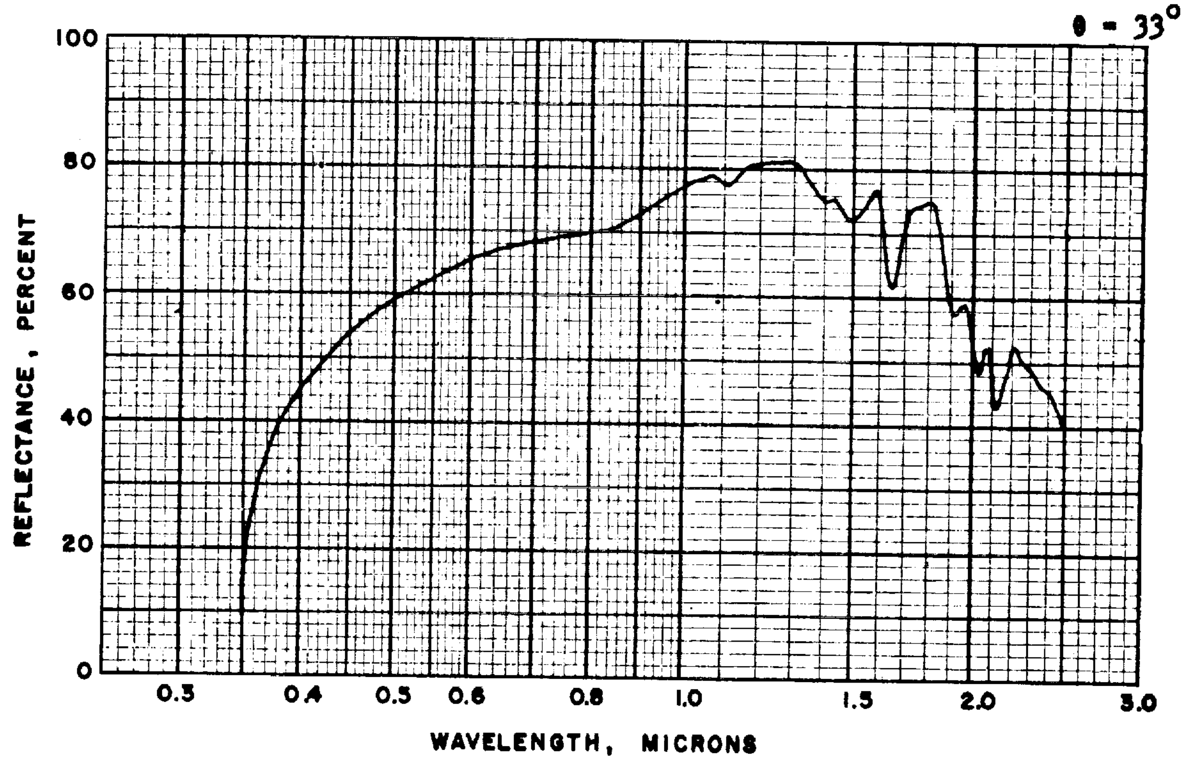

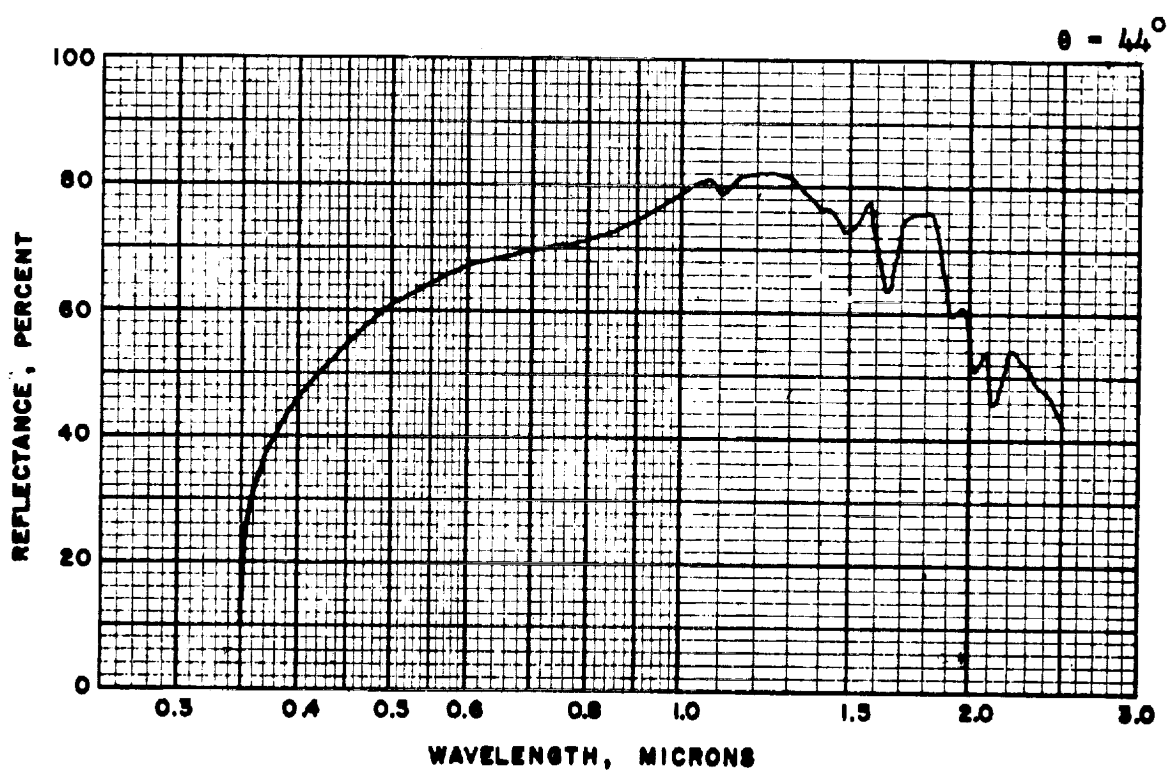

Figure 47 (Cont.): Sample 15B, Azimuthal Angle 45°, Angles of Incidence 33° and 44°

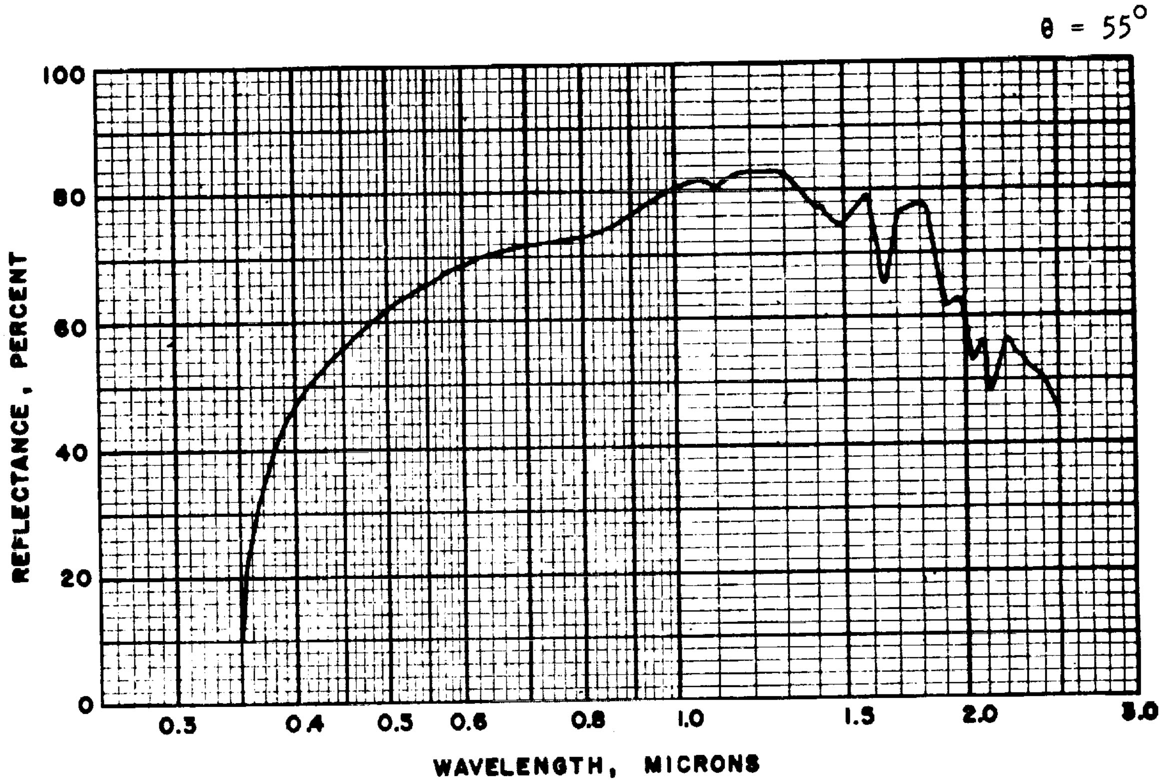

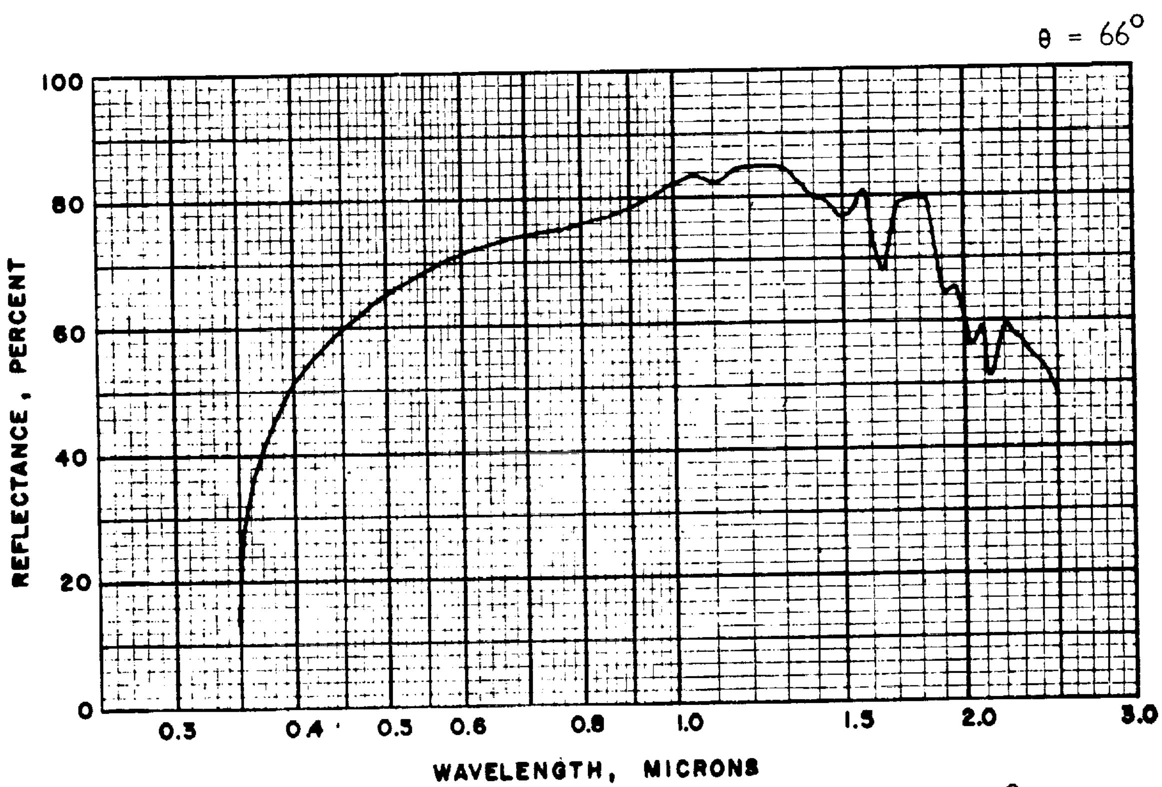

Figure 47 (Cont.): Sample 15B, Azimuthal Angle 45°, Angles of Incidence 55° and 66°

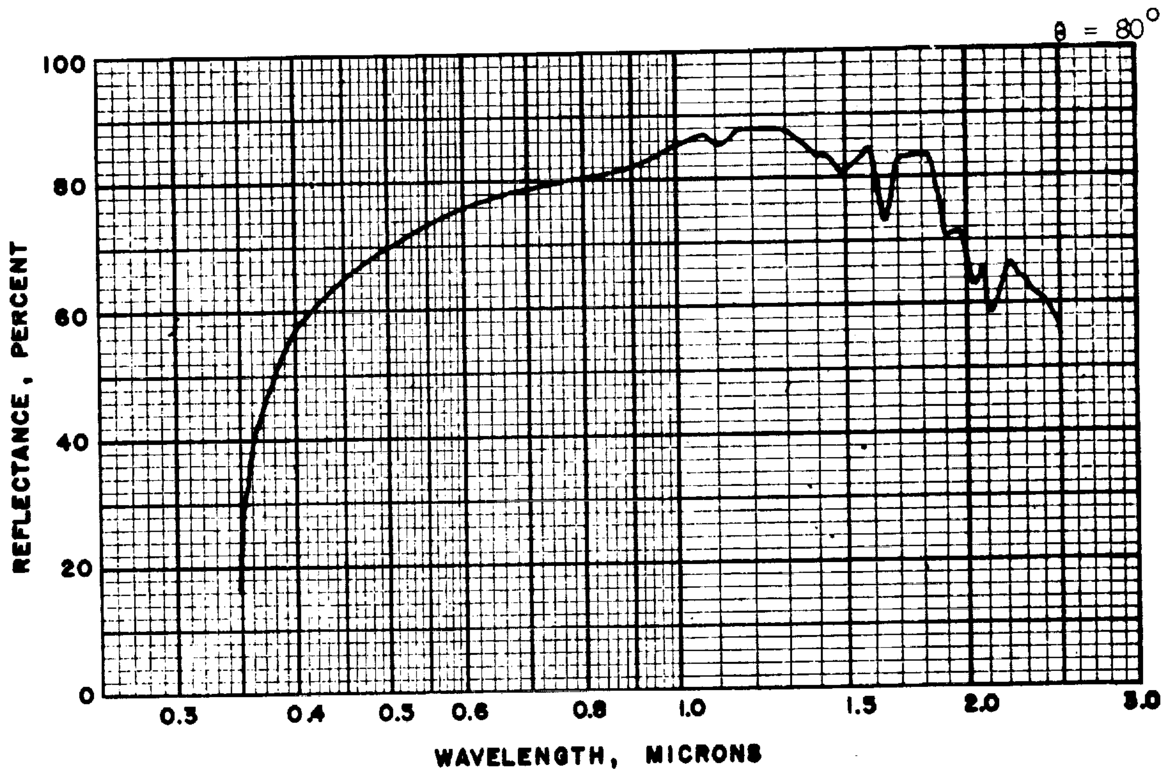

Figure 47 (Cont.): Sample 15B, Azimuthal Angle 45°, Angle of Incidence 80°

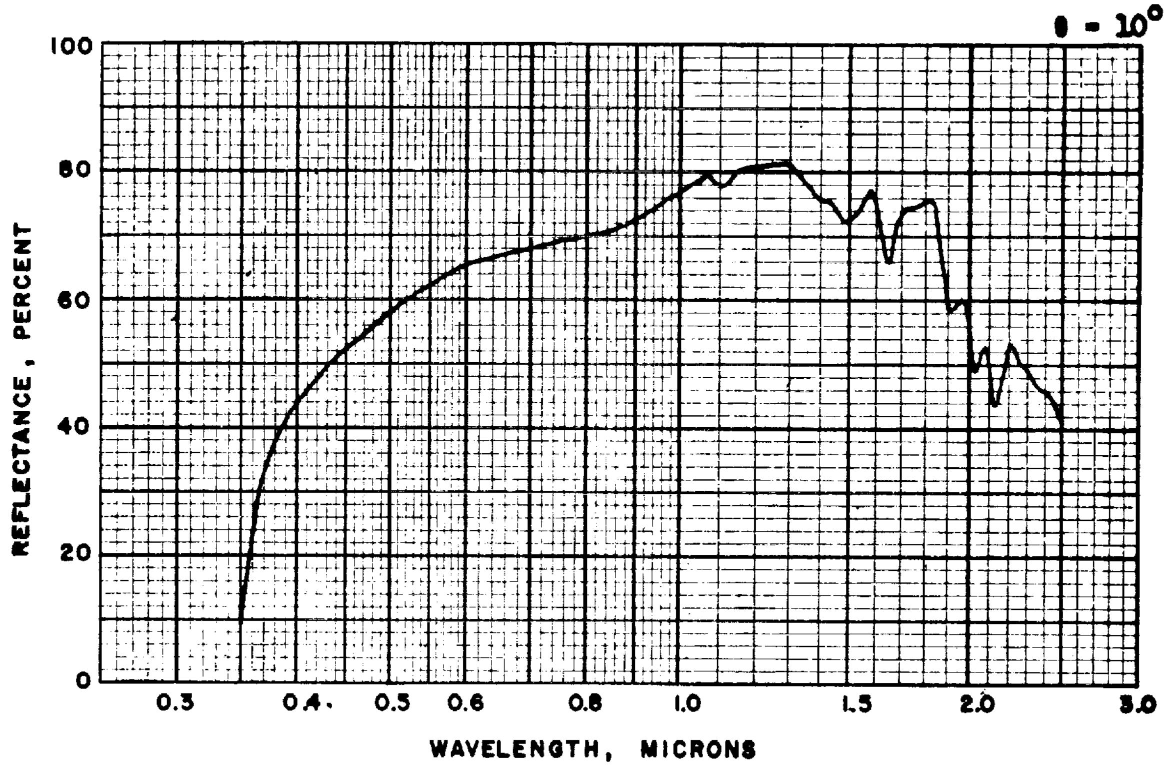

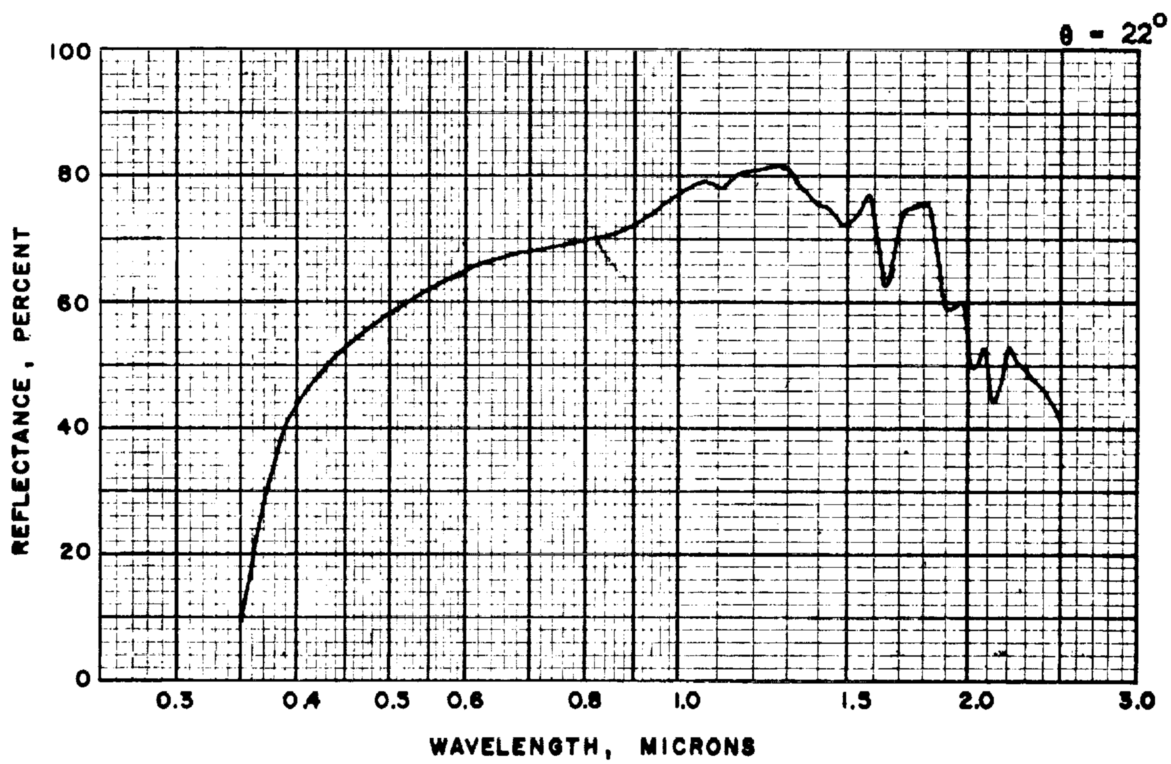

Figure 48: Sample 15B, Azimuthal Angle 60°, Angles of Incidence 10° and 22°

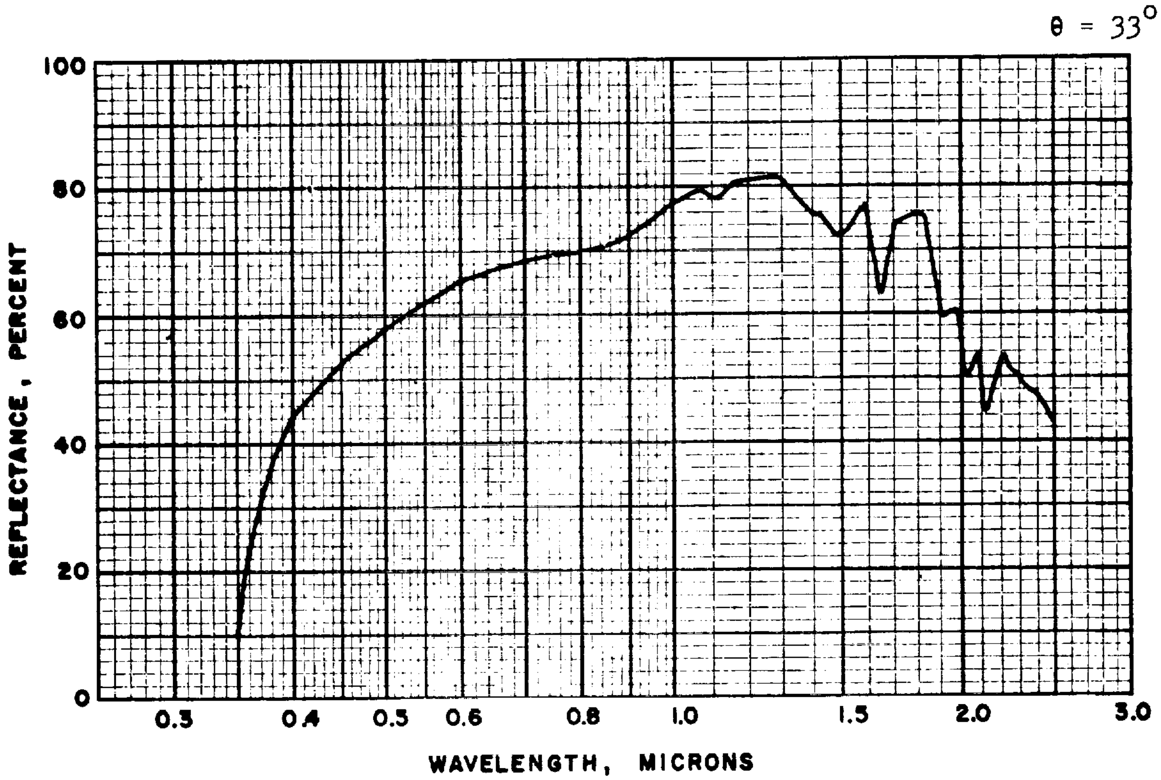

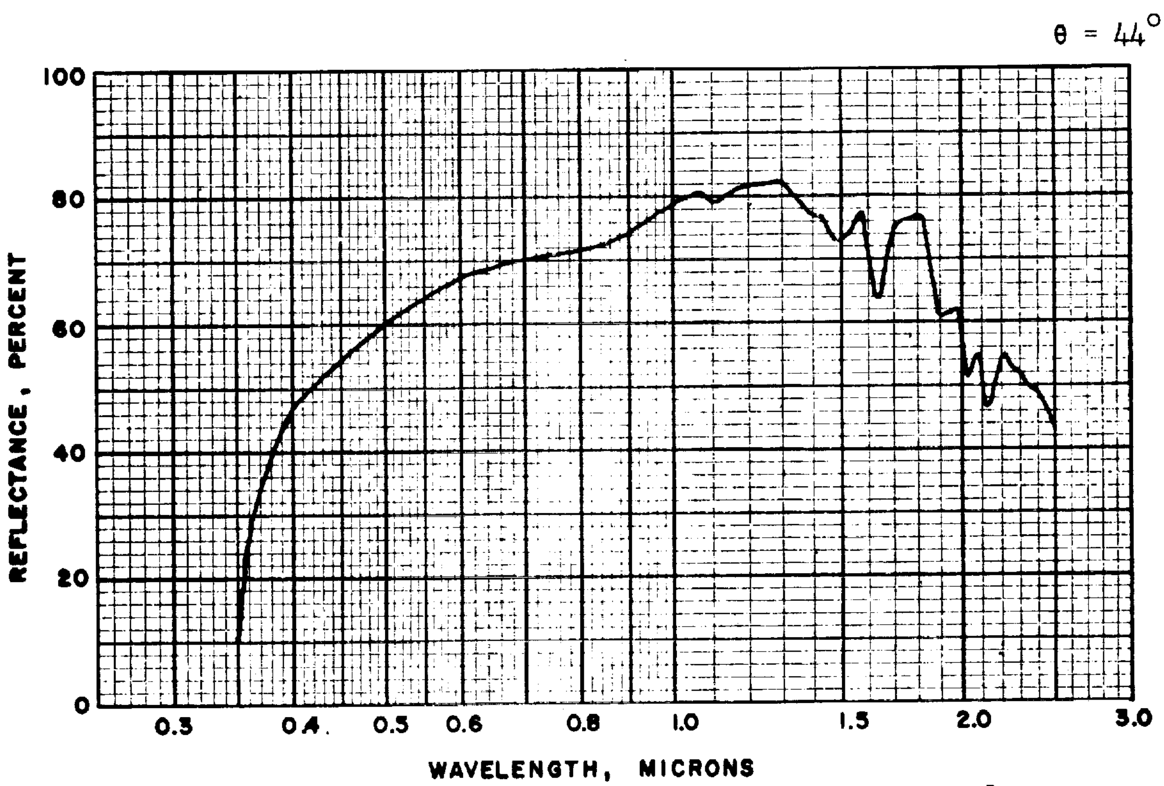

Figure 48 (Cont.): Sample 15B, Azimuthal Angle 60°, Angles of Incidence 33° and 44°

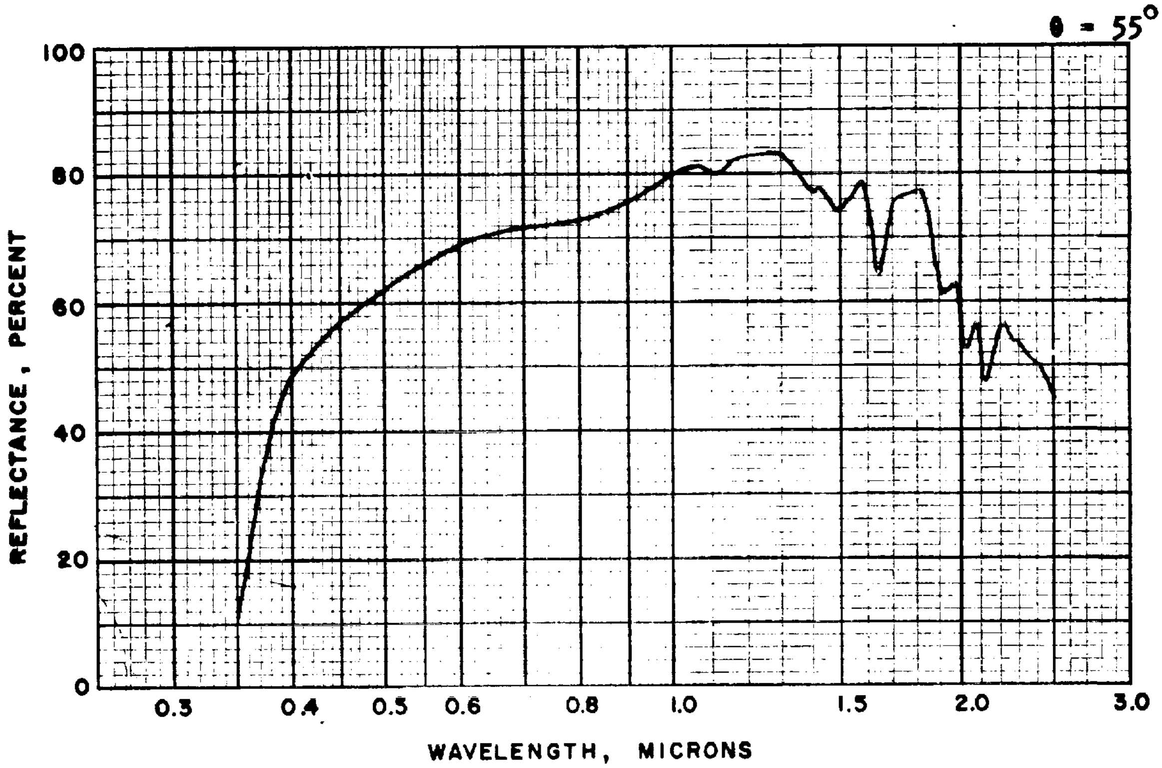

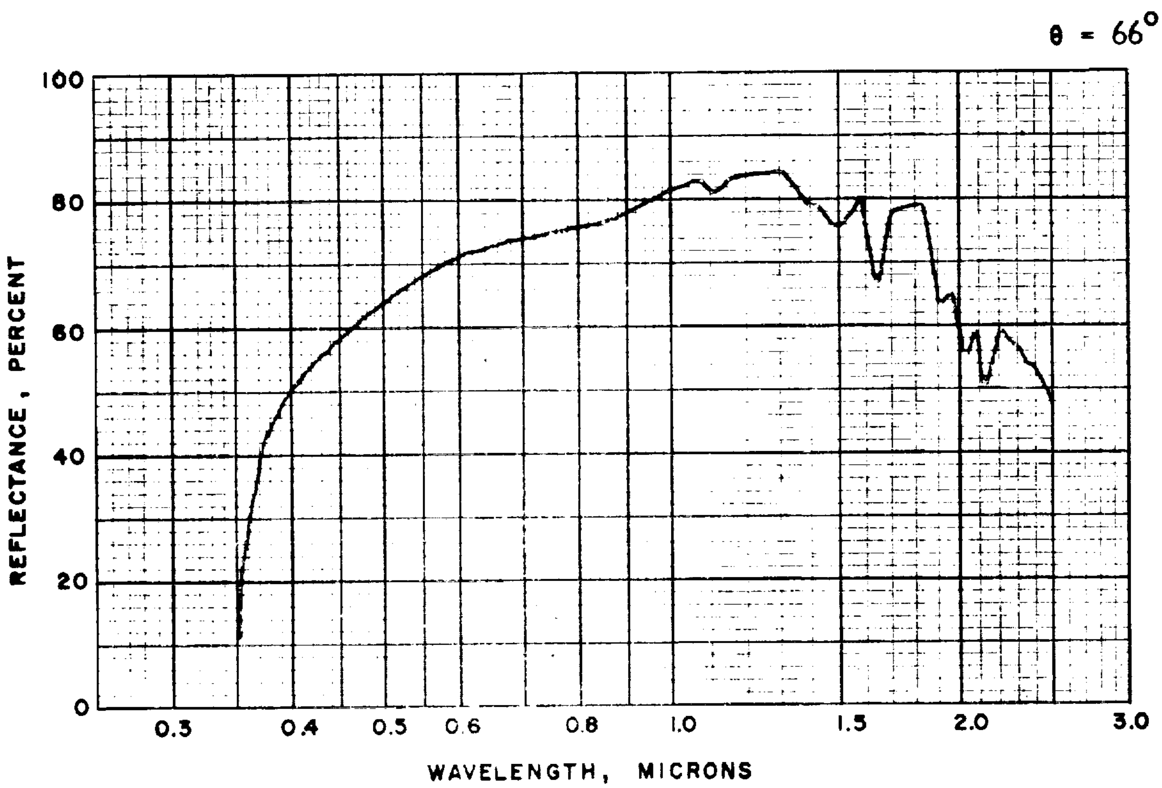

Figure 48 (Cont.): Sample 15B, Azimuthal Angle 60°, Angles of Incidence 55° and 66°

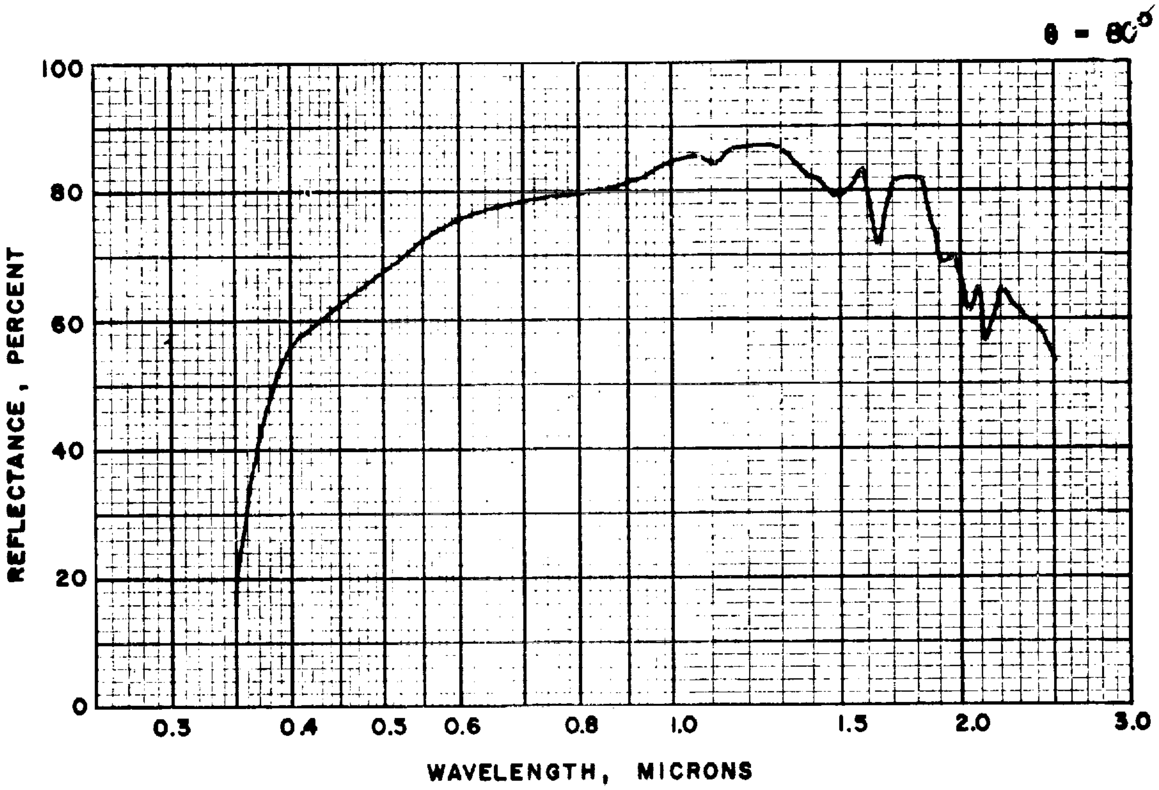

Figure 48 (Cont.): Sample 15B, Azimuthal Angle 60°
Angle of Incidence 80°

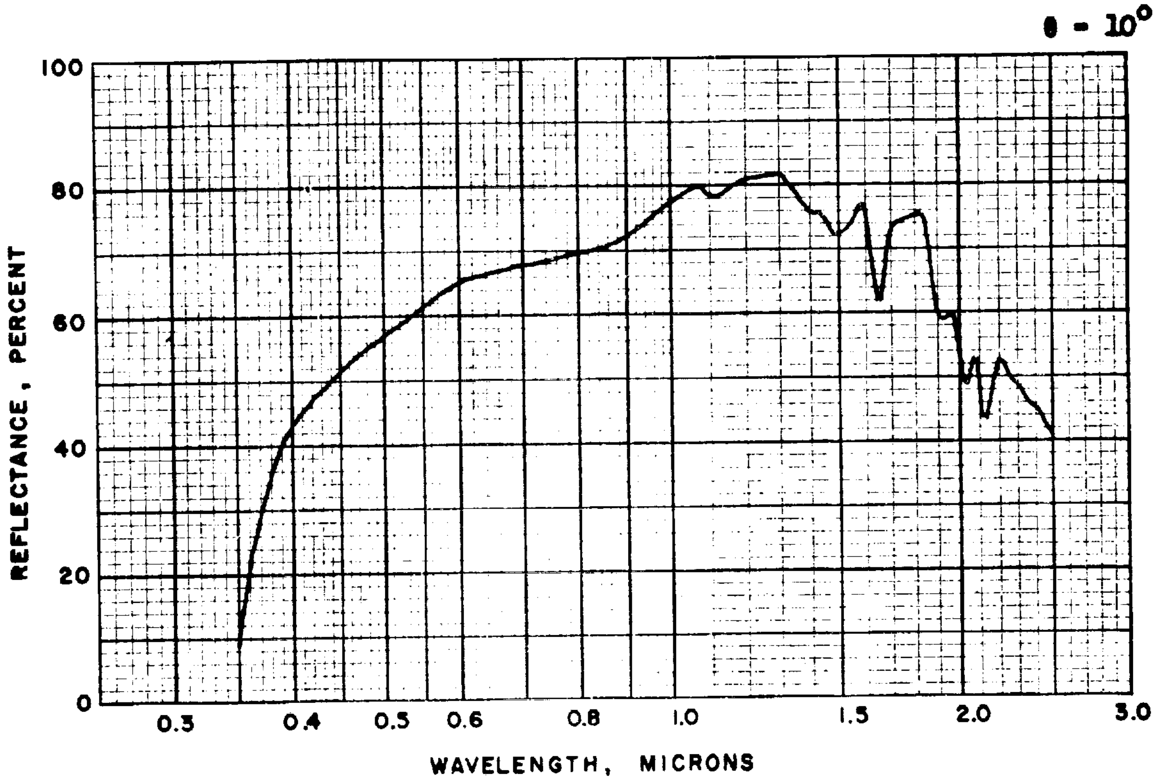

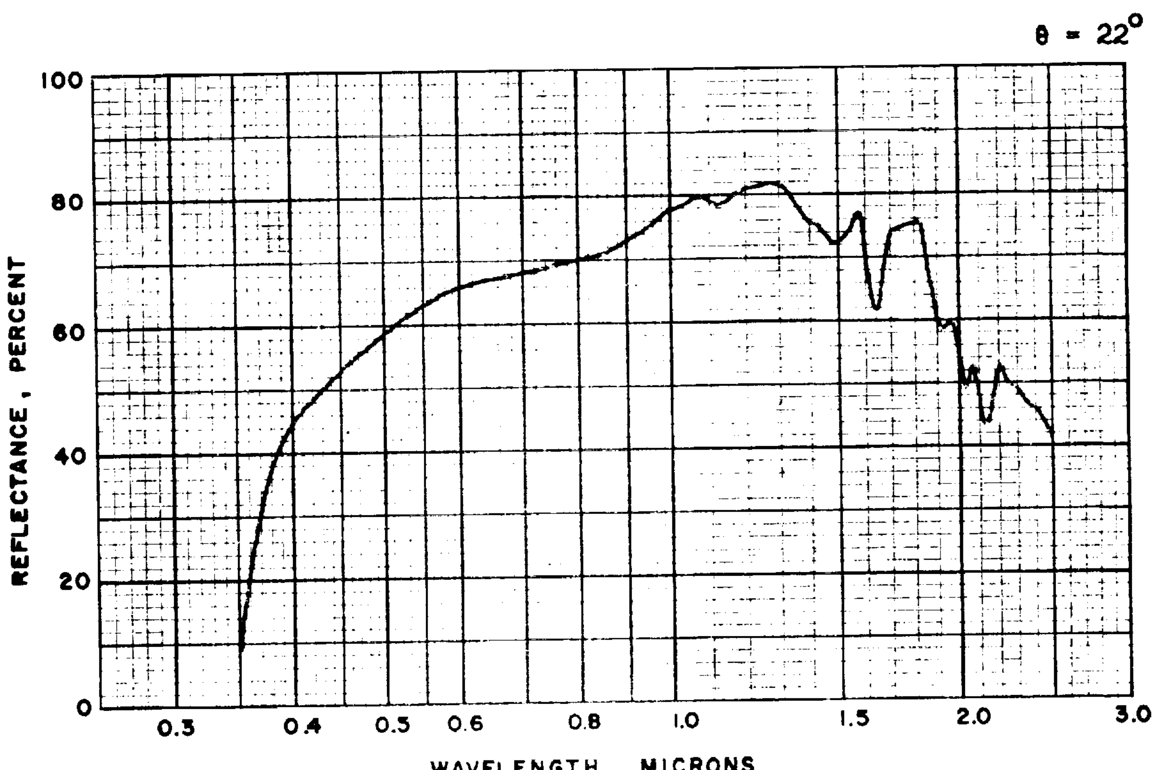

Figure 49: Sample 15B, Azimuthal Angle 90°, Angles of Incidence 10° and 22°

θ = 33°

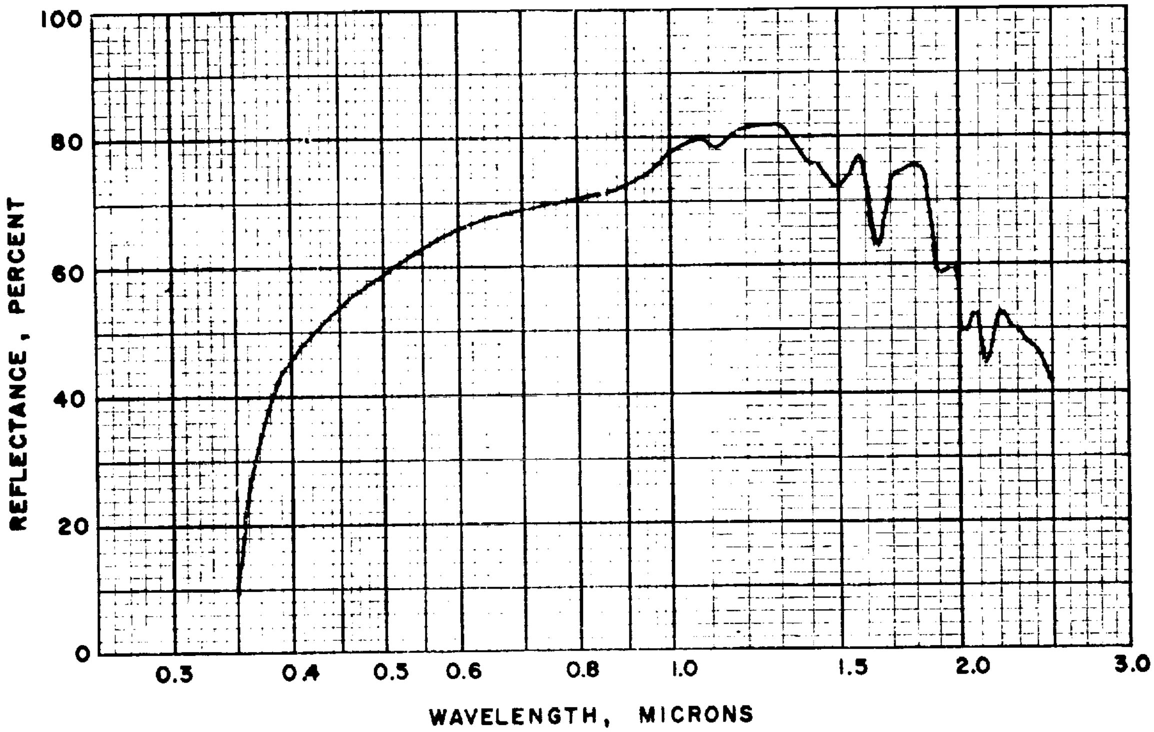

θ = 44°

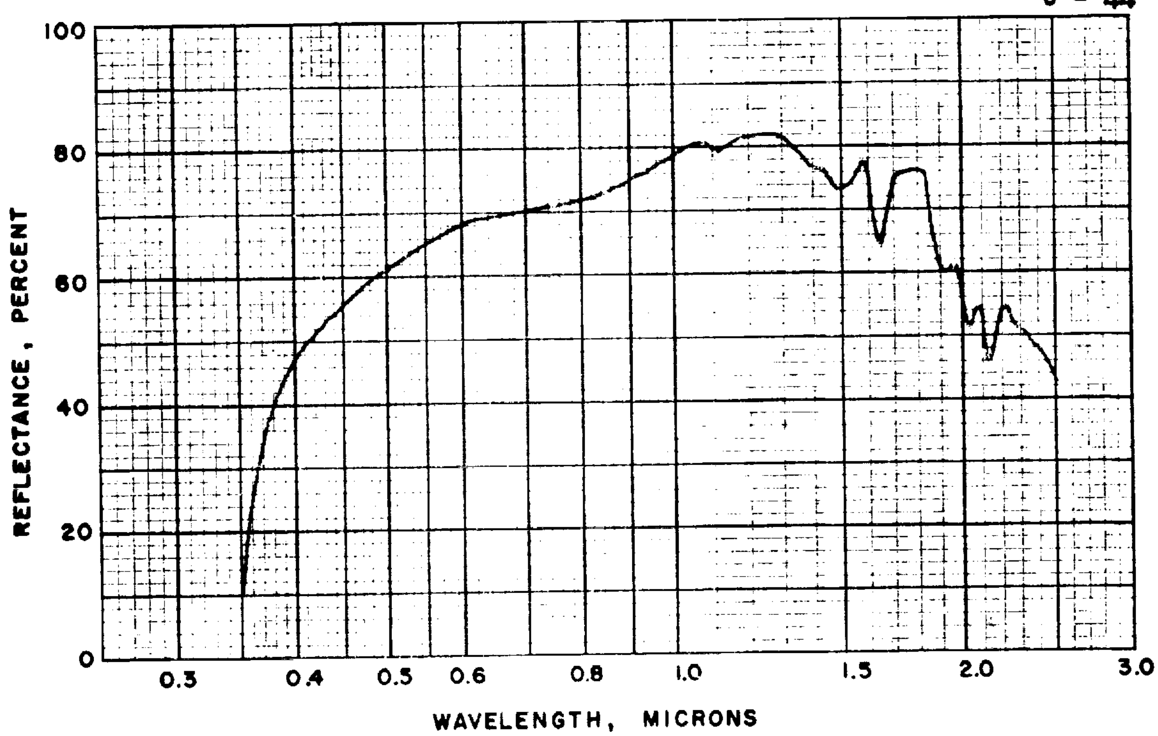

Figure 49 (Cont.): Sample 15B, Azimuthal Angle 90°, Angles of Incidence 33° and 44°

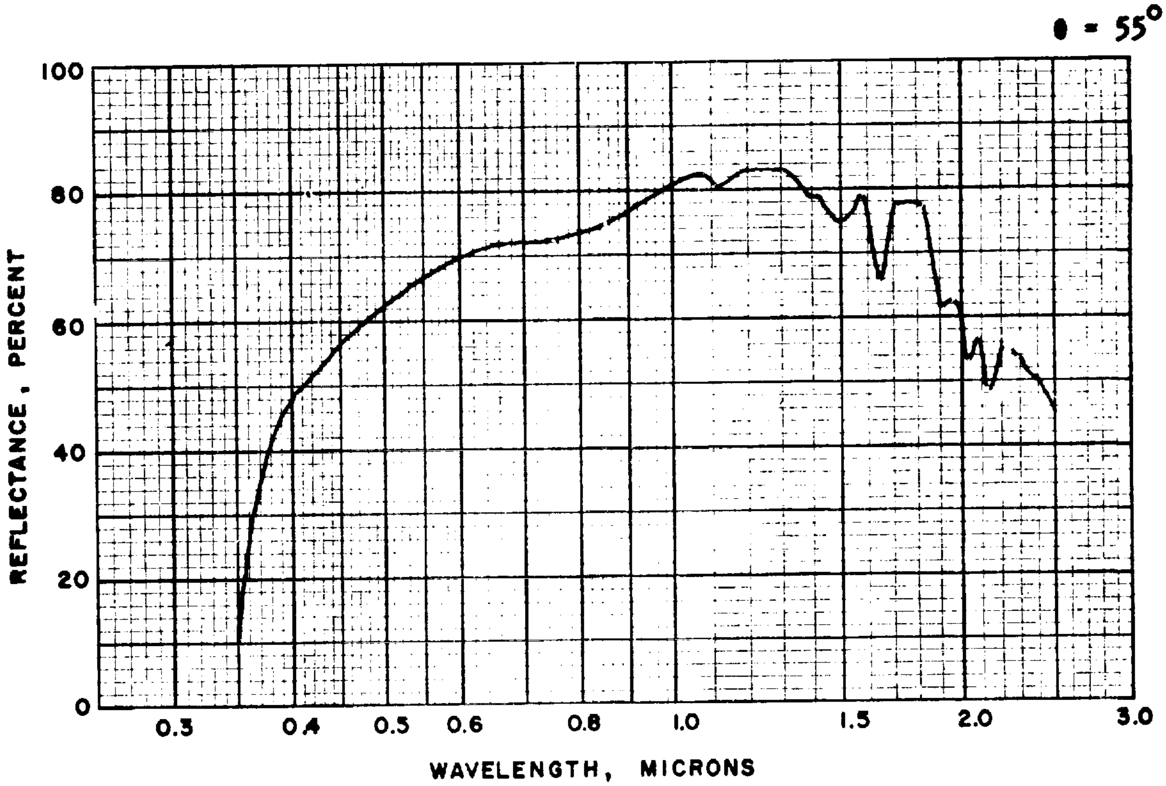

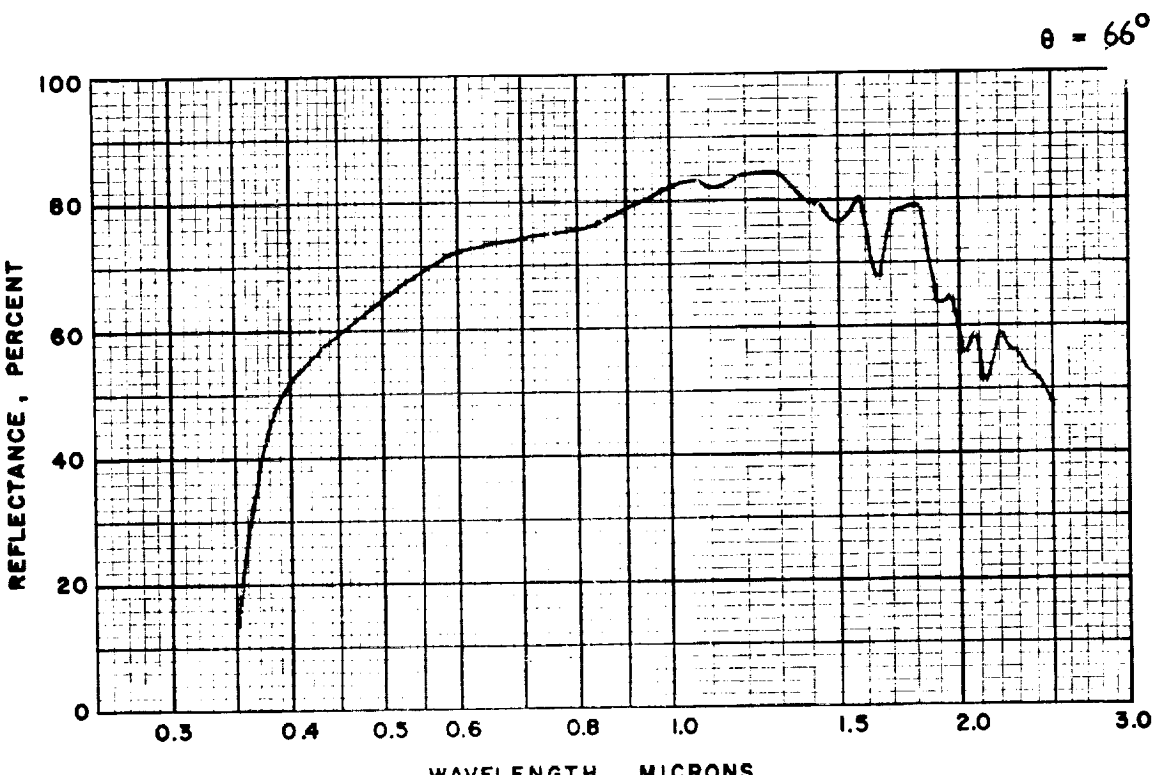

Figure 49 (Cont.): Sample 15B, Azimuthal Angle 90°, Angles of Incidence 55° and 66°

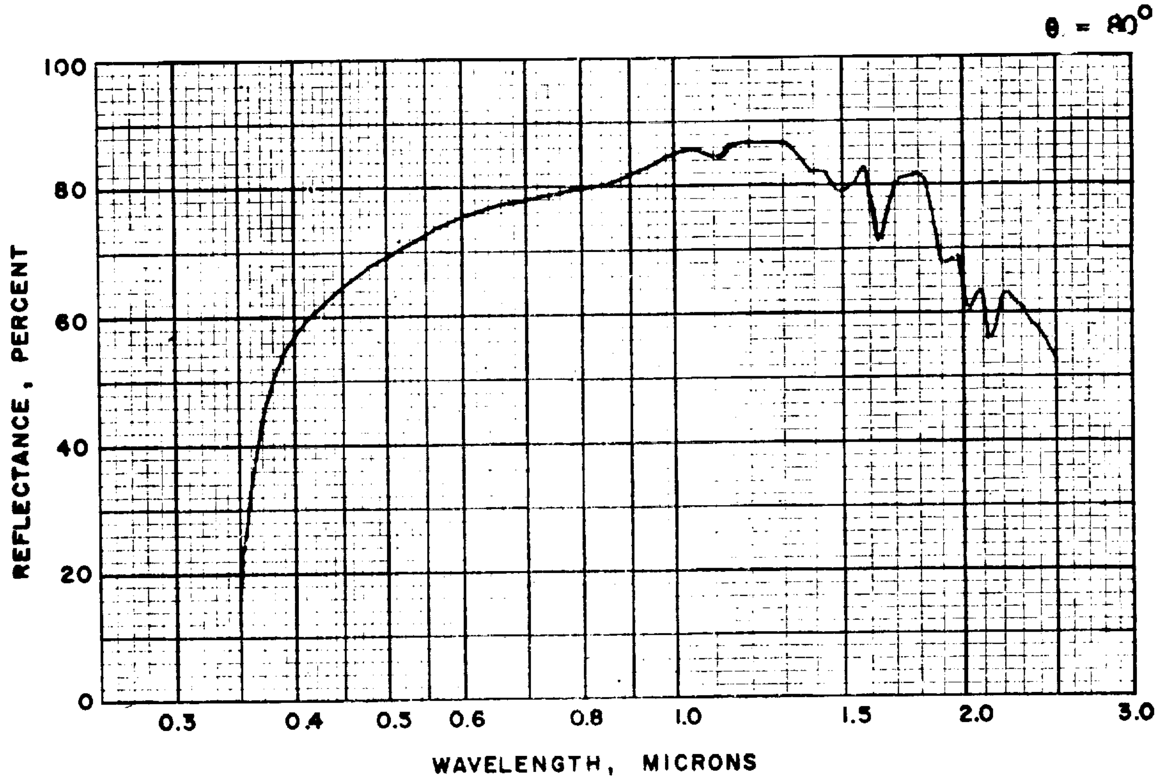

Figure 49 (Cont.): Sample 15B, Azimuthal Angle 90°, Angle of Incidence 80°

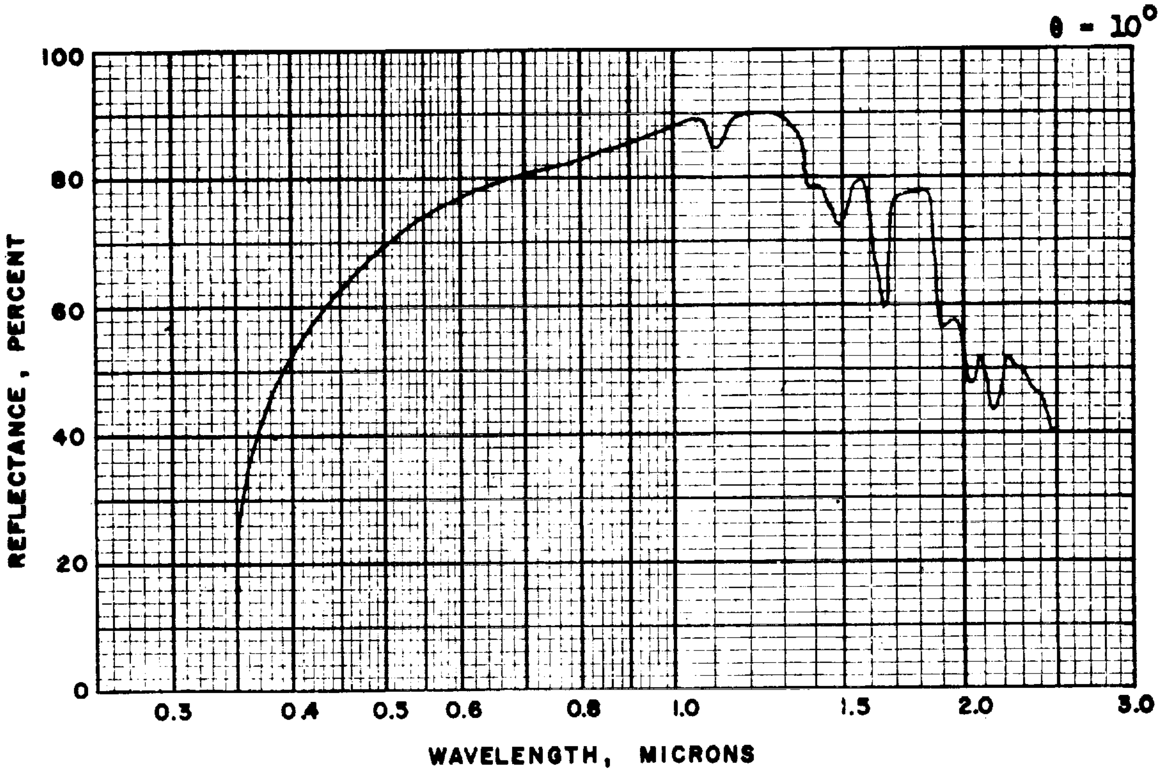

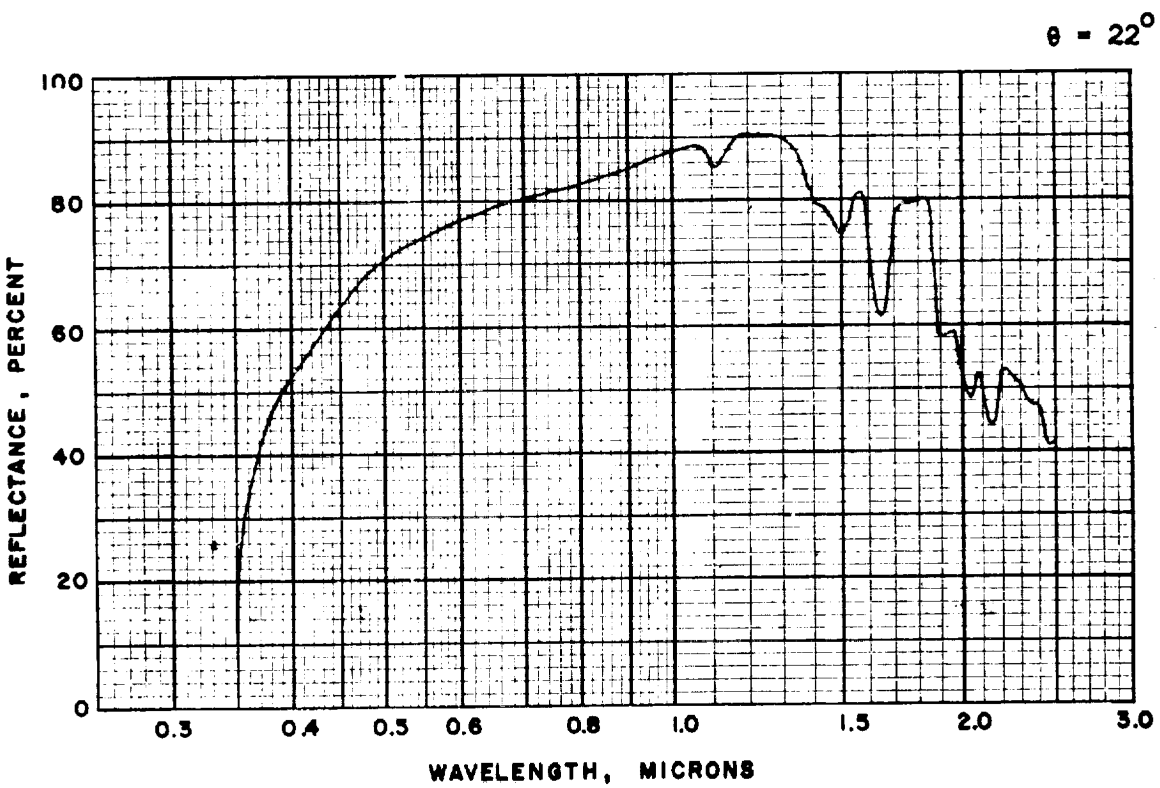

Figure 50: Sample 16, Azimuthal Angle 0°, Angles of Incidence 10° and 22°

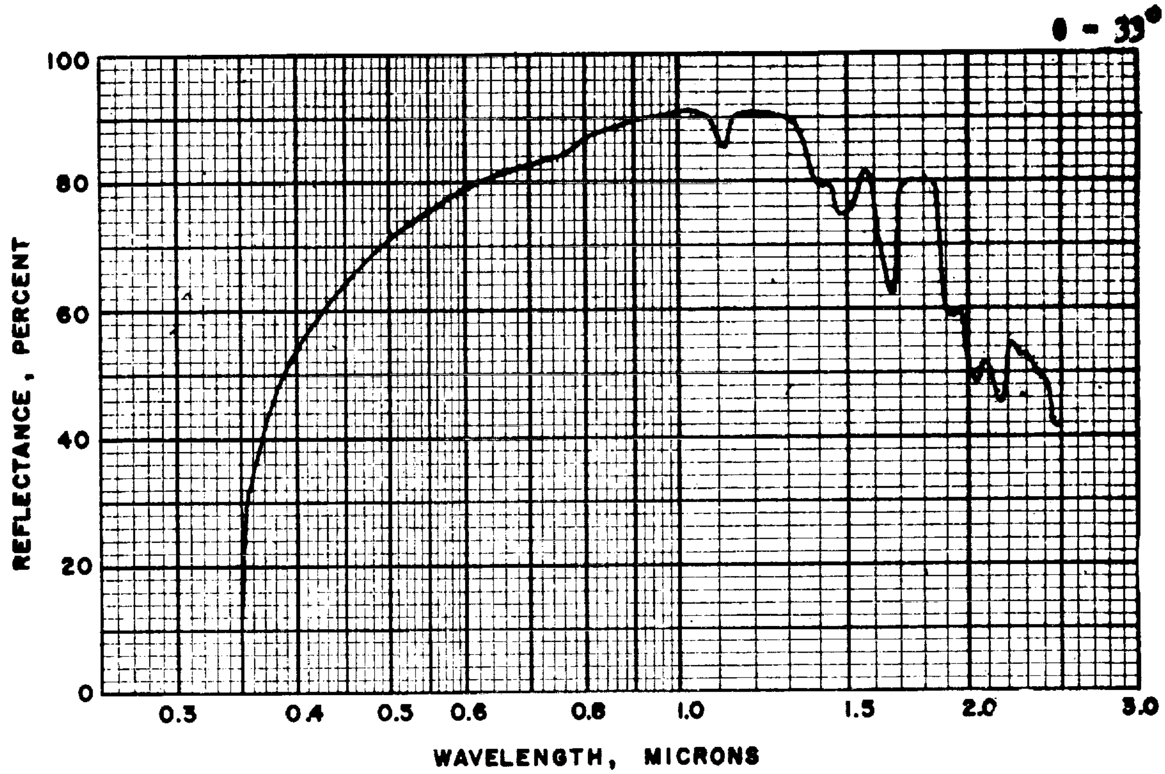

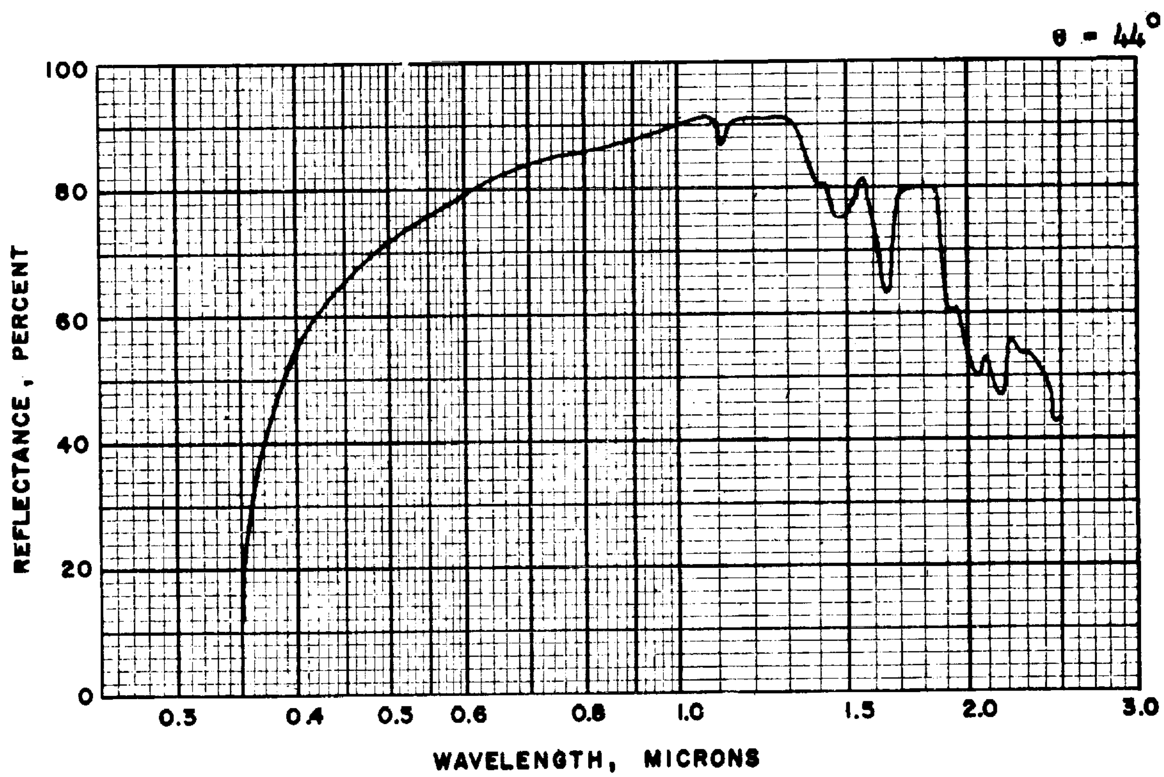

Figure 50 (Cont.): Sample 16, Azimuthal Angle 0°, Angles of Incidence 33° and 44°

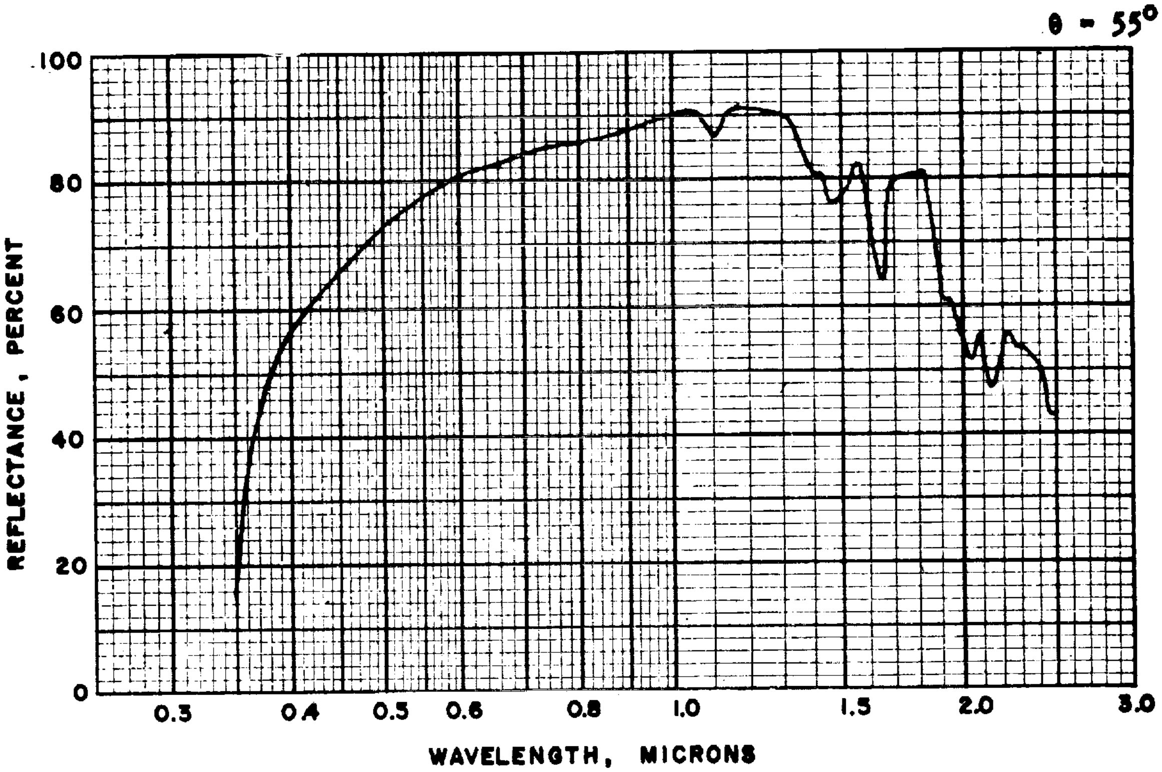

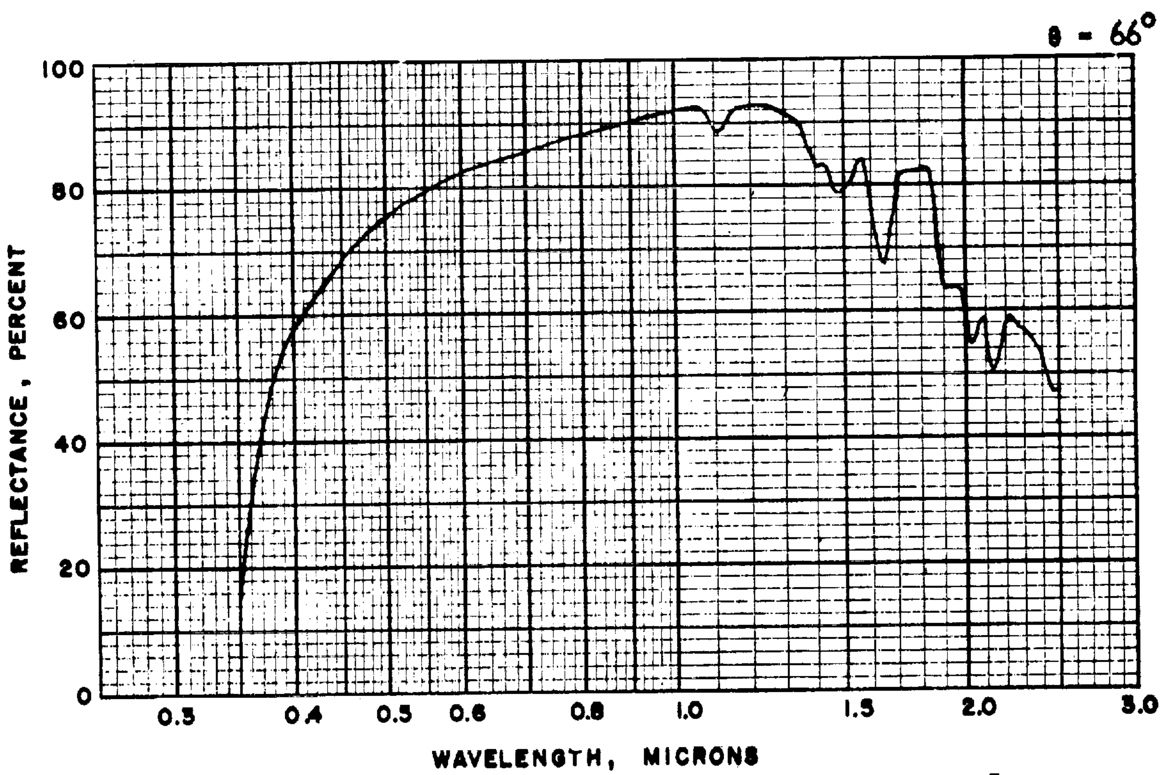

Figure 50 (Cont.): Sample 16, Azimuthal Angle 0°, Angles of Incidence 55° and 66°

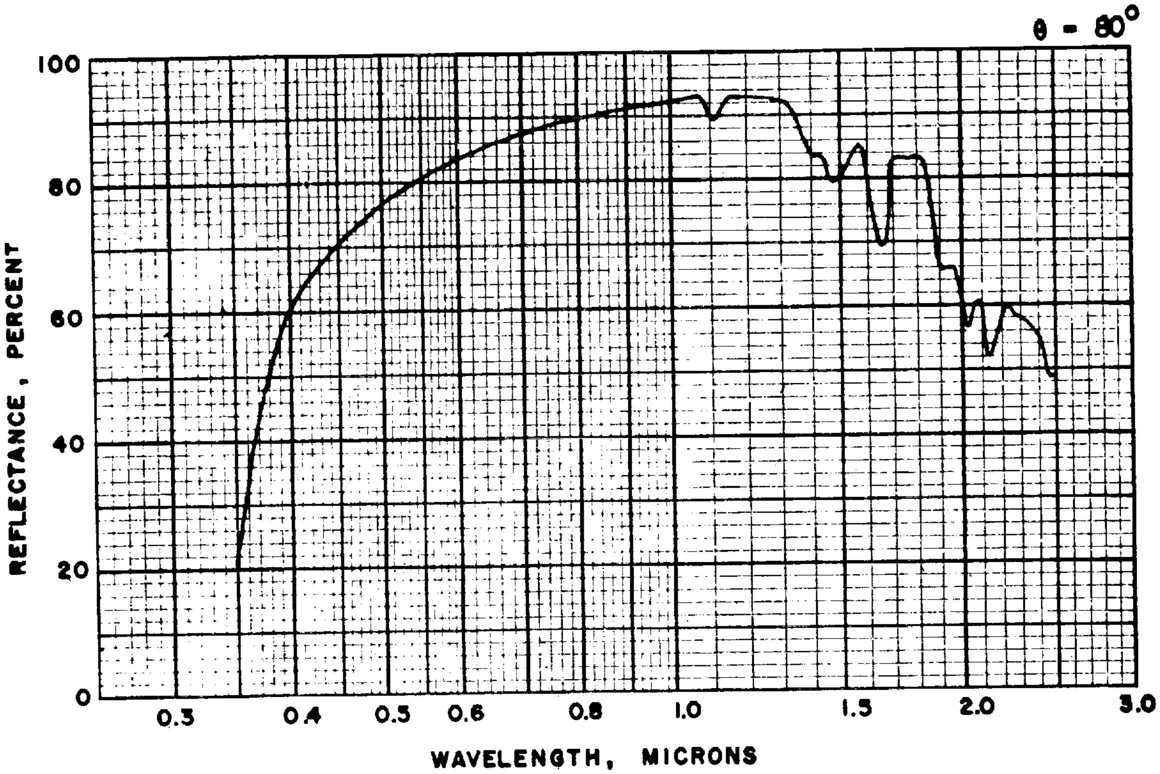

Figure 50 (Cont.): Sample 16, Azimuthal Angle 0°, Angle of Incidence 80°

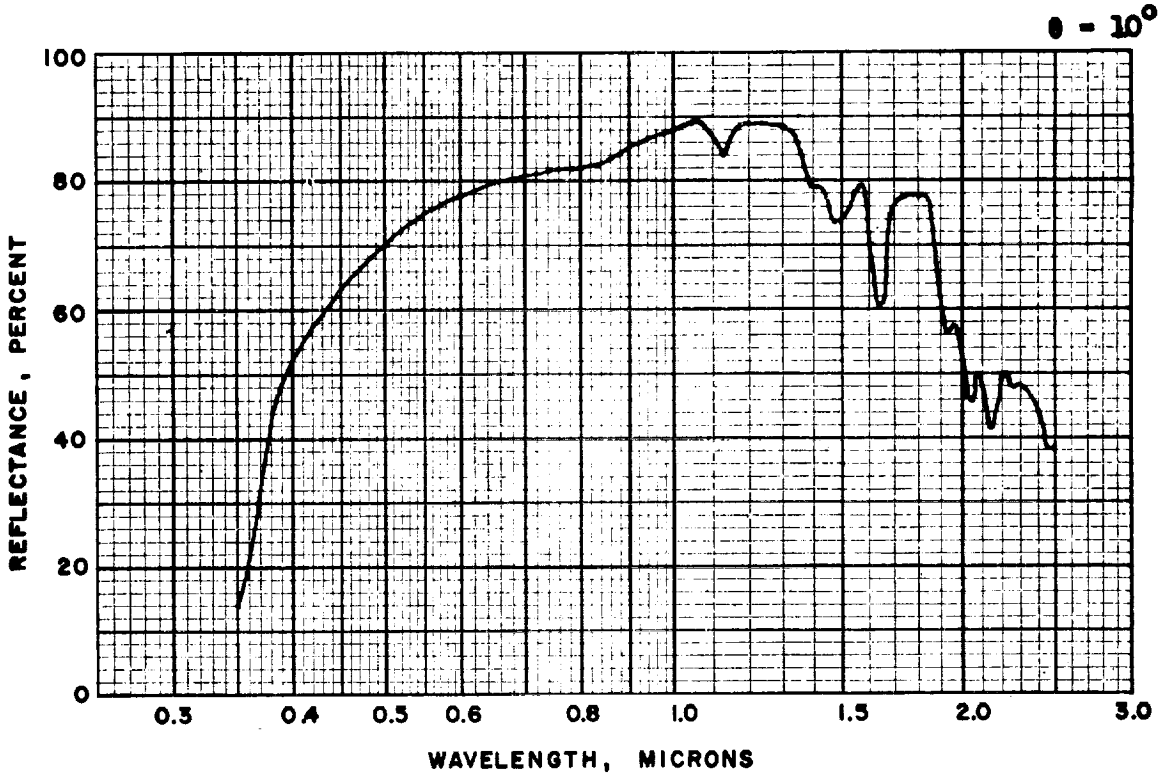

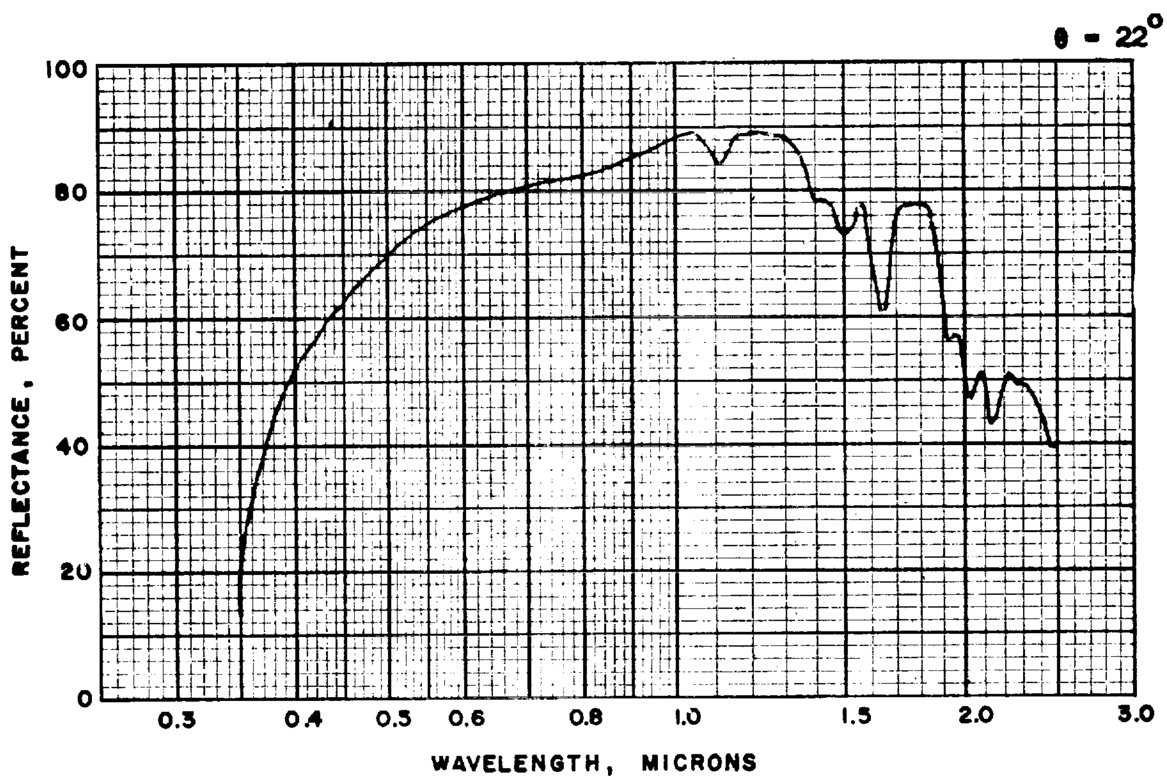

Figure 51: Sample 16, Azimuthal Angle 45°, Angles of Incidence 10° and 22°

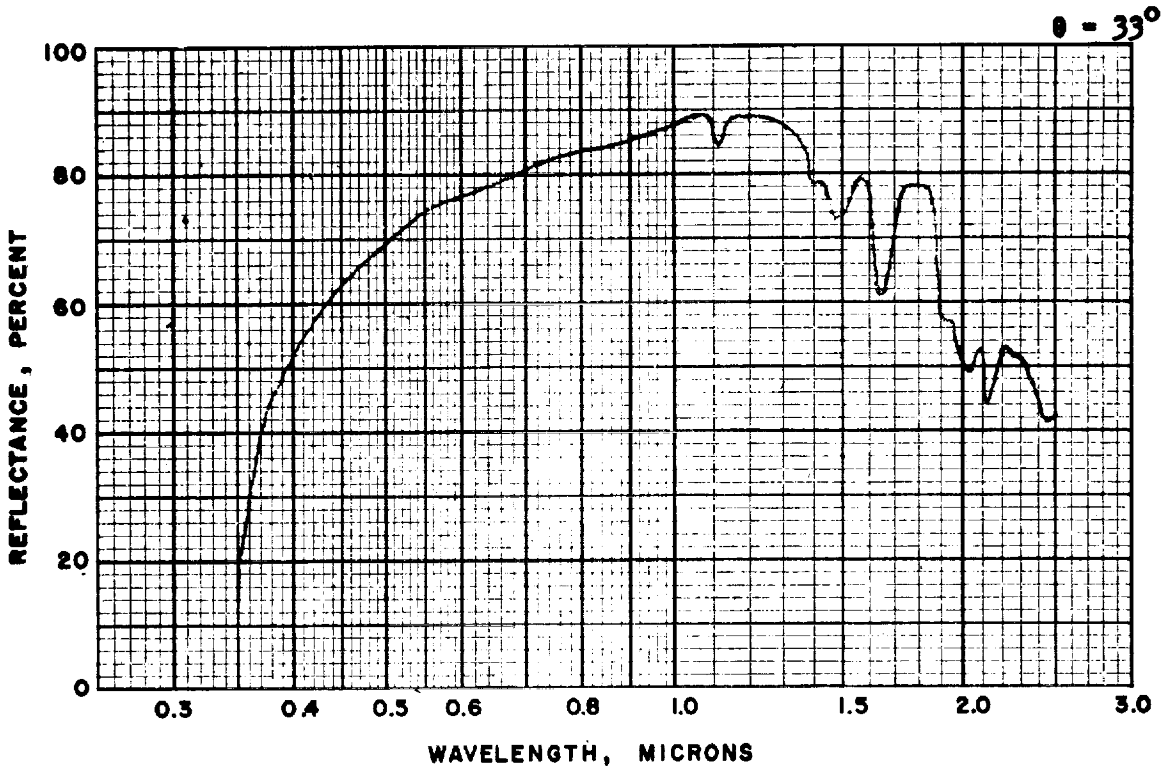

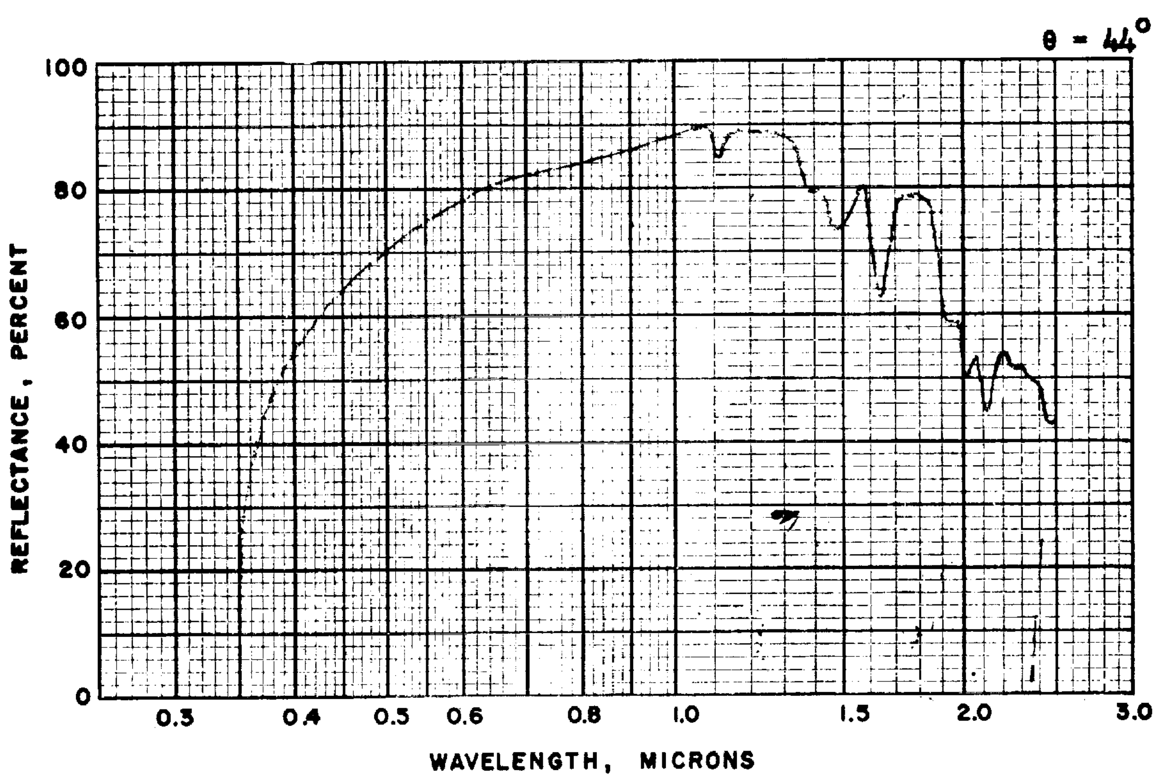

Figure 51 (Cont.): Sample 16, Azimuthal Angle 45°, Angles of Incidence 33° and 44°

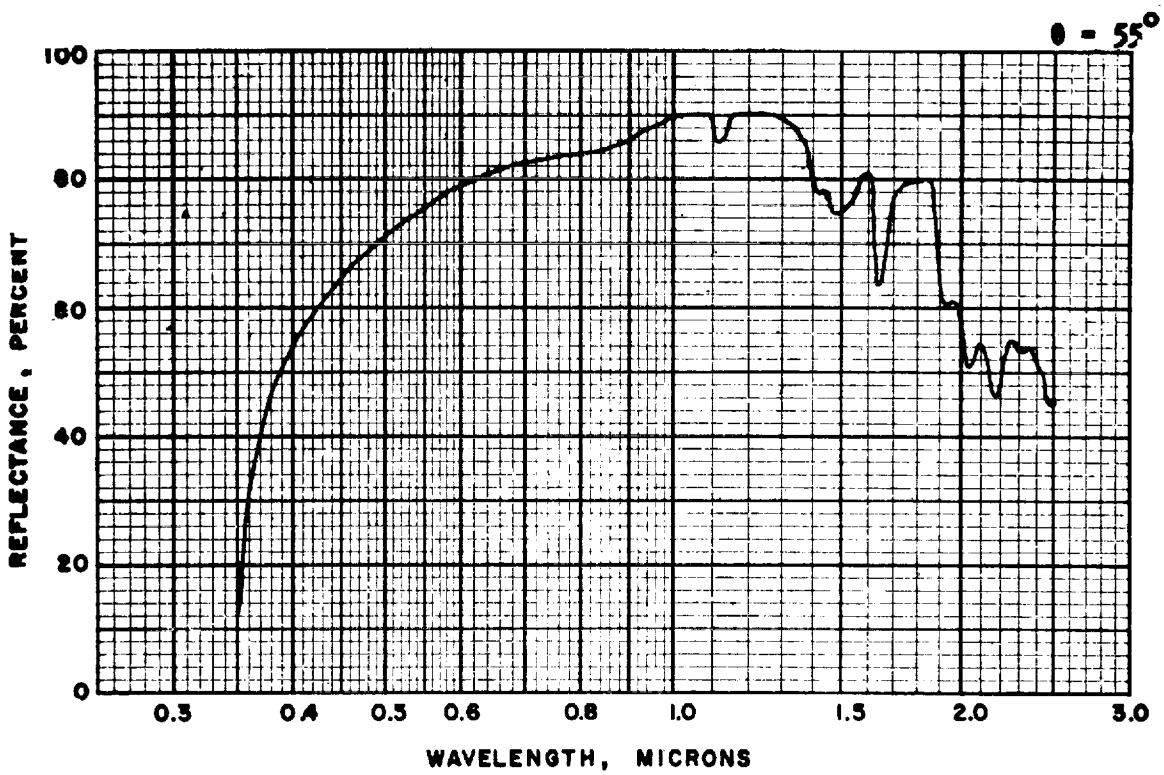

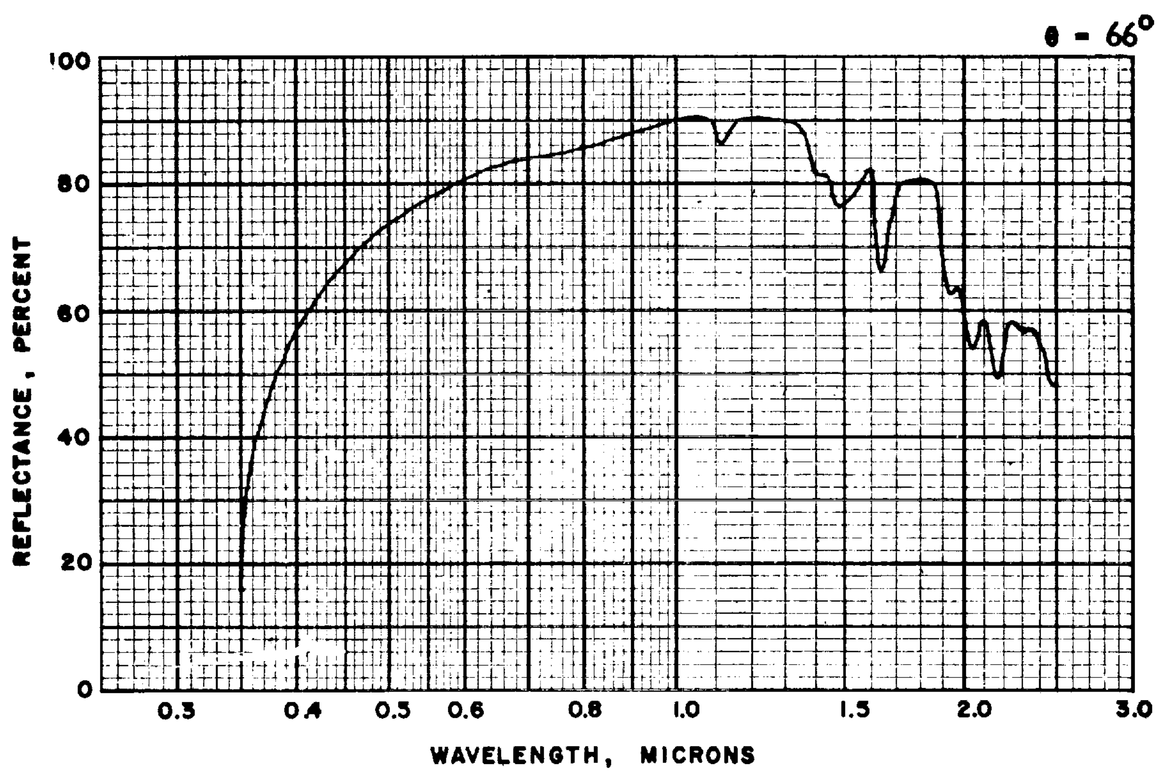

Figure 51 (Cont.): Sample 16, Azimuthal Angle 45°, Angles of Incidence 55° and 66°

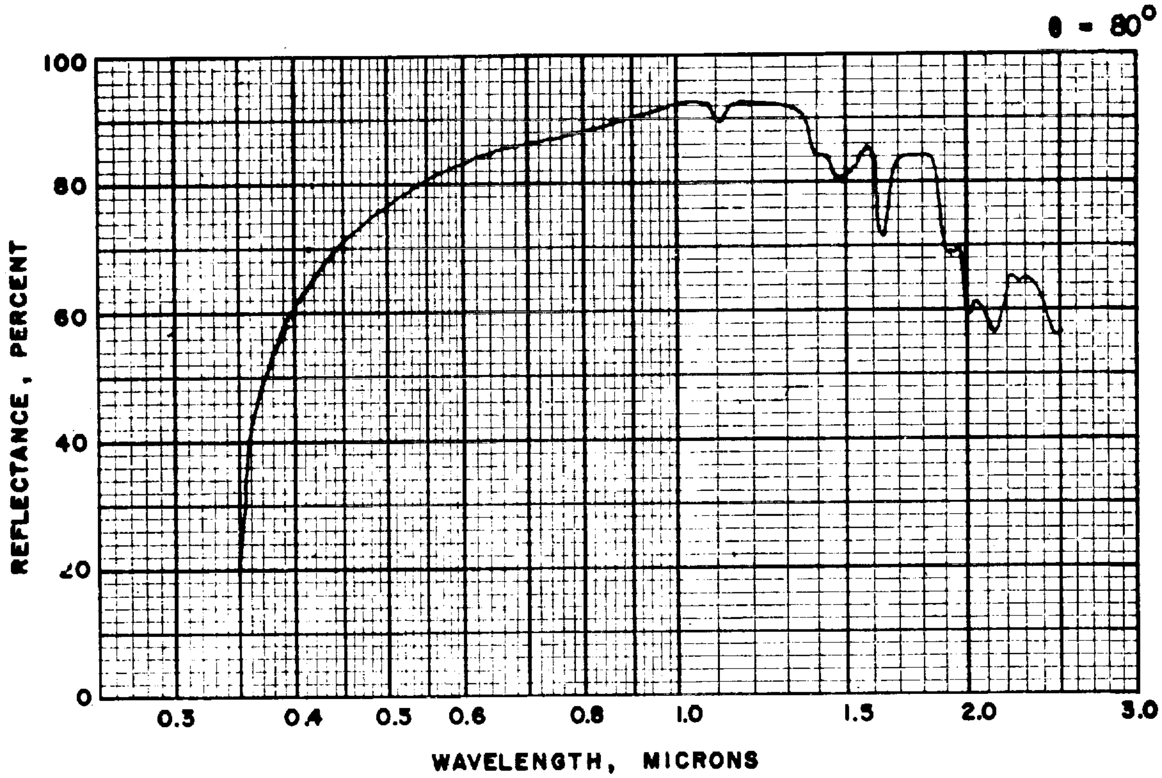

Figure 51 (Cont.): Sample 16, Azimuthal Angle 45°, Angle of Incidence 80°

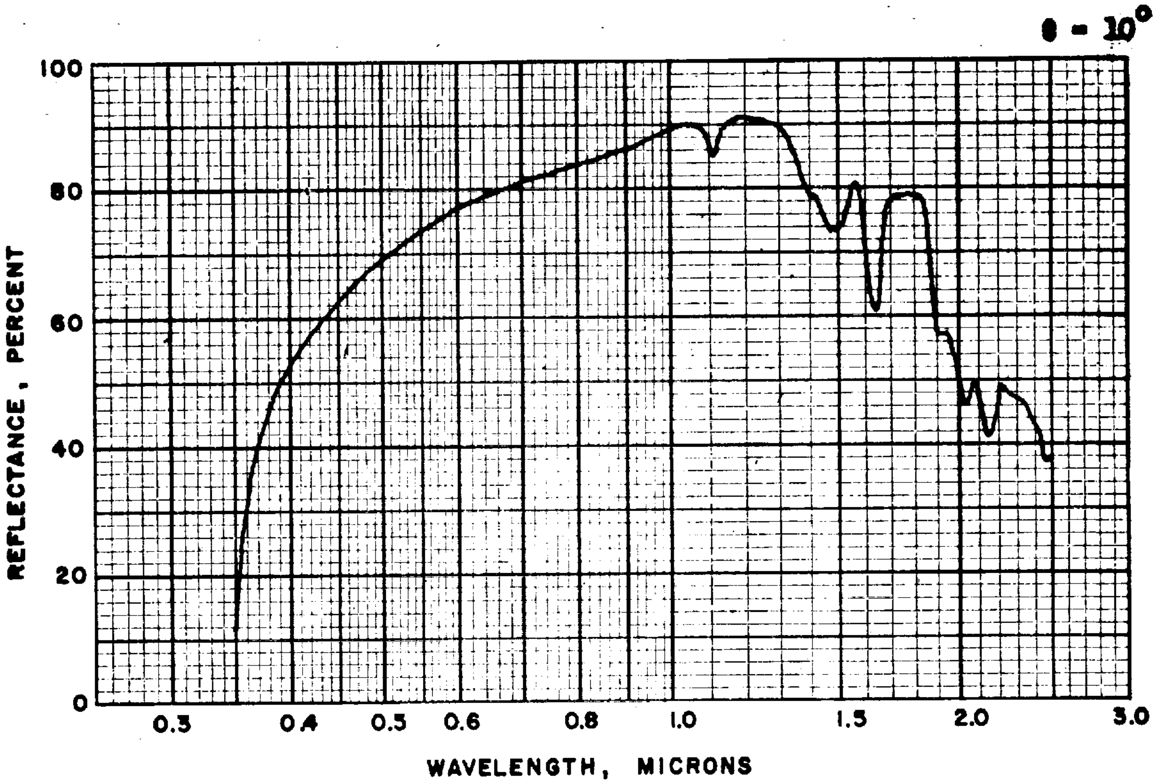

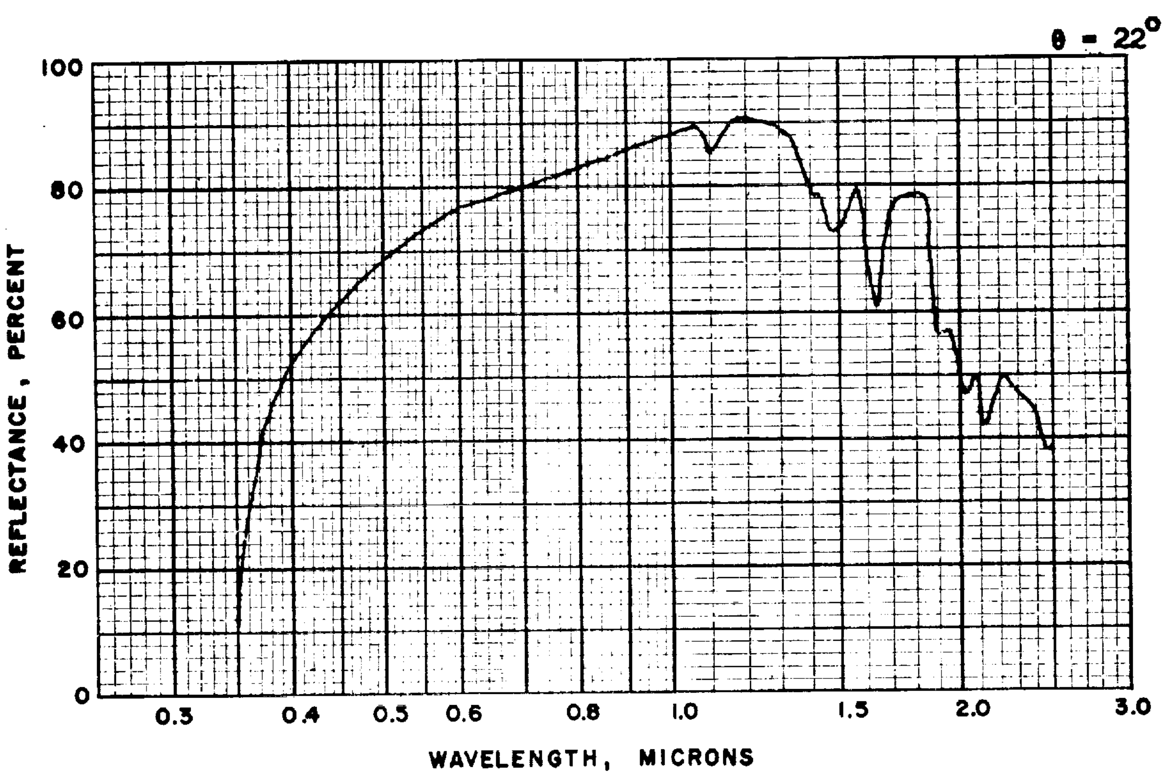

Figure 52: Sample 16, Azimuthal Angle 60°, Angles of Incidence 10° and 22°

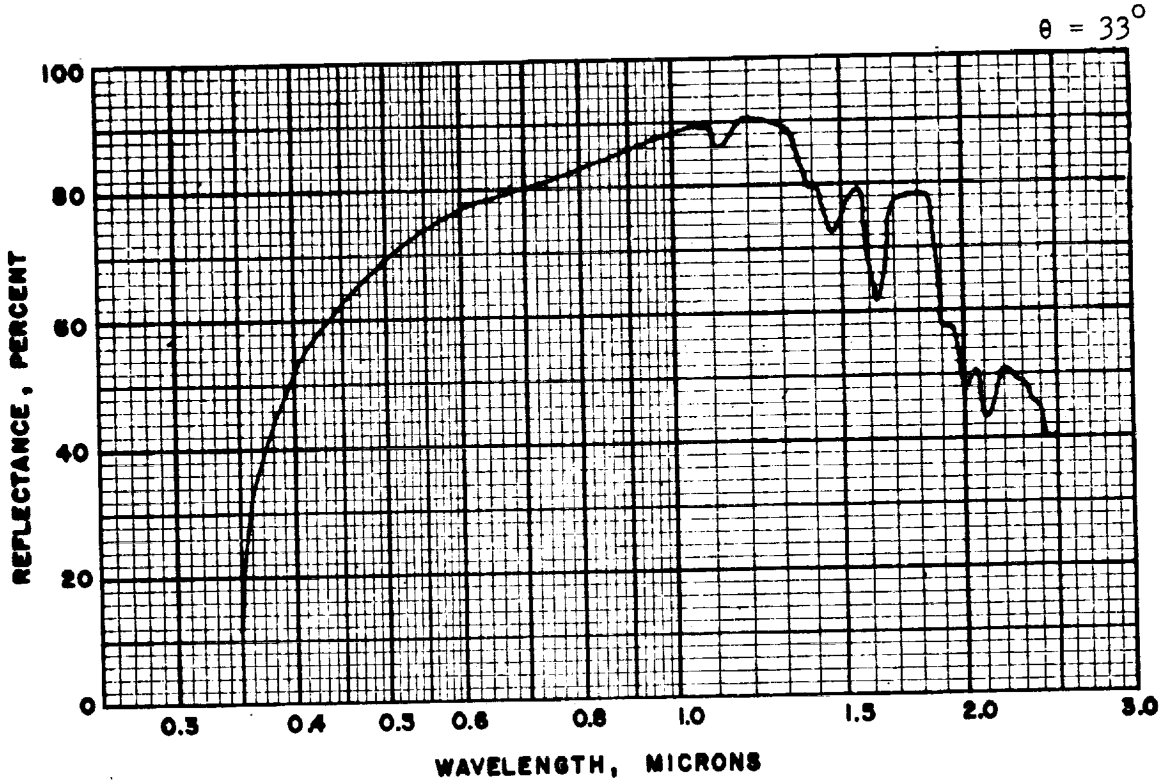

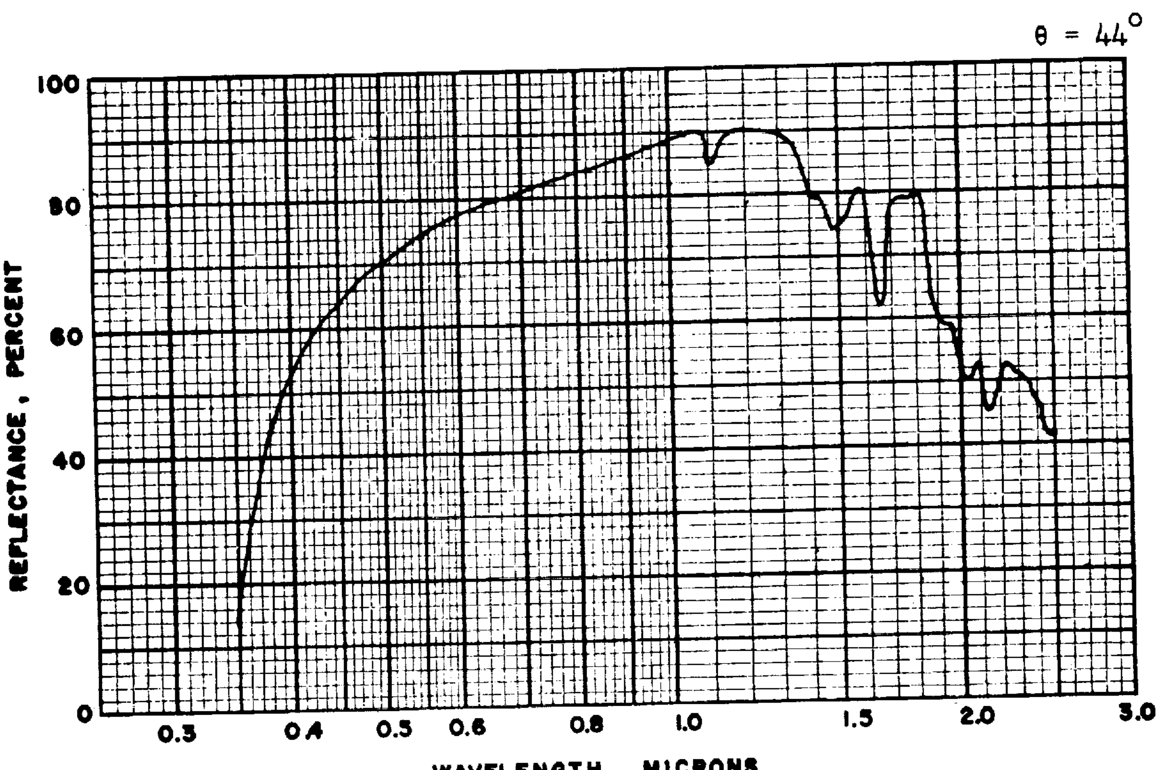

Figure 52 (Cont.): Sample 16, Azimuthal Angle 60°, Angles of Incidence 33° and 44°

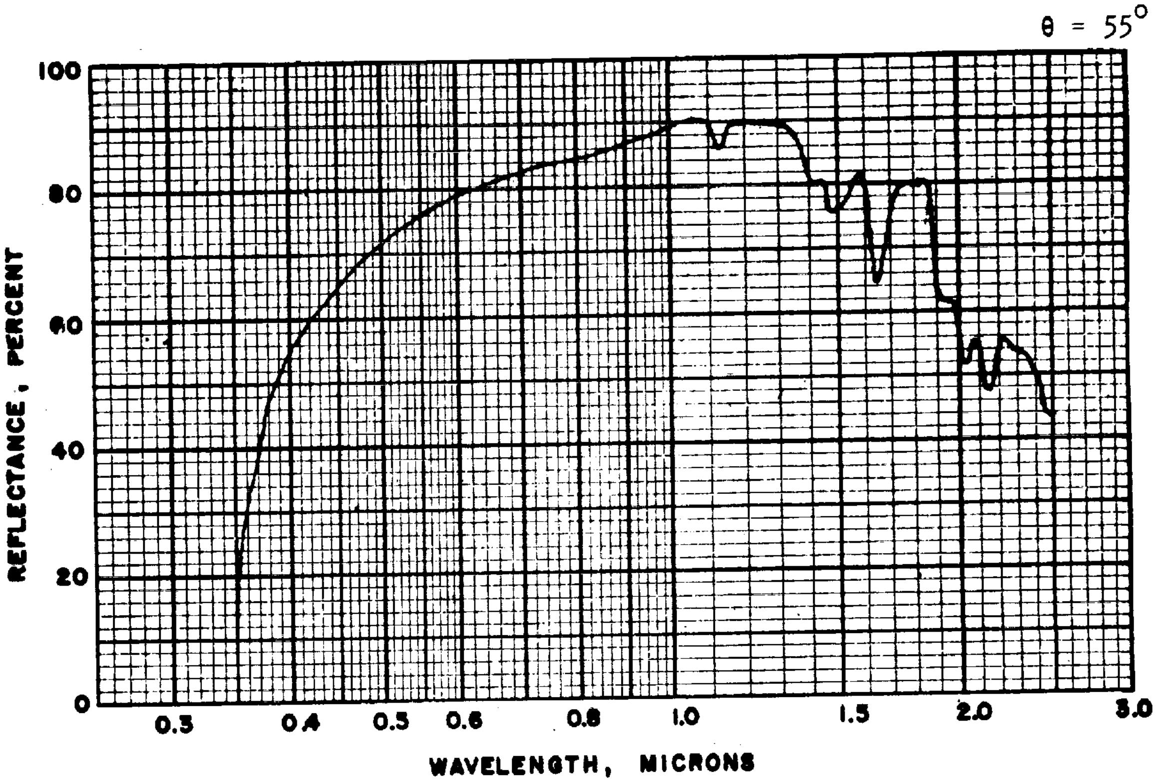

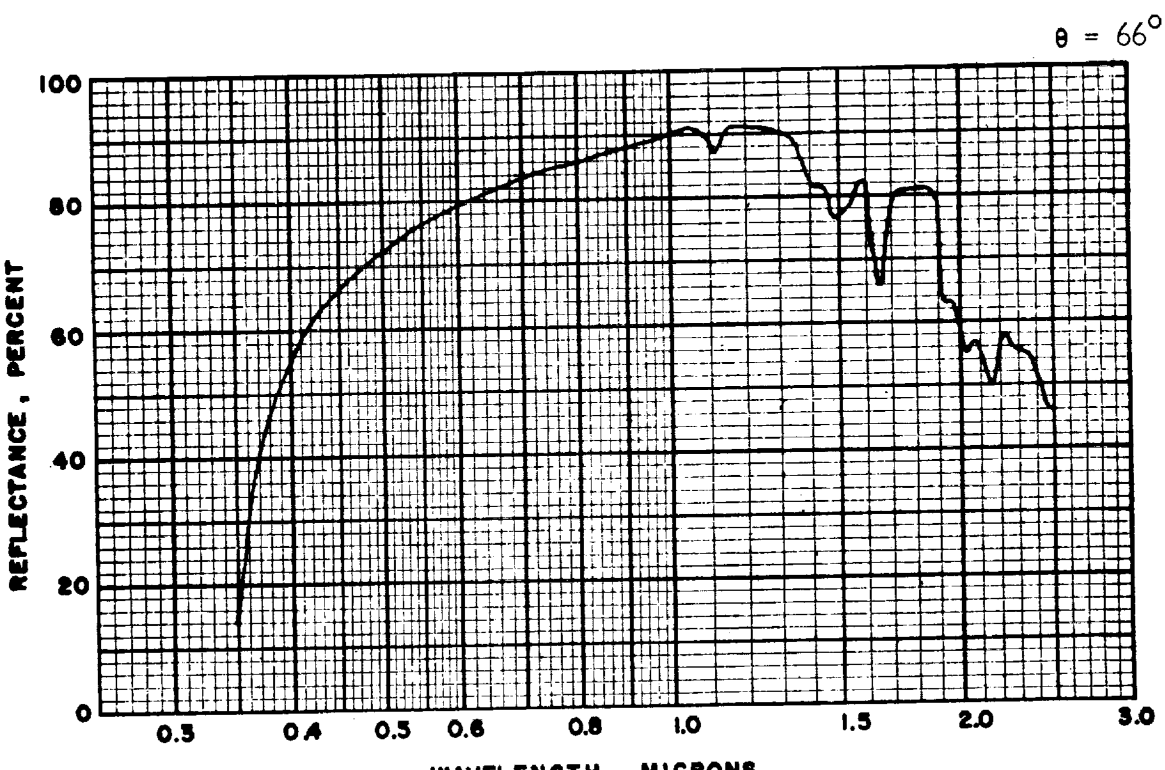

Figure 52 (Cont.): Sample 16, Azimuthal Angle 60°,
Angles of Incidence 55° and 66°

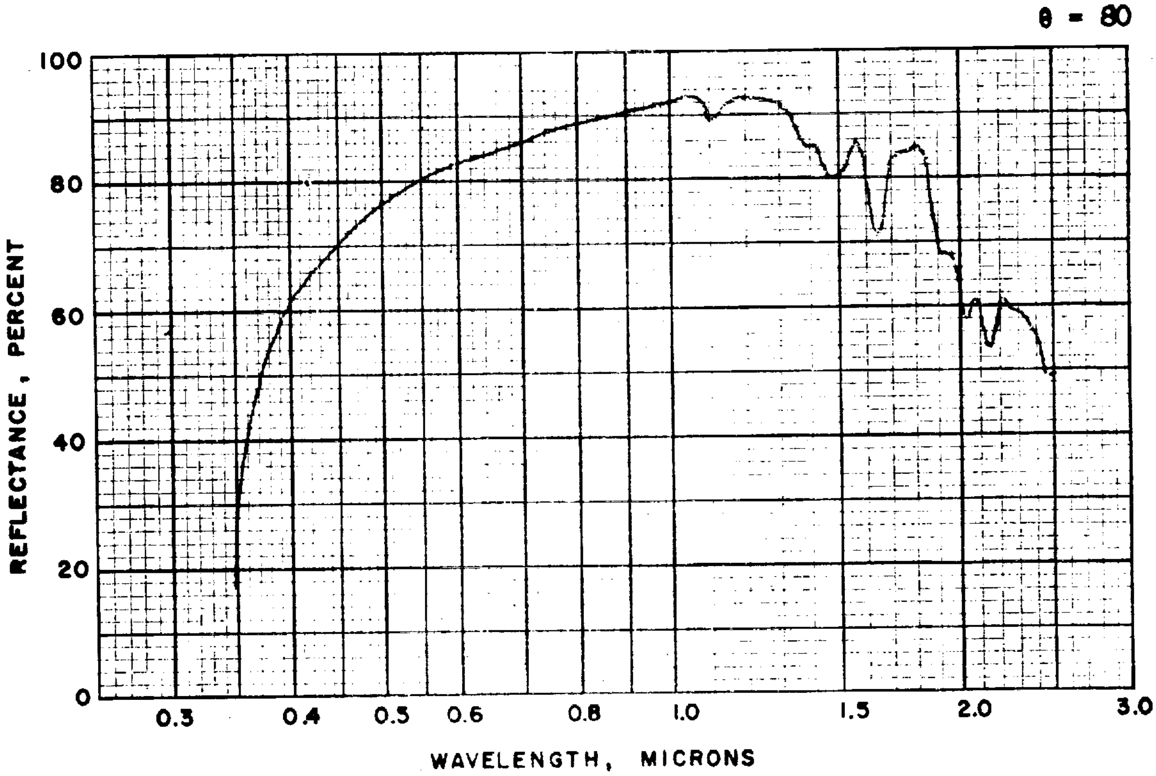

Figure 52 (Cont.): Sample 16, Azimuthal Angle 60°
Angle of Incidence 80°

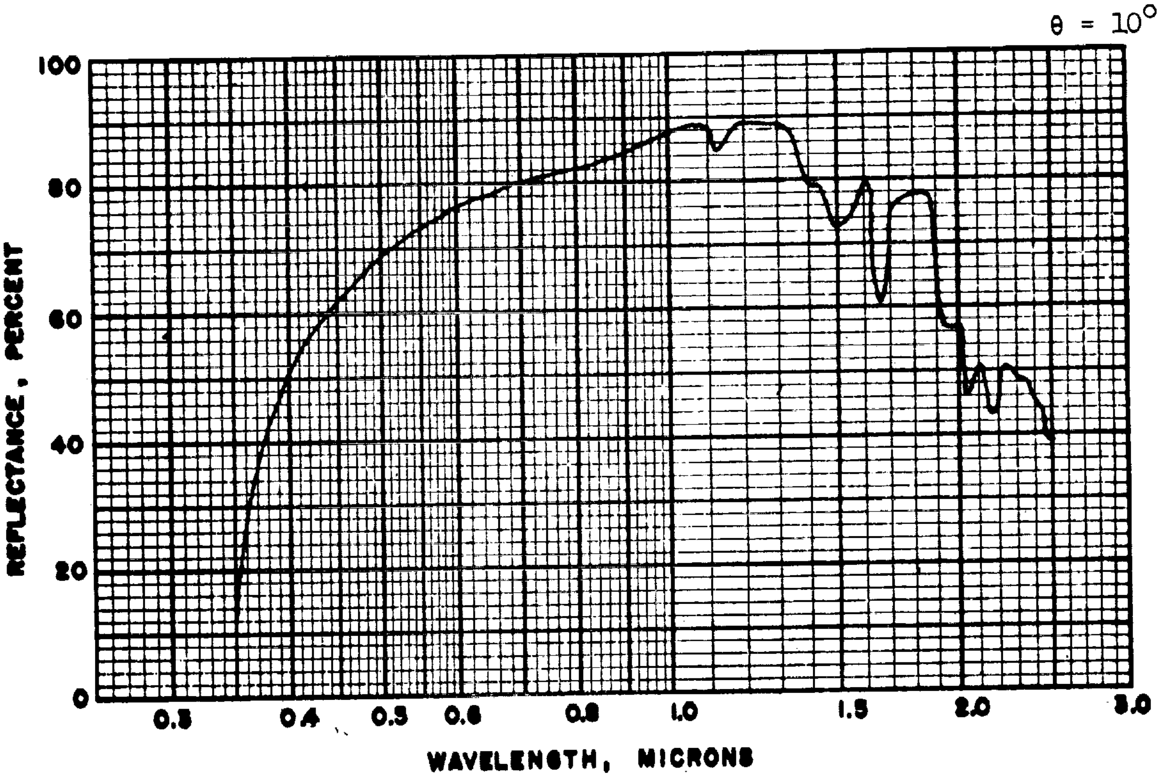

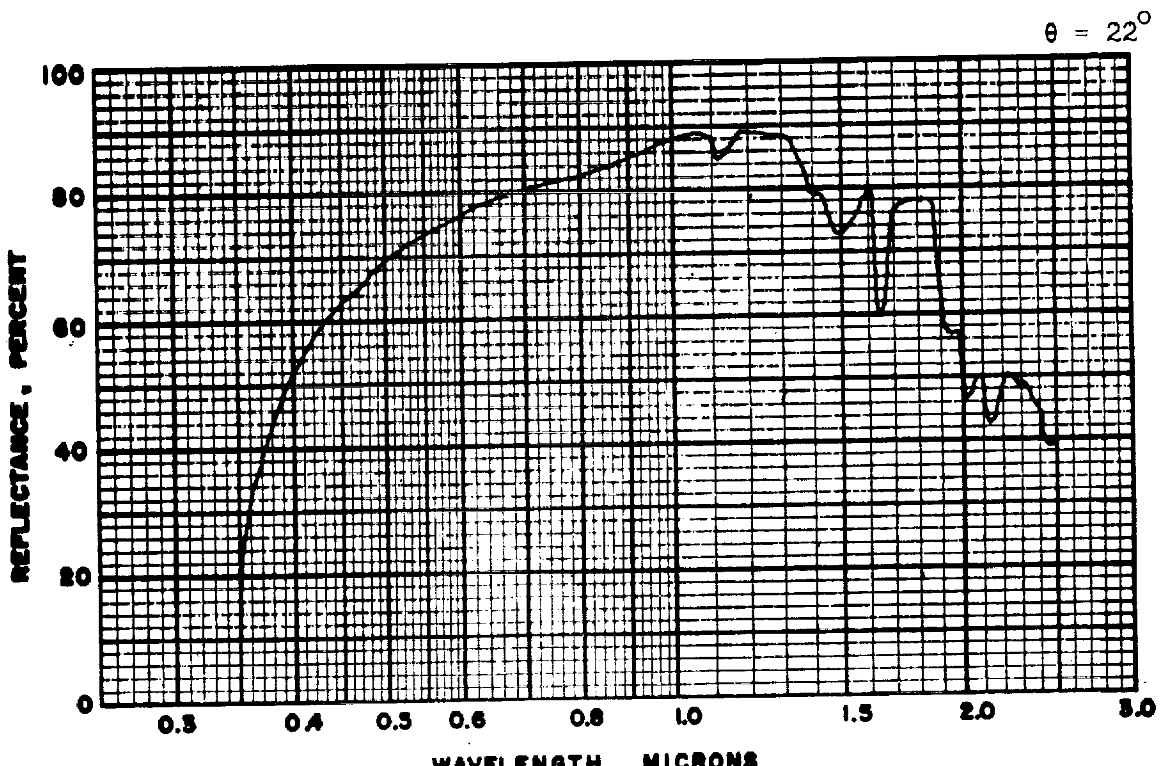

Figure 53: Sample 16, Azimuthal Angle 90°, Angles of Incidence 10° and 22°

θ = 33°

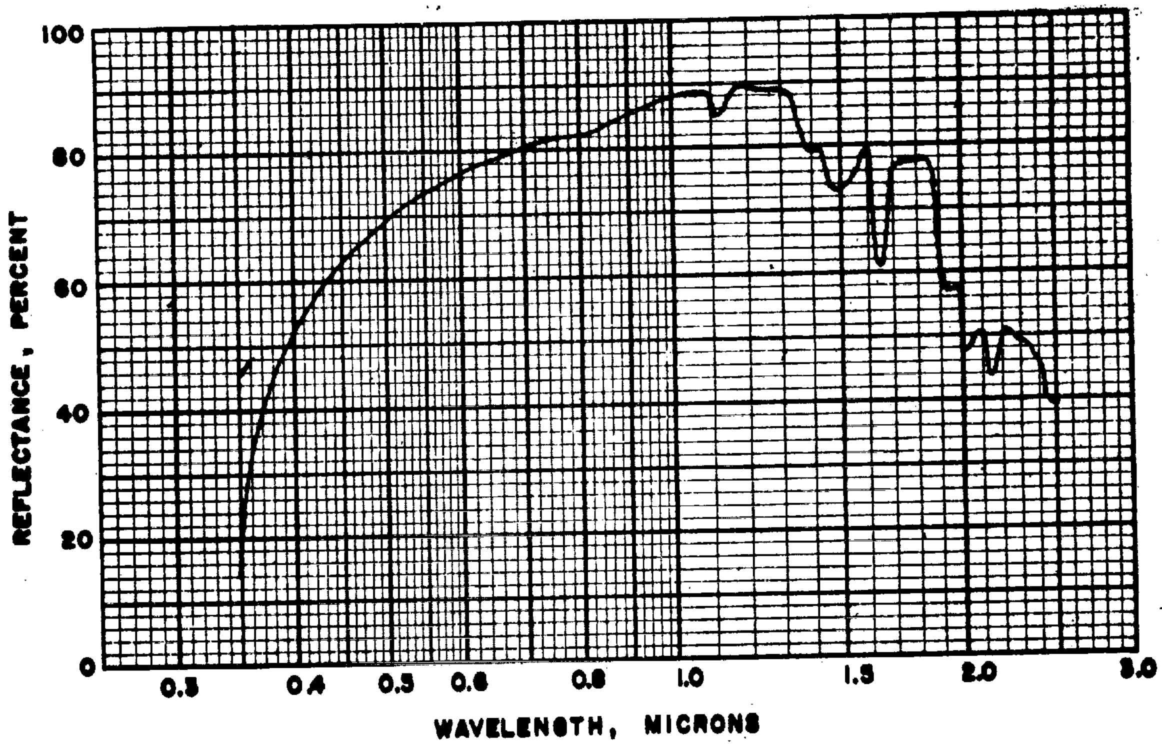

θ = 44°

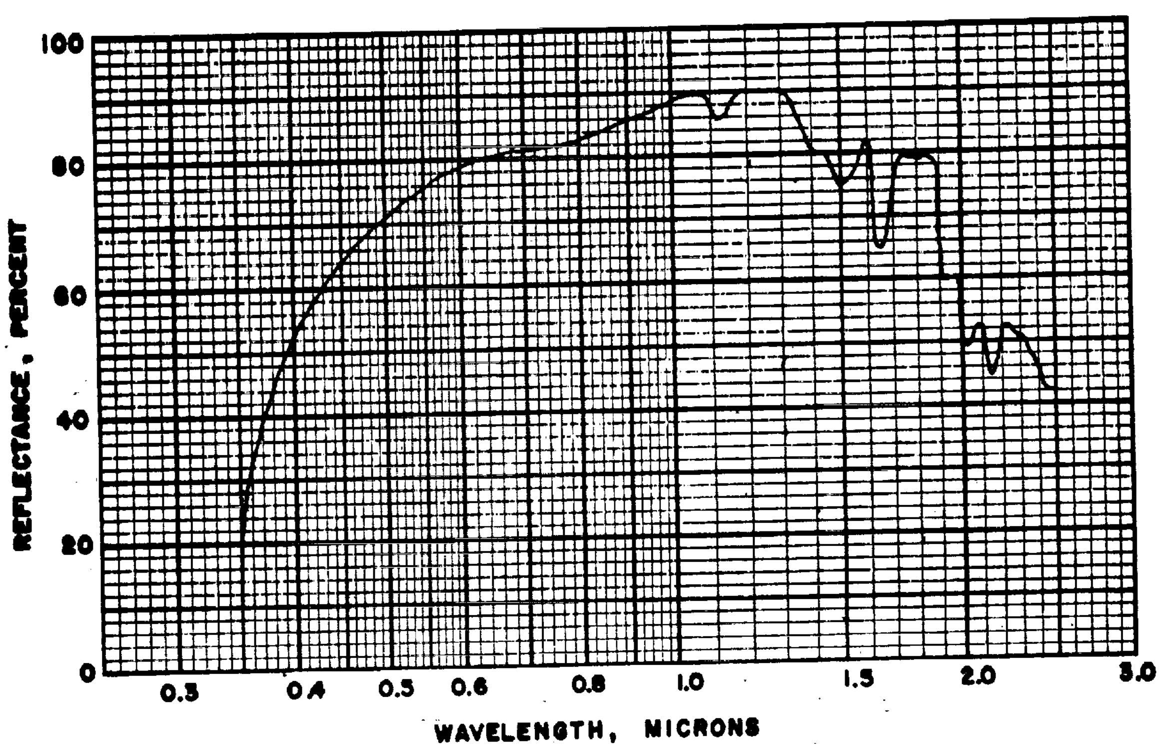

Figure 53: Sample 16, Azimuthal Angle 90°,
(Cont.) Angles of Incidence 33° and 44°

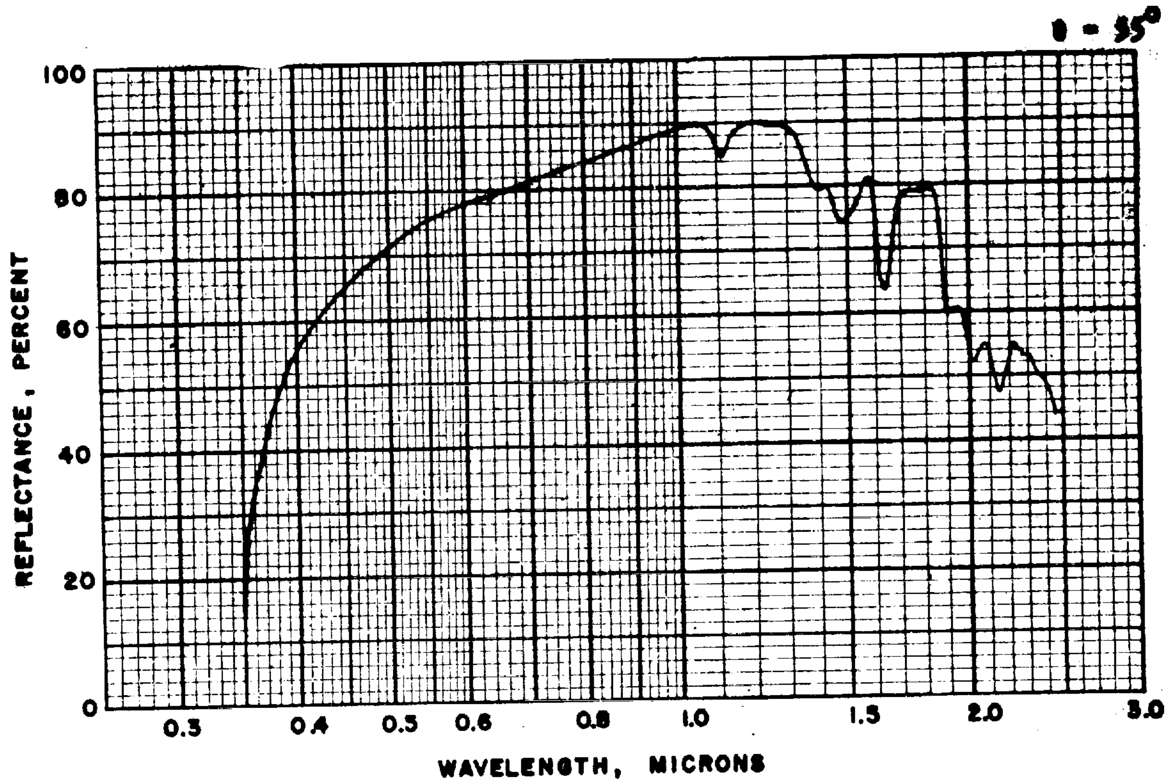

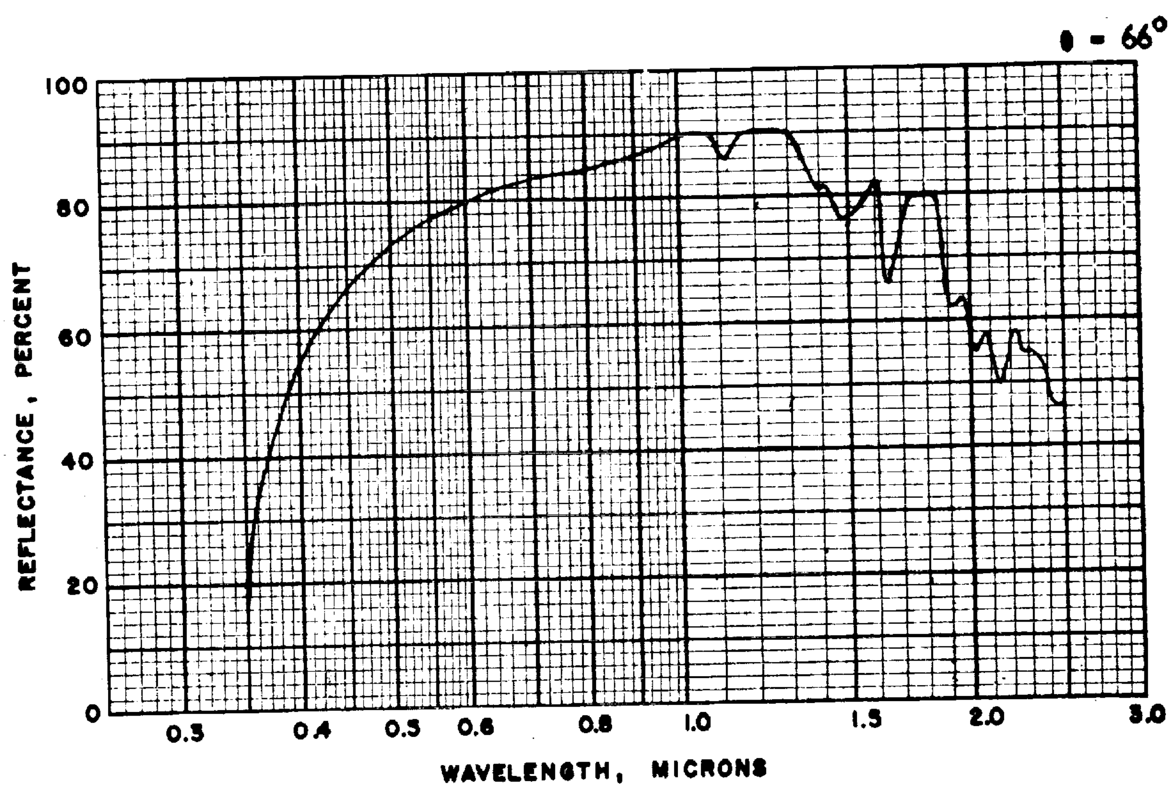

Figure 53: Sample 16, Azimuthal Angle 90°,
(Cont.) Angles of Incidence 55° and 66°

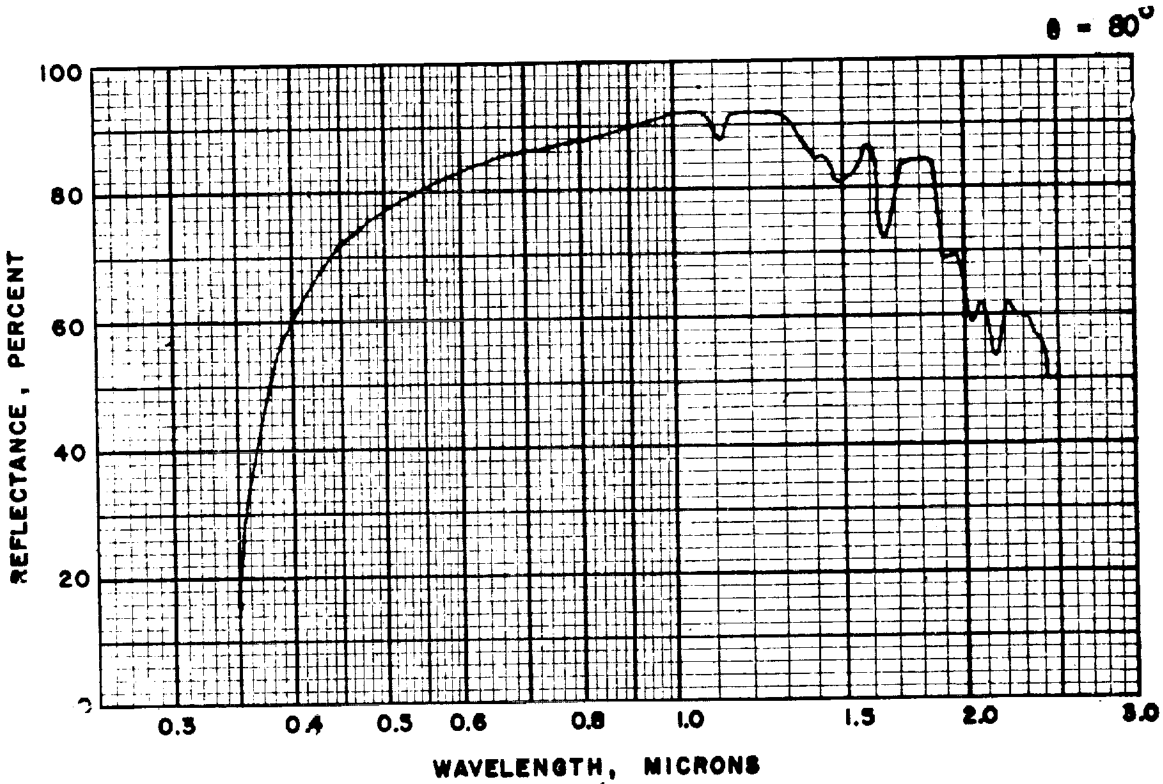

Figure 53: Sample 16, Azimuthal Angle 90°,
(Cont.) Angle of Incidence 80°

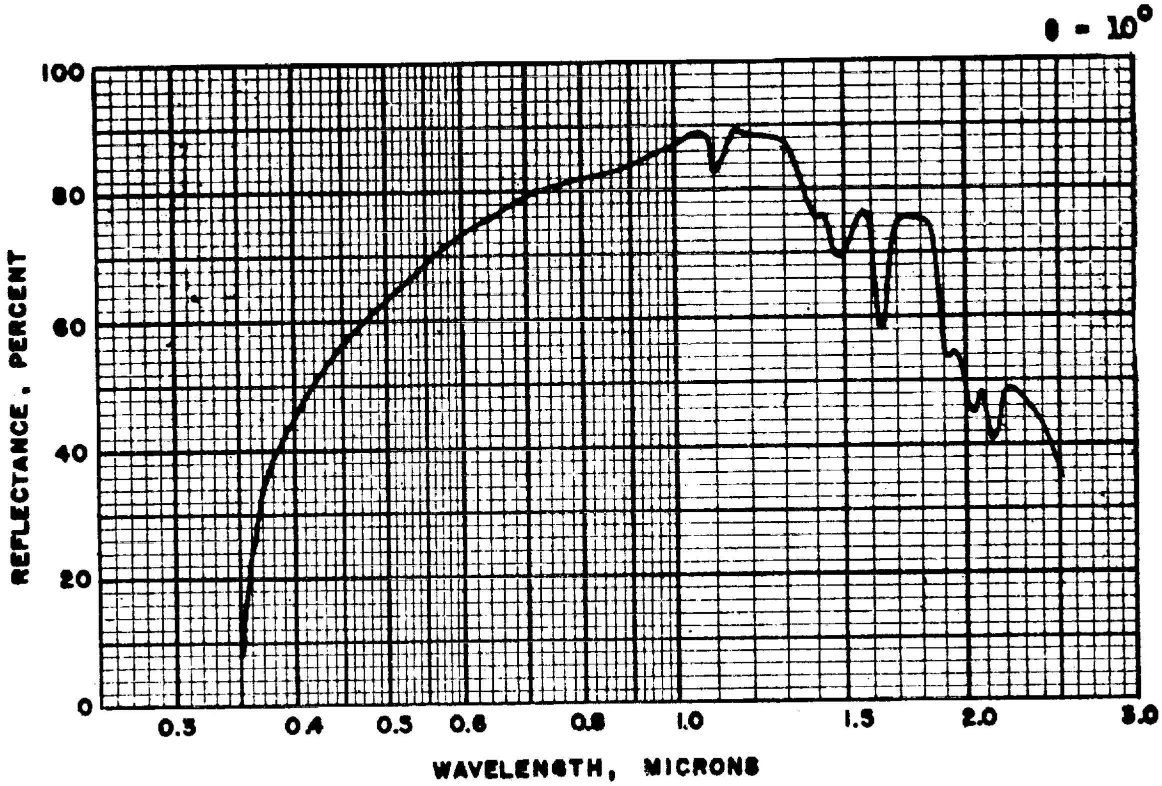

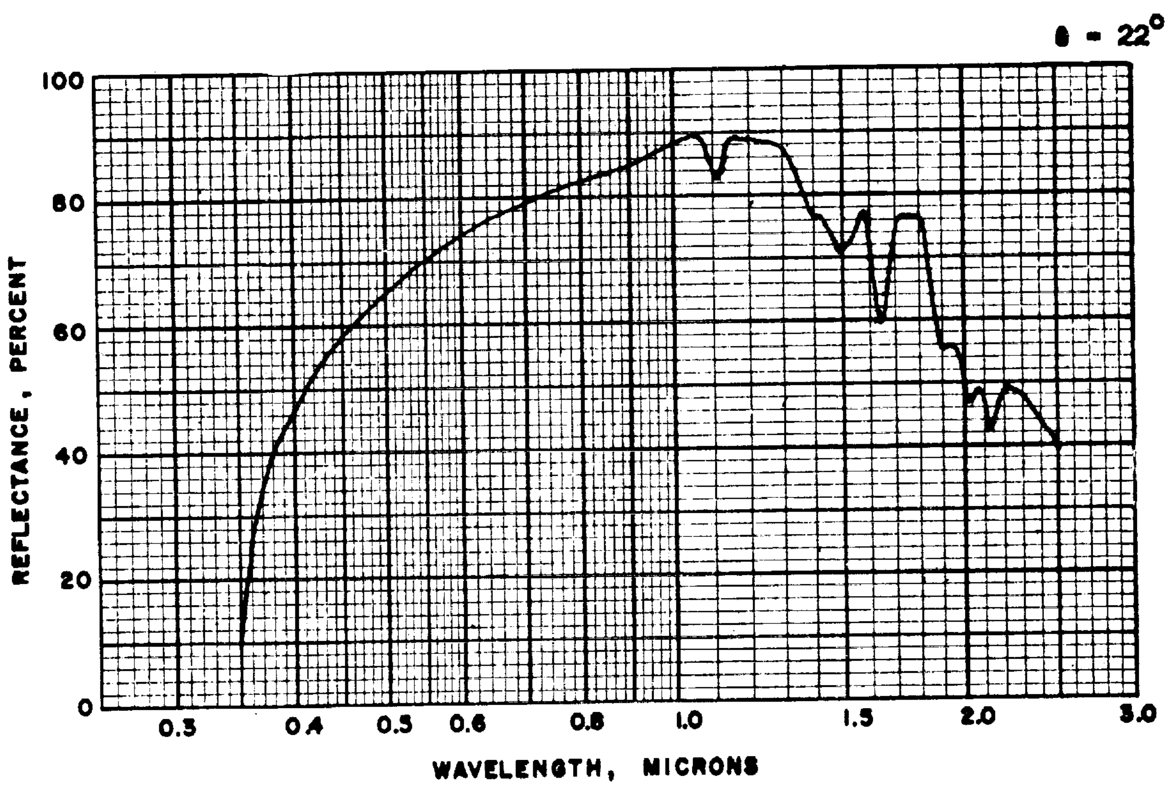

Figure 54: Sample 17, Azimuthal Angle 0°, Angles of Incidence 10° and 22°

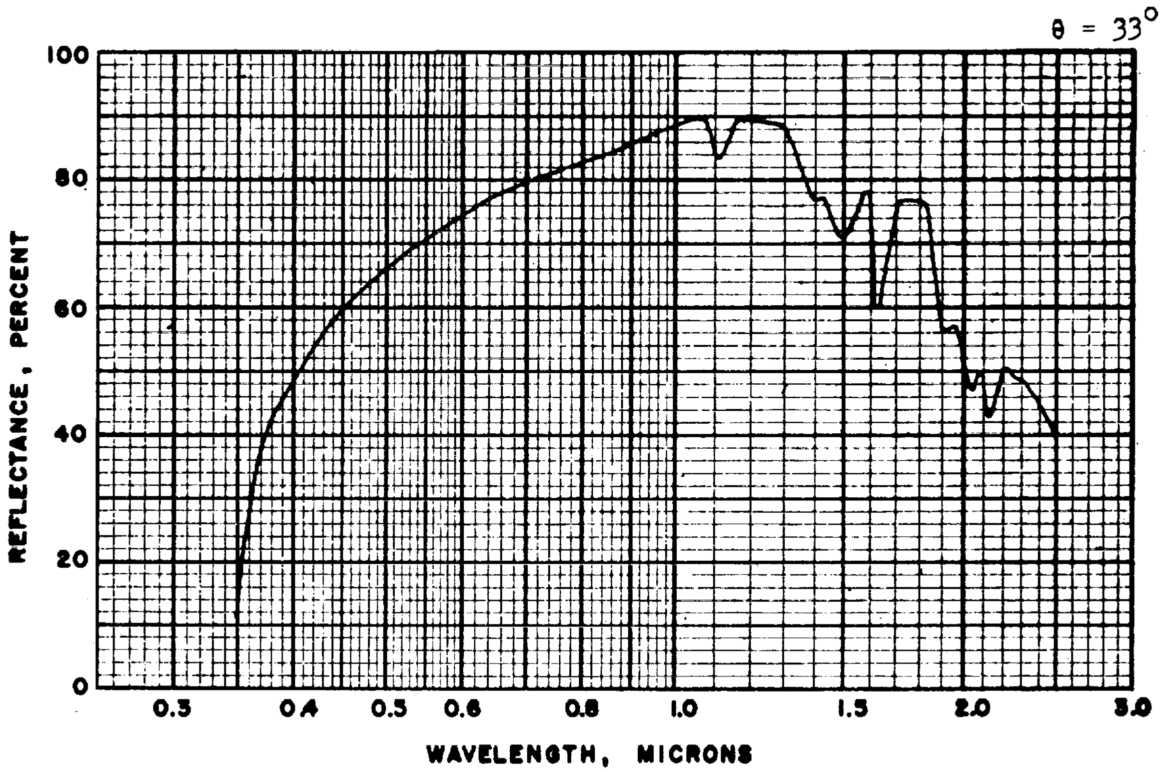

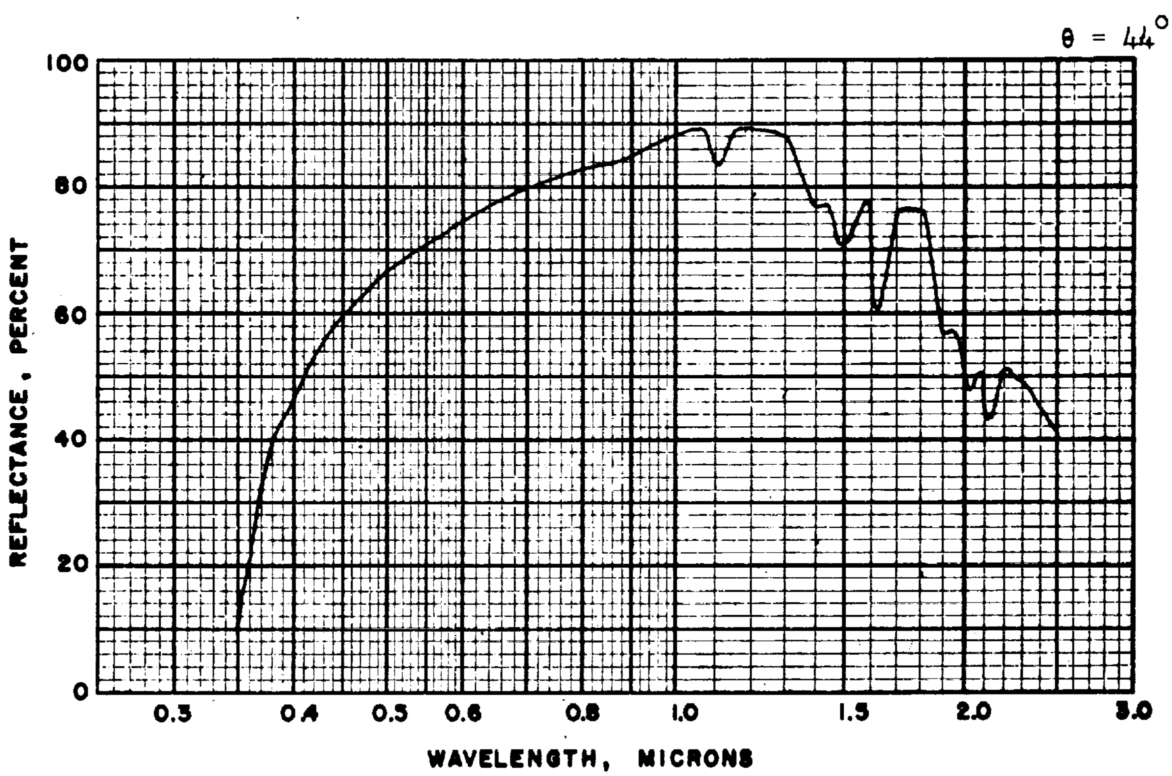

Figure 54 (Cont.): Sample 17, Azimuthal Angle 0°, Angles of Incidence 33° and 44°

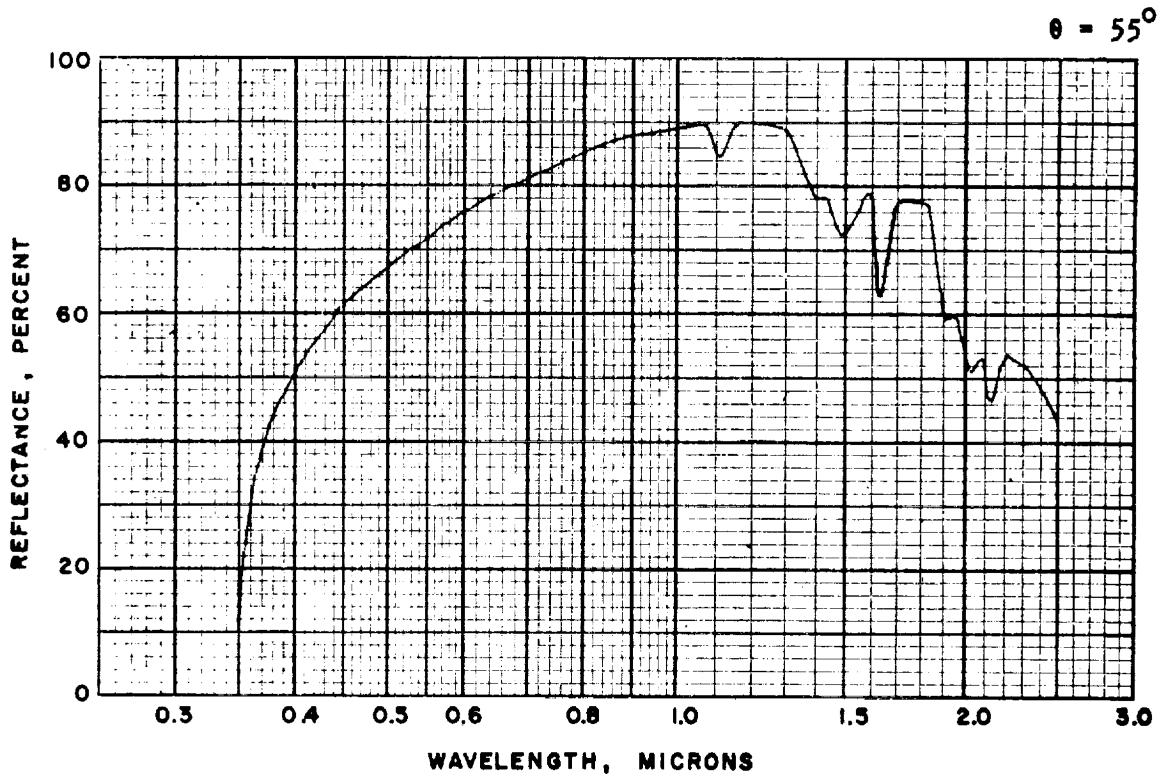

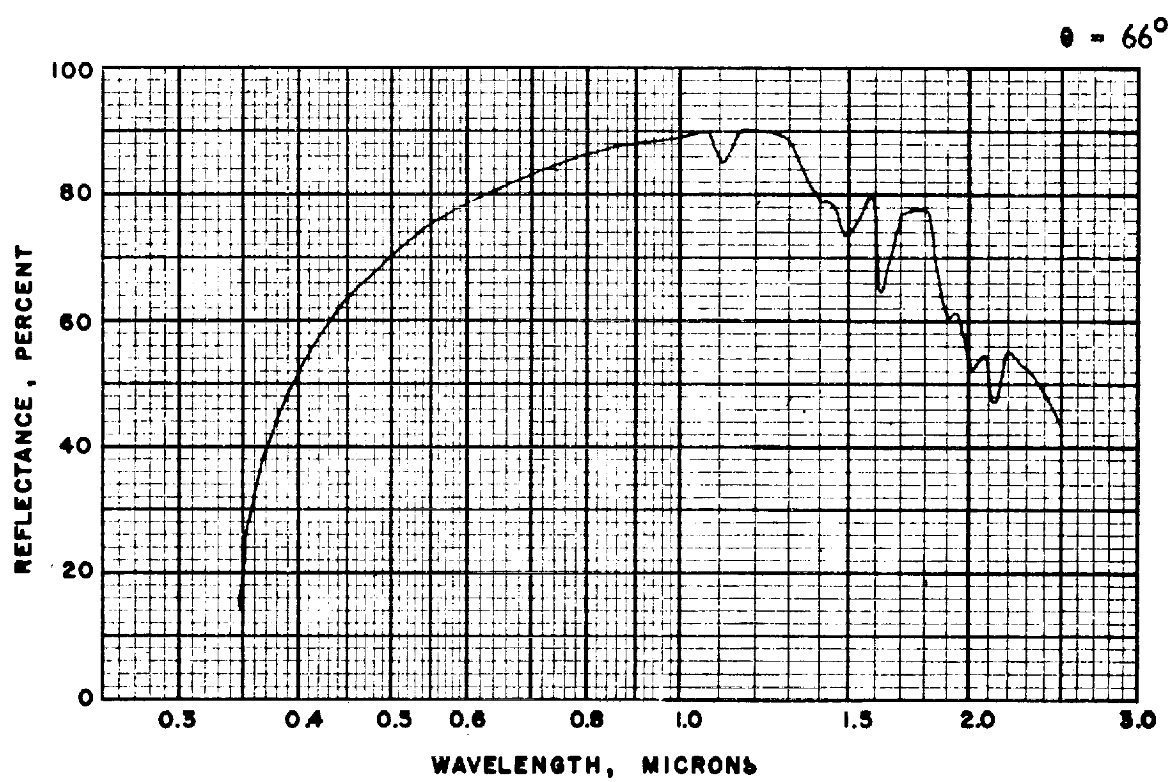

Figure 54 (Cont.): Sample 17, Azimuthal Angle 0°, Angles of Incidence 55° and 66°

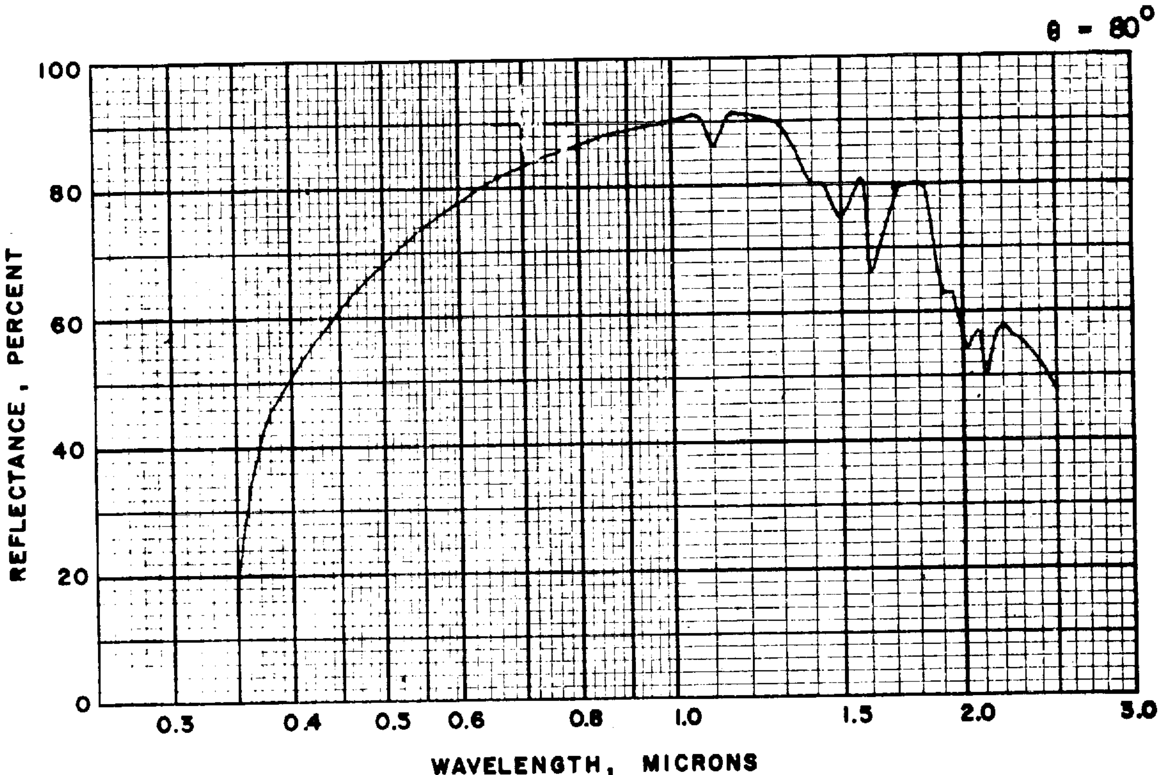

Figure 54 (Cont.): Sample 17, Azimuthal Angle 0°, Angle of Incidence 80°

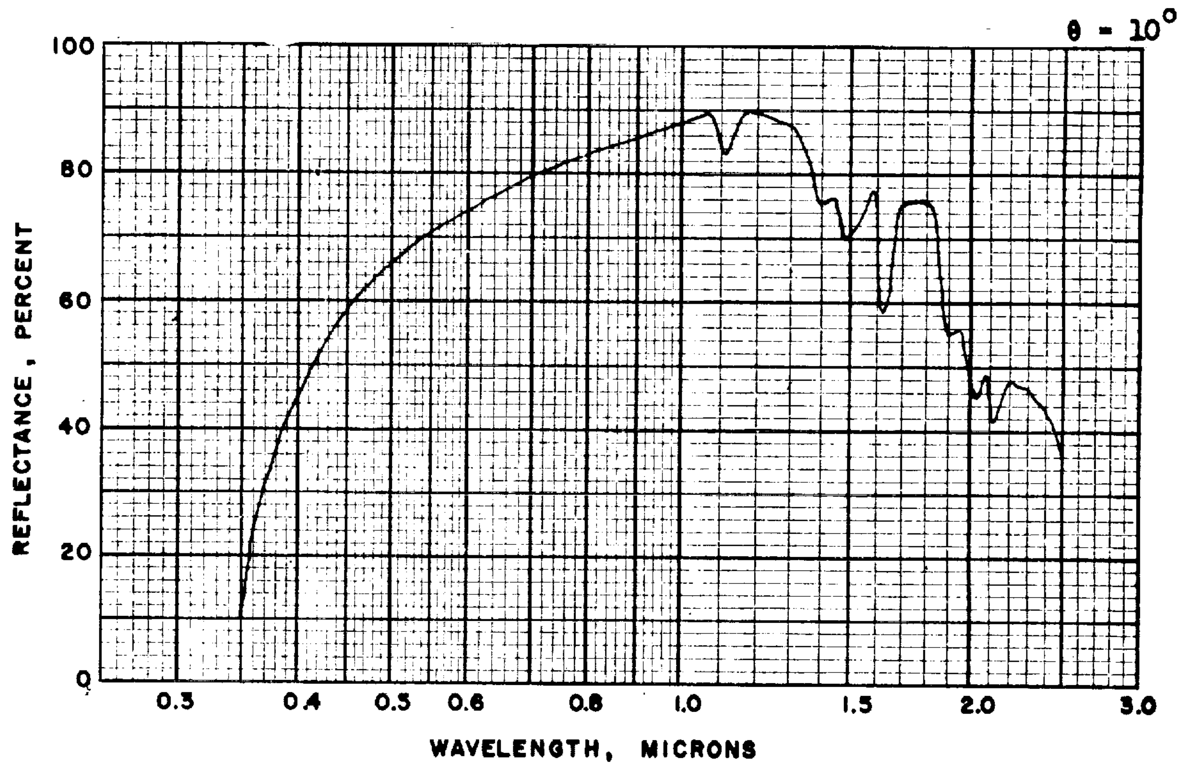

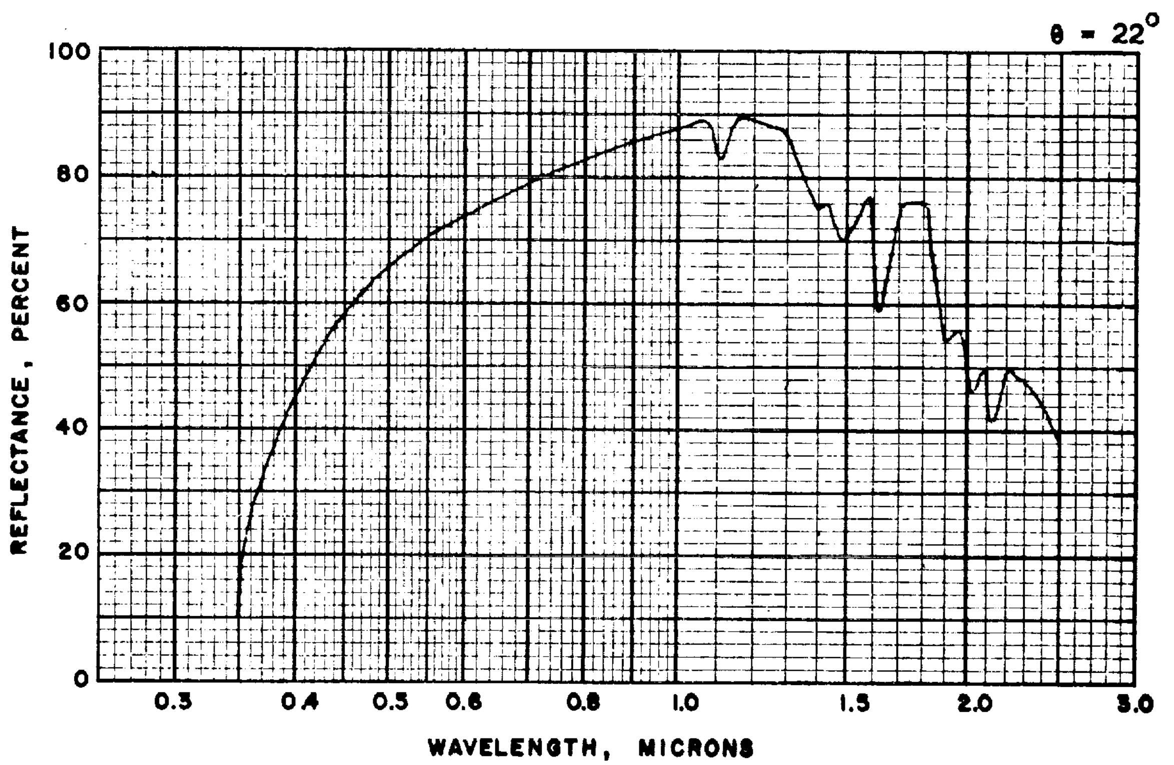

Figure 55: Sample 17, Azimuthal Angle 45°, Angles of Incidence 10° and 22°

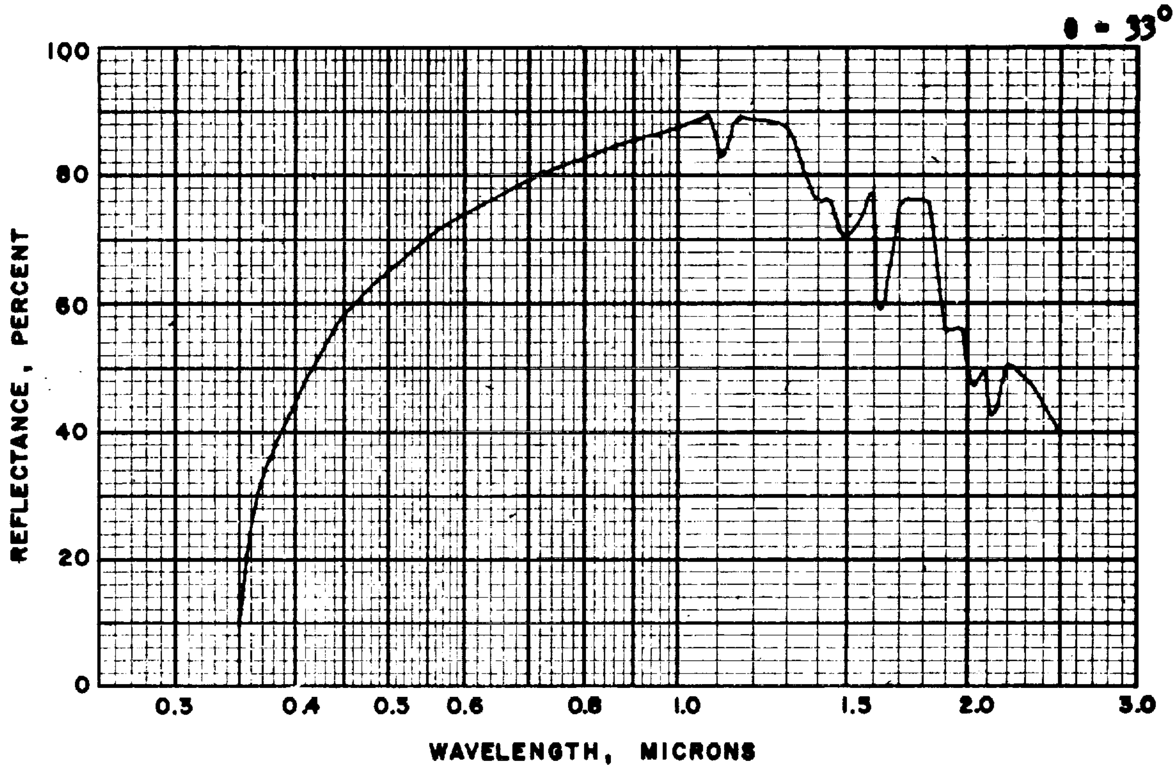

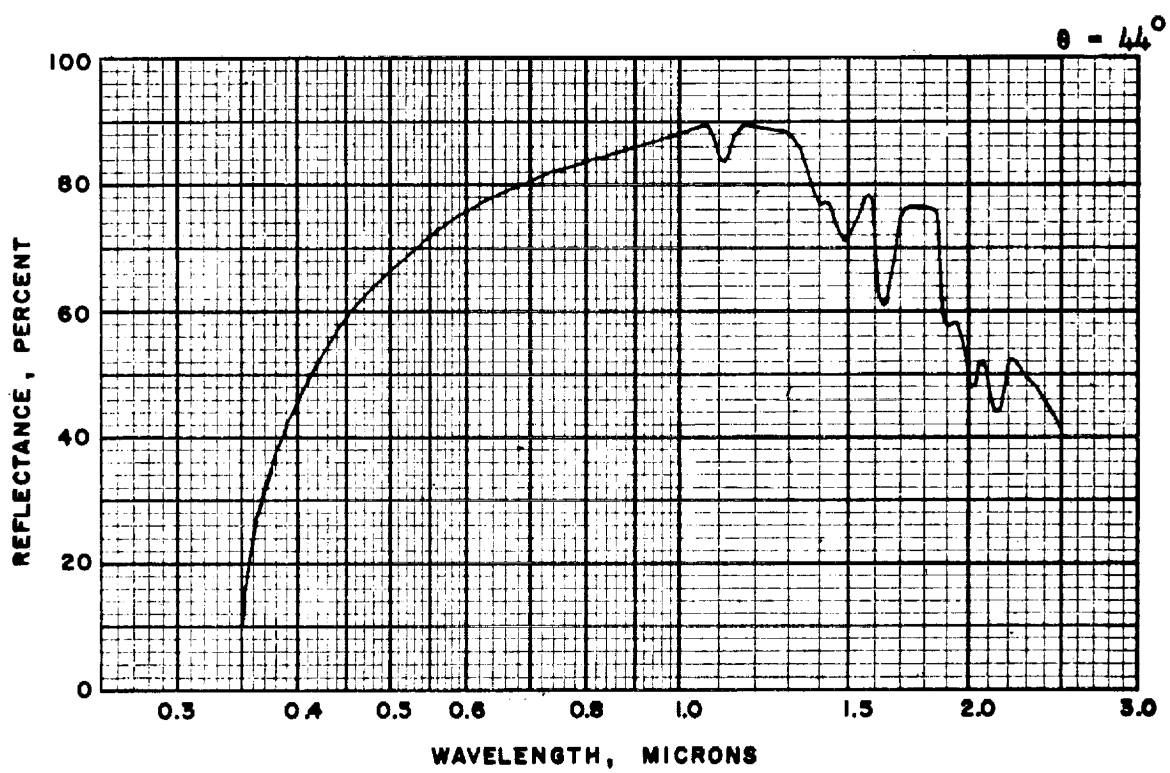

Figure 55 (Cont.): Sample 17, Azimuthal Angle 45°, Angles of Incidence 33° and 44°

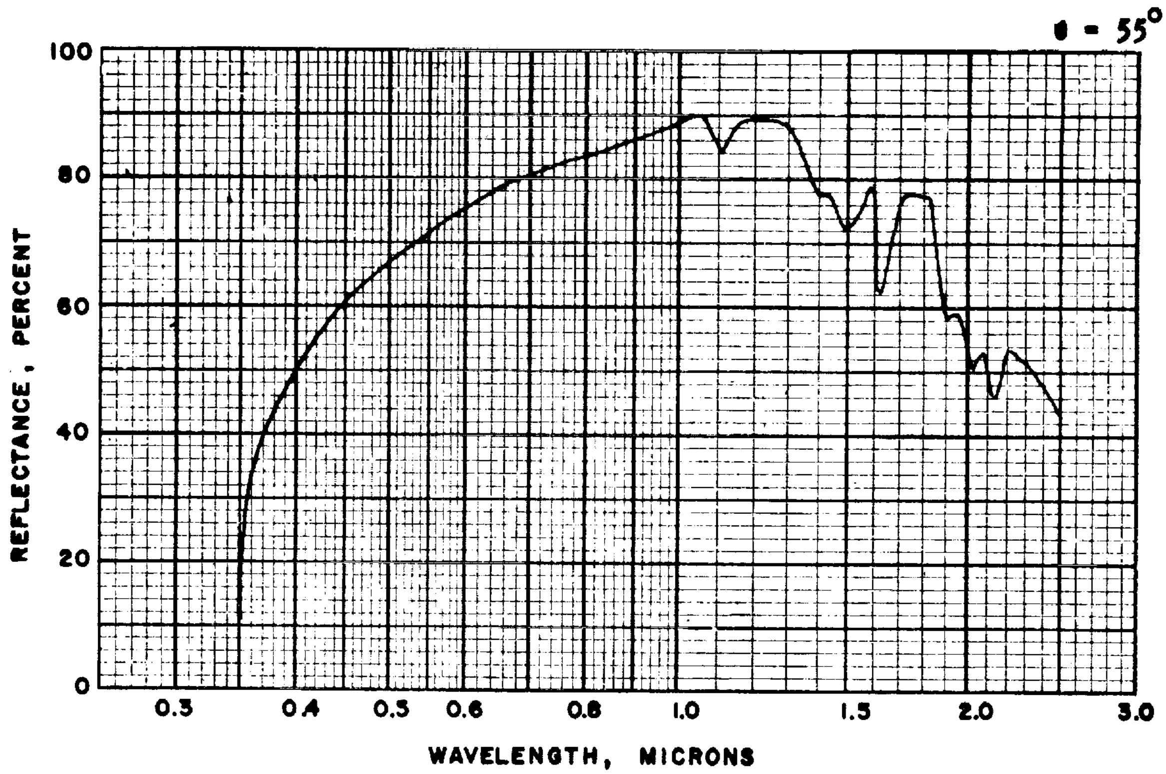

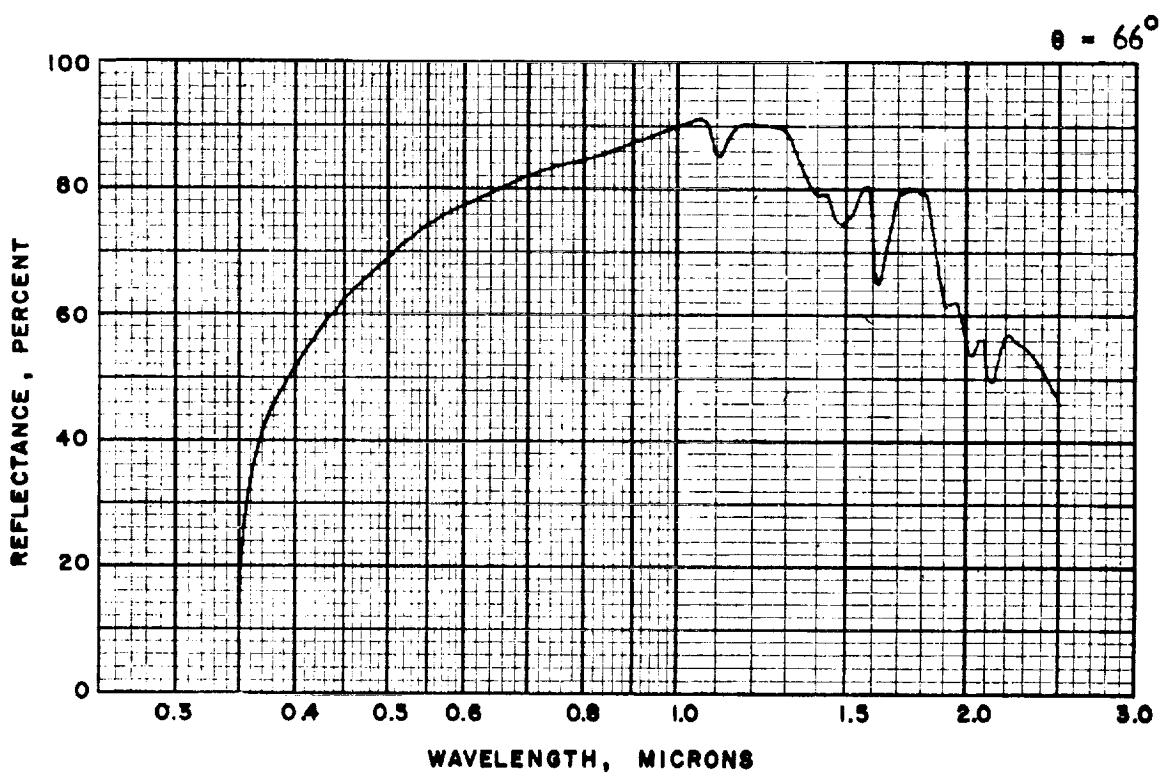

Figure 55 (Cont.): Sample 17, Azimuthal Angle 45°, Angles of Incidence 44° and 55°

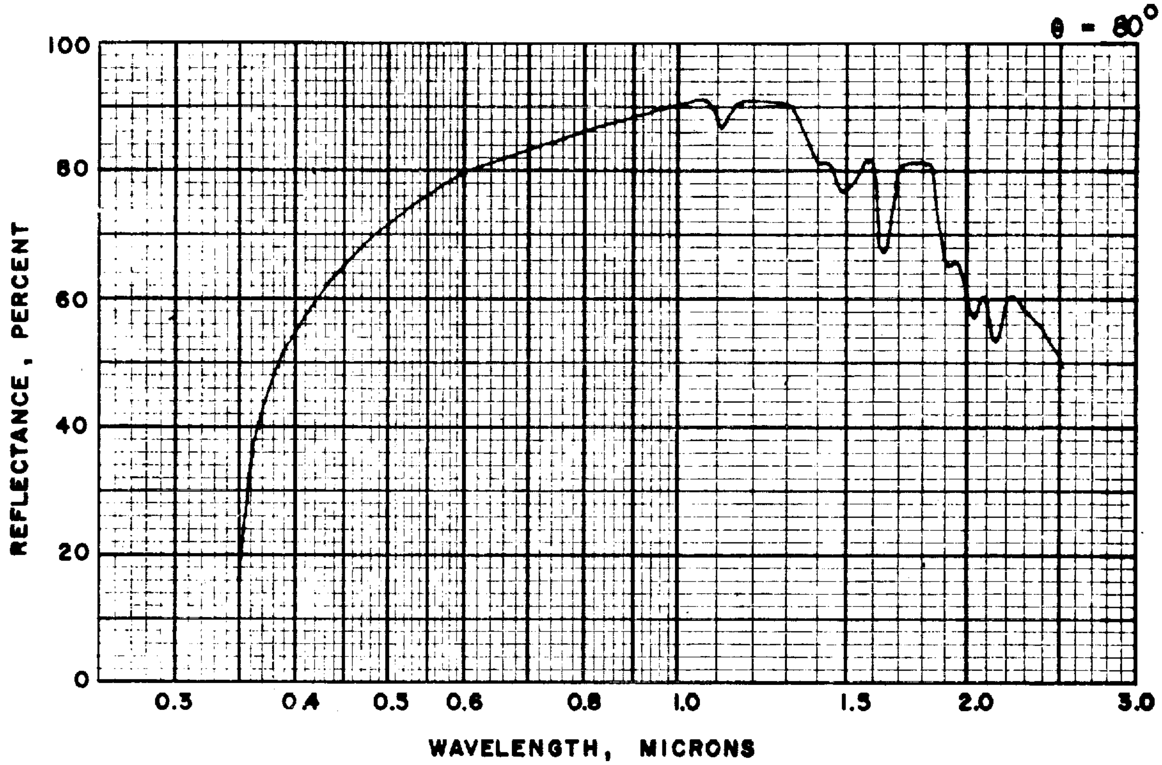

Figure 55 (Cont.): Sample 17, Azimuthal Angle 45°, Angle of Incidence 80°

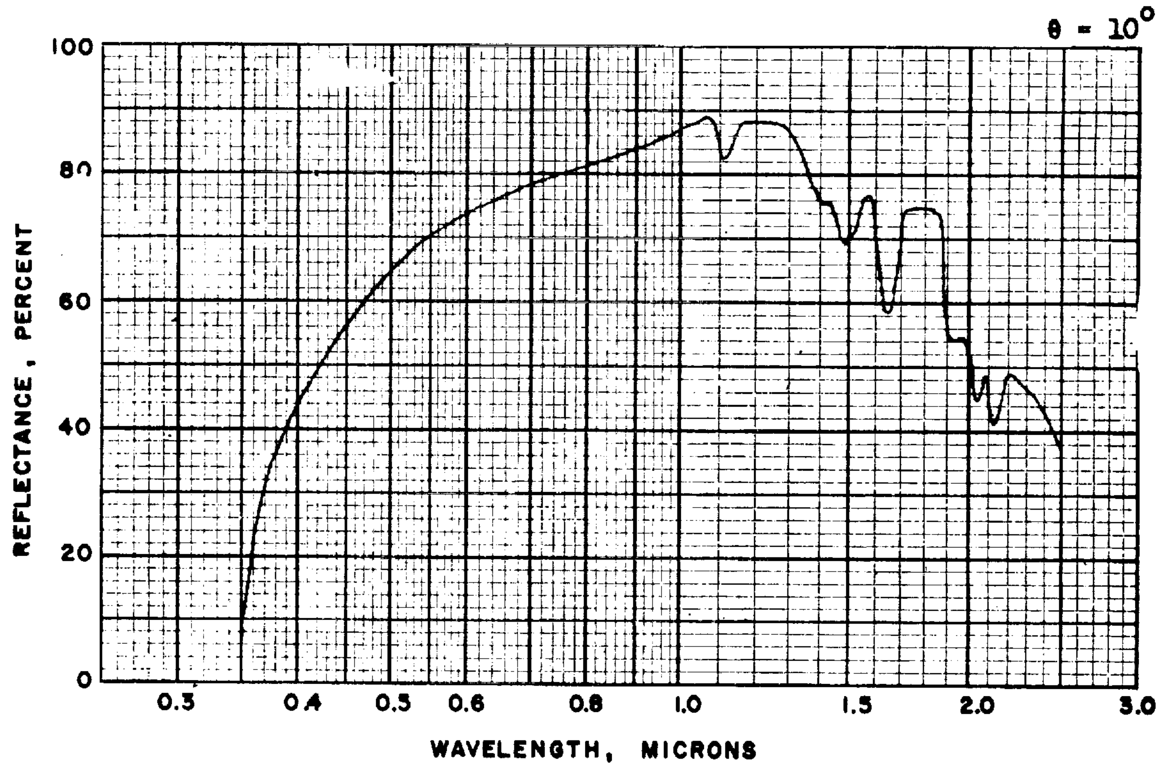

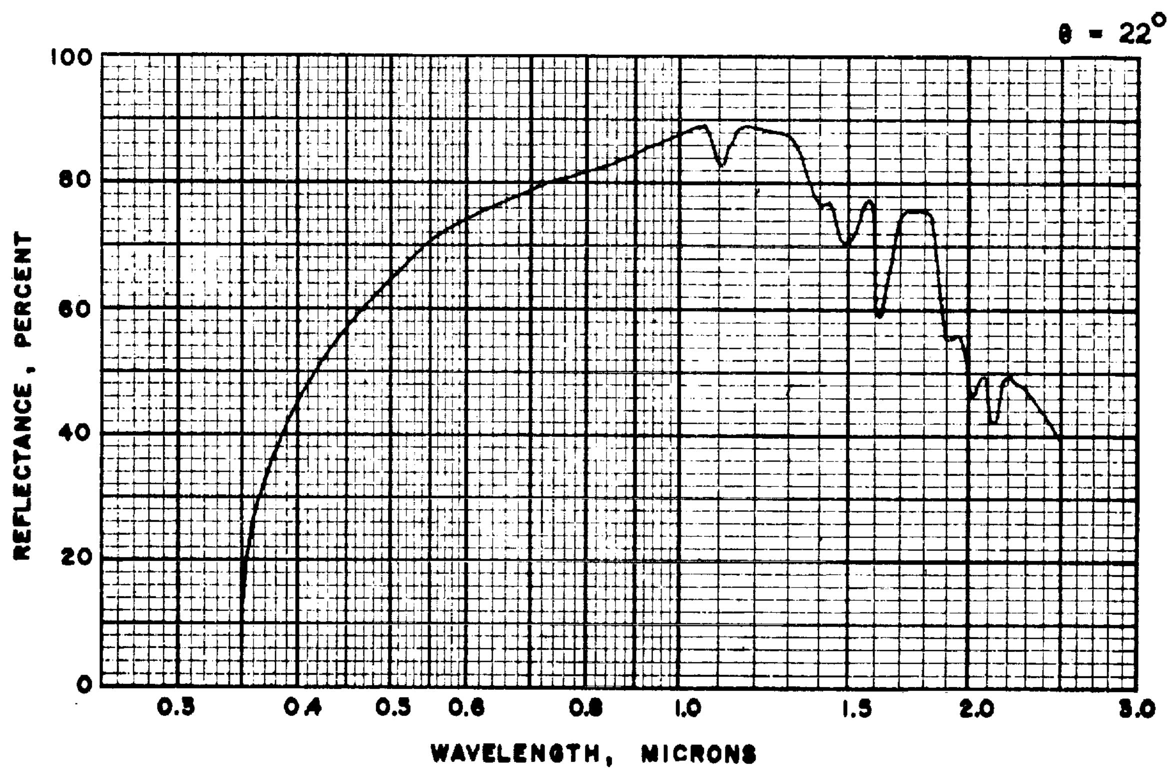

Figure 56: Sample 17, Azimuthal Angle 60°, Angles of Incidence 10° and 22°

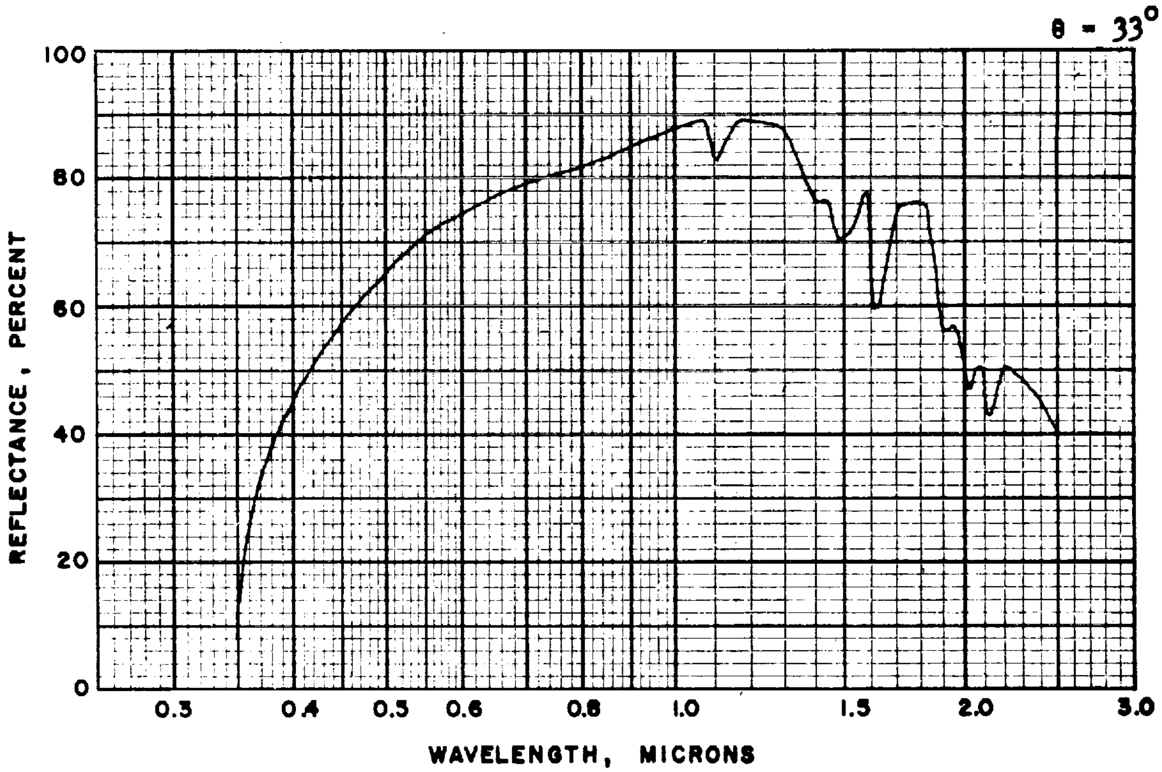

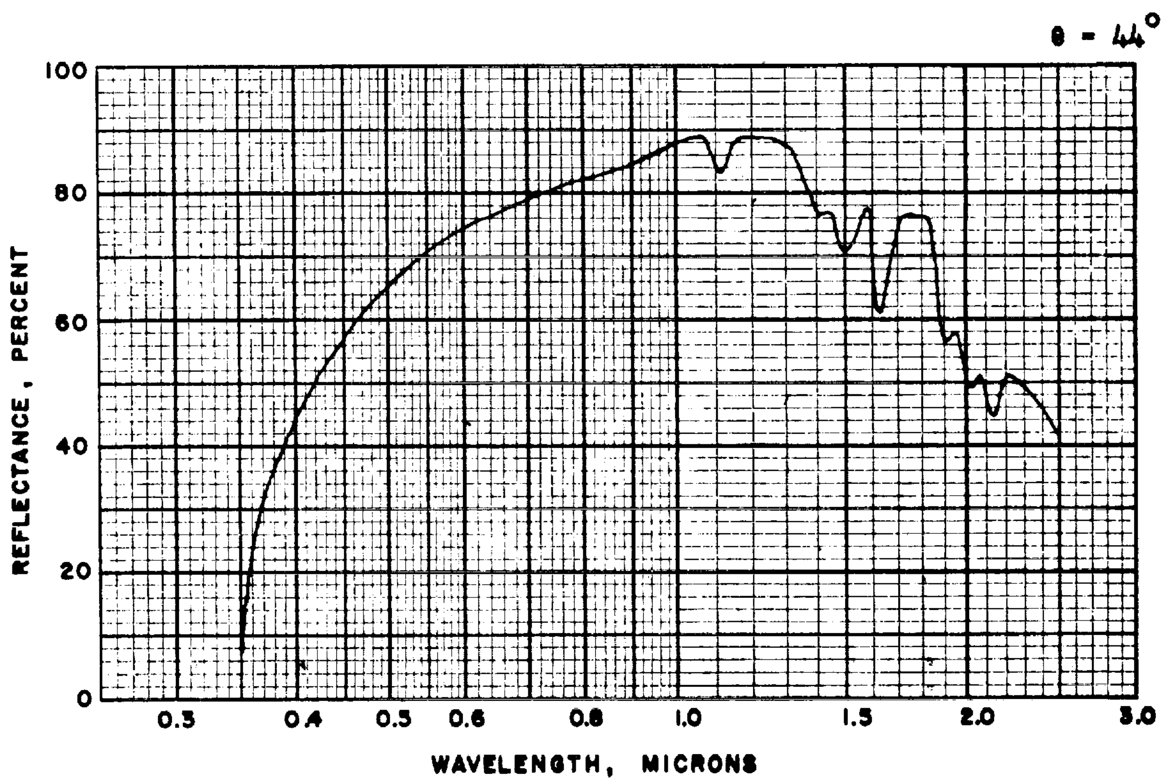

Figure 56 (Cont.): Sample 17, Azimuthal Angle 60°, Angles of Incidence 33° and 44°

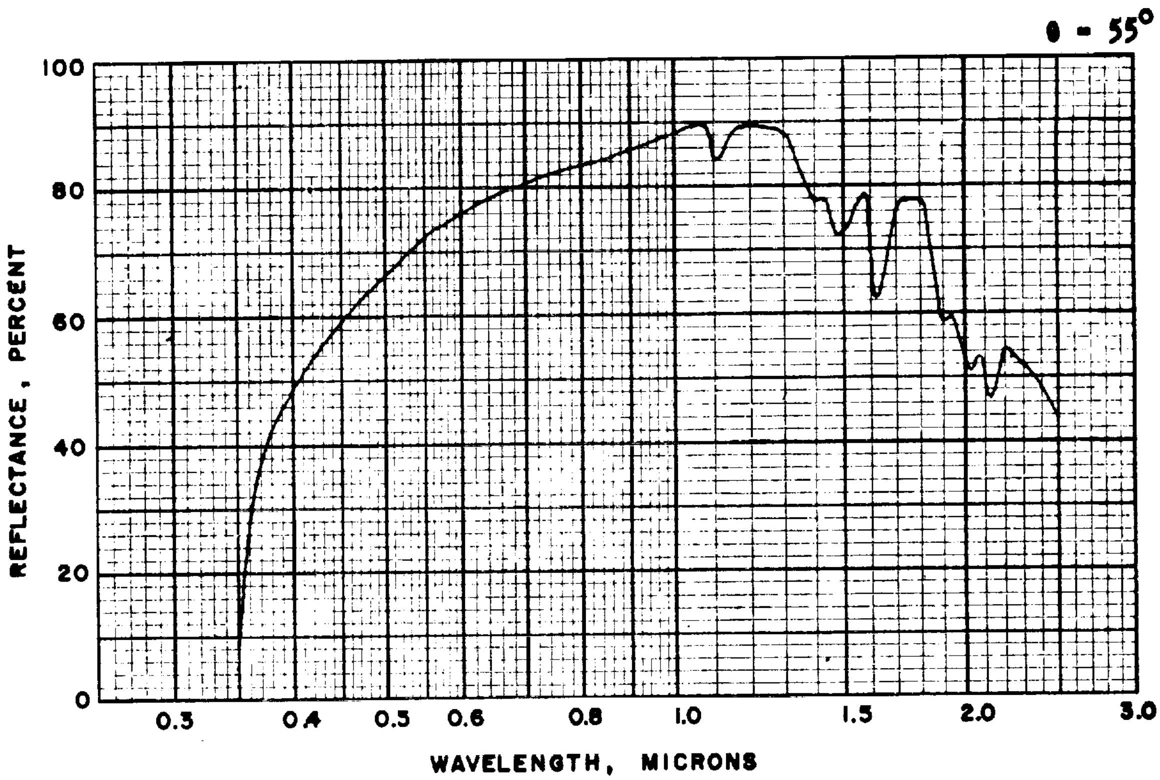

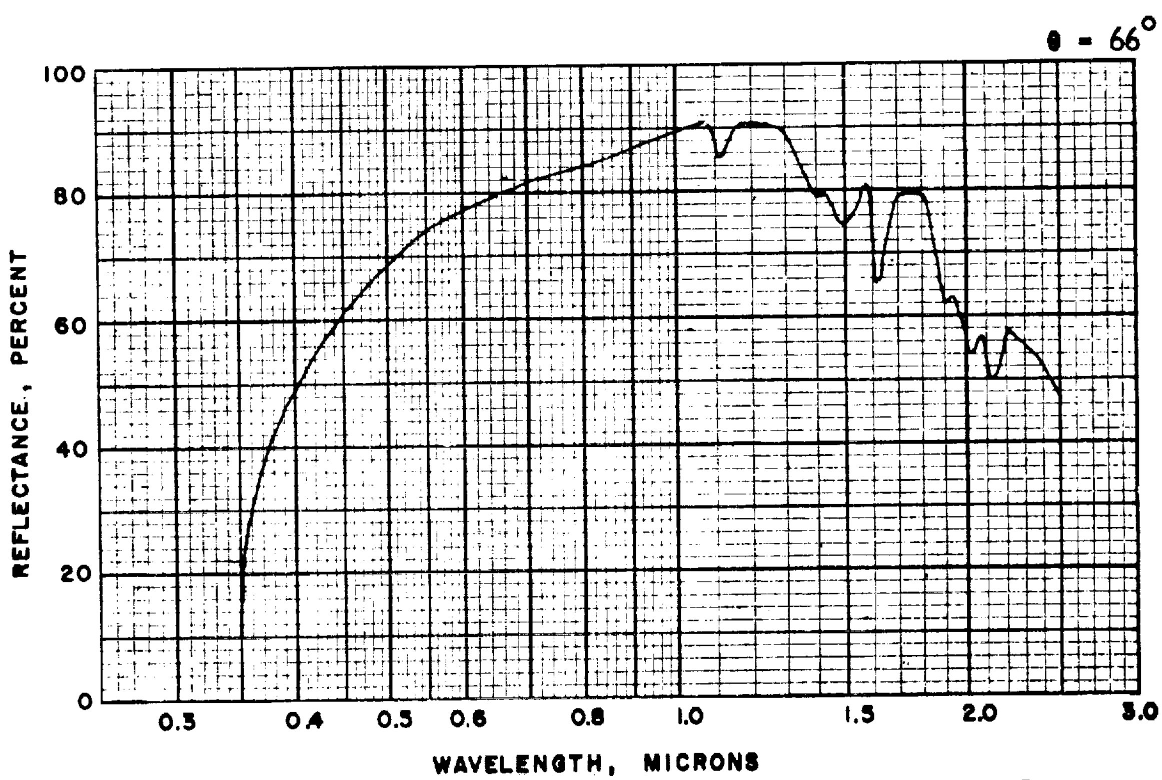

Figure 56 (Cont.): Sample 17, Azimuthal Angle 60°, Angles of Incidence 55° and 66°

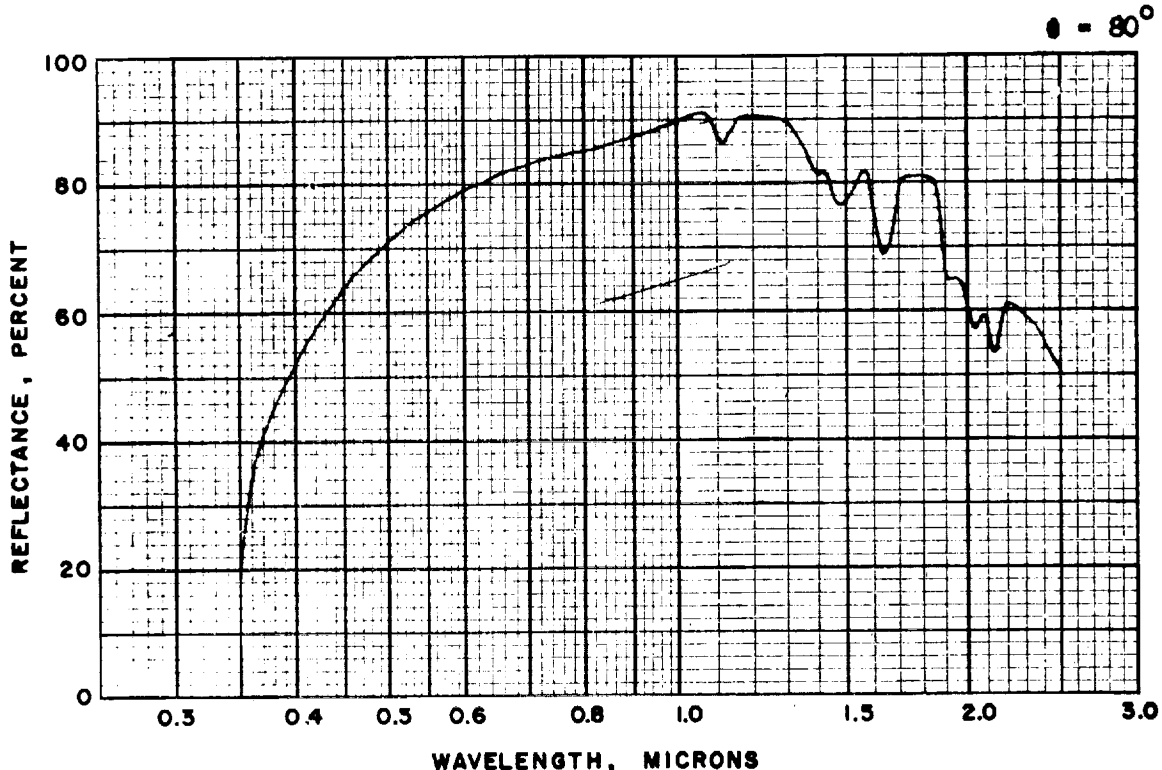

Figure 56 (Cont.): Sample 17, Azimuthal Angle 60°, Angle of Incidence 80°

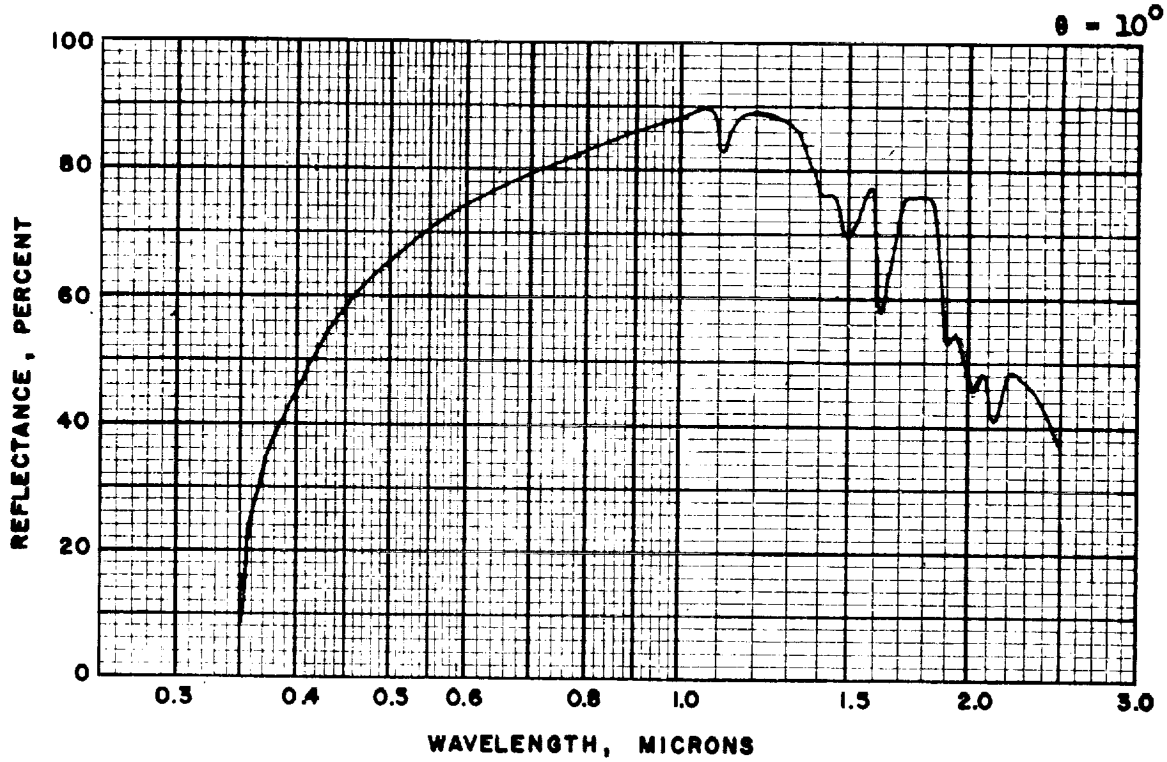

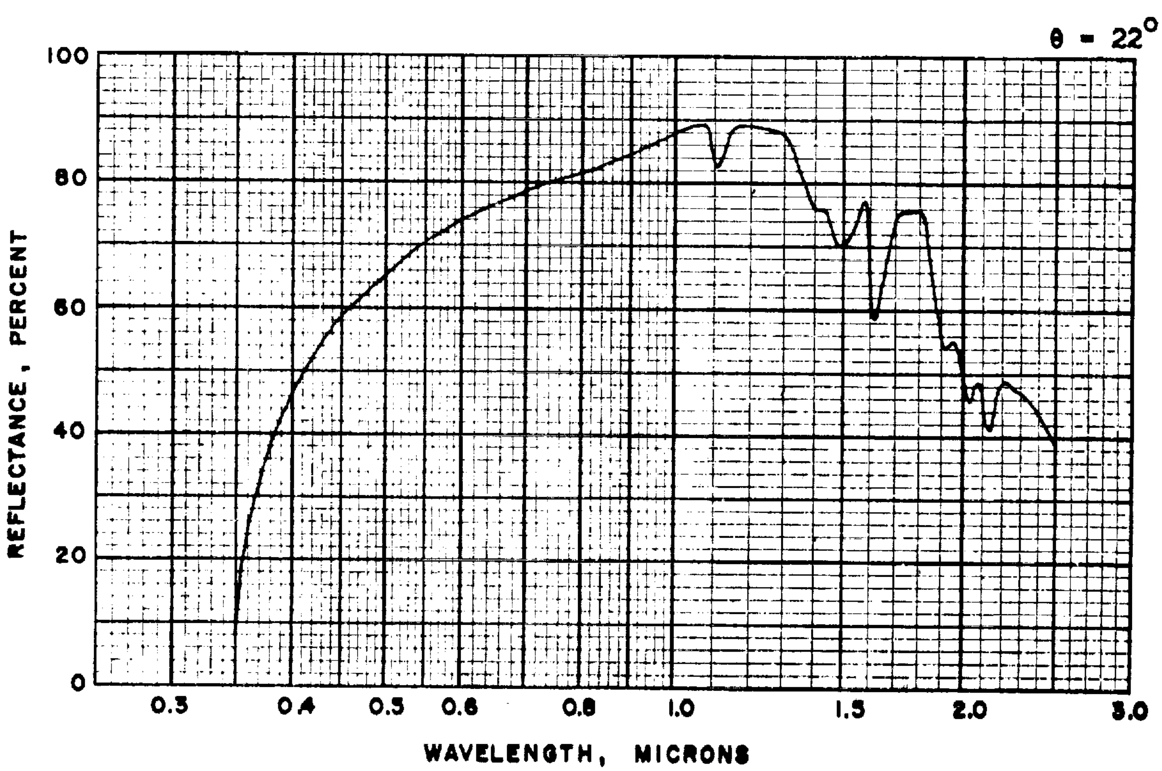

Figure 57: Sample 17, Azimuthal Angle 90°, Angles of Incidence 10° and 22°

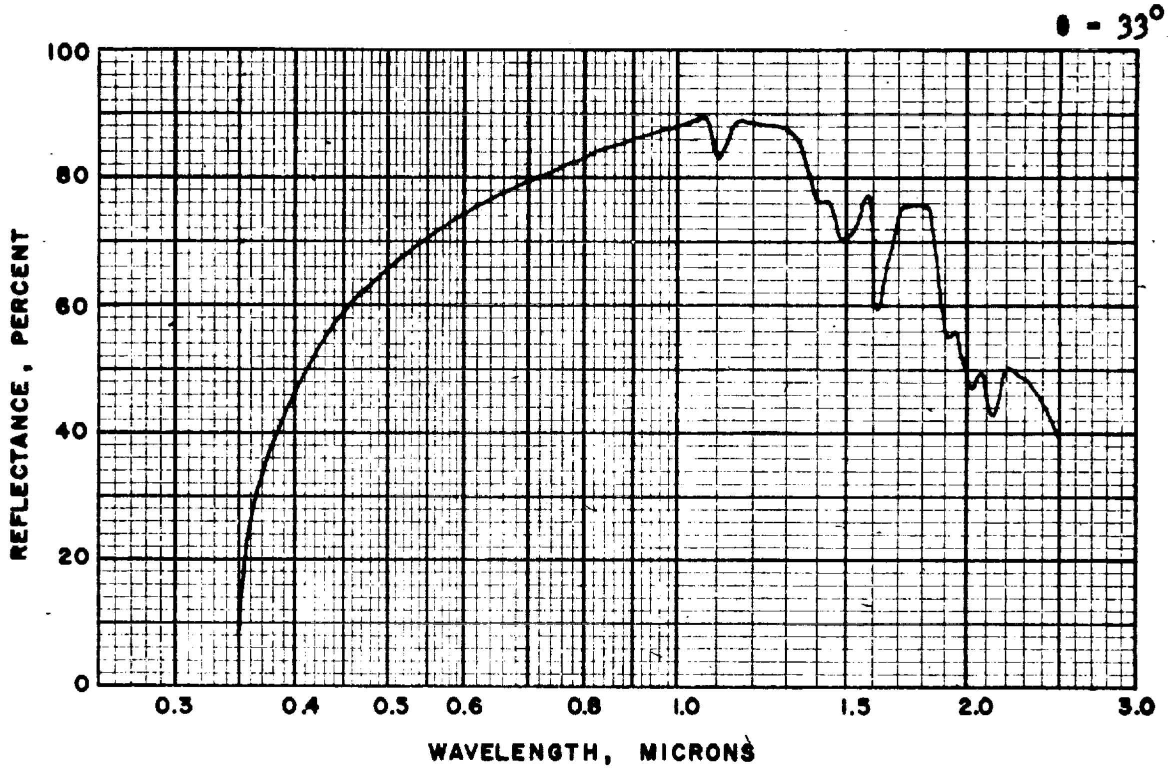

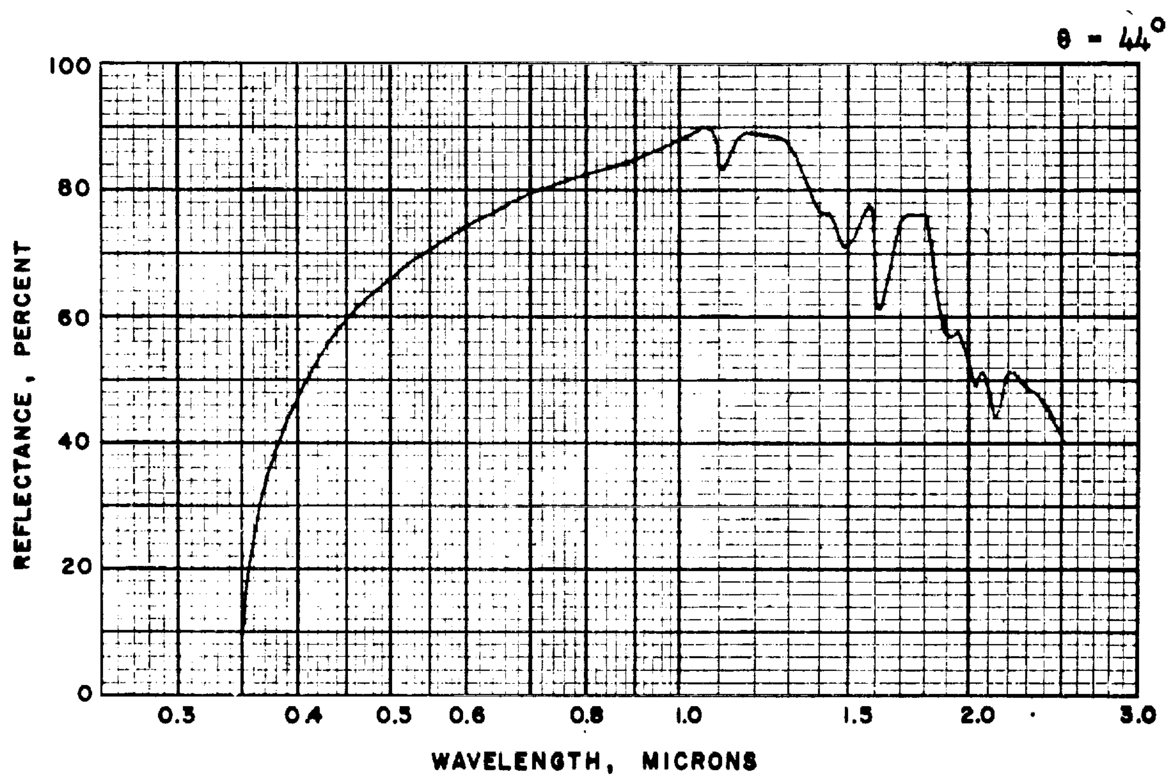

Figure 57 (Cont.): Sample 17, Azimuthal Angle 90°, Angles of Incidence 33° and 44°

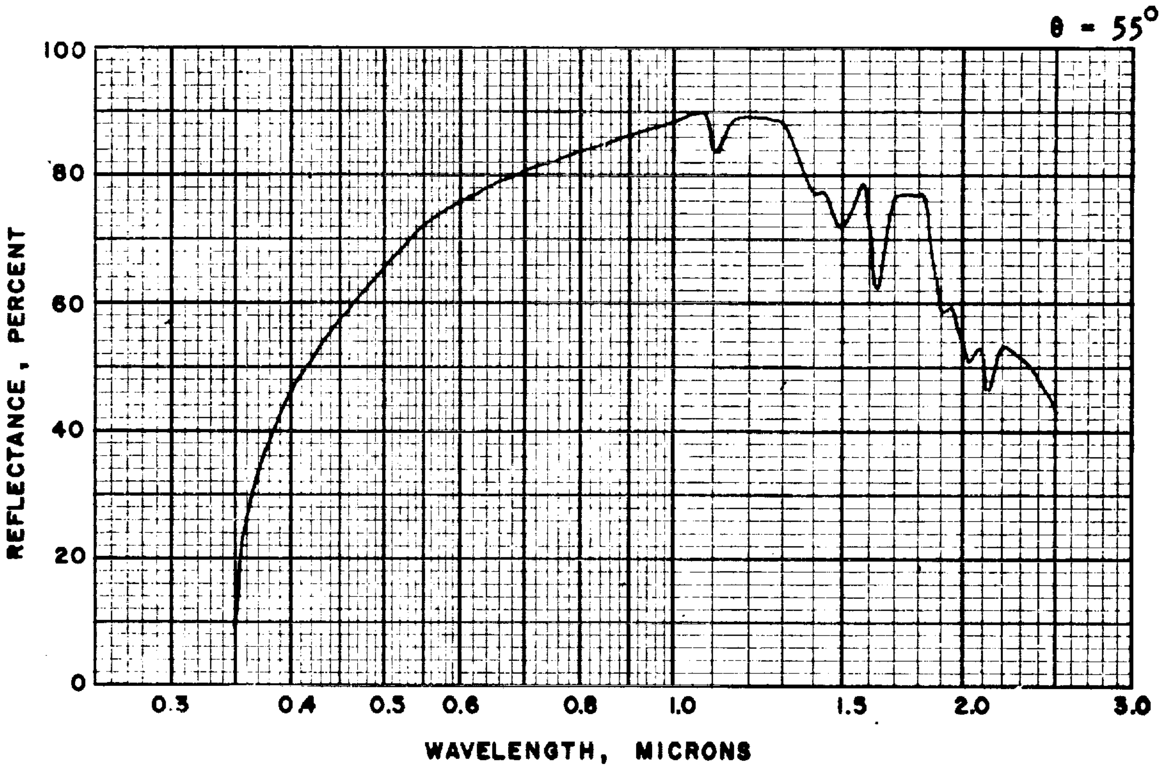

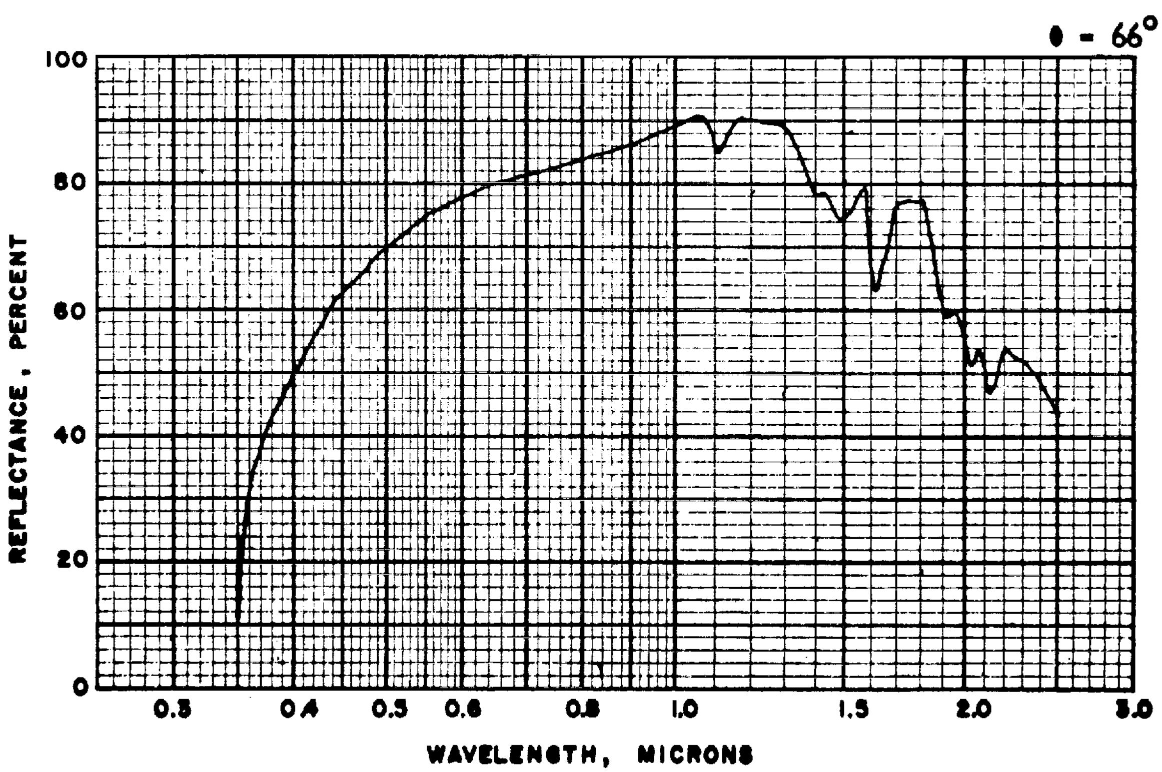

Figure 57 (Cont.): Sample 17, Azimuthal Angle 90°, Angles of Incidence 55° and 66°

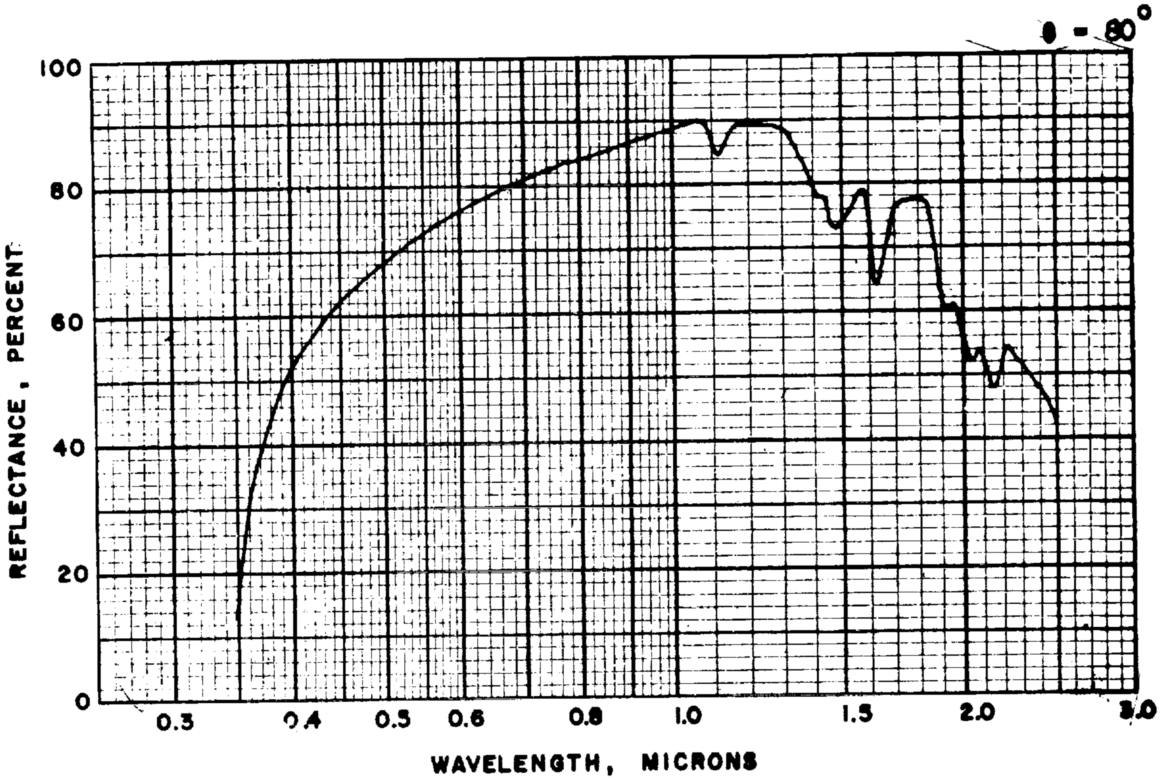

Figure 57 (Cont.): Sample 17, Azimuthal Angle 90°, Angle of Incidence 80°